U.S.NRC

United States Nuclear Regulatory Commission

Protecting People and the Environment

User's Manual for RESRAD-OFFSITE Code Version 4

Methodology and Models Used in RESRAD-OFFSITE Code

Office of Nuclear Regulatory Research

AVAILABILITY OF REFERENCE MATERIALS
IN NRC PUBLICATIONS

NRC Reference Material

As of November 1999, you may electronically access NUREG-series publications and other NRC records at the NRC's Library at www.nrc.gov/reading-rm.html. Publicly released records include, to name a few, NUREG-series publications; *Federal Register* notices; applicant, licensee, and vendor documents and correspondence; NRC correspondence and internal memoranda; bulletins and information notices; inspection and investigative reports; licensee event reports; and Commission papers and their attachments.

NRC publications in the NUREG series, NRC regulations, and Title 10, "Energy," in the *Code of Federal Regulations* may also be purchased from one of these two sources:

1. **The Superintendent of Documents**
   U.S. Government Publishing Office
   Washington, DC 20402-0001
   Internet: www.bookstore.gpo.gov
   Telephone: (202) 512-1800
   Fax: (202) 512-2104

2. **The National Technical Information Service**
   5301 Shawnee Road
   Alexandria, VA 22312-0002
   Internet: www.ntis.gov
   1-800-553-6847 or, locally, (703) 605-6000

A single copy of each NRC draft report for comment is available free, to the extent of supply, upon written request as follows:

Address: **U.S. Nuclear Regulatory Commission**
Office of Administration
Division of Resource Management & Analysis
Washington, DC 20555-0001
E-mail: distribution.resource@nrc.gov
Facsimile: (301) 415-2289

Some publications in the NUREG series that are posted at the NRC's Web site address www.nrc.gov/reading-rm/doc-collections/nuregs are updated periodically and may differ from the last printed version. Although references to material found on a Web site bear the date the material was accessed, the material available on the date cited may subsequently be removed from the site.

Non-NRC Reference Material

Documents available from public and special technical libraries include all open literature items, such as books, journal articles, transactions, *Federal Register* notices, Federal and State legislation, and congressional reports. Such documents as theses, dissertations, foreign reports and translations, and non-NRC conference proceedings may be purchased from their sponsoring organization.

Copies of industry codes and standards used in a substantive manner in the NRC regulatory process are maintained at—

The NRC Technical Library
Two White Flint North
11545 Rockville Pike
Rockville, MD 20852-2738

These standards are available in the library for reference use by the public. Codes and standards are usually copyrighted and may be purchased from the originating organization or, if they are American National Standards, from—

American National Standards Institute
11 West 42nd Street
New York, NY 10036-8002
Internet: www.ansi.org
(212) 642-4900

User's Manual for RESRAD-OFFSITE Code Version 4

Methodology and Models Used in RESRAD-OFFSITE Code

Prepared by:
ANL Team: C. Yu, RESRAD Project Manager
E. Gnanapragasam, J.-J. Cheng, D. LePoire,
S. Kamboj, and C. Wang

Argonne National Laboratory
9700 S. Cass Avenue
Lemont, IL 60439

NRC Team: S. Bush-Goddard, NRC Project Manager
C. Barr and B. Abu-Eid

Office of Nuclear Regulatory Research

ABSTRACT

The RESRAD-OFFSITE computer code evaluates radiological dose and excess cancer risk to an individual who is exposed while within and/or outside the area of initial (primary) contamination. The code considers releases from the primary contamination to the atmosphere, to surface runoff and to groundwater. It models the movement of the radionuclides, by groundwater and by air, from the primary contamination to the agricultural areas, pastures, a dwelling area, a well and a surface water body. It also simulates the accumulation of contaminants at those locations, where appropriate. Nine exposure pathways are considered in RESRAD-OFFSITE: direct exposure from contamination in soil, inhalation of particulates, inhalation of short-lived radon progeny, ingestion of plant food, meat, milk, aquatic foods, water and soil.

This document describes the processes modeled by the code; the data sources used in the modeling and the mathematical formulations of the processes are detailed in the Appendices. The sensitivity analysis feature and the probabilistic analysis feature are described. The options to model onsite exposure scenarios, to simulate the RESRAD-ONSITE code and the feature to compute area factors for regions of elevated contamination for offsite exposure scenarios are illustrated in the appendices. The benchmarking, verification and validation of the models in RESRAD-OFFSITE are described in this document.

TABLE OF CONTENTS

LIST OF FIGURES

LIST OF TABLES

ACKNOWLEDGMENTS

1 INTRODUCTION

RESRAD-OFFSITE is part of the RESRAD Family of Codes, which Argonne National Laboratory (Argonne) developed for the U.S. Department of Energy (DOE) and the U.S. Nuclear Regulatory Commission (NRC). The RESRAD Family of Codes includes five codes that are actively maintained and updated to run on various computer systems. These five codes are RESRAD-ONSITE, RESRAD-OFFSITE, RESRAD-BUILD, RESRAD-BIOTA, and RESRAD-RDD. Descriptions of these codes and their supporting documents are on the RESRAD website (http://resrad.evs.anl.gov). This report is Volume 1 of a NUREG/CR report that documents the methodology, models, and radionuclide-specific data used in RESRAD-OFFSITE, and it will also serve as RESRAD-OFFSITE's User's Manual. Volume 2 of the NUREG/CR is the User's Guide for RESRAD-OFFSITE Code Version 4, which describes how to use the RESRAD-OFFSITE code and contains screenshots and parameter information.

1.1   Genesis and Evolution of RESRAD-OFFSITE

The first code in the RESRAD Family is RESRAD-ONSITE, which evaluates the radiological dose and excess cancer risk to an individual who is exposed while residing or working in or directly above an area where the soil is contaminated with radionuclides (Gilbert et al. 1989; Yu et al. 1993, 2001). RESRAD-ONSITE was developed by Argonne's Environmental Assessment Division in the 1980s and has been widely used to assess radiologically contaminated sites since its release in 1989. Since then, RESRAD-ONSITE has undergone continuous improvement in response to feedback from users and sponsors.

The RESRAD team participated in many national and international model intercomparison studies in which RESRAD-ONSITE analyzed both hypothetical and actual contaminated site-based scenarios. The evolution of the RESRAD-OFFSITE code from RESRAD-ONSITE began in the 1990s during the International Atomic Energy Agency's (IAEA's) BIOsphere MOdel Validation Study II (BIOMOVS II), which compared radiological assessment models (Gnanapragasam and Yu 1997; IAEA 1996). This study required models to predict exposure to a receptor located outside the footprint of the primary contamination.

The RESRAD-OFFSITE code was first created by adding an offsite soil accumulation submodel (BIOMOVS II 1995) to the basic RESRAD-ONSITE modules. Then, an advective-dispersive groundwater transport submodel (BIOMOVS II 1996) was added. The ability to accept temporal information defining the releases from the contaminated soil was also added during this period. During the multimedia model comparison study, the advective-dispersive groundwater transport submodel was improved to better predict the transport of progeny produced in transit (Gnanapragasam et al. 2000). Subsequently, an atmospheric transport submodel and a surface water body accumulation submodel were added before the initial release of the code. The ability to model releases from the primary contamination that were delayed and/or distributed over time, the ability to model an equilibrium desorption release, and the ability to model transport by groundwater within the primary contamination were added for the release of version 3.1 (Yu et al. 2013; NUREG/CR-7127). The capability to model a submerged primary contamination and to offer a choice between the ICRP 38- and ICRP 107-based transformation data were added in Version 3.2. The option to model solubility-controlled release, diffusive release from contaminated material, and deposition of particulates over the catchment of the surface water body were added in Version 4.0. These enhancements allow application of RESRAD-OFFSITE for assessment of clean-up levels for complex decommissioning sites and performance of low-level radioactive waste disposal facilities.

Many of the submodels from RESRAD-ONSITE were modified before being incorporated into RESRAD-OFFSITE, which allowed the new code to model both onsite and offsite exposure scenarios. While both codes use analytical expressions and are not finite difference- or finite element-based codes, they use different computational algorithms. RESRAD-OFFSITE uses analytical expressions to compute the radionuclide transfer rates and radionuclide concentrations progressively over time based on those values at previous times. The time-integrated dose and time-integrated risk are computed using these concentrations. RESRAD-ONSITE numerically evaluates the analytical expressions for dose, risk, and concentration at any desired time after the site survey.

1.2   Overview of RESRAD-OFFSITE

The RESRAD-OFFSITE computer code evaluates radiological dose and excess cancer risk to an individual who is exposed while within and/or outside the area of initial (primary) contamination. The sources of water and the land-based locations of exposure can be outside the boundary of the primary contamination, as shown in Figure 1-1. They could be entirely within/on the boundary of the primary contamination, as shown in Figure 1-2, or, as shown in Figure 1-3, some exposure locations can be onsite, some can be offsite, and some can even straddle the site boundary.

The primary contamination, which is the source of all releases modeled by the code, is assumed to be within a layer of soil. The code considers releases of contaminants from the primary contamination to the atmosphere, to surface runoff, and to groundwater. It models the movement of the contaminants from the primary contamination to agricultural areas, pastures, a dwelling area, a well, and a surface water body. It also simulates the accumulation of contaminants at those locations, where appropriate. Any contribution of contaminants from the catchment to the surface water body and from the water sources to the land-based locations is also modeled.

Nine exposure pathways are considered in RESRAD-OFFSITE: direct exposure from contamination in soil, inhalation of particulates, inhalation of short-lived radon progeny, ingestion of plant food (i.e., vegetables, grain, and fruits), ingestion of meat, ingestion of milk, ingestion of aquatic foods, ingestion of water, and (incidental) ingestion of soil.
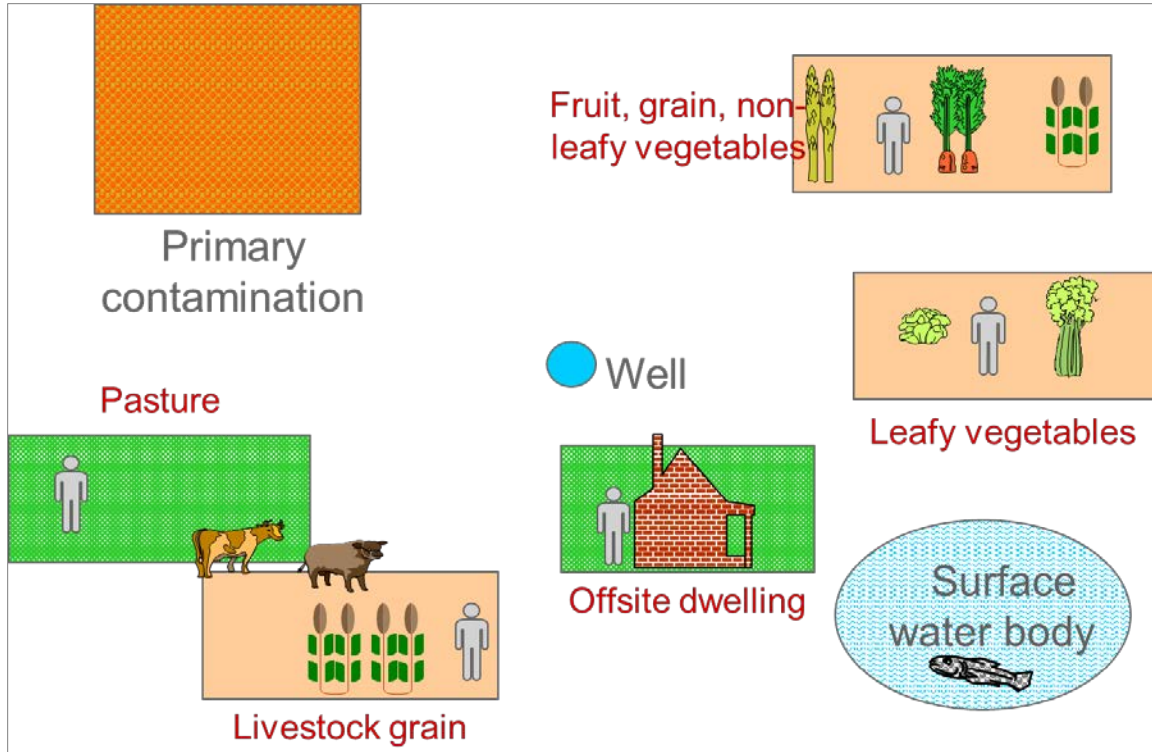
Figure 1-1   Exposure Locations for an Offsite Exposure Scenario
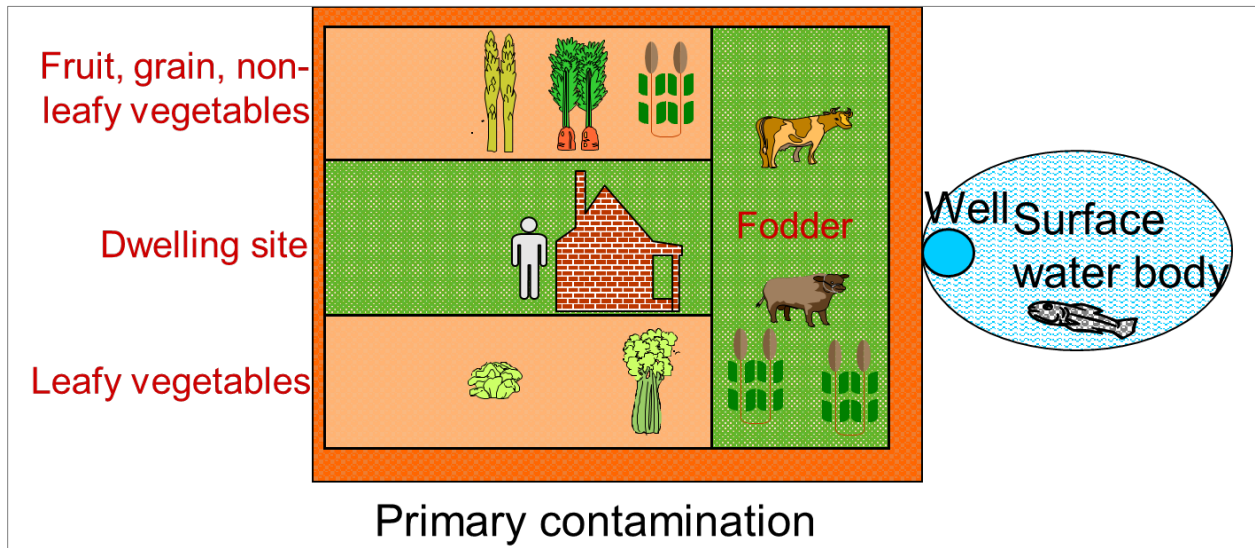
Figure 1-2   Exposure Locations for an Onsite Exposure Scenario
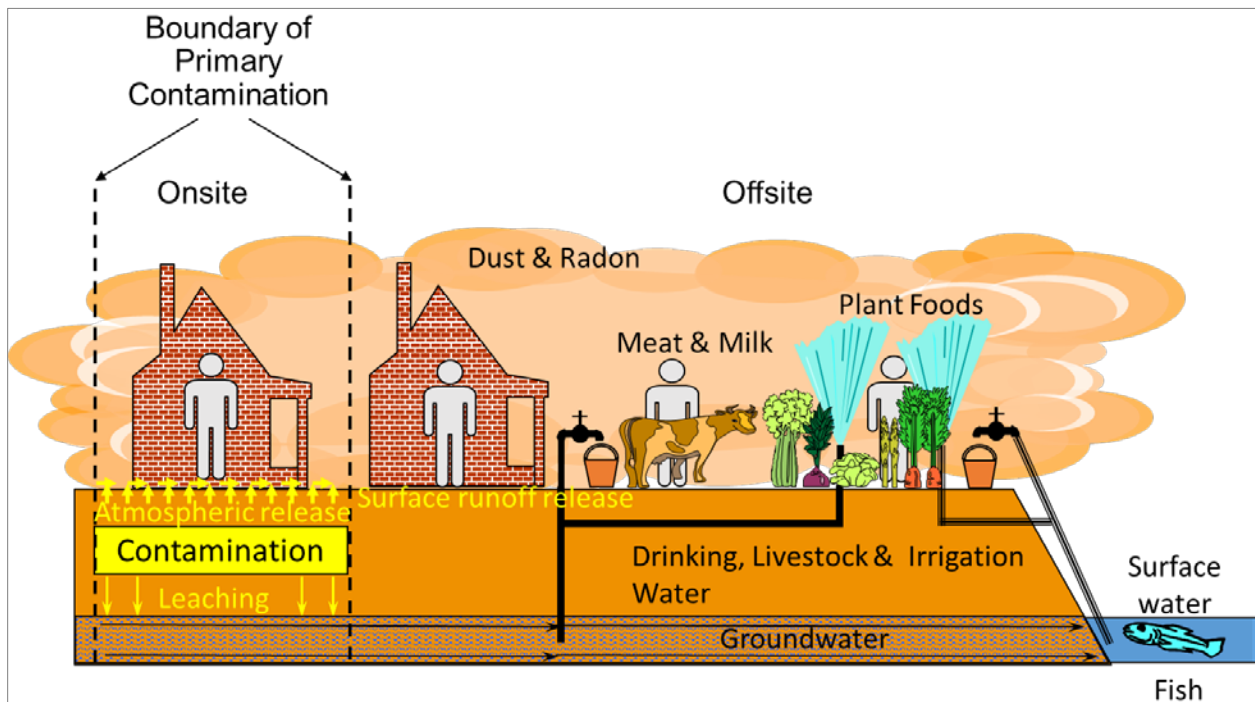
Figure 1-3 Environmental Pathways and Exposure Locations

1.3   Organization of Manual

Chapters 2 through 5 of this manual describe the process modeled by the code and the data sources used. Chapters 6 and 7 discuss sensitivity analyses and benchmarking, verification, and validation of the models and code. Chapter 8 is a list of references. Details about the formulations in the models and the information in the data sources are described in detail in Appendices A through J. Appendices K and L describe simulating RESRAD-ONSITE code using RESRAD-OFFSITE and the onside scenario template file. Appendix M describes benchmarking of the source term model in the RESRAD-OFFSITE code and the DUST-MS code. Appendix N presents the risk slope factor for radionuclides. Appendix O describes the feature in RESRAD-OFFSITE regarding generating the area factors. A user's guide that describes the user interface is included in Volume 2 of this NUREG/CR.

The information presented in this manual is organized as follows:

- Chapter 1: Introduction

- Chapter 2: Conceptualization of Primary Contamination and Releases

- Chapter 3: Exposure Pathways, Locations, and Scenarios

- Chapter 4: Calculation of Dose and Risk

- Chapter 5: Concentration of Radionuclides in Environmental Media

- Chapter 6: Deterministic Analysis, Sensitivity Analysis, and Uncertainty/Probabilistic Analysis

- Chapter 7: Verification, Benchmarking, and Validation

- Chapter 8: References

- Appendix A: Radionuclide Transformation Databases and Associated Dose Coefficient Libraries

- Appendix B: External Radiation from Contamination in Soil

- Appendix C: Exposure from Inhalation of Particulates

- Appendix D: Exposure from Inhalation of Short-Lived Radon Progeny

- Appendix E: Exposure from Ingestion of Vegetables, Meat, Milk, Aquatic Food, Water, and Incidental Ingestion of Soil

- Appendix F: Models for Tritium and Carbon-14

- Appendix G: Primary Contamination Model

- Appendix H: Groundwater Transport

- Appendix I: Atmospheric Transport

- Appendix J: Concentration in Environmental Media

- Appendix K: Simulating the RESRAD-ONSITE Code

- Appendix L: The Onsite Scenario Template File

- Appendix M: Example Applications and Benchmarking of the Source Term Model

- Appendix N: Slope Factor

- Appendix O: Area Factors for Offsite Exposure Scenarios

2 CONCEPTUALIZATION OF AND RELEASES FROM THE PRIMARY CONTAMINATION

This chapter describes the conceptualization of the initial location of the contamination, the releases that are modeled, the options available to model the release to infiltration, and the modeling of engineered barriers. Appendix G discusses models and equations for releases from the primary contamination in detail.

2.1   Location of Primary Contamination

The primary contamination, the initial location of radionuclides, is a layer of soil that is either directly contaminated or contains radionuclide-bearing material distributed within it. The code assumes that the primary contamination is uniformly contaminated and is of a constant thickness. There can be a layer of clean cover on top of the primary contamination. The primary contamination can be above the water table, it can straddle the water table, or it can be submerged with its top at the water table, as shown in Figure 2-1.
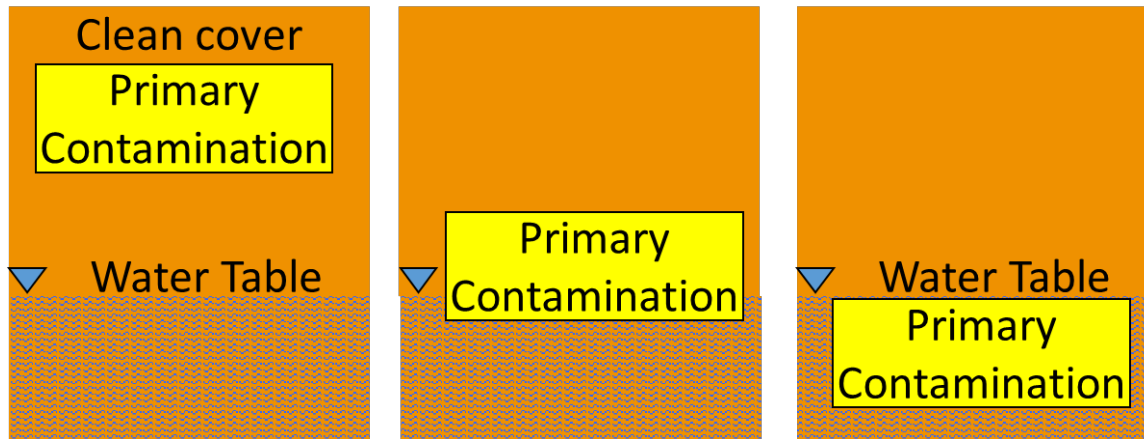
Figure 2-1   Location of Primary Contamination

2.2   Releases from the Primary Contamination

The three general releases modeled are (1) the leaching release to the water that infiltrates through the primary contamination; (2) the release of particulate, both respirable and total, to the air; and (3) the release of eroded material to runoff, as shown in Figure 2-2. The release of particulates to air and the release of eroded material to runoff occur from the surface soil layer. If there is initially a clean cover above the primary contamination, then the surface soil layer will not release radionuclides until it becomes contaminated. The code models mixing within a surface layer. As the cover erodes over time, the surface mixing layer can penetrate the primary contamination at some time in the future and become contaminated. Radionuclides will then be released with the particulates and eroded materials from the contaminated surface layer. The code computes the releases from the surface layer under the two transfer mechanisms described in Sections 2.4.2 and 2.4.3. It does not compute the releases from the surface layer under the third transfer mechanism (Section 2.4.1) for the reason described in Section 5.1.2. The leaching release will occur from both the contaminated mixing layer and the primary

contamination. The code computes the infiltration rate using an annual surface hydrology water balance involving precipitation and irrigation inflows and evapotranspiration, runoff, and infiltration outflows.
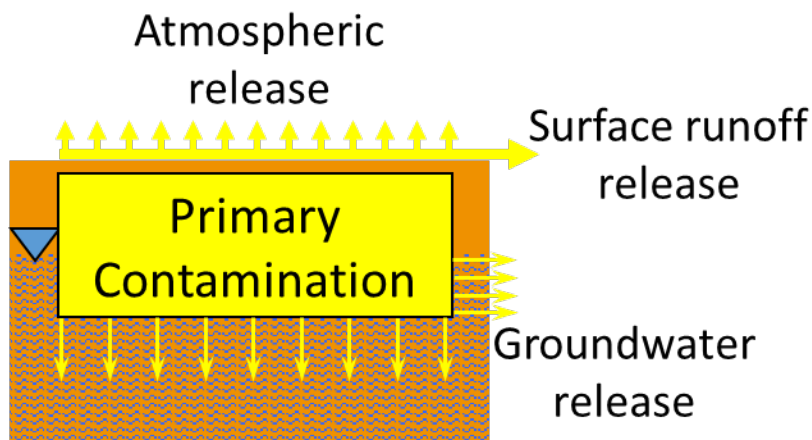
Figure 2-2   Three General Releases from the Primary Contamination

The code also models the release of gaseous forms for three specific cases: tritiated water vapor, carbon-14 in the form of carbon dioxide, and the radon isotopes. The release of tritiated water vapor is modeled in the same manner as evapotranspiration of soil moisture from a surface layer. The release of carbon-14 dioxide is based on an evasion rate that is input by the user. The diffusive release of radon gas through the primary contamination, any cover, and the foundations of any buildings occupied by the receptor is modeled numerically.

2.2.1   Mass Balance

Radiological decay (or transformations); the three general releases; and, when applicable, the gaseous release are interrelated. They all affect the amount of radionuclide in the primary contamination that is available for release or for later transformation. The code maintains mass balance of the nuclide inventory by considering the losses to transformation, the release to infiltration, the release to runoff, and, when applicable, the release of carbon-14 as carbon dioxide and hydrogen-3 in water. However, the code does not currently consider losses due to particulate releases to the atmosphere or the release of radon gas. All three conceptualizations (Section 2.3) and all three transfer mechanisms to infiltration (Section 2.4) maintain mass balance. Appendix G describes the verification of mass balance.

2.3   Conceptualization of Primary Contamination

RESRAD-OFFSITE offers a choice among the three methods of conceptualizing the primary contamination described in Sections 2.3.1 through 2.3.3, in addition to the RESRAD-ONSITE conceptualization described in Section 2.6. These three additional choices arise from the initial disposition of the radionuclides within the primary contamination (Figure 2-3) and, where applicable, whether advective-dispersive transport or diffusive transport dominates in the radionuclide-bearing material (Figure 2-4). The choice of conceptualization method applies to all the radionuclides in an input file and determines the choices for the infiltration release options that are described in subsequent sections.

2.3.1 Entire Site of Primary Contamination Is Contaminated

In this conceptualization, all the solids in the primary contamination are assumed to be contaminated. The initial activity concentrations of the radionuclides are specified in terms of the mass of the entire primary contamination. The radionuclides may be transferred from the solid phase to the aqueous phase (soil moisture) of the primary contamination according to any of the three transfer mechanisms available in the code (Section 2.4). The code models the one-dimensional advective-dispersive transport of the radionuclides from where radionuclides are transferred to the aqueous phase to the bottom of the primary contamination. The properties specified for the primary contamination are used to model the transfer of radionuclide to the soil moisture and the transport of the radionuclides through the primary contamination.
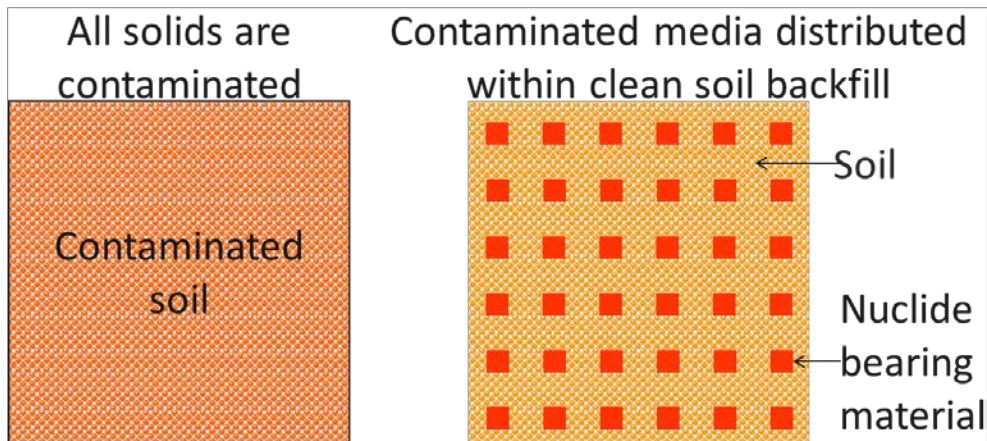
Figure 2-3   Conceptualization of the Initial Disposition of Radionuclides
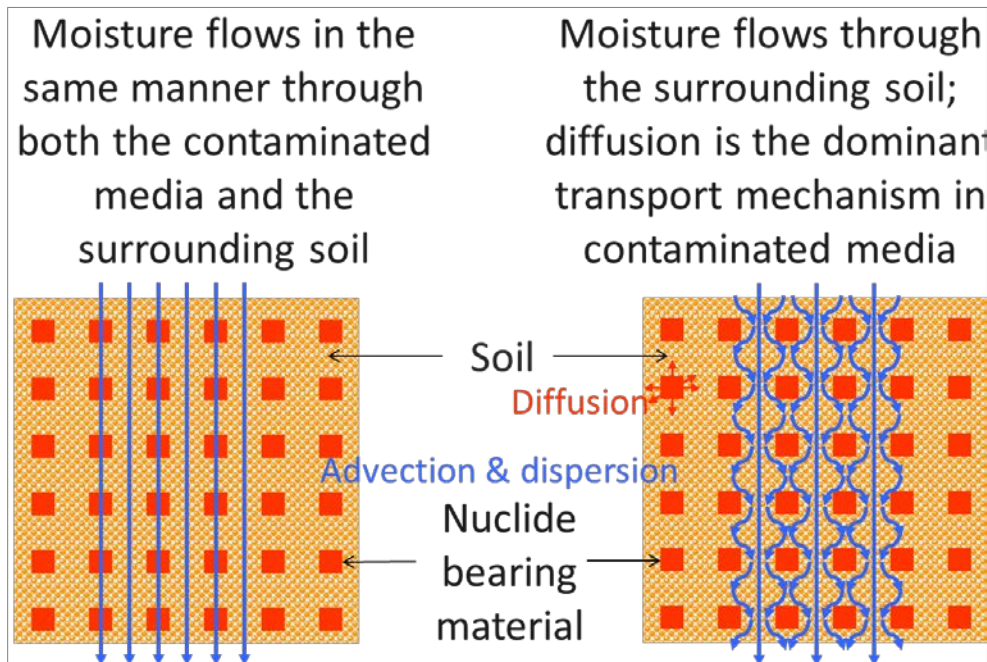
Figure 2-4   Flow of Moisture through the Primary Contamination

2.3.2 Radionuclide-Bearing Material Is as Conductive as the Surrounding Soil

The code assumes that the radionuclide-bearing material is distributed uniformly within the soil in the primary contamination. The soil is initially uncontaminated. The initial activity concentrations of the radionuclides are specified in terms of the mass of only the radionuclide-bearing material. Both the radionuclide-bearing material and the surrounding soil have similar properties with respect to the movement of water. However, the radionuclides can have different affinities to the radionuclide-bearing material and to the soil solids. These are quantified by the respective distribution coefficients. The radionuclides may be transferred from the radionuclide-bearing material to the aqueous phase of the primary contamination according to any of the three transfer mechanisms available in the code (Section 2.4). The code models the one-dimensional advective-dispersive transport of the radionuclides from where they are transferred to the aqueous phase to the bottom of the primary contamination. The properties specified for the primary contamination and for the radionuclide-bearing material are used to model the transfer of radionuclide to the soil moisture and the transport of the radionuclides through the primary contamination.

2.3.3 Diffusion Is the Dominant Transport Mechanism in the Radionuclide-Bearing Material

The code assumes that the radionuclide-bearing material is distributed uniformly within the soil in the primary contamination. The soil initially is not contaminated. The initial activity concentrations of the radionuclides are specified in terms of the mass of only the radionuclide-bearing material. The infiltrating water is assumed to travel through the soil and not through the nuclide-bearing material. However, at least some of the pores in the radionuclide-bearing material are assumed to contain water and diffusion is the dominant transport mechanism in the radionuclide bearing material. The radionuclides can have different affinities to the radionuclide-bearing material and to the soil solids. These are quantified by the respective distribution coefficients. The radionuclides may transfer from the solid phase of the radionuclide-bearing material to the aqueous phase of the radionuclide-bearing material by only equilibrium desorption characterized by the distribution coefficient in the radionuclide-bearing material. The code first models the diffusive transport of the radionuclides through the aqueous phase of the radionuclide-bearing material into the surrounding soil under the assumption that there is no advective transport within the radionuclide-bearing material. The properties of the radionuclide-bearing material are used to model the diffusive transport. The code then models the one-dimensional advective-dispersive transport of the radionuclides to the bottom of the primary contamination. The properties specified for the primary contamination are used to model the transport of the radionuclides through the primary contamination.

2.4 Transfer Mechanisms for Infiltration Release

The code has three mechanisms to model the transfer of radionuclides from the solid phase of the contamination to the aqueous phase—the soil moisture—of the contamination. Two of these are based on the equilibrium of the process determining the transfer, and the third is based on the system being so far from equilibrium that only the forward process is modeled.

2.4.1 Equilibrium Desorption

The radionuclide is modeled as being in linear desorption-adsorption equilibrium between the solid phase and the aqueous phase of the soil. The equilibrium is characterized by a constant ratio between the adsorbed concentration and the concentration in the aqueous phase, the

linear distribution coefficient of the radionuclide. Equilibrium is assumed to be attained instantaneously; under this assumption, the concentration of the radionuclide in the water that enters the primary contamination increases rapidly to the equilibrium concentration. Thus, the transfer of radionuclides from the solid to the aqueous phase will occur at the up-gradient edge of the contamination and not uniformly over the primary contamination (Figure 2-5).

The code models the advective-dispersive transport of the radionuclide over the primary contamination and computes the release out of the down-gradient edge of the primary contamination; however, it does not compute the concentration profile over the primary contamination. If the concentration profile over the transport distance were computed, it would shift away from the up-gradient edge because of the transfer from the solid phase to the aqueous phase, and it will be non-uniform, especially at the trailing edge of the profile, because of the dispersive component of transport (Figure 2-5). Although the adsorption-desorption equilibrium is assumed to be instantaneous, the release of the radionuclide from the down-gradient edge of the primary contamination will occur over an extended period determined by, among other things, the distribution coefficient of the radionuclide.
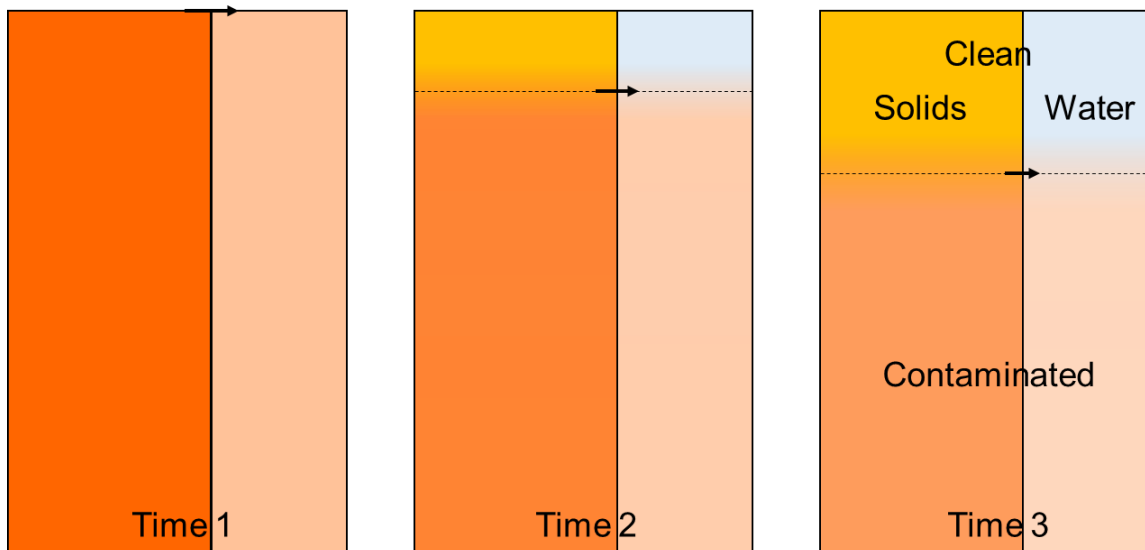
Figure 2-5   Schematic of the Conceptualization of the Equilibrium Desorption Release

2.4.2   Equilibrium Solubility

The code models the radionuclide as being in dissolution-precipitation equilibrium between the solid phase and the aqueous phase of the soil. The equilibrium is characterized by a total soluble concentration of the element. This choice applies to all the isotopes of the element, both radioactive and stable, that are present at the site. However, the code does not deal with stable isotopes and apportions the soluble concentration between the radioactive isotopes. The code assumes that equilibrium is attained slowly, with the concentration of the isotopes in the water that enters the primary contamination increasing gradually to the equilibrium concentration at the down-gradient edge of the primary contamination. The code assumes that the rate of transfer of each radioisotope will be uniform over the length of transport in the primary contamination at any time such that the concentration within the primary contamination is spatially uniform but changes over time as radionuclides are depleted due to transfer and

radiological transformations. (Figure 2-6). The rate of transfer can vary with time if the relative inventories of the isotopes of the element change with time due to radiological transformations. The code models the un-retarded advective-dispersive transport of the radionuclide over the primary contamination and computes the release out of the down-gradient edge of the primary contamination.
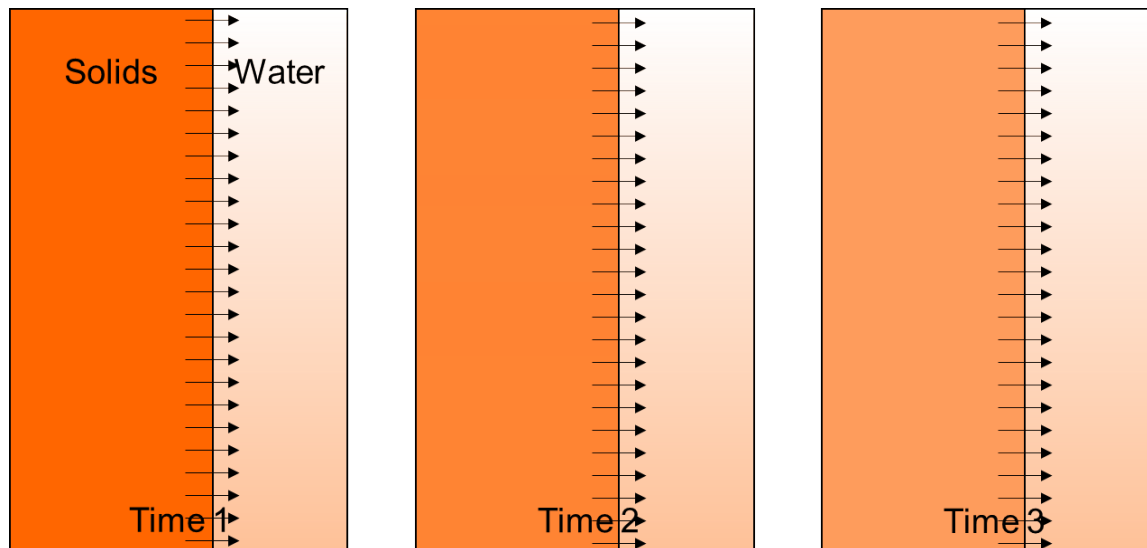
Figure 2-6   Schematic of the Conceptualization of the Equilibrium Dissolution Release

2.4.3   First-Order Rate-Controlled Release

The process that leads to the transfer of the radionuclide from the solid phase to the aqueous phase of the soil, whether it be through dissolution or desorption, is assumed to be so far from equilibrium that it can be characterized by a single forward transfer rate with the backward rate being negligible. The transfer rate is assumed to be proportional to the inventory of the radionuclide and the proportionality constant, the leach rate, is a user input. The rate of transfer of each radionuclide will be uniform over the length of transport in the primary contamination at any time, but it will vary with time as the inventory of the isotope changes with time due to transfer and radiological transformations (Figure 2-7). The thickness of the primary contamination is not affected by the transfer, and the concentration within the primary contamination is spatially uniform but changes over time. The code models the advective-dispersive transport of the radionuclide over the primary contamination and computes the release out of the down-gradient edge of the primary contamination.

2.4.4   Choice of Mechanisms for Radionuclides in a Transformation Chain

The transfer mechanism chosen for a radionuclide applies to all atoms of that radionuclide, regardless of whether they were initially present or whether they were produced by the radiological transformation of their parent radionuclide. The code can model different release mechanisms for different members of a transformation chain with three exceptions. If equilibrium solubility is chosen for an isotope of an element, that choice applies to all isotopes of that element (see Section 2.4.2); the progeny produced during the transport are not counted toward the soluble concentration, and the progeny produced by transformations of radionuclides undergoing equilibrium desorption transfer are modeled assuming they too are undergoing

equilibrium desorption transfer because of the way equilibrium desorption transfer is modeled by the code (see Section 5).
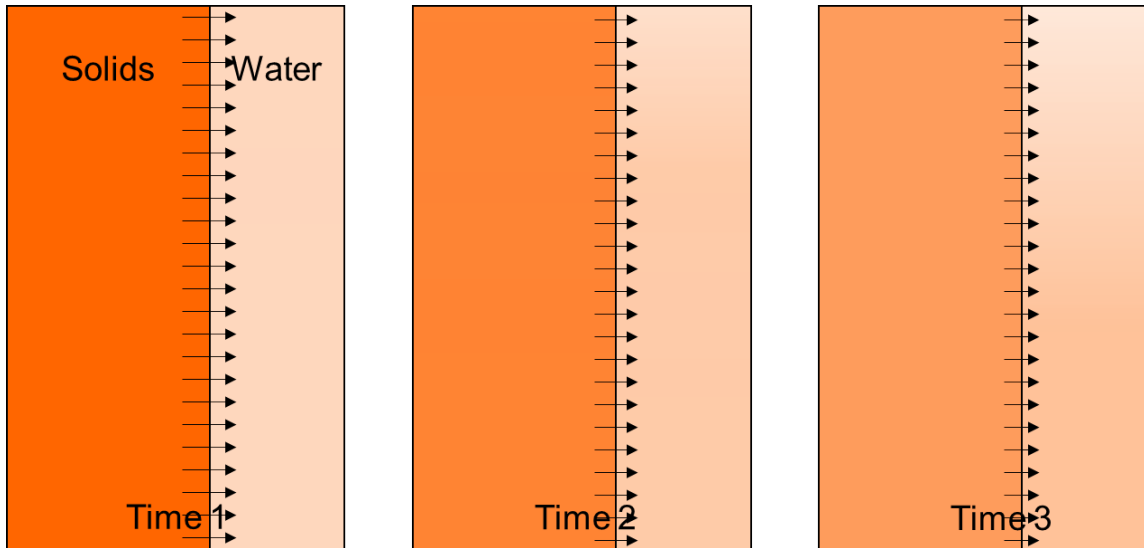
Figure 2-7 Schematic of First-Order Rate-Controlled Release

2.5   Temporal Changes in Release

The effects of engineered barriers—such as caps, containers, and others—can be modeled by temporally changing some of the inputs that affect the release. These inputs can be changed up to eight times or over eight intervals of time. This section describes the inputs that can be changed and the manner in which they can be changed over time.

2.5.1   Cumulative Fraction of Nuclide-Bearing Material that Is Releasable

When an engineered barrier is intact and effective, very little of the radionuclide-bearing material, if any at all, will have infiltration flowing through or past the radionuclide-bearing material. Over time, the engineered barrier will deteriorate and water will infiltrate through a part of the radionuclide-bearing material. The radionuclides contained in the part of the material through which water infiltrates will be susceptible to release. The code simulates the progressive deterioration and failure of the engineered barrier by specifying—at a number of times—the fraction of radionuclide-bearing material that is susceptible to release.

2.5.2   Leach Rate and Total Soluble Concentration

The chemical conditions in the waste and in the infiltrating water can change over time. This can lead to a change in the leach rate, the total soluble concentration, and the distribution coefficient. The code can accommodate changes in the leach rate and in the soluble concentration, but not changes in the distribution coefficient. The code cannot accommodate changes in the distribution coefficient because it does not compute the concentration profile of the radionuclides in the transport zones.

2.5.3   Manner in Which Changes Occur over Time

In the code, the releasable fraction, the leach rate, and the soluble concentration can be specified up to nine times. The first value specified will occur as a step function; the values will be zero prior to the first value and will change to the specified value at the specified time. For each of the subsequent changes, the user can specify whether the change in the value occurs gradually over the preceding time interval or stepwise at the specified time.

2.5.4   First-Order Leaching of the Same Radionuclide in Multiple Forms

Instead of the entire releasable fraction being subject to the same first-order leach rate, the user can choose to model a scenario in which up to nine different portions of the releasable material each undergo a different first-order rate-controlled release. In this case, each portion can become releasable at its own specific time and is released at its own specific leach rate. The releasable fraction and the leach rate of each portion remain constant over time.

2.6   RESRAD-ONSITE Conceptualization and Transfer Mechanism

When seen in light of the discussions in Sections 2.3 and 2.4, the conceptualization in RESRAD-ONSITE code can be viewed as one of the two conceptualizations described in Sections 2.6.1 and 2.6.2. RESRAD-OFFSITE retains this as the "RESRAD-ONSITE Exponential Release Model" choice of conceptualization of the primary contamination, and it is used by the "Simulate the RESRAD-ONSITE code" File menu option in the RESRAD-OFFSITE code. In addition to this "Simulate the RESRAD-ONSITE code" option, there is also an "onsite scenario template" option under the File menu. These options in RESRAD-OFFSITE code, described in Appendices K and L, increase the range of modeling options provided to users to fit their modeling needs. In both conceptualizations, all the solids in the primary contamination are assumed to be contaminated. The initial activity concentrations of the radionuclides are specified in terms of the mass of the entire primary contamination. The temporal changes described in Section 2.5 are not applicable for these conceptualizations.

2.6.1   First-Order Rate-Controlled Transfer without Transport

In this conceptualization, the code transfers the radionuclides to the soil moisture according to a user specified leach rate. These radionuclides are modeled as exiting the primary contamination immediately upon transfer to the soil moisture. The code imposes an upper limit to the user-specified leach rate.

2.6.2   Desorption-Adsorption Equilibrium Release from a Continuously Mixed Primary Contamination

In this conceptualization, the entire primary contamination is within the mixing layer and mixing occurs frequently enough to be modeled as continuously mixed. Transfer from the solid phase to the aqueous phase in the primary contamination takes place according to an instantaneous linear desorption-adsorption equilibrium. In this conceptualization, the expression for the temporal variation of the release is identical to that from a first-order rate-controlled release without transport. This conceptualization is similar to the conceptualization of the accumulation in the mixing layer at offsite locations.

3 EXPOSURE PATHWAYS, LOCATIONS, AND SCENARIOS

The RESRAD-OFFSITE computer code evaluates the radiological dose and excess cancer risk to an individual who is exposed while within or outside the area of initial (primary) contamination (Figure 3-1). The primary contamination, which is the source of all the releases modeled by the code, is assumed to be a layer of soil. The code considers releases of contaminants from the primary contamination to the atmosphere, to surface runoff, and to groundwater. It models the movement of the contaminants from the primary contamination to agricultural areas, pastures, a dwelling area, a well, and a surface water body. It also models the accumulation of contaminants at those locations, where appropriate. Any contribution of the contaminants from the water sources to the land-based locations is also modeled. Figure 3-2 depicts the primary and secondary contamination locations that contribute to exposure.

In RESRAD-OFFSITE, the general principles for computing exposure are the same as for RESRAD-ONSITE (Yu et al. 2001). The primary difference between the two codes is that RESRAD-OFFSITE uses media concentrations at the time of exposure, while RESRAD-ONSITE uses environmental transfer factors.
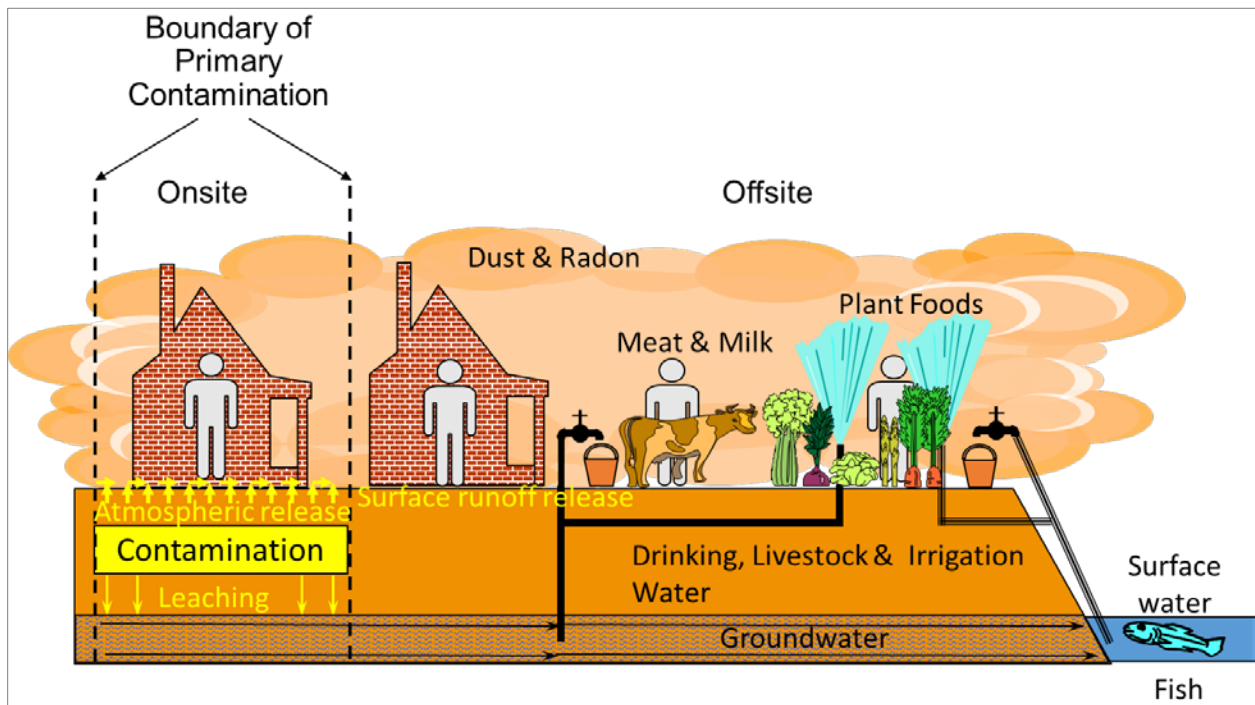
Figure 3-1   Environmental Pathways and Exposure Locations
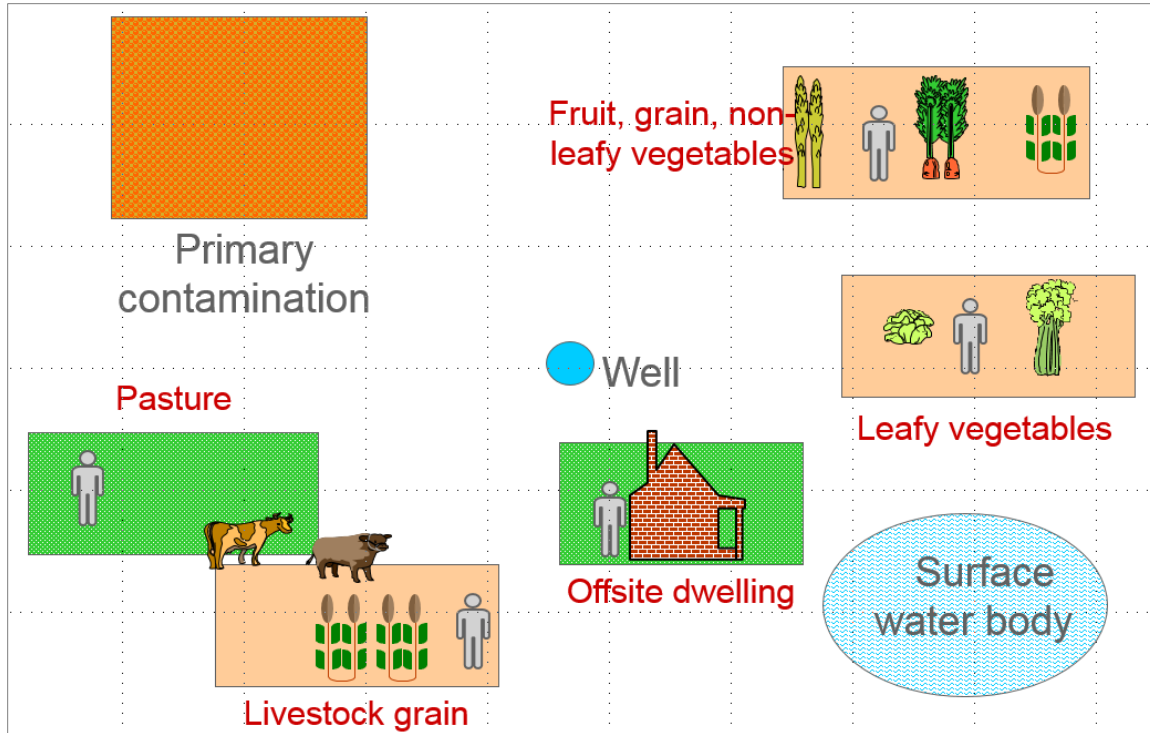
Figure 3-2   Primary and Secondary Contamination Locations

3.1   Identification of Exposure Pathways

Table 3-1 identifies potential exposure pathways. The three major headings in the table—
external radiation, inhalation, and ingestion—correspond to the three exposure pathways by
which the receptor is subjected or exposed to radiation. In the first pathway, exposure is due to
external radiation from radionuclides outside the body. In the second and third pathways,
exposure is due to internal radiation from radionuclides that an individual inhales or ingests.
These three types of exposure pathways correspond to the three kinds of dose conversion
coefficients discussed in Section 4.

For each exposure pathway, radionuclides can migrate from a source to a human exposure
location (Figure 3-2) via many environmental transport pathways. The human receptor can be
onsite and/or offsite, as shown in Figure 3-1.

The footnotes of Table 3-1 describe the major pathways RESRAD-OFFSITE uses to calculate
dose or risk. When calculating dose or risk, the code does not account for minor pathways (e.g.,
air submersion) for exposure because the dose or risk contribution from these pathways is
expected to be insignificant. The transport and dosimetry for gaseous airborne radionuclides
other than radon decay products (e.g., C-14 occurring in CO_2 or tritium occurring in tritiated
water vapor) require special consideration (see Appendix F). Some of the minor pathways
(e.g., air submersion) that are not considered in RESRAD-OFFSITE are considered in
RESRAD-BUILD (Yu et al. 2003).

Table 3-1   Potential Exposure Pathways

External radiation
    Ground shine
        Volume source[a,b]
    Air submersion
        Dust
        Radon and radon decay products
        Other gaseous airborne radionuclides
    Water immersion

Inhalation
    Dust[a]
    Radon and radon decay products[a]
    Other gaseous airborne radionuclides[a,c,d]

Ingestion
    Food
        Plant foods (vegetables, grains, and fruits)[a,e]
        Meat[a]
        Milk[a]
        Aquatic foods (fish, crustaceans, and mollusks)[a]
    Water
        Well water[a]
        Surface water[a]
    Soil[a]

[a]   Pathway used to calculate dose or risk in RESRAD-OFFSITE.

[b]   The surface source can be approximated by assuming a very thin layer of contamination (e.g., 0.1 cm).

[c]   Special model for tritium includes a 50% dose increase to account for dermal absorption of tritiated water. Inhalation of H-3 in particulate form is not considered; only inhalation of tritiated water vapor is considered.

[d]   Inhalation of C-14 in particulate form as well in carbon dioxide form is considered.

[e]   Special model for C-14 includes incorporation of CO_2 by photosynthesis.

3.2   External Radiation from Contamination in Soil

Gamma and beta radiation from radionuclides distributed in soil due to primary or secondary contamination are the dominant external radiation pathways and the only external radiation pathways taken into account in calculating dose or risk in RESRAD-OFFSITE. Figure 3-3 shows the direct external exposure locations and pathways RESRAD-OFFSITE considers for primary

contamination and areas of secondary contamination. For example, an indoor or outdoor receptor at the location of primary contamination is exposed directly to this primary contamination; the receptor located at an offsite dwelling is exposed both to primary contamination and to deposited contamination at the offsite dwelling (i.e., the secondary contamination at that location). Chapter 5 discusses how the contamination from the primary contamination is transported to areas of secondary contamination.
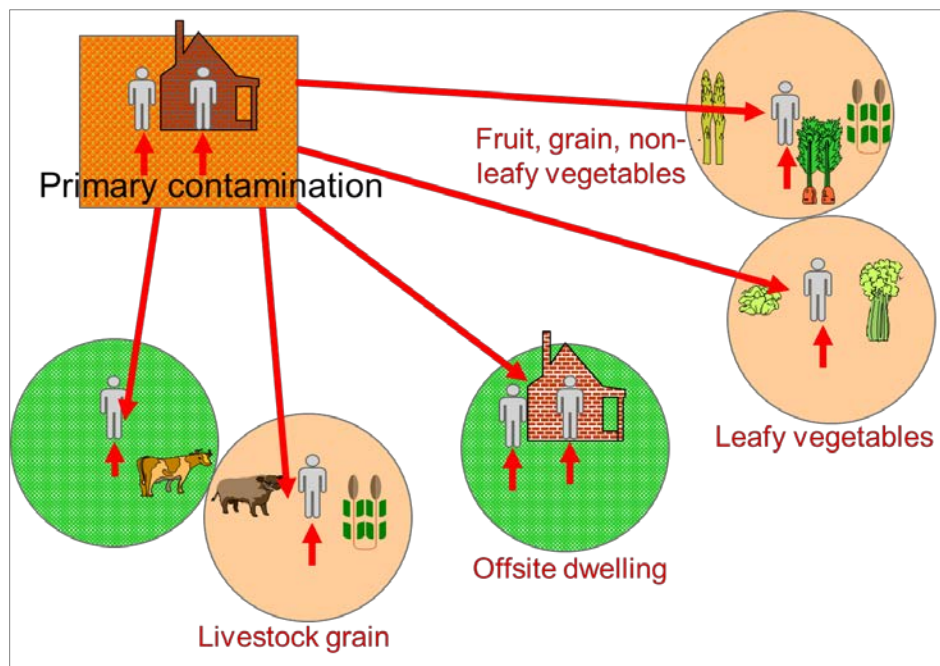
Figure 3-3   Direct External Exposure Locations and Pathways in RESRAD-OFFSITE

3.2.1   Exposure from Primary Contamination

RESRAD-OFFSITE models the external radiation from primary contamination in soil for the following situations:

- Exposure to radiation from the primary contamination while located indoors and outdoors on the primary contamination.

- Exposure to radiation from the primary contamination while located indoors and outdoors in an offsite dwelling that is outside the perimeter of the primary contamination.

- Exposure to radiation from the primary contamination in an offsite agricultural area that is outside the perimeter of the primary contamination while located outdoors.

3.2.2 Exposure from Secondary Contamination

RESRAD-OFFSITE models the external radiation from secondary contamination in soil for the following situations:

- Exposure to radiation from the accumulation in the soil in the offsite dwelling while indoors and outdoors in that dwelling.

- Exposure to radiation from the accumulation in the soil in an offsite agricultural area while outdoors in that area.

3.3 <u>Inhalation of Respirable Dust Particulates</u>

An inhalation pathway consists of two segments: (1) an airborne release and a dispersion segment that links the primary contamination with the respirable airborne radionuclides at an exposure location, and (2) an inhalation segment that links the airborne radionuclides with the exposed individual. The inhalation segment is characterized by an occupancy factor (equivalent fraction of time during which an individual inhales contaminated air) and a factor for the inhalation rate. Numerical values for these factors can be obtained using well-established procedures (ICRP 1975). There are two steps to modeling the airborne release and dispersion segment: (1) modeling the process by which radionuclides become airborne and (2) modeling the process by which the airborne radionuclides are transported to a human exposure location and diluted before inhalation. Details on calculating the air concentration of radionuclide attaching to respirable dust particles at onsite and offsite locations are discussed in Chapter 5. Special models for tritium as tritiated water vapor and C-14 as CO_2 are presented in Appendix F.

Figure 3-4 shows the inhalation exposure locations and pathways RESRAD-OFFSITE considers, from both primary contamination and areas of secondary contamination. For example, a receptor inside or outside at the primary contamination site is exposed to an air concentration there, and the receptor located at an offsite dwelling is exposed to an air concentration transported from the primary contamination, as well as an air concentration from secondary contamination.

3.3.1 Particulates and Gaseous Radionuclides from Primary Contamination

RESRAD-OFFSITE models the effects of inhaling contaminated particulates and gaseous radionuclides from primary contamination in the following situations:

- Inhalation of particulate matter and/or gaseous radionuclides released from the primary contamination while located indoors and outdoors in an onsite dwelling above the primary contamination.

- Inhalation of particulate matter and/or gaseous radionuclides released from the primary contamination and transported to the offsite dwelling site by the atmosphere while located indoors and outdoors in an offsite dwelling that is outside the perimeter of the primary contamination.

- Inhalation of particulate matter and/or gaseous radionuclides released from the primary contamination and transported to the offsite agricultural area while located outdoors in that offsite agricultural area.
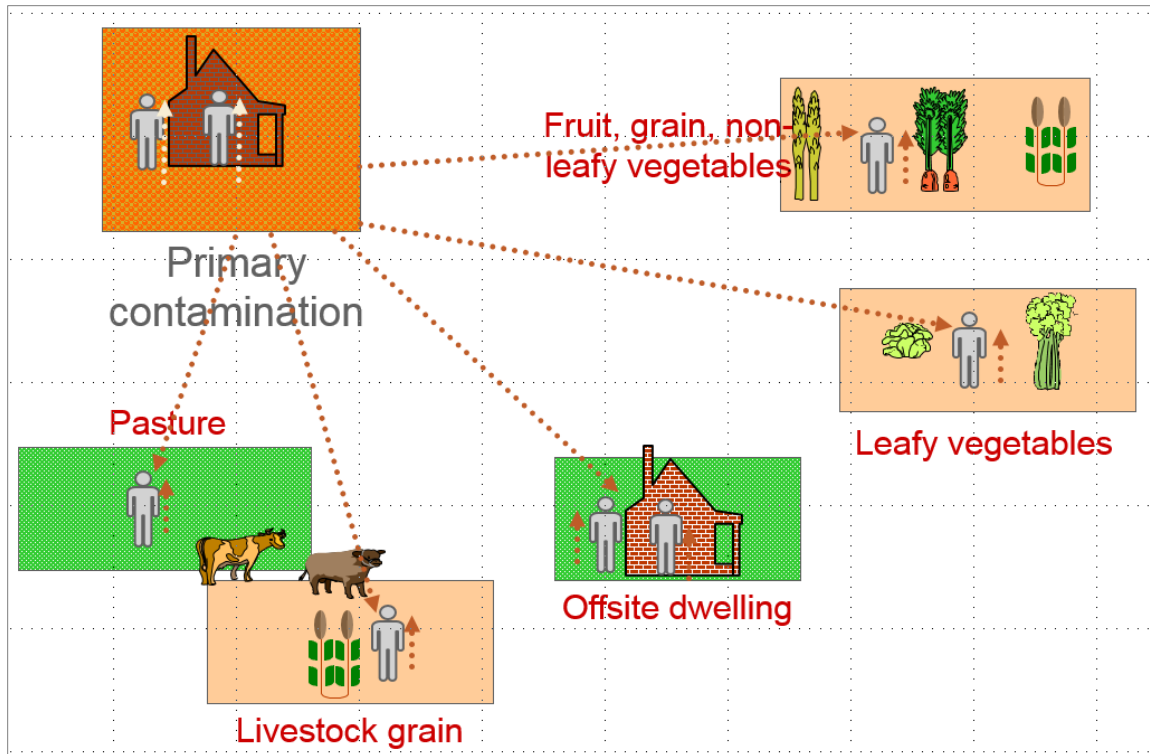
Figure 3-4   Inhalation Exposure Locations and Pathways in RESRAD-OFFSITE

3.3.2   Particulates and Gaseous Radionuclides from Secondary Contamination

RESRAD-OFFSITE models the effects of inhaling contaminated particulates and gaseous radionuclides from the secondary contamination for the following situations:

- Inhalation of re-suspended particulate matter and/or gaseous radionuclides from the secondary contamination at the offsite dwelling site while located indoors and outdoors there.

- Inhalation of re-suspended particulate matter and/or gaseous radionuclides from the secondary contamination at the agricultural areas and pasture location while located outdoors there.

3.4   Inhalation of Short-lived Radon progeny

For the radon pathway, inhalation dose results primarily from inhalation of radon decay products. For this pathway, the radon decay product air concentrations onsite and offsite are calculated. Quantitative details are presented in Appendix D.

3.4.1 Radon Emanating from Primary Contamination

RESRAD-OFFSITE models the effects of inhaling radon and its short-lived progeny emanating from primary contamination for the following situations:

- Inhalation of radon that emanated from the primary contamination and its short-lived progeny, while indoors and outdoors at the onsite dwelling location.

- Inhalation of radon that emanated from the primary contamination and was transported to the offsite dwelling site by the atmosphere, and its short-lived progeny that were produced during transport while indoors and outdoors at the offsite dwelling.

- Inhalation of radon that emanated from the primary contamination and was transported to the agricultural areas by the atmosphere, and its short-lived progeny that were produced during the transport while outdoors in the offsite agricultural area.

3.4.2 Radon Emanating from Secondary Contamination

RESRAD-OFFSITE models the effects of inhaling radon and its short-lived progeny emanating from secondary contamination for the following situations:

- Inhalation of radon that emanated from the secondary contamination and its progeny while indoors and outdoors at the offsite dwelling.

- Inhalation of radon that emanated from the secondary contamination and its progeny while outdoors in the offsite agricultural area.

3.4.3 Radon Outgassing from Household Water

RESRAD-OFFSITE models the effects of radon outgassing from household water for the following situation:

- Inhalation of radon released from contaminated water used inside a dwelling (both onsite and offsite dwellings) and its progeny.

3.5 Ingestion of Food and Water

RESRAD-OFFSITE assesses five food and water ingestion pathway categories: plant foods, meat, milk, aquatic foods, and water. The plant foods pathway activates when the crops consumed grow in primary or secondary contaminated areas. The meat and milk pathway activates when there is a potential of contamination in consumed meat or milk products. The aquatic food pathway occurs only in areas where the topography and soil characteristics are favorable for a manmade pond or any other surface water body. The water pathway activates when well or surface water is used for drinking. The well cannot be within the primary contamination, and the surface water body should not be on the primary contamination.

Plant foods are contaminated by root uptake while the roots grow in contaminated soil, foliar uptake from contaminated dust deposited on the foliage, and foliar uptake from contaminated irrigation water. Appendix F presents a special model to incorporate C-14 as CO_2 as a result of

photosynthesis in plant foods. The meat is contaminated when the meat animal ingests contaminated plant foods, water, and soil. The milk is contaminated when the milk-producing animal ingests contaminated plant foods, water, and soil. Contamination in surface water contaminates aquatic food. The offsite surface water body is contaminated by the influx of contaminated soil removed from the primary contamination and catchment areas by surface erosion, contaminated groundwater entering a surface water body, and dust from atmospheric transport. Concentrations in plant foods, meat, milk, aquatic food, surface water, and groundwater are discussed in Chapter 5.

3.5.1 Ingestion of Vegetables

Two types of plant foods consumed by humans include (1) leafy vegetables and (2) fruit, grain, and nonleafy vegetables. Adding the doses from both food types produces the total dose. RESRAD-OFFSITE models plant ingestion for the following situations:

- Ingestion of plants grown at the site of primary contamination and contaminated by root uptake and foliar deposition.

- Ingestion of plants grown at the site of secondary contamination and contaminated by root uptake and foliar deposition.

- Ingestion of plants irrigated with contaminated water.

3.5.2 Ingestion of Meat

Two types of plant foods consumed by the meat-producing animal include (1) grain and (2) pasture and silage.

RESRAD-OFFSITE models the ingestion of meat from an animal grazing at the site of primary contamination, and/or grazing at the site of secondary contamination, and/or consuming contaminated water.

3.5.3 Ingestion of Milk

Two types of plant foods consumed by a milk-producing cow include (1) grain and (2) pasture and silage.

RESRAD-OFFSITE models the ingestion of milk from a milk-producing cow grazing at the site of primary contamination, and/or grazing at the site of secondary contamination, and/or consuming contaminated water.

3.5.4 Ingestion of Aquatic Food

The aquatic food pathway describes the ingestion of fish, crustaceans, and mollusks from a nearby surface water body contaminated by radionuclides. The radionuclides in the surface water body come from three potential sources: (1) radionuclides in eroded soil from the primary contamination or the catchment area that is carried by runoff, (2) radionuclides in groundwater, and (3) deposition of airborne particulates.

3.5.5 Ingestion of Water

Both well water and surface water can be used for drinking. RESRAD-OFFSITE uses the fraction of well water blended with or supplemented by surface water to calculate the total contribution from the well and from the surface water.

3.6   Incidental Ingestion of Soil

The soil ingestion pathway corresponds to direct ingestion of contaminated soil. The surface soil at offsite locations is contaminated from deposition of contaminated particulates from the atmosphere and runoff and due to irrigation with contaminated water.

3.6.1 Exposure from Primary Contamination

RESRAD-OFFSITE models the soil ingestion from the site of primary contamination.

3.6.2 Exposure from Secondary Contamination

RESRAD-OFFSITE models the soil ingestion from the site of secondary contamination.

3.7   Exposure Scenarios

Exposure scenarios are patterns of human activity that can affect the release of radioactivity from the contamination and the amount of exposure received at the exposure location. This section describes the principal exposure scenarios that RESRAD-OFFSITE can model. Additional potential scenarios that require refinements and additional components for the code are also discussed, where appropriate. The four principal scenarios are rural resident farmer, urban resident, worker, and recreationist. The principal exposure scenarios can give rise to specific sub-scenarios, such as office worker, industrial worker, or construction worker within the worker scenario. Sections 3.7.1 through Section 3.7.4 list these possibilities. The pathways relevant to the various scenarios are summarized in Table 3-2 through Table 3-11.

As described in Travers (2003), the exposure scenarios that need to be considered for each site can be arrived at by determining the potential land use of that specific site and then considering the exposure groups of receptors that are relevant to each of those potential land uses. The land use of a site is governed by the zoning and planning of the municipality. Hence, a reliable exposure scenario can be developed by considering the municipality zoning district and future planning/development of the site.

Different combinations of land use and exposure group can lead to the same generic exposure scenario. For example, a maintenance worker in a public park or golf course and a resident maintenance worker in a large apartment complex would both fall under the generic maintenance worker scenario. These exposure scenarios would each have different input parameters to reflect the differences in land use and in activities these people perform. Thus, the land use/exposure group approach is necessary for conducting site-specific analyses and developing input values for the exposure scenarios.

This report focuses on the principal exposure scenarios that RESRAD-OFFSITE can model. It does not deal with the selection of exposure scenarios or parameter development for them. Thus, it does not use the land use/exposure group approach. Instead, it overviews the main generic exposure conditions associated with the principal exposure scenarios.

It is not practical to provide an exhaustive list of all the exposure scenarios that RESRAD-OFFSITE can model. Chapter 2 presents information that is useful in deciding whether this code can be used to model other exposure scenarios. Methods for developing site-specific scenarios and for modifying principal scenarios based on site characteristics are given in Chapter 5 and Appendix I of NUREG-1757 (Schmidt et al. 2006). The general scenarios given in Table I.3 of NUREG-1757, Volume 2, for sites with contamination in soil can be modeled using either the principal scenarios listed in Sections 3.7.1 through Section 3.7.4 or as a sub-scenario of one of the principal scenarios.

Table 3-2 Exposure Pathways Considered for a Rural Resident Farmer Scenario

| | Location of Contamination | | | |
Exposure Pathway	Dwelling Site	Agricultural Land and Pasture	Surface Water Body	Well
External radiation	Yes	Yes	No	NA[a]
Inhalation of dust particulates and gaseous radionuclides	Yes	Yes	NA	NA
Inhalation of short-lived radon progeny	Yes[b]	Yes[b]	Yes[b]	Yes[b]
Ingestion of vegetables, fruit, and grain	NA	Yes	Yes	Yes
Ingestion of meat	NA	Yes	Yes	Yes
Ingestion of milk	NA	Yes	Yes	Yes
Ingestion of aquatic food	NA	NA	Yes	NA
Ingestion of soil	Yes	Yes	NA	NA
Ingestion of water	NA	NA	Yes	Yes

[a] NA = not applicable.

[b] The radon pathway can be excluded for decommissioning of contaminated facilities and sites seeking unrestricted release under the NRC's license termination rule (Federal Register, July 21, 1997, at 62 FR 39083).

Table 3-3   Contamination Pathways Considered for a Rural Resident Farmer Scenario

| | Location of Contamination | | | |
	Dwelling Site	Agricultural Land and Pasture	Surface Water Body	Well
Contamination Pathway				
Deposition of dust from primary contamination	Yes	Yes	Yes	NA[a]
Interception of groundwater infiltrating from primary contamination	NA	NA	Yes	Yes
Surface runoff from primary contamination	Yes	Yes	Yes	NA
Surface runoff from catchment	No	No	Yes	NA
Irrigation water from well and/or surface water body	Yes	Yes	NA	NA

[a]   NA = not applicable.

Table 3-4   Exposure Pathways Considered for an Urban Resident Scenario

| | Location of Contamination | | | |
	Dwelling Site	Agricultural Land and Pasture	Surface Water Body	Well
Exposure Pathway				
External radiation	Yes	NA[a]	No	NA
Inhalation of dust particulates and gaseous radionuclides	Yes	NA	No	NA
Inhalation of short-lived radon progeny	Yes[b]	NA	Yes[b]	Yes[b]
Ingestion of vegetables, fruit, and grain	Maybe[c]	NA	Maybe	Maybe
Ingestion of meat	NA	NA	NA	NA
Ingestion of milk	NA	NA	NA	NA
Ingestion of aquatic food	NA	NA	Maybe	NA
Ingestion of soil	Yes	NA	NA	NA

Table 3-4 Exposure Pathways Considered for an Urban Resident Scenario(Cont.)

| | Location of Contamination | | | |
Exposure Pathway	Dwelling Site	Agricultural Land and Pasture	Surface Water Body	Well
Ingestion of water	NA	NA	Maybe	Maybe

[a] NA = not applicable.

[b] The radon pathway can be excluded for decommissioning of contaminated facilities and sites seeking unrestricted release under the NRC's license termination rule (Federal Register, July 21, 1997, at 62 FR 39083).

[c] Maybe = not suggested for the default scenario; can be considered, if appropriate.

Table 3-5   Contamination Pathways Considered for an Urban Resident Scenario

| | Location of Contamination | | | |
Contamination Pathway	Dwelling Site	Agricultural Land and Pasture	Surface Water Body	Well
Deposition of dust from primary contamination	Yes	NA[a]	Maybe[b]	NA
Interception of groundwater infiltrating from primary contamination	NA	NA	Maybe	Maybe
Surface runoff from primary contamination	NA	NA	Maybe	NA
Surface runoff from catchment	NA	NA	Maybe	NA
Irrigation water from well and/or surface water body	Maybe	Maybe	NA	NA

[a] NA = not applicable.

[b] Maybe = not suggested for the default scenario; can be considered, if appropriate.

Table 3-6   Exposure Pathways Considered for the Worker Scenario

Exposure Pathway	Location of Contamination			
	Work Site[a]	Agricultural Land[b]	Surface Water Body	Well
External radiation	Yes	Yes	NA[c]	NA
Inhalation of dust particulates and gaseous radionuclides	Yes	Yes	NA	NA
Inhalation of short-lived radon progeny	No[d]	No[d]	NA	NA
Ingestion of vegetables, fruit, and grain	NA	NA	NA	NA
Ingestion of meat	NA	NA	NA	NA
Ingestion of milk	NA	NA	NA	NA
Ingestion of aquatic food	NA	NA	NA	NA
Ingestion of soil	Yes	Yes	NA	NA
Ingestion of water	NA	NA	Maybe[e]	Maybe

[a]   For office worker, industrial worker, and construction worker scenarios.

[b]   For agricultural worker scenario.

[c]   NA = not applicable.

[d]   The radon pathway can be excluded for decommissioning of contaminated facilities and sites seeking unrestricted release under the NRC's license termination rule (Federal Register, July 21, 1997, at 62 FR 39083).

[e]   Maybe = not suggested for the default scenario; can be considered, if appropriate.

Table 3-7 Contamination Pathways Considered for the Worker Scenario

	Location of Contamination			
Contamination Pathway	Work Site[a]	Agricultural Land[b]	Surface Water Body	Well
Deposition of dust from primary contamination	Yes	Yes	Yes	NA[c]
Interception of groundwater infiltrating from primary contamination	NA	NA	Yes	Yes
Surface runoff from primary contamination	NA	No	Yes	NA
Surface runoff from catchment	NA	No	Yes	NA
Irrigation water from well and/or surface water body	NA	Yes	NA	NA

[a] For office worker, industrial worker, and construction worker scenarios.

[b] For agricultural worker scenario.

[c] NA = not applicable.

Table 3-8 Exposure Pathways Considered for a Sportsperson or Outdoorsperson Recreational Scenario

	Location of Contamination			
Exposure Pathway	Dwelling Site	Agricultural Land and Pasture Representing Forest or Other Outdoor Areas	Surface Water Body	Well to Represent a Spring
External radiation	NA[a]	Yes	No	NA
Inhalation of dust particulates and gaseous radionuclides	NA	Yes	No	NA
Inhalation of short-lived radon progeny Internal radiation	NA	Yes[b]	NA	NA

Table 3-8 Exposure Pathways Considered for a Sportsperson or Outdoorsperson Recreational Scenario (Cont.)

Exposure Pathway		Location of Contamination		
	Dwelling Site	Agricultural Land and Pasture Representing Forest or Other Outdoor Areas	Surface Water Body	Well to Represent a Spring
Ingestion of vegetables, fruit, and grain	NA	Maybe[c]	Maybe	Maybe
Ingestion of meat	NA	Yes	Yes	Yes
Ingestion of milk	NA	NA	NA	NA
Ingestion of aquatic food	NA	NA	Yes	NA
Ingestion of soil	NA	Yes	NA	NA
Ingestion of water	NA	NA	Maybe	Maybe

[a] NA = not applicable.

[b] The radon pathway can be excluded for decommissioning of contaminated facilities and sites seeking unrestricted release under the NRC's license termination rule (Federal Register, July 21, 1997, at 62 FR 39083).

[c] Maybe = not suggested for the default scenario; can be considered, if appropriate.

Table 3-9   Contamination Pathways Considered for a Sportsperson or Outdoorsperson Recreational Scenario

Contamination Pathway		Location of Contamination		
	Dwelling Site	Agricultural Land and Pasture (for forest)	Surface Water Body	Well to Represent a Spring
Deposition of dust from primary contamination	NA[a]	Yes	Yes	NA
Interception of groundwater infiltrating from primary contamination	NA	NA	Yes	Maybe[b]

Table 3-9 Contamination Pathways Considered for a Sportsperson or Outdoorsperson Recreational Scenario (Cont.)

	Location of Contamination			
Contamination Pathway	Dwelling Site	Agricultural Land and Pasture (for forest)	Surface Water Body	Well to Represent a Spring
Surface runoff from primary contamination	NA	No	Yes	NA
Surface runoff from catchment	NA	No	Yes	NA
Irrigation water from well and/or surface water body	NA	NA	NA	NA

a NA = not applicable.

b Maybe = not suggested for the default scenario; can be considered, if appropriate.

Table 3-10 Exposure Pathways Considered for the Park or Playfield Recreational Scenario

	Location of Contamination			
Exposure Pathway	Dwelling Site	Agricultural Land and Pasture (for park or playfield)	Surface Water Body	Well
External radiation	NAa	Yes	NA	NA
Inhalation of dust particulates and gaseous radionuclides	NA	Yes	NA	NA
Inhalation of short-lived radon progeny Internal radiation	NA	Yesb	NA	NA
Ingestion of vegetables, fruit, and grain	NA	NA	NA	NA
Ingestion of meat	NA	NA	NA	NA
Ingestion of milk	NA	NA	NA	NA

Table3-10 Exposure Pathways Considered for the Park or Playfield Recreational Scenario (Cont.)

Exposure Pathway	Dwelling Site	Agricultural Land and Pasture (for park or playfield)	Surface Water Body	Well
		Location of Contamination		
Ingestion of aquatic food	NA	NA	NA	NA
Ingestion of soil	NA	Yes	NA	NA
Ingestion of water	NA	NA	Maybe[c]	Maybe

[a] NA = not applicable.

[b] The radon pathway can be excluded for decommissioning of contaminated facilities and sites seeking unrestricted release under the NRC's license termination rule (Federal Register, July 21, 1997, at 62 FR 39083).

[c] Maybe = not suggested for the default scenario; can be considered, if appropriate.

Table 3-11   Contamination Pathways Considered for a Park or Playfield Recreational Scenario

Contamination Pathway	Dwelling Site	Agricultural Land and Pasture (for park or playfield)	Surface Water Body	Well
		Location of Contamination		
Deposition of dust from primary contamination	NA[a]	Yes	Yes	NA
Interception of groundwater infiltrating from primary contamination	NA	NA	Yes	Yes
Surface runoff from primary contamination	NA	No	Yes	NA
Surface runoff from catchment	NA	No	Yes	NA

Table 3-11 Contamination Pathways Considered for a Park or Playfield Recreational Scenario (Cont.)

| | Location of Contamination | | | |
Contamination Pathway	Dwelling Site	Agricultural Land and Pasture (for park or playfield)	Surface Water Body	Well
Irrigation water from well and/or surface water body	NA	Maybe[b]	NA	NA

[a] NA = not applicable.

[b] Maybe = not suggested for the default scenario; can be considered, if appropriate.

3.7.1   Rural Resident Farmer Scenario

The most conservative case that would result in the highest exposure would be a self-sufficient resident farmer-survivalist who produces all food to meet his dietary needs in the affected area. All exposure pathways would be active. A more likely variation would be the sub-scenario of a semi-self-sufficient resident farmer who purchases some food to meet his dietary needs from outside the affected area. Although we expect that all the pathways would still be active, the ingestion parameters would reflect the reduced reliance on food from the affected area. Depending on the location and topography, the farmer could obtain water primarily from a well or from a surface water body. It is also possible that some portion or all of the farmed areas and the dwelling would be located directly above the primary contamination.

A second variation of this principal scenario would arise if the extent of the impacted area was large. In this case, a significant portion of the food a person used to meet dietary needs would be produced in the affected area, although not by the same individual. The occupancy factor would need to decrease to reflect the applicable situation. For example, a person who lives elsewhere might pick the food at a cooperative farm or purchase it from a roadside stand or farmer's market.

3.7.2   Urban Resident Scenario

In the urban resident scenario, it is likely that the meat, milk, and aquatic food pathways would be inactive and that input appropriate for the location of the affected area would be used for modeling. Depending on the location of the water supply and the type of water treatment process, the drinking water and household water pathways might be inactive. If the resident's dwelling is a house, seasonal vegetable consumption from a home garden would be a possibility. If the dwelling is an apartment or townhome, the vegetable pathway might be inactive. The urban resident might work at a different location that was also in the affected area. Direct modeling of this variation is not currently possible, but an informed user can adjust the occupancy in the unused agricultural area to model this sub-scenario. The code can expand to include an offsite work area at a location different from the offsite dwelling when the dwelling model is refined.

3.7.3 Worker Scenario

In the worker scenario, the drinking water, vegetables, meat, milk, and aquatic food pathways would be inactive. The occupancy, shielding, inhalation, and incidental soil ingestion parameters would be different for various types of workers, for example, office worker, industrial worker, and construction worker. Either the offsite or the onsite dwelling location could be appropriate for these scenarios. The relevant agricultural area would be used to model a farm worker. A combined urban resident worker sub-scenario would be necessary if the worker also resided in an affected area.

3.7.4 Recreationist Scenario

Numerous recreational use scenarios are possible. They could range from an avid sportsperson or outdoorsperson who would obtain a significant portion of his meat and fish from the affected area to a person who would hike in an affected area for only a few hours in a year.

The vegetable, milk, and drinking water pathways would be turned off for the sportsperson/outdoorsperson scenario, although the ingestion of some wild berries, mushrooms, and spring water would be plausible. The ingestion rates for meat and aquatic food would depend on the available game and aquatic organisms at the location. All the water used by livestock would probably come from surface water. The irrigation rate should be set to reflect the situation modeled, because the foraging area would likely not be irrigated.

A person who routinely trains or exercises in an affected playfield or park, or a person who regularly spends time in a park, is another likely candidate for recreational exposure. The vegetable, meat, milk, aquatic food, and drinking water pathways would be turned off for this scenario. The park or playfield could be modeled as the outdoor occupancy of the offsite dwelling, since the park/playfield option is not available.

RESRAD-OFFSITE is not currently equipped to model a swimmer or boater. A module to compute the direct exposure from the contaminants in the lake would have to be added. A more detailed lake model, which considers potential stratification and turnover of the lake and the rate-controlled release from the sediments, might also be necessary.

4 CALCULATION OF DOSE AND RISK

RESRAD-OFFSITE calculates radionuclide concentrations in different environmental media as a function of time and then uses the concentrations in different environmental media to compute intake, dose, and risk. The total dose or risk is the sum of dose or risk from individual pathways.

The radiological doses and risks are all time-integrated quantities. The dose reported for a particular time is the dose over a period of 1 year beginning at the specified time. The risk reported for a particular time is the value over an exposure duration beginning at the specified time. The exposure duration for risk calculation is the length of time the receptor is exposed to radiation at the site. Hence, exposure duration may be different for different exposure scenarios.

RESRAD-OFFSITE finds the time-integrated dose (or risk) by performing a trapezoidal integration using the dose (or risk) rates at the beginning and end of the time interval and at all the calculation time points that fall within the time interval (1 year for dose and the exposure duration for risk). If the end of the time integration interval does not coincide with a calculation time point, the rate at the end is found by interpolating between the two calculation time points around it.

The total annual dose, $D(t)$, received by a member of the critical population group at time t following the radiological survey of the site (mSv/yr [mrem/yr]) is given by

$$D(t) = \sum_{i=1,n} \sum_{p} D_{ip}(t)$$

where $D_{ip}(t)$ is the annual dose received by a member of the critical population group beginning at time t from the ith principal radionuclide transported through the pth environmental pathway, together with its associated decay products (mSv/yr [mrem/yr]). $D(t)$ is the sum of annual doses over all active pathways, p, and the number of principal radionuclides present, n.

Principal radionuclides are radionuclides with half-lives greater than the cutoff half-life selected. In RESRAD-OFFSITE, the user can select any cutoff half-life greater than or equal to 10 minutes. The decay products of any principal radionuclide down to, but not including, the next principal radionuclide in its decay chain are called associated radionuclides. The code assumes that the associated radionuclides are in secular equilibrium with the preceding principal radionuclide during transport and at the point of exposure. Appendix A contains a detailed discussion on the radionuclide database used in RESRAD-OFFSITE.

The criterion for releasing a site for use without radiological restrictions is generally based on dose limit. For dose limit criteria, the site should not exceed the dose limit within the time horizon:

$$D(t) \leq D_L, t_r \leq t \leq t_h$$

where

$D(t)$ = annual dose received by a member of the critical population group at time t following the radiological survey of the site (mSv/yr [mrem/yr]) from all active pathways, p, and all principal radionuclides, n, present at a site,

D_L = basic dose limit,

t_r = time at which the site is released for use without radiological restrictions following the radiological survey, and

t_h = time horizon.

The time at which a radiological survey is performed is the time of origin, or time 0. The time at which a site is released after the radiological survey has been performed is the release time, or time t_r.

4.1   External Pathway Dose and Risk from Contamination in Soil

RESRAD-OFFSITE calculates external pathway dose/risk from primary contamination and secondary contamination for different situations, as discussed in Section 3.2. The exposure for each of the situations is computed as the product of the following:

- The dose conversion factor or slope factor for external radiation, for a volume source of infinite thickness and infinite area, from the chosen dose factor library ($[\text{mSv yr}^{-1}]/[\text{Bq g}^{-1}]$ or $[\text{risk yr}^{-1}]/[\text{Bq g}^{-1}]$);

- The concentration of the radionuclide in the soil (Bq g^{-1} [pCi g^{-1}]);

- An occupancy and indoor shielding factor to account for the time spent at the location and for the shielding from any building components while indoors;

- A cover and depth factor to account for the finite thickness of the contamination and for any intervening clean cover between the contamination and the receptor; and

- An area and shape factor to account for the finite area and shape of the contaminated soil and for the position (location) of the receptor in relation to the contaminated area.

All the above factors, except for the occupancy factor, depend on the radionuclide. The shape of the primary contamination can be specified to be circular or polygonal. The location of the onsite and offsite dwellings in relation to the primary contamination can also be specified. The offsite areas (dwelling and agricultural areas) are assumed to be circular, with the receptor located at the center of the circle, when calculating the exposure from external radiation. Detailed discussion on external dose calculation is included in Appendix B.

4.2   Inhalation Pathway Dose and Risk from Respirable Dust Particulates

The code calculates inhalation pathway dose/risk for each of the situations discussed in Section 3.3 as the product of the following:

- The dose conversion factor or slope factor for the radionuclide from the chosen dose factor library ($[\text{mSv Bq}^{-1}]$ or $[\text{risk Bq}^{-1}]$),

- An occupancy and indoor filtration factor to account for the time spent at the location and for the filtration of dust by any building components while indoors,

- The inhalation rate ($\text{m}^3\text{ yr}^{-1}$), and

- The concentration of the radionuclide in the air at the exposure location (Bq m^{-3}).

The inhalation of gaseous carbon-14 (CO_2) and hydrogen-3 in vapor form (H_2O) is also computed and reported under this exposure pathway. Thus, the inhalation exposure reported for carbon-14 includes exposure from both the particulate form and the gaseous form. Different dose conversion factors can be used for the two forms of carbon-14. The inhalation exposure reported for hydrogen-3 is for the vapor form only and includes a 50% increase to account for the absorption of ^3HHO through the skin at a rate equal to 50% of the breathing rate (ICRP 1979−1982). Appendix C contains a detailed discussion of inhalation dose calculation.

4.3   Inhalation Pathway Dose and Risk from Radon and Short-lived Progeny

Appendix D describes the methodology used to calculate the radon pathway. RESRAD-OFFSITE models exposure by using the concentration of radon and its short-lived progeny at indoor and/or outdoor locations; time spent indoors and/or outdoors; and radon and its progeny slope factors or radon dose conversion factors from the risk factor library or dose factor library.

4.4   Ingestion Pathway Dose and Risk from Food and Water

The exposure from the ingestion of water, plant-derived food, meat, milk, and aquatic food is computed as the product of the following:

- The dose conversion factor or slope factor for the radionuclide and food type from the chosen dose factor library ($[mSv\ Bq^{-1}]$ or risk library $[risk\ Bq^{-1}]$),

- The ingestion rate ($kg\ yr^{-1}$ or $L\ yr^{-1}$),

- The fraction of the food that was obtained from the contaminated areas, and

- The concentration of the radionuclide in the food ($Bq\ kg^{-1}$ or $Bq\ L^{-1}$).

4.5   Incidental Soil Ingestion Pathway Dose and Risk

The exposure from the incidental ingestion of soil is computed by summing the product of the following at the onsite location and at each of the offsite locations:

- The dose conversion factor or slope factor for the radionuclide from the chosen dose factor library ($[mSv\ Bq^{-1}]$ or $[risk\ Bq^{-1}]$),

- The incidental ingestion rate of soil ($g\ yr^{-1}$),

- The fraction of time spent at the onsite or offsite location, and

- The concentration of the radionuclide in the soil at the onsite or offsite location ($Bq\ g^{-1}$).

5 CONCENTRATIONS OF RADIONUCLIDES IN ENVIRONMENTAL MEDIA

The locations of contamination considered for each exposure pathway are discussed in Chapters 3 and 4. These locations are listed below with a brief indication of why the concentrations of radionuclides need to be evaluated at each location:

- Concentrations of radionuclides in the primary contamination (activity/g of porous medium in the primary contamination). These are used to compute the onsite exposure from external radiation, inhalation of radon progeny, and ingestion of vegetables, meat, and milk for exposure scenarios that are wholly or partially onsite; the exposure from external radiation at offsite exposure locations; and release from the primary contamination to infiltration.

- Concentrations of radionuclides in the surface soil at the primary contamination (activity/g of surface soil). These are used to compute the exposure from the inhalation of particulates; ingestion of vegetables, meat, and milk; incidental ingestion of soil for exposure scenarios that are wholly or partially onsite; and releases from the primary contamination to the atmosphere, to runoff and to infiltration.

- Concentrations of radionuclides contained in respirable particulates in the air above the primary contamination (activity/m^3 of air). These are used to compute the exposure from the inhalation of particulates at onsite exposure locations.

- Concentrations of radionuclides contained in all particulates in the air above the primary contamination (activity/m^3 of air). These are used to compute the deposition on the foliage for scenarios that are wholly or partially onsite.

- Concentrations of radionuclides contained in all particulates in the air above offsite exposure locations and above the catchment (activity/m^3 of air) due to release from the primary contamination. These are used to compute the deposition on the foliage, offsite exposure locations, surface water body, and catchment.

- Concentrations of radionuclides dissolved in a surface water body (activity/m^3 of water). These are used to compute the exposure from the use of water from the surface water body for cooking, drinking, and other household purposes; for irrigation; for livestock; and from the ingestion of aquatic food.

- Concentrations of radionuclides dissolved in well water (activity/m^3 of water). These are used to compute the exposure from the use of well water for cooking, drinking, and other household purposes; for irrigation; and for livestock.

- Concentrations of radionuclides in surface soil at offsite exposure locations (activity/g of surface soil). These are used to compute the exposure from external radiation; inhalation of particulates; inhalation of radon progeny; ingestion of vegetables, meat, and milk; and incidental ingestion of soil for exposure scenarios that are wholly or partially offsite.

- Concentrations of radionuclides contained in respirable particulates in the air above offsite exposure locations (activity/m³ of air) from both the release from the primary contamination and the local area of secondary contamination. These are used to compute the exposure from the inhalation of particulates at offsite exposure locations.

RESRAD-OFFSITE models the release of radionuclides from the primary contamination, the transport of the radionuclides that were released from the primary contamination to the locations of exposure, and the accumulation of the radionuclides at those exposure locations in order to compute the concentrations of the radionuclides at the locations listed above. These are described in the following sections (i.e., Sections 5.1, 5.2, and 5.3).

5.1 Concentrations at the Location of and Releases from the Primary Contamination

Section 2.3 of this manual describes different conceptualizations of the primary contamination available in the code. Section 2.4 describes different mechanisms available in the code to model the transfer of radionuclides from the solid to the aqueous phase of the contaminated media. This section describes how the code computes the concentrations of the radionuclides in the primary contamination and in the surface mixing layer and the releases to infiltration, surface runoff, and the atmosphere. The mathematics of these computations and detailed descriptions of the output files to which the calculated values are written are in Appendix G.

5.1.1 Concentrations of Radionuclides in the Release-Immune Part of Contaminated Media

Radionuclides in contaminated media that is isolated from the environment by intact and effective engineered barriers will be immune from release (Section 2.5). The concentrations of release-immune radionuclides are affected only by radiological transformation; the Bateman equations compute these concentrations as a function of time. The code does not output temporal values of the release-immune concentrations, but it outputs the sum of the release-immune and release-susceptible concentrations to the file SFSIN.DAT (Section G.16).

5.1.2 Concentrations of Radionuclides in the Release-Susceptible Part of Contaminated Media

Radionuclides in contaminated media that is subject to the environmental processes of infiltration, erosion, and/or mixing are susceptible to release. The concentrations of release-susceptible radionuclides are affected by transfer to infiltration and by radiological transformation. Release to the infiltrating water occurs uniformly over the primary contamination when the transfer mechanism is first-order rate controlled; it is modeled as being uniform under the equilibrium solubility transfer mechanism. Thus, the code uses a modified form of the Bateman equations to compute the release-susceptible concentrations of radionuclides for which the user selects the equilibrium solubility or the first-order rate-controlled transfer options. The code does not output the temporal values of the release-immune concentration, but it outputs the sum of the release-immune and release-susceptible concentrations to the file SFSIN.DAT (Section G.16).

The desorption-adsorption equilibrium of the radionuclide between the solid phase and the aqueous phase of the contaminated material is modeled as being achieved instantaneously. The transfer of the radionuclides occurs at the up-gradient part of the primary contamination

under this assumption; the concentration is not constant over the primary contamination. The code does not calculate the release-susceptible concentration profiles of the radionuclides for which the equilibrium desorption option is chosen; for these radionuclides, it only computes the release at the down-gradient edge of the primary contamination. Therefore, the releases of radionuclides in particulates to the air and in eroded material to runoff are not generally modeled for radionuclides for which the user chooses the equilibrium desorption transfer mechanism. The gaseous release of hydrogen-3, carbon-14, and the two isotopes of radon are also not generally modeled, if the equilibrium desorption transfer mechanism is chosen for those radionuclides.

5.1.3   Concentrations of Radionuclides Being Transported in the Primary Contamination

Concentration profiles of radionuclides during transport in the primary contamination are not currently computed by the code under any of the three transfer mechanism options.

5.1.4   Concentrations of Radionuclides in the Surface Soil Mixing Layer above the Primary Contamination

If the primary contamination has a clean cover on top of it, the surface soil layer will remain clean until the cover erodes and is of the same thickness as the mixing layer. The code computes the erosion rate using the universal soil-loss equation (Shen and Julien 1993).

As the cover continues to erode, increasing amounts of material from the primary contamination will mix into the surface soil mixing layer, and erosion will remove some of the mixed soil. Thus, the volume fraction of material from the primary contamination in the mixing layer will increase over time, but the fraction will not be linearly related to time. If the cover and the primary contamination have different densities, the density of the mixing layer will also change over time. The code models the volume fraction and the density by considering the changes in these quantities due to material from the primary contamination entering the mixing layer and the loss of mixed material from the mixing layer due to erosion. The code outputs the ratio of the concentration in the mixing layer to the concentration in the primary contamination to the file CZTHICK3.DAT (Section G.16).

5.1.5   Release of Particulates to the Atmosphere

Radionuclides in the surface soil layer at the top of the primary contamination can be released into the atmosphere because of human activity such as farming, or because of a non-anthropogenic process such as wind. The code models release into the air under the assumption that the rate of release of particulates from the surface soil layer to the air is equal to the rate of deposition of the particulates from the air to the surface soil layer. The code uses two user inputs, the mass loading of particulates in the air above the primary contamination and the deposition velocity of the particulates, to compute the release rate of the particulates. The release-susceptible concentrations of radionuclides in the surface layer and the release rate of the particulates are used to calculate the release rates of radionuclides associated with particulates. Both the release of radionuclides associated with respirable particulates and the release of radionuclides associated with all particulates are calculated. The code outputs the release associated with particulates to the atmosphere to the file AIFLUXIN.DAT (Section G.16).

5.1.6 Release of Eroded Material to Runoff

Radionuclides in the surface soil layer at the top of the primary contamination can be released to runoff following intense rainfall. The code computes the erosion rate of the surface layer using the universal soil-loss equation (Shen and Julien 1993) which takes into account user input values related to the erodibility of the soil, energy/intensity of the rainfall, length and slope of the surface, vegetation, agricultural practices, and conservation practices. The code uses the release-susceptible concentrations of radionuclides in the surface layer and the erosion rate to calculate the release rate of radionuclides to runoff. The code outputs the release associated with erosion to runoff to the file SWFLUXIN.DAT (Section G.16).

5.1.7 Equilibrium Desorption Release to Infiltration

Section 2.4.1 describes the equilibrium desorption transfer mechanism. The code assumes that equilibrium between the radionuclides adsorbed on the soil solids and the radionuclides in solution in the interstitial pore water is attained instantaneously and is characterized by a linear distribution coefficient. Under these assumptions, radionuclides transfer rapidly to the infiltrating water at the up-gradient edge of the primary contamination until the concentrations of radionuclides in the water reach values proportional to the concentrations that remain in the rest of the primary contamination. The proportionality constant is the distribution coefficient. Once the infiltrating moisture attains the equilibrium concentration, there is no further net transfer of radionuclides from the radionuclide-bearing material to the infiltrating water as it moves through the primary contamination. The advective-dispersive transport of radionuclides from where they are transferred to the down-gradient edge of the primary contamination is modeled to compute the release from the primary contamination. The releases at the down-gradient boundary are output to the file AQFLUXIN.DAT (Section G.16).

Because the concentration of radionuclides in the pore water is proportional to the concentration in the primary contamination at desorption-adsorption equilibrium characterized by the distribution coefficient, the rate of transfer is proportional to the concentration in the primary contamination while the duration of transfer is independent of the concentration in the primary contamination. Hence, the magnitude of the release, the concentration of the radionuclide in groundwater and computed dose vary linearly with the concentration of radionuclides in the primary contamination. This allows the code to extrapolate or interpolate the results of a single deterministic run to compute a derived concentration guideline level (DCGL). The DCGL is the activity concentration of a radionuclide in the contaminated medium that will ensure that the predicted dose from that radionuclide and the progeny that grow from its transformations stay within the specified dose limit over the time horizon.

5.1.8 Equilibrium Dissolution Release to Infiltration

Section 2.4.2 describes equilibrium dissolution release. The equilibrium is characterized by the total soluble concentration of the element. The soluble concentration of the element is apportioned between isotopes of the element in proportion to their inventories. The code assumes that radionuclides of each isotope transfer from the solid phase to the infiltrating water uniformly over the transport dimension of the primary contamination so that the concentration of the isotope attains its apportioned soluble concentration when the water reaches the down-gradient edge of the primary contamination. The rate of transfer is constant over the length of transport but varies over time as the relative inventory of the isotope changes because of the different half-lives of the isotopes and/or if the user specifies changes to the soluble concentration over time. The code models the un-retarded advective-dispersive transport of the

radionuclides from where they are transferred to the down-gradient edge of the primary contamination to compute the release from the primary contamination. The transfer from the solid phase to the soil moisture is output to the file AQTRANIN.DAT, and the release at the down-gradient boundary is output to the file AQFLUXIN.DAT. These two files are described in Section G.16.

Because the total soluble concentration of an isotope does not vary linearly with that isotope's concentration in the primary contamination, the rate of transfer, too, will not vary linearly with the concentration in the primary contamination. Furthermore, the duration of the transfer depends on the concentration in the primary contamination. Thus, the computed dose will not necessarily vary linearly with the concentration of the radionuclide in the primary contamination, and the code cannot compute the guideline by extrapolating the results of a single deterministic run.

5.1.9 First-Order Rate-Controlled Release to Infiltration

Section 2.4.3 describes first-order rate-controlled release. The radionuclide's rate of transfer from the solid phase of the primary contamination to the pore water is proportional to that radionuclide's concentration in the primary contamination and occurs uniformly over the transport length of the primary contamination. The code models the advective-dispersive transport of radionuclides from where they are transferred to the down-gradient edge of the primary contamination to compute the release from the primary contamination. The transfer from the solid phase to the soil moisture is output to the file AQTRANIN.DAT, and the release at the down-gradient boundary is output to the file AQFLUXIN.DAT. These two files are described in Section G.16.

Because the radionuclide's rate of transfer from the solid phase to the infiltration water is proportional to the radionuclide's concentration in the primary contamination, the computed dose will vary linearly with the concentration of the radionuclide in the primary contamination. This allows the code to extrapolate or interpolate the results of a single deterministic run to compute a DCGL. The DCGL is the activity concentration of a radionuclide in the contaminated medium that will ensure that the predicted dose from that radionuclide and its progeny stay within the specified dose limit within the time horizon.

5.1.10 Diffusion-Controlled Release to Infiltration

Section 2.3.3 describes diffusion-controlled release. Some of the pores of the nuclide-bearing material contain water. The code models radionuclides in the pore water as being in desorption-adsorption equilibrium with the radionuclides in the solid phase of the radionuclide-bearing material; the equilibrium is characterized by a linear distribution coefficient. The code assumes this pore water has a continuous connection within the radionuclide-bearing material and the initially clean soil surrounding the radionuclide-bearing material. The code models the diffusive transport of the radionuclide through the connected pore water in the nuclide-bearing material into the surrounding soil.

To compute the release from the primary contamination, the code models the advective-dispersive transport of radionuclides from where they enter the surrounding soil to the down-gradient edge of the primary contamination.

5.1.11 Gaseous Releases to the Atmosphere

The code models gaseous releases of hydrogen-3 and carbon-14 as occurring from the releasable inventory of radionuclides contained within the evasion layer. It assumes radionuclides below the evasion layer are unable to escape as water vapor or as carbon dioxide; the thickness of the evasion layer for carbon-14 is a user input, while that for hydrogen-3 is fixed in the code. The evasion rate, the fraction of the releasable inventory within the evasion layer released per unit time, is a user input for carbon-14, and the code computes the rate for hydrogen-3. The details of the computation appear in Appendices F and G.

The code numerically models diffusive transport of the radon isotopes, generated in the primary contamination, through the pores in the primary contamination and through any clean cover to determine the release of radon into the atmosphere. The release of radon into any building on or above the contaminated layer is modeled by including diffusion through the concrete floor of the building. Appendix D contains the details of these computations. The flux of radon is output to the file RadonFlux.OUT.

5.1.12 Concentrations of Radionuclides in Airborne Particulates above the Primary Contamination

The particulates in the air above the primary contamination are a mixture of particulates that originated from the primary contamination and particulates that blew in from elsewhere. The code uses the particle size and average wind speed to compute the fraction of particulates that came from the primary contamination. It then uses the mass load of the particulates above the primary contamination and the concentrations of radionuclides in the surface soil to compute the concentrations of radionuclides in particulates above the primary contamination. The code computes the concentrations of radionuclides in respirable particulates and in particulates of all sizes.

5.1.13 Concentrations of Gaseous Radionuclides above the Primary Contamination

The code computes the concentration of hydrogen-3 in the form of water vapor and the concentration of carbon-14 as carbon dioxide in the air above the primary contamination by assuming that the releases of these forms—described in Section 5.1.11—mix within a rectangular prism of air above the primary contamination.

The code calculates concentrations of radon isotopes and their short-lived progeny in the air above the primary contamination by assuming that releases of radon isotopes (Section 5.1.11) mix within a rectangular prism of air above the primary contamination. It also computes the ingrowth of the short-lived progeny as the radon is transported from various parts of the primary contamination to the onsite receptor.

5.2 Transport from Primary Contamination to Offsite Locations

The code models the atmospheric transport of the particulate and gas releases and the groundwater transport of the aqueous release to infiltration. It also accepts input of the fate of the erosion release to runoff. The offsite location to which transport is modeled can be an exposure location or it can be an intermediate location from which the radionuclides are transported by a different mechanism.

5.2.1 Atmospheric Transport

The code contains formulations to model the transport of radionuclides by wind, from the primary contamination to the locations of accumulation and exposure: the farmed areas, the offsite dwelling, the surface water body, and the catchment of the surface water body.

The code contains formulations for a sector-averaged Gaussian plume from a chronic release. It uses atmospheric conditions (joint frequency data of wind direction, wind speed, and stability class) in stability array (STAR) format; has three built-in options to compute the atmospheric dispersion coefficients; considers confinement of the plume by a stable layer with different mixing heights before and after noon; and accounts for both wet and dry deposition. It also considers buoyancy-induced dispersion, heat energy of the plume, wind speed corrections, and height adjustments for terrain that slopes up from the primary contamination to the offsite location. It models ingrowth of the three short-lived radon progeny during the atmospheric transport of radon.

These formulations are implemented in two different ways. The concentrations of radionuclides in the air at the offsite locations (for inhalation, foliar deposition, and deposition on the offsite locations) are computed using an implementation that has been in the code since the first version. The primary contamination and the offsite locations are split into a number of small rectangles with side lengths that are less than a user-specified value. The code computes the atmospheric transport from each congruent small rectangle in the source to each congruent small rectangle in the offsite location, then sums and averages the resulting concentrations over the offsite location. This implementation can be applied when the primary contamination and the offsite location do not overlap. The accuracy of the computations depends on the user-specified limit to the side length of the small rectangle. The code outputs the results of the atmospheric transport calculations to the file CHIOVERQ.OUT.

Because it is conceivable that the catchment area of the surface water body and the primary contamination could overlap, a new method to model atmospheric transport and deposition to and from overlapping areas is developed. The code calculates deposition from atmospheric transport from an increasing number of points within the primary contamination over the catchment until the results converge to within a user-specified criterion. The code outputs intermediate results of these calculations to SectorDepletedFraction.OUT. Appendix I describes the formulations and the output file.

5.2.2 Groundwater Transport

The code contains formulations to model the transport of radionuclides by ground water—vertically down the unsaturated layers and horizontally from the primary contamination—to the well and the surface water body.

The code models vertical transport in the unsaturated layers, which can include the primary contamination, by considering advective and dispersive transport in the vertical direction, radiological transformations that occur during the transport, and radionuclide-specific interactions between the solid and aqueous phases of the unsaturated layer. These formulations compute the transfers, i.e., the areally integrated flux, across the boundary between each adjacent pair of unsaturated zones and finally across the water table. The transfer across the water table is output to the file WTFLUXIN.DAT (Section G.16).

Transport in the saturated layers, which can include submerged primary contamination, is modeled by considering advective transport in the horizontal direction; longitudinal and transverse dispersive transport including reflections of the plume off the lower impermeable boundary and the water table, as necessary; radiological transformations that occur during transport; and radionuclide-specific interactions between the solid and aqueous phases of the saturated layer. The formulations can compute both the profile of the flux across a vertical plane surface and the profile of the concentration over a vertical plane. The areally integrated fluxes from the aquifer to the surface water body are output to the file GWtoSWBFLUX.DAT (Section G.16). The transverse profiles of the fluxes and concentrations of the radionuclides at the locations of the well and the surface water body are output to files PROFILEW.OUT and PROFILES.OUT. Appendix H describes the formulations.

5.2.3 Fate of Eroded Material in Runoff

The code does not model in detail the fate and transport of material eroded by runoff. Instead, it accepts user input specifying the fractions of the material eroded from the primary contamination and subsequently deposited at the offsite exposure locations and in a surface water body, as well as the fraction of material deposited on the catchment and subsequently washed out to the surface water body.

5.3   Accumulation and Concentrations at Offsite Locations

Concentrations at some of the offsite locations are obtained directly from the formulations for release and transport. The concentrations at other offsite locations also involve formulations for accumulation at the final and or intermediate locations.

5.3.1 Concentrations of Radionuclides in Well Water

The groundwater transport formulations compute the concentration profile of each radionuclide in the transverse plane—the plane perpendicular to the direction of groundwater flow—that contains the well. The code does not model any effects well pumping will have on this concentration profile. It estimates the concentration in the well water by finding the average concentration over the flow lines in the transverse section that are assumed to be intercepted by the well. This is described in Appendix H.

5.3.2 Concentrations of Radionuclides in a Surface Water Body

Concentrations of radionuclides in the surface water body are modeled by considering its water balance, sediment balance, and radionuclide balance. The processes considered in each balance are listed below. Appendix J describes the formulations.

The water balance considers the interception of groundwater by the surface water body, inflow of runoff and stream flow from the catchment into the surface water body, precipitation on the surface water body, evaporation from the surface water body, stream flow and extraction out of the surface water body, and infiltration from the surface water body into the aquifer (Figure 5-1).
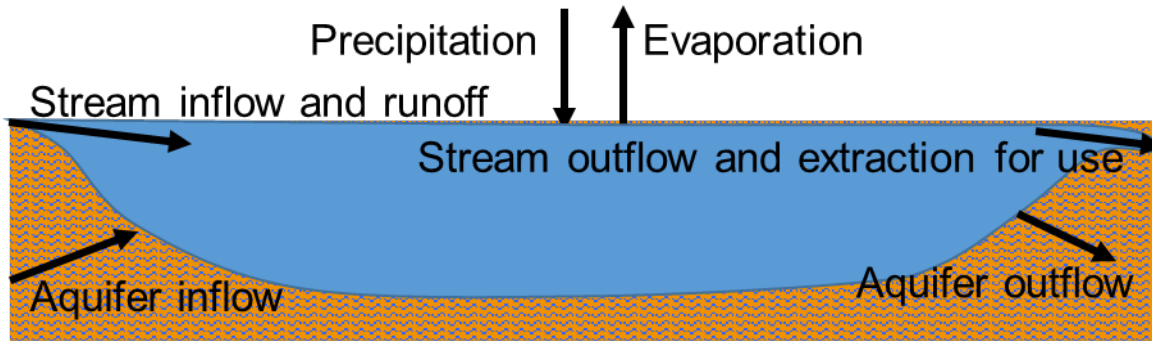
Figure 5-1   Water Balance of the Surface Water Body

The sediment balance considers the influx of eroded material from the catchment, removal of sediments with stream flow and extraction out of the surface water body, settling of suspended sediment, and changes in the amount of suspend sediment (Figure 5-2).
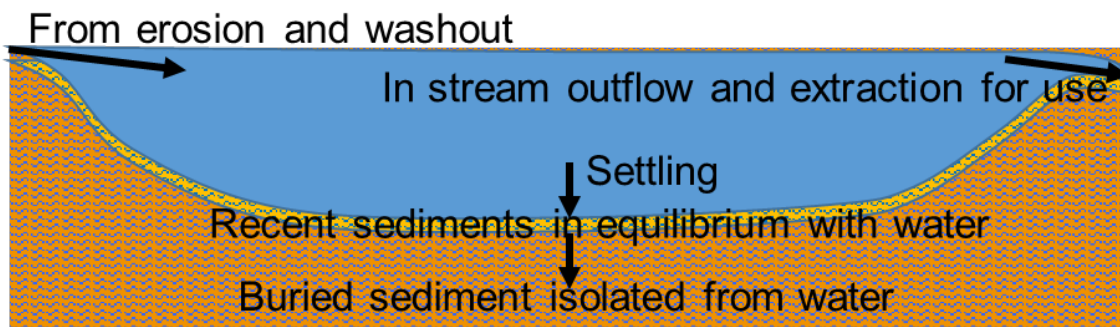
Figure 5-2   Sediment Balance of the Surface Water Body

The radionuclide balance includes the influx of radionuclides in the water that is intercepted from the aquifer, in the eroded particulates from the primary contamination, in the runoff from the catchment containing a fraction of the airborne contaminated particulates that were deposited there, and in the airborne particulates that are deposited directly on the surface water body; also considered are the removal of radionuclides with stream flow and extraction out of the surface water body, in the infiltration from the surface water body to the aquifer, and in the sediments that are isolated in the deeper layers of the bottom sediment; and finally the equilibrium partitioning of radionuclides between the water, the suspended sediments and the bottom sediments, and the effect of radiological transformations (Figure 5-3).

From deposition and
washout from atmosphere

From erosion and
washout from catchment

In stream outflow and
extraction for use

From aquifer inflow → Dissolved in water

In aquifer outflow

Ingrowth ← →Adsorbed on suspended sediments →

Decay

Adsorbed on recent sediments in equilibrium with water

Isolated in buried sediment
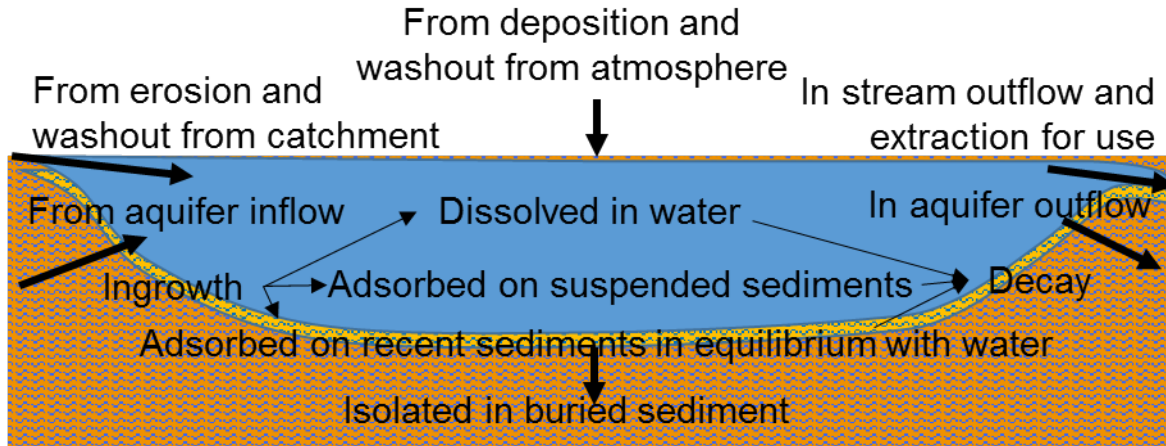
Figure 5-3   Radionuclide Balance in Surface Water Body

5.3.3   Concentrations of Radionuclides in Surface Soil at Offsite Locations

The code models the concentrations of the radionuclides in the surface soil layer at the offsite locations by considering the deposition of particulates containing radionuclides from the atmosphere, settling eroded material out of the runoff from the primary contamination, influx of radionuclide in irrigation applied to the offsite location, mixing of the surface layer, erosion of the surface layer, linear adsorption-desorption partitioning between the solid and aqueous phases of the surface layer, and radiological transformations of each radionuclide and its parent radionuclides Figure 5-4). The formulations are described in Appendix J, and the concentrations are available in the deterministic graphics viewer.

Influx (irrigation water, eroded material, particulates from air)

Lost to erosion

Mixing Layer

Parent
radionuclide → Radionuclide → Progeny
radionuclide

Linear adsorption / desorption leaching
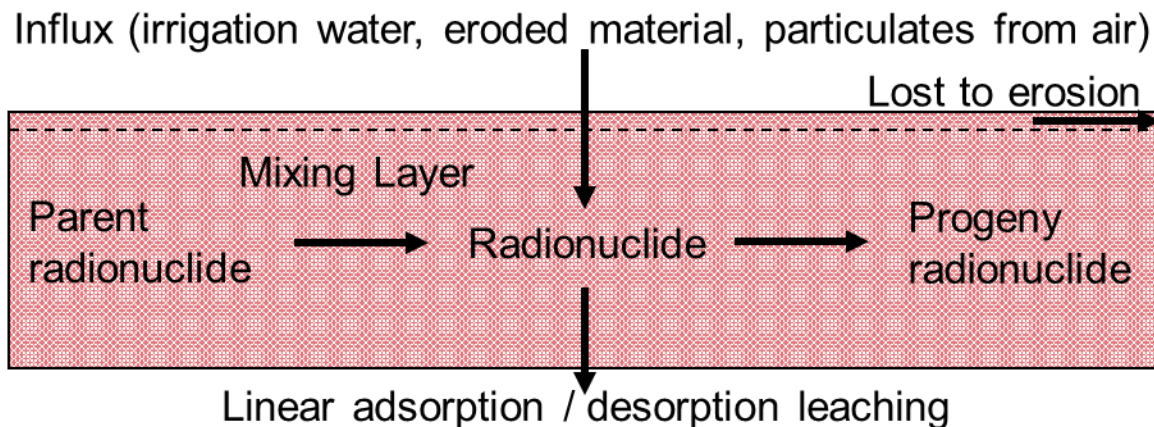
Figure 5-4   Radionuclide Balance in Offsite Mixing Layer

5.3.4 Concentrations of Radionuclides in Air in Particulates at Offsite Locations

The contaminated particulates in the air at the offsite locations are a mixture of the contaminated particulates released from the primary contamination and transported by the atmosphere, and the contaminated particulates released from secondary contamination at the offsite locations. The code computes the contribution of the former using the release rate of the radionuclide in particulates in Section 5.1.5 and the concentration to release rate ratio from the atmospheric transport in Section 5.2.1. It computes the contribution from the latter using the concentration of the radionuclide in the surface soil at the offsite location in Section 5.3.3 and the mass loading of particulates from the offsite location. Both the concentration of the radionuclide associated with respirable particulates and the concentration of the radionuclide associated with all the particulates are computed. The formulations are described in Appendix J, and the concentrations are available in the deterministic graphics viewer.

5.3.5 Concentrations of Radionuclides in Vegetables and in Livestock Feed

The code models the root uptake from the primary and secondary contaminations, the foliar interception of particulates released from the primary contamination but not from the secondary contamination, foliar interception of contaminated irrigation water, translocation of the radionuclides intercepted by the foliage to the edible part of the plant, and losses due to weathering. The code models two classes of vegetables and two classes of animal feed. The formulations are described in Appendix J, and the concentrations are available in the deterministic graphics viewer. The code also models the incorporation of carbon-14 into plants by photosynthesis from carbon dioxide released from the primary and secondary contamination.

5.3.6 Concentrations of Radionuclides in Meat and in Milk

The code computes concentrations of the radionuclide in meat and milk using transfer factors that are in essence ratios of the concentrations to the intake rates. It models the intake of radionuclides from ingesting livestock feed and water and the incidental ingestion of soil with the feed. The formulations are described in Appendix J, and the concentrations are available in the deterministic graphics viewer.

5.3.7 Concentrations of Radionuclides in Aquatic Food

The code computes concentrations of the radionuclide in two classes of aquatic food—fish and crustaceans—using transfer factors or bioaccumulation factors. This factor is simply the ratio of the concentration in the aquatic food to the concentration in the water where the fish lived. The formulations are described in Appendix J, and the concentrations are available in the deterministic graphics viewer.

6 UNCERTAINTY AND SENSITIVITY ANALYSIS TOOLS

RESRAD-OFFSITE code has built-in tools to study parameter sensitivity and uncertainty of calculated dose and risk. Both sensitivity analysis and uncertainty analysis help users to understand the effects of input parameters on model results. Once the important parameters are identified, resources might be focused to refine and understand their potential values.

Many factors may contribute to the uncertainty of predicted dose and risk. These factors include uncertainty of exposure scenarios, future use and zoning of the site, applicability of the models and their limitations, and uncertainty and variability of input parameters. Furthermore, user experiences and training may affect their interpretation of scenario and selection of parameter values. RESRAD-OFFSITE has built-in features to prevent users from misuse of the code such as setting and checking parameter bounds and prompting users when calculated quantities are outside normal ranges or design of the code. Among all these uncertainty factors, parameter uncertainty can be studied using the built-in sensitivity analysis and probabilistic uncertainty analysis tools.

6.1   Overview of Tools

Uncertainty and probabilistic analysis are used to determine the variation in predictions (dose, risk, or media concentrations) due to uncertainty in the values of some parameters and the probabilistic nature of other parameters. This type of analysis can also be used to identify input parameters that are responsible for much of the variation in output. Then the resources can focus on reducing any uncertainty in those parameters in order to efficiently reduce the variation in the predicted dose, risk, or media concentrations.

Deterministic sensitivity analysis is much simpler and quicker to set up, run, and interpret results because it considers the change of some result based on a discrete change in only one input parameter. Probabilistic uncertainty and sensitivity analyses are more comprehensive, but correspondingly more difficult and slower to set up, run, and interpret because multiple parameters can vary simultaneously based on both a probabilistic input distribution (e.g., normal, uniform, log-normal) and input correlations between input parameters.

With the capabilities of studying multiple parameters and their correlations simultaneously, probabilistic uncertainty analysis can address more complex aspects of parameter sensitivity, generate probabilistic results, and generate results based on regulatory standards. Regulatory guidance issued by the NRC for decommissioning nuclear facilities (NUREG-1757, Vol. 2) discusses consideration of peak of the mean (POM) and mean of the peak (MOP) outputs from probabilistic analyses for demonstrating compliance with regulatory standards for license termination found in 10 CFR Part 20, Subpart E.

6.2   Deterministic Sensitivity Analysis

Sensitivity of some model result, R, to an input parameter, x, is often defined as the fractional change in R given a small factional change in x (i.e., $[\Delta R/R]/[\,\Delta x/x]$). This sensitivity will in general depend on the value of the input parameter, x, the size of the increment in the input value (although hopefully this will be somewhat independent as the increment decreases), the value of all other input values (X), the time, and the specific result of interest. For regulatory purposes, the sensitivity value of interest might be the sensitivity of the peak total annual dose, with all parameters set at the agreed-upon use scenario (e.g., subsistence farming at the site).

The RESRAD-OFFSITE code does not calculate this sensitivity, but instead graphically show the result R as a function of time for three values of the input parameter of interest. The three input values are the base input value multiplied and divided by a user-provided factor (Figure 6-1). This allows a quick visual interpretation of the importance of the parameter along with its time, pathway, and nuclide dependence. Although the selection of the factor is not very important, since the default will indicate a good qualitative indication of whether the result is sensitive to the parameter, the factor might be chosen to match the potential range of the input value based on the uncertainty or variability of the parameter.

Figure 6-1   Form to Set Sensitivity Range

6.2.1   Examples

Some examples of expected sensitivities are helpful. Several are provided in Table 6-1.

Table 6-1   Examples of Deterministic Sensitivity Analysis Results

Scenario	Example Plot
If the result is directly proportional to the input R = ax, then the sensitivity is 1. The graphs would show that the result doubles if the input parameter doubles.	
Sometimes the time dependence of the result will change with a parameter's value (the graph shows the dependence of the timing of peak dose on precipitation rate). However, the DCGL is based on the peak dose, so in this case there is very little sensitivity of the result (peak dose) to the input (precipitation rate).	

6.2.2   Parameters to Determine Release Contributions

Sometimes it is easier to determine contributions of environmental transport/release or exposure pathways to the total dose, and then focus on the parameters that influence the dominant pathway. Table 6-2 lists parameters that different release and exposure pathways (air, water, external, erosion) are most sensitive to.

Table 6.2   Parameters That Determine Release Conditions

Release/Exposure Pathway	Variable
Erosion to pond	Sediment delivery ratio.
Release to air	Deposition velocity (in primary contamination form).
External dose	Direct external dose is split in the graphics by the "waterborne" and "direct and airborne" components. To distinguish the latter two, the deposition velocity (in the Nuclide form) can be used.
Release to groundwater and surface water	For transport pathways through the well, the well-water usage parameters can be set. For transport pathways to the surface water body (which can also be contaminated by air deposition and erosion), there are no specific parameters that control release to the pond without having a side effect on other pathways.

6.3   Uncertainty

6.3.1   Overview

Parameter uncertainty might arise from a lack of detailed characterization, the variability of a parameter, or problems forecasting future conditions. Although it would be nice to have a functional form of the uncertainty of the result, given the uncertainty of the inputs, this is rarely simple to do. In the simplest case, if the result is the product of two normally distributed input parameters, then the probability distribution of the result would be the convolution of the input. This would result in a normal distribution with a wider standard deviation.

In general, it is easier to construct the probability distribution of the result based on many standard calculations where each calculation is based on single values of the input. The values to use from the input distributions are based on their relative probability. There are two ways of doing this. The first is a standard random method (Monte Carlo) that generates a probability between 0 and 1 and then back-calculates the corresponding input value (i.e., the cumulative probability of the input being less than the identified value is the random number). A more refined way to select the input values, which gives the same statistically determined results but does not require as many calculations, is the Latin hypercube sampling (LHS) method (see the following section for discussion). A typical uncertainty/probabilistic analysis input/output is illustrated in Figure 6-2. The process starts on the left with the user specifying a series of probability distributions for inputs. When the code is run, these distributions are sampled to generate a series of complete set of RESRAD-OFFSITE input values. Each set is run, generating dose results which are saved. When all the sets have been run, the code performs statistical analysis on the set of results and prepares the data for the user to interactively explore the results.
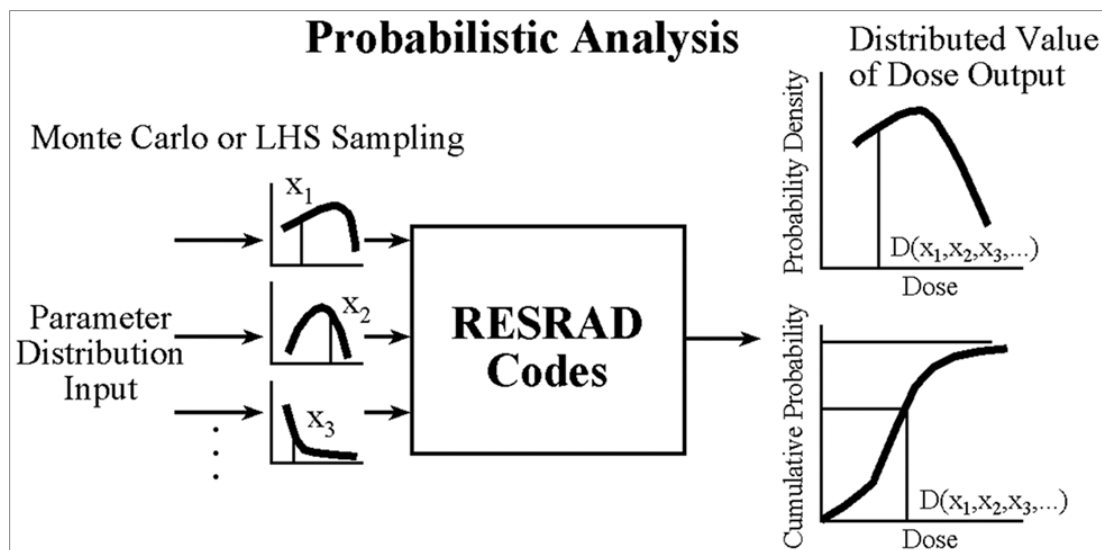
Figure 6-2   Uncertainty/Probabilistic Analysis

6.3.2   Input

Probability distributions for parameters. The users need to select the probability distribution function and the corresponding distribution parameters. Default distributions are available in RESRAD OFFSITE for many parameters. If default distributions are unavailable or it is appropriate to use site-specific information to develop parameter distributions, parameter distributions can be developed based on the following considerations:

- When available or important to the decision being made, site-specific information about the site, region, or some characteristics such as soil type should be used to develop the parameter distribution.

- A uniform distribution should be selected, if the relative probability is unknown but should be tested over a range. This also includes log-uniform, triangular, and normal distribution (Figure 6-3) as more information is gathered.

- A discrete distribution should be selected, if only specific values of the parameter are used (Figure 6-4). This, in conjunction with another parameter set with a smooth distribution, will lead to multiple distinct result curves to test its dependence on the two parameters.
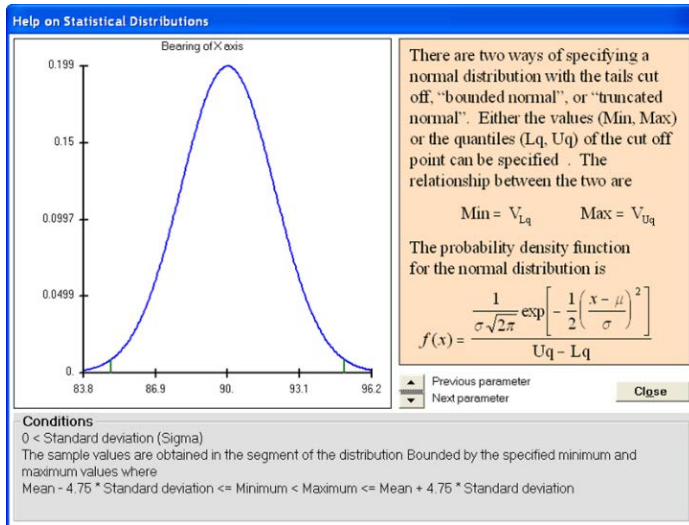
Figure 6-3   Specifying a Normal Distribution for Probabilistic Analysis
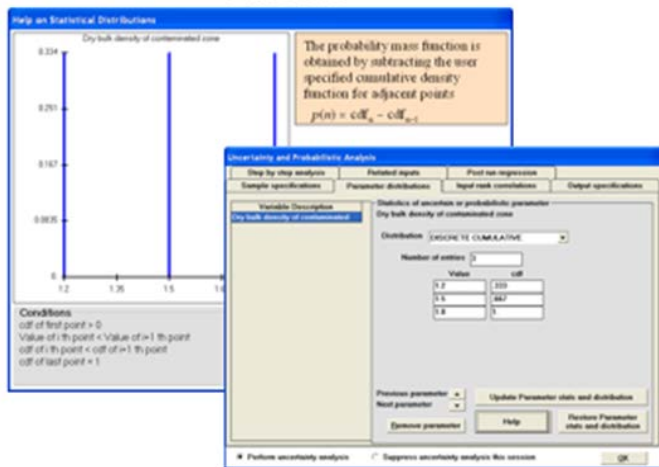
Figure 6-4   Specifying a Discrete Distribution for Probabilistic Analysis

Correlations between pairs of input parameters. This is based on rank correlation, so the correlation is between +1, fully positive correlation i.e., the highest value of one parameter matches with the highest value of the correlated parameter, to -1, where the highest values of one parameter are matched with the lowest of the second. Figure 6-5 shows an example of an input screen for specification of the correlation between two parameters. Precipitation rate and erosion rate are correlated with a positive rank correlation coefficient of 0.9. The following are some considerations when specifying correlations between parameters:

- No default nonzero correlations are specified (i.e., the user must provide input on parameter correlations).

- Some parameters are expected to be correlated, such as precipitation and erosion.

Figure 6-5   Specifying Input Correlations

- Distribution coefficients, Kds, should be considered for correlation, especially if the default distributions (very wide log-normal distribution with ranges of about 1 million) are used (Figure 6-6). If there is some commonality between the zones (e.g., the distribution coefficient is similar in the zones but just not known), then a positive correlation should be used between each pair of zones. For example, with a primary contaminated zone (PCZ), unsaturated zone (UZ), and saturated zone (SZ), correlations of the Kd in these zones should include PCZ/UZ, PCZ/SZ, and UZ/SZ. If this last correlation is not specified, the code might not be able to generate a usable sample.

Figure 6-6   Setting up Correlation among Three Related Parameters

- Another special case is the distribution coefficients for isotopes, which are assumed to be isotope-dependent, not just element-dependent (Figure 6-7). Therefore, if the distribution coefficients for uranium-238 and uranium-234 are set up for uncertainty analysis in a zone, then the Kd values would very likely need to be correlated (i.e., Kd(U238)/Kd(U234)).

Figure 6-7   Setting up Correlation among Isotopes

Number of Observations. This is the number of values that will be sampled from the distribution of each input parameter specified in the parameter distributions tab. This number must exceed the number of input parameters, if correlations are specified between inputs or if regression statistics are to be produced. The accuracy of the probabilistic predictions can be improved by increasing the number of observations.

Sampling Technique. The code offers a choice of two sampling techniques: LHS or Monte Carlo. In the LHS technique, the distribution is divided into equally probable segments, equal in number to the desired number of observations. Then a value is picked at random from each segment according to the probability density function within that segment. This ensures that the sample covers the entire range of the distribution, even when the number of samples is relatively small. In the Monte Carlo technique, the desired observations are each picked at random from the entire distribution according to the probability density function. When the number of samples is small, the sampled values do not represent the distribution as well as the values obtained using LHS.

Number of Repetitions. This is the number of times the analysis needs to be repeated in order to obtain a measure of the accuracy of the probabilistic predictions. Increasing the number of observations increases the accuracy of the probabilistic predictions, but a measure of the accuracy can be obtained only if the analysis is repeated. The closeness of the results, or the lack thereof, is an indication of the accuracy, or lack of accuracy, of the predictions.

Figure 6-8 shows the sampling of a normal distribution with eight observations and three repetitions, for a total of 24 points. Each repetition covers the range of inputs and is therefore considered a separate complete sample set.
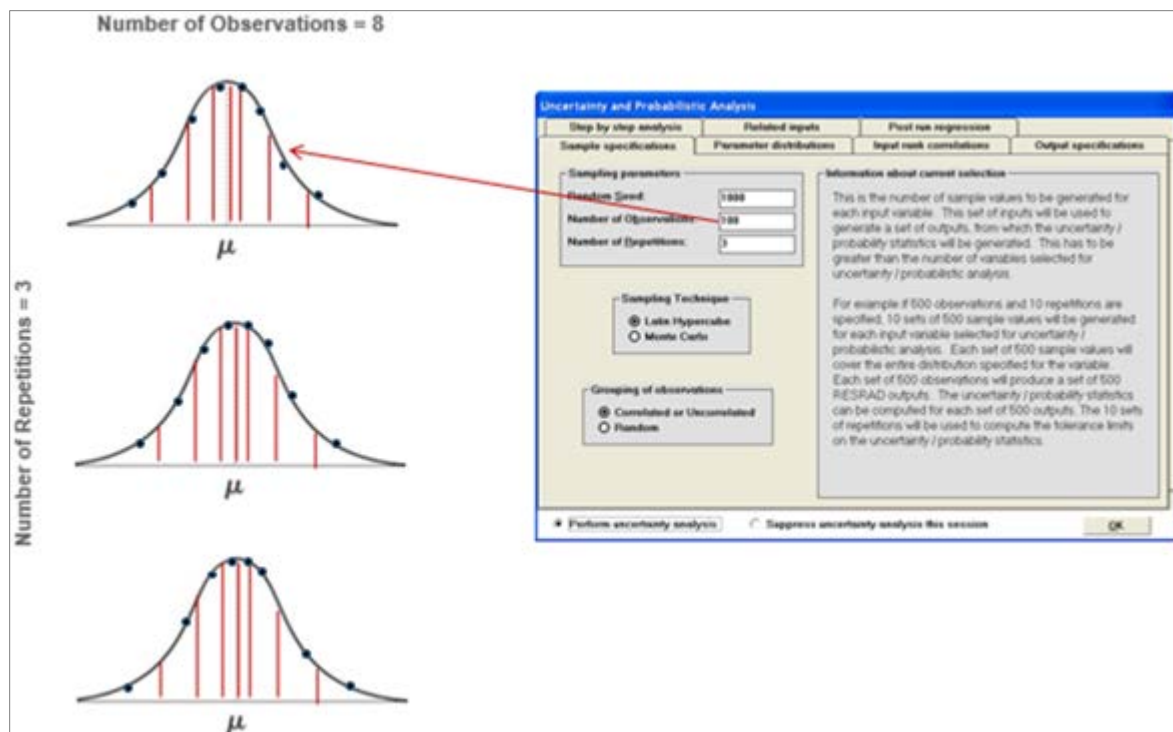
Figure 6-8   Setting up the Number of Observations and Repetitions

6.3.3   Example of Sampling

A simple example of the sampling process demonstrates what the RESRAD-OFFSITE code does. In this example, there is one parameter, the distribution coefficient of uranium-238 in the saturated zone, selected for uncertainty analysis. This distribution is shown at the top of Figure 6-9. It is very difficult to understand this distribution because it very skewed, so instead the cumulative probability distribution (Figure 6-9, middle) is shown. It is still difficult to determine the range of the first 80% of the distribution, so the x-axis is put on log-scale (Figure 6-9, bottom).

Note that the default probability distribution shown this way covers over 7 orders of magnitude from 0.1 to 1 million cm^3/g. This is a log-normal distribution. The input graphics will not show it this way, but the graphics in the output are more flexible.

Also note that the median value (50%) is slightly lower than 100 cm^3/g. The default value for this parameter is 50 cm^3/g.
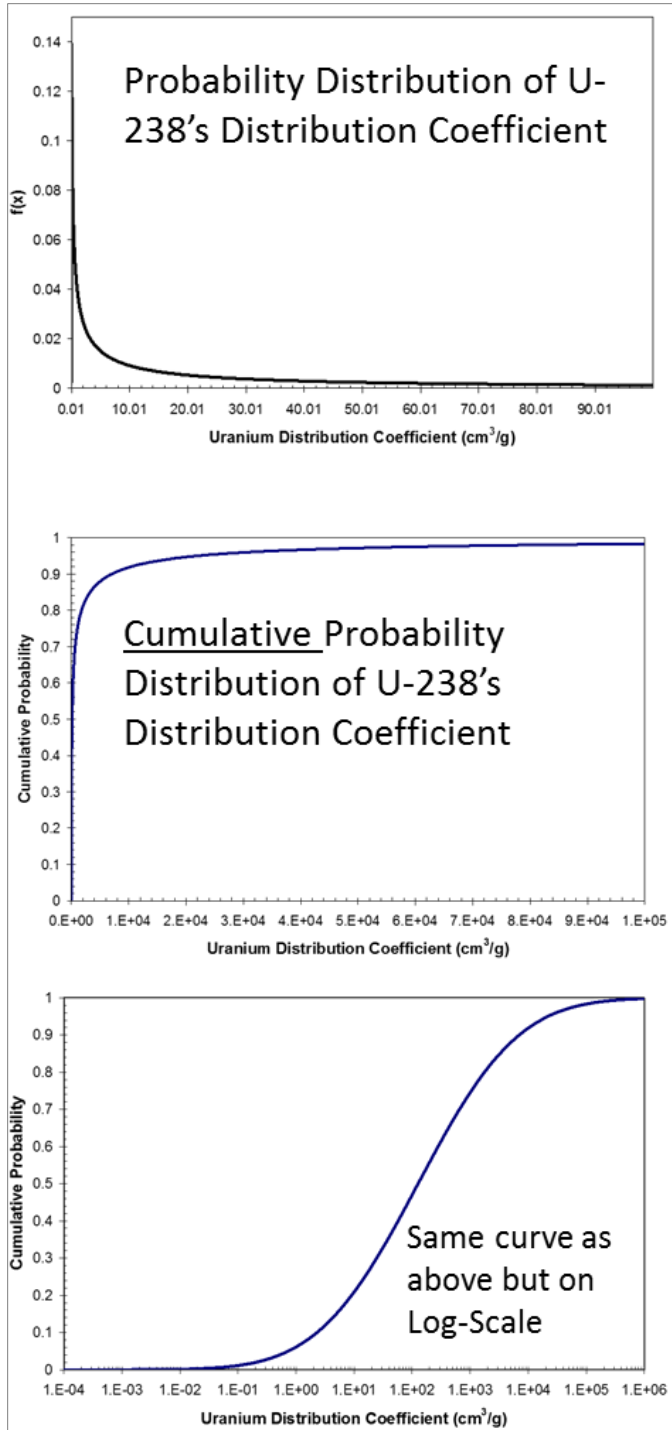
Figure 6-9   Different Ways to Display the Probability Distribution for Kd

The actual sampling with the default random seed is shown in Figure 6-10. Note that the x-scale covers just a subset of the one in Figure 6-9. The specific values of the Kd that were sampled are on the right of the plot. Because it used LHS sampling, there is one point for every 9% increment in the cumulative probability.
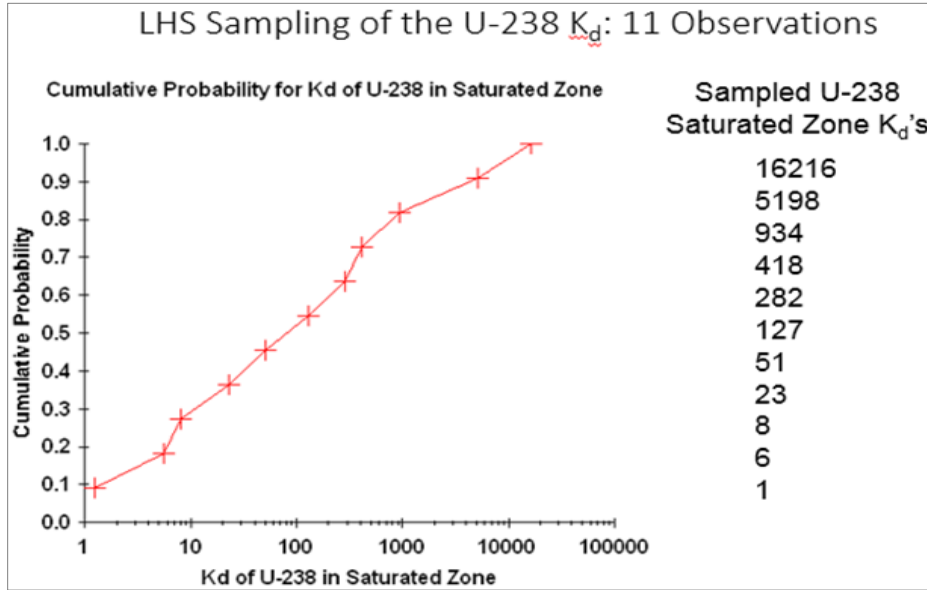
Figure 6-10   LHS Sampling of Probability Distribution from Figure 6-9

Then the RESRAD-OFFSITE deterministic model is run for each value of the distribution coefficient. Figure 6-11 shows the temporal plots of total dose for different distribution coefficients. It shows that the temporal dose profiles differ with the distribution coefficient.
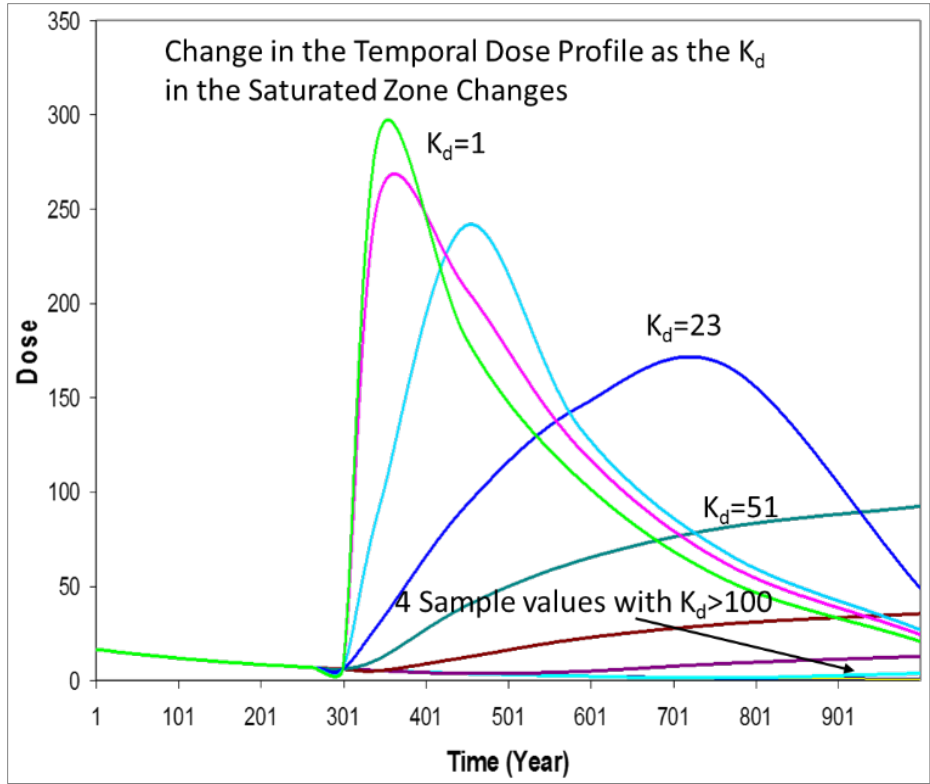
Figure 6-11   Change in Temporal Dose Profile as Kd in the Saturated Zone Changes

To perform a POM analysis, the mean (average) value of dose at each time is calculated (see Figure 6-12). Then the peak dose of this mean dose curve is identified. This dose rate is then used to determine the DCGL.
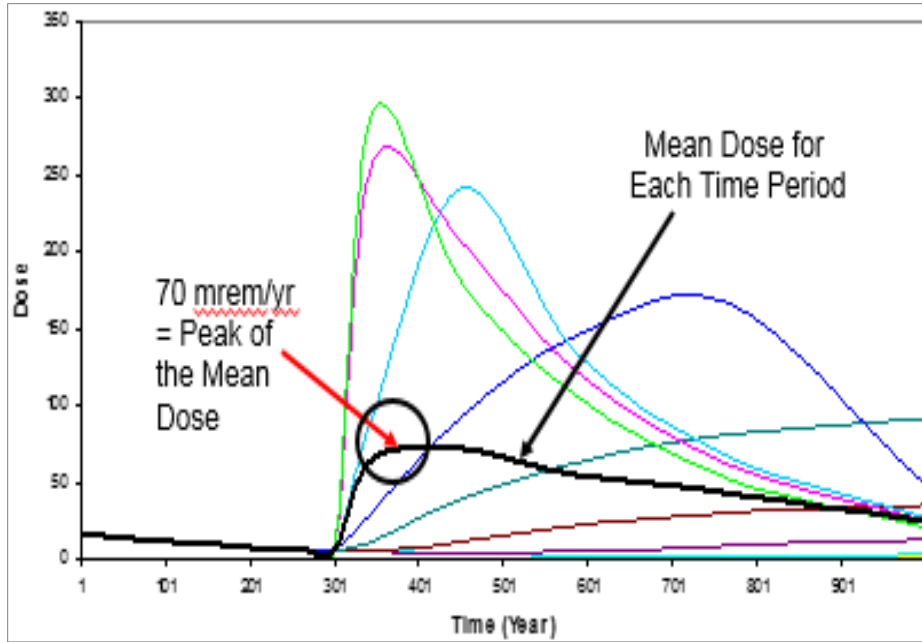
Figure 6-12   Peak of the Mean Calculation

To perform a MOP analysis, the peak dose value of each curve is identified (see Figure 6-13). Then the mean of the peak doses is calculated and used to determine the DCGL.

$$\frac{16.5+16.5+16.5+16.5+16.5+35.5+92.5+167+242+259+292}{11}$$

Mean of the
Peak Dose:
106 mrem/yr
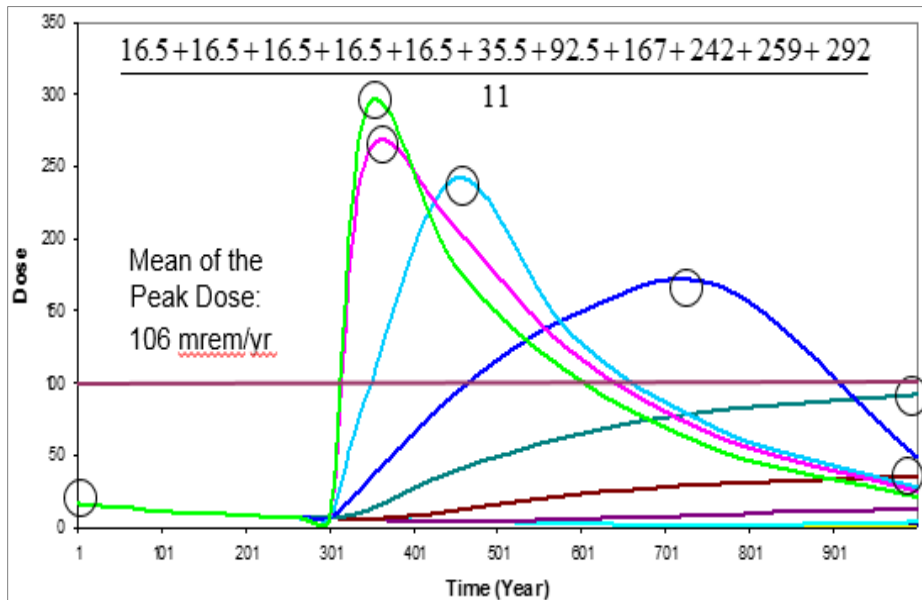
Figure 6-13   MOP Analysis

6.3.4 Results

Determining MOP. The cumulative distribution function (CDF) of the output can be used to obtain any desired percentile of the output (dose or risk). The value of the percentile can be obtained by keying in the desired percentile in the gray box in the x-axis frame on the right side of the Probabilistic/Uncertainty Outputs screen (Figure 6-14). This frame also displays the mean and the standard deviation of the output. Error ranges are shown where appropriate after a plus/minus symbol (±). (If the error range is less significant than the number of significant figures in the output, it will not be shown.)
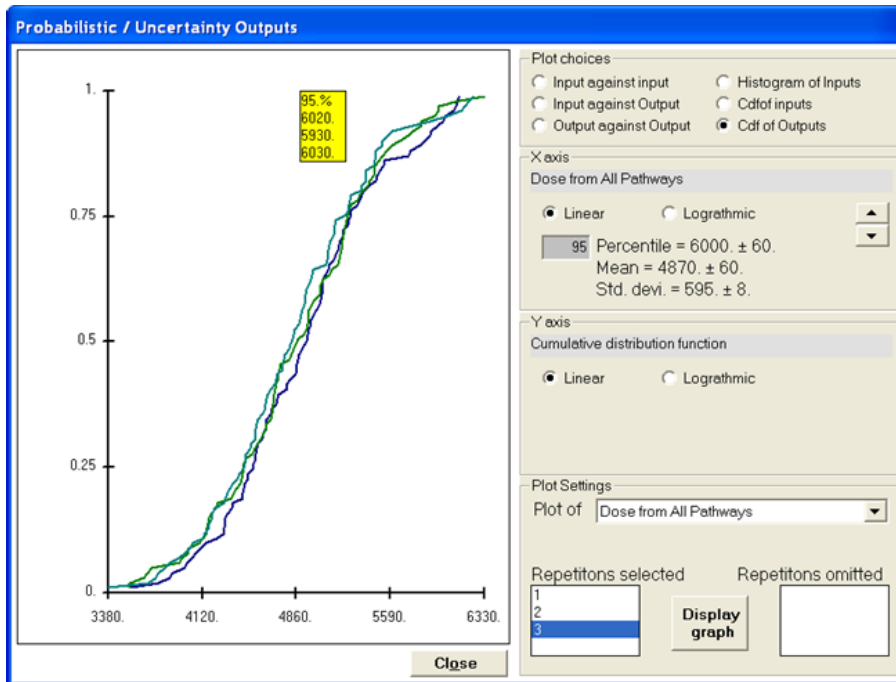
Figure 6-14   Determining the MOP with Uncertainty Results

Determining POM. The temporal plot shows the variation of the mean, median, and one other user-specifiable percentile of the total dose (dose summed over nuclides and pathways) with time. The plots for all repetitions can be displayed together, as shown in Figure 6-15, to see the variation among repetitions; plots of each repetition can also be displayed for clarity. The coordinates of any location on the plot will be displayed in the yellow box when the cursor moves to the desired point. The data from the plots for the corresponding year can be displayed by clicking the mouse; the data for each of the repetitions will be shown in the yellow box at the lower right of the form.
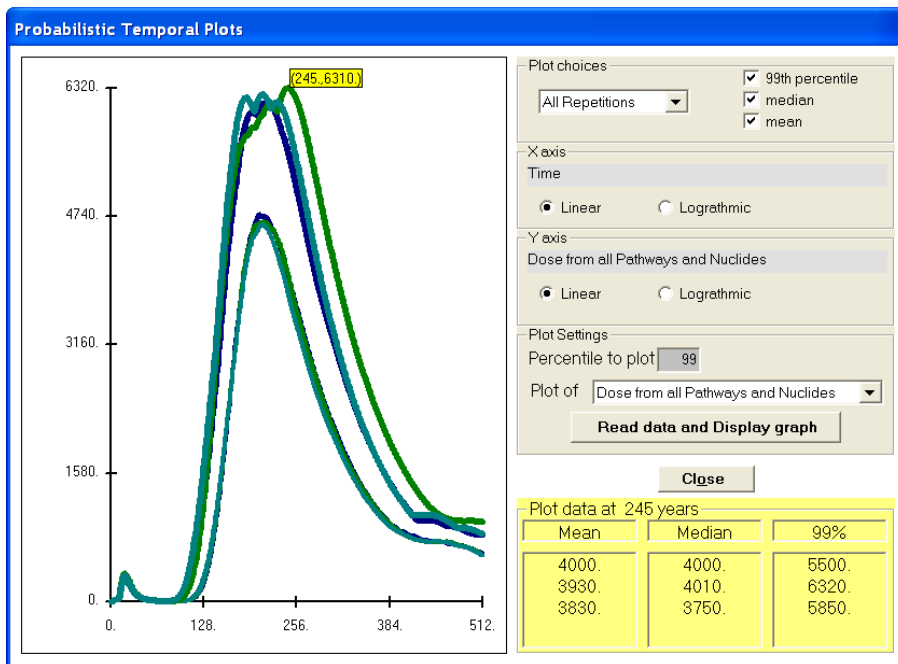
Figure 6-15   Determining POM with Uncertainty Results

Determining Sensitivity. Multiparameter sensitivity analysis can be performed using the uncertainty feature by allowing more than one parameter to vary at the same time. A parameter can be selected for this analysis by pressing Shift+F8 when the parameter is in focus. That parameter will be included in an uncertainty analysis with a uniform distribution ranging from 0.9 to 1.1 of its current deterministic value. The sensitivity of the dose or risk to the parameters is given by the standardized regression coefficient or the standardized rank regression coefficient.

The scatter plots of output against input are helpful in identifying the input parameters that have a significant influence on the output, especially when there are a few significant input parameters (Figure 6-16). However, it is not easy to visually pick out the important parameters when they are masked by the compounding effects (interference) of other equally important input parameters. The important parameters can be identified by using the regression coefficients listed in the linear regression report (Figure 6-17).

Determining Multi-parameter Dependence. The uncertainty analysis feature can also be used to see the variation of dose over the range of one parameter at various levels of another parameter. The scatter plot of output against input is useful for seeing this variation and the interaction between the inputs, as shown in Figure 6-18.

Probabilistic / Uncertainty Outputs

Plot choices
- Input against input
- Input against Output
- Output against Output
- Histogram of Inputs
- Cdf of inputs
- Cdf of Outputs

X axis
Thickness of contaminated zone
- Linear
- Logrithmic

95 Percentile = 2.17 ± 0.03
Mean = 2.01
Std. devi. = 0.0982 ± 0.0052

Y axis
Dose from All Pathways
- Linear
- Logrithmic

99 Percentile = 6240. ± 110.
Mean = 4870. ± 60.
Std. devi. = 595. ± 8.

Plot Settings
Plot of | Thickness of contaminated zone
against | Dose from All Pathways

Repetitons selected
1
2
3

Repetitons omitted

Display graph

Close

Figure 6-16   Displaying Input vs. Output Scatter Plot for an Input Parameter that has Positive Correlation with Results

MCSUMMAR.REP

Help

LineDraw 10   Page: 87

OFFSITE Regression and Correlation output   07/27/06 09:00 Page: Coef   1
Users Guide Output Screen Shots
usersGuideImp.ROF

:ients for peak All Pathways Dose

Coefficient =	PCC	PCC	PCC	SRC	SRC	SRC
Repetition =	1	2	3	1	2	3

:ion of Probabilistic Variable

	Sig Coeff	Sig Coeff	Sig Coeff	Sig Coeff	Sig Coeff	Sig Coeff
Leach Rate of Ra-226	7 -0.97	9 -0.94	7 -0.96	7 -0.26	9 -0.20	7 -0.29
Kd of Pb-210 in Saturated Zone	4 -0.98	5 -0.97	5 -0.97	4 -0.33	5 -0.32	5 -0.32
Kd of Ra-226 in Unsaturated Zone 1	14 -0.81	14 -0.69	14 -0.65	14 -0.09	14 -0.07	14 -0.07
Kd of Ra-226 in Saturated Zone	8 0.97	8 0.95	9 0.95	8 0.25	8 0.23	9 0.24
Precipitation	12 0.83	12 0.76	13 0.65	12 0.10	13 0.09	13 0.07
Length of contamination parallel to aquifer flow	5 0.98	3 0.98	3 0.98	5 0.32	3 0.36	3 0.36
Evapotranspiration coefficient in area of primary contamination	13 -0.81	13 -0.76	11 -0.80	13 -0.09	12 -0.09	11 -0.10
Thickness of contaminated zone	1 0.99	1 0.98	2 0.98	1 0.41	1 0.41	2 0.37
Dry bulk density of contaminated zone	2 0.98	2 0.98	1 0.98	2 0.38	2 0.41	1 0.40
Thickness (meters) of Unsaturated zone 1	15 -0.67	15 -0.60	15 -0.50	15 -0.06	15 -0.06	15 -0.05
Dry Bulk Density (grams/cm**3) of Unsaturated zone 1	11 -0.84	11 -0.78	12 -0.69	11 -0.10	11 -0.09	12 -0.07
Hydraulic Conductivity of saturated zone	6 -0.98	6 -0.97	6 -0.97	6 -0.31	6 -0.31	6 -0.29
Hydraulic Gradient of saturated zoneto well	3 -0.98	4 -0.98	4 -0.97	3 -0.33	4 -0.33	4 -0.34
Vertical lateral Dispersivity of saturated zoneto well	17 -0.12	17 -0.23	16 -0.19	17 -0.01	17 -0.02	16 -0.02
Water for Consumption by humans	9 0.97	7 0.96	8 0.95	9 0.25	7 0.26	8 0.24
Fraction of water from well for Consumption by humans	10 0.92	10 0.92	10 0.92	10 0.16	10 0.17	10 0.19
: in the direction parallel to aquifer flow from downgradient edge of contamination	16 -0.14	16 -0.33	17 -0.13	16 -0.01	16 -0.03	17 -0.01
R-SQUARE =	1.00	0.99	0.99	1.00	0.99	0.99

: set to zero if the dose is zero or the correlation matrix is singular.
RE varies between 0 and 1 and is called the coefficient of determination; it provides a measure of the
ion in the dependent variable (Dose) explained by regression on the independent variables.

Figure 6-17   Regression Analysis Results
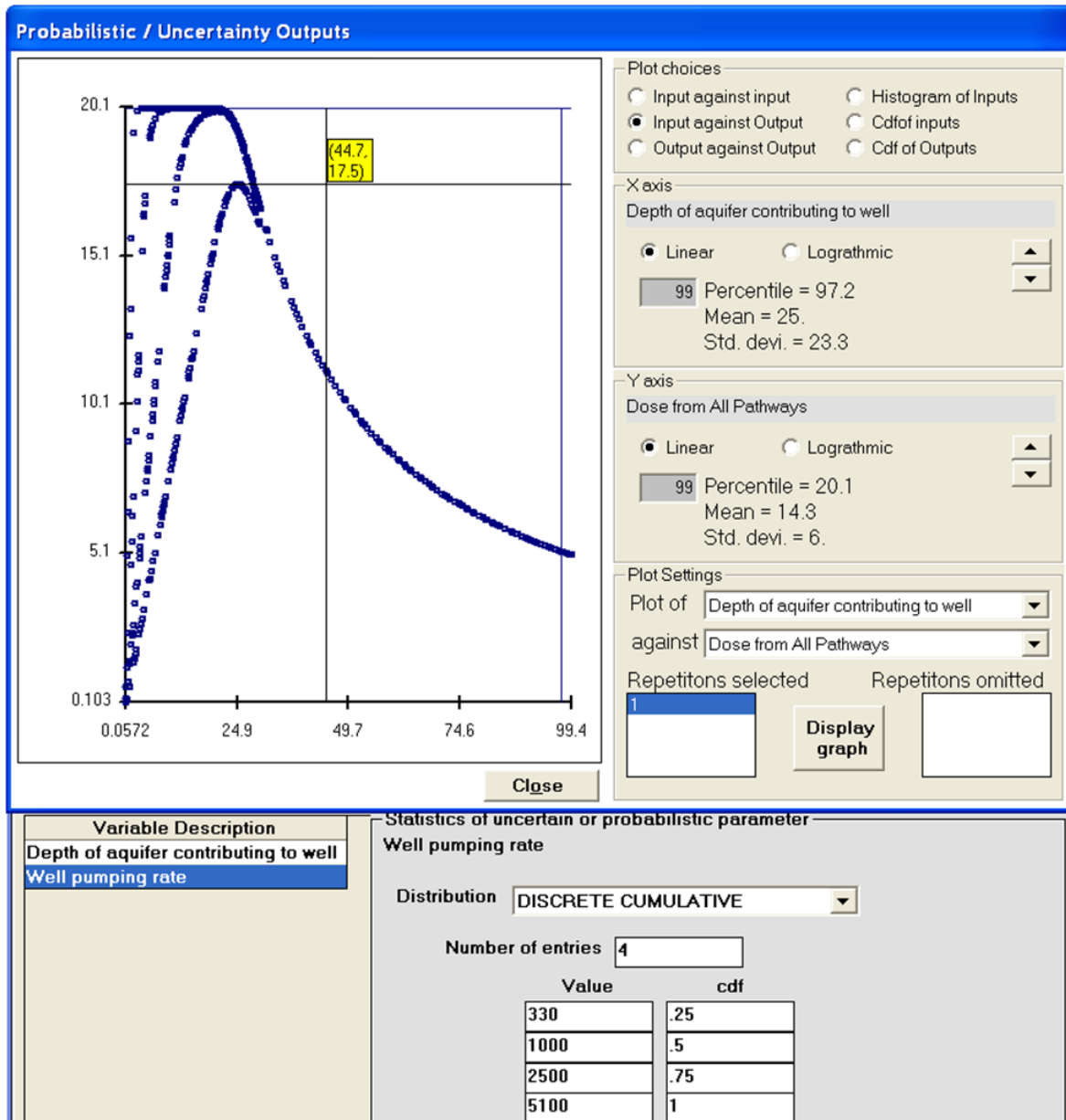
Figure 6-18   Using Discrete Probability Distributions to Find the Dependence of the Result on Two Input Parameters

7 VERIFICATION, BENCHMARKING, AND VALIDATION

The RESRAD-OFFSITE code was developed following the RESRAD program quality assurance (QA) and quality control (QC) procedures. Various components of the code were verified by separately developed spreadsheets, benchmarked against the RESRAD-ONSITE code for onsite exposures, benchmarked with peer codes for atmospheric transport and groundwater transport modeling, and benchmarked against the DUST-MS code (Sullivan 2006) concerning delayed and distributed releases of radionuclides from waste materials. The following sections provide additional discussion on each of these activities.

7.1   QA/QC Verification

Any beta version of the RESRAD-OFFSITE code was tested and verified prior to official release following the procedure described in the RESRAD Program Software Configuration Management Plan (SCMP) (Argonne 2018a). SCMP is part of the RESRAD Program Software Quality Assurance Plan (Argonne 2018b), which meets the requirements of DOE Order 414.1D (DOE 2011) and Argonne software QA guidance (Argonne 2017). Any revision made to the code was tested and/or verified by the programmer, task leader, and independent reviewers via different means, including interpreting and analyzing the results against physical principles and mathematical expectations, as well as comparing the results with independent spreadsheet calculations. The testing and verifications were documented with sufficient detail to be reproduced and tracked in the future. RESRAD-OFFSITE is currently being evaluated by the DOE safety software central registry review team for inclusion in the DOE safety software toolbox.

7.2   Activities for Databases and Programming Modules Shared with RESRAD-ONSITE

As previously mentioned, the RESRAD-OFFSITE code is an extension of the RESRAD-ONSITE code, and the two share the same radiological transformation, dose coefficients, cancer slope factors, biological transfer and uptake, and geochemical input databases, as well as many transport and exposure programming modules. RESRAD-ONSITE has already been extensively tested, verified, and validated, as documented in Chapter 5 of the RESRAD-ONSITE User's Manual and other documents (Yu et al. 2001; Halliburton NUS 1994; Cheng et al. 1995; Gnanapragasam et al. 2000; Mills et al. 1997; Whelan et al. 1999a,b). The conclusions of this testing, verification, and validation for the RESRAD-ONSITE code also apply to the RESRAD-OFFSITE code, for the components both codes share.

In addition to the ICRP-38 radiological transformation database, the ICRP-107 transformation database, the DCFPAK 3.02 and DOE STD dose coefficients, and the DCFPAK 3.02 cancer slope factors were incorporated into RESRAD-ONSITE and RESRAD-OFFSITE in 2014 and 2016, respectively. Testing of switching between the ICRP-38 and ICRP-107 databases and of the restriction imposed to allow the selection of only the corresponding DCF databases was conducted prior to the release of Version 7.2 of the RESRAD-ONSITE code and Version 3.2 of RESRAD-OFFSITE code. The testing was performed and documented following the RESRAD program QA/QC requirements.

7.3   Verifying and Benchmarking Onsite Exposures

Detailed benchmarking of the RESRAD-OFFSITE and RESRAD-ONSITE codes was conducted in 2006 (Yu et al. 2006) for an onsite exposure scenario that considered a farmer building a house, growing plant foods, and raising livestock on a contaminated area. In addition, this farmer also drew water for drinking and household activities, feeding livestock, and irrigating agricultural fields from an onsite well and caught fish from an onsite pond. All exposure pathways were considered for dose calculations.

Major differences were found in the radiation dose associated with the ingestion of food from the aquatic pathway, due to the more sophisticated surface water model implemented in RESRAD-OFFSITE. This new model considers the discharge of eroded soil to the surface water body, the residence time of water, and equilibrium adsorption-desorption of radionuclides between sediment and water. Other differences in radiation dose associated with the ingestion of groundwater and the inhalation pathway as well as in the radiation dose of carbon-14 and hydrogen-3 were also observed. These differences were attributed to the enhanced groundwater transport model in RESRAD-OFFSITE, which considers dispersion, and minor differences in the use of input parameter, the scheme of interpolation, and the number of time points for dose integration. By setting the dispersivity to zero and adjusting the input parameter values, these differences were eliminated or reduced, and the RESRAD-OFFSITE results agreed well with the RESRAD-ONSITE results. This benchmarking study was documented in Yu et al. (2006), which is available at the RESRAD website, http://resrad.evs.anl.gov.

Exercises comparing radiation doses calculated for an onsite exposure scenario by RESRAD-ONSITE and RESRAD-OFFSITE were routinely incorporated in RESRAD-OFFSITE training workshops to illustrate differences in the transport modeling and the use of input parameters between the two codes. These exercises used the Onsite Scenario Template File provided by RESRAD-OFFSITE. Where Am-241 was concerned, the largest difference was observed in the water-dependent plant ingestion dose due to the different uses of the annual irrigation rate. After adjusting the default irrigation rates that come with the template file, RESRAD-OFFSITE calculated a plant ingestion dose close to that calculated by RESRAD-ONSITE. Detailed discussions on the use of the Onsite Scenario Template File in RESRAD-OFFSITE and the comparisons with RESRAD-ONSITE are provided in Appendix K of this User's Manual.

7.4   Verifying the Modifications and Extensions beyond Onsite Exposures

To allow for evaluation of offsite radiation exposures, some existing modules of the RESRAD-ONSITE code were modified and new modules were added to develop the RESRAD-OFFSITE code. The calculations of these modified or added modules were verified with spreadsheets that implemented the same mathematical formulations. Detailed descriptions of these verifications are available (Yu et al. 2011). They involve four programming components of the RESRAD-OFFSITE code: (1) source term and releases, (2) groundwater transport, (3) atmospheric transport, and (4) accumulation at offsite locations and in food.

Verification of the source term and releases consisted of verifying the temporal variations in thickness and radionuclide concentration for the different layers of soil from the ground surface to the bottom of the contaminated zone, and in the flux of radionuclides released to the atmosphere, unsaturated zone, and surface water body. The verification of groundwater transport included verifying transport in the unsaturated zone, in the saturated zone to the surface water body, and in the saturated zone to a well. A decreasing and then an increasing triangular input flux generated the output flux at the end of the transport distance for

comparison. For atmospheric transport, the point-source-to-point-receptor normalized air concentrations (χ/Q values) were calculated for five different combinations of distance, direction, wind speed, and stability class, and each combination was coupled with six different cases of dispersion coefficient and dry/wet deposition. The accumulation in offsite soil was verified by considering the deposition of radionuclides with the atmospheric dust particles and irrigation water. Accumulation in the surface water body was also verified. Accumulation in different types of plant food was verified, via root uptake and foliar interception due to deposition of airborne dust particles and irrigation water. Similarly, the accumulation in meat and milk was verified, via ingestion of grain, pasture, and silage, as well as soil and water.

The verification showed that the calculation results from RESRAD-OFFSITE agreed with those from the spreadsheets.

7.5   Benchmarking the Air Dispersion Model

RESRAD-OFFSITE air transport modeling (Yu et al. 2006) was benchmarked in 2006 using CAP88-PC (Parks 1992) and ISCLT3 (EPA 1995). Downwind air concentrations were compared at receptor distances ranging from 100 to 80,000 m, associated with airborne releases from area sources of 10,000 and 40,000 m^2.

In general, good agreement was observed between RESRAD-OFFSITE and CAP88-PC regardless of an urban or rural setting, when dry/wet deposition was not considered. When dry/wet deposition was considered, the difference in air concentration was less than 10%, 20%, and 67% within a distance of 3,000, 10,000, and 80,000 m, respectively. RESRAD-OFFSITE was benchmarked with ISCLT3 only when dry/wet deposition was not considered. For a rural setting, good agreement was observed; for an urban setting, however, the difference ranged from 9.5% to 109% depending on downwind distance. Benchmarking of RESRAD-OFFSITE with ISCLT3 considering dry/wet deposition was not conducted because ISCLT3 uses a different approach with significantly different input data requirements. The causes of the differences in air concentrations were investigated and identified; these include differences in the approaches for area averaging and the use of different mathematical forms to estimate vertical dispersion as a function of downwind distance.

7.6   Benchmarking the Offsite Accumulation Models

The models to account for accumulation of radionuclides in soil at offsite locations due to atmospheric dust deposition and water irrigation were first developed during the International Atomic Energy Agency (IAEA) Biospheric Model Validation Study: Phase II (BIOMOVS II 1995, 1996) and were tested by participating in the Uranium Mill Tailings (UMT) Working Group's computer model comparison study. Developers of nine different computer models from different countries were involved in the study.

Exposure scenarios due to the long-term releases of contaminants from UMT were developed, and participants submitted predicted environmental media concentrations and radiation doses for comparison. Two receptors, located 2.5 and 7.5 km, respectively, from a hypothetical UMT pile (1,000 m × 500 m × 10 m), were concerned. The receptors planted lettuce and raised livestock for consumption. The pasturelands were not irrigated, but the lettuce fields were irrigated with either well water or lake water. The well water came from a well located 1,000 m from the down-gradient edge of the UMT pile. The lake water came from a lake 5 km from the UMT pile and recharged by a river situated 1,000 m from the down-gradient edge of the UMT pile and flowed through the lake.

The RESRAD predictions of radiation dose associated with the atmospheric release and dust deposition agreed well with those of other computer models. However, considerable differences were found in the predictions of radiation dose associated with the groundwater release and deposition of irrigation water. The associated peak and steady-state doses predicted by RESRAD agreed well with the predictions from most of the other models. Nevertheless, the breakthrough predicted by the RESRAD model occurred later, due to the differences in the formulation of the retardation factor. The predicted change in dose from the RESRAD model was sharper compared to the gradual change in other models, because other models accounted for longitudinal dispersion. Detailed information on this IAEA model comparison study is available (Gnanapragasam and Yu 1997; Gnanapragasam et al. 2000; BIOMOVS II 1995, 1996).

When the groundwater release and deposition models were implemented in RESRAD-OFFSITE after the BIOMOVS II exercise, it was modified to account for longitudinal dispersion. This modified groundwater transport model was benchmarked later with three multiple-pathway risk assessment models (see Section 7.7).

7.7   Benchmarking the Groundwater Transport Model

During BIOMOVS II, the models that account for accumulation of radionuclides in soil at offsite locations were developed, and the RESRAD-ONSITE modeling of groundwater transport was enhanced to allow for calculation of groundwater concentrations at offsite locations. The enhanced groundwater transport model was the early prototype of RESRAD-OFFSITE. The model comparison study based on the UMT exposure scenarios illuminated not only the differences in the soil accumulation model but also the differences in the groundwater transport model between the RESRAD code and the other participating codes.

Another benchmarking exercise that involved the enhanced groundwater transport model of RESRAD (now accounting for longitudinal dispersion) was the comparison study of multiple-pathway risk assessment models that spanned from 1997 to 2000 (Laniak et al. 1997; Mills et al. 1997; Whelan et al. 1999a, 1999b; Gnanapragasam et al. 2000). The other multiple-pathway models involved in the comparison were PRESTO, MMSOILS, and MEPAS. The comparison study considered the release of strontium-90 and uranium-234 from a contaminated soil source and required the prediction of concentrations of strontium-90, uranium-234, and the progeny of uranium-234 (e.g., thorium-230 and radium-226) in the groundwater aquifer as functions of time and distance. A scheme that allowed for better consideration of longitudinal dispersion and nuclide-specific transport rate for progeny radionuclides was developed and tested in this study.

In general, the concentration profiles predicted by PRESTO were quite different from those predicted by RESRAD, MEPAS, and MMSOILS, because PRESTO did not account for longitudinal dispersion. Among RESRAD, MEPAS, and MMSOILS, good agreement with the concentration profiles of strontium-90 and uranium-234 was observed, if the same formulation for the retardation factor was used. However, discrepancies were significant with the concentration profiles of thorium-230 and radium-226, because each code adopted different assumptions to simplify and solve the governing equations analytically. The predicted concentration profiles of thorium-230 and radium-226 from the three codes also deviated from those associated with the exact solutions, which were obtained by carrying out the complicated calculations pertaining to the mathematical solutions of the governing equations with the use of spreadsheets. When the transport zone was subdivided into smaller subzones according to the scheme developed during this study, the enhanced groundwater transport model of RESRAD

produced much improved results for thorium-230 and radium-226; in other words, they were in better agreement with the exact solutions (Gnanapragasam et al. 2000).

After this comparison study, the RESRAD-OFFSITE code was improved to allow the unsaturated and saturated zones to be subdivided, if chosen by the user; when this option is selected, the scheme to improve the predictions of progeny nuclide concentrations is automatically implemented. The implementation of the scheme in RESRAD-OFFSITE was successful, as tested by applying it to analyze the scenario considered in the comparison study of multiple-pathway risk assessment models. The produced groundwater concentration profiles for uranium-234, thorium-230, and radium-226 agreed well with the concentration profiles associated with the exact solutions (Yu et al. 2006).

7.8   Benchmarking the New Source Term Model

The RESRAD-OFFSITE code was originally designed to analyze potential radiation exposures from a contaminated soil source. From 2011 to 2013, under the sponsorship of NRC, the source term was expanded to include non-soil sources that could be containerized and protected from contact with soil water by engineering barriers. New features were added to allow consideration of delayed and distributed contact of the source material with water over time, and to select a release-controlled mechanism to estimate the release rates of radionuclides from the source material. In addition to the new features, transport analysis of the released radionuclides from the release point to the bottom of the contaminate zone was incorporated in the code. The new source term model is available in RESRAD-OFFSITE Versions 3.1 and 3.2.

The new source term model was benchmarked by comparing the calculated release rates of radionuclides across the bottom of the contaminated zone, from RESRAD-OFFSITE and from DUST-MS and GoldSim. Five different cases for which radionuclide release rates were calculated were developed; they had different sources of radionuclides, contaminated zone dimensions, and water infiltration rates. The benchmarking with DUST-MS involved radionuclide release rates based on uniform dissolution and equilibrium desorption. DUST-MS does not have provisions to consider a first-order rate-controlled mechanism. Overall, very good agreement was observed with the calculated release rates; the minor disagreement observed was attributed to numerical dispersion, which is typical for numerical analysis codes such as DUST-MS. Radionuclide release rates corresponding to the uniform dissolution, equilibrium desorption, and first-order rate-controlled mechanisms were compared when benchmarking RESRAD-OFFSITE with GoldSim. The results from both codes exhibited good agreement. The report Yu et al. 2013 documents these benchmarking activities and includes detailed discussions.

The source term model was further enhanced over the past 2 years, resulting in more flexibility and new features being incorporated, including up to nine time periods for specifying change in the releasable fraction and two more release-controlled mechanisms: diffusion-controlled and solubility-controlled (available in Version 4.0). Example applications of the available features were developed to evaluate the disposal of different types of wastes—activated metal, grouted and non-grouted transuranic wastes, and sealed sources—to a near surface trench.

Radionuclide release rates across the bottom of the trench were obtained with RESRAD-OFFSITE and DUST-MS. Comparison of the release rates showed that RESRAD-OFFSITE produced very close results to DUST-MS when the releases were controlled by uniform dissolution, instantaneous desorption (no adsorption to the waste materials), or solubility. When the releases were controlled by instantaneous desorption (with adsorption to the waste materials) and diffusion, the release rates of parent nuclide predicted by RESRAD-OFFSITE agreed well with those predicted by DUST-MS. However, the release rates of progeny nuclides

showed discrepancies. The actual cause of discrepancy is not clear, but it could be due to the different assumptions the two codes employ to handle the ingrowth of progenies during diffusion. Appendix M of this report provides detailed discussions on the example applications of the latest source term model, as well as a comparison of the release rates of radionuclides predicted by RESRAD-OFFSITE and by DUST-MS.

7.9   Other and Future Activities

The RESRAD-OFFSITE code, determined to be appropriate for simulating the behavior of naturally occurring radioactive material (NORM) in the environment, was used by the NORM Working Group under the IAEA Environmental Modeling for Radiation Safety (EMRAS) Program. The EMRAS NORM working group tested RESRAD-OFFSITE's ability to evaluate radiation exposures associated with NORM releases via different pathways, including the inhalation of radon and its progeny. Three sets of hypothetical scenarios were developed for the testing, involving a point source, an area source, and an area source plus a river. RESRAD-OFFSITE was selected to evaluate the two scenarios involving an area source. The area source was 1,000 m long, 1,000 m wide, and 10 m thick. RESRAD-OFFSITE calculated radiation doses incurred by a resident building a house at the center of the contaminated area and at a distance of 1,000 m from the edge of the area source. In addition to RESRAD-OFFSITE, DOSDIM + HYDRUS (used together to analyze the scenarios) were also selected for testing. According to the IAEA report for this exercise (IAEA 2007), the general agreement between DOSDIM and RESRAD-OFFSITE was good, considering the different modeling approaches adopted by the two codes.

Following the conclusion of the EMRAS program, IAEA carried out the Phase II of the EMRAS program, i.e., EMRAS II, in 2009. RESRAD-OFFSITE (as well as RESRAD-ONSITE) was extensively used by the EMRAS II Work Group 2 (WG2)—i.e., NORM and Nuclear Legacy Sites WG—participants in several scenarios. The benchmarking results are included in the EMRAS II WG 2 reports. The pre-publication report of the EMRAS II WG 2 report, entitled *Modelling Approaches for Management and Remediation at NORM and Nuclear Legacy Sites*, is available at the EMRAS II website (http://www-ns.iaea.org/projects/emras/emras2/default.asp).

After the EMRAS II, IAEA started a new program in 2012, i.e., Modelling and Data for Radiological Assessments (MODARIA) Program. RESRAD-OFFSITE was used in the MODARIA WG3 (NORM and Legacy Sites) for several benchmarking scenarios. The results of MODARIA WG3 are being reviewed and will be published at the IAEA MODARIA website (http://www-ns.iaea.org/projects/modaria/default.asp).

Currently, RESRAD-OFFSITE is used by the participants of the new IAEA MODARIA II Program's WG1 (Decision Making and NORM and Legacy Sites Working Group). The MODARIA II WG1 information is at the IAEA MODARIA II website (https://www-ns.iaea.org/projects/modaria/modaria2.asp). Testing, verification, and validation of RESRAD-OFFSITE will continue in the future when relevant datasets are available.

8 REFERENCES

Argonne (Argonne National Laboratory), 2017, *Argonne National Laboratory Quality Assurance Program Plan* (AQAPP), Lemont, IL.

Argonne, 2018a, *RESRAD Program Software Configuration Management Plan*, Environmental Science Division, Lemont, IL.

Argonne, 2018b, *RESRAD Program Software Quality Assurance Plan*, Environmental Science Division, Lemont, IL.

BIOMOVS II, 1995, *Long-Term Contaminant Migration and Impacts from Uranium Mill Tailings —Comparison of Computer Models Using a Hypothetical Dataset*, BIOMOVS II Technical Report No. 4, Biosphere Model Validation Study Steering Committee, Swedish Radiation Protection Institute, Stockholm, Sweden.

BIOMOVS II, 1996, *Long-Term Contaminant Migration and Impacts from Uranium Mill Tailings —Comparison of Computer Models Using a Realistic Dataset*, BIOMOVS II Technical Report No. 5, Biosphere Model Validation Study Steering Committee, Swedish Radiation Protection Institute, Stockholm, Sweden.

Cheng, J.-J., J.G. Droppo, E.R. Faillace, E. Gnanapragasam, R. Johns, G. Laniak, C. Lew, W. Mills, L. Owens, D.L. Strenge, J.F. Sutherland, G. Whelan, and C. Yu, 1995, *Benchmarking Analysis of Three Multimedia Models: RESRAD, MMSOILS, and MEPAS*, DOE/ORO-2033, U.S. Department of Energy, Washington, D.C.

DOE (U.S. Department of Energy), 2011, DOE Order 414.1D, Quality Assurance, April 25.

EPA (U.S. Environmental Protection Agency), 1995, *User's Guide for the Industrial Source Complex (ISC3) Dispersion Models, Vols. 1 & 2*, EPA-454/B-95-003a and -003b, prepared by Pacific Environmental Services, Inc., Research Triangle Park, N.C., for the EPA Office of Air Quality Planning and Standards, Research Triangle Park, North Carolina, September.

Gilbert, T.L., C. Yu, Y.C. Yuan, A.J. Zielen, M.J. Jusko, and A. Wallo, 1989, A Manual for Implementing Residual Radioactive Material Guidelines, ANL/ES-160, DOE/CH/8901, prepared by Energy and Environmental Systems Division, Argonne National Laboratory, Argonne, Illinois, Office of Remedial Action and Waste Technology.

Gnanapragasam, E., and C. Yu, 1997, *Analysis of BIOMOVS II Uranium Mill Tailings Scenario 1.07 with the RESRAD Computer Code*, ANL/EAD/TM-66, Argonne National Laboratory, Lemont, Ill.

Gnanapragasam, E., C. Yu et al., Comparison of Multimedia Model Predictions for a Contaminant Plume Migration Scenario, *J. Contaminant Hydrology*, 46(1-2): 17-38, 2000.

Halliburton NUS Corporation, 1994, *Verification of RESRAD. A Code for Implementing Residual Radioactive Material Guidelines, Version 5.03*, HNUS-ARPD-94-174, Gaithersburg, Maryland.

IAEA (International Atomic Energy Agency), 1996, Long Term Contaminant Migration and Impacts from Uranium Mill Tailings, *Comparison of Computer Models Using a Realistic Dataset*, BIOMOVS II Technical Report Number 5, Biosphere Model Validation Study II Program.

IAEA, 2007, *Modelling the Transfer of Radionuclides from Naturally Occurring Radioactive Material (NORM)*, report of the NORM Working Group of ERMAS II, Environmental Modelling for Radiation Safety II Program.

ICRP (International Commission on Radiological Protection), 1975, *Report of the Task Group on Reference Man, ICRP Publication 23*, a report by a Task Group of Committee 2 of the International Commission on Radiological Protection, adopted by the Commission in October 1974, Pergamon Press, New York, N.Y.

ICRP, 1979, *Limits for Intakes of Radionuclides by Workers*, ICRP Publication 30, Part 1, a report of Committee 2 of the International Commission on Radiological Protection, adopted by the Commission in July 1978, Annals of the ICRP, Pergamon Press, New York, N.Y.

ICRP, 1980, *Limits for Intakes of Radionuclides by Workers*, ICRP Publication 30, Part 2, a report of Committee 2 of the International Commission on Radiological Protection, adopted by the Commission in July 1978, Annals of the ICRP, Pergamon Press, New York, N.Y.

ICRP, 1981, *Limits for Intakes of Radionuclides by Workers*, ICRP Publication 30, Part 3, a report of Committee 2 of the International Commission on Radiological Protection, adopted by the Commission in July 1978, Annals of the ICRP, Pergamon Press, New York, N.Y.

ICRP, 1982, *Limits for Intakes of Radionuclides by Workers*, ICRP Publication 30, Index, Annals of the ICRP, Pergamon Press, New York, N.Y.

Laniak, G.F., J.G. Droppo, E.R. Faillace, E.K. Gnanapragasam, W.B. Mills, D.L. Strenge, G.Whelan, and C. Yu, 1997, "An Overview of the Multimedia Benchmarking Analysis for ThreeRisk Assessment Models: RESRAD, MMSOILS, and MEPAS," *Risk Analysis* 17,203–214.

M Mills, W.B., J.J. Cheng, J.G. Droppo, Jr., E.R. Faillace, E.K. Gnanapragasam, R.A. Johns, G.F. Laniak, C.S. Lew, D.L. Strenge, J.F. Sutherland, G. Whelan, and C. Yu, 1997, "Multimedia Benchmarking Analysis for Three Risk Assessment Models: RESRAD, MMSOILS, and MEPAS," *Risk Analysis* 17(2):187–201.

Parks, B.S., 1992, *User's Guide for CAP88-PC, Version 1.0*, EPA 402-B-92-001, prepared by U.S. Environmental Protection Agency, Office of Radiation Programs, Las Vegas, Nevada, for the U.S. Department of Energy, March.

Shen, H.W., and P.Y. Julien, 1993, "Erosion and Sediment Transport" in *Handbook of Hydrology*, D.R. Maidment (ed.), McGraw-Hill Inc.

Schmidt, D.W., K.L. Banovac, J.T. Buckley, D.W. Esh, R.L. Johnson, J.J. Kottan, C.A. McKenney, T.G. McLaughlin, and S. Schneider, 2006, *Consolidated NMSSDecommissioning Guidance*, NUREG-1757, Vol. 2, Rev. 1, U.S. Nuclear RegulatoryCommission, Washington, D.C., September.

Sullivan, T.M., 2006, *DUSTMS-D Disposal Unit Source Term−Multiple Species-Distributed Failure Data Input Guide*, BNL-75554-2006, Brookhaven National Laboratory, Upton, New York, January.

Travers, W.D., 2003, "Results of Evaluations for Realistic Exposure Scenarios," Attachment 6 to Results of the License Termination Rule Analysis, Paper SECY-03-0069, U.S. Nuclear Regulatory Commission, Washington, D.C., May.

Whelan, G., J.P. McDonald, E.K. Gnanapragasam, G.F. Laniak, C.S. Lew, W.B. Mills, and C. Yu, 1999a, "Benchmarking of the Saturated-Zone Module Associated with Three Risk Assessment Models: RESRAD, MMSOILS, and MEPAS," *Environmental Engineering Science* 16(1):67−80.

Whelan, G., J.P. McDonald, E.K. Gnanapragasam, G.F. Laniak, C.S. Lew, W.B. Mills, and C. Yu, 1999b, "Benchmarking of the Vadose-Zone Module Associated with Three Risk Assessment Models: RESRAD, MMSOILS, and MEPAS," *Environmental Engineering Science* 16(1):81−91.

Yu, C., A.J. Zielen, J.-J. Cheng, Y.C. Yuan, L.G. Jones, D.J. LePoire, Y.Y. Wang, C.O. Loureiro, E. Gnanapragasam, E. Faillace, A. Wallo III, W.A. Williams, and H. Peterson, Jr., 1993, *Manual for Implementing Residual Radioactive Material Guidelines Using RESRAD, Version 5.0*, Working Draft For Comment, ANL/EAD/LD-2, Argonne National Laboratory, Argonne, Illinois.

Yu, C., A.J. Zielen, J.-J. Cheng, D.J. LePoire, E. Gnanapragasam, S. Kamboj, J. Arnish, A. Wallo III, W.A. Williams, and H. Peterson, 2001, *User's Manual for RESRAD Version 6*, ANL/EAD-4, Environmental Assessment Division, Argonne National Laboratory, Lemont, Illinois.

Yu, C., D.J. LePoire, J-J. Cheng, E. Gnanapragasam, S. Kamboj, J. Arnish, B.M. Biwer, A.J. Zielen, W.A. Williams, A. Wallo III, and H.T. Peterson, Jr., 2003, *User's Manual for RESRAD-BUILD Version 3*, ANL/EAD/03-1, June.

Yu, C., E. Gnanapragasam, J.-J. Cheng, and B. Biwer, 2006, *Benchmarking of RESRAD-OFFSITE: Transition from RESRAD (onsite) to RESRAD-OFFSITE and Comparison of the RESRAD-OFFSITE Predictions with Peer Codes*, ANL/EVS/TM/06-3, DOE/EH-0708, Argonne National Laboratory, Lemont, Illinois, May.

Yu, C., E.K. Gnanapragasam, J.-J. Cheng, S. Kamboj, B.M. Biwer, and D. J. LePoire, 2011, *Verification of RESRAD-OFFSITE*, NUREG/CR-7038, ANL-10/27, Argonne National Laboratory, Lemont, Illinois, February.

Yu, C., E.K. Gnanapragasam, J.-J. Cheng, S. Kamboj, and S.Y. Chen, 2013, *New Source Term Model for the RESRAD-OFFSITE Code Version 3*, NUREG/CR-7127, ANL/EVS/TM/11-5, Argonne National Laboratory, Lemont, Illinois, June.

APPENDIX A:
RADIONUCLIDE TRANSFORMATION DATABASES, ASSOCIATED DOSE FACTOR LIBRARIES, AND DOSE ESTIMATION METHODOLOGY

This appendix discusses the radionuclide transformation databases, dose factor libraries, and dose estimation methodology in the RESRAD-OFFSITE code.

A.1   Radionuclide Transformation Databases in RESRAD-OFFSITE

The user has an option to select the International Commission of Radiological Protection (ICRP) Publication 107-based or ICRP Publication 38-based radionuclide transformation database. Some radionuclides in the transformation database have a long decay chain with multiple progeny. The code first generates all the threads in the decay chain. A thread is defined as a unique decay sequence starting with the selected radionuclide and continuing to the last radionuclide in the decay chain that decays to a stable isotope. One way of performing calculations is to do a separate calculation for each thread and combine the contributions of each thread at the end. In general, this process will take a very long time. RESRAD-OFFSITE uses the concept of principal and associated radionuclides to reduce computation time. In RESRAD-OFFSITE, threads that only include short-lived progeny (less than cutoff half-life) are combined in a single thread (condensed thread). Section E.4 has examples of threads and condensed threads in the long decay chains.

As mentioned in Chapter 4, the user can select a cutoff half-life from the values in the list (180, 30, 7, or 1 day[s]) or type in a value that is not less than 10 minutes. Radionuclides in the decay chain with half-lives greater than the cutoff half-life are considered principal radionuclides, and those with half-lives less than the cutoff half-life are considered associated radionuclides. The associated radionuclides are assumed to be in secular equilibrium with the preceding principal radionuclide in the same decay chain. The dose contributions of associated radionuclides are included in that of the preceding principal radionuclide, by adding their dose coefficients to the dose coefficient of the preceding principal radionuclide and then using the summed dose coefficient to calculate internal dose.

RESRAD-OFFSITE explicitly models the movement and concentration of the principal radionuclide in the environment. Some of the decay threads of a radionuclide will be identical when viewed from the perspective of the principal radionuclides. The threads with the same sequence of principal radionuclides can be combined into one condensed thread. This reduces computation time. Chapter 5 has examples of threads and condensed treads.

A.1.1   ICRP Publication 38 Database

ICRP Publication 38 (ICRP 38) (ICRP 1983) contains radionuclide decay data for 838 nuclides. For each radionuclide, the emissions are given by type, energy, and yield. The decay modes include alpha decay, beta decay (beta plus and beta minus), electron capture, isomeric transition, and spontaneous fission.

Table A.1-1 lists principal and associated radionuclides condensed thread fractions used in dose or risk calculations for the ICRP-38 radionuclide transformation database using a 30 day half-life cutoff.

Table A.1-1 Principal and Associated Radionuclides with a Cutoff Half-Life of 30 Day in ICRP-38 Database

Principal Radionuclide[a]		Associated Decay Chain[b]	Terminal Nuclide or Radionuclide[c]		
Species	Half-Life (yr)		Species	Half-Life (yr)	Fraction
Ac-227+D	2.177E+01	(Th-227 9.8620E-01), Ra-223, Rn-219, Po-215, Pb-211, Bi-211, (Tl-207 9.9720E-01), (Po-211 2.8000E-03), (Fr-223 1.3800E-02)	Pb-207	*	
Ag-105	1.123E-01	—[d]	Pd-105	*	
Ag-108m+D	1.270E+02	(Ag-108 8.9000E-02)	Pd-108, Cd-108	*	
Ag-110m+D	6.842E-01	(Ag-110 1.3300E-02)	Cd-110, Pd-110	*	
Al-26	7.160E+05	—	Mg-26	*	
Am-241	4.322E+02	—	Np-237	2.140E+06	
Am-242m+D	1.520E+02	Am-242	Cm-242	4.457E-01	8.231E-01
Am-242m+D1	1.520E+02	Am-242	Pu-242	3.763E+05	1.722E-01
Am-242m+D2	1.520E+02	Np-238	Pu-238	8.774E+01	4.760E-03
Am-243+D	7.380E+03	—	Pu-239	2.407E+04	
As-73	2.198E-01	—	Ge-73	*	
Au-195	5.010E-01	—	Pt-195	*	
Ba-133	1.074E+01	—	Cs-133	*	
Be-10	1.600E+06	—	B-10	*	
Be-7	1.459E-01	—	Li-7	*	
Bi-207	3.800E+01	—	Pb-207	*	
Bi-210m+D	3.000E+06	Tl-206	Pb-206	*	
Bk-247	1.380E+03	—	Am-243m+D	7.380E+03	
Bk-249	8.761E-01	—	SF		4.700E-10
Bk-249	8.761E-01	—	Cf-249	3.506E+02	1.000E+00
Bk-249+D	8.761E-01	—	Cm-245	8.500E+03	1.450E-05
C-14	5.730E+03	—	N-14	*	
Ca-41	1.400E+05	—	K-41	*	
Ca-45	4.463E-01	—	Sc-45	*	
Cd-109	1.270E+00	—	Ag-109	*	
Cd-113	9.300E+15	—	In-113	*	
Cd-113m	1.360E+01	—	In-113	*	
Cd-115m	1.221E-01	—	In-115	5.100E+15	

Table A.1-1 Principal and Associated Radionuclides with a Cutoff Half-Life of 30 Day in ICRP-38 Database (Cont.)

Principal Radionuclide[a]		Associated Decay Chain[b]	Terminal Nuclide or Radionuclide[c]		
Species	Half-Life (yr)		Species	Half-Life (yr)	Fraction
Ce-139	3.769E-01	—	La-139	*	
Ce-141	8.898E-02	—	Pr-141	*	
Ce-144+D	7.784E-01	(Pr-144m 0.0178), Pr-144	Nd-144	*	
Cf-248	9.131E-01	—	SF		2.900E-05
Cf-248	9.131E-01	—	Cm-244	1.811E+01	1.000E+00
Cf-249	3.506E+02	—	SF		5.200E-09
Cf-249	3.506E+02	—	Cm-245	8.500E+03	1.000E+00
Cf-250	1.308E+01	—	SF		7.700E-04
Cf-250	1.308E+01	—	Cm-246	4.730E+03	9.992E-01
Cf-251	8.980E+02	—	Cm-247+D	1.560E+07	
Cf-252	2.638E+00	—	SF		3.092E-02
Cf-252	2.638E+00	—	Cm-248	3.390E+05	9.691E-01
Cl-36	3.010E+05	—	Ar-36, S-36	*	
Cm-241	8.980E-02	—	Am-241	4.322E+02	9.900E-01
Cm-241	8.980E-02	—	Pu-237	1.240E-01	1.000E-02
Cm-242	4.457E-01	—	SF		6.800E-08
Cm-242	4.457E-01	—	Pu-238	8.774E+01	1.000E+00
Cm-243	2.850E+01	—	Am-243	7.380E+03	2.400E-03
Cm-243	2.850E+01	—	Pu-239	2.407E+04	9.976E-01
Cm-244	1.811E+01	—	SF		1.350E-06
Cm-244	1.811E+01	—	Pu-240	6.537E+03	1.000E+00
Cm-245	8.500E+03	—	Pu-241	1.440E+01	1.000E+00
Cm-246	4.730E+03	—	SF		2.614E-04
Cm-246	4.730E+03	—	Pu-242	3.763E+05	9.997E-01
Cm-247+D	1.560E+07	Pu-243	Am-243+D	7.380E+03	
Cm-248	3.390E+05	—	SF		8.260E-02
Cm-248	3.390E+05	—	Pu-244	8.260E+07	9.174E-01
Co-56	2.156E-01	—	Fe-56	*	
Co-57	7.417E-01	—	Fe-57	*	
Co-58	1.938E-01	—	Fe-58	*	
Co-60	5.271E+00	—	Ni-60	*	
Cs-134	2.062E+00	—	Ba-134, Xe-134	*	
Cs-135	2.300E+06	—	Ba-135	*	
Cs-137+D	3.000E+01	(Ba-137m 0.946)	Ba-137	*	
Dy-159	3.953E-01	—	Tb-159	*	
Es-254+D	7.548E-01	Bk250	Cf-250	1.308E+01	1.000E+00
Eu-148	1.492E-01	—	Sm-148	*	
Eu-148	1.492E-01	—	Pm-144	9.938E-01	9.400E-09
Eu-149	2.549E-01	—	Sm-149	*	
Eu-150b	3.420E+01	—	Sm-150	*	

Table A.1-1 Principal and Associated Radionuclides with a Cutoff Half-Life of 30 Day in ICRP-38 Database (Cont.)

Principal Radionuclide[a]			Terminal Nuclide or Radionuclide[c]		
Species	Half-Life (yr)	Associated Decay Chain[b]	Species	Half-Life (yr)	Fraction
Eu-152	1.333E+01	—	Sm-152		7.208E-01
Eu-152	1.333E+01	—	Gd-152	1.080E+14	2.792E-01
Eu-154	8.800E+00	—	Gd-154, Sm-154	*	
Eu-155	4.960E+00	—	Gd-155	*	
Fe-55	2.700E+00	—	Mn-55	*	
Fe-59	1.219E-01	—	Co-59	*	
Fe-60+D	1.000E+05	Co-60m	Ni-60	*	2.500E-03
Fe-60+D1	1.000E+05	Co-60m	Co-60	5.271E+00	9.975E-01
Fm-257+D	2.752E-01	Cf-253, Es-253	SF		8.673E-08
Fm-257+D1	2.752E-01	Cf-253, (Es-253 9.9690E-01), (Cm-249 3.1000E-03)	Bk-249		1.000E+00
Gd-146+D	1.322E-01	Eu-146	Sm-146	1.030E+08	
Gd-148	9.300E+01	—	Sm-144	*	
Gd-151	3.285E-01	—	Eu-151	*	
Gd-151	3.285E-01	—	Sm147	0.000E+00	
Gd-152	1.080E+14	—	Sm-148	*	
Gd-153	6.626E-01	—	Eu-153	*	
Ge-68+D	7.885E-01	Ga-68	Zn-68	*	
H-3	1.235E+01	—	He-3	*	
Hf-172+D	1.870E+00	Lu-172	Yb-172	*	
Hf-175	1.917E-01	—	Lu-175	*	
Hf-178m	3.100E+01	—	Hf-178	*	
Hf-181	1.161E-01	—	Ta-181	*	
Hf-182	9.000E+06	—	Ta-182	3.149E-01	
Hg-194+D	2.600E+02	Au-194	Pt-194	*	
Hg-203	1.276E-01	—	Tl-203	*	
Ho-166m	1.200E+03	—	Er-166	*	
I-125	1.647E-01	—	Te-125	*	
I-129	1.570E+07	—	Xe-129	*	
In-114m+D	1.356E-01	(In-114 0.957)	Cd-114, Sn-114	*	
In-115	5.100E+15	—	Sn-115	*	
Ir-192	2.027E-01	—	Os-192, Pt-192	*	
Ir-192m	2.410E+02	—	Ir-192	2.027E-01	
Ir-194m	4.682E-01	—	Pt-194	*	
K-40	1.280E+09	—	Ca-40, Ar-40	*	
La-137	6.000E+04	—	Ba-137	*	

Table A.1-1 Principal and Associated Radionuclides with a Cutoff Half-Life of 30 Day in ICRP-38 Database (Cont.)

Principal Radionuclide[a]			Terminal Nuclide or Radionuclide[c]		
Species	Half-Life (yr)	Associated Decay Chain[b]	Species	Half-Life (yr)	Fraction
La-138	1.350E+11	—	Ba-138, Ce-138	*	
Lu-173	1.370E+00	—	Yb-173	*	
Lu-174	3.310E+00	—	Yb-174	*	
Lu-174m	3.888E-01	—	Yb-174	*	7.000E-03
Lu-174m	3.888E-01	—	Lu-174	3.310E+00	9.930E-01
Lu-176	3.600E+10	—	Hf-176	*	
Lu-177m+D	4.405E-01	(Lu-177 0.21)	Hf-177	*	
Md-258	1.506E-01		Es-254	7.548E-01	1.000E+00
Mn-53	3.700E+06	—	Cr-53	*	
Mn-54	8.556E-01	—	Cr-54	*	
Mo-93	3.500E+03	—	Nb-93	*	
Na-22	2.602E+00	—	Ne-22	*	
Nb-93m	1.360E+01	—	Nb-93	*	
Nb-94	2.030E+04	—	Mo-94	*	
Nb-95	9.624E-02	—	Mo-95	*	
Ni-59	7.500E+04	—	Co-59	*	
Ni-63	9.600E+01	—	Cu-63	*	
Np-235	1.084E+00	—	U-235	7.038E+08	1.000E+00
Np-235	1.084E+00	—	Pa-231	3.276E+04	1.400E-05
Np-236a	1.150E+05	—	U-236		9.110E-01
Np-236a	1.150E+05	—	Pu-236	2.851E+00	8.900E-02
Np-237+D	2.140E+06	Pa-233	U-233	1.585E+05	
Os-185	2.574E-01	—	Re-185	*	
Os-194+D	6.000E+00	Ir-194	Pt-194	*	
Pa-231	3.276E+04	—	Ac-227+D	2.177E+01	
Pb-202+D	3.000E+05	Tl-202	Hg-202	*	
Pb-205	1.430E+07	—	Tl-205	*	
Pb-210+D	2.230E+01	Bi-210	Po-210	3.789E-01	
Pd-107	6.500E+06	—	Ag-107	*	
Pm-143	7.255E-01	—	Nd-143	*	
Pm-144	9.938E-01	—	Nd-144	*	
Pm-145	1.770E+01	—	Nd-145	*	
Pm-146	5.530E+00	—	Nd-146	*	6.410E-01
Pm-146	5.530E+00	—	Sm-146	1.030E+08	3.590E-01
Pm-147	2.623E+00	—	Sm-147	1.060E+11	
Pm-148m+D	1.131E-01	(Pm-148 0.046)	Sm-148	*	
Po-210	3.789E-01	—	Pb-206	*	
Pt-193	5.000E+01	—	Ir-193	*	
Pu-236	2.851E+00	—	SF		8.100E-10

Table A.1-1 Principal and Associated Radionuclides with a Cutoff Half-Life of 30 Day in ICRP-38 Database (Cont.)

Principal Radionuclide[a]			Terminal Nuclide or Radionuclide[c]		
Species	Half-Life (yr)	Associated Decay Chain[b]	Species	Half-Life (yr)	Fraction
Pu-236	2.851E+00	—	U-232	7.200E+01	1.000E+00
Pu-237	1.240E-01	—	Np-237+D	2.140E+06	1.000E+00
Pu-237	1.240E-01	—	U-233	1.585E+05	5.000E-05
Pu-238	8.774E+01	—	SF		1.840E-09
Pu-238	8.774E+01	—	U-234	2.445E+05	1.000E+00
Pu-239	2.407E+04	—	U-235	7.038E+08	
Pu-240	6.537E+03	—	SF		4.950E-08
Pu-240	6.537E+03	—	U-236	2.342E+07	1.000E+00
Pu-241	1.440E+01	—	Am-241	4.322E+02	1.000E+00
Pu-241+D	1.440E+01	(U-237 0.0000245)	Np-237	2.140E+06	2.450E-05
Pu-242	3.763E+05	—	SF		5.500E-06
Pu-242	3.763E+05	—			
Pu-242	3.763E+05	—	U-238	4.468E+09	1.000E+00
Pu-244	8.260E+07	—	SF		1.250E-03
Pu-244+D	8.260E+07	(U-240 0.9988), (Np-240m 0.9988)	Pu-240	6.537E+03	9.988E-01
Ra-226+D	1.600E+03	Rn-222,Po-218, (Pb-214 9.9980E-01), Bi-214, (Po-214 9.9980E-01), (Tl-210 2.0000E-04), (At-218 2.0000E-04)	Pb-210	2.230E+01	
Ra-228+D	5.750E+00	Ac-228	Th-228+D	1.913E+00	
Rb-83+D	2.360E-01	(Kr-83m 0.76199)	Kr-83	*	
Rb-84	8.972E-02	—	Sr-84, Kr-84	*	
Rb-87	4.700E+10	—	Sr-87	*	
Re-184	1.040E-01	—	W-184	*	
Re-184m	4.517E-01	—	W-184	*	2.530E-01
Re-184m	4.517E-01	—	Re-184	1.040E-01	7.470E-01
Re-186m+D	2.000E+05	Re-186	W-186, Os-186	*	
Re-187	5.000E+10	—	Os-187	*	
Rh-101	3.200E+00	—	Ru-101	*	
Rh-102	2.900E+00	—	Ru-102	*	
Rh-102m	5.667E-01	—	Ru-102, Pd-102	*	9.500E-01
Rh-102m	5.667E-01	—	Rh-102	2.900E+00	5.000E-02
Ru-103+D	1.075E-01	(Rh-103m 0.997)	Rh-103	*	
Ru-106+D	1.008E+00	Rh-106	Pd-106	*	
S-35	2.394E-01	—	Cl-35	*	
Sb-124	1.648E-01	—	Te-124	*	

Table A.1-1 Principal and Associated Radionuclides with a Cutoff Half-Life of 30 Day in ICRP-38 Database (Cont.)

| Principal Radionuclide[a] | | Associated Decay Chain[b] | Terminal Nuclide or Radionuclide[c] | | |
Species	Half-Life (yr)		Species	Half-Life (yr)	Fraction
Sb-125	2.770E+00	—	Te-125	*	7.720E-01
Sb-125	2.770E+00	—	Te-125m	1.588E-01	2.280E-01
Sc-46	2.295E-01	—	Ti-46	*	
Se-75	3.280E-01	—	As-75	*	
Se-79	6.500E+04	—	Br-79	*	
Si-32+D	4.500E+02	P-32	S-32	*	
Sm-145	9.309E-01	—	Pm-145	1.770E+01	
Sm-146	1.030E+08	—	Nd-142	*	
Sm-147	1.060E+11	—	Nd-143	*	
Sm-151	9.000E+01	—	Eu-151	*	
Sn-113+D	3.151E-01	In-113m	In-113	*	
Sn-119m	8.022E-01	—	Sn-119	*	
Sn-121m+D	5.500E+01	(Sn-121 0.776)	Sb-121	*	
Sn-123	3.537E-01	—	Sb-123	*	
Sn-126+D	1.000E+05	Sb-126m, (Sb-126 0.14)	Te-126	*	
Sr-85	1.775E-01	—	Rb-85	*	
Sr-89	1.383E-01	—	Y-89	*	
Sr-90+D	2.912E+01	Y-90	Zr-90	*	
Ta-179	1.820E+00	—	Hf-179	*	
Ta-180	1.000E+13	—	W-180	*	
Ta-182	3.149E-01	—	W-182	*	
Tb-157	1.500E+02	—	Gd-157	*	
Tb-158	1.500E+02	—	Gd-158, Dy-158	*	
Tb-160	1.979E-01	—	Dy-160	*	
Tc-95m+D	1.670E-01	(Tc-95 0.04)	Mo-95	*	
Tc-97	2.600E+06	—	Mo-97	*	
Tc-97m	2.382E-01	—	Tc-97	2.600E+06	
Tc-98	4.200E+06	—	Ru-98	*	
Tc-99	2.130E+05	—	Ru-99	*	
Te-121m+D	4.216E-01	(Te-121 0.886)	Sb-121	*	
Te-123	1.000E+13	—	Sb-123	*	
Te-123m	3.277E-01	—	Te-123	1.000E+13	
Te-125m	1.588E-01	—	Te-125	*	
Te-127m+D	2.984E-01	(Te-127 0.976)	I-127	*	
Te-129m+D	9.199E-02	(Te-129 0.35)	I-129	1.570E+07	
Th-228+D	1.913E+00	Ra-224, Rn-220, Po-216, Pb-212, Bi-212, (Po-212 0.6407), (Tl-208 0.3593)	Pb-208	*	

Table A.1-1 Principal and Associated Radionuclides with a Cutoff Half-Life of 30 Day in ICRP-38 Database (Cont.)

Principal Radionuclide[a]			Terminal Nuclide or Radionuclide[c]		
Species	Half-Life (yr)	Associated Decay Chain[b]	Species	Half-Life (yr)	Fraction
Th-229+D	7.340E+03	Ra-225, Ac-225, Fr-221, At-217, Bi-213, (Po-213 0.9784), (Tl-209 0.0216), Pb-209	Bi-209	*	
Th-230	7.700E+04	—	Ra-226+D	1.600E+03	
Th-232	1.405E+10	—	Ra-228+D	5.750E+00	
Ti-44+D	4.730E+01	Sc-44	Ca-44	*	
Tl-204	3.779E+00	—	Pb-204, Hg-204	*	
Tm-170	3.521E-01	—	Er-170, Yb-170	*	
Tm-171	1.920E+00	—	Yb-171	*	
U-232	7.200E+01	—	Th-228+D	1.913E+00	
U-233	1.585E+05	—	Th-229+D	7.340E+03	
U-234	2.445E+05	—	Th-230	7.700E+04	
U-235+D	7.038E+08	—	Pa-231	3.276E+04	
U-236	2.342E+07	—	Th-232	1.405E+10	
U-238	4.468E+09	—	SF		5.400E-05
U-238+D	4.468E+09	Th-234, (Pa-234m 0.998), (Pa-234 0.0033)	U-234	2.445E+05	1
V-49	9.035E-01	—	Ti-49	*	
W-181	3.318E-01	—	Ta-181	*	
W-185	2.056E-01	—	Re-185	*	
W-188+D	1.900E-01	Re-188	Os-188	*	
Y-88	2.920E-01	—	Sr-88	*	
Y-91	1.602E-01	—	Zr-91	*	
Yb-169	8.764E-02	—	Tm-169	*	
Zn-65	6.678E-01	—	Cu-65	*	
Zr-88	2.283E-01	—	Y-88	2.920E-01	
Zr-93	1.530E+06	—	Nb-93m	1.360E+01	
Zr-95+D	1.752E-01	(Nb-95m 0.007)	Nb-95	9.624E-02	

[a] Radionuclides with half-lives greater than 30 days. If short-lived progeny are involved, the +D symbol is added along with the radionuclide name (e.g., Ac-227+D). To distinguish between different associated radionuclides or terminal radionuclides, different +D (for example +D, +D1, etc.) indicators are used (Appendix E.4).

[b] The associated progeny with half-lives shorter than 30 days are listed. If a branching fraction is anything other than 1, it is listed along with the radionuclide in the bracket.

Footnotes continued on next page.

^c   The principal radionuclide or stable nuclide that terminates an associated decay chain. Stable nuclides are indicated by an asterisk (*) in place of the half-life. If a radionuclide has spontaneous fission, it is indicated by SF. If the branching fraction is anything other than 1, the fraction is listed.

[d]   Indicates there is no associated radionuclide.

A.1.2   ICRP Publication 107 Database

ICRP Publication 107 (ICRP 107) includes radionuclide transformation data for 1,252 nuclides. For some isomers, the notation in ICRP 107 has changed from ICRP-38 notations. In ICRP 107, isomers of energy above the ground state are identified by appending "m," "n," "p," or "q" to the mass number, whereas the information during the preparation of ICRP 38 was insufficient to identify the ground and excited states of a few radionuclides. Several radionuclides that did not have sufficient information were assigned an *ad-hoc* designation based on their physical half-life. Table A.1-2 shows the correspondence between the ICRP-38 and ICRP-107 isomers. Some radionuclides in ICRP 38 are not in the ICRP-107 database (see footnote b in Table A.1-2). If any of the radionuclides not in ICRP 107 were selected using the ICRP-38 radionuclide transformation data and if the transformation database is later changed to ICRP 107, an alert message will be displayed and these nuclides will be deleted from the analysis. Principal and associated radionuclide condensed thread fractions used in dose or risk calculations for the ICRP-107 radionuclide database are listed in Table A.1-3 for a 30-day half-life cutoff.

Table A.1-2   Identification of ICRP-38 and ICRP 107 Isomers

ICRP-38 Notation[a,b]		ICRP-107 Notation[a]	
ICRP 38[c]	$T_{1/2}$	ICRP 107	$T_{1/2}$
Nb-89a	66 m	Nb-89m	66 m
Nb-89b	122 m	Nb-89	2.03 h
Nb-98	51.5 m	Nb-98m	51.3 m
Rh-102	2.9 y	Rh-102m	3.742 y
Rh-102m	207 d	Rh-102	207 d
In-110a	69.1 m	In-110m	69.1 m
In-110b	4.9 h	In-110	4.9 h
Sb-120a	15.89 m	Sb-120	15.89 m
Sb-120b	5.76 d	Sb-120m	5.76 d
Sb-124n	20.2 m	Sb-124n[d]	20.2 m
Sb-128a	10.4 m	Sb-128m	10.4 m
Sb-128b	9.01 h	Sb-128	9.01 h
Eu-150a	12.62 h	Eu-150m	12.8 h
Eu-150b	34.2 y	Eu-150	36.9 y
Tb-156n	5.0 h	Tb-156n[d]	5.3 h
Tb-156m	24.4 h	Tb-156m	24.4 h

Table A.1-2 Identification of ICRP-38 and ICRP 107 Isomers (Cont.)

ICRP-38 Notation[a,b]		ICRP-107 Notation[a]	
ICRP 38[c]	$T_{1/2}$	ICRP 107	$T_{1/2}$
Ta-178a	9.31 m	Ta-178	9.31 m
Ta-178b	2.2 h	Ta-178m	2.36 h
Ta-180m	8.1 h	Ta-180	8.152 h
Ta-180	1.0E13 y	Ta-180m	—[e]
Re-182a	12.7 h	Re-182m	12.7 h
Re-182b	64.0 h	Re-182	64.0 h
Ir-186b	1.75 h	Ir-186m	1.92 h
Ir-186a	15.8 h	Ir-186	16.64 h
Ir-190m	1.2 h	Ir-190m	1.120 h
Ir-190n	3.1 h	Ir-190n	3.087 h
Ir-192m	241 y	Ir-192n[d]	241 y
Np-236b	22.5 h	Np-236m	22.5 h
Np-236a	115E3 y	Np-236	1.54E5 y
Es-250	2.1 h	Es-250m	2.22 h

[a] Half-life ($T_{1/2}$) units: m—minute(s); h—hour(s); d—day(s); y—year(s).

[b] Nb-97m (60 s), W-176 (2.3 h), Re-177 (14 m), Ta-180m (8.1 h), Md-257 (5.2 h), and Md-258 (55 d) were in ICRP 38 ($T_{1/2}$ values from ICRP-38) but are not in ICRP 107.

[c] Ad-hoc notation "a" and "b" used in ICRP-38 database.

[d] Metastable state of higher energy than the first metastable state.

[e] Ta-180m, $T_{1/2}$ in excess of 1.2E15 y; decay has not been observed (i.e., observationally stable).

Table A.1-3 Principal and Associated Radionuclides with a Cutoff Half-Life of 30 Days in ICRP-107 Database

Principal Radionuclide[a]	Half-Life (yr)	Associated Decay Chain[b]	Terminal Nuclide or Radionuclide[c]		
			Species	Half-Life (yr)	Fraction
Ac-227+D	2.177E+01	(Th-227 9.8620E-01) (Ra-223 1.0000E+00) (Rn-219 1.0000E+00) Po-215 Pb-211 Bi-211 (Tl-207 9.9724E-01) (Po-211 2.7600E-03) (Fr-223 1.3800E-02) (At-219 8.2800E-07) (Bi-215 8.2800E-07)	Pb-207	*	
Ag-105	1.130E-01	—[d]	Pd-105	*	
Ag-108m+D	4.180E+02	(Ag-108 8.7000E-02)	Pd-108, Cd-108	*	
Ag-110m+D	6.838E-01	(Ag-110 1.3600E-02)	Cd-110, Pd-110	*	
Al-26	7.170E+05	—	Mg-26	*	
Am-241	4.322E+02	—	Np-237	2.144E+06	
Am-242m+D	1.410E+02	Am-242	Cm-242	4.457E-01	0.823278
Am-242m+D1	1.410E+02	Am-242	Pu-242	3.750E+05	0.172221
Am-242m+D2	1.410E+02	Np-238	Pu-238	8.770E+01	0.0045
Am-243+D	7.370E+03	Np-239	Pu-239	2.411E+04	
As-73	2.198E-01	—	Ge-73	*	
Au-195	5.095E-01	—	Pt-195	*	
Ba-133	1.052E+01	—	Cs-133	*	
Be-10	1.510E+06	—	B-10	*	
Be-7	1.457E-01	—	Li-7	*	
Bi-207	3.290E+01	—	Pb-207	*	
Bi-208	3.680E+05	—	Pb-208	*	
Bi-210m+D	3.040E+06	Tl-206	Pb-206	*	
Bk-247	1.380E+03	—	Am-243m	7.370E+03	
Bk-249	9.035E-01	—	Cf-249	3.510E+02	0.999986
Bk-249+D	9.035E-01	Am-245	Cm-245	8.500E+03	1.45E-05
C-14	5.700E+03	—	N-14	*	
Ca-41	1.020E+05	—	K-41	*	
Ca-45	4.454E-01	—	Sc-45	*	
Cd-109	1.263E+00	—	Ag-109	*	
Cd-113	7.700E+15	—	In-113	*	
Cd-113m	1.410E+01	—	In-113	*	0.9986
Cd-113m	1.410E+01	—	Cd-113	7.700E+15	0.0014
Cd-115m+D	1.221E-01	In-115m	In-115	4.410E+14	5.29E-06
Cd-115m+D1	1.221E-01	(In-115m 1.0049E-04)	In-115	4.410E+14	0.999995
Ce-139	3.768E-01	—	La-139	*	

Table A.1-3 Principal and Associated Radionuclides with a Cutoff Half-Life of 30 Days in ICRP-107 Database (Cont.)

Principal Radionuclide[a]	Half-Life (yr)	Associated Decay Chain[b]	Terminal Nuclide or Radionuclide[c]		
			Species	Half-Life (yr)	Fraction
Ce-141	8.900E-02	—	Pr-141	*	
Ce-144+D	7.800E-01	(Pr-144m 9.7699E-03) (Pr-144 9.9999E-01)	Nd-144	2.290E+15	
Cf-248	9.144E-01	—	SF		0.000029
Cf-248	9.144E-01	—	Cm-244	1.810E+01	0.999971
Cf-249	3.510E+02	—	SF		5.02E-09
Cf-249	3.510E+02	—	Cm-245	8.500E+03	1
Cf-250	1.308E+01	—	SF		0.00077
Cf-250	1.308E+01	—	Cm-246	4.760E+03	0.99923
Cf-251	9.000E+02	—	Cm-247	1.560E+07	
Cf-252	2.645E+00	—	SF		0.03092
Cf-252	2.645E+00	—	Cm-248	3.480E+05	0.96908
Cf-254	1.656E-01	—	SF		0.9969
Cf-254	1.656E-01	—	Cm-250	8.300E+03	0.0031
Cl-36	3.010E+05	—	Ar-36, S-36	*	
Cm-241	8.980E-02	—	Am-241	4.322E+02	0.99
Cm-241	8.980E-02	—	Pu-237	1.238E-01	0.01
Cm-242	4.457E-01	—	SF		6.37E-08
Cm-242	4.457E-01	—	Pu-238	8.770E+01	1.0024
Cm-243	2.910E+01	—	Am-243	7.370E+03	0.0024
Cm-243	2.910E+01	—	Pu-239	2.411E+04	0.9976
Cm-244	1.810E+01	—	SF		1.37E-06
Cm-244	1.810E+01	—	Pu-240	6.564E+03	0.999999
Cm-245	8.500E+03	—	SF		6.1E-09
Cm-245	8.500E+03	—	Pu-241	1.435E+01	1
Cm-246	4.760E+03	—	SF		0.000263
Cm-246	4.760E+03	—	Pu-242	3.750E+05	0.999737
Cm-247+D	1.560E+07	Pu-243	Am-243	7.370E+03	
Cm-248	3.480E+05	—	SF		0.0839
Cm-248	3.480E+05	—	Pu-244	8.000E+07	0.9161
Cm-250	8.300E+03	—	SF		0.74
Cm-250+D	8.300E+03	Pu-246, Am-246m	Cm-246	4.760E+03	0.18
Cm-250+D1	8.300E+03	Bk-250	Cf-250	1.308E+01	0.08
Co-56	2.114E-01	—	Fe-56	*	
Co-57	7.440E-01	—	Fe-57	*	
Co-58	1.940E-01	—	Fe-58	*	
Co-60	5.271E+00	—	Ni-60	*	
Cs-134	2.065E+00	—	Ba-134, Ce-134	*	
Cs-135	2.300E+06	—	Ba-135	*	
Cs-137+D	3.017E+01	(Ba-137m 9.4399E-01)	Ba-137	*	

Table A.1-3 Principal and Associated Radionuclides with a Cutoff Half-Life of 30 Days in ICRP-107 Database (Cont.) (Cont.)

Principal Radionuclide[a]	Half-Life (yr)	Associated Decay Chain[b]	Terminal Nuclide or Radionuclide[c]		
			Species	Half-Life (yr)	Fraction
Dy-154	3.000E+06	—	Gd-150	1.790E+06	1
Dy-159	3.953E-01	—	Tb-159	*	
Es-254+D	7.548E-01	(Bk-250 1.0000E+00) (Fm-254 1.7390E-06)	Cf-250	1.308E+01	1
Es-254+D1	7.548E-01	(Fm-254 3.3196E-02)	SF		
Es-255+D	1.090E-01	(Fm-255 4.6800E-03)	SF		4.521E-5
Es-255+D1	1.090E-01	(Fm-255 9.2000E-01) (Bk-251 8.0004E-02)	Cf-251	9.000E+02	0.99995
Eu-148	1.492E-01	—	Sm-148	7.000E+15	1
Eu-148	1.492E-01	—	Pm-144	9.938E-01	9.4E-09
Eu-149	2.549E-01	—	Sm-149	*	
Eu-150	3.690E+01	—	Sm-150	*	
Eu-152	1.354E+01	—	Sm-152	*	0.721
Eu-152	1.354E+01	—	Gd-152	1.080E+14	0.279
Eu-154	8.593E+00	—	Gd-154, Sm-154	*	
Eu-155	4.761E+00	—	Gd-155	*	
Fe-55	2.737E+00	—	Mn-55	*	
Fe-59	1.218E-01	—	Co-59	*	
Fe-60+D	1.500E+06	Co-60m	Ni-60	*	0.0024
Fe-60+D1	1.500E+06	Co-60m	Co-60	5.271E+00	0.9976
Fm-257+D	2.752E-01	(Cf-253 4.2159E-05) (Es-253 4.2159E-05)	SF		0.0021
Fm-257+D1	2.752E-01	Cf-253 (Es-253 9.9690E-01) (Cm-249 3.1000E-03)	Bk-249	9.035E-01	0.9979
Gd-146+D	1.322E-01	Eu-146	Sm-146	1.030E+08	
Gd-148	7.460E+01	—	Sm-144	*	
Gd-150	1.790E+06	—	Sm-146	1.030E+08	1
Gd-151	3.395E-01	—	Eu-151	*	1
Gd-151	3.395E-01	—	Sm-147	1.060E+11	1E-08
Gd-152	1.080E+14	—	Sm-148	7.000E+15	
Gd-153	6.582E-01	—	Eu-153	*	
Ge-68+D	7.418E-01	Ga-68	Zn-68	*	
H-3	1.232E+01	—	He-3	*	
Hf-172+D	1.870E+00	Lu-172m Lu-172	Yb-172	*	
Hf-174	2.000E+15	—	Yb-170	*	
Hf-175	1.917E-01	—	Lu-175	*	
Hf-178m	3.100E+01	—	Hf-178	*	
Hf-181	1.161E-01	—	Ta-181	*	

Table A.1-3 Principal and Associated Radionuclides with a Cutoff Half-Life of 30 Days in ICRP-107 Database (Cont.) (Cont.)

| Principal Radionuclide[a] | Half-Life (yr) | Associated Decay Chain[b] | Terminal Nuclide or Radionuclide[c] | | |
			Species	Half-Life (yr)	Fraction
Hf-182	9.000E+06	—	Ta-182	3.133E-01	
Hg-194+D	4.400E+02	Au-194	Pt-194	*	
Hg-203	1.276E-01	—	Tl-203	*	
Ho-163	4.570E+03	—	Dy-163	*	
Ho-166m	1.200E+03	—	Er-166	*	
I-125	1.626E-01	—	Te-125	*	
I-129	1.570E+07	—	Xe-129	*	
In-114m+D	1.356E-01	(In-114 9.6750E-01)	Cd-114, Sn-114	*	
In-115	4.410E+14	—	Sn-115	*	
Ir-192	2.021E-01	—	Os-192, Pt-192	*	
Ir-192n	2.410E+02	—	Ir-192	2.021E-01	
Ir-194m	4.682E-01	—	Pt-194	*	
K-40	1.251E+09	—	Ca-40, Ar-40	*	
La-137	6.000E+04	—	Ba-137	*	
La-138	1.020E+11	—	Ba-138, Ce-138	*	
Lu-173	1.370E+00	—	Yb-173	*	
Lu-174	3.310E+00	—	Yb-174	*	
Lu-174m	3.888E-01	—	Yb-174	*	0.0062
Lu-174m	3.888E-01	—	Lu-174	3.310E+00	0.9938
Lu-176	3.850E+10	—	Hf-176	*	*
Lu-177m+D	4.392E-01	(Lu-177 2.1700E-01)	Hf-177	*	
Mn-53	3.700E+06	—	Cr-53	*	
Mn-54	8.545E-01	—	Cr-54	*	
Mo-93	4.000E+03	—	Nb-93	*	0.12
Mo-93	4.000E+03	—	Nb-93m	1.613E+01	0.88
Na-22	2.602E+00	—	Ne-22	*	
Nb-91	6.800E+02	—	Zr-91	*	
Nb-91m	1.666E-01	—	Zr-91	*	0.034
Nb-91m	1.666E-01	—	Nb-91	6.800E+02	0.966
Nb-92	3.470E+07	—	Zr-92	*	
Nb-93m	1.613E+01	—	Nb-93	*	
Nb-94	2.030E+04	—	Mo-94	*	
Nb-95	9.580E-02	—	Mo-95	*	
Nd-144	2.290E+15	—	Ce-140	*	
Ni-59	1.010E+05	—	Co-59	*	
Ni-63	1.001E+02	—	Cu-63	*	
Np-235	1.084E+00	—	Pa-231	3.276E+04	0.000026
Np-235+D	1.084E+00	(U-235m 3.9934E-03)	U-235	7.040E+08	0.999974
Np-236	1.540E+05	—	U-236	2.342E+07	0.8734
Np-236	1.540E+05	—	Pu-236	2.858E+00	0.125

Table A.1-3 Principal and Associated Radionuclides with a Cutoff Half-Life of 30 Days in ICRP-107 Database (Cont.) (Cont.)

Principal Radionuclide[a]	Half-Life (yr)	Associated Decay Chain[b]	Terminal Nuclide or Radionuclide[c]		
			Species	Half-Life (yr)	Fraction
Np-236+D	1.540E+05	Pa-232	Th-232	1.405E+10	4.8E-08
Np-236+D1	1.540E+05	Pa-232	U-232	6.890E+01	0.0016
Np-237+D	2.144E+06	Pa-233	U-233	1.592E+05	
Os-185	2.563E-01	—	Re-185	*	
Os-186	2.000E+15	—	W-182	*	
Os-194+D	6.000E+00	Ir-194	Pt-194	*	
Pa-231	3.276E+04	—	Ac-227	2.177E+01	
Pb-202+D	5.250E+04	(Tl-202 9.9000E-01)	Hg-202	*	
Pb-205	1.530E+07	—	Tl-205	*	
Pb-210+D	2.220E+01	Bi-210	Po-210	3.789E-01	0.999999
Pb-210+D1	2.220E+01	(Bi-210 9.8581E-01) Tl-206 (Hg-206 1.4190E-02)	Pb-206	*	1.34E-06
Pd-107	6.500E+06	—	Ag-107	*	
Pm-143	7.255E-01	—	Nd-143	*	
Pm-144	9.938E-01	—	Nd-144	2.290E+15	
Pm-145	1.770E+01	—	Nd-145	*	
Pm-146	5.530E+00	—	Nd-146	*	
Pm-146	5.530E+00	—	Sm-146	1.030E+08	
Pm-147	2.623E+00	—	Sm-147	1.060E+11	
Pm-148m+D	1.130E-01	(Pm-148 4.2000E-02)	Sm-148	7.000E+15	
Po-208	2.898E+00	—	Pb-204	*	
Po-208	2.898E+00	—	Bi-208	3.68E+05	2.23E-05
Po-209	1.020E+02	—	Pb-205	1.530E+07	0.9952
Po-209w	1.020E+02	—	Bi-209	*	0.0048
Po-210	3.789E-01	—	Pb-206	*	
Pt-190	6.500E+11	—	Os-186	2.000E+15	1
Pt-193	5.000E+01	—	Ir-193	*	
Pu-236	2.858E+00	—	SF		1.37E-09
Pu-236	2.858E+00	—	U-232	6.890E+01	1
Pu-237	1.238E-01	—	Np-237	2.144E+06	0.999958
Pu-237	1.238E-01	—	U-233	1.592E+05	0.000042
Pu-238	8.770E+01	—	SF		1.85E-09
Pu-238	8.770E+01	—	U-234	2.455E+05	1
Pu-239+D	2.411E+04	(U-235m 9.9940E-01)	U-235	7.040E+08	
Pu-240	6.564E+03	—	SF		5.75E-08
Pu-240	6.564E+03	—	U-236	2.342E+07	1
Pu-241	1.435E+01	—	Am-241	4.322E+02	0.999976
Pu-241+D	1.435E+01	U-237	Np-237	2.144E+06	2.45E-05
Pu-242	3.750E+05	—	SF		5.54E-06

Table A.1-3 Principal and Associated Radionuclides with a Cutoff Half-Life of 30 Days in ICRP-107 Database (Cont.) (Cont.)

Principal Radionuclide[a]	Half-Life (yr)	Associated Decay Chain[b]	Terminal Nuclide or Radionuclide[c]		
			Species	Half-Life (yr)	Fraction
Pu-242	3.750E+05	—	U-238	4.468E+09	1.88E-06
Pu-244	8.000E+07	—	SF		0.00121
Pu-244+D	8.000E+07	U-240 Np-240m (Np-240 1.1000E-03)	Pu-240	6.564E+03	0.99879
Ra-226+D	1.600E+03	Rn-222 Po-218 (Pb-214 9.9980E-01) (Bi-214 1.0000E+00) (Po-214 9.9979E-01) (Tl-210 2.1000E-04) (At-218 2.0000E-04) (Rn-218 2.0000E-07)	Pb-210	2.220E+01	1
Ra-228+D	5.750E+00	Ac-228	Th-228	1.912E+00	
Rb-83+D	2.360E-01	(Kr-83m 7.4292E-01)	Kr-83	*	
Rb-84	8.972E-02	—	Sr-84, Kr-84	*	
Rb-87	4.923E+10	—	Sr-87	*	
Re-183	1.917E-01	—	W-183	*	
Re-184	1.040E-01	—	W-184	*	
Re-184m	4.627E-01	—	W-184	*	0.246
Re-184m	4.627E-01	—	Re-184	1.040E-01	0.754
Re-186m+D	2.000E+05	Re-186	W-186	*	0.0747
Re-186m+D1	2.000E+05	Re-186	Os-186	2.000E+15	0.9253
Re-187	4.120E+10	—	Os-187	*	
Rh-101	3.300E+00	—	Ru-101	*	
Rh-102	5.667E-01	—	Ru-102, Pd-102	*	
Rh-102m	3.742E+00	—	Ru-102	*	0.99767
Rh-102m	3.742E+00	—	Rh-102	5.667E-01	0.00233
Ru-103+D	1.075E-01	(Rh-103m 9.8755E-01)	Rh-103	*	
Ru-106+D	1.023E+00	Rh-106	Pd-106	*	
S-35	2.396E-01	—	Cl-35	*	
Sb-124	1.648E-01	—	Te-124	*	
Sb-125	2.759E+00	—	Te-125	*	0.76864
Sb-125	2.759E+00	—	Te-125m	1.572E-01	0.23136
Sc-46	2.294E-01	—	Ti-46	*	
Se-75	3.279E-01	—	As-75	*	
Se-79	2.950E+05	—	Br-79	*	
Si-32+D	1.320E+02	P-32	S-32	*	
Sm-145	9.309E-01	—	Pm-145	1.770E+01	
Sm-146	1.030E+08	—	Nd-142	*	
Sm-147	1.060E+11	—	Nd-143	*	
Sm-148	7.000E+15	—	Nd-144	2.290E+15	

Table A.1-3 Principal and Associated Radionuclides with a Cutoff Half-Life of 30 Days in ICRP-107 Database (Cont.) (Cont.)

Principal Radionuclide[a]	Half-Life (yr)	Associated Decay Chain[b]	Terminal Nuclide or Radionuclide[c]		
			Species	Half-Life (yr)	Fraction
Sm-151	9.000E+01	—	Eu-151	*	
Sn-113+D	3.151E-01	(In-113m 9.9998E-01)	In-113	*	
Sn-119m	8.025E-01	—	Sn-119	*	
Sn-121m+D	4.390E+01	(Sn-121 7.7600E-01)	Sb-121	*	
Sn-123	3.537E-01	—	Sb-123	*	
Sn-126+D	2.300E+05	Sb-126m (Sb-126 1.4000E-01)	Te-126	*	
Sr-85	1.775E-01	—	Rb-85	*	
Sr-89	1.383E-01	—	Y-89	*	
Sr-90+D	2.879E+01	Y-90	Zr-90	*	
Ta-179	1.820E+00	—	Hf-179	*	
Ta-182	3.133E-01	—	W-182	*	
Tb-157	7.100E+01	—	Gd-157	*	
Tb-158	1.800E+02	—	Gd-158, Dy-158	*	
Tb-160	1.979E-01	—	Dy-160	*	
Tc-95m+D	1.670E-01	(Tc-95 3.8800E-02)	Mo-95	*	
Tc-97	2.600E+06	—	Mo-97	*	
Tc-97m	2.467E-01	—	Tc-97	2.600E+06	
Tc-98	4.200E+06	—	Ru-98	*	
Tc-99	2.111E+05	—	Ru-99	*	
Te-121m+D	4.216E-01	(Te-121 8.8600E-01)	Sb-121	*	
Te-123	6.000E+14	—	Sb-123	*	
Te-123m	3.265E-01	—	Te-123	6.000E+14	
Te-125m	1.572E-01	—	Te-125	*	
Te-127m+D	2.984E-01	(Te-127 9.7600E-01)	I-127	*	
Te-129m+D	9.199E-02	(Te-129 6.3000E-01)	I-129	1.570E+07	
Th-228+D	1.912E+00	Ra-224 Rn-220 Po-216 Pb-212 Bi-212 (Po-212 6.4060E-01) (Tl-208 3.5940E-01)	Pb-208	*	
Th-229+D	7.340E+03	Ra-225 Ac-225 Fr-221 At-217 Bi-213 (Po-213 9.7910E-01) Pb-209 (Tl-209 2.0900E-02)	Bi-209	*	
Th-230	7.538E+04	—	Ra-226	1.600E+03	1
Th-232	1.405E+10	—	Ra-228	5.750E+00	
Ti-44+D	6.000E+01	Sc-44	Ca-44	*	
Tl-204	3.780E+00	—	Pb-204, Hg-204	*	
Tm-168	2.549E-01	—	Er-168, Yb-168	*	

Table A.1-3 Principal and Associated Radionuclides with a Cutoff Half-Life of 30 Days in ICRP-107 Database (Cont.) (Cont.)

Principal Radionuclide[a]	Half-Life (yr)	Associated Decay Chain[b]	Terminal Nuclide or Radionuclide[c] Species	Terminal Nuclide or Radionuclide[c] Half-Life (yr)	Terminal Nuclide or Radionuclide[c] Fraction
Tm-170	3.521E-01	—	Er-170, Yb-170	*	
Tm-171	1.920E+00	—	Yb-171	*	
U-232	6.890E+01	—	Th-228	1.912E+00	
U-233	1.592E+05	—	Th-229	7.340E+03	
U-234	2.455E+05	—	Th-230	7.538E+04	1
U-235+D	7.040E+08	Th-231	Pa-231	3.276E+04	
U-236	2.342E+07	—	Th-232	1.405E+10	
U-238	4.468E+09	—	SF		5.45E-07
U-238+D	4.468E+09	Th-234 Pa-234m (Pa-234 1.6000E-03)	U-234	2.455E+05	0.999999
V-49	9.035E-01	—	Ti-49	*	
V-50	1.500E+17	—	Ti-50	*	
W-181	3.318E-01	—	Ta-181	*	
W-185	2.056E-01	—	Re-185	*	
W-188+D	1.910E-01	Re-188	Os-188	*	
Y-88	2.920E-01	—	Sr-88	*	
Y-91	1.602E-01	—	Zr-91	*	
Yb-169	8.768E-02	—	Tm-169	*	
Zn-65	6.682E-01	—	Cu-65	*	
Zr-88	2.283E-01	—	Y-88	2.920E-01	
Zr-93	1.530E+06	—	Nb-93	*	0.025
Zr-93	1.530E+06	—	Nb-93m	1.613E+01	0.975
Zr-95+D	1.753E-01	Nb-95m	Mo-95	*	0.000605
Zr-95+D1	1.753E-01	(Nb-95m 1.0203E-02)	Nb-95	9.580E-02	0.999395

[a] Radionuclides with half-lives longer than 30 days. If short-lived progeny are involved, the +D symbol is added along with the radionuclide name (e.g., Ac-227+D). To distinguish between different associated radionuclides or terminal radionuclides, different +D (for example +D, +D1, etc.) indicators are used.

[b] The associated progeny with half-lives shorter than 30 days are listed. If the branching fraction is anything other than 1, it is listed along with the radionuclide in the bracket.

[c] The principal radionuclide or stable nuclide that terminates an associated decay chain. Stable nuclides are indicated by an asterisk (*) in place of the half-life. If a radionuclide has spontaneous fission, it is indicated by SF. If the branching fraction is anything other than 1, the fraction is listed.

[d] Indicates there is no associated radionuclide.

A.2   Dose Coefficient Libraries

Three sets of dose coefficient libraries are available in RESRAD-OFFSITE. Two sets of dose coefficient libraries are based on the ICRP-38 radionuclide transformation database, and one dose coefficient library is based on the ICRP-107 radionuclide transformation database. Users can also create their own libraries starting with the base libraries available for the ICRP-38 and ICRP-107 transformation databases. The external dose coefficient library is automatically selected based on the internal dose library selection. For example, if the Federal Guidance Report No. 11 (FGR-11) (Eckerman et al. 1988) internal dose library is chosen, the external dose library used is Federal Guidance Report No. 12 (FGR 12) (Eckerman and Ryman 1993). Both the internal and the external dose libraries will come from the user-created library when a user-created library is selected.

A.2.1   FGR-12 and FGR-11 Libraries

The FGR-12 and FGR-11 dose coefficient libraries are based on the ICRP-38 radionuclide transformation database and use the ICRP-26 dose estimation methodology (see Section A.3). FGR-12 lists dose coefficients for external exposure to photons and electrons emitted by radionuclides distributed in air, water, and soil. Dose coefficients for external exposure relate the doses to organs and tissues of the body to the concentrations of radionuclides in environmental media. The RESRAD-OFFSITE code uses only dose coefficients for exposure to contaminated soil. Table A.2-1 lists the dose coefficients and fitting parameters (see Appendix B for additional information on the need for fitting parameters to assess dose from external or direct radiation) used in the code for radionuclides with a 30-day half-life cutoff in external pathway dose calculations. The dose coefficients for principal radionuclides with half-lives longer than 30 days and their associated progeny are included in Table A.2-1.

Table A.2-1   Effective Dose Equivalent Conversion Factors for External Gamma Radiation from Contaminated Soil and Fitting Parameters to Calculate Depth and Cover Factors (30-day Half-Life Cutoff from FGR 12)

Radionuclide	Volume Dose Coefficients[a] (mSv/yr per Bq/g)	Fitting Parameters[b]			
		CF_A	CF_B	CF_KA (cm^2/g)	CF_KB (cm^2/g)
Ac-225	1.72E-02	0.908	0.092	1.51E-01	1.66E+00
Ac-227	1.34E-04	0.913	0.087	1.60E-01	2.58E+00
Ac-228	1.62E+00	0.09	0.91	1.18E+00	8.30E-02
Ag-105	7.88E-01	0.919	0.081	9.90E-02	1.41E+00
Ag-108	3.09E-02	0.906	0.094	9.20E-02	1.28E+00
Ag-108m	2.61E+00	0.928	0.072	9.70E-02	1.44E+00
Ag-110	6.06E-02	0.919	0.081	9.60E-02	1.36E+00
Ag-110m	4.64E+00	0.09	0.91	1.17E+00	8.30E-02
Al-26	4.71E+00	0.914	0.086	7.50E-02	1.15E+00
Am-241	1.18E-02	0.836	0.164	3.13E-01	2.88E+00

Table A.2-1 Effective Dose Equivalent Conversion Factors for External Gamma Radiation from Contaminated Soil and Fitting Parameters to Calculate Depth and Cover Factors (30-day Half-Life Cutoff from FGR 12) (Cont.)

Radionuclide	Volume Dose Coefficients[a] (mSv/yr per Bq/g)	CF_A	CF_B	CF_KA (cm²/g)	CF_KB (cm²/g)
Am-242	1.35E-02	0.08	0.92	2.56E+00	1.78E-01
Am-242m	4.57E-04	0.704	0.296	1.83E-01	6.62E+00
Am-243	3.84E-02	0.884	0.116	2.38E-01	1.98E+00
Am-245	3.91E-02	0.926	0.074	1.37E-01	1.68E+00
As-73	2.55E-03	0.812	0.188	3.66E-01	2.35E+00
At-217	4.79E-04	0.922	0.078	1.00E-01	1.36E+00
At-218	1.58E-03	0.814	0.186	3.71E-01	2.88E+00
Au-194	1.76E+00	0.079	0.921	1.29E+00	8.40E-02
Au-195	5.61E-02	0.877	0.123	2.38E-01	1.89E+00
Ba-133	5.35E-01	0.08	0.921	1.64E+00	1.13E-01
Ba-137m	9.75E-01	0.928	0.072	9.50E-02	1.41E+00
Be-10	2.91E-04	0.855	0.145	1.64E-01	2.12E+00
Be-7	7.78E-02	0.922	0.078	1.00E-01	1.37E+00
Bi-207	2.54E+00	0.08	0.92	1.31E+00	8.70E-02
Bi-210	9.75E-04	0.868	0.132	1.33E-01	1.71E+00
Bi-210m	3.72E-01	0.919	0.081	1.14E-01	1.33E+00
Bi-211	6.92E-02	0.066	0.934	1.58E+00	1.13E-01
Bi-212	3.17E-01	0.073	0.927	1.36E+00	8.60E-02
Bi-213	2.07E-01	0.916	0.084	9.90E-02	1.32E+00
Bi-214	2.65E+00	0.087	0.913	1.15E+00	7.50E-02
Bk-247	1.18E-01	0.896	0.104	1.37E-01	1.43E+00
Bk-249	1.26E-06	0.555	0.445	2.60E-01	3.54E+00
Bk-250	1.50E+00	0.074	0.926	1.35E+00	8.60E-02
C-14	3.64E-06	0.642	0.358	2.94E-01	3.39E+00
Ca-41	0.00E+00	0	1	0.00E+00	0.00E+00
Ca-45	1.69E-05	0.252	0.748	2.74E+00	2.26E-01
Cd-109	3.97E-03	0.653	0.347	2.05E-01	4.77E+00
Cd-113	3.07E-05	0.79	0.21	2.10E-01	2.65E+00
Cd-113m	1.75E-04	0.848	0.152	1.68E-01	2.18E+00
Cd-115m	4.01E-02	0.087	0.913	1.24E+00	8.40E-02
Ce-139	1.72E-01	0.918	0.082	1.42E-01	1.90E+00
Ce-141	8.58E-02	0.93	0.07	1.56E-01	1.81E+00
Ce-144	1.94E-02	0.901	0.099	1.62E-01	1.87E+00
Cf-248	3.37E-05	0.82	0.18	8.60E+00	1.20E+00
Cf-249	5.00E-01	0.92	0.08	1.06E-01	1.37E+00
Cf-250	3.20E-05	0.82	0.18	8.60E+00	1.20E+00
Cf-251	1.42E-01	0.917	0.083	1.41E-01	1.70E+00
Cf-252	4.75E-05	0.65	0.35	7.26E+00	1.82E-01
Cf-253	2.08E-05	0.749	0.251	2.20E-01	3.25E+00
Cl-36	6.46E-04	0.889	0.111	1.33E-01	1.90E+00
Cm-241	7.12E-01	0.906	0.094	1.03E-01	1.30E+00

Table A.2-1 Effective Dose Equivalent Conversion Factors for External Gamma Radiation from Contaminated Soil and Fitting Parameters to Calculate Depth and Cover Factors (30-day Half-Life Cutoff from FGR 12) (Cont.)

Radionuclide	Volume Dose Coefficients[a] (mSv/yr per Bq/g)	Fitting Parameters[b]			
		CF_A	CF_B	CF_KA (cm^2/g)	CF_KB (cm^2/g)
Cm-242	4.62E-05	0.224	0.776	1.70E-01	8.40E+00
Cm-243	1.58E-01	0.925	0.075	1.35E-01	1.68E+00
Cm-244	3.40E-05	0.007	0.993	8.46E+02	2.19E+00
Cm-245	9.19E-02	0.079	0.921	1.86E+00	1.65E-01
Cm-246	3.14E-05	0.087	0.913	4.58E-01	8.60E+00
Cm-247	4.81E-01	0.922	0.078	1.05E-01	1.37E+00
Cm-248	2.37E-05	0.733	0.267	1.04E+01	1.22E+00
Cm-249	3.10E-02	0.916	0.084	9.70E-02	1.30E+00
Co-56	6.36E+00	0.096	0.904	1.01E+00	7.10E-02
Co-57	1.35E-01	0.929	0.071	1.60E-01	1.69E+00
Co-58	1.61E+00	0.923	0.077	9.00E-02	1.34E+00
Co-60	4.38E+00	0.076	0.924	1.28E+00	7.80E-02
Co-60m	6.67E-03	0.12	0.88	1.17E+00	7.90E-02
Cs-134	2.56E+00	0.927	0.073	9.30E-02	1.38E+00
Cs-135	1.04E-05	0.725	0.275	2.51E-01	3.03E+00
Cs-137	2.03E-04	0.848	0.152	1.57E-01	2.05E+00
Dy-159	1.49E-02	0.8	0.2	4.80E-01	3.01E+00
Es-253	4.76E-04	0.122	0.878	3.65E+00	1.11E-01
Es-254	3.49E-03	0.773	0.227	1.42E-01	4.60E+00
Eu-146	4.17E+00	0.078	0.922	1.33E+00	8.70E-02
Eu-148	3.55E+00	0.919	0.081	9.00E-02	1.31E+00
Eu-149	5.45E-02	0.84	0.16	1.16E-01	1.72E+00
Eu-150b	2.36E+00	0.925	0.075	9.70E-02	1.42E+00
Eu-152	1.89E+00	0.09	0.91	1.19E+00	8.40E-02
Eu-154	2.08E+00	0.09	0.91	1.17E+00	8.30E-02
Eu-155	4.92E-02	0.862	0.138	1.91E-01	1.55E+00
Fe-55	0.00E+00	0	1	0.00E+00	0.00E+00
Fe-59	2.07E+00	0.072	0.928	1.32E+00	8.20E-02
Fe-60	3.03E-06	0.61	0.39	3.12E-01	3.48E+00
Fm-257	1.16E-01	0.922	0.078	1.49E-01	1.84E+00
Fr-221	4.15E-02	0.939	0.061	1.32E-01	1.69E+00
Fr-223	5.35E-02	0.86	0.14	1.33E-01	1.57E+00
Ga-68	1.52E+00	0.927	0.073	9.90E-02	1.42E+00
Gd-146	2.17E-01	0.882	0.118	1.64E-01	1.82E+00
Gd-148	0.00E+00	0	1	0.00E+00	0.00E+00
Gd-151	4.70E-02	0.822	0.178	1.37E-01	1.78E+00
Gd-152	0.00E+00	0	1	0.00E+00	0.00E+00
Gd-153	6.61E-02	0.823	0.177	1.99E-01	1.94E+00
Ge-68	2.15E-07	0.99	0.01	3.20E+01	1.20E+00
H-3	0.00E+00	0	0	0.00E+00	0.00E+00
Hf-172	6.72E-02	0.823	0.177	2.37E-01	1.90E+00

Table A.2-1 Effective Dose Equivalent Conversion Factors for External Gamma Radiation from Contaminated Soil and Fitting Parameters to Calculate Depth and Cover Factors (30-day Half-Life Cutoff from FGR 12) (Cont.)

Radionuclide	Volume Dose Coefficients[a] (mSv/yr per Bq/g)	Fitting Parameters[b]			
		CF_A	CF_B	CF_KA (cm²/g)	CF_KB (cm²/g)
Hf-175	5.04E-01	0.083	0.917	1.50E+00	1.13E-01
Hf-178m	3.52E+00	0.915	0.085	1.03E-01	1.34E+00
Hf-181	8.23E-01	0.912	0.088	1.02E-01	1.33E+00
Hf-182	3.37E-01	0.93	0.07	1.21E-01	1.51E+00
Hg-194	2.97E-06	0.99	0.01	2.20E+01	1.20E+00
Hg-203	3.41E-01	0.93	0.07	1.18E-01	1.50E+00
Ho-166m	2.78E+00	0.081	0.919	1.33E+00	9.30E-02
I-125	4.47E-03	0.854	0.146	3.45E+00	4.42E-01
I-129	3.50E-03	0.435	0.565	7.14E-01	3.58E+00
In-113m	3.88E-01	0.927	0.073	1.07E-01	1.47E+00
In-114	4.79E-03	0.077	0.923	1.37E+00	7.90E-02
In-114m	1.31E-01	0.91	0.09	9.90E-02	1.46E+00
In-115	1.09E-04	0.828	0.172	1.70E-01	2.25E+00
Ir-192	1.25E+00	0.931	0.069	1.08E-01	1.49E+00
Ir-192m	2.03E-01	0.932	0.068	1.41E-01	1.61E+00
Ir-194	1.48E-01	0.918	0.082	9.70E-02	1.30E+00
Ir-194m	3.69E+00	0.922	0.078	1.00E-01	1.35E+00
K-40	2.81E-01	0.084	0.916	1.17E+00	7.20E-02
Kr-83m	8.18E-06	0.013	0.987	9.85E+02	1.90E+00
La-137	3.81E-03	0.4	0.6	6.10E-01	3.15E+00
La-138	2.15E+00	0.09	0.91	1.13E+00	7.60E-02
Lu-172	3.11E+00	0.09	0.91	1.21E+00	8.30E-02
Lu-173	1.13E-01	0.825	0.175	1.33E-01	1.43E+00
Lu-174	1.55E-01	0.157	0.843	1.10E+00	8.25E-02
Lu-174m	3.95E-02	0.71	0.29	1.40E-01	1.32E+00
Lu-176	6.82E-01	0.93	0.07	1.20E-01	1.58E+00
Lu-177	4.29E-02	0.924	0.076	1.38E-01	1.62E+00
Lu-177m	1.35E+00	0.916	0.084	1.18E-01	1.43E+00
Md-258	6.16E-04	0.61	0.39	2.40E-01	5.55E+00
Mn-53	0.00E+00	0	1	0.00E+00	0.00E+00
Mn-54	1.39E+00	0.085	0.915	1.22E+00	8.80E-02
Mo-93	1.60E-04	0.999	0.001	1.06E+01	9.19E-01
Na-22	3.70E+00	0.074	0.926	1.34E+00	8.70E-02
Nb-93m	2.81E-05	0.999	0.001	1.06E+01	9.19E-01
Nb-94	2.62E+00	0.928	0.072	9.10E-02	1.39E+00
Nb-95	1.27E+00	0.075	0.925	1.36E+00	9.10E-02
Nb-95m	8.64E-02	0.945	0.055	1.27E-01	1.99E+00
Ni-59	0.00E+00	0	1	0.00E+00	0.00E+00
Ni-63	0.00E+00	0	1	0.00E+00	0.00E+00
Np-235	8.74E-04	0.828	0.172	1.90E-01	6.75E+00
Np-236a	1.25E-01	0.065	0.935	2.20E+00	1.72E-01

Table A.2-1 Effective Dose Equivalent Conversion Factors for External Gamma Radiation from Contaminated Soil and Fitting Parameters to Calculate Depth and Cover Factors (30-day Half-Life Cutoff from FGR 12) (Cont.)

Radionuclide	Volume Dose Coefficients[a] (mSv/yr per Bq/g)	Fitting Parameters[b]			
		CF_A	CF_B	CF_KA (cm^2/g)	CF_KB (cm^2/g)
Np-237	2.11E-02	0.897	0.103	1.85E-01	2.58E+00
Np-238	9.29E-01	0.083	0.917	1.24E+00	8.40E-02
Np-239	2.04E-01	0.925	0.075	1.39E-01	1.64E+00
Np-240m	5.45E-01	0.921	0.079	9.00E-02	1.35E+00
Os-185	1.13E+00	0.083	0.917	1.36E+00	9.30E-02
Os-194	3.15E-04	0.78	0.22	5.20E-01	3.36E+00
P-32	3.19E-03	0.9	0.1	1.28E-01	1.74E+00
Pa-231	5.15E-02	0.93	0.07	1.16E-01	2.02E+00
Pa-233	2.76E-01	0.925	0.075	1.18E-01	1.52E+00
Pa-234	3.12E+00	0.085	0.915	1.24E+00	8.80E-02
Pa-234m	2.42E-02	0.916	0.084	9.10E-02	1.39E+00
Pb-202	1.67E-06	0.99	0.01	2.57E+01	1.20E+00
Pb-205	1.91E-06	0.99	0.01	2.51E+01	1.20E+00
Pb-209	2.09E-04	0.852	0.148	1.63E-01	2.14E+00
Pb-210	6.61E-04	0.804	0.196	4.93E-01	4.04E+00
Pb-211	8.28E-02	0.926	0.074	9.60E-02	1.42E+00
Pb-212	1.90E-01	0.927	0.073	1.31E-01	1.59E+00
Pb-214	3.62E-01	0.08	0.921	1.39E+00	1.11E-01
Pd-107	0.00E+00	0	1	0.00E+00	0.00E+00
Pm-143	4.79E-01	0.92	0.08	9.30E-02	1.49E+00
Pm-144	2.50E+00	0.927	0.073	9.60E-02	1.45E+00
Pm-145	7.93E-03	0.59	0.41	4.00E-01	2.60E+00
Pm-146	1.19E+00	0.928	0.072	9.70E-02	1.48E+00
Pm-147	1.35E-05	0.773	0.227	2.09E-01	2.80E+00
Pm-148	9.95E-01	0.075	0.925	1.31E+00	8.20E-02
Pm-148m	3.25E+00	0.079	0.921	1.33E+00	9.30E-02
Po-210	1.41E-05	0.927	0.073	9.00E-02	1.38E+00
Po-211	1.29E-02	0.922	0.078	9.00E-02	1.33E+00
Po-212	0.00E+00	0	1	0.00E+00	0.00E+00
Po-213	0.00E+00	0	1	0.00E+00	0.00E+00
Po-214	1.39E-04	0.084	0.916	1.23E+00	8.80E-02
Po-215	2.75E-04	0.915	0.085	1.00E-01	1.28E+00
Po-216	2.82E-05	0.084	0.916	1.24E+00	8.80E-02
Po-218	1.53E-05	0.082	0.918	1.25E+00	8.80E-02
Pr-144	6.82E-02	0.082	0.918	1.26E+00	7.90E-02
Pr-144m	3.88E-03	0.532	0.468	1.29E-01	2.11E+00
Pt-193	1.53E-06	0.99	0.01	2.49E+01	1.20E+00
Pu-236	6.16E-05	0.405	0.595	1.57E-01	8.36E+00
Pu-237	4.37E-02	0.076	0.924	2.20E+00	1.84E-01
Pu-238	4.09E-05	0.297	0.703	1.96E-01	9.12E+00
Pu-239	7.98E-05	0.8	0.2	1.35E-01	6.75E+00

Table A.2-1 Effective Dose Equivalent Conversion Factors for External Gamma Radiation from Contaminated Soil and Fitting Parameters to Calculate Depth and Cover Factors (30-day Half-Life Cutoff from FGR 12) (Cont.)

Radionuclide	Volume Dose Coefficients[a] (mSv/yr per Bq/g)	Fitting Parameters[b]			
		CF_A	CF_B	CF_KA (cm²/g)	CF_KB (cm²/g)
Pu-240	3.97E-05	0.298	0.702	2.18E-01	9.00E+00
Pu-241	1.60E-06	0.079	0.921	2.80E+00	1.76E-01
Pu-242	3.46E-05	0.331	0.669	2.11E-01	8.98E+00
Pu-243	2.15E-02	0.881	0.119	1.73E-01	1.70E+00
Pu-244	2.04E-05	0.008	0.992	8.46E+02	1.90E+00
Ra-223	1.63E-01	0.905	0.095	1.30E-01	1.38E+00
Ra-224	1.38E-02	0.943	0.057	1.27E-01	1.74E+00
Ra-225	2.98E-03	0.708	0.292	5.80E-01	3.44E+00
Ra-226	8.58E-03	0.932	0.068	1.35E-01	1.64E+00
Ra-228	0.00E+00	0	1	0.00E+00	0.00E+00
Rb-83	7.93E-01	0.916	0.084	9.60E-02	1.29E+00
Rb-84	1.52E+00	0.085	0.915	1.24E+00	8.80E-02
Rb-87	3.81E-05	0.787	0.213	2.15E-01	2.63E+00
Re-184	1.41E+00	0.918	0.082	9.00E-02	1.35E+00
Re-184m	5.50E-01	0.908	0.092	1.01E-01	1.35E+00
Re-186	2.11E-02	0.906	0.094	1.64E-01	1.68E+00
Re-186m	7.47E-03	0.796	0.204	2.75E-01	1.96E+00
Re-187	0.00E+00	0	1	0.00E+00	0.00E+00
Re-188	8.68E-02	0.897	0.103	9.90E-02	1.23E+00
Rh-101	3.31E-01	0.932	0.068	1.34E-01	1.73E+00
Rh-102	3.51E+00	0.919	0.081	9.00E-02	1.29E+00
Rh-102m	7.68E-01	0.925	0.075	9.80E-02	1.35E+00
Rh-103m	6.57E-05	0.79	0.21	7.30E+00	1.22E+00
Rh-106	3.49E-01	0.927	0.073	9.60E-02	1.41E+00
Rn-219	8.33E-02	0.08	0.921	1.34E+00	1.11E-01
Rn-220	6.21E-04	0.926	0.074	9.70E-02	1.41E+00
Rn-222	6.36E-04	0.922	0.078	9.80E-02	1.34E+00
Ru-103	7.42E-01	0.922	0.078	1.00E-01	1.35E+00
Ru-106	0.00E+00	0	1	0.00E+00	0.00E+00
S-35	4.02E-06	0.34	0.66	3.31E+00	2.90E-01
Sb-124	3.16E+00	0.077	0.923	1.28E+00	7.90E-02
Sb-125	6.61E-01	0.922	0.078	9.80E-02	1.44E+00
Sb-126	4.62E+00	0.075	0.925	1.38E+00	9.30E-02
Sb-126m	2.52E+00	0.927	0.073	9.60E-02	1.40E+00
Sc-44	3.57E+00	0.079	0.921	1.31E+00	8.70E-02
Sc-46	3.43E+00	0.073	0.927	1.35E+00	8.60E-02
Se-75	5.35E-01	0.069	0.931	1.55E+00	1.24E-01
Se-79	5.03E-06	0.662	0.338	2.86E-01	3.29E+00
Si-32	9.60E-06	0.722	0.278	2.52E-01	3.02E+00
Sm-145	1.84E-02	0.666	0.334	4.30E-01	2.66E+00
Sm-146	0.00E+00	0	1	0.00E+00	0.00E+00

Table A.2-1 Effective Dose Equivalent Conversion Factors for External Gamma Radiation from Contaminated Soil and Fitting Parameters to Calculate Depth and Cover Factors (30-day Half-Life Cutoff from FGR 12) (Cont.)

Radionuclide	Volume Dose Coefficients[a] (mSv/yr per Bq/g)	Fitting Parameters[b]			
		CF_A	CF_B	CF_KA (cm²/g)	CF_KB (cm²/g)
Sm-147	0.00E+00	0	1	0.00E+00	0.00E+00
Sm-151	2.66E-07	0.033	0.967	8.27E-01	6.15E+00
Sn-113	8.03E-03	0.807	0.193	1.25E-01	3.82E+00
Sn-119m	8.13E-04	0.733	0.267	5.09E+00	1.22E+00
Sn-121	5.30E-05	0.8	0.2	1.87E-01	2.39E+00
Sn-121m	5.30E-04	0.8	0.2	3.53E+00	4.42E-01
Sn-123	1.37E-02	0.083	0.917	1.37E+00	8.70E-02
Sn-126	3.98E-02	0.89	0.11	2.12E-01	2.23E+00
Sr-85	8.03E-01	0.92	0.08	9.70E-02	1.34E+00
Sr-89	2.45E-03	0.9	0.1	1.28E-01	1.77E+00
Sr-90	1.90E-04	0.848	0.152	1.70E-01	2.15E+00
Ta-179	1.56E-02	0.824	0.176	3.24E-01	2.12E+00
Ta-180	7.57E-01	0.92	0.08	1.18E-01	1.49E+00
Ta-182	2.15E+00	0.079	0.921	1.32E+00	8.40E-02
Tb-157	7.83E-04	0.792	0.208	5.20E-01	3.20E+00
Tb-158	1.28E+00	0.083	0.917	1.34E+00	8.70E-02
Tb-160	1.87E+00	0.077	0.923	1.33E+00	8.70E-02
Tc-95	1.30E+00	0.925	0.075	9.00E-02	1.39E+00
Tc-95m	1.06E+00	0.925	0.075	9.60E-02	1.41E+00
Tc-97	2.19E-04	0.999	0.001	9.40E+00	9.19E-01
Tc-97m	5.15E-04	0.52	0.48	1.89E-01	7.70E+00
Tc-98	2.32E+00	0.926	0.074	9.30E-02	1.38E+00
Tc-99	3.39E-05	0.787	0.213	2.11E-01	2.63E+00
Te-121	8.99E-01	0.924	0.076	9.70E-02	1.46E+00
Te-121m	2.90E-01	0.93	0.07	1.18E-01	1.70E+00
Te-123	1.77E-03	0.013	0.987	1.24E+02	1.90E+00
Te-123m	1.70E-01	0.934	0.066	1.45E-01	1.98E+00
Te-125m	4.10E-03	0.776	0.224	3.48E+00	3.70E-01
Te-127	7.72E-03	0.913	0.087	1.03E-01	1.36E+00
Te-127m	1.47E-03	0.278	0.722	1.60E-01	3.30E+00
Te-129	8.94E-02	0.922	0.078	1.00E-01	1.54E+00
Te-129m	5.00E-02	0.91	0.09	9.30E-02	1.70E+00
Th-227	1.41E-01	0.917	0.083	1.21E-01	1.47E+00
Th-228	2.15E-03	0.912	0.088	1.56E-01	2.31E+00
Th-229	8.68E-02	0.912	0.088	1.66E-01	1.82E+00
Th-230	3.27E-04	0.863	0.137	1.87E-01	4.11E+00
Th-231	9.85E-03	0.87	0.13	1.95E-01	3.26E+00
Th-232	1.41E-04	0.815	0.185	2.08E-01	5.76E+00
Th-234	6.51E-03	0.896	0.104	2.09E-01	2.08E+00
Ti-44	9.70E-02	0.882	0.118	2.39E-01	1.86E+00
Tl-202	6.77E-01	0.907	0.093	1.02E-01	1.31E+00

**Table A.2-1 Effective Dose Equivalent Conversion Factors for External Gamma
Radiation from Contaminated Soil and Fitting Parameters to Calculate
Depth and Cover Factors (30-day Half-Life Cutoff from FGR 12) (Cont.)**

Radionuclide	Volume Dose Coefficients[a] (mSv/yr per Bq/g)	Fitting Parameters[b]			
		CF_A	CF_B	CF_KA (cm^2/g)	CF_KB (cm^2/g)
Tl-204	1.10E-03	0.868	0.132	2.07E-01	1.88E+00
Tl-206	2.08E-03	0.9	0.1	1.33E-01	1.83E+00
Tl-207	5.35E-03	0.908	0.092	9.70E-02	1.46E+00
Tl-208	6.21E+00	0.096	0.904	9.60E-01	6.30E-02
Tl-209	3.50E+00	0.079	0.921	1.26E+00	7.90E-02
Tm-170	4.04E-03	0.848	0.152	2.20E-01	1.82E+00
Tm-171	3.02E-04	0.815	0.185	3.32E-01	2.16E+00
U-232	2.44E-04	0.809	0.191	1.75E-01	6.12E+00
U-233	3.78E-04	0.889	0.111	1.39E-01	4.28E+00
U-234	1.09E-04	0.723	0.277	1.94E-01	7.34E+00
U-235	1.95E-01	0.933	0.067	1.38E-01	1.65E+00
U-236	5.81E-05	0.593	0.407	1.98E-01	8.40E+00
U-237	1.43E-01	0.904	0.096	1.49E-01	1.65E+00
U-238	2.79E-05	0.397	0.603	4.30E-01	1.01E+01
U-240	3.85E-04	0.49	0.51	3.90E-01	6.46E+00
V-49	0.00E+00	0	1	0.00E+00	0.00E+00
W-181	2.07E-02	0.83	0.17	3.08E-01	2.04E+00
W-185	1.17E-04	0.848	0.152	1.88E-01	2.22E+00
W-188	2.62E-03	0.917	0.083	1.21E-01	1.46E+00
Y-88	4.80E+00	0.096	0.904	9.90E-01	7.10E-02
Y-90	6.46E-03	0.907	0.093	1.18E-01	1.65E+00
Y-91	8.79E-03	0.097	0.903	1.31E+00	8.80E-02
Yb-169	2.98E-01	0.872	0.128	1.44E-01	1.54E+00
Zn-65	1.00E+00	0.073	0.927	1.33E+00	8.40E-02
Zr-88	6.06E-01	0.927	0.073	1.05E-01	1.47E+00
Zr-93	0.00E+00	0	1	0.00E+00	0.00E+00
Zr-95	1.22E+00	0.93	0.07	9.30E-02	1.44E+00

[a] Volume dose coefficients assume infinite thickness.

[b] Fitting parameters are used in depth and cover factor calculations (see
Appendix B).

A dose coefficient for inhalation in FGR 11 is the dose/exposure ratio for the committed effective dose equivalent that is incurred by an individual from exposure by inhalation of the radionuclide in contaminated dust. Inhalation dose coefficients depend on the size of the particle and inhalation class. The inhalation class for inhaled radioactive material is defined according to its rate of clearance from the lung. The three inhalation classes, D, W, and Y, correspond to retention half-times of less than 10 days, 10 to 100 days, and more than 100 days, respectively. FGR-11 Table 2.1 lists exposure-to-dose conversion factors for inhalation. The dose coefficients are for the dust particles with an activity median aerodynamic diameter (AMAD) of 1 µm. The

table lists dose equivalent conversion factors for organ or tissue and committed effective dose equivalent conversion factors based on the ICRP-26 methodology (see Section A.3).

A dose coefficient for ingestion in the FGR 11 is the dose/exposure ratio for the committed effective dose equivalent that an individual incurs from intake by ingestion of the radionuclide. The ingestion dose coefficients depend on the element's chemical form, which determines what fraction of a radionuclide entering the gastrointestinal tract will reach the body fluid. FGR-11 Table 2.2 includes exposure-to-dose conversion factors for ingestion. The table lists dose equivalent conversion factors for organ or tissue and committed effective dose equivalent conversion factor based on the ICRP-26 methodology (see Section A.3). Some elements (antimony, tungsten, mercury, uranium, and plutonium) have different fractional uptakes based on different chemical forms that result in different ingestion dose coefficients. When using the default settings, the RESRAD-OFFSITE code uses the most restrictive dose coefficients.

Table A.2-2 lists the default inhalation and ingestion dose coefficients used in the RESRAD-OFFSITE code for a 30-day half-life cutoff.

Table A.2-2 Default Inhalation and Ingestion Dose Coefficients for 30-day Cutoff Half-Life from FGR 11

Radionuclide[a]	Associated Decay Chain[b]	Inhalation[c] (mSv/Bq)	Ingestion[d] (mSv/Bq)
Ac-227+D	(Th-227 9.8620E-01), Ra-223, Rn-219, Po-215, Pb-211, Bi-211, (Tl-207 9.9720E-01), (Po-211 2.8000E-03), (Fr-223 1.3800E-02)	1.82E+00	4.00E-03
Ag-105	—[e]	1.26E-06	5.51E-07
Ag-108m+D	(Ag-108 8.9000E-02)	7.65E-05	2.06E-06
Ag-110m+D	(Ag-110 1.3300E-02)	2.17E-05	2.92E-06
Al-26	—	2.15E-05	3.95E-06
Am-241	—	1.20E-01	9.84E-04
Am-242m+D	Am-242	1.15E-01	9.49E-04
Am-242m+D1	Am-242	1.15E-01	9.49E-04
Am-242m+D2	Np-238	1.15E-01	9.50E-04
Am-243+D	—	1.19E-01	9.79E-04
As-73	—	9.35E-07	1.91E-07
Au-195	—	3.51E-06	2.87E-07
Ba-133	—	2.11E-06	9.19E-07
Be-10	—	9.57E-05	1.26E-06
Be-7	—	8.68E-08	3.46E-08
Bi-207	—	5.41E-06	1.48E-06
Bi-210m+D	Tl-206	2.05E-03	2.59E-05
Bk-247	—	1.55E-01	1.27E-03
Bk-249	—	3.76E-04	3.24E-06
Bk-249+D	—	3.76E-04	3.29E-06
C-14 particulate	—	5.65E-07	5.65E-07
C-14 gaseous	—	6.35E-09	None

Table A.2-2 Default Inhalation and Ingestion Dose Coefficients for 30-day Cutoff Half-Life from FGR 11 (Cont.)

Radionuclide[a]	Associated Decay Chain[b]	Inhalation[c] (mSv/Bq)	Ingestion[d] (mSv/Bq)
Ca-41	—	3.65E-07	3.43E-07
Ca-45	—	1.79E-06	8.54E-07
Cd-109	—	3.08E-05	3.54E-06
Cd-113	—	4.51E-04	4.70E-05
Cd-113m	—	4.14E-04	4.35E-05
Cd-115m	—	1.95E-05	4.38E-06
Ce-139	—	2.45E-06	3.08E-07
Ce-141	—	2.42E-06	7.84E-07
Ce-144+D	(Pr-144m 0.0178), Pr-144	1.01E-04	5.71E-06
Cf-248	—	1.37E-02	9.03E-05
Cf-249	—	1.56E-01	1.28E-03
Cf-250	—	7.08E-02	5.76E-04
Cf-251	—	1.59E-01	1.31E-03
Cf-252	—	4.24E-02	2.92E-04
Cl-36	—	5.92E-06	8.19E-07
Cm-241	—	3.97E-05	1.21E-06
Cm-242	—	4.68E-03	3.11E-05
Cm-243	—	8.30E-02	6.78E-04
Cm-244	—	6.70E-02	5.46E-04
Cm-245	—	1.23E-01	1.01E-03
Cm-246	—	1.22E-01	1.00E-03
Cm-247+D	—	1.12E-01	9.24E-04
Cm-248	Pu-243	4.46E-01	3.68E-03
Co-56	—	1.07E-05	3.41E-06
Co-57	—	2.45E-06	3.19E-07
Co-58	—	2.95E-06	9.68E-07
Co-60	—	5.92E-05	7.27E-06
Cs-134	—	1.25E-05	1.98E-05
Cs-135	—	1.23E-06	1.91E-06
Cs-137+D	(Ba-137m 0.946)	8.62E-06	1.35E-05
Dy-159	—	6.57E-07	1.20E-07
Es-254+D	Bk-250	1.11E-02	8.48E-05
Eu-148	—	3.87E-06	1.55E-06
Eu-149	—	5.11E-07	1.24E-07
Eu-150b	—	7.24E-05	1.72E-06
Eu-152	—	5.97E-05	1.75E-06
Eu-154	—	7.73E-05	2.58E-06
Eu-155	—	1.12E-05	4.14E-07
Fe-55	—	7.27E-07	1.64E-07
Fe-59	—	4.00E-06	1.81E-06
Fe-60+D	Co-60m	2.02E-04	4.11E-05
Fe-60+D1	Co-60m	2.02E-04	4.11E-05
Fm-257+D	Cf-253, Es-253	8.24E-03	5.37E-05

Table A.2-2 Table A.2-2 Default Inhalation and Ingestion Dose Coefficients for 30-day Cutoff Half-Life from FGR 11 (Cont.)

Radionuclide[a]	Associated Decay Chain[b]	Inhalation[c] (mSv/Bq)	Ingestion[d] (mSv/Bq)
Fm-257+D1	Cf-253, (Es-253 9.9690E-01), (Cm-249 3.1000E-03)	8.24E-03	5.37E-05
Gd-146+D	Eu-146	1.14E-05	2.66E-06
Gd-148	—	8.92E-02	5.89E-05
Gd-151	—	2.40E-06	2.23E-07
Gd-152	—	6.57E-02	4.35E-05
Gd-153	—	6.43E-06	3.16E-07
Ge-68+D	Ga-68	1.40E-05	3.82E-07
H-3	—	1.73E-08	1.73E-08
Hf-172+D	Lu-172	8.73E-05	2.74E-06
Hf-175	—	1.51E-06	4.92E-07
Hf-178m	—	6.65E-04	5.68E-06
Hf-181	—	4.16E-06	1.27E-06
Hf-182	—	8.97E-04	4.30E-06
Hg-194+D	Au-194	4.92E-05	7.84E-05
Hg-203	—	1.98E-06	3.08E-06
Ho-166m	—	2.09E-04	2.18E-06
I-125	—	6.54E-06	1.04E-05
I-129	—	4.70E-05	7.46E-05
In-114m+D	(In-114 0.957)	2.40E-05	4.62E-06
In-115	—	1.01E-03	4.27E-05
Ir-192	—	7.62E-06	1.55E-06
Ir-192m	—	1.04E-04	4.24E-07
Ir-194m	—	1.85E-05	2.46E-06
K-40	—	3.35E-06	5.03E-06
La-137	—	2.37E-05	1.23E-07
La-138	—	3.70E-04	1.59E-06
Lu-173	—	6.08E-06	2.95E-07
Lu-174	—	1.07E-05	3.00E-07
Lu-174m	—	6.87E-06	5.76E-07
Lu-176	—	1.79E-04	1.98E-06
Lu-177m+D	(Lu-177 0.21)	2.00E-05	2.11E-06
Md-258	—	4.46E-03	3.19E-05
Mn-53	—	1.35E-07	2.92E-08
Mn-54	—	1.81E-06	7.49E-07
Mo-93	—	7.68E-06	3.65E-07
Na-22	—	2.07E-06	3.11E-06
Nb-93m	—	7.89E-06	1.41E-07
Nb-94	—	1.12E-04	1.93E-06
Nb-95	—	1.57E-06	6.95E-07
Ni-59	—	7.30E-07	5.68E-08
Ni-63	—	1.70E-06	1.56E-07
Np-235	—	1.12E-06	6.57E-08
Np-236a	—	2.81E-02	2.34E-04

Table A.2-2 Default Inhalation and Ingestion Dose Coefficients for 30-day Cutoff Half-Life from FGR 11 (Cont.)

Radionuclide[a]	Associated Decay Chain[b]	Inhalation[c] (mSv/Bq)	Ingestion[d] (mSv/Bq)
Np-237+D	Pa-233	1.46E-01	1.20E-03
Os-185	—	2.81E-06	6.11E-07
Os-194+D	Ir-194	1.82E-04	4.38E-06
Pa-231	—	3.46E-01	2.87E-03
Pb-202+D	Tl-202	2.68E-05	1.09E-05
Pb-205	—	1.06E-06	4.41E-07
Pb-210+D	Bi-210	3.73E-03	1.45E-03
Pd-107	—	3.46E-06	4.03E-08
Pm-143	—	2.95E-06	2.78E-07
Pm-144	—	1.45E-05	1.17E-06
Pm-145	—	8.24E-06	1.28E-07
Pm-146	—	3.97E-05	9.92E-07
Pm-147	—	1.06E-05	2.84E-07
Pm-148m+D	(Pm-148 0.046)	6.24E-06	2.21E-06
Po-210	—	2.54E-03	5.14E-04
Pt-193	—	6.14E-08	3.22E-08
Pu-236	—	3.92E-02	3.16E-04
Pu-237	—	5.32E-07	1.20E-07
Pu-238	—	1.06E-01	8.65E-04
Pu-239	—	1.16E-01	9.57E-04
Pu-240	—	1.16E-01	9.57E-04
Pu-241	—	2.23E-03	1.85E-05
Pu-241+D	(U-237 0.0000245)	2.23E-03	1.93E-05
Pu-242	—	1.11E-01	9.08E-04
Pu-244	—	1.09E-01	8.97E-04
Pu-244+D	(U-240 0.9988), (Np-240m 0.9988)	1.09E-01	8.99E-04
Ra-226+D	Rn-222,Po-218, (Pb-214 9.9980E-01), Bi-214, (Po-214 9.9980E-01), (Tl-210 2.0000E-04), (At-218 2.0000E-04)	2.32E-03	3.57E-04
Ra-228+D	Ac-228	1.37E-03	3.90E-04
Rb-83+D	(Kr-83m 0.76199)	1.33E-06	2.08E-06
Rb-84	—	1.76E-06	2.70E-06
Rb-87	—	8.73E-07	1.33E-06
Re-184	—	1.39E-06	5.92E-07
Re-184m	—	3.97E-06	7.97E-07
Re-186m+D	Re-186	1.06E-05	1.88E-06
Re-187	—	1.47E-08	2.57E-09
Rh-101	—	1.07E-05	6.27E-07
Rh-102	—	3.24E-05	2.81E-06
Rh-102m	—	1.29E-05	1.27E-06
Ru-103+D	(Rh-103m 0.997)	2.42E-06	8.27E-07
Ru-106+D	Rh-106	1.29E-04	7.41E-06
S-35	—	6.70E-07	1.98E-07

Table A.2-2 Default Inhalation and Ingestion Dose Coefficients for 30-day Cutoff Half-Life from FGR 11 (Cont.)

Radionuclide[a]	Associated Decay Chain[b]	Inhalation[c] (mSv/Bq)	Ingestion[d] (mSv/Bq)
Sb-124	—	6.81E-06	2.73E-06
Sb-125	—	3.30E-06	7.60E-07
Sc-46	—	8.00E-06	1.73E-06
Se-75	—	2.29E-06	2.60E-06
Se-79	—	2.66E-06	2.35E-06
Si-32+D	P-32	2.77E-04	2.96E-06
Sm-145	—	2.97E-06	2.46E-07
Sm-146	—	2.23E-02	5.51E-05
Sm-147	—	2.02E-02	5.00E-05
Sm-151	—	8.11E-06	1.05E-07
Sn-113+D	In-113m	2.90E-06	8.61E-07
Sn-119m	—	1.69E-06	3.76E-07
Sn-121m+D	(Sn-121 0.776)	3.22E-06	6.08E-07
Sn-123	—	8.78E-06	2.27E-06
Sn-126+D	Sb-126m, (Sb-126 0.14)	2.73E-05	5.70E-06
Sr-85	—	1.36E-06	5.35E-07
Sr-89	—	1.12E-05	2.50E-06
Sr-90+D	Y-90	3.54E-04	4.13E-05
Ta-179	—	1.76E-06	7.38E-08
Ta-180	—	6.62E-05	9.81E-07
Ta-182	—	1.21E-05	1.76E-06
Tb-157	—	2.49E-06	3.35E-08
Tb-158	—	6.92E-05	1.19E-06
Tb-160	—	6.76E-06	1.82E-06
Tc-95m+D	(Tc-95 0.04)	1.05E-06	3.97E-07
Tc-97	—	2.68E-07	4.62E-08
Tc-97m	—	1.32E-06	3.35E-07
Tc-98	—	6.19E-06	1.32E-06
Tc-99	—	2.25E-06	3.95E-07
Te-121m+D	(Te-121 0.886)	4.76E-06	2.48E-06
Te-123	—	2.84E-06	1.13E-06
Te-123m	—	2.87E-06	1.53E-06
Te-125m	—	1.97E-06	9.92E-07
Te-127m+D	(Te-127 0.976)	5.90E-06	2.41E-06
Te-129m+D	(Te-129 0.35)	6.48E-06	2.93E-06
Th-228+D	Ra-224, Rn-220, Po-216, Pb-212, Bi-212, (Po-212 0.6407), (Tl-208 0.3593)	9.33E-02	2.19E-04
Th-229+D	Ra-225, Ac-225, Fr-221, At-217, Bi-213, (Po-213 0.9784), (Tl-209 0.0216), Pb-209	5.86E-01	1.09E-03
Th-230	—	8.81E-02	1.48E-04
Th-232	—	4.43E-01	7.38E-04

Table A.2-2 Default Inhalation and Ingestion Dose Coefficients for 30-day Cutoff Half-Life from FGR 11 (Cont.)

Radionuclide[a]	Associated Decay Chain[b]	Inhalation[c] (mSv/Bq)	Ingestion[d] (mSv/Bq)
Ti-44+D	Sc-44	2.76E-04	6.63E-06
Tl-204	—	6.51E-07	9.08E-07
Tm-170	—	7.11E-06	1.43E-06
Tm-171	—	2.47E-06	1.16E-07
U-232	—	1.78E-01	3.54E-04
U-233	—	3.65E-02	7.81E-05
U-234	—	3.57E-02	7.65E-05
U-235+D	—	3.32E-02	7.23E-05
U-236	—	3.38E-02	7.27E-05
U-238	—	3.19E-02	6.89E-05
U-238+D	Th-234, (Pa-234m 0.998), (Pa-234 0.0033)	3.19E-02	7.26E-05
V-49	—	9.32E-08	1.66E-08
W-181	—	4.08E-08	9.30E-08
W-185	—	2.03E-07	5.38E-07
W-188+D	Re-188	1.65E-06	3.37E-06
Y-88	—	7.60E-06	1.62E-06
Y-91	—	1.32E-05	2.57E-06
Yb-169	—	2.18E-06	8.11E-07
Zn-65	—	5.51E-06	3.89E-06
Zr-88	—	6.57E-06	4.03E-07
Zr-93	—	8.68E-05	4.49E-07
Zr-95+D	Nb-95m 0.007	6.38E-06	1.02E-06

[a] Dose coefficients for entries labeled by +D are aggregated dose coefficients for intake of principal radionuclide together with associated radionuclides in the decay chain in secular equilibrium.

[b] The associated radionuclide in the decay chain and their fractions, if the fraction is less than 1.

[c] Inhalation dose coefficients are for most restricted inhalation class and for an AMAD of 1 μm.

[d] Ingestion dose coefficients are for the most restricted chemical type.

[e] Indicate there is no associated radionuclide.

A.2.2   ICRP-60 and ICRP-72 Libraries

ICRP-60 and ICRP-72 (ICRP 1996) dose coefficient libraries are based on the ICRP-38 radionuclide transformation database and use the ICRP-60 dose estimation methodology (see Section A.3). The dose coefficients for six age groups (infant, 1, 5, 10, 15, and adult) are available. Table A.2-3 lists the dose coefficients and fitting parameters used in the RESRAD-OFFSITE code for radionuclides with a 30-day half-life cutoff in external pathway dose calculations. The dose coefficients for principal radionuclides with half-lives longer than 30 days and their associated progeny radionuclides are included in Table A.2-3. Appendix B discusses the fitting parameters.

ICRP-60 uses newer biokinetic models in calculating inhalation and ingestion dose coefficients for six different age groups (3 months, 1 year, 5 year, 10 year, 15 year, and adult). Inhalation class types D (days), W (week), and Y (year) in ICRP 26/30 are replaced with F (fast), M (medium), S (slow), and V (very fast), as applied to gases and vapors in ICRP 60.

Table A.2-4 lists the default inhalation and ingestion dose coefficients from ICRP Publication 72 used in the code for a 30-day cutoff half-life.

Table A.2-3 Effective Dose Coefficients in ICRP-60/ICRP-72 Libraries for External Gamma Radiation from Contaminated Soil and Fitting Parameters Used to Calculate Depth and Cover Factors, 30-day Half-Life Cutoff

Nuclide	Volume Dose Coefficients[a] (mSv/yr per Bq/g)	Fitting Parameters[b]			
		CF_A	CF_B	CF_KA (cm^2/g)	CF_KB (cm^2/g)
Ac-225	1.56E-02	0.914	0.086	1.59E-01	1.77E+00
Ac-227	1.21E-04	0.913	0.087	1.61E-01	2.56E+00
Ac-228	1.53E+00	0.915	0.085	8.44E-02	1.36E+00
Ag-105	7.32E-01	0.906	0.094	9.95E-02	1.27E+00
Ag-108	3.10E-02	0.87	0.131	1.01E-01	6.35E+00
Ag-108m	2.44E+00	0.915	0.085	9.43E-02	1.33E+00
Ag-110	6.41E-02	0.825	0.175	9.69E-02	4.13E+00
Ag-110m	4.38E+00	0.918	0.082	8.56E-02	1.31E+00
Al-26	4.47E+00	0.913	0.087	7.63E-02	1.20E+00
Am-241	1.01E-02	0.836	0.164	3.14E-01	2.88E+00
Am-242	1.22E-02	0.908	0.092	1.75E-01	2.80E+00
Am-242m	3.89E-04	0.745	0.255	1.88E-01	6.65E+00
Am-243	3.37E-02	0.88	0.12	2.38E-01	2.01E+00
Am-245	3.60E-02	0.924	0.076	1.38E-01	3.08E+00
As-73	2.13E-03	0.78	0.22	3.56E-01	2.25E+00
At-217	4.47E-04	0.926	0.074	1.03E-01	1.53E+00
At-218	1.32E-03	0.821	0.179	3.81E-01	3.19E+00
Au-194	1.67E+00	0.911	0.09	8.13E-02	1.24E+00
Au-195	4.91E-02	0.87	0.13	2.38E-01	1.90E+00
Ba-133	4.92E-01	0.911	0.089	1.13E-01	1.53E+00
Ba-137m	9.14E-01	0.916	0.084	9.38E-02	1.34E+00
Be-10	2.74E-04	0.83	0.17	1.69E-01	2.23E+01
Be-7	7.27E-02	0.915	0.085	9.97E-02	1.33E+00
Bi-207	2.39E+00	0.91	0.09	8.63E-02	1.26E+00
Bi-210	1.48E-03	0.53	0.47	1.36E-01	1.58E+01
Bi-210m	3.45E-01	0.919	0.081	1.14E-01	1.41E+00
Bi-211	6.41E-02	0.923	0.077	1.11E-01	1.49E+00
Bi-212	3.01E-01	0.919	0.081	8.44E-02	1.96E+00
Bi-213	1.94E-01	0.919	0.081	1.03E-01	2.19E+00

Table A.2-3 3   Effective Dose Coefficients in ICRP-60/ICRP-72 Libraries for External Gamma Radiation from Contaminated Soil and Fitting Parameters Used for Calculate Depth and Cover Factors, 30-day Half-Life Cutoff (Cont.)

Nuclide	Volume Dose Coefficients[a] (mSv/yr per Bq/g)	Fitting Parameters[b]			
		CF_A	CF_B	CF_KA (cm^2/g)	CF_KB (cm^2/g)
Bi-214	2.52E+00	0.916	0.084	7.69E-02	1.31E+00
Bk-247	1.07E-01	0.914	0.086	1.46E-01	1.69E+00
Bk-249	1.02E-06	0.55	0.45	2.39E-01	3.39E+00
Bk-250	1.42E+00	0.909	0.091	8.24E-02	1.22E+00
C-14	2.99E-06	0.655	0.345	2.88E-01	3.38E+00
Ca-41	0.00E+00	0.918	0.082	6.77E-02	1.13E+00
Ca-45	1.45E-05	0.77	0.23	2.31E-01	2.81E+00
Cd-109	3.31E-03	0.7	0.3	2.12E-01	4.78E+00
Cd-113	2.66E-05	0.79	0.21	2.06E-01	2.53E+00
Cd-113m	1.63E-04	0.82	0.18	1.69E-01	1.83E+01
Cd-115m	3.98E-02	0.884	0.116	8.63E-02	5.64E+00
Ce-139	1.57E-01	0.926	0.074	1.46E-01	2.06E+00
Ce-141	7.83E-02	0.934	0.066	1.55E-01	2.06E+00
Ce-144	1.75E-02	0.91	0.09	1.67E-01	2.01E+00
Cf-248	2.36E-05	0.05	0.95	6.25E-01	7.83E+00
Cf-249	4.65E-01	0.921	0.079	1.08E-01	1.46E+00
Cf-250	2.25E-05	0.05	0.95	6.25E-01	7.84E+00
Cf-251	1.30E-01	0.92	0.08	1.45E-01	1.78E+00
Cf-252	7.98E-01	0.917	0.083	7.44E-02	1.21E+00
Cf-253	1.78E-05	0.77	0.23	2.25E-01	3.25E+00
Cl-36	6.77E-04	0.778	0.222	1.28E-01	2.31E+01
Cm-241	6.62E-01	0.912	0.088	1.08E-01	1.41E+00
Cm-242	3.48E-05	0.27	0.73	1.63E-01	8.68E+00
Cm-243	1.45E-01	0.923	0.077	1.37E-01	1.71E+00
Cm-244	2.42E-05	0.05	0.95	3.13E-01	8.75E+00
Cm-245	8.28E-02	0.92	0.08	1.70E-01	1.88E+00
Cm-246	2.25E-05	0.13	0.87	6.25E-01	9.19E+00
Cm-247	4.47E-01	0.916	0.084	1.06E-01	1.35E+00
Cm-248	2.29E+00	0.916	0.084	7.38E-02	1.19E+00
Cm-249	2.91E-02	0.92	0.08	9.81E-02	3.34E+00
Co-56	6.06E+00	0.912	0.088	7.25E-02	1.15E+00
Co-57	1.23E-01	0.92	0.08	1.59E-01	1.68E+00
Co-58	1.52E+00	0.903	0.097	8.69E-02	1.17E+00
Co-60	4.16E+00	0.914	0.086	7.69E-02	1.21E+00
Co-60m	6.26E-03	0.887	0.113	8.07E-02	1.32E+00
Cs-134	2.40E+00	0.911	0.089	9.00E-02	1.26E+00
Cs-135	8.74E-06	0.75	0.25	2.63E-01	3.13E+00
Cs-137	2.26E-04	0.7	0.3	1.63E-01	1.36E+01
Dy-159	1.21E-02	0.69	0.31	4.13E-01	2.36E+00
Es-253	4.35E-04	0.886	0.114	1.13E-01	3.35E+00
Es-254	3.07E-03	0.79	0.21	1.41E-01	4.25E+00

Table A.2-3   Effective Dose Coefficients in ICRP-60/ICRP-72 Libraries for External Gamma Radiation from Contaminated Soil and Fitting Parameters Used for Calculate Depth and Cover Factors, 30-day Half-Life Cutoff (Cont.)

Nuclide	Volume Dose Coefficients[a] (mSv/yr per Bq/g)	Fitting Parameters[b]			
		CF_A	CF_B	CF_KA (cm^2/g)	CF_KB (cm^2/g)
Eu-146	3.93E+00	0.916	0.084	8.62E-02	1.31E+00
Eu-148	3.33E+00	0.904	0.096	8.81E-02	1.18E+00
Eu-149	4.95E-02	0.862	0.138	1.21E-01	1.86E+00
Eu-150b	2.21E+00	0.916	0.084	9.58E-02	1.36E+00
Eu-152	1.79E+00	0.904	0.096	8.29E-02	1.19E+00
Eu-154	1.97E+00	0.915	0.085	8.31E-02	1.32E+00
Eu-155	4.37E-02	0.88	0.12	1.94E-01	1.81E+00
Fe-55	0.00E+00	0.925	0.075	1.01E-01	1.40E+00
Fe-59	1.96E+00	0.905	0.095	7.75E-02	1.12E+00
Fe-60	2.46E-06	0.61	0.39	2.96E-01	3.39E+00
Fm-257	1.06E-01	0.93	0.07	1.55E-01	2.01E+00
Fr-221	3.82E-02	0.937	0.063	1.31E-01	1.75E+00
Fr-223	4.90E-02	0.867	0.133	1.35E-01	2.88E+00
Ga-68	1.42E+00	0.916	0.084	9.81E-02	1.55E+00
Gd-146	1.95E-01	0.897	0.103	1.69E-01	2.03E+00
Gd-148	0.00E+00	0.822	0.178	1.99E-01	1.93E+00
Gd-151	4.21E-02	0.85	0.15	1.46E-01	1.98E+00
Gd-152	0.00E+00	0.918	0.082	8.36E-02	1.27E+00
Gd-153	5.76E-02	0.83	0.17	2.06E-01	1.97E+00
Ge-68	3.50E-07	0.002	0.998	9.38E-01	3.71E+01
H-3	0.00E+00	1	0	0.00E+00	0.00E+00
Hf-172	5.86E-02	0.78	0.22	2.13E-01	1.68E+00
Hf-175	4.65E-01	0.911	0.089	1.13E-01	1.48E+00
Hf-178m	3.27E+00	0.921	0.079	1.08E-01	1.46E+00
Hf-181	7.63E-01	0.917	0.083	1.08E-01	1.41E+00
Hf-182	3.12E-01	0.914	0.086	1.17E-01	1.36E+00
Hg-194	2.88E-06	0.002	0.998	4.75E-01	2.46E+01
Hg-203	3.16E-01	0.914	0.086	1.14E-01	1.36E+00
Ho-166m	2.61E+00	0.915	0.085	9.43E-02	1.33E+00
I-125	3.23E-03	0.2	0.8	6.25E-01	3.69E+00
I-129	2.60E-03	0.402	0.598	6.35E-01	3.56E+00
In-113m	3.60E-01	0.924	0.076	1.08E-01	1.49E+00
In-114	4.55E-03	0.912	0.088	7.72E-02	1.33E+00
In-114m	1.22E-01	0.913	0.087	1.03E-01	1.48E+00
In-115	9.65E-05	0.846	0.154	1.81E-01	6.56E+00
Ir-192	1.16E+00	0.928	0.072	1.11E-01	1.49E+00
Ir-192m	1.86E-01	0.929	0.071	1.43E-01	1.65E+00
Ir-194	1.42E-01	0.9	0.1	9.81E-02	3.13E+00
Ir-194m	3.44E+00	0.915	0.085	9.88E-02	1.33E+00
K-40	2.69E-01	0.924	0.076	7.56E-02	2.22E+00
Kr-83m	6.82E-06	0.052	0.948	3.63E-01	1.74E+01

Table A.2-3   Effective Dose Coefficients in ICRP-60/ICRP-72 Libraries for External Gamma Radiation from Contaminated Soil and Fitting Parameters Used for Calculate Depth and Cover Factors, 30-day Half-Life Cutoff (Cont.)

| Nuclide | Volume Dose Coefficients[a] (mSv/yr per Bq/g) | Fitting Parameters[b] | | | |
		CF_A	CF_B	CF_KA (cm^2/g)	CF_KB (cm^2/g)
La-137	2.84E-03	0.407	0.593	6.35E-01	3.25E+00
La-138	2.04E+00	0.907	0.093	7.55E-02	1.14E+00
Lu-172	2.94E+00	0.904	0.096	8.28E-02	1.18E+00
Lu-173	1.02E-01	0.844	0.156	1.39E-01	1.56E+00
Lu-174	1.45E-01	0.864	0.136	8.44E-02	1.25E+00
Lu-174m	3.49E-02	0.709	0.291	1.37E-01	1.31E+00
Lu-176	6.31E-01	0.918	0.082	1.18E-01	1.46E+00
Lu-177	3.92E-02	0.919	0.081	1.37E-01	1.66E+00
Lu-177m	1.25E+00	0.915	0.085	1.19E-01	1.49E+00
Md-258	5.04E-04	0.644	0.356	2.39E-01	5.43E+00
Mn-53	0.00E+00	0.919	0.081	8.18E-02	1.24E+00
Mn-54	1.31E+00	0.909	0.091	8.60E-02	1.23E+00
Mo-93	1.13E-04	0.002	0.998	3.13E-01	1.09E+01
Na-22	3.48E+00	0.919	0.081	8.54E-02	1.32E+00
Nb-93m	1.99E-05	0.002	0.998	3.13E-01	1.09E+01
Nb-94	2.47E+00	0.913	0.087	8.75E-02	1.28E+00
Nb-95	1.20E+00	0.91	0.09	8.81E-02	1.23E+00
Nb-95m	7.93E-02	0.937	0.063	1.27E-01	1.83E+00
Ni-59	0.00E+00	0.844	0.156	1.20E-01	1.30E+00
Ni-63	0.00E+00	0.925	0.075	9.77E-02	1.39E+00
Np-235	7.63E-04	0.843	0.157	1.94E-01	6.50E+00
Np-236a	1.13E-01	0.916	0.084	1.67E-01	1.88E+00
Np-237	1.88E-02	0.9	0.1	1.88E-01	2.55E+00
Np-238	8.79E-01	0.911	0.089	8.31E-02	1.29E+00
Np-239	1.86E-01	0.918	0.082	1.37E-01	1.65E+00
Np-240m	5.15E-01	0.916	0.084	9.00E-02	1.81E+00
Os-185	1.06E+00	0.908	0.092	9.25E-02	1.29E+00
Os-194	2.53E-04	0.64	0.36	4.19E-01	2.57E+00
P-32	5.51E-03	0.475	0.525	1.25E-01	9.19E+00
Pa-231	4.76E-02	0.93	0.07	1.18E-01	2.03E+00
Pa-233	2.55E-01	0.923	0.077	1.20E-01	1.57E+00
Pa-234	2.94E+00	0.914	0.086	8.81E-02	1.31E+00
Pa-234m	2.67E-02	0.78	0.22	8.94E-02	5.50E+00
Pb-202	1.99E-06	0.002	0.998	7.50E-01	3.04E+01
Pb-205	2.22E-06	0.002	0.998	5.63E-01	2.97E+01
Pb-209	2.04E-04	0.802	0.198	1.69E-01	2.43E+01
Pb-210	5.35E-04	0.89	0.11	5.72E-01	6.88E+00
Pb-211	7.88E-02	0.921	0.079	9.56E-02	3.74E+00
Pb-212	1.75E-01	0.937	0.063	1.34E-01	1.91E+00
Pb-214	3.36E-01	0.917	0.083	1.11E-01	1.49E+00
Pd-107	0.00E+00	0.932	0.068	1.13E-01	1.51E+00

Table A.2-3   Effective Dose Coefficients in ICRP-60/ICRP-72 Libraries for External Gamma Radiation from Contaminated Soil and Fitting Parameters Used for Calculate Depth and Cover Factors, 30-day Half-Life Cutoff (Cont.)

Nuclide	Volume Dose Coefficients[a] (mSv/yr per Bq/g)	Fitting Parameters[b]			
		CF_A	CF_B	CF_KA (cm^2/g)	CF_KB (cm^2/g)
Pm-143	4.50E-01	0.904	0.096	8.94E-02	1.33E+00
Pm-144	2.34E+00	0.911	0.089	9.31E-02	1.30E+00
Pm-145	6.26E-03	0.57	0.43	3.91E-01	2.56E+00
Pm-146	1.12E+00	0.914	0.086	9.44E-02	1.36E+00
Pm-147	1.17E-05	0.79	0.21	2.13E-01	2.81E+00
Pm-148	9.45E-01	0.917	0.083	8.13E-02	1.56E+00
Pm-148m	3.05E+00	0.908	0.092	9.13E-02	1.24E+00
Po-210	1.33E-05	0.912	0.088	8.75E-02	1.26E+00
Po-211	1.21E-02	0.916	0.084	9.00E-02	1.33E+00
Po-212	0.00E+00	1	0	0.00E+00	0.00E+00
Po-213	0.00E+00	1	0	0.00E+00	0.00E+00
Po-214	1.31E-04	0.914	0.086	8.88E-02	1.28E+00
Po-215	2.56E-04	0.919	0.081	1.03E-01	1.38E+00
Po-216	2.66E-05	0.916	0.084	8.88E-02	1.33E+00
Po-218	1.44E-05	0.916	0.084	8.75E-02	1.31E+00
Pr-144	7.22E-02	0.832	0.168	7.94E-02	3.84E+00
Pr-144m	3.25E-03	0.56	0.44	1.21E-01	2.16E+00
Pt-193	1.71E-06	0.002	0.998	5.63E-01	2.85E+01
Pu-236	4.90E-05	0.456	0.544	1.75E-01	8.56E+00
Pu-237	3.93E-02	0.928	0.072	1.89E-01	2.31E+00
Pu-238	3.15E-05	0.33	0.67	1.96E-01	9.19E+00
Pu-239	7.12E-05	0.824	0.176	1.33E-01	6.56E+00
Pu-240	3.05E-05	0.33	0.67	1.96E-01	9.19E+00
Pu-241	1.44E-06	0.922	0.078	1.78E-01	2.75E+00
Pu-242	2.69E-05	0.36	0.64	1.94E-01	9.03E+00
Pu-243	1.92E-02	0.894	0.106	1.81E-01	1.98E+00
Pu-244	3.73E-02	0.915	0.085	7.38E-02	1.22E+00
Ra-223	1.50E-01	0.916	0.084	1.33E-01	1.61E+00
Ra-224	1.28E-02	0.937	0.063	1.28E-01	1.66E+00
Ra-225	2.33E-03	0.666	0.334	5.72E-01	3.19E+00
Ra-226	7.88E-03	0.927	0.073	1.36E-01	1.64E+00
Ra-228	0.00E+00	1	0	0.00E+00	0.00E+00
Rb-83	7.42E-01	0.925	0.075	9.88E-02	1.49E+00
Rb-84	1.42E+00	0.914	0.086	8.87E-02	1.31E+00
Rb-87	3.29E-05	0.8	0.2	2.13E-01	2.66E+00
Re-184	1.33E+00	0.908	0.092	8.88E-02	1.28E+00
Re-184m	5.15E-01	0.897	0.103	9.88E-02	1.28E+00
Re-186	1.95E-02	0.887	0.113	1.63E-01	5.06E+00
Re-186m	6.37E-03	0.856	0.144	3.13E-01	2.55E+00
Re-187	0.00E+00	0.904	0.096	1.26E-01	1.49E+00
Re-188	8.44E-02	0.88	0.12	1.05E-01	3.75E+00

Table A.2-3 Effective Dose Coefficients in ICRP-60/ICRP-72 Libraries for External Gamma Radiation from Contaminated Soil and Fitting Parameters Used for Calculate Depth and Cover Factors, 30-day Half-Life Cutoff (Cont.)

Nuclide	Volume Dose Coefficients[a] (mSv/yr per Bq/g)	Fitting Parameters[b]			
		CF_A	CF_B	CF_KA (cm²/g)	CF_KB (cm²/g)
Rh-101	3.04E-01	0.927	0.073	1.36E-01	1.69E+00
Rh-102	3.29E+00	0.915	0.085	9.00E-02	1.31E+00
Rh-102m	7.17E-01	0.906	0.094	9.38E-02	1.33E+00
Rh-103m	4.60E-05	0.11	0.89	6.25E-01	6.78E+00
Rh-106	3.37E-01	0.898	0.102	9.50E-02	2.33E+00
Rn-219	7.73E-02	0.925	0.075	1.11E-01	1.49E+00
Rn-220	5.76E-04	0.925	0.075	9.88E-02	1.49E+00
Rn-222	5.91E-04	0.926	0.074	1.01E-01	1.49E+00
Ru-103	6.92E-01	0.915	0.085	9.94E-02	1.33E+00
Ru-106	0.00E+00	0.925	0.075	9.56E-02	1.52E+00
S-35	3.32E-06	0.67	0.33	2.81E-01	3.29E+00
Sb-124	3.00E+00	0.907	0.093	7.75E-02	1.16E+00
Sb-125	6.16E-01	0.919	0.081	1.00E-01	1.44E+00
Sb-126	4.34E+00	0.909	0.091	9.00E-02	1.26E+00
Sb-126m	2.36E+00	0.914	0.086	9.38E-02	1.40E+00
Sc-44	3.37E+00	0.909	0.091	8.56E-02	1.29E+00
Sc-46	3.24E+00	0.915	0.085	8.24E-02	1.27E+00
Se-75	4.95E-01	0.932	0.068	1.26E-01	1.67E+00
Se-79	4.16E-06	0.68	0.32	2.88E-01	3.31E+00
Si-32	8.08E-06	0.733	0.267	2.56E-01	2.98E+00
Sm-145	1.48E-02	0.6	0.4	3.69E-01	2.42E+00
Sm-146	0.00E+00	0.925	0.075	1.01E-01	1.40E+00
Sm-147	0.00E+00	0.919	0.081	8.72E-02	1.30E+00
Sm-151	1.83E-07	0.04	0.96	6.25E-01	6.38E+00
Sn-113	7.17E-03	0.825	0.175	1.20E-01	3.56E+00
Sn-119m	5.71E-04	0.1	0.9	6.25E-01	4.54E+00
Sn-121	4.65E-05	0.82	0.18	1.96E-01	2.46E+00
Sn-121m	3.89E-04	0.3	0.7	6.25E-01	3.94E+00
Sn-123	1.43E-02	0.83	0.17	8.50E-02	8.00E+00
Sn-126	3.52E-02	0.88	0.12	2.10E-01	2.06E+00
Sr-85	7.48E-01	0.918	0.082	9.88E-02	1.38E+00
Sr-89	4.09E-03	0.49	0.51	1.25E-01	1.03E+01
Sr-90	1.75E-04	0.858	0.142	1.88E-01	1.97E+01
Ta-179	1.32E-02	0.82	0.18	3.25E-01	2.18E+00
Ta-180	6.97E-01	0.917	0.083	1.19E-01	1.52E+00
Ta-182	2.03E+00	0.906	0.094	8.06E-02	1.19E+00
Tb-157	6.26E-04	0.7	0.3	4.69E-01	2.61E+00
Tb-158	1.20E+00	0.908	0.092	8.63E-02	1.28E+00
Tb-160	1.77E+00	0.907	0.093	8.40E-02	1.20E+00
Tc-95	1.23E+00	0.916	0.084	8.94E-02	1.31E+00
Tc-95m	9.95E-01	0.911	0.089	9.38E-02	1.28E+00

Table A.2-3   Effective Dose Coefficients in ICRP-60/ICRP-72 Libraries for External Gamma Radiation from Contaminated Soil and Fitting Parameters Used for Calculate Depth and Cover Factors, 30-day Half-Life Cutoff (Cont.)

Nuclide	Volume Dose Coefficients[a] (mSv/yr per Bq/g)	Fitting Parameters[b]			
		CF_A	CF_B	CF_KA (cm^2/g)	CF_KB (cm^2/g)
Tc-97	1.53E-04	0.002	0.998	3.13E-01	9.62E+00
Tc-97m	4.15E-04	0.582	0.418	1.98E-01	7.81E+00
Tc-98	2.18E+00	0.904	0.096	8.94E-02	1.17E+00
Tc-99	2.94E-05	0.8	0.2	2.13E-01	2.63E+00
Te-121	8.38E-01	0.921	0.079	9.81E-02	1.46E+00
Te-121m	2.68E-01	0.923	0.077	1.19E-01	1.59E+00
Te-123	1.26E-03	0.13	0.87	6.25E-01	4.04E+00
Te-123m	1.55E-01	0.924	0.076	1.45E-01	1.78E+00
Te-125m	3.01E-03	0.25	0.75	3.88E-01	3.63E+00
Te-127	7.22E-03	0.922	0.078	1.08E-01	4.50E+00
Te-127m	1.13E-03	0.34	0.66	1.86E-01	3.54E+00
Te-129	8.49E-02	0.907	0.093	9.88E-02	3.59E+00
Te-129m	4.75E-02	0.9	0.1	9.25E-02	2.93E+00
Th-227	1.30E-01	0.927	0.073	1.24E-01	1.72E+00
Th-228	1.94E-03	0.913	0.087	1.59E-01	2.31E+00
Th-229	7.83E-02	0.91	0.09	1.67E-01	1.86E+00
Th-230	2.90E-04	0.862	0.138	1.87E-01	3.88E+00
Th-231	8.69E-03	0.872	0.128	1.96E-01	3.09E+00
Th-232	1.23E-04	0.815	0.185	2.06E-01	5.38E+00
Th-234	5.76E-03	0.891	0.109	2.09E-01	2.07E+00
Ti-44	8.49E-02	0.863	0.137	2.38E-01	1.74E+00
Tl-202	6.26E-01	0.912	0.088	1.08E-01	1.41E+00
Tl-204	1.05E-03	0.81	0.19	2.13E-01	1.63E+01
Tl-206	3.41E-03	0.5	0.5	1.31E-01	1.11E+01
Tl-207	6.21E-03	0.735	0.265	9.88E-02	1.04E+01
Tl-208	5.91E+00	0.911	0.089	6.63E-02	1.10E+00
Tl-209	3.31E+00	0.91	0.09	7.75E-02	1.24E+00
Tl-210	4.49E+00	0.913	0.087	7.88E-02	1.29E+00
Tm-170	3.81E-03	0.785	0.215	2.13E-01	9.36E+00
Tm-171	2.55E-04	0.8	0.2	3.25E-01	2.15E+00
U-232	2.15E-04	0.82	0.18	1.75E-01	5.81E+00
U-233	3.42E-04	0.889	0.111	1.39E-01	3.88E+00
U-234	9.30E-05	0.75	0.25	1.97E-01	7.38E+00
U-235	1.78E-01	0.928	0.072	1.38E-01	1.68E+00
U-236	4.81E-05	0.62	0.38	2.00E-01	8.39E+00
U-237	1.30E-01	0.914	0.086	1.54E-01	1.88E+00
U-238	2.15E-05	0.46	0.54	5.00E-01	1.11E+01
U-240	3.01E-04	0.51	0.49	3.88E-01	6.39E+00
V-49	0.00E+00	0.921	0.079	1.02E-01	1.37E+00
W-181	1.76E-02	0.79	0.21	2.88E-01	1.86E+00
W-185	1.04E-04	0.86	0.14	1.94E-01	2.53E+00

Table A.2-3   Effective Dose Coefficients in ICRP-60/ICRP-72 Libraries for External Gamma Radiation from Contaminated Soil and Fitting Parameters Used for Calculate Depth and Cover Factors, 30-day Half-Life Cutoff (Cont.)

Nuclide	Volume Dose Coefficients[a] (mSv/yr per Bq/g)	Fitting Parameters[b]			
		CF_A	CF_B	CF_KA (cm^2/g)	CF_KB (cm^2/g)
W-188	2.41E-03	0.932	0.068	1.26E-01	1.79E+00
Y-88	4.57E+00	0.912	0.088	7.25E-02	1.14E+00
Y-90	1.09E-02	0.52	0.48	1.25E-01	6.56E+00
Y-91	1.03E-02	0.735	0.265	8.88E-02	8.44E+00
Yb-169	2.70E-01	0.887	0.113	1.49E-01	1.71E+00
Zn-65	9.50E-01	0.909	0.091	7.88E-02	1.18E+00
Zr-88	5.61E-01	0.92	0.08	1.08E-01	1.38E+00
Zr-93	0.00E+00	0.918	0.082	7.53E-02	1.19E+00
Zr-95	1.15E+00	0.908	0.092	8.94E-02	1.21E+00

[a]   Volume dose coefficients assume infinite thickness.

[b]   Fitting parameters are used in depth and cover factor calculations (see Appendix B).

Table A.2-4   Default Inhalation and Ingestion Dose Coefficients for 30-day Cutoff Half-Life from ICRP 72 for Adult

Radionuclide[a]	Associated Decay Chain[b]	Inhalation[c] (mSv/Bq)	Ingestion[d] (mSv/Bq)
Ac-227+D	(Th-227 9.8620E-01), Ra-223, Rn-219, Po-215, Pb-211, Bi-211, (Tl-207 9.9720E-01), (Po-211 2.8000E-03), (Fr-223 1.3800E-02)	5.69E-01	1.21E-03
Ag-105	—[e]	8.10E-07	4.70E-07
Ag-108m+D	(Ag-108 8.9000E-02)	3.70E-05	2.30E-06
Ag-110m+D	(Ag-110 1.3300E-02)	1.20E-05	2.80E-06
Al-26	—	2.00E-05	3.50E-06
Am-241	—	9.60E-02	2.00E-04
Am-242m+D	Am-242	9.20E-02	1.90E-04
Am-242m+D1	Am-242	9.20E-02	1.90E-04
Am-242m+D2	Np-238	9.20E-02	1.91E-04
Am-243+D	—	9.60E-02	2.01E-04
As-73	—	1.00E-06	2.60E-07
Au-195	—	1.70E-06	2.50E-07
Ba-133	—	1.00E-05	1.50E-06
Be-10	—	3.50E-05	1.10E-06
Be-7	—	5.50E-08	2.80E-08
Bi-207	—	5.60E-06	1.30E-06

Table A.2-4 Default Inhalation and Ingestion Dose Coefficients for 30-day Cutoff Half-Life from ICRP 72 for Adult (Cont.)

Radionuclide[a]	Associated Decay Chain[b]	Inhalation[c] (mSv/Bq)	Ingestion[d] (mSv/Bq)
Bi-210m+D	Tl-206	3.40E-03	1.50E-05
Bk-247	—	6.90E-02	3.50E-04
Bk-249	—	1.60E-04	9.70E-07
Bk-249+D	—	1.60E-04	1.03E-06
C-14 particulates	—	5.80E-06	5.80E-07
C-14 gaseous	—	6.20E-09	None
Ca-41	—	1.80E-07	1.90E-07
Ca-45	—	3.70E-06	7.10E-07
Cd-109	—	8.10E-06	2.00E-06
Cd-113	—	1.20E-04	2.50E-05
Cd-113m	—	1.10E-04	2.30E-05
Cd-115m	—	7.70E-06	3.30E-06
Ce-139	—	1.90E-06	2.60E-07
Ce-141	—	3.80E-06	7.10E-07
Ce-144+D	(Pr-144m 0.0178), Pr-144	5.30E-05	5.25E-06
Cf-248	—	8.80E-03	2.80E-05
Cf-249	—	7.00E-02	3.50E-04
Cf-250	—	3.40E-02	1.60E-04
Cf-251	—	7.10E-02	3.60E-04
Cf-252	—	2.00E-02	9.00E-05
Cl-36	—	7.30E-06	9.30E-07
Cm-241	—	3.70E-05	9.10E-07
Cm-242	—	5.90E-03	1.20E-05
Cm-243	—	6.90E-02	1.50E-04
Cm-244	—	5.70E-02	1.20E-04
Cm-245	—	9.90E-02	2.10E-04
Cm-246	—	9.80E-02	2.10E-04
Cm-247+D	—	9.00E-02	1.90E-04
Cm-248	Pu-243	3.60E-01	7.70E-04
Co-56	—	6.70E-06	2.50E-06
Co-57	—	1.00E-06	2.10E-07
Co-58	—	2.10E-06	7.40E-07
Co-60	—	3.10E-05	3.40E-06
Cs-134	—	2.00E-05	1.90E-05
Cs-135	—	8.60E-06	2.00E-06
Cs-137+D	(Ba-137m 0.946)	3.90E-05	1.30E-05
Dy-159	—	3.70E-07	1.00E-07
Es-254+D	Bk250	8.60E-03	2.81E-05
Eu-148	—	2.60E-06	1.30E-06
Eu-149	—	2.90E-07	1.00E-07
Eu-150b	—	5.30E-05	1.30E-06
Eu-152	—	4.20E-05	1.40E-06
Eu-154	—	5.30E-05	2.00E-06

Table A.2-4 Default Inhalation and Ingestion Dose Coefficients for 30-day Cutoff Half-Life from ICRP 72 for Adult (Cont.)

Radionuclide[a]	Associated Decay Chain[b]	Inhalation[c] (mSv/Bq)	Ingestion[d] (mSv/Bq)
Eu-155	—	6.90E-06	3.20E-07
Fe-55	—	7.70E-07	3.30E-07
Fe-59	—	4.00E-06	1.80E-06
Fe-60+D	Co-60m	2.80E-04	1.10E-04
Fe-60+D1	Co-60m	2.80E-04	1.10E-04
Fm-257+D	Cf-253, Es-253	1.11E-02	2.25E-05
Fm-257+D1	Cf-253, (Es-253 9.9690E-01), (Cm-249 3.1000E-03)	1.11E-02	2.25E-05
Gd-146+D	Eu-146	7.20E-06	2.26E-06
Gd-148	—	2.60E-02	5.60E-05
Gd-151	—	8.60E-07	2.00E-07
Gd-152	—	1.90E-02	4.10E-05
Gd-153	—	2.10E-06	2.70E-07
Ge-68+D	Ga-68	1.41E-05	1.40E-06
H-3	—	2.60E-07	4.20E-08
Hf-172+D	Lu-172	3.36E-05	2.30E-06
Hf-175	—	1.20E-06	4.10E-07
Hf-178m	—	2.60E-04	4.70E-06
Hf-181	—	5.00E-06	1.10E-06
Hf-182	—	3.10E-04	3.00E-06
Hg-194+D	Au-194	4.02E-05	5.14E-05
Hg-203	—	7.00E-06	1.90E-06
Ho-166m	—	1.20E-04	2.00E-06
I-125	—	1.40E-05	1.50E-05
I-129	—	9.60E-05	1.10E-04
In-114m+D	(In-114 0.957)	9.30E-06	4.10E-06
In-115	—	3.90E-04	3.20E-05
Ir-192	—	6.60E-06	1.40E-06
Ir-192m	—	3.90E-05	3.10E-07
Ir-194m	—	1.30E-05	2.10E-06
K-40	—	2.10E-06	6.20E-06
La-137	—	8.70E-06	8.10E-08
La-138	—	1.50E-04	1.10E-06
Lu-173	—	2.40E-06	2.60E-07
Lu-174	—	4.20E-06	2.70E-07
Lu-174m	—	4.20E-06	5.30E-07
Lu-176	—	7.00E-05	1.80E-06
Lu-177m+D	(Lu-177 0.21)	1.63E-05	1.81E-06
Md-258	—	5.90E-03	1.30E-05
Mn-53	—	5.40E-08	3.00E-08
Mn-54	—	1.50E-06	7.10E-07
Mo-93	—	2.30E-06	3.10E-06
Na-22	—	1.30E-06	3.20E-06
Nb-93m	—	1.80E-06	1.20E-07

Table A.2-4 Default Inhalation and Ingestion Dose Coefficients for 30-day Cutoff Half-Life from ICRP 72 for Adult (Cont.)

Radionuclide[a]	Associated Decay Chain[b]	Inhalation[c] (mSv/Bq)	Ingestion[d] (mSv/Bq)
Nb-94	—	4.90E-05	1.70E-06
Nb-95	—	1.80E-06	5.80E-07
Ni-59	—	8.30E-07	6.30E-08
Ni-63	—	2.00E-06	1.50E-07
Np-235	—	6.30E-07	5.30E-08
Np-236a	—	8.00E-03	1.70E-05
Np-237+D	Pa-233	5.00E-02	1.11E-04
Os-185	—	1.60E-06	5.10E-07
Os-194+D	Ir-194	8.56E-05	3.70E-06
Pa-231	—	1.40E-01	7.10E-04
Pb-202+D	Tl-202	1.22E-05	9.25E-06
Pb-205	—	8.50E-07	2.80E-07
Pb-210+D	Bi-210	5.69E-03	6.91E-04
Pd-107	—	5.90E-07	3.70E-08
Pm-143	—	1.50E-06	2.30E-07
Pm-144	—	8.20E-06	9.70E-07
Pm-145	—	3.60E-06	1.10E-07
Pm-146	—	2.10E-05	9.00E-07
Pm-147	—	5.00E-06	2.60E-07
Pm-148m+D	(Pm-148 0.046)	5.80E-06	1.82E-06
Po-210	—	4.30E-03	1.20E-03
Pt-193	—	2.10E-08	3.10E-08
Pu-236	—	4.00E-02	8.70E-05
Pu-237	—	3.90E-07	1.00E-07
Pu-238	—	1.10E-01	2.30E-04
Pu-239	—	1.20E-01	2.50E-04
Pu-240	—	1.20E-01	2.50E-04
Pu-241	—	2.30E-03	4.80E-06
Pu-241+D	(U-237 0.0000245)	2.30E-03	5.56E-06
Pu-242	—	1.10E-01	2.40E-04
Pu-244	—	1.10E-01	2.40E-04
Pu-244+D	(U-240 0.9988), (Np-240m 0.9988)	1.10E-01	2.41E-04
Ra-226+D	Rn-222, Po-218, (Pb-214 9.9980E-01), Bi-214, (Po-214 9.9980E-01), (Tl-210 2.0000E-04), (At-218 2.0000E-04)	9.53E-03	2.80E-04
Ra-228+D	Ac-228	1.60E-02	6.90E-04
Rb-83+D	(Kr-83m 0.76199)	6.90E-07	1.90E-06
Rb-84	—	1.00E-06	2.80E-06
Rb-87	—	5.00E-07	1.50E-06
Re-184	—	1.90E-06	1.00E-06
Re-184m	—	6.50E-06	1.50E-06
Re-186m+D	Re-186	1.31E-05	3.70E-06
Re-187	—	6.30E-09	5.10E-09

Table A.2-4 Default Inhalation and Ingestion Dose Coefficients for 30-day Cutoff Half-Life from ICRP 72 for Adult (Cont.)

Radionuclide[a]	Associated Decay Chain[b]	Inhalation[c] (mSv/Bq)	Ingestion[d] (mSv/Bq)
Rh-101	—	5.40E-06	5.50E-07
Rh-102	—	1.70E-05	2.60E-06
Rh-102m	—	7.10E-06	1.20E-06
Ru-103+D	(Rh-103m 0.997)	3.00E-06	7.34E-07
Ru-106+D	Rh-106	6.60E-05	7.00E-06
S-35	—	1.90E-06	7.70E-07
Sb-124	—	8.60E-06	2.50E-06
Sb-125	—	1.20E-05	1.10E-06
Sc-46	—	6.80E-06	1.50E-06
Se-75	—	1.30E-06	2.60E-06
Se-79	—	6.80E-06	2.90E-06
Si-32+D	P-32	1.13E-04	2.96E-06
Sm-145	—	1.60E-06	2.10E-07
Sm-146	—	1.10E-02	5.40E-05
Sm-147	—	9.60E-03	4.90E-05
Sm-151	—	4.00E-06	9.80E-08
Sn-113+D	In-113m	2.72E-06	7.58E-07
Sn-119m	—	2.20E-06	3.40E-07
Sn-121m+D	(Sn-121 0.776)	4.68E-06	5.59E-07
Sn-123	—	8.10E-06	2.10E-06
Sn-126+D	Sb-126m, (Sb-126 0.14)	2.85E-05	5.07E-06
Sr-85	—	8.10E-07	5.60E-07
Sr-89	—	7.90E-06	2.60E-06
Sr-90+D	Y-90	1.62E-04	3.07E-05
Ta-179	—	5.60E-07	6.50E-08
Ta-180	—	2.60E-05	8.40E-07
Ta-182	—	1.00E-05	1.50E-06
Tb-157	—	1.20E-06	3.40E-08
Tb-158	—	4.60E-05	1.10E-06
Tb-160	—	7.00E-06	1.60E-06
Tc-95m+D	(Tc-95 0.04)	1.20E-06	5.67E-07
Tc-97	—	1.80E-06	6.80E-08
Tc-97m	—	4.10E-06	5.50E-07
Tc-98	—	4.50E-05	2.00E-06
Tc-99	—	1.30E-05	6.40E-07
Te-121m+D	(Te-121 0.886)	6.15E-06	2.68E-06
Te-123	—	1.20E-05	4.40E-06
Te-123m	—	5.10E-06	1.40E-06
Te-125m	—	4.20E-06	8.70E-07
Te-127m+D	(Te-127 0.976)	9.94E-06	2.47E-06
Te-129m+D	(Te-129 0.35)	7.93E-06	3.04E-06
Th-228+D	Ra-224, Rn-220, Po-216, Pb-212, Bi-212, (Po-212 0.6407), (Tl-208 0.3593)	4.36E-02	1.43E-04

Table A.2-4 Default Inhalation and Ingestion Dose Coefficients for 30-day Cutoff Half-Life from ICRP 72 for Adult (Cont.)

Radionuclide[a]	Associated Decay Chain[b]	Inhalation[c] (mSv/Bq)	Ingestion[d] (mSv/Bq)
Th-229+D	Ra-225, Ac-225, Fr-221, At-217, Bi-213, (Po-213 0.9784), (Tl-209 0.0216), Pb-209	2.56E-01	6.13E-04
Th-230	—	1.00E-01	2.10E-04
Th-232	—	1.10E-01	2.30E-04
Ti-44+D	Sc-44	1.20E-04	6.15E-06
Tl-204	—	3.90E-07	1.20E-06
Tm-170	—	7.00E-06	1.30E-06
Tm-171	—	1.40E-06	1.10E-07
U-232	—	3.70E-02	3.30E-04
U-233	—	9.60E-03	5.10E-05
U-234	—	9.40E-03	4.90E-05
U-235+D	—	8.50E-03	4.73E-05
U-236	—	8.70E-03	4.70E-05
U-238	—	8.00E-03	4.50E-05
U-238+D	Th-234, (Pa-234m 0.998), (Pa-234 0.0033)	8.01E-03	4.84E-05
V-49	—	3.40E-08	1.80E-08
W-181	—	2.70E-08	7.60E-08
W-185	—	1.20E-07	4.40E-07
W-188+D	Re-188	1.11E-06	3.50E-06
Y-88	—	4.40E-06	1.30E-06
Y-91	—	8.90E-06	2.40E-06
Yb-169	—	3.00E-06	7.10E-07
Zn-65	—	2.20E-06	3.90E-06
Zr-88	—	3.60E-06	4.50E-07
Zr-93	—	2.50E-05	1.10E-06
Zr-95+D	Nb-95m 0.007	5.91E-06	9.54E-07

[a] Dose coefficients for entries labeled with +D are aggregated dose coefficients for intake of principal radionuclide together with associated radionuclides in the decay chain in secular equilibrium.

[b] The associated radionuclide in the decay chain and their fractions, if the fraction is less than 1.

[c] Inhalation dose coefficients are for most restricted inhalation class and for an AMAD of 1 µm.

[d] Ingestion dose coefficients are for most restricted chemical type.

[e] Indicate no associated radionuclide.

A.2.3 Dose Coefficient File Package 3.02 Libraries

Dose Coefficient File Package (DCFPAK) 3.02 libraries use the ICRP-107 (ICRP 2008) radionuclide transformation database and ICRP-60 dose estimation methodology (see Section A.3). The dose coefficients for six age groups (infant, 1, 5, 10, 15, and adult) and for a

reference person are available. The reference person is defined as a hypothetical aggregation of human (male and female) physical and physiological characteristics arrived at by international consensus for standardizing radiation dose calculations. The reference person dose coefficients are derived using age-specific dose coefficients coupled with information on the age and gender structure of the U.S. population in 2000 census data and age- and gender-specific intakes (DOE 2011).

Table A.2-5 lists the dose coefficients and fitting parameters from the DCFPAK3.02 libraries used in RESRAD-OFFSITE for radionuclides with a 30-day half-life cutoff in external pathway dose calculations. The dose coefficients for principal radionuclides with half-lives longer than 30 days and their associated progeny radionuclides are included in Table A.2-5. Appendix B discusses the fitting parameters. Table A.2-6 lists the default inhalation and ingestion dose coefficients from DCFPAK 3.02 libraries used in the code for a 30-day half-life cutoff.

Table A.2-5 Effective Dose Coefficients in DCFPAK3.02 Libraries for External Gamma Radiation from Contaminated Soil and Fitting Parameters Used to Calculate Depth and Cover Factors, 30-day Half-life Cutoff

Nuclide	Volume Dose Coefficients[a] (mSv/yr per Bq/g)	Fitting Parameters[b]			
		CF_A	CF_B	CF_KA (cm^2/g)	CF_KB (cm^2/g)
Ac-225	1.43E-02	0.091	0.909	1.73E+00	1.47E-01
Ac-227	7.07E-05	0.165	0.835	5.57E+00	1.66E-01
Ac-228	1.36E+00	0.119	0.881	1.01E+00	8.05E-02
Ag-105	7.17E-01	0.097	0.903	1.24E+00	9.95E-02
Ag-108	3.19E-02	0.135	0.865	5.94E+00	9.82E-02
Ag-108m	2.43E+00	0.098	0.902	1.18E+00	9.31E-02
Ag-110	6.41E-02	0.184	0.816	3.94E+00	9.52E-02
Ag-110m	4.40E+00	0.12	0.88	9.30E-01	8.03E-02
Al-26	4.46E+00	0.134	0.866	8.14E-01	6.97E-02
Am-241	1.01E-02	0.175	0.825	2.46E+00	3.08E-01
Am-242	1.22E-02	0.08	0.92	3.15E+00	1.80E-01
Am-242m	2.87E-04	0.317	0.683	6.80E+00	1.75E-01
Am-243	3.47E-02	0.123	0.877	1.97E+00	2.38E-01
Am-245	3.59E-02	0.073	0.927	3.17E+00	1.39E-01
Am-246m	1.57E+00	0.109	0.891	1.09E+00	8.04E-02
As-73	2.11E-03	0.188	0.812	2.47E+00	3.74E-01
At-217	3.21E-04	0.086	0.914	1.39E+00	1.13E-01
At-218	1.51E-05	0.482	0.518	5.31E+00	1.14E-01
At-219	0.00E+00	0	1	0.00E+00	0.00E+00
Au-194	1.62E+00	0.139	0.861	8.27E-01	7.55E-02
Au-195	4.85E-02	0.133	0.867	1.86E+00	2.36E-01
Ba-133	4.92E-01	0.085	0.915	1.59E+00	1.14E-01
Ba-137m	9.14E-01	0.097	0.903	1.20E+00	9.05E-02
Be-10	2.74E-04	0.169	0.831	2.26E+01	1.68E-01
Be-7	7.32E-02	0.091	0.909	1.25E+00	9.96E-02

Table A.2-5 Effective Dose Coefficients in DCFPAK3.02 Libraries for External Gamma Radiation from Contaminated Soil and Fitting Parameters Used to Calculate Depth and Cover Factors, 30-day Half-life Cutoff (Cont.)

Nuclide	Volume Dose Coefficients[a] (mSv/yr per Bq/g)	Fitting Parameters[b]			
		CF_A	CF_B	CF_KA (cm²/g)	CF_KB (cm²/g)
Bi-207	2.38E+00	0.119	0.881	9.84E-01	8.19E-02
Bi-208	4.77E+00	0.148	0.852	6.31E-01	5.47E-02
Bi-210	1.48E-03	0.465	0.535	1.59E+01	1.42E-01
Bi-210m	3.51E-01	0.078	0.922	1.46E+00	1.15E-01
Bi-211	6.51E-02	0.083	0.917	1.38E+00	1.10E-01
Bi-212	1.69E-01	0.097	0.903	2.18E+00	8.31E-02
Bi-213	1.86E-01	0.08	0.92	2.30E+00	1.04E-01
Bi-214	2.47E+00	0.125	0.875	9.15E-01	7.13E-02
Bi-215	3.70E-01	0.09	0.91	1.92E+00	9.75E-02
Bk-247	1.60E-01	0.086	0.914	1.56E+00	1.38E-01
Bk-249	1.72E-06	0.292	0.708	3.19E+00	1.58E-01
Bk-250	1.44E+00	0.118	0.882	9.64E-01	7.90E-02
Bk-251	8.38E-02	0.075	0.925	2.74E+00	1.60E-01
C-14	2.99E-06	0.344	0.656	3.38E+00	2.91E-01
Ca-41	0.00E+00	0	1	0.00E+00	0.00E+00
Ca-45	1.44E-05	0.231	0.769	2.82E+00	2.30E-01
Cd-109	3.29E-03	0.302	0.698	4.76E+00	2.07E-01
Cd-113	2.61E-05	0.205	0.795	2.59E+00	2.08E-01
Cd-113m	2.43E-04	0.143	0.857	1.53E+01	1.49E-01
Cd-115m	5.76E-02	0.113	0.887	4.31E+00	8.29E-02
Ce-139	1.57E-01	0.08	0.92	1.95E+00	1.44E-01
Ce-141	7.88E-02	0.071	0.929	1.92E+00	1.53E-01
Ce-144	1.71E-02	0.09	0.91	1.92E+00	1.62E-01
Cf-248	5.81E-04	0.128	0.872	3.51E+00	7.41E-02
Cf-249	4.56E-01	0.079	0.921	1.42E+00	1.09E-01
Cf-250	1.65E-02	0.13	0.87	9.40E-01	6.83E-02
Cf-251	1.25E-01	0.074	0.926	1.80E+00	1.49E-01
Cf-252	7.67E-01	0.137	0.863	8.30E-01	6.74E-02
Cf-253	1.70E-04	0.353	0.647	3.96E-01	5.88E+00
Cf-254	2.83E+01	0.14	0.86	8.20E-01	6.71E-02
Cl-36	6.56E-04	0.219	0.781	2.38E+01	1.33E-01
Cm-241	6.61E-01	0.092	0.908	1.34E+00	1.07E-01
Cm-242	3.48E-05	0.287	0.713	1.46E-01	8.44E+00
Cm-243	1.45E-01	0.077	0.923	1.70E+00	1.37E-01
Cm-244	5.40E-05	0.434	0.566	7.77E+00	8.27E-02
Cm-245	9.54E-02	0.08	0.92	1.85E+00	1.67E-01
Cm-246	6.11E-03	0.118	0.882	1.15E+00	6.89E-02
Cm-247	4.46E-01	0.081	0.919	1.39E+00	1.07E-01
Cm-248	2.21E+00	0.138	0.862	8.36E-01	6.72E-02
Cm-249	2.91E-02	0.081	0.919	3.33E+00	9.76E-02
Cm-250	2.24E+01	0.14	0.86	8.25E-01	6.72E-02
Co-56	6.16E+00	0.147	0.853	7.19E-01	6.56E-02

Table A.2-5 Effective Dose Coefficients in DCFPAK3.02 Libraries for External Gamma Radiation from Contaminated Soil and Fitting Parameters Used to Calculate Depth and Cover Factors, 30-day Half-life Cutoff (Cont.)

Nuclide	Volume Dose Coefficients[a] (mSv/yr per Bq/g)	Fitting Parameters[b]			
		CF_A	CF_B	CF_KA (cm²/g)	CF_KB (cm²/g)
Co-57	1.23E-01	0.072	0.928	1.78E+00	1.63E-01
Co-58	1.52E+00	0.107	0.893	1.05E+00	8.63E-02
Co-60	4.16E+00	0.131	0.869	8.17E-01	7.17E-02
Co-60m	6.06E-03	0.181	0.819	8.59E-01	7.11E-02
Cs-134	2.40E+00	0.105	0.895	1.09E+00	8.82E-02
Cs-135	2.12E-05	0.219	0.781	2.67E+00	2.19E-01
Cs-137	2.35E-04	0.307	0.693	1.34E+01	1.59E-01
Dy-154	0.00E+00	0	1	0.00E+00	0.00E+00
Dy-159	1.22E-02	0.254	0.746	2.66E+00	4.48E-01
Es-253	4.29E-04	0.095	0.905	2.78E+00	1.13E-01
Es-254	2.92E-03	0.2	0.8	4.21E+00	1.40E-01
Es-255	1.16E-03	0.152	0.848	8.05E-01	6.67E-02
Eu-146	3.79E+00	0.123	0.877	9.19E-01	7.92E-02
Eu-148	3.41E+00	0.11	0.89	1.04E+00	8.64E-02
Eu-149	5.20E-02	0.148	0.852	1.73E+00	1.16E-01
Eu-150	2.30E+00	0.099	0.901	1.18E+00	9.35E-02
Eu-152	1.82E+00	0.128	0.872	9.03E-01	7.90E-02
Eu-154	1.97E+00	0.123	0.877	9.28E-01	7.92E-02
Eu-155	4.41E-02	0.114	0.886	1.84E+00	1.98E-01
Fe-55	1.66E-10	0.07	0.93	1.77E+00	1.63E-01
Fe-59	1.95E+00	0.129	0.871	8.47E-01	7.36E-02
Fe-60	6.56E-06	0.294	0.706	3.11E+00	2.65E-01
Fm-254	1.18E-02	0.128	0.872	1.01E+00	6.83E-02
Fm-255	1.45E-03	0.269	0.731	5.25E+00	1.96E-01
Fm-257	1.68E-01	0.101	0.899	1.40E+00	1.17E-01
Fr-221	3.60E-02	0.069	0.931	1.67E+00	1.30E-01
Fr-223	4.75E-02	0.138	0.862	2.90E+00	1.33E-01
Ga-68	1.42E+00	0.084	0.916	1.56E+00	9.83E-02
Gd-146	1.97E-01	0.117	0.883	1.83E+00	1.64E-01
Gd-148	0.00E+00	0	1	0.00E+00	0.00E+00
Gd-150	0.00E+00	0	1	0.00E+00	0.00E+00
Gd-151	4.96E-02	0.15	0.85	1.83E+00	1.39E-01
Gd-152	0.00E+00	0	1	0.00E+00	0.00E+00
Gd-153	5.76E-02	0.173	0.827	1.96E+00	2.01E-01
Ge-68	3.05E-07	0	1	0.00E+00	3.73E+01
H-3	0.00E+00	0	1	0.00E+00	0.00E+00
Hf-172	5.40E-02	0.185	0.815	1.84E+00	2.20E-01
Hf-174	0.00E+00	0	1	0.00E+00	0.00E+00
Hf-175	4.41E-01	0.092	0.908	1.44E+00	1.14E-01
Hf-178m	3.11E+00	0.088	0.912	1.33E+00	1.06E-01
Hf-181	7.32E-01	0.088	0.912	1.35E+00	1.06E-01
Hf-182	3.12E-01	0.071	0.929	1.59E+00	1.22E-01

Table A.2-5 Effective Dose Coefficients in DCFPAK3.02 Libraries for External Gamma Radiation from Contaminated Soil and Fitting Parameters Used to Calculate Depth and Cover Factors, 30-day Half-life Cutoff (Cont.)

Nuclide	Volume Dose Coefficients[a] (mSv/yr per Bq/g)	Fitting Parameters[b]			
		CF_A	CF_B	CF_KA (cm²/g)	CF_KB (cm²/g)
Hg-194	2.08E-06	0	1	1.10E-02	2.46E+01
Hg-203	3.15E-01	0.073	0.927	1.54E+00	1.19E-01
Hg-206	1.66E-01	0.074	0.926	2.40E+00	1.14E-01
Ho-163	0.00E+00	0	1	0.00E+00	0.00E+00
Ho-166m	2.42E+00	0.107	0.893	1.08E+00	9.12E-02
I-125	3.24E-03	0.285	0.715	8.47E-01	4.01E+00
I-129	2.62E-03	0.468	0.532	7.65E-01	3.83E+00
In-113m	3.64E-01	0.081	0.919	1.43E+00	1.07E-01
In-114	1.10E-02	0.374	0.626	7.26E+00	9.77E-02
In-114m	1.01E-01	0.088	0.912	1.50E+00	1.05E-01
In-115	9.74E-05	0.157	0.843	6.74E+00	1.79E-01
In-115m	2.16E-01	0.073	0.927	1.62E+00	1.13E-01
Ir-192	1.16E+00	0.081	0.919	1.40E+00	1.07E-01
Ir-192n	4.15E-04	0.133	0.867	3.57E+00	1.98E-01
Ir-194	1.43E-01	0.1	0.9	3.11E+00	9.82E-02
Ir-194m	3.44E+00	0.091	0.909	1.25E+00	9.84E-02
K-40	2.70E-01	0.095	0.905	1.81E+00	7.18E-02
Kr-83m	6.31E-06	0.203	0.797	9.00E-01	2.02E+01
La-137	2.89E-03	0.447	0.553	6.70E-01	3.42E+00
La-138	2.04E+00	0.142	0.858	7.64E-01	6.98E-02
Lu-172	3.04E+00	0.126	0.874	9.22E-01	7.92E-02
Lu-172m	3.75E-07	0.196	0.804	1.68E+01	6.62E-01
Lu-173	1.56E-01	0.149	0.851	1.47E+00	1.34E-01
Lu-174	1.27E-01	0.203	0.797	9.21E-01	7.79E-02
Lu-174m	3.26E-02	0.26	0.74	1.48E+00	1.59E-01
Lu-176	6.16E-01	0.073	0.927	1.60E+00	1.21E-01
Lu-177	3.92E-02	0.077	0.923	1.69E+00	1.38E-01
Lu-177m	1.25E+00	0.083	0.917	1.50E+00	1.21E-01
Mn-53	0.00E+00	0	1	0.00E+00	0.00E+00
Mn-54	1.31E+00	0.114	0.886	9.90E-01	8.35E-02
Mo-93	1.11E-04	0	1	1.01E-03	1.09E+01
Na-22	3.48E+00	0.119	0.881	9.38E-01	8.04E-02
Nb-91	2.46E-03	0.104	0.896	4.99E+00	9.98E-02
Nb-91m	4.08E-02	0.108	0.892	1.22E+00	7.58E-02
Nb-92	2.33E+00	0.107	0.893	1.06E+00	8.59E-02
Nb-93m	1.97E-05	0	1	1.01E-03	1.09E+01
Nb-94	2.44E+00	0.107	0.893	1.06E+00	8.55E-02
Nb-95	1.19E+00	0.104	0.896	1.09E+00	8.68E-02
Nb-95m	8.18E-02	0.064	0.936	1.94E+00	1.25E-01
Nd-144	0.00E+00	0	1	0.00E+00	0.00E+00
Ni-59	2.31E-05	0.093	0.907	1.22E+00	9.73E-02
Ni-63	0.00E+00	0	1	0.00E+00	0.00E+00

Table A.2-5 Effective Dose Coefficients in DCFPAK3.02 Libraries for External Gamma Radiation from Contaminated Soil and Fitting Parameters Used to Calculate Depth and Cover Factors, 30-day Half-life Cutoff (Cont.)

Nuclide	Volume Dose Coefficients[a] (mSv/yr per Bq/g)	Fitting Parameters[b]			
		CF_A	CF_B	CF_KA (cm²/g)	CF_KB (cm²/g)
Np-235	5.10E-04	0.168	0.832	7.02E+00	1.88E-01
Np-236	1.35E-01	0.076	0.924	1.95E+00	1.63E-01
Np-237	1.81E-02	0.106	0.894	2.44E+00	1.86E-01
Np-238	9.34E-01	0.116	0.884	1.01E+00	7.92E-02
Np-239	1.96E-01	0.078	0.922	1.70E+00	1.40E-01
Np-240	1.58E+00	0.109	0.891	1.10E+00	8.74E-02
Np-240m	4.96E-01	0.091	0.909	1.72E+00	8.93E-02
Os-185	1.02E+00	0.109	0.891	1.11E+00	9.08E-02
Os-186	0.00E+00	0	1	0.00E+00	0.00E+00
Os-194	5.96E-04	0.289	0.711	2.91E+00	4.67E-01
P-32	5.50E-03	0.479	0.521	1.28E-01	9.25E+00
Pa-231	4.35E-02	0.078	0.922	1.83E+00	1.18E-01
Pa-232	1.45E+00	0.116	0.884	9.86E-01	8.41E-02
Pa-233	2.75E-01	0.08	0.92	1.52E+00	1.20E-01
Pa-234	2.24E+00	0.115	0.885	1.02E+00	8.48E-02
Pa-234m	3.40E-02	0.187	0.813	5.17E+00	8.75E-02
Pb-202	1.92E-06	0	1	1.10E-02	3.08E+01
Pb-205	1.95E-06	0	1	1.10E-02	3.08E+01
Pb-209	2.04E-04	0.206	0.794	2.34E+01	1.67E-01
Pb-210	5.65E-04	0.228	0.772	3.72E+00	4.71E-01
Pb-211	9.95E-02	0.088	0.912	2.93E+00	9.40E-02
Pb-212	1.71E-01	0.081	0.919	1.54E+00	1.30E-01
Pb-214	3.40E-01	0.079	0.921	1.55E+00	1.13E-01
Pd-107	0.00E+00	0	1	0.00E+00	0.00E+00
Pm-143	4.50E-01	0.108	0.892	1.19E+00	8.79E-02
Pm-144	2.34E+00	0.101	0.899	1.16E+00	9.16E-02
Pm-145	6.16E-03	0.375	0.625	2.85E+00	4.55E-01
Pm-146	1.11E+00	0.099	0.901	1.21E+00	9.28E-02
Pm-147	1.17E-05	0.218	0.782	2.74E+00	2.09E-01
Pm-148	9.44E-01	0.105	0.895	1.26E+00	7.76E-02
Pm-148m	3.04E+00	0.101	0.899	1.14E+00	9.08E-02
Po-208	3.03E-05	0.106	0.894	1.15E+00	9.58E-02
Po-209	8.99E-03	0.122	0.878	9.94E-01	8.91E-02
Po-210	1.53E-05	0.116	0.884	9.85E-01	8.39E-02
Po-211	1.27E-02	0.113	0.887	1.01E+00	8.51E-02
Po-212	0.00E+00	0	1	0.00E+00	0.00E+00
Po-213	5.86E-05	0.105	0.895	1.08E+00	8.61E-02
Po-214	1.30E-04	0.104	0.896	1.08E+00	8.59E-02
Po-215	2.56E-04	0.086	0.914	1.31E+00	1.03E-01
Po-216	2.40E-05	0.11	0.89	1.02E+00	8.46E-02
Po-218	2.49E-09	0.238	0.762	2.80E+00	2.30E-01
Pr-144	6.67E-02	0.191	0.809	3.67E+00	7.71E-02

Table A.2-5 Effective Dose Coefficients in DCFPAK3.02 Libraries for External Gamma Radiation from Contaminated Soil and Fitting Parameters Used to Calculate Depth and Cover Factors, 30-day Half-life Cutoff (Cont.)

Nuclide	Volume Dose Coefficients[a] (mSv/yr per Bq/g)	Fitting Parameters[b]			
		CF_A	CF_B	CF_KA (cm^2/g)	CF_KB (cm^2/g)
Pr-144m	4.46E-03	0.349	0.651	2.03E+00	9.58E-02
Pt-190	0.00E+00	0	1	0.00E+00	0.00E+00
Pt-193	1.18E-06	0	1	1.10E-02	2.86E+01
Pu-236	4.65E-05	0.485	0.515	1.79E-01	8.65E+00
Pu-237	3.98E-02	0.084	0.916	2.03E+00	1.84E-01
Pu-238	3.00E-05	0.34	0.66	2.00E-01	9.43E+00
Pu-239	7.47E-05	0.191	0.809	6.19E+00	1.37E-01
Pu-240	3.05E-05	0.366	0.634	1.87E-01	9.14E+00
Pu-241	1.41E-06	0.082	0.918	1.93E+00	1.75E-01
Pu-242	1.53E-04	0.183	0.817	5.96E+00	7.50E-02
Pu-243	1.93E-02	0.116	0.884	1.84E+00	1.78E-01
Pu-244	3.33E-02	0.133	0.867	8.89E-01	6.79E-02
Pu-246	1.41E-01	0.084	0.916	1.77E+00	1.43E-01
Ra-223	1.57E-01	0.092	0.908	1.49E+00	1.31E-01
Ra-224	1.34E-02	0.065	0.935	1.67E+00	1.26E-01
Ra-225	2.41E-03	0.231	0.769	4.10E+00	6.44E-01
Ra-226	8.58E-03	0.066	0.934	1.77E+00	1.39E-01
Ra-228	1.78E-05	0	1	0.00E+00	1.30E+01
Rb-83	7.22E-01	0.096	0.904	1.20E+00	9.60E-02
Rb-84	1.40E+00	0.102	0.898	1.13E+00	8.72E-02
Rb-87	3.65E-05	0.2	0.8	2.57E+00	2.10E-01
Re-183	1.24E-01	0.132	0.868	1.60E+00	1.60E-01
Re-184	1.33E+00	0.119	0.881	1.02E+00	8.53E-02
Re-184m	5.05E-01	0.125	0.875	1.07E+00	9.58E-02
Re-186	1.94E-02	0.107	0.893	5.24E+00	1.63E-01
Re-186m	6.56E-03	0.191	0.809	2.10E+00	2.82E-01
Re-187	0.00E+00	0	1	0.00E+00	0.00E+00
Re-188	8.89E-02	0.116	0.884	3.72E+00	1.07E-01
Rh-101	3.27E-01	0.069	0.931	1.77E+00	1.36E-01
Rh-102	7.47E-01	0.092	0.908	1.32E+00	9.50E-02
Rh-102m	3.31E+00	0.106	0.894	1.07E+00	8.73E-02
Rh-103m	4.27E-05	0.127	0.873	7.76E-01	6.87E+00
Rh-106	3.38E-01	0.106	0.894	2.25E+00	9.39E-02
Rn-218	1.15E-03	0.097	0.903	1.18E+00	9.23E-02
Rn-219	8.03E-02	0.077	0.923	1.46E+00	1.13E-01
Rn-220	9.39E-04	0.094	0.906	1.21E+00	9.62E-02
Rn-222	5.76E-04	0.084	0.916	1.34E+00	9.97E-02
Ru-103	7.32E-01	0.088	0.912	1.29E+00	9.94E-02
Ru-106	0.00E+00	0	1	0.00E+00	0.00E+00
S-35	3.30E-06	0.33	0.67	3.29E+00	2.82E-01
Sb-124	3.05E+00	0.13	0.87	8.53E-01	7.27E-02
Sb-125	6.26E-01	0.097	0.903	1.25E+00	9.66E-02

Table A.2-5 Effective Dose Coefficients in DCFPAK3.02 Libraries for External Gamma Radiation from Contaminated Soil and Fitting Parameters Used to Calculate Depth and Cover Factors, 30-day Half-life Cutoff (Cont.)

Nuclide	Volume Dose Coefficients[a] (mSv/yr per Bq/g)	Fitting Parameters[b]			
		CF_A	CF_B	CF_KA (cm²/g)	CF_KB (cm²/g)
Sb-126	4.22E+00	0.1	0.9	1.15E+00	9.05E-02
Sb-126m	2.36E+00	0.096	0.904	1.28E+00	9.25E-02
Sc-44	3.36E+00	0.105	0.895	1.12E+00	8.42E-02
Sc-46	3.24E+00	0.126	0.874	8.84E-01	7.73E-02
Se-75	4.89E-01	0.072	0.928	1.59E+00	1.25E-01
Se-79	3.44E-06	0.338	0.662	3.35E+00	2.94E-01
Si-32	9.70E-06	0.254	0.746	2.95E+00	2.46E-01
Sm-145	1.44E-02	0.366	0.634	2.57E+00	4.06E-01
Sm-146	0.00E+00	0	1	0.00E+00	0.00E+00
Sm-147	0.00E+00	0	1	0.00E+00	0.00E+00
Sm-148	0.00E+00	0	1	0.00E+00	0.00E+00
Sm-151	1.96E-07	0.036	0.964	9.74E-01	6.33E+00
Sn-113	8.03E-03	0.155	0.845	3.62E+00	1.24E-01
Sn-119m	7.42E-04	0.107	0.893	7.29E-01	4.58E+00
Sn-121	4.77E-05	0.182	0.818	2.43E+00	1.94E-01
Sn-121m	3.91E-04	0.254	0.746	5.20E-01	3.77E+00
Sn-123	1.43E-02	0.177	0.823	7.75E+00	8.58E-02
Sn-126	3.52E-02	0.115	0.885	2.15E+00	2.11E-01
Sr-85	7.32E-01	0.095	0.905	1.21E+00	9.66E-02
Sr-89	4.11E-03	0.497	0.503	1.28E-01	1.04E+01
Sr-90	1.75E-04	0.164	0.836	1.72E+01	1.71E-01
Ta-179	1.02E-02	0.168	0.832	2.27E+00	3.30E-01
Ta-182	2.03E+00	0.135	0.865	8.58E-01	7.57E-02
Tb-157	1.15E-03	0.247	0.753	2.95E+00	5.06E-01
Tb-158	1.21E+00	0.118	0.882	1.02E+00	8.28E-02
Tb-160	1.77E+00	0.121	0.879	9.51E-01	8.09E-02
Tc-95	1.23E+00	0.113	0.887	1.01E+00	8.51E-02
Tc-95m	1.02E+00	0.098	0.902	1.17E+00	9.28E-02
Tc-97	1.49E-04	0	1	1.01E-03	9.66E+00
Tc-97m	4.11E-04	0.418	0.582	7.77E+00	1.92E-01
Tc-98	2.18E+00	0.103	0.897	1.09E+00	8.90E-02
Tc-99	2.98E-05	0.205	0.795	2.57E+00	2.10E-01
Te-121	8.38E-01	0.09	0.91	1.31E+00	9.61E-02
Te-121m	2.69E-01	0.077	0.923	1.61E+00	1.18E-01
Te-123	2.17E-06	0.419	0.581	1.18E+00	5.33E+00
Te-123m	1.55E-01	0.069	0.931	1.94E+00	1.45E-01
Te-125m	3.00E-03	0.214	0.786	2.95E-01	3.50E+00
Te-127	7.22E-03	0.078	0.922	4.61E+00	1.08E-01
Te-127m	1.11E-03	0.326	0.674	1.84E-01	3.51E+00
Te-129	8.89E-02	0.09	0.91	3.55E+00	9.99E-02
Te-129m	4.77E-02	0.101	0.899	3.00E+00	9.19E-02
Th-227	1.53E-01	0.076	0.924	1.61E+00	1.25E-01

Table A.2-5 Effective Dose Coefficients in DCFPAK3.02 Libraries for External Gamma Radiation from Contaminated Soil and Fitting Parameters Used to Calculate Depth and Cover Factors, 30-day Half-life Cutoff (Cont.)

Nuclide	Volume Dose Coefficients[a] (mSv/yr per Bq/g)	Fitting Parameters[b]			
		CF_A	CF_B	CF_KA (cm^2/g)	CF_KB (cm^2/g)
Th-228	1.96E-03	0.09	0.91	2.24E+00	1.60E-01
Th-229	7.78E-02	0.089	0.911	1.83E+00	1.67E-01
Th-230	2.99E-04	0.137	0.863	3.79E+00	1.84E-01
Th-231	8.78E-03	0.119	0.881	3.10E+00	2.01E-01
Th-232	1.29E-04	0.179	0.821	5.13E+00	2.28E-01
Th-234	6.26E-03	0.119	0.881	1.94E+00	2.07E-01
Ti-44	8.78E-02	0.121	0.879	1.90E+00	2.43E-01
Tl-202	6.26E-01	0.101	0.899	1.24E+00	1.04E-01
Tl-204	1.13E-03	0.189	0.811	1.52E+01	2.13E-01
Tl-206	3.45E-03	0.498	0.502	1.11E+01	1.32E-01
Tl-207	6.46E-03	0.262	0.738	1.02E+01	9.64E-02
Tl-208	5.86E+00	0.144	0.856	7.06E-01	6.05E-02
Tl-209	3.48E+00	0.139	0.861	8.35E-01	7.21E-02
Tl-210	4.53E+00	0.128	0.872	9.04E-01	7.34E-02
Tm-168	1.81E+00	0.109	0.891	1.11E+00	9.08E-02
Tm-170	3.07E-03	0.217	0.783	1.10E+01	2.14E-01
Tm-171	2.43E-04	0.187	0.813	2.23E+00	3.34E-01
U-232	1.95E-04	0.183	0.817	5.66E+00	1.75E-01
U-233	2.48E-04	0.118	0.882	4.08E+00	1.40E-01
U-234	9.34E-05	0.253	0.747	7.17E+00	1.95E-01
U-235	1.89E-01	0.067	0.933	1.77E+00	1.40E-01
U-235m	0.00E+00	0	1	0.00E+00	0.00E+00
U-236	4.75E-05	0.362	0.638	8.47E+00	2.07E-01
U-237	1.29E-01	0.094	0.906	1.73E+00	1.52E-01
U-238	4.63E-05	0.346	0.654	7.47E+00	1.30E-01
U-240	4.04E-03	0.1	0.9	2.86E+00	1.69E-01
V-49	0.00E+00	0	1	0.00E+00	0.00E+00
V-50	2.42E+00	0.141	0.859	7.38E-01	6.68E-02
W-181	1.73E-02	0.171	0.829	2.10E+00	3.14E-01
W-185	1.00E-04	0.153	0.847	2.42E+00	1.86E-01
W-188	2.40E-03	0.08	0.92	1.56E+00	1.23E-01
Y-88	4.57E+00	0.142	0.858	7.29E-01	6.61E-02
Y-90	1.09E-02	0.498	0.502	1.17E-01	6.25E+00
Y-91	9.44E-03	0.284	0.716	8.52E+00	9.01E-02
Yb-169	2.80E-01	0.129	0.871	1.59E+00	1.48E-01
Zn-65	9.44E-01	0.127	0.873	8.64E-01	7.53E-02
Zr-88	5.45E-01	0.079	0.921	1.42E+00	1.07E-01
Zr-93	0.00E+00	0	1	0.00E+00	0.00E+00
Zr-95	1.14E+00	0.103	0.897	1.09E+00	8.82E-02

[a] Volume dose coefficients assume infinite thickness.

[b] Fitting parameters are used in depth and cover factor calculations (see Appendix B).

Table A.2-6   Default Inhalation and Ingestion Dose Coefficients for 30-day Half-Life Cutoff from DCFPAK3.02 for Adult

Radionuclide[a]	Associated Decay Chain[b]	Inhalation[c] (mSv/Bq)	Ingestion[d] (mSv/Bq)
Ac-227+D	(Th-227 9.8620E-01) (Ra-223 1.0000E+00) (Rn-219 1.0000E+00) Po-215 Pb-211 Bi-211 (Tl-207 9.9724E-01) (Po-211 2.7600E-03) (Fr-223 1.3800E-02) (At-219 8.2800E-07) (Bi-215 8.2800E-07)	1.75E-01	4.34E-04
Ag-105	—[e]	8.15E-07	4.62E-07
Ag-108m+D	(Ag-108 8.7000E-02)	3.85E-05	2.35E-06
Ag-110m+D	(Ag-110 1.3600E-02)	1.25E-05	2.82E-06
Al-26	—	1.09E-04	3.49E-06
Am-241	—	9.64E-02	2.04E-04
Am-242m+D	Am-242	9.16E-02	1.90E-04
Am-242m+D1	Am-242	9.16E-02	1.90E-04
Am-242m+D2	Np-238	9.16E-02	1.91E-04
Am-243+D	Np-239	9.57E-02	2.04E-04
As-73	—	1.36E-06	2.59E-07
Au-195	—	1.79E-06	2.65E-07
Ba-133	—	1.04E-05	1.54E-06
Be-10	—	3.47E-05	1.14E-06
Be-7	—	5.58E-08	2.80E-08
Bi-207	—	3.88E-05	1.28E-06
Bi-208	—	3.67E-05	1.16E-06
Bi-210m+D	Tl-206	9.90E-03	1.50E-05
Bk-247	—	1.67E-01	3.50E-04
Bk-249	—	4.18E-04	9.93E-07
Bk-249+D	Am-245	4.18E-04	1.06E-06
C-14 particulates	—	5.73E-06	5.81E-07
C-14 gaseous	—	6.24E-09	None
Ca-41	—	2.13E-07	2.27E-07
Ca-45	—	3.64E-06	7.09E-07
Cd-109	—	8.13E-06	2.00E-06
Cd-113	—	1.19E-04	2.45E-05
Cd-113m	—	1.12E-04	2.34E-05
Cd-115m+D	In-115m	7.70E-06	3.38E-06
Cd-115m+D1	(In-115m 1.0049E-04)	7.64E-06	3.29E-06
Ce-139	—	1.93E-06	2.64E-07
Ce-141	—	3.76E-06	7.14E-07
Ce-144+D	(Pr-144m 9.7699E-03) (Pr-144 9.9999E-01)	5.28E-05	5.28E-06

Table A.2-6   Default Inhalation and Ingestion Dose Coefficients for 30-day Half-Life Cutoff from DCFPAK3.02 for Adult (Cont.)

Radionuclide[a]	Associated Decay Chain[b]	Inhalation[c] (mSv/Bq)	Ingestion[d] (mSv/Bq)
Cf-248	—	1.13E-02	2.83E-05
Cf-249	—	1.68E-01	3.51E-04
Cf-250	—	7.53E-02	1.61E-04
Cf-251	—	1.71E-01	3.58E-04
Cf-252	—	3.68E-02	9.05E-05
Cf-254	—	4.31E-02	4.02E-04
Cl-36	—	3.79E-05	9.28E-07
Cm-241	—	3.72E-05	9.25E-07
Cm-242	—	5.92E-03	1.17E-05
Cm-243	—	6.99E-02	1.50E-04
Cm-244	—	5.71E-02	1.23E-04
Cm-245	—	9.85E-02	2.08E-04
Cm-246	—	9.81E-02	2.07E-04
Cm-247+D	Pu-243	9.00E-02	1.91E-04
Cm-248	—	3.62E-01	7.75E-04
Cm-250	—	2.46E+00	5.30E-03
Cm-250+D	Pu-246, Am-246m	2.46E+00	5.30E-03
Cm-250+D1	Bk-250	2.46E+00	5.30E-03
Co-56	—	6.64E-06	2.53E-06
Co-57	—	1.00E-06	2.11E-07
Co-58	—	2.11E-06	7.48E-07
Co-60	—	3.08E-05	3.42E-06
Cs-134	—	2.04E-05	1.93E-05
Cs-135	—	1.17E-05	2.65E-06
Cs-137+D	(Ba-137m 9.4399E-01)	3.94E-05	1.36E-05
Dy-154	—	2.58E-02	5.57E-05
Dy-159	—	4.56E-07	1.06E-07
Es-254+D	(Bk-250 1.0000E+00) (Fm-254 1.7390E-06)	1.03E-02	2.83E-05
Es-254+D1	(Fm-254 3.3196E-02)	1.03E-02	2.81E-05
Es-255+D	(Fm-255 4.6800E-03)	4.56E-03	5.97E-06
Es-255+D1	(Fm-255 9.200E-01) (Bk-251 8.0004E-02)	4.83E-03	8.31E-06
Eu-148	—	3.61E-06	1.30E-06
Eu-149	—	5.34E-07	1.61E-07
Eu-150	—	1.28E-04	1.25E-06
Eu-152	—	9.33E-05	1.34E-06
Eu-154	—	1.07E-04	1.97E-06
Eu-155	—	1.24E-05	3.32E-07
Fe-55	—	7.82E-07	3.31E-07
Fe-59	—	4.03E-06	1.79E-06
Fe-60+D	Co-60m	2.90E-04	1.16E-04
Fe-60+D1	Co-60m	2.90E-04	1.16E-04

Table A.2-6 Default Inhalation and Ingestion Dose Coefficients for 30-day Half-Life Cutoff from DCFPAK3.02 for Adult (Cont.)

Radionuclide[a]	Associated Decay Chain[b]	Inhalation[c] (mSv/Bq)	Ingestion[d] (mSv/Bq)
Fm-257+D	(Cf-253 4.2159E-05) (Es-253 4.2159E-05)	8.37E-03	1.63E-05
Fm-257+D1	Cf-253 (Es-253 9.9690E-01) (Cm-249 3.1000E-03)	1.31E-02	2.38E-05
Gd-146+D	Eu-146	7.87E-06	2.16E-06
Gd-148	—	2.53E-02	5.47E-05
Gd-150	—	2.42E-02	5.23E-05
Gd-151	—	1.17E-06	2.27E-07
Gd-152	—	1.90E-02	4.10E-05
Gd-153	—	2.40E-06	2.79E-07
Ge-68+D	Ga-68	3.08E-05	1.38E-06
H-3	—	2.62E-07	4.19E-08
Hf-172+D	Lu-172m Lu-172	3.47E-05	2.39E-06
Hf-174	—	3.06E-02	2.55E-04
Hf-175	—	1.40E-06	4.04E-07
Hf-178m	—	2.22E-04	3.97E-06
Hf-181	—	5.94E-06	1.11E-06
Hf-182	—	2.94E-04	2.83E-06
Hg-194+D	Au-194	4.07E-05	5.17E-05
Hg-203	—	7.02E-06	1.91E-06
Ho-163	—	2.65E-07	2.88E-09
Ho-166m	—	2.81E-04	1.97E-06
I-125	—	1.40E-05	1.55E-05
I-129	—	9.81E-05	1.08E-04
In-114m+D	(In-114 9.6750E-01)	1.35E-05	4.14E-06
In-115	—	3.91E-04	3.27E-05
Ir-192	—	6.61E-06	1.37E-06
Ir-192n	—	5.81E-05	9.15E-07
Ir-194m	—	1.20E-05	2.06E-06
K-40	—	8.47E-05	6.15E-06
La-137	—	8.94E-06	8.40E-08
La-138	—	1.56E-04	1.09E-06
Lu-173	—	4.57E-06	3.66E-07
Lu-174	—	7.22E-06	2.85E-07
Lu-174m	—	4.39E-06	5.45E-07
Lu-176	—	1.52E-04	1.81E-06
Lu-177m+D	(Lu-177 2.1700E-01)	1.63E-05	1.83E-06
Mn-53	—	3.37E-07	2.98E-08
Mn-54	—	3.27E-06	7.21E-07
Mo-93	—	2.23E-06	2.89E-06
Na-22	—	2.91E-05	3.17E-06
Nb-91	—	1.84E-06	4.39E-08
Nb-91m	—	4.19E-06	4.10E-07

Table A.2-6   Default Inhalation and Ingestion Dose Coefficients for 30-day Half-Life Cutoff from DCFPAK3.02 for Adult (Cont.)

Radionuclide[a]	Associated Decay Chain[b]	Inhalation[c] (mSv/Bq)	Ingestion[d] (mSv/Bq)
Nb-92	—	2.71E-05	1.02E-06
Nb-93m	—	1.91E-06	1.29E-07
Nb-94	—	4.86E-05	1.73E-06
Nb-95	—	1.75E-06	5.87E-07
Nd-144	—	1.90E-02	4.08E-05
Ni-59	—	8.18E-07	6.23E-08
Ni-63	—	2.00E-06	1.55E-07
Np-235	—	7.26E-07	5.66E-08
Np-235+D	(U-235m 3.9934E-03)	7.26E-07	5.66E-08
Np-236	—	1.15E-02	2.48E-05
Np-236+D	Pa-232	1.15E-02	2.55E-05
Np-236+D1	Pa-232	1.15E-02	2.55E-05
Np-237+D	Pa-233	4.97E-02	1.08E-04
Os-185	—	1.56E-06	5.03E-07
Os-186	—	4.17E-03	3.20E-05
Os-194+D	Ir-194	8.60E-05	3.81E-06
Pa-231	—	2.30E-01	4.79E-04
Pb-202+D	(Tl-202 9.9000E-01)	4.97E-05	1.61E-05
Pb-205	—	8.24E-07	2.71E-07
Pb-210+D	Bi-210	5.75E-03	6.97E-04
Pb-210+D1	(Bi-210 9.8581E-01) Tl-206 (Hg-206 1.4190E-02)	5.75E-03	6.97E-04
Pd-107	—	6.08E-07	3.84E-08
Pm-143	—	2.88E-06	2.35E-07
Pm-144	—	1.71E-05	9.86E-07
Pm-145	—	8.04E-06	1.11E-07
Pm-146	—	4.40E-05	8.96E-07
Pm-147	—	6.98E-06	2.61E-07
Pm-148m+D	(Pm-148 4.2000E-02)	5.78E-06	1.87E-06
Po-208	—	6.75E-03	1.52E-03
Po-209	—	9.44E-03	1.51E-03
Po-210	—	4.28E-03	1.21E-03
Pt-190	—	5.17E-03	6.94E-06
Pt-193	—	6.69E-07	3.56E-08
Pu-236	—	4.08E-02	8.89E-05
Pu-237	—	3.88E-07	1.12E-07
Pu-238	—	1.08E-01	2.28E-04
Pu-239+D	(U-235m 9.9940E-01)	1.19E-01	2.51E-04
Pu-240	—	1.19E-01	2.51E-04
Pu-241	—	2.28E-03	4.74E-06
Pu-241+D	U-237	2.29E-03	5.52E-06
Pu-242	—	1.13E-01	2.39E-04
Pu-244	—	1.12E-01	2.38E-04

Table A.2-6   Default Inhalation and Ingestion Dose Coefficients for 30-day Half-Life Cutoff from DCFPAK3.02 for Adult (Cont.)

Radionuclide[a]	Associated Decay Chain[b]	Inhalation[c] (mSv/Bq)	Ingestion[d] (mSv/Bq)
Pu-244+D	U-240 Np-240m (Np-240 1.1000E-03)	1.12E-01	2.39E-04
Ra-226+D	Rn-222 Po-218 (Pb-214 9.9980E-01) (Bi-214 1.0000E+00) (Po-214 9.9979E-01) (Tl-210 2.1000E-04) (At-218 2.0000E-04) (Rn-218 2.0000E-07)	9.54E-03	2.80E-04
Ra-228+D	Ac-228	1.61E-02	6.96E-04
Rb-83+D	(Kr-83m 7.4292E-01)	1.37E-06	1.77E-06
Rb-84	—	2.88E-06	2.81E-06
Rb-87	—	1.57E-05	1.53E-06
Re-183	—	3.56E-06	9.64E-07
Re-184	—	2.32E-06	1.01E-06
Re-184m	—	1.02E-05	1.48E-06
Re-186m+D	Re-186	6.20E-05	3.66E-06
Re-186m+D1	Re-186	6.20E-05	3.66E-06
Re-187	—	3.92E-08	4.79E-09
Rh-101	—	5.12E-06	5.50E-07
Rh-102	—	7.27E-06	1.19E-06
Rh-102m	—	1.98E-05	2.76E-06
Ru-103+D	(Rh-103m 9.8755E-01)	2.86E-06	7.18E-07
Ru-106+D	Rh-106	6.65E-05	7.02E-06
S-35	—	1.86E-06	7.74E-07
Sb-124	—	8.57E-06	2.55E-06
Sb-125	—	1.20E-05	1.15E-06
Sc-46	—	6.75E-06	1.47E-06
Se-75	—	1.32E-06	2.58E-06
Se-79	—	6.31E-06	2.74E-06
Si-32+D	P-32	1.15E-04	2.98E-06
Sm-145	—	2.85E-06	2.12E-07
Sm-146	—	2.53E-02	5.42E-05
Sm-147	—	2.31E-02	4.95E-05
Sm-148	—	1.98E-02	4.26E-05
Sm-151	—	9.27E-06	9.89E-08
Sn-113+D	(In-113m 9.9998E-01)	4.03E-06	7.77E-07
Sn-119m	—	3.41E-06	3.53E-07
Sn-121m+D	(Sn-121 7.7600E-01)	1.51E-05	5.64E-07
Sn-123	—	1.29E-05	2.11E-06
Sn-126+D	Sb-126m (Sb-126 1.4000E-01)	1.59E-04	5.21E-06
Sr-85	—	8.07E-07	5.50E-07

Table A.2-6 Default Inhalation and Ingestion Dose Coefficients for 30-day Half-Life Cutoff from DCFPAK3.02 for Adult (Cont.)

Radionuclide[a]	Associated Decay Chain[b]	Inhalation[c] (mSv/Bq)	Ingestion[d] (mSv/Bq)
Sr-89	—	7.96E-06	2.57E-06
Sr-90+D	Y-90	1.58E-04	3.03E-05
Ta-179	—	4.90E-07	6.00E-08
Ta-182	—	1.03E-05	1.52E-06
Tb-157	—	3.22E-06	3.90E-08
Tb-158	—	1.05E-04	1.12E-06
Tb-160	—	8.32E-06	1.62E-06
Tc-95m+D	(Tc-95 3.8800E-02)	1.21E-06	5.77E-07
Tc-97	—	1.78E-06	6.81E-08
Tc-97m	—	4.17E-06	5.49E-07
Tc-98	—	4.25E-05	1.86E-06
Tc-99	—	1.33E-05	6.42E-07
Te-121m+D	(Te-121 8.8600E-01)	6.28E-06	2.76E-06
Te-123	—	3.75E-06	1.36E-06
Te-123m	—	5.07E-06	1.37E-06
Te-125m	—	4.12E-06	8.70E-07
Te-127m+D	(Te-127 9.7600E-01)	9.96E-06	2.52E-06
Te-129m+D	(Te-129 6.3000E-01)	7.90E-06	3.02E-06
Th-228+D	Ra-224 Rn-220 Po-216 Pb-212 Bi-212 (Po-212 6.4060E-01) (Tl-208 3.5940E-01)	4.33E-02	1.43E-04
Th-229+D	Ra-225 Ac-225 Fr-221 At-217 Bi-213 (Po-213 9.7910E-01) Pb-209 (Tl-209 2.0900E-02)	2.55E-01	6.37E-04
Th-230	—	1.02E-01	2.14E-04
Th-232	—	1.10E-01	2.31E-04
Ti-44+D	Sc-44	1.27E-04	6.16E-06
Tl-204	—	1.90E-05	1.19E-06
Tm-168	—	5.07E-06	1.04E-06
Tm-170	—	9.14E-06	1.31E-06
Tm-171	—	2.13E-06	1.06E-07
U-232	—	3.69E-02	3.34E-04
U-233	—	9.59E-03	5.12E-05
U-234	—	9.40E-03	4.95E-05
U-235+D	Th-231	8.47E-03	4.70E-05
U-236	—	8.68E-03	4.66E-05
U-238	—	8.04E-03	4.46E-05
U-238+D	Th-234 Pa-234m (Pa-234 1.6000E-03)	8.04E-03	4.80E-05
V-49	—	6.82E-08	1.84E-08
V-50	—	6.48E-05	3.41E-06
W-181	—	2.86E-07	8.64E-08
W-185	—	3.87E-06	4.44E-07

Table A.2-6   Default Inhalation and Ingestion Dose Coefficients for 30-day Half-Life Cutoff from DCFPAK3.02 for Adult (Cont.)

Radionuclide[a]	Associated Decay Chain[b]	Inhalation[c] (mSv/Bq)	Ingestion[d] (mSv/Bq)
W-188+D	Re-188	1.61E-05	3.45E-06
Y-88	—	6.13E-06	1.30E-06
Y-91	—	8.94E-06	2.37E-06
Yb-169	—	3.41E-06	8.20E-07
Zn-65	—	2.24E-06	3.92E-06
Zr-88	—	3.62E-06	4.41E-07
Zr-93	—	2.41E-05	1.07E-06
Zr-95+D	Nb-95m	6.78E-06	1.58E-06
Zr-95+D1	(Nb-95m 1.0203E-02)	5.90E-06	9.73E-07

[a]   Dose coefficients for entries labeled with +D are aggregated dose coefficients for intake of the principal radionuclide together with associated radionuclides in the decay chain in secular equilibrium.

[b]   The associated radionuclide in the decay chain and their fractions, if the fraction is less than 1.

[c]   Inhalation dose coefficients are for most restricted inhalation class and for an AMAD of 1 μm.

[d]   Ingestion dose coefficients are for most restricted chemical type.

[e]   Indicate no associated radionuclide.

A.2.4   User Libraries

Users can also create their own dose coefficient libraries starting with the base libraries available in the DCF Editor. For example, if the inhalation class for a radionuclide is different from the default inhalation class, the user can choose an inhalation dose coefficient based on the known inhalation class. The user can create a user library using the DCF Editor. The User's guide discusses how to create a user library.

A.3   Dose Estimation Methodology

The absorbed dose is a fundamental dosimetric quantity in radiological protection. To estimate the total whole-body dose from external and internal radiation exposure, doses are estimated separately from external and internal exposure and later added. Doses are initially estimated for different organs/tissues, multiplied by organ/tissue weighting factors, and added to estimate an external or internal dose. Organ/tissue doses depend on the absorbed dose and quality factors/radiation weighting factors. The radiation weighting factors depend on the radiation type and energy. Table A.3-1 and Table A.3-2 show the organ/tissue weighting factors and quality factors/radiation weighting factors used in ICRP 26 and ICRP 60. The tissue/organ weighting factors were further updated in ICRP 103. The ICRP-103 methodology-based DCFs are currently not available. Table A.3-3 shows the different dose terms used in ICRP 26 and ICRP 60.

Table A.3-1 Tissue Weighting Factors in ICRP 26 and ICRP 60

	Weighting Factors	
Organ/Tissue	ICRP 26	ICRP 60
Gonads	0.25	0.20
Breast	0.15	0.05
Colon	-[a]	0.12
Red Marrow	0.12	0.12
Lungs	0.12	0.12
Stomach	-[a]	0.12
Urinary Bladder	-[a]	0.05
Liver	-[a]	0.05
Esophagus	-[a]	0.05
Thyroid	0.03	0.05
Bone Surface	0.03	0.01
Skin	-[a]	0.01
Remainder	0.30[b]	0.05[c,d]

[a] Weighting factor not assigned in ICRP 26.

[b] The value 0.30 is applied to the average dose among the five remaining organs or tissues receiving the highest dose, excluding the skin, lens of the eye, and the extremities.

[c] The remainder is composed of the following tissues and organs: adrenals, brain, small intestine, upper large intestine, kidney, muscle, pancreas, spleen, thymus, and uterus.

[d] The value 0.05 is applied to the average dose to the remainder tissue group. However, if a member of the remainder receives a dose in excess of the highest dose in any of the twelve organs for which weighting factors are specified, a weighting factor of 0.025 is applied to that organ and a weighting factor of 0.025 is applied to the average dose in the rest of the remainder.

Sources: ICRP (1977) and ICRP (1991).

Table A.3-2 Quality Factors in ICRP 26 and Radiation Weighting Factors in ICRP 60

Radiation Type and Energy Range	ICRP-26 Quality Factor	ICRP-60 Radiation Weighting Factor[a]
Photons, all energies	1	1
Electrons and muons, all energies[b]	1	1
Neutrons[c]		
<10 keV	-	5
10 keV to 100 keV	-	10
>100 Kev to 2 MeV	-	20
>2 MeV to 20 MeV	-	10
>20 MeV	-	5
Protons, other than recoil protons, energy >2 MeV	1	5
Alpha particles, fission fragments, heavy nuclei	20	20

[a] All values relate to the radiation incident on the body or, for internal sources, emitted from the source.

[b] Excluding Auger electrons emitted from nuclei bound to DNA.

[c] In ICRP 26, quality factor for neutrons was recommended to be 10 for unknown energies, otherwise to be calculated, and a value of 2.3 for thermal neutrons.

Source: ICRP (1991).

A.3.1 ICRP-26 Methodology

In ICRP 26, tissue dose was estimated at a point in an organ or tissue and was defined as dose equivalent, H, which was the product of absorbed dose in the organ/tissue, quality factor, and a modifying factor, N, (with a recommended value of 1). When organ/tissue doses multiplied by organ/tissue weighting factors were added over all organs/tissues, the sum was defined as effective dose equivalent (EDE). ICRP-26 used quantity-committed dose equivalent to define a dose to a given organ or tissue from a single intake of radionuclide material as the integral of effective dose up to 50 years after intake. When organ doses multiplied by organ/tissue weighting factors were added over all tissues/organs, the sum was defined as the committed effective dose equivalent (CEDE). Total effective dose equivalent (TEDE) is sum of EDE from external radiation and CEDE from internal radiation.

Table A.3-3　Dose Terms Used in ICRP 26 and ICRP 60

Type of Dose	Dose Quantity	
	ICRP 26/ICRP 30	ICRP 60
Organ/tissue dose	Absorbed dose in tissue or organ, D_T	Absorbed dose in tissue or organ, D_T
Absorbed organ/tissue dose adjusted for radiation type	Dose equivalent in tissue or organ T, $H_T = D_T \times Q \times N^a$	Equivalent dose in tissue or organ T, $H_T = \sum_R W_R \times D_{T,R}$ (average absorbed dose in tissue T from radiation type R)
Committed organ/tissue dose (over a period of time following intake)	Committed dose equivalent, $H_{T,50}$	Committed equivalent dose, $H_{T,50}$
Whole-body dose	Effective dose equivalent (EDE), $H_E = \sum_T W_T \times H_T$	Effective dose (E), $E = \sum_T W_T \times H_T$
Whole-body committed dose (internal only)	Committed effective dose equivalent (CEDE) $= \sum_T W_T \times H_{T,50}$	Committed effective dose (CED), $E_{50} = \sum_T W_T \times H_{T,50}$
Total committed whole-body dose	Total effective dose equivalent (TEDE) = EDE (ext.) + CEDE (int)	Total effective dose (TED) = E (ext) + CED (int)

[a]　N is the product of all other modifying factors that might take account, for example, of absorbed dose rate and fractionation.

A.3.2　ICRP-60 Methodology

In ICRP-60, tissue dose was an average dose over an organ or tissue and was defined as equivalent dose, H_T, which was the product of absorbed dose and radiation weighting factor (WR). When organ/tissue doses multiplied by organ/tissue weighting factors were added over all organs/tissues, the sum was defined as effective dose (E). ICRP 60 used quantity-committed dose equivalent to define a dose to a given organ or tissue from a single intake of radionuclide material as the integral of effective dose up to 70 years after intake for children and 50 years after intake for adults. When organ doses multiplied by organ/tissue weighting factors were added over all tissues/organs, the sum was defined as committed effective dose (E*i*), were *i* is the integration time (in years) following the intake; for an adult, this is 50. Total effective dose (TED) is the sum of E from external radiation and E50 from internal radiation for an adult.

ICRP 60 uses newer biokinetic models to calculate DCFs for six different age groups (3 months, 1 year, 5 years, 10 years, 15 years, and adult). Inhalation class types D (days), W (weeks), and Y (years) in ICRP 26 and ICRP 30 are replaced with F (fast), M (medium), S (slow), and V (very fast) in ICRP 60. The type V applies to gases and vapors.

A.4   References

DOE (U.S. Department of Energy), 2011, *DOE Standard: Derived Concentration Technical Standard,* DOE-STD-1196-2011, Washington, D.C., April.

Eckerman, K.F., A.B. Wolbarst, and Allan C.B. Richardson, 1988, *Limiting Values of Radionuclide Intake and Air Concentration and Dose Conversion Factors for Inhalation, Submersion, and Ingestion*, EPA-520/1-88-020, Federal Guidance Report 11, prepared by Oak Ridge National Laboratory, Oak Ridge, Tenn., for U.S. Environmental Protection Agency, Office of Radiation Programs, Washington, D.C.

Eckerman, K.F., and J.C. Ryman, 1993, *External Exposure to Radionuclides in Air, Water, and Soil, Exposure to Dose Coefficients for General Application, Based on the 1987 Federal Radiation Protection Guidance*, EPA 402-R-93-076, Federal Guidance Report 12, prepared by Oak Ridge National Laboratory, Oak Ridge, Tenn., for U.S. Environmental Protection Agency, Office of Radiation and Indoor Air, Washington, D.C.

ICRP (International Commission on Radiological Protection), 1977, *Recommendations of the International Commission on Radiological Protection,* Publication 26, Annals of the ICRP, 1(2), Pergamon Press, New York, N.Y.

ICRP, 1983, *Radionuclide Transformations: Energy and Intensity of Emissions*, Publication 38, Annals of the ICRP, Vols. 11–13, Pergamon Press, New York, N.Y.

ICRP, 1991, *1990 Recommendations of the International Commission on Radiological Protection,* Publication 60, Annals of the ICRP, 21(1-3), Pergamon Press, New York, N.Y.

ICRP, 1996, *Age-Dependent Doses to Members of the Public from Intake of Radionuclides: Part 5—Compilation of Ingestion and Inhalation Dose Coefficients*, Publication 72, Annals of the ICRP, Vol. 26(1), Pergamon Press, New York, N.Y.

ICRP, 2008, *Nuclear Decay Data for Dosimetric Calculations,* Publication 107, Pergamon Press, New York, N.Y.

APPENDIX B:
EXTERNAL RADIATION FROM CONTAMINATION IN SOIL

This appendix presents models, formulas, and data for calculating dose from an external exposure pathway. Exposure to external radiation occurs primarily as a result of spending time on top of or close to a contaminated area where radionuclides emanate radiation.

The external dose or risk from the external exposure pathway for the principal radionuclide at time *t* following the radiological survey is the sum of the products of the external dose coefficient or the external slope factor of each decay product, the soil concentration of each decay product, radionuclide-specific contaminated source geometry factors, and the occupancy and shielding factor. Section B.1 discusses dose and risk coefficients, Appendix A provides tables of dose coefficients (DCFs) for the external exposure pathway, and Appendix N provides tables of slope factors (SFs) for the external exposure pathway. Section B.2 provides models and formulas for calculating the source geometry factors and the occupancy and shielding factor. Chapter 5 discusses concentrations of radionuclides in soil at different exposure locations. The value listed for the external dose in the summary report is the total of the time-integrated dose for 1 year incurred at different exposure locations (see Chapter 4 for a detailed discussion). The value listed for the external risk in the risk report is the total of the time-integrated risk for the exposure duration incurred at different exposure locations.

B.1   Dose and Risk Coefficients

The dose coefficient *DCFi* for the external exposure pathway is the annual dose received from exposure to radiation from the *i*th principal radionuclide present at the unit concentration in a uniformly contaminated area of infinite depth and lateral extent. The dose is calculated at a distance of 1 m above the ground surface.

The cancer risk at a certain time due to external exposure is estimated using the SFs, which are the excess cancer risks per year of exposure per unit of soil concentration, also in a uniformly contaminated area of infinite depth and lateral extent.

Both DCFs and SFs are derived on the assumption that there is no cover material on top of the contaminated soil.

B.2   Source Geometry Factors

The standard source associated with the default DCFs and SFs in the RESRAD-OFFSITE database is a contaminated area of infinite depth and lateral extent with no cover. To adjust the default DCFs or SFs for an actual contaminated area, which can have any depth, shape, cover, and size, a depth-and-cover factor function and an area-and-shape factor function were developed and used in RESRAD-OFFSITE.

Regression analysis was used to develop a depth factor function to express the radiation attenuation by soils for radionuclides. It includes three independent nuclei-specific parameters whose values were determined by fitting the function with the DCFs for a source of an infinite lateral extent but of a finite depth of 0, 1, 5, and 15 cm, which are available in FGR 12, ICRP 60, or DCFPAK 3.02. A depth-and-cover factor function was then derived based on the depth factor function by considering both dose contribution and attenuation from different depths.

To model external radiation for actual geometries (i.e., finite irregular areas), an area factor was derived using the point-kernel method. This factor depends not only on the lateral extent of the contamination but also on source depth, cover thickness, and gamma energies (Kamboj et al. 1998). A shape factor corrects for a noncircular shape.

The external dose for an individual radionuclide i with concentration $C_i(t)$ at time t for the external exposure pathway is expressed as

$$D_{ext,i}(t) = DCF_{ext,i} \times FO \times FS_i(t) \times FA_i(t) \times FCD_i(t) \times C_i(t) \qquad \text{(B.1)}$$

where

$\quad DCF_{ext.i}$ = external dose coefficient for radionuclide i (mSv/yr per Bq/g),
$\quad FO$ = occupancy and shielding factor (dimensionless),
$\quad FS_i(t)$ = shape factor (dimensionless),
$\quad FA_i(t)$ = area factor (dimensionless),
$\quad FCD_i(t)$ = depth-and-cover factor (dimensionless), and
$\quad C_i(t)$ = concentration of radionuclide i at time t (Bq/g).

The external risk for an individual radionuclide i with concentration $C_i(t)$ at time t for the external exposure pathway is expressed as

$$SF_{ext,i}(t) = SF_{ext,i} \times FO \times FS_i(t) \times FA_i(t) \times FCD_i(t) \times C_i(t) \qquad \text{(B.2)}$$

where $SF_{ext.i}$ = external risk coefficient for radionuclide i (risk/yr per Bq/g).

The occupancy and shielding factor accounts for the fraction of a year that an individual is located at a specific area of concern (i.e., within the primary contaminated area or on top of a secondary contaminated area) and the reduction in the external exposure rate afforded by buildings or other structures while the individual is indoors. It is expressed as

$$FO = f_{otd} + (f_{ind} \times F_{sh}) \qquad \text{(B.3)}$$

where

$\quad f_{otd}$ = fraction of a year spent outdoors, on contaminated area;
$\quad f_{ind}$ = fraction of a year spent indoors, on contaminated area; and
$\quad F_{sh}$ = indoor shielding factor for external gamma (0.7, dimensionless).

The fraction of time outdoors is defined as the average fraction of time during which an individual stays outdoors on the contaminated area. The fraction of time spent indoors is defined as the average fraction of time during which an individual stays inside a building. (Note: All time spent at an agricultural field is outdoors.) The default shielding factor of 0.7 implies that the indoor levels of external radiation are 30% lower than the outdoor levels. This value will likely be conservative for situations involving low- to moderate-energy gamma emitters or when applied to well-shielded buildings. In situations in which indoor exposure to the external gamma pathway is important, separate runs may be performed for low- and high-energy gamma emitters, by applying an appropriate indoor shielding factor in each case.

B.2.1 Depth-and-Cover Factor

The depth factor (FD_i) is based on the regression analysis of the dose coefficients (DCF_i) as a function of depth to the following function:

$$FD_i = \frac{DCF_i[T_s=T(t)]}{DCF_i(T_s=\infty)} = 1 - A_i e^{-100 KA_i \rho_b{}^{ca} T(t)} - B_i e^{-100 KB_i \rho_b{}^{ca} T(t)} \qquad \text{(B.4)}$$

where

$DCF_i\,[T_s = T(t)]$ = DCF of radionuclide i for a source with different contamination depths over time (mSv/yr per Bq/g),

$T(t)$ = depth of contamination at time t (m),

$DCF_i\,[T_s = \underline{\infty}\,]$ = DCF of radionuclide i for the standard source with an infinite depth (mSv/yr per Bq/g),

$\rho_b{}^{ca}$ = bulk density of soil material in the contaminated area (g/cm^3),

$A_i,\ B_i$ = fit parameters (dimensionless), and

$KA_i,\ KB_i$ = fit parameters (cm^2/g).

The following constraints were put on the four fitting parameters:

1. All the parameters were forced to be positive,
2. $A_i + B_i = 1$, and
3. In the limit source depth, $T \rightarrow 0$, $DCF_i\,(T_s = 0)$ should be consistent with the contaminated surface DCF.

The values of the four fit parameters (A_i, B_i, KA_i, and KB_i) were determined for all radionuclides and saved in the RESRAD-OFFSITE database for each of the three external dose factor libraries, FGR-12, ICRP-60, and DCFPAK 3.02. Parameters A_i, B_i, KA_i, and KB_i for the three databases for principal radionuclides based on a 30-day half-life cutoff and their decay progeny radionuclides are shown in Appendix A in Tables A.2-1, A.2-3, and A.2-5. The contamination depth in agricultural and dwelling areas is not time-dependent (it is assumed to be the same as the mixing or plowing depth at all times) and does not have any cover.

The time dependence of the primary contamination thickness (i.e., depth) is given by

$$T_{pc}(t) = T_{pc}(0) \text{ when } t \le t_{\text{cv}}, \text{ and} \qquad \text{(B.5)}$$

$$T_{pc}(t) = T_{pc}(0) - \mathcal{E}_{pc}(t - t_{cv}) \text{ when } t > t_{\text{cv}}, \qquad \text{(B.6)}$$

where

$T_{pc}(t)$ = thickness of the primary contamination at time t (m),

$T_{pc}(0)$ = initial thickness of the primary contamination (2 m),

t = time since the site was characterized (yr),

t_{cv} = $T_{cv}(0)/\mathcal{E}_{cv}$ = time to erode the cover (yr),

$T_{cv}(0)$ = initial thickness of the cover (m),

$\mathcal{E}_{cv}$ = rate at which the cover is eroded (m yr^{-1}), and

$\mathcal{E}_{pc}$ = rate at which the primary contamination is eroded (m yr^{-1}).

Erosion rates for both the cover and the primary contamination are calculated using the universal soil-loss equation. Section 12.10 of the *Handbook of Hydrology* (Shen and Julien 1993) has figures and tables for the first five factors in the following expression for erosion rate,

$$\mathcal{E} = 224 \times R \times K \times LS \times C \times P/(\rho \times 10^6) \qquad \text{(B.7)}$$

where

ε = erosion rate (m yr-1),
R = annual rainfall erosion index, the rainfall erosivity factor, or the rainfall and runoff factor (yr⁻¹),
K = soil erodibility factor (tons/acre),
LS = slope length-steepness factor (dimensionless),
C = cropping management factor or the cover and management factor (dimensionless),
P = conservation practice factor or the support practice factor (dimensionless),
224 = to convert tons per acre to grams per square meter (g m⁻² [tons/acre]⁻¹),
ρ = dry bulk density of the soil (g [cm]⁻³), and
10^6 = to convert per cubic centimeter to per cubic meter ([cm]³ m⁻³).

The following depth and cover factor (FCD_i) for primary contamination was derived based on the depth factor function, by considering both the dose contribution and attenuation from different depths:

$$FCD_i = \frac{DCF_i[T_c=T_{cv}(t),T_s=T_{pc}(t)]}{DCF_i(T_c=0,T_s=\infty)} \tag{B.8}$$

$$= A_i e^{-100KA_i\rho_b^{cv}\ T_{cv}(t)}\left(1 - e^{-100KA_i\rho_b^{pc}T_{pc}(t)}\right) + B_i e^{-100KB_i\rho_b^{cv}T_{cv}(t)}(1 - e^{-100KB_i\rho_b^{pc}T_{pc}(t)})$$

where

$T_{cv}(t)$ = cover depth at time t (m),
ρ_b^{cv} = bulk density of cover material (g/cm³),
$T_{pc}(t)$ = thickness of primary contamination at time t (m), and
ρ_b^{pc} = bulk density of primary contamination at time t (g/cm³).

B.2.2 Area and Shape Factors

The energy-dependent area factor, FA_γ' (E_γ), can be derived by considering the point-kernel dose integral, $D(R, t_a, C_d (t), T(t))$, over the source thickness ($T(t)$), radius (R), distance from the receptor midpoint to the plane of the source and air interface (T_a), and the thickness of the shielding material ($C_d(t)$) for the geometry depicted in Figure B-1. The area factor is the ratio of the dose integrals for the geometry being considered and the infinite slab geometry.
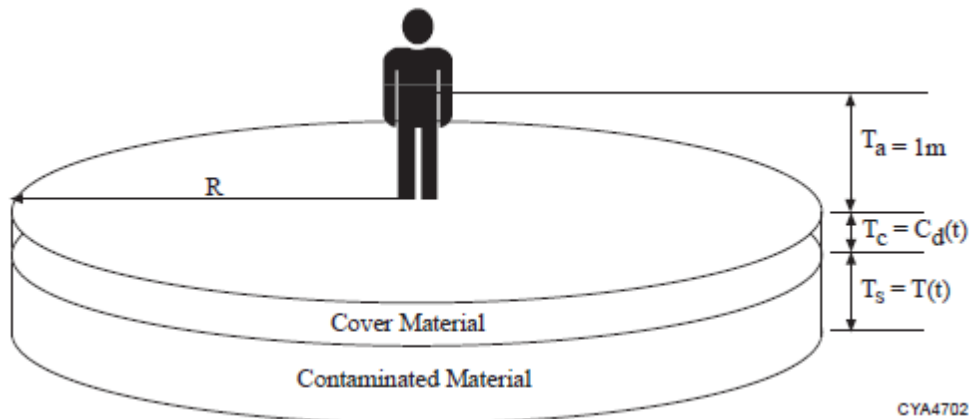

Figure B-1 Exposure Geometry Considered for Area Factor Calculations

$$FA'_\gamma = \frac{D[R=r, T_a=1m, T_c=C_d(t), T_s=T(t)]}{D[R=\infty, T_a=1m, T_c=C_d(t), T_s=T(t)]},$$ (B.9)

where the function *D* is the dose rate evaluated using the point-kernel method (Figure B-2).
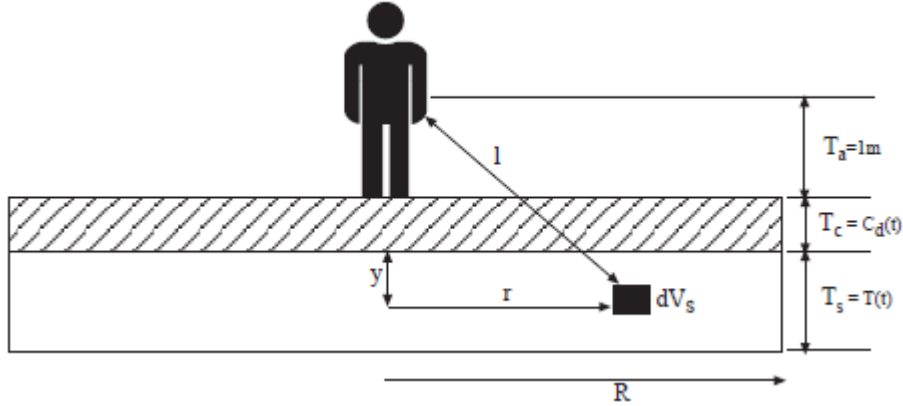

Figure B-2 Cross-Section of Exposure Geometry Showing Element of Integration for Area Factor Calculation

$$D[R, R_{Ra}, C_d(t), T(t)] = K \int_{V_s} e^{-z} \frac{B(z)}{4\pi l^2} dV$$ (B.10)

where

$z = \frac{\mu_a T_a + \mu_c C_d(t) + \mu_s y}{T_a + C_d(t) + y} l;$

$l^2 = r^2 + (T_a + C_d(t) + y^2)$

$dV_S = 2\pi r y\, dr dy;$

μ_a = attenuation coefficient for air (energy-dependent);

μ_c = attenuation coefficient for the cover material (energy-dependent);

μ_s = attenuation coefficient of the source material (energy-dependent);

$B(z)$ = buildup factor (G-P Method [Trubey 1991]) for length measured in mean free paths, *z* (energy-dependent); and

K = energy-dependent conversion factor (for uniform photon slab sources in soil with thickness of 5 mean free path from Table 3 in Chen 1991).

The volume integral can be written more explicitly as

$$\int_0^{T_s} dy \int_0^R \frac{e^{-z} B(z)}{4\pi l^2} 2\pi r dr.$$ (B.11)

Note that in the inner integral

$$\frac{dz}{z} = \frac{dl}{l} = \frac{r\, dr}{l^2}.$$ (B.12)

The volume integral can then be written as

$$1/2 \int_0^{T_s} dy \int_{Z_0}^{Z_f} \frac{e^{-z} B(z)}{z} dz,$$ (B.13)

where

$$Z_0 = \mu_a T_a + \mu_c C_d(t) + \mu_s t \ \text{ and}$$

$$Z_f = Z_0 \sqrt{1 + \frac{R^2}{(T_a + C_d(t) + y)^2}}$$

The photon energies and yields of different radionuclides were obtained by condensing ICRP Publication 38 (ICRP-38) (ICRP 1983) and ICRP Publication 107 (ICRP-107) (ICRP 2008) photon spectra.

For ICRP-38 radionuclides, the algorithm was chosen to analyze the full spectra and repeatedly combine the photons with the smallest relative ratio in their energies. The yield of the resultant photon is the sum of the two photons, and the energy is the yield-weighted energy of the two photons. This combining of pairs of photons was repeated until the closest pair had an energy ratio larger than 3. This resulted in four or fewer collapsed photons for all radionuclides processed. More information on the collapsed photons and their photon fraction appear in the external exposure model used in the RESRAD code for various geometries of contaminated soil (Kamboj et al. 1998). Table B-1 shows the collapsed photon energies and yields for ICRP-38 radionuclides with half-life of at least 30 days and their shorter-lived progeny.

A somewhat different approach is used to collapse the photon spectra from ICRP 107. The Oak Ridge National Laboratory (ORNL) file ICRP-07.RAD contains energy and yield data for all radiations emitted for each nuclear transformation of the ICRP-107 set of radionuclides. There are 11 possible radiation types (ICODE 1 to 11) in this file. The external exposure pathway uses 1 through 5: gammas, x-rays, annihilation photons, β+, β-. For β emissions, the bremsstrahlung energy yield, y', is taken to be: $y' = (y)(\text{MeV})(0.0175)$ where y is the β yield per decay and MeV is the energy.

For the ICRP-107 radionuclide transformation database, all nuclides with total ICODE 1-5 photons greater than four are condensed to four photons. Nuclides with ICODE 1-5 that have total four or less photons are not condensed. Each nuclide's full spectra (ICODE 1-5) is sorted by increasing energy. The two photons with the closest energy ratio are condensed into a single photon with a yield-weighted energy and sum of the two yields. This conserves energy. The process is repeated until four condensed photons represent the original spectra. Table B-2 shows the collapsed photon energies and yields for ICRP-107 radionuclides with half-lives of at least 30 days, as well as their shorter-lived progeny.

The energy-dependent area factor $FA_\gamma'(E_\gamma)$ is computed for each radionuclide's gamma energy (for pure beta emitters by their average bremsstrahlung energy) by interpolation from tabulated values of FA_γ'. The discrete value of each of the four variables used in pre-calculation of the area factor is listed in Table B-3.

The radionuclide-specific area factor, FA_i, is obtained by combining the energy-dependent area factors weighted by their photon fraction, FPT_γ, and the dose contribution at the reference point:

$$FA_i = \frac{\sum_\gamma FA_\gamma'(E_\gamma) FPT_\gamma D_{slab}(E_\gamma)}{\sum_\gamma FPT_\gamma D_{slab}(E_\gamma)} \tag{B.14}$$

where $D_{slab}(E_\gamma)$ = dose from the infinite slab geometry.

A shape factor, FS_i, is used to correct a noncircular contaminated area based on an ideally circular zone. The shape factor of a circular contaminated area is 1.0. For an irregularly shaped contaminated area, the shape factor is obtained by enclosing the irregularly shaped contaminated area in a circle, multiplying the area factor of each annulus by the fraction of the annulus area that is contaminated, summing the products, and dividing by the area factor of a circular primary contamination that is equivalent in area:

$$FS_i = \frac{\sum_{j=1}^{n} f_j [FA_{i1}(A_j) - FA_{i1}(A_{j-1})]}{FA_{i1}[\sum_{j=1}^{n} f_j (A_j - A_{j-1})]}$$ (B.15)

where

f_j = fraction of annular area, j, which is contaminated, and

$FA_i(A_j)$ = area factor for area A_j.

Table B-1 Collapsed Photon Energies (MeV) and Fractions for ICRP-38 Radionuclides with Half-Life of at least 30 Days and their Shorter-Lived Progeny

Nuclide	EPT(1)	EPT(2)	EPT(3)	EPT(4)	FPT(1)	FPT(2)	FPT(3)	FPT(4)
Ac-225	4.55E-01	1.12E-01	1.40E-02	0.00E+00	2.10E-03	1.32E-01	1.64E-01	0.00E+00
Ac-227	1.47E-02	4.65E-02	1.12E-01	3.53E-01	7.40E-03	1.38E-05	1.08E-03	7.87E-06
Ac-228	1.53E-02	1.06E-01	3.50E-01	1.01E+00	4.20E-01	1.51E-01	3.70E-01	8.15E-01
Ag-105	4.11E-01	6.40E-02	2.16E-02	1.62E-01	1.22E+00	1.05E-01	8.19E-01	2.28E-08
Ag-108	1.08E+00	5.79E-01	2.16E-02	6.26E-01	2.35E-04	2.98E-02	1.51E-02	1.07E-02
Ag-108m	5.91E-01	7.92E-02	2.16E-02	0.00E+00	2.72E+00	6.78E-02	6.56E-01	0.00E+00
Ag-110	6.67E-01	2.17E-02	1.19E+00	0.00E+00	4.59E-02	2.22E-03	2.07E-02	0.00E+00
Ag-110m	8.57E-01	1.33E-01	0.00E+00	0.00E+00	3.21E+00	1.15E-03	0.00E+00	0.00E+00
Al-26	2.94E+00	1.79E+00	5.11E-01	5.44E-01	2.40E-03	1.02E+00	1.64E+00	7.78E-03
Am-241	5.96E-02	1.68E-02	0.00E+00	0.00E+00	3.59E-01	6.65E-01	0.00E+00	0.00E+00
Am-242	1.75E-02	4.28E-02	1.06E-01	1.91E-01	3.12E-01	5.24E-04	1.22E-01	2.77E-03
Am-242m	1.51E-01	1.01E-01	5.22E-02	1.74E-02	5.19E-04	2.06E-03	2.31E-03	2.71E-01
Am-243	7.52E-02	4.34E-02	1.64E-02	0.00E+00	6.70E-01	5.69E-02	1.92E-01	0.00E+00
Am-245	1.75E-02	4.56E-02	1.11E-01	2.54E-01	1.02E-01	9.91E-04	1.24E-01	7.05E-02
As-73	5.34E-02	1.00E-02	1.19E-03	0.00E+00	1.05E-01	1.04E+00	2.11E-02	0.00E+00
At-217	5.94E-01	2.59E-01	7.88E-02	1.21E-02	4.00E-04	2.30E-04	1.38E-04	5.42E-05
At-218	5.32E-02	1.55E-02	1.30E-02	1.08E-02	6.59E-02	2.93E-02	1.23E-01	1.07E-01
Au-194	1.04E-02	6.84E-02	3.60E-01	1.50E+00	2.78E-01	7.93E-01	9.15E-01	4.55E-01
Au-195	7.18E-02	3.09E-02	1.05E-02	0.00E+00	1.10E+00	7.52E-03	5.34E-01	0.00E+00
Ba-133	3.41E-01	7.93E-02	3.17E-02	4.54E-03	9.76E-01	3.85E-01	1.20E+00	1.45E-01
Ba-137m	6.62E-01	3.29E-02	0.00E+00	0.00E+00	8.98E-01	7.49E-02	0.00E+00	0.00E+00
Be-10	2.52E-01	0.00E+00	0.00E+00	0.00E+00	4.41E-03	0.00E+00	0.00E+00	0.00E+00
Be-7	4.78E-01	0.00E+00	0.00E+00	0.00E+00	1.03E-01	0.00E+00	0.00E+00	0.00E+00
Bi-207	1.18E-02	7.67E-02	5.70E-01	1.12E+00	3.30E-01	7.47E-01	9.78E-01	8.21E-01
Bi-210	3.89E-01	0.00E+00	0.00E+00	0.00E+00	6.81E-03	0.00E+00	0.00E+00	0.00E+00
Bi-210m	6.40E-01	2.81E-01	7.45E-02	1.15E-02	3.12E-02	8.05E-01	1.33E-01	5.79E-02
Bi-211	1.14E-02	7.45E-02	1.75E-01	3.51E-01	9.46E-03	2.54E-02	8.55E-06	1.27E-01
Bi-212	1.16E-02	5.23E-02	7.48E-01	1.62E+00	7.99E-02	1.58E-02	1.75E-01	3.66E-02

Table B-1 Collapsed Photon Energies (MeV) and Fractions for ICRP-38 Radionuclides with Half-Life of at least 30 Days and their Shorter-Lived Progeny (Cont.)

Nuclide	EPT(1)	EPT(2)	EPT(3)	EPT(4)	FPT(1)	FPT(2)	FPT(3)	FPT(4)
Bi-213	1.25E-02	8.10E-02	4.37E-01	9.42E-01	1.66E-02	4.10E-02	2.87E-01	7.94E-03
Bi-214	1.54E+00	6.43E-01	8.11E-02	7.75E-01	7.16E-01	6.25E-01	1.94E-02	1.12E-02
Bk-247	2.65E-01	9.33E-02	1.91E-02	1.45E-02	1.60E-01	6.43E-01	9.60E-02	8.09E-02
Bk-249	1.69E-02	3.30E-02	1.09E-01	3.24E-01	8.30E-08	5.76E-04	1.45E-07	2.06E-07
Bk-250	1.01E+00	1.16E-01	1.89E-02	3.07E-01	8.76E-01	1.16E-02	2.46E-01	4.52E-03
C-14	4.95E-02	0.00E+00	0.00E+00	0.00E+00	8.65E-04	0.00E+00	0.00E+00	0.00E+00
Ca-41	3.59E-03	3.31E-03	3.31E-03	0.00E+00	1.30E-02	7.47E-02	3.75E-02	0.00E+00
Ca-45	1.25E-02	4.46E-03	4.09E-03	7.72E-02	2.66E-06	2.81E-07	2.21E-06	1.35E-03
Cd-109	8.80E-02	2.26E-02	3.09E-03	0.00E+00	3.61E-02	1.01E+00	8.62E-02	0.00E+00
Cd-113	9.33E-02	0.00E+00	0.00E+00	0.00E+00	1.63E-03	0.00E+00	0.00E+00	0.00E+00
Cd-113m	1.85E-01	0.00E+00	0.00E+00	0.00E+00	3.24E-03	0.00E+00	0.00E+00	0.00E+00
Cd-115m	9.95E-01	1.48E-01	6.13E-01	0.00E+00	2.21E-02	1.65E-04	1.06E-02	0.00E+00
Ce-139	1.66E-01	3.42E-02	4.88E-03	0.00E+00	7.91E-01	8.13E-01	1.04E-01	0.00E+00
Ce-141	1.45E-01	3.69E-02	5.28E-03	1.49E-01	4.80E-01	1.70E-01	2.15E-02	2.54E-03
Ce-144	5.38E-03	3.70E-02	8.14E-02	1.34E-01	1.70E-02	1.12E-01	2.69E-02	1.08E-01
Cf-248	4.30E-02	2.30E-02	1.92E-02	1.48E-02	1.58E-04	8.27E-03	3.62E-02	2.77E-02
Cf-249	3.73E-01	1.11E-01	1.77E-02	0.00E+00	8.60E-01	8.10E-02	2.93E-01	0.00E+00
Cf-250	4.29E-02	2.30E-02	1.92E-02	1.48E-02	1.48E-04	7.87E-03	3.45E-02	2.63E-02
Cf-251	1.96E-01	1.11E-01	6.74E-02	1.78E-02	3.07E-01	5.13E-01	1.16E-02	7.61E-01
Cf-252	1.60E-01	1.00E-01	4.34E-02	1.80E-02	1.94E-05	1.29E-04	1.48E-04	6.57E-02
Cf-253	1.48E-02	1.99E-02	5.00E-02	7.94E-02	4.71E-04	7.76E-04	5.67E-06	1.39E-03
Cl-36	5.11E-01	2.47E-03	2.31E-03	2.79E-01	2.97E-04	7.64E-05	1.23E-03	4.79E-03
Cm-241	4.74E-01	1.16E-01	1.72E-02	0.00E+00	8.05E-01	8.82E-01	1.01E+00	0.00E+00
Cm-242	1.21E-01	4.41E-02	1.69E-02	0.00E+00	4.27E-05	3.21E-04	1.07E-01	0.00E+00
Cm-243	2.52E-01	1.05E-01	1.67E-02	0.00E+00	2.88E-01	4.94E-01	5.76E-01	0.00E+00
Cm-244	4.28E-02	2.16E-02	1.80E-02	1.42E-02	2.60E-04	1.09E-02	4.93E-02	3.96E-02
Cm-245	1.74E-01	1.08E-01	1.67E-02	0.00E+00	6.60E-02	6.81E-01	6.16E-01	0.00E+00
Cm-246	4.45E-02	2.16E-02	1.80E-02	1.42E-02	2.80E-04	9.73E-03	4.40E-02	3.51E-02
Cm-247	3.93E-01	1.06E-01	5.91E-02	1.69E-02	7.87E-01	3.64E-02	6.98E-03	1.12E-01
Cm-248	4.40E-02	2.16E-02	1.80E-02	1.42E-02	2.02E-04	7.44E-03	3.36E-02	2.69E-02

Table B-1 Collapsed Photon Energies (MeV) and Fractions for ICRP-38 Radionuclides with Half-Life of at least 30 Days and their Shorter-Lived Progeny (Cont.)

Nuclide	EPT(1)	EPT(2)	EPT(3)	EPT(4)	FPT(1)	FPT(2)	FPT(3)	FPT(4)
Cm-249	5.80E-01	1.19E-01	1.79E-02	2.77E-01	3.17E-02	6.12E-03	3.27E-03	4.76E-03
Co-56	2.41E+00	1.02E+00	5.11E-01	6.25E-01	5.97E-01	1.90E+00	3.98E-01	2.11E-03
Co-57	6.68E-01	1.24E-01	1.44E-02	6.48E-03	1.89E-03	9.62E-01	9.19E-02	5.72E-01
Co-58	6.48E-03	2.01E-01	7.42E-01	1.67E+00	2.66E-01	5.28E-04	1.30E+00	5.17E-03
Co-60	1.25E+00	9.85E-02	0.00E+00	0.00E+00	2.00E+00	1.68E-03	0.00E+00	0.00E+00
Co-60m	7.01E-03	5.86E-02	6.02E-01	1.32E+00	3.23E-01	2.07E-02	2.60E-05	2.59E-03
Cs-134	6.98E-01	2.01E-01	0.00E+00	0.00E+00	2.23E+00	2.74E-03	0.00E+00	0.00E+00
Cs-135	6.73E-02	0.00E+00	0.00E+00	0.00E+00	1.18E-03	0.00E+00	0.00E+00	0.00E+00
Cs-137	4.25E-01	1.73E-01	2.04E-01	0.00E+00	5.40E-02	9.46E-01	3.27E-03	0.00E+00
Dy-159	4.58E-02	6.75E-03	0.00E+00	0.00E+00	9.58E-01	1.80E-01	0.00E+00	0.00E+00
Es-253	3.96E-01	1.10E-01	4.19E-02	1.84E-02	6.43E-04	4.55E-04	7.27E-04	4.28E-02
Es-254	3.10E-01	5.81E-02	1.81E-02	1.10E-03	4.24E-03	3.49E-02	8.55E-01	3.00E-01
Eu-146	8.00E-01	4.11E-02	6.35E-01	0.00E+00	3.09E+00	7.36E-01	5.38E-04	0.00E+00
Eu-148	6.74E-01	4.11E-02	4.05E-01	0.00E+00	3.18E+00	7.90E-01	1.06E-05	0.00E+00
Eu-149	3.30E-01	4.11E-02	2.25E-02	6.05E-03	9.27E-02	7.74E-01	4.42E-03	1.37E-01
Eu-150b	9.71E-01	4.31E-01	4.11E-02	0.00E+00	4.55E-01	2.37E+00	8.18E-01	0.00E+00
Eu-152	1.09E+00	2.55E-01	4.11E-02	3.85E-01	8.63E-01	7.13E-01	7.56E-01	1.46E-03
Eu-154	1.00E+00	1.42E-01	4.40E-02	3.73E-01	1.16E+00	4.77E-01	2.75E-01	3.96E-03
Eu-155	6.51E-03	2.55E-02	4.48E-02	9.41E-02	6.96E-02	3.77E-03	2.56E-01	5.17E-01
Fe-55	6.49E-03	5.89E-03	0.00E+00	0.00E+00	3.35E-02	2.49E-01	0.00E+00	0.00E+00
Fe-59	1.18E+00	1.80E-01	1.32E-01	0.00E+00	9.98E-01	4.00E-02	2.05E-03	0.00E+00
Fe-60	4.91E-02	0.00E+00	0.00E+00	0.00E+00	8.60E-04	0.00E+00	0.00E+00	0.00E+00
Fm-257	2.13E-01	1.18E-01	6.36E-02	1.87E-02	1.38E-01	5.77E-01	1.88E-02	6.45E-01
Fr-221	3.82E-01	2.17E-01	8.46E-02	1.31E-02	2.35E-03	1.26E-01	2.85E-02	2.13E-02
Fr-223	1.45E-02	6.20E-02	2.53E-01	7.92E-01	3.59E-01	5.19E-01	6.77E-02	8.89E-03
Ga-68	1.11E+00	5.11E-01	8.33E-01	0.00E+00	3.65E-02	1.78E+00	1.29E-02	0.00E+00
Gd-146	1.28E-01	4.25E-02	6.26E-03	0.00E+00	1.32E+00	1.85E+00	3.11E-01	0.00E+00
Gd-148	0.00E+00	0.00E+00	0.00E+00	0.00E+00	0.00E+00	0.00E+00	0.00E+00	0.00E+00
Gd-151	2.02E-01	4.25E-02	2.15E-02	6.35E-03	1.35E-01	8.17E-01	2.32E-02	2.30E-01
Gd-152	0.00E+00	0.00E+00	0.00E+00	0.00E+00	0.00E+00	0.00E+00	0.00E+00	0.00E+00

Table B-1 Collapsed Photon Energies (MeV) and Fractions for ICRP-38 Radionuclides with Half-Life of at least 30 Days and their Shorter-Lived Progeny (Cont.)

Nuclide	EPT(1)	EPT(2)	EPT(3)	EPT(4)	FPT(1)	FPT(2)	FPT(3)	FPT(4)
Gd-153	9.84E-02	4.25E-02	6.26E-03	0.00E+00	5.34E-01	1.22E+00	2.09E-01	0.00E+00
Ge-68	1.03E-02	9.24E-03	1.11E-03	0.00E+00	5.42E-02	3.86E-01	6.29E-03	0.00E+00
H-3	5.68E-03	0.00E+00	0.00E+00	0.00E+00	9.94E-05	0.00E+00	0.00E+00	0.00E+00
Hf-172	1.24E-01	5.69E-02	2.40E-02	8.32E-03	1.61E-01	1.54E+00	2.00E-01	6.82E-01
Hf-175	3.46E-01	9.22E-02	5.53E-02	8.35E-03	9.12E-01	2.66E-02	8.95E-01	2.34E-01
Hf-178m	4.96E-01	2.59E-01	7.21E-02	8.64E-03	3.01E+00	2.83E+00	1.78E+00	5.56E-01
Hf-181	4.63E-01	1.04E-01	8.93E-03	1.19E-01	1.01E+00	8.40E-01	1.48E-01	2.08E-03
Hf-182	8.92E-03	5.88E-02	1.45E-01	2.70E-01	4.69E-02	1.44E-01	9.88E-02	8.00E-01
Hg-194	1.36E-02	1.15E-02	9.71E-03	8.49E-03	2.74E-02	1.20E-01	9.55E-02	3.65E-03
Hg-203	1.15E-02	5.77E-02	7.45E-02	2.79E-01	5.44E-02	1.01E-03	1.34E-01	8.15E-01
Ho-166m	7.22E-01	2.15E-01	5.77E-02	1.82E-02	2.03E+00	1.14E+00	5.25E-01	3.01E-04
I-125	3.55E-02	2.81E-02	3.92E-03	0.00E+00	6.67E-02	1.40E+00	1.24E-01	0.00E+00
I-129	3.96E-02	3.04E-02	4.28E-03	4.89E-02	7.51E-02	7.00E-01	6.76E-02	8.55E-04
In-113m	3.92E-01	2.47E-02	0.00E+00	0.00E+00	6.42E-01	2.45E-01	0.00E+00	0.00E+00
In-114	1.30E+00	5.51E-01	2.37E-02	7.77E-01	2.01E-03	1.46E-04	3.88E-03	1.35E-02
In-114m	6.41E-01	1.90E-01	2.46E-02	3.41E-03	8.72E-02	1.54E-01	3.69E-01	4.46E-02
In-115	1.52E-01	0.00E+00	0.00E+00	0.00E+00	2.66E-03	0.00E+00	0.00E+00	0.00E+00
Ir-192	9.14E-01	3.71E-01	6.83E-02	1.84E-01	3.60E-03	2.17E+00	1.39E-01	3.00E-03
Ir-192m	1.61E-01	0.00E+00	0.00E+00	0.00E+00	1.00E-01	0.00E+00	0.00E+00	0.00E+00
Ir-194	9.36E-01	3.22E-01	6.84E-02	8.23E-01	4.10E-02	1.59E-01	8.60E-03	1.41E-02
Ir-194m	1.01E+00	4.81E-01	8.35E-02	6.98E-02	3.60E-02	4.73E-01	2.53E-01	1.22E-03
K-40	1.46E+00	5.85E-01	0.00E+00	0.00E+00	1.07E-01	9.14E-03	0.00E+00	0.00E+00
Kr-83m	3.22E-02	1.28E-02	9.40E-03	1.61E-03	5.09E-04	1.63E-01	5.64E-02	2.58E-02
La-137	3.29E-02	5.63E-03	4.68E-03	0.00E+00	7.24E-01	5.37E-03	8.02E-02	0.00E+00
La-138	1.44E+00	7.88E-01	3.29E-02	9.49E-02	6.71E-01	3.29E-01	4.10E-01	5.47E-04
Lu-172	8.07E-03	5.79E-02	1.86E-01	9.32E-01	4.09E-01	1.28E+00	2.49E-01	1.89E+00
Lu-173	6.06E-01	2.57E-01	5.61E-02	8.06E-03	1.26E-02	1.67E-01	1.37E+00	3.04E-01
Lu-174	8.07E-03	5.50E-02	1.74E-01	1.24E+00	2.69E-01	8.70E-01	5.10E-07	6.11E-02
Lu-174m	9.92E-01	2.31E-01	5.51E-02	8.39E-03	6.98E-03	1.13E-02	9.01E-01	4.92E-01
Lu-176	8.65E-03	5.71E-02	8.83E-02	2.58E-01	2.10E-01	3.29E-01	1.31E-01	1.79E+00

Table B-1 Collapsed Photon Energies (MeV) and Fractions for ICRP-38 Radionuclides with Half-Life of at least 30 Days and their Shorter-Lived Progeny (Cont.)

Nuclide	EPT(1)	EPT(2)	EPT(3)	EPT(4)	FPT(1)	FPT(2)	FPT(3)	FPT(4)
Lu-177	8.64E-03	5.74E-02	1.14E-01	2.11E-01	3.03E-02	5.89E-02	6.68E-02	1.14E-01
Lu-177m	8.58E-03	5.69E-02	1.83E-01	3.58E-01	4.50E-01	1.39E+00	2.39E+00	1.35E+00
Md-258	7.50E-02	2.52E-02	2.09E-02	1.59E-02	7.43E-03	3.64E-02	1.50E-01	1.02E-01
Mn-53	5.95E-03	5.41E-03	0.00E+00	0.00E+00	2.91E-02	2.25E-01	0.00E+00	0.00E+00
Mn-54	8.35E-01	5.41E-03	0.00E+00	0.00E+00	1.00E+00	2.26E-01	0.00E+00	0.00E+00
Mo-93	1.69E-02	2.21E-03	0.00E+00	0.00E+00	6.28E-01	2.60E-02	0.00E+00	0.00E+00
Na-22	1.27E+00	5.11E-01	2.17E-01	0.00E+00	9.99E-01	1.80E+00	3.40E-03	0.00E+00
Nb-93m	1.69E-02	2.18E-03	0.00E+00	0.00E+00	1.10E-01	2.09E-02	0.00E+00	0.00E+00
Nb-94	8.71E-01	7.03E-01	1.66E-01	0.00E+00	1.00E+00	1.00E+00	2.90E-03	0.00E+00
Nb-95	7.66E-01	4.33E-02	0.00E+00	0.00E+00	1.00E+00	7.58E-04	0.00E+00	0.00E+00
Nb-95m	2.35E-01	1.69E-02	0.00E+00	0.00E+00	2.59E-01	4.46E-01	0.00E+00	0.00E+00
Ni-59	7.65E-03	6.93E-03	0.00E+00	0.00E+00	4.09E-02	3.02E-01	0.00E+00	0.00E+00
Ni-63	1.71E-02	0.00E+00	0.00E+00	0.00E+00	3.00E-04	0.00E+00	0.00E+00	0.00E+00
Np-235	1.00E-01	5.08E-02	1.61E-02	0.00E+00	7.57E-03	1.44E-03	3.90E-01	0.00E+00
Np-236a	1.60E-01	1.01E-01	1.61E-02	1.13E-01	2.39E-01	7.65E-01	1.30E+00	1.76E-04
Np-237	1.71E-01	8.96E-02	2.94E-02	1.56E-02	1.81E-02	2.05E-01	1.40E-01	5.81E-01
Np-238	9.95E-01	1.08E-01	1.69E-02	3.53E-01	5.48E-01	9.79E-03	3.56E-01	3.90E-03
Np-239	2.60E-01	1.05E-01	1.67E-02	1.25E-01	3.31E-01	7.37E-01	5.81E-01	2.06E-03
Np-240m	1.69E-02	9.28E-02	5.95E-01	1.52E+00	4.60E-01	1.31E-02	4.84E-01	3.15E-02
Os-185	6.77E-01	1.75E-01	6.26E-02	9.53E-03	9.87E-01	1.54E-02	7.28E-01	2.36E-01
Os-194	1.04E-02	2.28E-02	4.31E-02	6.80E-02	7.33E-02	3.75E-04	2.32E-02	4.10E-04
P-32	6.95E-01	0.00E+00	0.00E+00	0.00E+00	1.22E-02	0.00E+00	0.00E+00	0.00E+00
Pa-231	3.04E-01	9.26E-02	2.88E-02	1.48E-02	1.10E-01	1.73E-02	1.02E-01	7.02E-01
Pa-233	3.19E-01	9.91E-02	1.59E-02	7.53E-02	5.01E-01	3.79E-01	4.40E-01	1.11E-03
Pa-234	1.61E-02	1.11E-01	2.64E-01	8.70E-01	1.14E+00	9.30E-01	3.45E-01	1.96E+00
Pa-234m	1.59E-02	9.97E-02	3.01E-01	8.93E-01	5.59E-03	5.03E-03	7.97E-04	2.52E-02
Pb-202	1.46E-02	1.23E-02	1.03E-02	8.95E-03	9.16E-04	4.31E-02	1.53E-01	6.04E-03
Pb-205	1.46E-02	1.23E-02	1.03E-02	8.95E-03	2.08E-03	4.84E-02	1.58E-01	6.25E-03
Pb-209	1.98E-01	0.00E+00	0.00E+00	0.00E+00	3.46E-03	0.00E+00	0.00E+00	0.00E+00
Pb-210	1.08E-02	1.30E-02	1.55E-02	4.65E-02	9.81E-02	1.12E-01	2.68E-02	4.05E-02

Table B-1 Collapsed Photon Energies (MeV) and Fractions for ICRP-38 Radionuclides with Half-Life of at least 30 Days and their Shorter-Lived Progeny (Cont.)

Nuclide	EPT(1)	EPT(2)	EPT(3)	EPT(4)	FPT(1)	FPT(2)	FPT(3)	FPT(4)
Pb-211	8.20E-01	4.09E-01	7.85E-02	4.65E-01	3.83E-02	4.53E-02	7.26E-03	7.92E-03
Pb-212	2.43E-01	7.94E-02	1.21E-02	1.07E-01	4.81E-01	3.74E-01	1.44E-01	1.74E-03
Pb-214	1.22E-02	7.79E-02	3.20E-01	6.66E-01	1.30E-01	2.33E-01	6.52E-01	3.32E-02
Pd-107	9.26E-03	0.00E+00	0.00E+00	0.00E+00	1.62E-04	0.00E+00	0.00E+00	0.00E+00
Pm-143	7.42E-01	3.82E-02	5.50E-03	0.00E+00	3.85E-01	7.62E-01	1.04E-01	0.00E+00
Pm-144	6.27E-01	3.82E-02	0.00E+00	0.00E+00	2.44E+00	7.80E-01	0.00E+00	0.00E+00
Pm-145	7.12E-02	3.82E-02	6.73E-03	5.51E-03	2.83E-02	7.42E-01	9.12E-03	1.18E-01
Pm-146	5.95E-01	3.82E-02	2.52E-01	0.00E+00	1.23E+00	4.89E-01	1.51E-03	0.00E+00
Pm-147	1.21E-01	4.11E-02	6.02E-03	6.20E-02	2.85E-05	2.18E-05	3.56E-06	1.08E-03
Pm-148	1.27E+00	5.53E-01	8.42E-01	0.00E+00	3.47E-01	2.44E-01	1.26E-02	0.00E+00
Pm-148m	6.20E-01	1.13E-01	4.07E-02	1.66E-01	3.21E+00	6.08E-02	1.11E-01	2.54E-03
Po-210	8.02E-01	0.00E+00	0.00E+00	0.00E+00	1.06E-05	0.00E+00	0.00E+00	0.00E+00
Po-211	7.31E-01	3.28E-01	7.67E-02	0.00E+00	1.06E-02	3.24E-05	1.93E-04	0.00E+00
Po-212	0.00E+00	0.00E+00	0.00E+00	0.00E+00	0.00E+00	0.00E+00	0.00E+00	0.00E+00
Po-213	0.00E+00	0.00E+00	0.00E+00	0.00E+00	0.00E+00	0.00E+00	0.00E+00	0.00E+00
Po-214	8.00E-01	2.98E-01	0.00E+00	0.00E+00	1.04E-04	5.00E-07	0.00E+00	0.00E+00
Po-215	4.39E-01	7.67E-02	0.00E+00	0.00E+00	4.00E-04	1.07E-05	0.00E+00	0.00E+00
Po-216	8.06E-01	0.00E+00	0.00E+00	0.00E+00	2.10E-05	0.00E+00	0.00E+00	0.00E+00
Po-218	8.37E-01	7.05E-02	0.00E+00	0.00E+00	1.09E-05	2.47E-07	0.00E+00	0.00E+00
Pr-144	1.99E+00	6.97E-01	1.22E+00	0.00E+00	1.08E-02	1.49E-02	2.11E-02	0.00E+00
Pr-144m	5.33E-03	3.69E-02	5.90E-02	7.54E-01	9.55E-02	3.04E-01	7.90E-04	1.21E-03
Pt-193	1.28E-02	1.07E-02	9.17E-03	8.04E-03	2.58E-02	1.10E-01	7.23E-02	2.63E-03
Pu-236	5.86E-01	1.12E-01	4.76E-02	1.61E-02	5.10E-06	1.30E-04	6.90E-04	1.27E-01
Pu-237	1.03E-01	5.95E-02	1.64E-02	0.00E+00	4.11E-01	3.25E-02	4.93E-01	0.00E+00
Pu-238	5.50E-02	1.61E-02	0.00E+00	0.00E+00	4.77E-04	1.11E-01	0.00E+00	0.00E+00
Pu-239	3.84E-01	1.19E-01	5.00E-02	1.61E-02	6.66E-05	1.91E-04	2.99E-04	4.17E-02
Pu-240	1.08E-01	4.52E-02	1.61E-02	0.00E+00	7.54E-05	4.50E-04	1.06E-01	0.00E+00
Pu-241	5.24E-03	1.60E-02	4.36E-02	1.07E-01	9.16E-05	6.25E-05	1.83E-07	1.44E-05
Pu-242	1.03E-01	4.49E-02	1.61E-02	0.00E+00	7.94E-05	3.60E-04	8.79E-02	0.00E+00
Pu-243	1.73E-02	4.17E-02	8.53E-02	3.76E-01	1.37E-01	8.56E-03	2.41E-01	7.30E-03

Table B-1 Collapsed Photon Energies (MeV) and Fractions for ICRP-38 Radionuclides with Half-Life of at least 30 Days and their Shorter-Lived Progeny (Cont.)

Nuclide	EPT(1)	EPT(2)	EPT(3)	EPT(4)	FPT(1)	FPT(2)	FPT(3)	FPT(4)
Pu-244	4.30E-02	2.03E-02	1.70E-02	1.35E-02	2.50E-04	8.63E-03	3.83E-02	2.82E-02
Ra-223	3.04E-01	9.67E-02	1.33E-02	0.00E+00	2.33E-01	6.23E-01	2.25E-01	0.00E+00
Ra-224	5.63E-01	2.41E-01	8.56E-02	1.36E-02	1.10E-04	3.91E-02	4.24E-03	3.70E-03
Ra-225	1.26E-02	1.61E-02	4.00E-02	9.46E-02	5.76E-02	8.49E-02	2.90E-01	1.65E-03
Ra-226	1.86E-01	8.56E-02	1.37E-02	0.00E+00	3.29E-02	6.17E-03	7.67E-03	0.00E+00
Ra-228	6.67E-03	9.86E-03	0.00E+00	0.00E+00	6.21E-07	1.73E-04	0.00E+00	0.00E+00
Rb-83	5.32E-01	1.25E-02	0.00E+00	0.00E+00	9.34E-01	6.25E-01	0.00E+00	0.00E+00
Rb-84	1.90E+00	7.25E-01	1.28E-02	5.88E-01	7.80E-03	1.24E+00	3.97E-01	2.64E-03
Rb-87	1.11E-01	0.00E+00	0.00E+00	0.00E+00	1.95E-03	0.00E+00	0.00E+00	0.00E+00
Re-184	8.52E-01	2.53E-01	6.89E-02	9.22E-03	9.48E-01	3.09E-02	1.05E+00	3.18E-01
Re-184m	8.56E-01	2.46E-01	7.04E-02	9.32E-03	2.50E-01	4.08E-01	1.01E+00	4.42E-01
Re-186	7.03E-01	1.01E-01	9.60E-03	3.51E-01	5.08E-04	1.96E-01	4.65E-02	5.75E-03
Re-186m	9.93E-02	5.91E-02	4.03E-02	9.76E-03	1.06E-02	1.87E-01	5.00E-02	5.31E-01
Re-187	6.60E-04	0.00E+00	0.00E+00	0.00E+00	1.16E-05	0.00E+00	0.00E+00	0.00E+00
Re-188	9.89E-03	1.33E-01	7.10E-01	1.69E+00	2.92E-02	1.96E-01	5.33E-02	2.18E-03
Rh-101	3.27E-01	1.62E-01	1.97E-02	0.00E+00	1.33E-01	1.29E+00	8.09E-01	0.00E+00
Rh-102	6.81E-01	1.97E-02	1.02E-01	0.00E+00	3.12E+00	6.64E-01	1.69E-09	0.00E+00
Rh-102m	5.36E-01	1.97E-02	5.13E-01	0.00E+00	8.92E-01	4.26E-01	2.85E-03	0.00E+00
Rh-103m	3.98E-02	2.06E-02	2.78E-03	2.45E-03	6.99E-04	7.87E-02	3.54E-02	1.10E-03
Rh-106	1.16E+00	5.48E-01	1.42E+00	0.00E+00	2.82E-02	3.14E-01	2.47E-02	0.00E+00
Rn-219	3.25E-01	8.44E-02	1.26E-02	0.00E+00	1.68E-01	1.90E-02	9.65E-03	0.00E+00
Rn-220	5.50E-01	8.11E-02	0.00E+00	0.00E+00	7.00E-04	1.25E-05	0.00E+00	0.00E+00
Rn-222	5.10E-01	8.11E-02	0.00E+00	0.00E+00	7.80E-04	1.62E-05	0.00E+00	0.00E+00
Ru-103	5.03E-01	9.99E-02	0.00E+00	0.00E+00	9.30E-01	1.26E-03	0.00E+00	0.00E+00
Ru-106	1.00E-02	0.00E+00	0.00E+00	0.00E+00	1.76E-04	0.00E+00	0.00E+00	0.00E+00
S-35	4.88E-02	0.00E+00	0.00E+00	0.00E+00	8.55E-04	0.00E+00	0.00E+00	0.00E+00
Sb-124	9.81E-01	6.24E-01	0.00E+00	0.00E+00	1.85E+00	6.70E-03	0.00E+00	0.00E+00
Sb-125	5.17E-01	1.76E-01	2.87E-02	1.28E-01	7.77E-01	7.89E-02	5.14E-01	1.52E-03
Sb-126	6.40E-01	4.25E-01	0.00E+00	0.00E+00	4.43E+00	4.71E-03	0.00E+00	0.00E+00
Sb-126m	1.48E+00	5.96E-01	6.84E-01	0.00E+00	3.43E-03	2.59E+00	1.02E-02	0.00E+00

Table B-1 Collapsed Photon Energies (MeV) and Fractions for ICRP-38 Radionuclides with Half-Life of at least 30 Days and their Shorter-Lived Progeny (Cont.)

Nuclide	EPT(1)	EPT(2)	EPT(3)	EPT(4)	FPT(1)	FPT(2)	FPT(3)	FPT(4)
Sc-44	2.65E+00	1.16E+00	5.11E-01	6.32E-01	1.16E-03	1.01E+00	1.89E+00	1.04E-02
Sc-46	1.12E+00	8.89E-01	1.12E-01	0.00E+00	1.00E+00	1.00E+00	1.96E-03	0.00E+00
Se-75	2.14E-01	1.07E-02	0.00E+00	0.00E+00	1.82E+00	5.55E-01	0.00E+00	0.00E+00
Se-79	5.58E-02	0.00E+00	0.00E+00	0.00E+00	9.77E-04	0.00E+00	0.00E+00	0.00E+00
Si-32	6.47E-02	0.00E+00	0.00E+00	0.00E+00	1.13E-03	0.00E+00	0.00E+00	0.00E+00
Sm-145	4.14E-02	5.80E-03	0.00E+00	0.00E+00	1.54E+00	2.15E-01	0.00E+00	0.00E+00
Sm-146	0.00E+00	0.00E+00	0.00E+00	0.00E+00	0.00E+00	0.00E+00	0.00E+00	0.00E+00
Sm-147	0.00E+00	0.00E+00	0.00E+00	0.00E+00	0.00E+00	0.00E+00	0.00E+00	0.00E+00
Sm-151	5.18E-03	6.32E-03	7.71E-03	2.05E-02	8.59E-06	9.44E-04	1.43E-04	6.36E-04
Sn-113	2.55E-01	2.47E-02	3.42E-03	0.00E+00	1.85E-02	7.25E-01	5.56E-02	0.00E+00
Sn-119m	6.57E-02	2.51E-02	4.31E-03	3.57E-03	1.94E-04	4.40E-01	7.36E-03	1.08E-01
Sn-121	1.14E-01	0.00E+00	0.00E+00	0.00E+00	2.00E-03	0.00E+00	0.00E+00	0.00E+00
Sn-121m	3.72E-02	2.69E-02	3.58E-03	1.21E-01	1.85E-02	1.53E-01	4.17E-02	4.73E-04
Sn-123	1.09E+00	5.22E-01	0.00E+00	0.00E+00	6.34E-03	9.10E-03	0.00E+00	0.00E+00
Sn-126	3.83E-03	2.61E-02	4.26E-02	8.36E-02	9.52E-02	3.70E-01	5.00E-03	5.57E-01
Sr-85	5.14E-01	1.36E-02	0.00E+00	0.00E+00	9.80E-01	5.87E-01	0.00E+00	0.00E+00
Sr-89	9.09E-01	5.83E-01	0.00E+00	0.00E+00	9.30E-05	1.02E-02	0.00E+00	0.00E+00
Sr-90	1.96E-01	0.00E+00	0.00E+00	0.00E+00	3.43E-03	0.00E+00	0.00E+00	0.00E+00
Ta-179	5.71E-02	1.07E-02	9.09E-03	7.87E-03	5.39E-01	1.79E-02	9.38E-02	8.12E-02
Ta-180	2.78E-01	9.30E-02	5.71E-02	8.64E-03	1.76E+00	1.73E-01	9.08E-01	4.02E-01
Ta-182	9.27E-03	7.09E-02	1.99E-01	1.18E+00	2.31E-01	1.01E+00	2.96E-01	9.88E-01
Tb-157	4.40E-02	8.03E-03	6.56E-03	5.36E-03	5.69E-02	1.78E-02	1.12E-01	1.02E-03
Tb-158	6.56E-03	5.08E-02	1.86E-01	9.38E-01	2.26E-01	1.00E+00	1.04E-01	7.74E-01
Tb-160	1.01E+00	2.81E-01	6.23E-02	2.24E-01	9.84E-01	3.88E-01	3.45E-01	3.62E-03
Tc-95	7.81E-01	1.78E-02	0.00E+00	0.00E+00	1.00E+00	6.63E-01	0.00E+00	0.00E+00
Tc-95m	7.27E-01	2.05E-01	1.78E-02	3.01E-01	7.36E-01	6.26E-01	6.61E-01	2.61E-05
Tc-97	1.78E-02	2.34E-03	0.00E+00	0.00E+00	6.35E-01	2.87E-02	0.00E+00	0.00E+00
Tc-97m	9.65E-02	1.87E-02	2.46E-03	0.00E+00	3.14E-03	4.92E-01	3.14E-02	0.00E+00
Tc-98	6.99E-01	1.56E-01	0.00E+00	0.00E+00	2.02E+00	2.73E-03	0.00E+00	0.00E+00
Tc-99	1.01E-01	0.00E+00	0.00E+00	0.00E+00	1.77E-03	0.00E+00	0.00E+00	0.00E+00

Table B-1 Collapsed Photon Energies (MeV) and Fractions for ICRP-38 Radionuclides with Half-Life of at least 30 Days and their Shorter-Lived Progeny (Cont.)

Nuclide	EPT(1)	EPT(2)	EPT(3)	EPT(4)	FPT(1)	FPT(2)	FPT(3)	FPT(4)
Te-121	5.60E-01	2.69E-02	0.00E+00	0.00E+00	9.94E-01	7.53E-01	0.00E+00	0.00E+00
Te-121m	1.09E+00	2.12E-01	2.79E-02	3.91E-03	2.66E-02	8.15E-01	5.26E-01	7.31E-02
Te-123	2.69E-02	3.74E-03	0.00E+00	0.00E+00	7.26E-01	5.90E-02	0.00E+00	0.00E+00
Te-123m	1.59E-01	2.81E-02	3.94E-03	0.00E+00	8.42E-01	4.93E-01	7.28E-02	0.00E+00
Te-125m	1.09E-01	3.55E-02	2.81E-02	3.95E-03	2.74E-03	6.63E-02	1.16E+00	1.27E-01
Te-127	4.11E-01	2.06E-01	3.69E-02	2.24E-01	1.13E-02	1.00E-03	1.11E-03	3.90E-03
Te-127m	3.95E-03	2.86E-02	2.53E-01	6.49E-01	6.19E-02	3.80E-01	1.06E-04	1.56E-04
Te-129	4.26E-03	2.78E-02	4.46E-01	9.77E-01	5.85E-02	1.57E-01	1.10E-01	1.07E-02
Te-129m	3.95E-03	2.81E-02	1.05E-01	6.96E-01	4.12E-02	2.87E-01	1.48E-03	4.51E-02
Th-227	7.54E-01	2.65E-01	7.23E-02	1.44E-02	2.29E-04	3.36E-01	2.07E-01	4.22E-01
Th-228	2.15E-01	1.46E-01	8.47E-02	1.45E-02	3.01E-03	1.93E-03	1.25E-02	9.04E-02
Th-229	1.73E-01	9.02E-02	3.35E-02	1.43E-02	1.64E-01	6.12E-01	4.61E-02	7.61E-01
Th-230	2.53E-01	1.51E-01	6.85E-02	1.45E-02	1.12E-04	5.37E-04	3.89E-03	8.10E-02
Th-231	1.59E-01	8.53E-02	1.72E-02	7.87E-02	4.93E-03	1.15E-01	8.78E-01	1.35E-03
Th-232	1.26E-01	9.04E-02	5.90E-02	1.45E-02	4.30E-04	1.31E-04	1.91E-03	7.99E-02
Th-234	9.34E-02	6.33E-02	1.56E-02	4.65E-02	5.82E-02	3.83E-02	9.83E-02	7.59E-04
Ti-44	1.47E-01	7.84E-02	6.78E-02	4.13E-03	1.00E-03	9.47E-01	8.77E-01	1.96E-01
Tl-202	1.11E-02	7.24E-02	1.85E-01	4.41E-01	2.90E-01	7.85E-01	2.92E-09	9.24E-01
Tl-204	9.94E-03	1.22E-02	7.24E-02	2.44E-01	3.52E-03	3.55E-03	1.45E-02	4.16E-03
Tl-206	1.17E-02	7.67E-02	5.36E-01	8.03E-01	2.69E-04	7.17E-04	9.39E-03	5.50E-05
Tl-207	8.98E-01	5.70E-01	7.67E-02	4.94E-01	2.40E-03	1.00E-04	4.85E-05	8.62E-03
Tl-208	2.61E+00	5.83E-01	7.67E-02	5.76E-01	9.98E-01	1.30E+00	7.23E-02	9.80E-03
Tl-209	1.57E+00	4.67E-01	1.09E-01	6.59E-01	9.84E-01	8.11E-01	1.02E+00	1.15E-02
Tl-210	2.00E+00	-2.00E+00	-2.00E+00	-2.00E+00	-2.00E+00	-2.00E+00	-2.00E+00	-2.00E+00
Tm-170	8.07E-03	5.35E-02	8.43E-02	3.17E-01	3.67E-02	4.55E-02	3.26E-02	5.54E-03
Tm-171	7.92E-03	9.84E-03	2.51E-02	5.53E-02	3.24E-03	2.54E-04	4.35E-04	1.12E-02
U-232	2.98E-01	1.22E-01	5.77E-02	1.53E-02	7.22E-05	9.49E-04	2.10E-03	1.26E-01
U-233	2.76E-01	1.09E-01	4.22E-02	1.53E-02	4.99E-04	1.32E-03	1.26E-03	6.53E-02
U-234	1.16E-01	5.32E-02	1.53E-02	0.00E+00	4.99E-04	1.18E-03	1.05E-01	0.00E+00
U-235	3.83E-01	1.68E-01	1.52E-02	0.00E+00	1.37E-03	9.02E-01	2.71E-01	0.00E+00

Table B-1 Collapsed Photon Energies (MeV) and Fractions for ICRP-38 Radionuclides with Half-Life of at least 30 Days and their Shorter-Lived Progeny (Cont.)

Nuclide	EPT(1)	EPT(2)	EPT(3)	EPT(4)	FPT(1)	FPT(2)	FPT(3)	FPT(4)
U-236	1.10E-01	4.94E-02	1.66E-02	1.29E-02	2.33E-04	7.74E-04	6.34E-02	3.52E-02
U-237	1.66E-02	5.97E-02	1.03E-01	2.14E-01	6.77E-01	3.50E-01	5.42E-01	2.57E-01
U-238	4.96E-02	1.91E-02	1.61E-02	1.29E-02	6.97E-04	1.02E-02	4.56E-02	3.10E-02
U-240	1.38E-02	1.82E-02	4.40E-02	1.02E-01	1.59E-01	2.56E-01	1.69E-02	1.78E-03
V-49	4.93E-03	4.51E-03	0.00E+00	0.00E+00	2.29E-02	1.76E-01	0.00E+00	0.00E+00
W-181	1.48E-01	5.88E-02	8.96E-03	6.21E-03	1.38E-03	6.51E-01	2.06E-01	9.75E-03
W-185	9.31E-03	1.18E-02	6.25E-02	1.27E-01	1.25E-04	1.00E-05	4.60E-04	2.43E-03
W-188	9.71E-03	6.32E-02	1.01E-01	2.67E-01	1.39E-03	3.08E-03	1.80E-03	6.30E-03
Y-88	1.84E+00	8.96E-01	1.44E-02	3.55E-01	1.00E+00	9.39E-01	6.01E-01	1.36E-05
Y-90	1.61E-02	2.08E-03	9.35E-01	0.00E+00	1.05E-04	3.90E-06	1.64E-02	0.00E+00
Y-91	1.20E+00	6.04E-01	0.00E+00	0.00E+00	3.00E-03	1.05E-02	0.00E+00	0.00E+00
Yb-169	1.79E-01	5.39E-02	7.80E-03	0.00E+00	1.03E+00	2.25E+00	4.54E-01	0.00E+00
Zn-65	1.12E+00	5.11E-01	8.14E-03	1.43E-01	5.08E-01	2.92E-02	3.86E-01	3.65E-05
Zr-88	3.93E-01	1.52E-02	0.00E+00	0.00E+00	1.00E+00	6.29E-01	0.00E+00	0.00E+00
Zr-93	1.96E-02	0.00E+00	0.00E+00	0.00E+00	3.44E-04	0.00E+00	0.00E+00	0.00E+00
Zr-95	7.42E-01	1.18E-01	0.00E+00	0.00E+00	9.96E-01	2.02E-03	0.00E+00	0.00E+00

Table B-2 Collapsed Photon Energies (MeV) and Fractions for ICRP-107 Radionuclides with Half-Life of at least 30 Days and their Shorter-Lived Progeny

Nuclide	EPT(1)	EPT(2)	EPT(3)	EPT(4)	FPT(1)	FPT(2)	FPT(3)	FPT(4)
Ac-225	6.06E-05	4.23E-04	1.22E-02	1.25E-01	7.33E-02	8.28E-06	2.32E-03	1.10E-03
Ac-227	8.17E-05	4.79E-04	1.10E-02	1.14E-01	4.26E-02	5.95E-06	5.80E-04	5.70E-06
Ac-228	8.24E-05	1.35E-02	1.06E-01	7.96E-01	1.02E-01	4.11E-03	1.19E-03	1.07E-02
Ag-105	7.86E-06	2.80E-03	2.64E-02	4.09E-01	9.36E-02	6.32E-04	9.28E-03	1.20E-02
Ag-108	7.88E-06	3.37E-04	2.03E-02	5.92E-01	2.06E-03	4.11E-07	1.96E-04	4.19E-04
Ag-108m	8.23E-06	2.81E-03	2.68E-02	5.90E-01	8.16E-02	5.52E-04	7.25E-03	2.71E-02
Ag-110	8.26E-06	3.41E-04	2.03E-02	8.27E-01	2.52E-04	5.11E-08	2.39E-05	6.68E-04
Ag-110m	1.35E-05	3.76E-04	2.13E-02	8.59E-01	1.99E-03	5.07E-07	1.37E-04	3.21E-02
Al-26	3.10E-07	6.89E-06	1.24E-03	1.00E+00	6.16E-19	7.67E-03	4.61E-05	2.67E-02
Am-241	7.44E-05	3.34E-03	3.71E-02	3.42E-01	1.12E-01	7.46E-04	7.62E-03	3.87E-07
Am-242	7.54E-05	5.63E-04	1.54E-02	1.08E-01	7.37E-02	1.29E-05	3.48E-03	1.24E-03
Am-242m	7.23E-05	5.56E-04	3.56E-03	1.83E-02	8.67E-02	1.52E-05	5.88E-04	2.62E-03
Am-243	7.44E-05	3.35E-03	6.09E-02	6.55E-01	6.02E-02	4.03E-04	9.51E-03	1.50E-07
Am-245	7.76E-05	5.81E-04	1.53E-02	1.64E-01	2.62E-02	4.72E-06	1.17E-03	1.93E-03
Am-246m	7.76E-05	5.79E-04	2.85E-02	9.62E-01	6.90E-02	1.26E-05	3.80E-03	1.01E-02
As-73	1.21E-05	1.05E-04	1.16E-03	1.41E-02	2.21E-01	2.92E-06	4.55E-04	1.11E-02
At-217	3.25E-05	3.56E-04	1.08E-02	2.40E-01	5.08E-05	4.37E-09	1.55E-06	1.01E-05
At-218	1.10E+00	0.00E+00	0.00E+00	0.00E+00	1.92E-07	0.00E+00	0.00E+00	0.00E+00
At-219	0.00E+00	0.00E+00	0.00E+00	0.00E+00	0.00E+00	0.00E+00	0.00E+00	0.00E+00
Au-194	1.01E-05	2.88E-04	5.11E-02	7.38E-01	1.44E-01	8.81E-06	1.11E-02	1.33E-02
Au-195	1.01E-05	2.90E-04	9.21E-03	7.18E-02	3.06E-01	1.87E-05	6.30E-03	1.08E-02
Ba-133	2.19E-05	4.27E-03	4.32E-02	3.41E-01	2.09E-01	1.72E-03	1.60E-02	9.76E-03
Ba-137m	1.86E-05	4.44E-03	3.29E-02	6.62E-01	1.37E-02	1.06E-04	7.53E-04	8.97E-03
Be-10	2.52E-01	0.00E+00	0.00E+00	0.00E+00	4.42E-05	0.00E+00	0.00E+00	0.00E+00
Be-7	4.78E-01	0.00E+00	0.00E+00	0.00E+00	1.04E-03	0.00E+00	0.00E+00	0.00E+00
Bi-207	2.66E-05	3.42E-04	5.39E-02	8.22E-01	1.41E-01	1.14E-05	1.13E-02	1.80E-02
Bi-208	2.66E-05	3.43E-04	4.72E-02	2.61E+00	1.29E-01	1.03E-05	7.55E-03	1.00E-02
Bi-210	2.07E-05	3.27E-04	1.02E-02	3.89E-01	3.76E-08	2.81E-12	1.04E-09	6.81E-05

Table B-2 Collapsed Photon Energies (MeV) and Fractions for ICRP-107 Radionuclides with Half-Life of at least 30 Days and their Shorter-Lived Progeny (Cont.)

Nuclide	EPT(1)	EPT(2)	EPT(3)	EPT(4)	FPT(1)	FPT(2)	FPT(3)	FPT(4)
Bi-210m	2.07E-05	3.27E-04	1.03E-02	2.68E-01	2.47E-02	1.85E-06	6.84E-04	9.69E-03
Bi-211	2.07E-05	3.27E-04	1.02E-02	3.05E-01	4.17E-03	3.11E-07	1.15E-04	1.55E-03
Bi-212	2.08E-05	2.27E-03	1.74E-02	8.74E-01	4.05E-02	1.48E-04	8.80E-04	1.25E-03
Bi-213	3.84E-05	3.70E-04	1.11E-02	4.04E-01	6.26E-03	5.74E-07	2.00E-04	3.24E-03
Bi-214	3.84E-05	3.70E-04	5.79E-02	1.11E+00	3.14E-03	2.89E-07	3.01E-04	1.33E-02
Bi-215	3.84E-05	3.70E-04	1.11E-02	3.63E-01	2.67E-02	2.45E-06	8.54E-04	7.15E-03
Bk-247	7.22E-05	5.57E-04	1.49E-02	1.47E-01	4.83E-02	8.20E-06	2.19E-03	9.76E-03
Bk-249	7.22E-05	3.52E-03	3.24E-02	2.38E-01	1.57E-07	1.13E-09	5.68E-06	2.77E-08
Bk-250	7.46E-05	6.20E-04	1.67E-02	9.92E-01	5.07E-02	1.04E-05	2.62E-03	9.03E-03
Bk-251	7.45E-05	6.28E-04	1.55E-02	1.26E-01	1.43E-01	2.92E-05	6.06E-03	6.56E-03
C-14	4.95E-02	0.00E+00	0.00E+00	0.00E+00	8.65E-06	0.00E+00	0.00E+00	0.00E+00
Ca-41	3.01E-06	2.62E-05	2.69E-04	3.31E-03	2.19E-14	3.73E-02	1.45E-05	1.22E-03
Ca-45	6.75E-06	3.51E-04	4.17E-03	7.72E-02	1.42E-06	5.32E-10	3.10E-08	1.35E-05
Cd-109	1.21E-05	3.68E-04	3.04E-03	2.48E-02	1.45E-01	3.52E-05	1.06E-03	1.05E-02
Cd-113	9.26E-02	0.00E+00	0.00E+00	0.00E+00	1.62E-05	0.00E+00	0.00E+00	0.00E+00
Cd-113m	1.72E-05	3.99E-04	2.12E-02	1.90E-01	8.18E-05	2.42E-08	5.78E-06	3.46E-05
Cd-115m	8.13E-06	4.32E-04	2.38E-02	9.00E-01	2.06E-05	3.63E-09	1.16E-06	4.38E-04
Ce-139	2.11E-05	7.29E-04	4.90E-03	9.87E-02	1.50E-01	8.26E-05	1.22E-03	1.61E-02
Ce-141	1.56E-05	7.99E-04	5.30E-03	1.17E-01	2.46E-02	1.95E-05	2.56E-04	6.59E-03
Ce-144	1.56E-05	8.00E-04	5.32E-03	8.97E-02	1.40E-02	1.09E-05	1.42E-04	2.16E-03
Cf-248	7.77E-05	5.78E-04	1.61E-02	1.04E+00	1.97E-02	3.59E-06	9.67E-04	3.06E-06
Cf-249	7.76E-05	5.80E-04	1.56E-02	3.51E-01	5.80E-02	1.06E-05	2.72E-03	9.22E-03
Cf-250	7.77E-05	1.60E-02	1.32E-01	1.04E+00	1.50E-02	7.42E-04	1.21E-05	9.35E-05
Cf-251	7.76E-05	5.81E-04	1.54E-02	1.41E-01	1.35E-01	2.44E-05	6.12E-03	8.11E-03
Cf-252	7.77E-05	5.78E-04	5.96E-02	1.05E+00	1.49E-02	2.73E-06	1.39E-03	4.33E-03
Cf-253	7.55E-05	6.51E-04	4.25E-03	2.01E-02	6.05E-02	1.31E-05	5.10E-04	2.11E-03
Cf-254	7.77E-05	3.59E-03	4.15E-02	9.73E-01	5.08E-05	3.70E-07	7.98E-03	1.75E-01
Cl-36	1.33E-06	1.29E-05	2.29E-03	2.91E-01	2.69E-17	7.46E-04	1.31E-05	5.06E-05
Cm-241	7.21E-05	5.68E-04	1.46E-02	2.87E-01	3.02E-01	5.20E-05	1.14E-02	1.69E-02
Cm-242	7.20E-05	5.37E-04	1.50E-02	1.64E-01	2.58E-02	4.22E-06	1.19E-03	4.61E-07

Table B-2 Collapsed Photon Energies (MeV) and Fractions for ICRP-107 Radionuclides with Half-Life of at least 30 Days and their Shorter-Lived Progeny (Cont.)

Nuclide	EPT(1)	EPT(2)	EPT(3)	EPT(4)	FPT(1)	FPT(2)	FPT(3)	FPT(4)
Cm-243	7.20E-05	5.53E-04	1.40E-02	1.59E-01	2.06E-01	3.44E-05	6.20E-03	7.85E-03
Cm-244	7.21E-05	1.50E-02	1.28E-01	1.05E+00	2.21E-02	1.02E-03	3.16E-07	1.63E-07
Cm-245	7.20E-05	1.44E-02	1.15E-01	1.12E+00	1.60E-01	6.62E-03	8.53E-03	6.66E-10
Cm-246	7.21E-05	1.51E-02	1.36E-01	1.05E+00	1.76E-02	8.16E-04	3.80E-06	3.43E-05
Cm-247	7.20E-05	5.36E-04	1.45E-02	3.80E-01	5.18E-03	8.33E-07	2.32E-04	8.24E-03
Cm-248	7.20E-05	5.37E-04	8.15E-02	1.06E+00	1.65E-02	2.71E-06	2.64E-03	1.24E-02
Cm-249	7.82E-05	6.45E-04	4.86E-03	4.81E-01	8.51E-02	1.68E-05	5.04E-04	4.24E-04
Cm-250	7.20E-05	3.39E-03	2.74E-02	9.59E-01	4.46E-03	3.02E-05	3.70E-03	1.41E-01
Co-56	1.25E-05	6.52E-04	6.43E-03	1.25E+00	4.64E-02	6.27E-05	2.42E-03	2.91E-02
Co-57	1.25E-05	6.52E-04	7.57E-03	1.25E-01	1.05E-01	1.42E-04	6.40E-03	9.65E-03
Co-58	1.25E-05	6.52E-04	6.43E-03	7.46E-01	4.88E-02	6.59E-05	2.54E-03	1.31E-02
Co-60	1.45E-05	7.33E-03	9.59E-02	1.25E+00	1.50E-05	1.09E-06	1.68E-05	2.00E-02
Co-60m	1.35E-05	7.24E-04	1.02E-02	1.31E+00	5.22E-02	8.84E-05	3.26E-03	2.51E-05
Cs-134	1.86E-05	4.44E-03	3.28E-02	6.97E-01	1.48E-03	1.15E-05	8.62E-05	2.23E-02
Cs-135	8.94E-02	0.00E+00	0.00E+00	0.00E+00	1.56E-05	0.00E+00	0.00E+00	0.00E+00
Cs-137	1.86E-05	6.87E-04	4.67E-03	2.06E-01	4.46E-08	2.05E-11	3.25E-10	3.30E-05
Dy-154	0.00E+00	0.00E+00	0.00E+00	0.00E+00	0.00E+00	0.00E+00	0.00E+00	0.00E+00
Dy-159	1.38E-05	1.67E-04	6.22E-03	4.58E-02	1.10E-01	4.89E-06	2.14E-03	9.63E-03
Es-253	7.85E-05	6.07E-04	1.73E-02	3.98E-01	7.24E-03	1.40E-06	3.09E-04	6.45E-06
Es-254	7.84E-05	1.60E-02	3.10E-01	7.36E+00	3.28E-01	1.06E-02	4.24E-05	1.58E-12
Es-255	8.17E-02	5.34E-01	1.79E+00	7.36E+00	1.38E-05	3.82E-06	2.65E-06	2.36E-09
Eu-146	1.45E-05	1.45E-04	3.54E-02	8.35E-01	9.45E-02	2.89E-06	8.91E-03	2.84E-02
Eu-148	1.45E-05	1.45E-04	3.56E-02	6.74E-01	1.01E-01	3.09E-06	9.44E-03	3.26E-02
Eu-149	1.46E-05	1.46E-04	3.25E-02	3.27E-01	1.67E-01	5.25E-06	1.04E-02	9.83E-04
Eu-150	1.45E-05	1.45E-04	3.54E-02	5.20E-01	1.03E-01	3.17E-06	9.56E-03	2.93E-02
Eu-152	1.46E-05	1.46E-04	3.49E-02	7.13E-01	1.04E-01	3.20E-06	9.04E-03	1.61E-02
Eu-154	1.94E-05	6.01E-03	1.08E-01	9.89E-01	4.32E-02	7.96E-04	7.41E-03	1.18E-02
Eu-155	1.94E-05	1.62E-04	6.03E-03	7.77E-02	4.62E-02	1.85E-06	8.42E-04	7.80E-03
Fe-55	1.15E-05	5.84E-04	5.92E-03	1.26E-01	6.05E-02	6.51E-05	2.69E-03	1.28E-11
Fe-59	1.35E-05	7.24E-04	6.96E-03	1.14E+00	3.24E-05	5.47E-08	1.99E-06	1.04E-02

Table B-2 Collapsed Photon Energies (MeV) and Fractions for ICRP-107 Radionuclides with Half-Life of at least 30 Days and their Shorter-Lived Progeny (Cont.)

Nuclide	EPT(1)	EPT(2)	EPT(3)	EPT(4)	FPT(1)	FPT(2)	FPT(3)	FPT(4)
Fe-60	6.47E-02	0.00E+00	0.00E+00	0.00E+00	1.13E-05	0.00E+00	0.00E+00	0.00E+00
Fm-254	7.46E-05	6.20E-04	1.81E-02	1.04E+00	1.66E-02	3.41E-06	8.73E-04	6.69E-05
Fm-255	7.47E-05	1.70E-02	3.72E-01	7.36E+00	2.24E-01	8.96E-03	2.05E-06	1.15E-11
Fm-257	7.45E-05	6.24E-04	1.61E-02	1.74E-01	1.79E-01	3.65E-05	8.33E-03	7.92E-03
Fr-221	4.43E-05	3.86E-04	1.17E-02	1.92E-01	7.19E-03	7.15E-07	2.46E-04	1.51E-03
Fr-223	7.13E-05	2.90E-03	4.35E-02	3.28E-01	9.45E-02	4.92E-04	8.28E-03	7.20E-04
Ga-68	1.64E-05	9.71E-04	8.69E-03	5.25E-01	5.22E-03	1.51E-05	4.57E-04	1.83E-02
Gd-146	1.42E-05	1.54E-04	5.79E-03	7.88E-02	2.23E-01	7.80E-06	3.66E-03	3.17E-02
Gd-148	0.00E+00	0.00E+00	0.00E+00	0.00E+00	0.00E+00	0.00E+00	0.00E+00	0.00E+00
Gd-150	0.00E+00	0.00E+00	0.00E+00	0.00E+00	0.00E+00	0.00E+00	0.00E+00	0.00E+00
Gd-151	1.43E-05	1.58E-04	5.86E-03	6.76E-02	1.88E-01	6.90E-06	2.88E-03	1.02E-02
Gd-152	0.00E+00	0.00E+00	0.00E+00	0.00E+00	0.00E+00	0.00E+00	0.00E+00	0.00E+00
Gd-153	1.42E-05	1.54E-04	5.81E-03	5.94E-02	1.51E-01	5.31E-06	2.48E-03	1.75E-02
Ge-68	1.58E-05	1.04E-04	1.06E-03	9.32E-03	6.20E-02	9.62E-07	1.51E-04	4.29E-03
H-3	5.68E-03	0.00E+00	0.00E+00	0.00E+00	9.94E-07	0.00E+00	0.00E+00	0.00E+00
Hf-172	1.40E-05	2.12E-04	7.54E-03	5.97E-02	2.66E-01	1.72E-05	6.63E-03	1.69E-02
Hf-174	0.00E+00	0.00E+00	0.00E+00	0.00E+00	0.00E+00	0.00E+00	0.00E+00	0.00E+00
Hf-175	1.40E-05	2.11E-04	7.52E-03	1.94E-01	1.12E-01	7.22E-06	2.85E-03	1.81E-02
Hf-178m	1.94E-05	2.20E-04	7.81E-03	3.11E-01	2.16E-01	1.53E-05	5.98E-03	7.19E-02
Hf-181	2.50E-05	2.31E-04	8.07E-03	2.97E-01	6.05E-02	4.55E-06	1.76E-03	1.79E-02
Hf-182	2.51E-05	2.30E-04	8.06E-03	2.29E-01	1.88E-02	1.39E-06	5.70E-04	1.04E-02
Hg-194	1.11E-05	5.59E-05	3.07E-04	9.24E-03	1.55E-01	4.84E-08	1.03E-05	2.75E-03
Hg-203	2.07E-05	3.27E-04	1.02E-02	2.50E-01	2.32E-02	1.74E-06	6.40E-04	9.48E-03
Hg-206	2.07E-05	3.27E-04	1.02E-02	2.76E-01	1.59E-02	1.19E-06	4.37E-04	4.49E-03
Ho-163	1.53E-05	2.46E-05	1.90E-04	1.30E-03	4.21E-02	1.80E-09	3.72E-06	1.70E-05
Ho-166m	1.35E-05	1.87E-04	4.21E-02	5.31E-01	8.76E-02	5.24E-06	7.24E-03	3.00E-02
I-125	1.36E-05	5.34E-04	3.91E-03	2.84E-02	2.50E-01	7.27E-05	1.49E-03	1.48E-02
I-129	1.66E-05	6.09E-04	4.28E-03	3.13E-02	1.11E-01	4.53E-05	8.11E-04	7.89E-03
In-113m	8.13E-06	4.33E-04	2.29E-02	3.92E-01	5.09E-02	8.96E-06	2.72E-03	6.49E-03
In-114	1.71E-05	3.99E-04	2.20E-02	8.14E-01	3.69E-04	1.08E-07	3.90E-05	1.57E-04

Table B-2 Collapsed Photon Energies (MeV) and Fractions for ICRP-107 Radionuclides with Half-Life of at least 30 Days and their Shorter-Lived Progeny (Cont.)

Nuclide	EPT(1)	EPT(2)	EPT(3)	EPT(4)	FPT(1)	FPT(2)	FPT(3)	FPT(4)
In-114m	8.33E-06	4.31E-04	2.20E-02	3.23E-01	1.08E-01	1.96E-05	4.14E-03	2.20E-03
In-115	1.53E-01	0.00E+00	0.00E+00	0.00E+00	2.67E-05	0.00E+00	0.00E+00	0.00E+00
In-115m	8.13E-06	4.33E-04	2.28E-02	3.36E-01	7.05E-02	1.24E-05	3.71E-03	4.59E-03
Ir-192	1.70E-05	2.81E-04	9.25E-03	3.54E-01	2.49E-02	1.70E-06	6.45E-04	2.31E-02
Ir-192n	4.56E-05	2.74E-04	9.31E-03	7.78E-02	1.41E-01	1.46E-05	5.74E-03	7.53E-05
Ir-194	1.01E-05	2.88E-04	9.43E-03	4.58E-01	1.84E-03	1.14E-07	4.31E-05	2.24E-03
Ir-194m	1.01E-05	2.88E-04	9.51E-03	4.65E-01	5.78E-02	3.60E-06	1.37E-03	5.02E-02
K-40	1.70E-05	2.02E-04	2.95E-03	1.38E+00	3.85E-03	1.19E-06	9.53E-05	1.18E-03
Kr-83m	1.94E-05	1.41E-04	1.57E-03	1.19E-02	1.11E-01	4.44E-06	3.75E-04	2.08E-03
La-137	1.86E-05	6.87E-04	4.68E-03	3.29E-02	1.34E-01	6.12E-05	9.66E-04	7.39E-03
La-138	1.86E-05	4.43E-03	3.30E-02	1.22E+00	8.79E-02	6.61E-04	3.88E-03	1.00E-02
Lu-172	8.66E-06	2.02E-04	7.34E-03	5.61E-01	2.02E-01	1.19E-05	4.88E-03	3.48E-02
Lu-172m	1.40E-05	2.10E-04	7.18E-03	4.19E-02	8.46E-02	5.30E-06	1.94E-03	3.76E-07
Lu-173	8.63E-06	2.02E-04	7.30E-03	8.99E-02	1.92E-01	1.13E-05	4.53E-03	2.00E-02
Lu-174	8.65E-06	2.02E-04	4.20E-02	1.24E+00	1.42E-01	8.37E-06	1.22E-02	5.24E-04
Lu-174m	1.39E-05	2.12E-04	3.74E-02	9.91E-01	2.59E-01	1.67E-05	1.51E-02	5.77E-05
Lu-176	1.94E-05	2.20E-04	7.88E-03	2.18E-01	9.36E-02	6.66E-06	2.69E-03	2.20E-02
Lu-177	1.94E-05	2.20E-04	7.87E-03	1.47E-01	1.28E-02	9.10E-07	3.67E-04	2.39E-03
Lu-177m	1.84E-05	2.19E-04	7.77E-03	1.97E-01	1.94E-01	1.35E-05	5.39E-03	5.06E-02
Mn-53	6.39E-06	9.95E-05	5.25E-04	5.43E-03	6.41E-02	7.17E-07	5.36E-05	2.42E-03
Mn-54	6.39E-06	5.19E-04	5.43E-03	8.35E-01	6.42E-02	5.44E-05	2.42E-03	1.00E-02
Mo-93	5.83E-06	2.05E-04	2.17E-03	1.69E-02	1.09E-01	6.65E-06	3.67E-04	6.26E-03
Na-22	5.11E-01	1.27E+00	2.15E-01	8.35E-01	1.80E-02	9.99E-03	3.39E-05	8.04E-08
Nb-91	6.52E-06	1.84E-04	1.53E-02	5.11E-01	1.20E-01	5.51E-06	6.63E-03	3.14E-05
Nb-91m	5.86E-06	2.04E-04	1.68E-02	1.20E+00	1.09E-01	6.62E-06	5.71E-03	2.02E-04
Nb-92	6.52E-06	1.84E-04	1.53E-02	7.48E-01	1.20E-01	5.52E-06	6.42E-03	2.00E-02
Nb-93m	5.83E-06	2.05E-04	2.15E-03	1.69E-02	9.26E-02	5.71E-06	3.03E-04	1.12E-03
Nb-94	6.85E-06	2.27E-04	1.69E-02	7.87E-01	2.91E-04	2.32E-08	2.05E-05	1.98E-02
Nb-95	6.85E-06	2.26E-03	2.88E-02	7.66E-01	1.49E-04	6.05E-07	1.75E-05	9.99E-03
Nb-95m	5.83E-06	2.05E-04	1.60E-02	2.34E-01	7.54E-02	4.62E-06	4.45E-03	2.68E-03

Table B-2 Collapsed Photon Energies (MeV) and Fractions for ICRP-107 Radionuclides with Half-Life of at least 30 Days and their Shorter-Lived Progeny (Cont.)

Nuclide	EPT(1)	EPT(2)	EPT(3)	EPT(4)	FPT(1)	FPT(2)	FPT(3)	FPT(4)
Nd-144	0.00E+00	0.00E+00	0.00E+00	0.00E+00	0.00E+00	0.00E+00	0.00E+00	0.00E+00
Ni-59	1.35E-05	7.24E-04	6.96E-03	5.11E-01	5.41E-02	9.05E-05	3.26E-03	3.04E-07
Ni-63	1.74E-02	0.00E+00	0.00E+00	0.00E+00	3.05E-06	0.00E+00	0.00E+00	0.00E+00
Np-235	7.54E-05	5.11E-04	1.33E-02	9.76E-02	1.32E-01	1.91E-05	4.20E-03	5.42E-05
Np-236	7.52E-05	5.03E-04	1.42E-02	1.20E-01	3.63E-01	5.36E-05	1.56E-02	1.12E-02
Np-237	7.65E-05	4.84E-04	3.18E-03	3.69E-02	1.65E-01	2.27E-05	9.68E-04	9.05E-03
Np-238	7.20E-05	5.37E-04	1.75E-02	9.92E-02	8.52E-02	1.40E-05	4.04E-03	5.86E-03
Np-239	7.19E-05	5.56E-04	1.42E-02	1.51E-01	2.22E-01	3.69E-05	7.07E-03	1.15E-02
Np-240	7.20E-05	5.37E-04	1.50E-02	5.59E-01	2.39E-01	3.91E-05	1.10E-02	1.86E-02
Np-240m	7.20E-05	5.36E-04	1.50E-02	6.52E-01	7.63E-02	1.25E-05	3.51E-03	4.98E-03
Os-185	3.76E-05	8.48E-03	6.47E-02	6.76E-01	8.56E-02	2.84E-03	7.39E-03	9.48E-03
Os-186	0.00E+00	0.00E+00	0.00E+00	0.00E+00	0.00E+00	0.00E+00	0.00E+00	0.00E+00
Os-194	4.52E-05	2.78E-04	2.00E-03	1.81E-02	6.66E-02	6.75E-06	3.18E-04	2.29E-03
P-32	6.95E-01	0.00E+00	0.00E+00	0.00E+00	1.22E-04	0.00E+00	0.00E+00	0.00E+00
Pa-231	7.95E-05	4.61E-04	1.50E-02	2.55E-01	2.13E-01	2.63E-05	7.25E-03	1.27E-03
Pa-232	7.55E-05	4.99E-04	1.42E-02	6.79E-01	1.28E-01	1.87E-05	5.53E-03	1.37E-02
Pa-233	7.55E-05	5.02E-04	1.37E-02	2.24E-01	1.63E-01	2.34E-05	6.23E-03	9.53E-03
Pa-234	7.55E-05	4.99E-04	1.40E-02	5.61E-01	2.55E-01	3.71E-05	1.08E-02	2.59E-02
Pa-234m	7.57E-05	1.38E-02	1.00E-01	8.86E-01	2.03E-03	8.14E-05	5.25E-05	3.07E-04
Pb-202	2.07E-05	3.24E-04	2.29E-03	1.06E-02	1.07E-01	7.61E-06	3.71E-04	2.07E-03
Pb-205	2.07E-05	3.24E-04	2.29E-03	1.06E-02	1.09E-01	7.69E-06	3.75E-04	2.09E-03
Pb-209	1.97E-01	0.00E+00	0.00E+00	0.00E+00	3.46E-05	0.00E+00	0.00E+00	0.00E+00
Pb-210	3.25E-05	3.61E-04	2.48E-03	1.73E-02	1.18E-01	1.01E-05	4.84E-04	2.79E-03
Pb-211	3.25E-05	3.57E-04	5.38E-02	5.88E-01	2.20E-03	1.90E-07	1.69E-04	1.14E-03
Pb-212	3.25E-05	3.56E-04	1.08E-02	1.71E-01	5.56E-02	4.79E-06	1.70E-03	8.36E-03
Pb-214	3.25E-05	3.58E-04	1.07E-02	2.71E-01	5.73E-02	4.94E-06	1.61E-03	9.31E-03
Pd-107	9.58E-03	0.00E+00	0.00E+00	0.00E+00	1.68E-06	0.00E+00	0.00E+00	0.00E+00
Pm-143	1.52E-05	1.34E-04	3.34E-02	7.42E-01	1.06E-01	2.51E-06	8.95E-03	3.85E-03
Pm-144	1.52E-05	1.34E-04	3.34E-02	6.26E-01	1.08E-01	2.54E-06	9.15E-03	2.45E-02
Pm-145	1.52E-05	1.34E-04	5.20E-03	3.92E-02	1.19E-01	2.84E-06	1.44E-03	7.79E-03

Table B-2 Collapsed Photon Energies (MeV) and Fractions for ICRP-107 Radionuclides with Half-Life of at least 30 Days and their Shorter-Lived Progeny (Cont.)

Nuclide	EPT(1)	EPT(2)	EPT(3)	EPT(4)	FPT(1)	FPT(2)	FPT(3)	FPT(4)
Pm-146	1.52E-05	1.34E-04	3.34E-02	5.88E-01	7.13E-02	1.68E-06	6.01E-03	1.24E-02
Pm-147	1.45E-05	1.45E-04	5.58E-03	6.30E-02	2.83E-06	8.64E-11	4.26E-08	1.13E-05
Pm-148	1.45E-05	1.45E-04	3.64E-02	9.78E-01	2.54E-04	7.75E-09	2.43E-05	5.98E-03
Pm-148m	1.47E-05	1.43E-04	5.49E-03	5.95E-01	1.51E-02	4.35E-07	2.18E-04	3.35E-02
Po-208	3.25E-05	3.59E-04	1.06E-02	3.54E-01	7.58E-06	6.53E-10	2.03E-07	5.97E-07
Po-209	2.67E-05	3.65E-04	1.06E-02	3.76E-01	4.26E-02	6.94E-06	3.03E-05	1.63E-04
Po-210	2.66E-05	3.41E-04	5.54E-02	8.03E-01	1.55E-08	1.25E-12	1.40E-09	1.21E-07
Po-211	2.66E-05	3.41E-04	5.54E-02	7.35E-01	3.31E-05	2.67E-09	3.00E-06	1.11E-04
Po-212	0.00E+00	0.00E+00	0.00E+00	0.00E+00	0.00E+00	0.00E+00	0.00E+00	0.00E+00
Po-213	2.66E-05	3.41E-04	5.62E-02	7.79E-01	2.13E-07	1.71E-11	1.98E-08	4.80E-07
Po-214	2.66E-05	3.41E-04	5.51E-02	7.97E-01	1.41E-07	1.14E-11	1.26E-08	1.04E-06
Po-215	2.66E-05	3.42E-04	1.06E-02	4.29E-01	1.98E-06	1.61E-10	5.85E-08	4.11E-06
Po-216	2.66E-05	3.41E-04	5.54E-02	8.05E-01	2.42E-08	1.95E-12	2.18E-09	1.90E-07
Po-218	7.14E-02	0.00E+00	0.00E+00	0.00E+00	2.50E-09	0.00E+00	0.00E+00	0.00E+00
Pr-144	1.52E-05	1.34E-04	3.35E-02	1.23E+00	7.59E-06	1.78E-10	6.53E-07	4.45E-04
Pr-144m	1.56E-05	4.94E-03	3.69E-02	9.52E-01	1.06E-01	1.12E-03	2.98E-03	1.72E-05
Pt-190	0.00E+00	0.00E+00	0.00E+00	0.00E+00	0.00E+00	0.00E+00	0.00E+00	0.00E+00
Pt-193	4.48E-05	2.80E-04	2.00E-03	1.00E-02	8.98E-02	9.24E-06	4.13E-04	2.09E-03
Pu-236	7.55E-05	4.98E-04	1.44E-02	5.85E-01	3.18E-02	4.66E-06	1.39E-03	5.26E-08
Pu-237	7.44E-05	5.23E-04	1.40E-02	1.00E-01	1.44E-01	2.20E-05	5.51E-03	4.48E-03
Pu-238	7.55E-05	4.98E-04	1.43E-02	7.97E-01	2.94E-02	4.31E-06	1.28E-03	3.85E-09
Pu-239	7.54E-05	5.31E-04	1.34E-02	3.85E-01	2.98E-02	4.50E-06	6.18E-04	6.29E-07
Pu-240	7.55E-05	4.98E-04	1.43E-02	1.02E+00	2.77E-02	4.05E-06	1.21E-03	7.85E-09
Pu-241	7.54E-05	5.19E-04	6.45E-03	1.07E-01	5.78E-06	8.50E-10	1.08E-06	1.42E-07
Pu-242	7.55E-05	4.98E-04	1.43E-02	1.09E+00	2.37E-02	3.47E-06	1.03E-03	7.07E-07
Pu-243	7.21E-05	5.63E-04	1.48E-02	9.23E-02	3.88E-02	6.64E-06	1.56E-03	2.57E-03
Pu-244	7.56E-05	1.44E-02	9.66E-01	7.36E+00	1.97E-02	8.62E-04	2.07E-04	5.66E-08
Pu-246	7.22E-05	5.60E-04	3.59E-03	9.22E-02	1.30E-01	2.22E-05	8.90E-04	1.54E-02
Ra-223	5.01E-05	4.10E-04	1.11E-02	1.54E-01	1.47E-01	1.62E-05	3.04E-03	8.90E-03
Ra-224	5.01E-05	4.02E-04	1.21E-02	2.27E-01	1.27E-03	1.34E-07	4.55E-05	4.56E-04

Table B-2 Collapsed Photon Energies (MeV) and Fractions for ICRP-107 Radionuclides with Half-Life of at least 30 Days and their Shorter-Lived Progeny (Cont.)

Nuclide	EPT(1)	EPT(2)	EPT(3)	EPT(4)	FPT(1)	FPT(2)	FPT(3)	FPT(4)
Ra-225	7.96E-05	4.49E-04	2.99E-03	3.21E-02	4.51E-02	5.48E-06	2.46E-04	4.42E-03
Ra-226	5.01E-05	4.02E-04	1.22E-02	1.71E-01	2.69E-03	2.87E-07	9.72E-05	4.25E-04
Ra-228	7.95E-05	4.67E-04	3.02E-03	1.55E-02	6.36E-02	8.45E-06	2.78E-04	1.59E-03
Rb-83	1.94E-05	1.57E-03	1.27E-02	5.32E-01	8.04E-02	2.87E-04	5.68E-03	9.10E-03
Rb-84	1.94E-05	1.57E-03	1.28E-02	7.26E-01	4.68E-02	1.72E-04	3.87E-03	1.25E-02
Rb-87	1.15E-01	0.00E+00	0.00E+00	0.00E+00	2.02E-05	0.00E+00	0.00E+00	0.00E+00
Re-183	3.12E-05	2.42E-04	8.22E-03	8.76E-02	2.22E-01	1.80E-05	6.65E-03	1.73E-02
Re-184	3.13E-05	8.29E-03	6.90E-02	8.33E-01	1.18E-01	3.82E-03	1.05E-02	9.79E-03
Re-184m	3.53E-05	8.29E-03	1.20E-01	8.56E-01	1.69E-01	5.35E-03	1.41E-02	2.45E-03
Re-186	3.85E-05	2.54E-04	8.68E-03	1.08E-01	1.60E-02	1.43E-06	5.67E-04	2.05E-03
Re-186m	3.76E-05	2.54E-04	8.41E-03	5.72E-02	2.22E-01	1.94E-05	6.44E-03	2.52E-03
Re-187	6.18E-04	0.00E+00	0.00E+00	0.00E+00	1.08E-07	0.00E+00	0.00E+00	0.00E+00
Re-188	4.41E-05	2.63E-04	8.94E-03	2.70E-01	9.60E-03	9.23E-07	3.64E-04	2.64E-03
Rh-101	8.91E-06	2.80E-04	1.85E-02	1.77E-01	1.03E-01	1.33E-05	8.32E-03	1.54E-02
Rh-102	8.91E-06	2.79E-04	1.85E-02	5.35E-01	5.59E-02	7.21E-06	4.60E-03	9.32E-03
Rh-102m	8.91E-06	2.80E-04	1.87E-02	6.80E-01	9.06E-02	1.17E-05	7.39E-03	3.15E-02
Rh-103m	9.96E-06	3.07E-04	2.73E-03	2.07E-02	6.87E-02	1.13E-05	4.18E-04	7.43E-04
Rh-106	7.86E-06	3.37E-04	2.03E-02	6.59E-01	1.27E-04	2.54E-08	1.22E-05	3.67E-03
Rn-218	3.84E-05	3.70E-04	5.66E-02	6.09E-01	3.00E-06	2.78E-10	2.76E-07	1.24E-05
Rn-219	3.84E-05	3.71E-04	1.13E-02	2.98E-01	3.78E-03	3.52E-07	1.23E-04	1.96E-03
Rn-220	3.84E-05	3.70E-04	1.12E-02	5.42E-01	3.48E-06	3.22E-10	1.13E-07	1.16E-05
Rn-222	3.84E-05	3.71E-04	1.12E-02	5.01E-01	2.76E-06	2.56E-10	8.95E-08	7.76E-06
Ru-103	9.96E-06	2.66E-03	3.31E-02	5.03E-01	1.24E-03	7.49E-06	1.61E-04	9.85E-03
Ru-106	1.00E-02	0.00E+00	0.00E+00	0.00E+00	1.76E-06	0.00E+00	0.00E+00	0.00E+00
S-35	4.87E-02	0.00E+00	0.00E+00	0.00E+00	8.53E-06	0.00E+00	0.00E+00	0.00E+00
Sb-124	1.36E-05	3.75E-03	2.87E-02	9.81E-01	7.68E-04	4.85E-06	4.62E-05	1.89E-02
Sb-125	1.36E-05	3.75E-03	2.87E-02	4.85E-01	8.49E-02	5.36E-04	5.43E-03	8.70E-03
Sb-126	1.36E-05	5.34E-04	2.58E-02	6.40E-01	3.75E-03	1.10E-06	2.40E-04	4.31E-02
Sb-126m	1.24E-05	3.59E-03	2.80E-02	5.98E-01	1.81E-02	1.05E-04	1.37E-04	2.60E-02
Sc-44	3.84E-06	3.65E-05	3.69E-03	7.37E-01	2.58E-15	2.07E-03	8.11E-05	2.91E-02

Table B-2 Collapsed Photon Energies (MeV) and Fractions for ICRP-107 Radionuclides with Half-Life of at least 30 Days and their Shorter-Lived Progeny (Cont.)

Nuclide	EPT(1)	EPT(2)	EPT(3)	EPT(4)	FPT(1)	FPT(2)	FPT(3)	FPT(4)
Sc-46	8.00E-06	4.05E-04	4.52E-03	1.00E+00	1.85E-05	9.22E-09	4.99E-07	2.00E-02
Se-75	1.42E-05	1.25E-03	1.06E-02	2.15E-01	8.88E-02	2.11E-04	5.46E-03	1.78E-02
Se-79	5.29E-02	0.00E+00	0.00E+00	0.00E+00	9.26E-06	0.00E+00	0.00E+00	0.00E+00
Si-32	6.86E-02	0.00E+00	0.00E+00	0.00E+00	1.20E-05	0.00E+00	0.00E+00	0.00E+00
Sm-145	1.48E-05	1.39E-04	3.63E-02	4.92E-01	1.82E-01	4.88E-06	1.76E-02	3.33E-07
Sm-146	0.00E+00	0.00E+00	0.00E+00	0.00E+00	0.00E+00	0.00E+00	0.00E+00	0.00E+00
Sm-147	0.00E+00	0.00E+00	0.00E+00	0.00E+00	0.00E+00	0.00E+00	0.00E+00	0.00E+00
Sm-148	0.00E+00	0.00E+00	0.00E+00	0.00E+00	0.00E+00	0.00E+00	0.00E+00	0.00E+00
Sm-151	1.43E-05	1.62E-04	1.04E-03	1.15E-02	9.08E-04	3.51E-08	1.11E-06	1.84E-05
Sn-113	8.13E-06	4.33E-04	2.30E-02	2.55E-01	1.41E-01	2.48E-05	7.92E-03	2.11E-04
Sn-119m	1.09E-05	4.71E-04	3.59E-03	2.51E-02	2.45E-01	4.98E-05	1.10E-03	5.74E-03
Sn-121	1.16E-01	0.00E+00	0.00E+00	0.00E+00	2.02E-05	0.00E+00	0.00E+00	0.00E+00
Sn-121m	1.12E-05	4.75E-04	3.53E-03	2.82E-02	1.09E-01	2.44E-05	4.97E-04	1.74E-03
Sn-123	1.22E-05	4.99E-04	3.72E-03	7.54E-01	1.64E-06	4.05E-10	8.96E-09	1.55E-04
Sn-126	1.22E-05	5.05E-04	3.78E-03	6.04E-02	2.13E-01	5.09E-05	1.05E-03	9.32E-03
Sr-85	1.53E-05	1.43E-04	1.30E-02	5.14E-01	9.07E-02	3.07E-06	6.08E-03	9.57E-03
Sr-89	5.30E-06	1.67E-04	1.45E-02	5.88E-01	1.08E-07	3.74E-12	5.34E-09	1.03E-04
Sr-90	1.96E-01	0.00E+00	0.00E+00	0.00E+00	3.43E-05	0.00E+00	0.00E+00	0.00E+00
Ta-179	1.93E-05	2.23E-04	7.72E-03	5.72E-02	9.44E-02	6.71E-06	2.30E-03	4.14E-03
Ta-182	3.13E-05	8.32E-03	9.99E-02	1.18E+00	8.78E-02	2.81E-03	1.29E-02	9.87E-03
Tb-157	1.95E-05	1.69E-04	6.14E-03	4.40E-02	9.65E-02	4.26E-06	1.44E-03	1.04E-03
Tb-158	1.90E-05	6.05E-03	6.38E-02	9.38E-01	1.48E-01	2.70E-03	1.12E-02	7.80E-03
Tb-160	1.37E-05	1.73E-04	4.86E-02	8.04E-01	5.16E-02	2.53E-06	4.52E-03	1.37E-02
Tc-95	6.85E-06	2.27E-04	1.69E-02	7.79E-01	1.01E-01	8.03E-06	7.02E-03	1.01E-02
Tc-95m	6.88E-06	2.28E-04	1.69E-02	4.87E-01	1.03E-01	8.27E-06	7.02E-03	1.39E-02
Tc-97	6.85E-06	2.28E-04	2.30E-03	1.78E-02	1.00E-01	7.99E-06	3.94E-04	6.31E-03
Tc-97m	7.88E-06	2.53E-04	2.43E-03	1.92E-02	8.97E-02	9.17E-06	4.02E-04	4.90E-03
Tc-98	8.91E-06	2.79E-04	1.85E-02	6.99E-01	3.90E-04	5.03E-08	3.25E-05	2.02E-02
Tc-99	8.91E-06	2.79E-04	2.58E-03	1.01E-01	8.45E-07	1.09E-10	4.43E-09	1.78E-05
Te-121	1.22E-05	4.99E-04	2.50E-02	5.60E-01	1.36E-01	3.36E-05	8.33E-03	9.94E-03

Table B-2 Collapsed Photon Energies (MeV) and Fractions for ICRP-107 Radionuclides with Half-Life of at least 30 Days and their Shorter-Lived Progeny (Cont.)

Nuclide	EPT(1)	EPT(2)	EPT(3)	EPT(4)	FPT(1)	FPT(2)	FPT(3)	FPT(4)
Te-121m	1.33E-05	5.29E-04	2.45E-02	2.40E-01	1.48E-01	4.18E-05	6.14E-03	8.42E-03
Te-123	1.22E-05	4.98E-04	3.62E-03	2.69E-02	1.07E-01	2.71E-05	5.26E-04	1.26E-05
Te-123m	1.36E-05	5.35E-04	3.89E-03	1.11E-01	1.41E-01	4.10E-05	8.19E-04	1.33E-02
Te-125m	1.36E-05	5.34E-04	3.90E-03	2.86E-02	2.43E-01	7.10E-05	1.44E-03	1.23E-02
Te-127	1.53E-05	3.91E-03	3.58E-02	3.54E-01	1.77E-04	1.24E-06	1.40E-05	1.62E-04
Te-127m	1.36E-05	3.73E-03	2.86E-02	4.85E-01	1.21E-01	7.36E-04	3.77E-03	2.56E-06
Te-129	1.52E-05	5.81E-04	2.15E-02	4.94E-01	1.04E-01	3.39E-05	2.25E-03	1.26E-03
Te-129m	1.36E-05	3.74E-03	2.84E-02	6.96E-01	7.75E-02	4.74E-04	2.77E-03	4.54E-04
Th-227	7.12E-05	4.33E-04	1.26E-02	1.93E-01	1.76E-01	2.06E-05	6.42E-03	6.33E-03
Th-228	7.13E-05	1.29E-02	1.13E-01	8.25E-01	2.78E-02	1.08E-03	1.79E-04	2.23E-09
Th-229	7.12E-05	4.39E-04	1.32E-02	1.10E-01	2.95E-01	3.45E-05	9.81E-03	7.47E-03
Th-230	7.13E-05	1.29E-02	8.36E-02	5.77E-01	2.44E-02	9.46E-04	4.61E-05	4.68E-10
Th-231	7.65E-05	4.92E-04	3.19E-03	2.65E-02	2.44E-01	3.38E-05	1.37E-03	9.32E-03
Th-232	7.12E-05	4.32E-04	2.89E-03	1.64E-02	2.26E-02	2.68E-06	1.15E-04	7.87E-04
Th-234	7.65E-05	4.88E-04	1.32E-02	7.99E-02	3.49E-02	4.75E-06	1.19E-03	1.09E-03
Ti-44	6.75E-06	3.51E-04	4.09E-03	7.32E-02	8.35E-02	3.10E-05	1.83E-03	1.90E-02
Tl-202	1.47E-05	3.14E-04	9.88E-03	2.72E-01	1.35E-01	9.32E-06	3.44E-03	1.70E-02
Tl-204	1.47E-05	3.15E-04	9.78E-03	1.07E-01	3.89E-03	2.68E-07	9.35E-05	2.04E-04
Tl-206	2.66E-05	3.41E-04	1.05E-02	5.05E-01	1.24E-04	9.94E-09	3.57E-06	1.03E-04
Tl-207	2.66E-05	3.41E-04	1.05E-02	5.86E-01	8.61E-06	6.90E-10	2.50E-07	1.13E-04
Tl-208	2.66E-05	3.41E-04	5.59E-02	1.46E+00	1.23E-02	9.88E-07	1.13E-03	2.30E-02
Tl-209	2.66E-05	3.41E-04	1.05E-02	7.05E-01	3.48E-02	2.80E-06	1.03E-03	3.05E-02
Tl-210	2.66E-05	3.42E-04	1.08E-02	8.82E-01	7.79E-02	6.47E-06	2.36E-03	3.16E-02
Tm-168	1.36E-05	1.88E-04	6.90E-03	3.81E-01	1.50E-01	9.01E-06	3.73E-03	3.26E-02
Tm-170	8.74E-06	2.01E-04	7.38E-03	8.84E-02	1.37E-02	8.14E-07	3.39E-04	6.38E-04
Tm-171	8.66E-06	2.01E-04	7.33E-03	5.42E-02	1.66E-03	9.79E-08	4.04E-05	1.11E-04
U-232	8.23E-05	4.64E-04	1.36E-02	8.18E-02	3.22E-02	4.26E-06	1.33E-03	2.92E-05
U-233	8.23E-05	1.37E-02	1.56E-01	1.04E+00	1.85E-02	6.90E-04	1.28E-05	1.80E-09
U-234	8.23E-05	4.64E-04	1.44E-02	5.05E-01	2.95E-02	3.90E-06	1.23E-03	5.38E-09
U-235	8.22E-05	4.86E-04	1.29E-02	1.69E-01	1.44E-01	1.93E-05	3.66E-03	9.54E-03

Table B-2 Collapsed Photon Energies (MeV) and Fractions for ICRP-107 Radionuclides with Half-Life of at least 30 Days and their Shorter-Lived Progeny (Cont.)

Nuclide	EPT(1)	EPT(2)	EPT(3)	EPT(4)	FPT(1)	FPT(2)	FPT(3)	FPT(4)
U-235m	7.65E-05	0.00E+00	0.00E+00	0.00E+00	1.00E-12	0.00E+00	0.00E+00	0.00E+00
U-236	8.23E-05	4.64E-04	3.07E-03	1.57E-02	2.68E-02	3.54E-06	1.49E-04	9.67E-04
U-237	7.44E-05	5.30E-04	1.42E-02	1.14E-01	2.30E-01	3.56E-05	8.00E-03	1.15E-02
U-238	8.24E-05	1.40E-02	1.06E+00	7.36E+00	2.16E-02	8.97E-04	7.86E-08	2.51E-11
U-240	7.44E-05	5.25E-04	1.38E-02	9.72E-02	9.57E-02	1.46E-05	3.41E-03	4.74E-04
V-49	8.00E-06	9.08E-05	4.14E-04	4.52E-03	7.20E-02	9.86E-07	3.46E-05	1.90E-03
V-50	8.00E-06	4.44E-03	7.51E-02	1.42E+00	5.98E-02	1.61E-03	2.24E-06	1.00E-02
W-181	2.49E-05	2.31E-04	7.65E-03	5.90E-02	1.24E-01	9.21E-06	2.71E-03	6.45E-03
W-185	3.76E-05	2.51E-04	8.51E-03	1.17E-01	4.32E-05	3.76E-09	1.49E-06	2.83E-05
W-188	3.75E-05	2.54E-04	8.41E-03	1.87E-01	5.62E-04	4.92E-08	1.68E-05	1.10E-04
Y-88	2.09E-05	1.80E-03	1.43E-02	1.38E+00	8.32E-02	2.94E-04	5.96E-03	1.94E-02
Y-90	6.52E-06	1.84E-04	1.53E-02	9.33E-01	1.39E-05	6.36E-10	7.79E-07	1.63E-04
Y-91	6.52E-06	1.84E-04	2.04E-03	7.23E-01	1.40E-07	6.40E-12	4.00E-10	1.32E-04
Yb-169	1.35E-05	1.96E-04	7.02E-03	9.05E-02	3.04E-01	2.06E-05	6.80E-03	3.59E-02
Zn-65	9.87E-06	8.80E-04	8.09E-03	1.08E+00	4.82E-02	1.19E-04	3.77E-03	5.34E-03
Zr-88	5.30E-06	1.68E-04	1.45E-02	3.93E-01	1.34E-01	4.67E-06	6.58E-03	9.73E-03
Zr-93	1.91E-02	3.02E-02	0.00E+00	0.00E+00	3.27E-06	1.32E-07	0.00E+00	0.00E+00
Zr-95	5.83E-06	2.04E-04	1.61E-02	7.41E-01	1.60E-04	9.82E-09	1.02E-05	9.89E-03

Table B-3 Dependent Variables and Discrete Values Used in Area Factor Calculations

Variables	Units	Values
Photon energy	keV	10, 12.5, 15, 20, 30, 40, 50, 60, 80, 100, 150, 200, 300, 400, 500, 600, 800, 1,000, 1,500, 2,000, 3,000, 4,000, 5,000
Source thickness	m	0.001, 0.005, 0.015, 0.05, 0.15, 0.5
Cover thickness	m	0.0, 0.001, 0.005, 0.015, 0.05, 0.15, 0.5
Source radius	m	0.564, 1.784, 2.523, 3.989, 5.642, 7.979, 12.62, 17.84, 39.89, 56.42, 178.4, 564.2

B.3   References

Chen, S.Y., 1991, "Calculation of Effective Dose Equivalent Responses for External Exposure from Residual Photon Emitters in Soil," *Health Physics* 60(3): 411–426.

ICRP (International Commission on Radiological Protection), 1983, *Radionuclide Transformations: Energy and Intensity of Emissions*, Publication 38, Annals of the ICRP, Vols. 11–13, Pergamon Press, New York, N.Y.

ICRP, 2008, *Nuclear Decay Data for Dosimetric Calculations,* Publication 107, Pergamon Press, New York, N.Y.

Kamboj, S., C. Yu, and D.J. LePoire, 1998, *External Exposure Model Used in the RESRAD Code for Various Geometries of Contaminated Soil,* ANL/EAD/TM-84, prepared by Argonne National Laboratory, Lemont, Ill., for U.S. Department of Energy, Washington, D.C.

Shen, H.W., and P.Y. Julien, 1993, "Erosion and Sediment Transport" in *Handbook of Hydrology,* D.R. Maidment (ed.), McGraw-Hill Inc.

Trubey, D.K., 1991, *New Gamma-Ray Buildup Factor Data for Point Kernel Calculations: ANS-6.4.3 Standard Reference Data*, NUREG-5740, ORNL/RSIC-49, Oak Ridge National Laboratory, Oak Ridge, Tenn., Aug.

APPENDIX C:
INHALATION PATHWAY FACTORS

This appendix describes the methodology RESRAD-OFFSITE implements to calculate radiation dose and cancer risk associated with exposure through the inhalation pathway. The general principles for computing the exposure, radiation dose, and cancer risk are the same as those for RESRAD-ONSITE (Yu et al. 2001). For most radionuclides that exist in solid forms, the reported dose (risk) for the inhalation pathway is for the inhalation of airborne particulates with radionuclides attaching to them. For carbon-14, which is considered to exist in a solid form and as $^{14}CO_2$, the reported dose (risk) for the inhalation pathway is for the inhalation of airborne particulates as well as $^{14}CO_2$. When hydrogen-3 is concerned, the reported dose (risk) for the inhalation pathway includes the inhalation and dermal absorption of ^3HHO vapor (with the dose or risk from dermal absorption being 50% of that from inhalation), because hydrogen-3 converts to ^3HHO in the environment. Like the other pathways, the reported dose (risk) of the inhalation pathway accounts for the combined exposures incurred both onsite and offsite.

In addition to the methodology used to calculate radiation dose and cancer risk associated with inhalation exposure, this appendix also presents the methodology to estimate the onsite and offsite air concentrations of radionuclides that attach to particulates. Appendix F describes the methodology for calculating the concentrations of gaseous carbon-14 ($^{14}CO_2$) and hydrogen-3 (^3HHO) in the air, as well as in the other environmental media, fodder/crops, animal products, and aquatic foods. After the air concentrations of $^{14}CO_2$ and ^3HHO are calculated, the equations presented in this appendix (Section C.3) are used to calculate the radiation dose and cancer risk associated with the exposures to them.

C.1   Onsite Air Concentration of Radionuclides that Attach to Particulates

The outdoor air concentration of radionuclides that attach to particulates above the primary contaminated area (i.e., onsite) is calculated using the same formulation [Equation (C.1)] as in RESRAD-ONSITE:

$$C_{k,onsite}^{rep-du}(t) = A_{sc,k,onsite}(t)\, ML_{onsite}\, f_{rep-du,onsite}\, FA_{air,onsite} \qquad (C.1)$$

$$A_{sc,k,onsite}(t) = A_{pc,k}(t) f_{vm}(t) \rho_{pc} / \rho_{mix}(t) \qquad (C.2)$$

where

$C_{k,onsite}^{rep-du}(t)$ = air concentration of radionuclide k attaching to respirable dust particles above the primary contaminated area (Bq/m^3 or pCi/m^3),

$A_{sc,k,onsite}(t)$ = activity concentration of radionuclide k in surface soil of the primary contaminated area (Bq/g or pCi/g),

ML_{onsite} = average mass loading of all dust particles in the air above the primary contaminated area (g/m^3),

$f_{rep-du,onsite}$ = fraction of respirable dust particles to total dust particles in the air,

$FA_{air,onsite}$ = area factor for the airborne dust particles (i.e., fraction of airborne dust particles from the primary contaminated area),

$A_{pc,k}(t)$ = activity concentration of radionuclide k in the primary contaminated zone (Bq/g or pCi/g),

$f_{vm}(t)$ = fraction of primary contamination in the surface mixing layer,

ρ_{pc} = bulk soil density of the primary contaminated zone (g/cm^3), and

$\rho_{mix}(t)$ = bulk soil density of the surface mixing layer (g/cm^3).

Particles in the surface layer of soil in the primary contaminated area are assumed to be re-suspended into the air by wind disturbance and various human activities. In the air, the contaminated soil (dust) particles mix homogeneously with uncontaminated dust particles blown in by wind from the surrounding uncontaminated areas. In Equation (C.1), ML_{onsite} represents the total dust loading in the air above the primary contaminated area, which is multiplied by the fraction of respirable dust particles to the total dust particles, $f_{rep-du,onsite}$, to produce the respirable dust loading above the primary contaminated area. The area factor, $FA_{air,onsite}$, is defined as the ratio of the airborne dust loading from a finite area source (i.e., the primary contamination) to the airborne dust loading from an infinite area source. Therefore, the product of the respirable dust loading above the primary contamination ($ML_{onsite} \times f_{rep-du}$) and $FA_{air,onsite}$ gives the respirable dust loading from the primary contaminated area.

The methodology for calculating $FA_{air,onsite}$ is the same as that used in RESRAD-ONSITE. It employs the Gaussian plume model combined with contaminant removal processes, such as dry and wet deposition of particulates. Chang et al. (1998) details the methodology and provides the values of area factors for various combinations of particle size (1, 2, 5, 10, and 30 μm) and wind speed (1, 2, 5, and 10 m/s) as a function of the square root of the contaminated area (1–10^5 m) [see Equation (C.3)]. They assume a particle density of 2.65 g/cm^3, a neutral atmospheric stability, a 1-mm raindrop diameter, and a 1-m/yr annual precipitation rate:

$$FA_{air} = \frac{a}{1+b(\sqrt{A})^c} \tag{C.3}$$

where

A = area of the finite source (m^2), and
a, b, c = least-square regression coefficients.

For a respirable particle size of 1 μm assumed in RESRAD-ONSITE and RESRAD-OFFSITE, the regression coefficients for Equation (C.3) are given in Table C-1. RESRAD-OFFSITE will calculate an area factor by interpolation, if the input average wind speed is not listed in Table C-1.

Table C-1 Coefficients for the Inhalation Pathway Area Factor for a Particle Size of 1 μm

Wind Speed (m/s)	Least-Squares Regression Coefficient		
	a	b	c
1	1.9005	14.1136	-0.2445
2	1.6819	25.5076	-0.2278
5	0.7837	31.5283	-0.2358
10	0.1846	14.6689	-0.2627

Source: Chang et al. (1998).

Equation (C2) relates the activity concentration of radionuclide *k* in surface soil, $A_{sc,k}$, to the activity concentration of radionuclide *k* in the primary contaminated zone and is obtained from Equation (G.67) in Appendix G.

C.2 Offsite Air Concentration of Radionuclides Attaching to Particulates

Outdoor air concentration of radionuclide *k* above an offsite location is made up of two components. The first component accounts for the contaminated soil (dust) particles that are released to the air from the primary contaminated area and then blown by wind to arrive at the offsite location. The second component accounts for the resuspension of contaminated soil (dust) particles from the secondary contamination source formed at the offsite location. The secondary contamination source forms over time due to the deposition of contaminated dust particles from the air, the deposition of contaminated irrigation water to soils, and the contaminated soil eroding from the primary contamination and accumulating offsite.

$$C_{k,offsite}^{rep-du}(t) = \overline{C_{k,onsite \to offsite}^{rep-du}}(t) + A_{sc,k,offsite}(t)\, ML_{offsite}\, f_{rep-du,offsite}$$

$$= Q_k^{rep-du}(t) \times \overline{(\chi/Q)_{rep-du}} + A_{sc,k,offsite}(t)\, ML_{offsite}\, f_{rep-du,offsite} \qquad (C.4)$$

where

$C_{k,offsite}^{rep-du}(t)$ = air concentration of radionuclide *k* attaching to respirable dust particles above the offsite location (Bq/m^3 or pCi/m^3),

$\overline{C_{k,onsite \to offsite}^{rep-du}}(t)$ = average air concentration of radionuclide *k* attaching to respirable dust particles over the offsite area of concern, due to release from the primary contaminated area (Bq/m^3 or pCi/m^3),

$A_{sc,k,offsite}(t)$ = cumulative activity concentration of radionuclide *k* in surface soil of the offsite location (Bq/g or pCi/g),

$ML_{offsite}$ = average mass loading of dust particles in the air above the offsite area (g/m^3),

$f_{rep-du,offsite}$ = fraction of respirable dust particles to total dust particles in the air at the offsite location,

$Q_k^{rep-du}(t)$ = air release rate of radionuclide *k* attaching to respirable dust particles from the primary contaminated area (Bq/yr or pCi/yr), and

$(\chi/Q)_{rep-du}$ = averaged atmospheric transport factor for respirable dust particles released from the primary contaminated area to the offsite area (yr/m^3).

The air concentration of radionuclide *k* attaching to respirable dust particles at an offsite location, $C_{k,onsite \to offsite}^{rep-du}$, is determined by the release rate of radionuclide *k* attaching to respirable dust particles from the primary contaminated area, Q_k^{rep-du}, and the χ/Q value determined by the Gaussian plume dispersion model for respirable particles, $(\chi/Q)_{rep-du}$. The χ/Q is the atmospheric transport factor representing the ratio of air concentration at a downwind location to the release rate from a point source. To calculate radiation dose or cancer risk incurred by a receptor at an offsite area, which could be the offsite dwelling or any of the four farmed areas, an integration scheme is used to obtain the average air concentration, $\overline{C_{k,onsite \to offsite}^{rep-du}}$, over the offsite area. This integration scheme involves subdividing the primary

contaminated area and the offsite area into small rectangles based on grid spacing specified by the user, calculating the χ/Q transport factor representing the transport from each subdivision of the primary contamination to each subdivision of the offsite area, and combining these results to obtain a spatially integrated value. Appendix I provides detailed discussions on the Gaussian plume dispersion model implemented in RESRAD-OFFSITE, as well as discussions on the integration scheme (see Section I.10.1).

The release rate of radionuclide *k* attaching to respirable dust particles is calculated with the following equation:

$$Q_k^{rep-du}(t) = C_{k,onsite}^{rep-du} \times A \times v_{rep-du} \times 3.15576 \times 10^7 \tag{C.5}$$

where

A = area of the primary contamination (m^2),
V_{rep-du} = deposition velocity of respirable dust particles (m/s), and
3.15576×10^7 = unit conversion factor (s/yr).

The equation is based on the assumption of equilibrium between deposition and resuspension. Note that RESRAD-OFFSITE uses two deposition velocities, one for respirable particles and the other for all particles. To calculate inhalation exposure, the deposition velocity of respirable particles is used in Equation (C.5).

The concentration of radionuclide *k* in surface soil of an offsite location, $A_{sc,k,offsite}(t)$, is determined by taking into account cumulative depositions from the air, from water irrigation, and from erosion from the primary contaminated area, as well as radiological ingrowth and decay, erosion, and leaching that would occur simultaneously with the accumulation contributed by the three depositions above. Detailed formulations to calculate $A_{sc,k,offsite}(t)$ are discussed and provided in Section J.1. The air concentration resulting from resuspension of soil (dust) particles at the offsite location is estimated by multiplying $A_{sc,k,offsite}(t)$ with the mass loading of dust particles, $ML_{offsite}$, and the fraction of respirable particles to all particles, $f_{rep-du,offsite}$. Unlike the resuspension at the onsite location [see Equation (C.1)], Equation (C.4) for an offsite location does not include an area factor, FA_{air}, because not all of the airborne particulates blown from outside the offsite area of concern are clean (i.e., not contaminated; some are from the primary contaminated area). To consider clean particles blown from the surrounding areas, a value lower than the actual mass loading may be specified for the input parameter $ML_{offsite}$.

C.3   Calculation of Radiation Dose and Cancer Risk from Inhalation of Airborne Radionuclides

In RESRAD-OFFSITE, the general principles for computing radiation exposure are the same as for RESRAD-ONSITE (Yu et al. 2001). The primary difference between the two codes is that RESRAD-OFFSITE calculates and uses media concentrations at the time of exposure, while RESRAD-ONSITE relates media concentrations at the time of exposure to the initial soil concentrations and environmental transfer factors. The dose (risk) resulting from exposure incurred at the primary contaminated area and at each of the offsite areas are summed and reported together.

The following equation is used to calculate the radiation dose from inhalation of airborne radionuclides:

$$Dose_{inh,k}(t) = FI_{inh} \times \left[(f_{otd,onsite} + f_{ind,onsite} \times F_{dust}) \times \int_t^{t+1} C^{air}_{k,onsite}(t)\, dt + \right.$$

$$\left. \Sigma_{offsite} (f_{otd,offsite} + f_{ind,offsite} \times F_{dust}) \times \int_t^{t+1} C^{air}_{k,offsite}(t)\, dt \right] \times DC_{inh,k} \qquad (C.6)$$

where

$Dose_{inh,k}(t)$	=	radiation dose from inhalation of airborne radionuclide k, either attaching to respirable dust particles or in gaseous form (mSv/yr or mrem/yr);
FI_{inh}	=	annual intake of air (i.e., annual inhalation rate, m³/yr);
$f_{otd,onsite}$	=	fraction of time spent outdoors at the primary contaminated area;
$f_{ind,onsite}$	=	fraction of time spent indoors at the primary contaminated area;
F_{dust}	=	indoor dust filtration factor;
$C^{air}_{k,onsite}(t)$	=	air concentration of radionuclide k above the primary contaminated area, [= $C^{rep-du}_{k,onsite}(t)$ if attaching to particulates] (pCi/m³ or Bq/m³);
$f_{otd,offsite}$	=	fraction of time spent outdoors at an offsite area;
$f_{ind,offsite}$	=	fraction of time spent indoors at an offsite area;
$C^{air}_{k,offsite}(t)$	=	air concentration of radionuclide k above an offsite area, [= $C^{rep-du}_{k,offsite}(t)$ if attaching to particulates] (pCi/m³ or Bq/m³);
$DC_{inh,k}$	=	inhalation dose coefficient for radionuclide k (mSv/Bq or mrem/pCi).

The summation in Equation (C.6) is performed over all the offsite areas where the receptor of concern would spend time, including the dwelling area and the four agriculture areas. The value of $f_{ind,offsite}$ at the four agriculture areas is 0, because agricultural activities are considered to be conducted outdoors. The inhalation dose coefficient, $DC_{inh,k}$, would depend on the chemical form of radionuclide k (see discussions in Appendix A). For radionuclides that attach to particulates, RESRAD-OFFSITE uses the most conservative DC_{inh} as the default for dose calculation. Users have the option of choosing a different dose coefficient. However, for the inhalation of gaseous carbon-14 and hydrogen-3, users cannot change the DC_{inh} used by RESRAD-OFFSITE; they are DC_{inh} for $^{14}CO_2$ and HTO, respectively.

To calculate the potential cancer risk associated with the inhalation of airborne radionuclides, the following equation is used by RESRAD-OFFSITE:

$$Risk_{inh,k}(t) = FI_{inh} \times \left[(f_{otd,onsite} + f_{ind,onsite} \times F_{dust}) \times \int_t^{t+ED} C^{air}_{k,onsite}(t)\, dt + \right.$$

$$\left. \Sigma_{offsite} (f_{otd,offsite} + f_{ind,offsite} \times F_{dust}) \times \int_t^{t+ED} C^{air}_{k,offsite}(t)\, dt \right] \times Sf_{inh,k} \qquad (C.7)$$

where

$Risk_{inh,k}(t)$	=	cancer risk from inhalation of radionuclide k, either attaching to respirable dust particles or in gaseous form,
ED	=	exposure duration (yr), and
$Sf_{inh,k}$	=	inhalation slope factor for radionuclide k (1/Bq or 1/pCi).

The summation in Equation (C.7) is also performed over all the offsite areas where the receptor of concern would spend time, including the dwelling area and the four agriculture areas. The inhalation slope factor, $Sf_{inh,k}$, would depend on the chemical form of radionuclide k (see discussions in Appendix A). For radionuclides that attach to particulates, RESRAD-OFFSITE uses the most conservative Sf_{inh} as the default for cancer risk calculation. Users have the option of choosing a different slope factor. However, for the inhalation of gaseous carbon-14 and hydrogen-3, users cannot change the Sf_{inh} used by RESRAD-OFFSITE; they are Sf_{inh} for $^{14}CO_2$ and HTO, respectively.

In RESRAD-OFFSITE, both radiation dose and cancer risk reported in text reports or graphical forms are time-integrated quantities. The dose reported for a particular time is the dose over a period of 1 year beginning at that time. Likewise, the risk reported for a particular time is the value over an exposure duration, *ED*, beginning at that time.

C.4 <u>References</u>

Chang, Y.-S., C. Yu, and S.K. Wang, 1998, *Evaluation of the Area Factor Used in the RESRAD Code for the Estimation of Airborne Contaminant Concentrations of Finite Area Sources*, ANL/EAD/TM-82, Argonne National Laboratory, Lemont, Ill., Sept.

Yu, C., A.J. Zielen, J.-J. Cheng, D.J. LePoire, E. Gnanapragasam, S. Kamboj, J. Arnish, A. Wallo III, W.A. Williams, and H. Peterson, 2001, *User's Manual for RESRAD Version 6*, ANL/EAD-4, Argonne National Laboratory

APPENDIX D:
RADON PATHWAY MODEL

RESRAD-OFFSITE considers radon exposure at both onsite and offsite locations. The modeling for onsite exposures are the same as that implemented in RESRAD-ONSITE, which considers diffusion of radon gas. This gas is generated in the primary contaminated zone, through soils and building foundation, respectively, and gets into the outdoor and indoor environment. This model also considers emanation of radon gas from contaminated household water into the residence, as well as building ventilation (i.e., air exchange between indoors and outdoors) that affects the indoor radon level. The modeling for offsite exposures also considers the diffusion of radon gas generated in the secondary contamination zone, which passes through soils and the building foundation, similar to the onsite exposures; however, for the outdoor radon level, the impact of radon exhalation from the primary contaminated zone, which is blown by wind to offsite locations, is also factored in. This potential increase in outdoor radon levels at offsite locations can increase the indoor radon level because radon gas and its decay progeny can infiltrate to the indoor space. The contribution to indoor radon due to the emanation of radon gas from contaminated household water is also considered at offsite locations, just as it is at onsite locations.

RESRAD-OFFSITE evaluates the concentrations of two radon isotopes—Rn-222 and Rn-220 (thoron)—that occur naturally and result in radiation exposures due to their alpha-emitting decay products. Rn-222 is the most common of the radon isotopes. Thoron has a decay half-life of 55.6 seconds, and its concentration in the air is usually low. Dosimetric considerations suggest that the dose to the lung from thoron progeny is, for an equal concentration of inhaled alpha energy, a factor of 3 less than that from Rn-222 progeny. However, in some DOE remedial action sites, high concentrations of Th-232 and Ra-228 (precursors of thoron) are present. In these circumstances, exposure to Rn-220 and its decay products may be predominant. Therefore, the Rn-220 exposure pathway also is included in RESRAD-OFFSITE.

This appendix provides detailed discussions on the formulations used to estimate the radon levels by RESRAD-OFFSITE. It is based on Appendix C of the RESRAD-ONSITE User's Manual (Yu et al. 2001) with necessary revisions to update the radiation dose conversions and reflect additional considerations incorporated in the RESRAD-OFFSITE code to evaluate exposures at offsite locations.

D.1   Onsite Radon Levels

RESRAD-OFFSITE includes a generalized radon pathway model for estimating the amount of radon released, its concentrations in both indoor and outdoor air, and the concentrations of its progeny due to radiological decay and ingrowth.

D.1.1   Radon Exhalation

Radon forms continually in the ground and migrates from radium-contaminated soil. Radon in soil gas near buildings can move into houses by diffusion or through cracks or holes in the foundation by convection. Radon progeny, however, are chemically active and attach to soil particles, and consequently do not move significantly in the ground. The movement of radon atoms through the pores may be caused by diffusion or convection. The size distribution and configuration of the pore spaces, as well as their moisture content and spatial distribution, are key parameters in determining the radon diffusion rate. Fractures or holes as small as 0.5 mm in

building foundations are enough to allow convective migration. Convective movement of soil gas and the respective transport of radon within the soil and near the subsurface structure of the building can be induced by pressure differences created by meteorological factors and operational conditions of the house. These factors and conditions are highly time-dependent and practically unpredictable. Consequently, the rate of radon exhalation to the outdoor environment and the infiltration into indoor air usually vary with time and cannot be readily quantified. However, the effect of the diurnal atmospheric pressure variation on the radon exhalation rate has been shown to be insignificant when averaged over long periods (Yuan and Roberts 1981).

When soil is assumed to be horizontally infinite and homogeneous, and the convective flow of the soil gas in the porous matrix of the soil is neglected, the radon flux J [the amount of radon activity crossing a unit area of soil surface per unit of time, Bq/($m^2 \times$ s) or pCi/($m^2 \times$ s)], can be mathematically related to the gradient of the radon concentration in the pore space, C, by the Fickian diffusion equation:

$$J = p_t D \frac{dC}{dz}$$ (D.1)

where

p_t = total porosity,
D = diffusion coefficient of radon in soil (m^2/s),
C = radon concentration in the pore space (Bq/m^3 or pCi/m^3), and
z = axial distance in the direction of diffusion (m).

Equation (D.1) can also relate the radon flux crossing a unit area of building foundation or cover layer on top of the contaminated zone to the radon concentration gradient in the pore space of the foundation or cover material. In that case, D is the diffusion coefficient of radon in the foundation or cover material.

Considering mass balance, the change in pore space radon concentration, C, with time within radium-contaminated soil, the cover material, or the foundation of a building can be related to the one-dimensional diffusion flux as follows:

$$\frac{d(p_t C)}{dt} = -\frac{d}{dz}(J) - p_t \lambda C + p_t Q$$ (D.2)

or

$$\frac{dC}{dt} = \frac{d}{dz}\left(D \frac{dC}{dz}\right) - \lambda C + Q$$ (D.3)

where

t = time (s),
λ = radon decay constant ($1/s$), and
Q = radon source term into the pore space [Bq/($m^3 \times$ s) or pCi/($m^3 \times$ s)].

Assuming steady state, Equation (D.3) can be written as follows:

$$-\frac{d}{dz}\left(D \frac{dC}{dz}\right) + \lambda C = Q$$ (D.4)

Q is zero in the cover material or the foundation of a building. In contaminated soil, it can be evaluated by the following expression:

$$Q = \frac{\varepsilon \rho_b S_{Ra} \lambda}{p_t}$$ (D.5)

where

ε = radon emanation coefficient (dimensionless),
ρ_b = bulk density of the contaminated soil (g/cm^3), and
S_{Ra} = radium concentration in soil (Bq/kg or pCi/kg).

The emanation coefficient ε represents the fraction of radon generated by radium decay that escapes from the soil particles. Radon enters air-filled pores in the soil primarily from the recoil of radon atoms during radium decay. The contribution from diffusion through the solid mineral grains is less important because most of the radon atoms decay before escaping. Observed values of ε range from about 0.01 to 0.80 (Mueller Associates, Inc. 1986). The observed emanation coefficient depends on many factors, including the mineral composition of the soil, porosity, particle size distribution, and moisture content.

The radium concentration in soil, S_{Ra}, is the radon precursor principal radionuclide concentration in the contaminated soil. Its value depends on the specific radon isotope considered. For Rn-222 or Rn-220, respectively, S_{Ra}, represents the Ra-226 or Th-228 concentration in soil. (The immediate parent of Rn-220 is Ra-224, which is an associated radionuclide assumed to be in equilibrium with its principal parent radionuclide Th-228).

The boundary conditions used in RESRAD-OFFSITE for solving Equation (D.4) are as follows:

- $C(Z_a) = 0$, the radon concentration at either the air-ground or the floor-indoor air interface, Z_a, is zero;

- $J(0) = 0$, the radon flux is zero at the bottom of the boundary; and

- $C(z)$ and $J(z)$, the radon concentration and flux, respectively, are continuous across medium interfaces in the ground.

RESRAD-OFFSITE solves Equations (D.1) and (D.4), together with the above boundary conditions, numerically for the vertical profiles of C and J using a finite-difference method. The radon flux, J, is then evaluated with Equation (D.1) at two distinct locations: (1) J_{out}, the outdoor flux at the interface between the ground surface and the atmosphere, and (2) J_{in}, the indoor flux at the interface between the floor (i.e., the foundation surface) and the indoor air.

In estimating the radon flux, the choice of a value for the diffusion coefficient, D, is critical. Values of D have been measured experimentally for a variety of materials (Nazaroff and Nero 1988; Rogers and Nielson 1991). Reported values for different soils and building materials are summarized in the *RESRAD Data Collection Handbook* (Yu et al. 2015). Because the moisture content has such a dominant effect on D (i.e., much smaller effects on D are from other soil properties), D correlates with moisture content as (Rogers and Nielson 1991):

$$D = (1.1 \times 10^{-5})\, p_t \exp\left(-6\, R_s p_t - 6\, R_s^{14 p_t}\right)$$ (D.6)

where 1.1×10^{-5} is the radon diffusion coefficient in air (m^2/s) and R_s is the saturation ratio, defined as the ratio of water content over the total porosity. This correlation is based primarily on laboratory data for earthen materials and is used in RESRAD-OFFSITE as a default approach for the diffusion coefficient, if no measured data are available for the site of interest.

Nevertheless, site-specific diffusion coefficients should be obtained whenever possible, especially for materials other than soil.

D.1.1.1   Outdoor Radon Concentrations

In general, the outdoor radon concentration is relatively low compared with the indoor radon concentration, and the average on top of a radium-contaminated area is more significantly dependent on the area of the contamination and average wind speed than other meteorological parameters. Therefore, RESRAD-OFFSITE simplifies the air dispersion model with the following considerations and conservative assumptions to estimate the outdoor radon concentration above a contaminated zone due to radon exhalation:

- The annual average estimates are appropriate.

- An average wind speed, calculated with the input joint frequency data, conservatively represents annual average wind speed.

- The receptor and the residency are at the geometric center of the contaminated area.

- The vertical dimension of the plume (for radon emission from the ground surface) is bounded, and a uniform concentration exists along the vertical plane for the downwind distance the plume travels toward the receptor.

- Radon exhalations from ground surfaces are uniform.

Based on the above considerations and assumptions, the annual average radon concentration above the contaminated area can be calculated as:

$$C_{out}^{Rn} = \frac{J_{out}F_{ao}}{H_{mix}^{Rn}} \frac{1 - \exp\left(-\frac{\lambda_{Rn}\sqrt{A}}{2V_{wind}}\right)}{\lambda_{Rn}} \tag{D.7}$$

where

$$
\begin{aligned}
C_{out}^{Rn} &= \text{annual average outdoor radon concentration (Bq/m}^3 \text{ or pCi/m}^3), \\
J_{out} &= \text{radon flux at the soil surface outdoors [Bq/(m}^2 \times \text{s) or pCi/(m}^2 \times \text{s)]}, \\
H_{mix}^{Rn} &= \text{height to which the radon plume is uniformly mixed (m)}, \\
F_{ao} &= \text{outdoor area factor (dimensionless)}, \\
\lambda_{Rn} &= \text{radon decay constant (1/s)}, \\
A &= \text{area of the contaminated zone (m}^2), \text{ and} \\
V_{wind} &= \text{annual average wind speed (m/s)}.
\end{aligned}
$$

The outdoor area factor, F_{ao}, is a correction factor to adjust for the lateral dispersion effect for a small contaminated area and is given by the formula

$$F_{ao} = \begin{array}{ll} \frac{A}{100}, & 0 \leq A \leq 100 \; m^2 \\ 1.0, & A \geq 100 \; m^2. \end{array} \tag{D.8}$$

The onsite outdoor Rn-222 concentration flux ratio is limited by a value of 500 s/m for a very large area of contamination—a value corresponding to the ratio of the radon concentration to the flux level generally observed in the natural environment. The onsite Rn-220 concentration, $C_{out,onsite}^{Rn-220}$, to flux ratio is limited by a value of 10 s/m for sites with a very large area of contamination—a value also based on the natural environment:

$$C_{out,onsite}^{Rn-222} \leq 500\, J_{out,onsite}^{Rn-222}, \tag{D.9}$$

and

$$C_{out,onsite}^{Rn-220} \leq 10\, J_{out,onsite}^{Rn-220}. \tag{D.10}$$

D.1.1.2   Outdoor Radon Progeny Concentrations

The decay and ingrowth of the short-lived radon progeny in the outdoor air are calculated based on an average transit time from the source to the receptor. For outdoor radon, the most important removal processes are dilution by wind and radioactive decay. Other processes, such as deposition of radon progeny on ground surfaces, are insignificant because the transport distances from the radon sources to the receptors are relatively short (i.e., up to a few hundred meters). The average transit time *t* during which radioactive decay occurs is approximated by dividing the average distance of the contaminated area by the annual average wind speed V_{wind}; that is, $t = (\sqrt{A}/2)/V_{wind}$, where $\sqrt{A}$ is the effective length of the contaminated area.

The outdoor concentration of the radon progeny in the air is calculated by

$$C_{out}^n = \frac{J_{out}F_{ao}}{H_{mix}^{Rn}} \sum_{i=1}^n A_{(i,n)} \left[\frac{1-\exp\left(-\frac{\lambda_i \sqrt{A}}{2V_{wind}}\right)}{\lambda_i} \right] \tag{D.11}$$

where

C_{out}^n = annual average outdoor *n*th radon progeny concentration (Bq/m³ or pCi/m³),
λ_i = *i*th radon progeny decay constant (1/s),
$A_{(i,n)}$ = $\frac{\lambda_2 \ldots \lambda_n}{(\lambda_1 - \lambda_i) \ldots (\lambda_n - \lambda_i)}, n \neq i$, and
$A_{(1,1)}$ = 1.

The index *n* is for radon and its progeny. For the Rn-222 decay chain, $n = 1, 2, 3$, and 4 represent Rn-222, Po-218, Pb-214, and Bi-214, respectively; for the Rn-220 decay chain, $n = 1, 2, 3$, and 4 represent Rn-220, Po-216, Pb-212, and Bi-212, respectively. In RESRAD-OFFSITE, the onsite outdoor concentrations of Rn-220 progeny Pb-212 and Bi-212 are limited by the following constraints:

$$C_{out,onsite}^{Pb-212} \leq 0.015\, C_{out,onsite}^{Rn-220}, \tag{D.12}$$

and

$$C_{out,onsite}^{Bi-212} \leq 0.015\, C_{out,onsite}^{Rn-220}. \tag{D.13}$$

This limit corrects the approximation made by Equation (D.11) for a very large area of contamination. The concentration ratio of 0.015 for Pb-212 and Bi-212 to Rn-220 is the value generally expected in the natural environment where an infinite area of contamination is almost reached.

D.1.1.3 Indoor Radon Concentration

Indoor radon levels depend on many parameters, including building characteristics, geographic area, and meteorological conditions (Nazaroff and Nero 1988; Cohen 1991). In RESRAD-OFFSITE, the radon concentration indoors is determined by assuming a balance between the rate of radon entry from sources and its rate of removal. Radon enters a house by exhalation from the ground through the foundation floor and below-grade walls, by the inflow of outdoor air brought in by ventilation, and by the use of water. The rate of radon removal in a house is affected by processes such as air exchange and radioactive decay. Under steady-state conditions, the radon gain from exhalation and ventilation inflow equals the radon loss by decay and ventilation outflow. In the current version of RESRAD-OFFSITE, a steady-state one-compartment model is used to determine the radon concentration indoors.

Under the steady-state, single-compartment model, the mass balance of radon inside a home can be expressed as

$$\frac{dC_{in}^{Rn}}{dt} = \frac{J_{in}A_{floor}F_{ai}}{V} - (\lambda_{Rn} + \lambda_{vent})C_{in}^{Rn} + \lambda_{vent}C_{out}^{Rn} = 0 \qquad (D.14)$$

where

$\quad C_{in}^{Rn}$ = average indoor radon concentration (Bq/m^3 or pCi/m^3),

$\quad J_{in}$ = radon flux from a floor built on the contaminated area [Bq/(m$^2 \times$ s) or pCi/(m$^2 \times$ s)],

$\quad A_{floor}$ = interior surface area of the house floor (assumed to be 100 m^2),

$\quad F_{ai}$ = indoor area factor (dimensionless),

$\quad V$ = interior volume of the house (m^3), and

$\quad \lambda_{vent}$ = ventilation rate of the house (1/s).

The indoor area factor, F_{ai}, is the fraction of the foundation area that is built on the contaminated area and is given by the following formula:

$$F_{ai} = \begin{cases} 1.0, & \text{when } A = A_{floor}, \\ \dfrac{A}{A_{floor}}, & \text{when } A < A_{floor}, \\ 1 + \dfrac{4D_h}{\sqrt{A_{floor}}}, & \text{when } A > A_{floor}. \end{cases} \qquad (D.15)$$

where D_h = depth of the foundation wall below and within the contaminated zone (m).

The radon flux, J_{in}, from the floor built on the contaminated area is calculated by solving Equations (D.1) and (D.4) and by assuming that the floor is a concrete slab that is 15 cm thick (default), with a default radon diffusion coefficient of 3.0 × 10^{-7} m^2/s. The default radon diffusion coefficient for the concrete slab is a conservative value compared to the value the U.S. Nuclear Regulatory Commission (1980) uses: 6.0 × 10^{-9} m^2/s. It accounts for possible cracks and other penetrations that may develop in the foundation as the house ages. Cohen (1991) has investigated the variation of Rn-222 levels in homes in relation to the age of the house. For the more than 30,000 homes investigated, variations were within 36% of the mean.

The solution for Equation (D.14) for the indoor radon concentration, C_{in}^{Rn}, can be written as follows:

$$C_{in}^{Rn} = \frac{\left(\frac{J_{in}F_{ai}}{H} + \lambda_{vent}C_{out}^{Rn}\right)}{(\lambda_{Rn} + \lambda_{vent})} \qquad (D.16)$$

where $H = V/A_{floor}$ (m) is the ratio of the interior volume of the house to the floor area of the house. For a single-story house, H is the ceiling height. Because the ventilation rate, λ_{vent}, is much greater than the Rn-222 decay rate, the indoor Rn-222 concentration would be very sensitive to the air exchange rate of a house. The ventilation rate is not an important factor for Rn-220 because of its high decay rate. The ventilation rate (i.e., air exchange rate) is usually expressed as air changes per hour and expresses the average number of times in an hour the interior volume of the house is replaced by the inflow volume of outside air. In RESRAD-OFFSITE, the input hourly air exchange rate is divided by 3,600 (the number of seconds in an hour) to obtain the λ_{vent} value used in Equation (D.16).

In RESRAD-OFFSITE, the onsite indoor radon concentration, $C_{in,onsite}^{Rn}$, is first calculated with Equation (D.16). This indoor radon concentration, along with the outdoor radon concentration calculated with Equation (D.7), is attributed to the airborne component or water-independent component of the radon exposure pathway. Subsequently, depending on the usage of groundwater in the house, the indoor radon concentration from water's contribution is also calculated (see discussion in Section D.1.2), which is attributed to the waterborne component or water-dependent component of the radon exposure pathway. The final indoor radon concentration is the sum of the indoor radon concentrations attributed to the water-independent and water-dependent components.

D.1.1.4   Indoor Radon Progeny Concentrations

Removal by ventilation and plate-out of radon progeny on surfaces within a house becomes important for indoor radon. Inside a house, the decay products may plate out on any available surface. In an enclosed space with complex surfaces, such as a room with walls and furniture, plate-out and detachment are complicated, and data are not readily available. The rate of plate-out can be specified in terms of the ratio of the amount deposited on a surface from the air (in atoms removed per unit area per unit time) to the concentration in the air (in atoms per unit volume). This ratio is usually called the deposition velocity.

The plate-out process was recently reviewed by Knutson et al. (1983) and Bodansky et al. (1987). The suggested values of the plate-out deposition velocity range from 0.05 cm/s for the highly reactive unattached fraction to 0.00075 cm/s for the fraction that has already attached to the aerosol in a house. For a room with a floor area of 3 m × 4 m and a ceiling height of 2 m, these deposition velocities correspond to removal rates of 0.065 per minute for the unattached fraction and 0.00090 per minute for the attached fraction. These removal rates range between 0.3 and 1.0 interior volume per hour, which correspond to removal rates of 0.005 to 0.0167 per minute. The unattached fraction *f* in the home has a range of about 1% to 10% (National Research Council 1991). RESRAD-OFFSITE does not consider plate-out to calculate radon progeny in a home. This approach is conservative because by neglecting plate-out, the indoor air concentrations of radon progeny are overestimated.

The indoor air concentrations of the radon progeny are calculated by a mass balance equation:

$$\frac{dC_{in}^n}{dt} = \lambda_n C_{in}^{n-1} + \lambda_{vent} C_{out}^n - (\lambda_n + \lambda_{vent}) C_{in}^n \qquad (D.17)$$

where $n = 1$ for radon; $C_{in,onsite}^{Rn}$ is calculated using Equation (D.16) for the radon indoor concentration; $n = 2$, 3, and 4 for the radon progeny (Po-218, Pb-214, and Bi-214 for the Rn-222 decay chain, and Po-216, Pb-212, and Bi-212 for the Rn-220 decay chain); and C_{in}^n and C_{out}^n are the nth radon progeny concentration indoors and outdoors, respectively, in units of Bq/m³ or pCi/m³. Under steady-state conditions, the mass balance equation above can be solved for C_{in}^n ($n = 2$, 3, and 4) as follows:

$$C_{in}^n = \frac{\lambda_n C_{in}^{n-1} + \lambda_{vent} C_{out}^n}{\lambda_n + \lambda_{vent}} \qquad (D.18)$$

D.1.2 Radon Emanation from Water

Groundwater or surface water that contains radium can add to the amount of radon in the air indoors, if the water is used for household activities. Radon partitions between air and water in a ratio of about 4 to 1 at 20°C in the environment under equilibrium conditions (Nazaroff and Nero 1988). When water is used, a large portion of the dissolved radon can escape. Various studies (Mueller Associates, Inc., 1986; Bodansky et al. 1987) on correlating the Rn-222 concentrations in the air of typical homes ($C_{in,water}^{Rn}$) with the concentrations in water supplies (C_w^{Rn}) have indicated that the ratios $C_{in,water}^{Rn}/C_w^{Rn}$ are on the general order of 10^{-4}. This value implies that water containing 10,000 pCi/L of radon would typically increase the indoor Rn-222 concentration by 1 pCi/L. The ratio derived under typical conditions with the equation used by the EPA (EPA 1984) also approximates the value of 10^{-4}.

Lawrence et al. (1992) revealed that the contribution of radon-222 from domestic water wells to indoor air in Colorado houses approaches 10^{-3} in homes with a high Rn-222 concentration in their water. This value is an order of magnitude greater than the ratio of 10^{-4} the EPA derived with their equation. One reason for this could be that the derivation with the EPA equation assumed that indoor air is perfectly mixed; therefore, the entire volume of air in a house was used to calculate the ratio. In reality, the distribution of Rn-222 in homes from water usage is highly uneven and dependent on the location of water outlets. Rn-222 concentrations are expected to be higher in rooms where water is accessible and frequently used (e.g., bathroom and kitchen) than in rooms where no water outlets exist. Because the half-life of Rn-220 is only 55.6 s, the concentration of Rn-220 from water usage would be much lower than that for an equal concentration of Rn-222 in water.

D.1.2.1   Indoor Radon Concentration

To estimate radon concentrations in the air from radon-contaminated water in homes, $C_{in,water}^{Rn}$, RESRAD-OFFSITE assumes that the air-to-water concentration ratio is 1.0×10^{-3} for Rn-222 as shown in Equation D.19; for Rn-220, it calculates the ratio with Equation D.20:

$$\frac{C_{in,water}^{Rn-222}}{C_w^{Rn-222}} = 1.0 \times 10^{-3} \qquad (D.19)$$

$$\frac{C_{in,water}^{Rn-220}}{C_w^{Rn-220}} = 1.0 \times 10^{-3} \times \left(\frac{\lambda_{vent} + \lambda_{Rn-222}}{\lambda_{vent} + \lambda_{Rn-220}} \right) \times F \qquad (D.20)$$

where F = the fraction of household water from the site (i.e., contamination fraction of household water).

The indoor radon concentration calculated with Equation (D.19) or Equation (D.20) is attributed to the waterborne or water-dependent component of the radon exposure pathway. It is added to the radon concentration attributed to the airborne or water-independent component [calculated with Eq. (D.16)] to determine the final indoor radon concentration.

D.1.2.2   Indoor Radon Progeny Concentrations

The indoor radon progeny concentration due to the use of radon-contaminated water, $C_{in,water}^n$, is calculated with Equation (D.21). This equation implies a steady state in the mass of a progeny in the indoor air; in other words, the generation rate of the progeny due to radioactive decay of the preceding progeny is equivalent to the depletion rate of the progeny due to radioactive decay and due to the outflow of the indoor air:

$$C_{in,water}^n = \frac{\lambda_n C_{in,water}^{n-1}}{\lambda_n + \lambda_{vent}} \quad \left(for\ n = 2, 3, 4;\ C_{in,water}^1 = C_{in,water}^{Rn-222}\ or\ C_{in,water}^{Rn-220}\right) \qquad \text{(D.21)}$$

The indoor radon progeny concentration calculated with Equation (D.21) is attributed to the waterborne or water-dependent component of the radon exposure pathway. It is added to the radon progeny concentration attributed to the airborne or water-independent component [calculated with Equation (D.18)] to determine the final indoor radon progeny concentration.

D.2   Offsite Radon Levels

For offsite locations, radon and radon progeny concentrations attributed to the water-independent and water-dependent components of the radon exposure pathway are modeled separately. The equations discussed in Sections D.1.2.1 and D.1.2.2 for indoor radon and radon progeny concentrations due to water use are applied to model the water-dependent component. For the water-independent component, the indoor and outdoor radon and radon progeny concentrations are contributed not only from radon exhalation from the secondary contamination source that forms at the offsite location, but also from radon exhalation from the primary contamination source that is blown by wind to the offsite locations. Therefore, the equations discussed in Sections D.1.1.1 through D.1.1.4 require modifications, as described in Sections D.2.1 through D.2.5.

D.2.1   Radon Exhalation

At an offsite location (i.e., an agricultural area, a livestock feed growing area, or a dwelling area), the modeling of radon diffusion is performed with the secondary soil contamination formed at that area. Equation (D.4) provides the radon concentration profile in the pore space (of soil or building foundation). Then the radon concentration gradient at either the interface between the ground surface and the atmosphere or the interface between the floor (i.e., the foundation surface) and the indoor air is calculated to obtain radon flux to the outdoor atmosphere, $J_{out,offsite}$, or to the inside of the dwelling, $J_{in,offsite}$, according to Equation (D.1).

D.2.2 Outdoor Radon Concentration

The average outdoor radon concentration contributed by radon exhalation from the secondary contamination source, $C_{out,second}^{Rn}$, is calculated with Equation (D.7), where J_{out} refers to $J_{out,offsite}$ and A refers to the offsite area of concern. The average outdoor radon concentration contributed by radon exhalation from the primary contamination source, $\overline{C_{a,Rn,offsite}}$, is determined by the Gaussian plume dispersion modeling with an integration scheme, as detailed in Appendix I. The Gaussian plume dispersion modeling involves the use of the radon exhalation rate from the primary contamination, $J_{out,offsite} \times A$ (where A refers to the area of the primary contamination); χ/Q values for radon, obtained with a deposition velocity of 0 m/s; and radioactive decay over the transport distance. The final outdoor radon concentration is the sum of the contributions from both contamination sources:

$$C_{out,offsite}^{Rn} = C_{out,second}^{Rn} + \overline{C_{a,Rn,offsite}} \tag{D.22}$$

The restriction Equation (D.9) or (D.10) imposed on the onsite outdoor radon concentration does not apply to limit the offsite outdoor radon concentration.

D.2.3 Outdoor Radon Progeny Concentrations

The outdoor radon progeny concentration at an offsite location is also modeled to result from radon exhalation from the primary contamination source and the secondary contamination source. The contribution from the secondary contamination source, $C_{out,second}^{n}$ ($n = 2, 3,$ or 4), is calculated with Equation (D.11), where J_{out} refers to $J_{out,offsite}$ and A refers to the offsite area of concern. The contribution from the primary contamination source, $\overline{C_{a,Rn\ progeny\ n,offsite}}$, like the radon concentration, is determined by the Gaussian plume dispersion model with an integration scheme, as detailed in Appendix I. Gaussian plume dispersion modeling involves the use of the radon exhalation rate from the primary contamination, $J_{out,offsite} \times A$ (where A refers to the area of the primary contamination); the χ/Q values for the radon progeny, obtained with a deposition velocity of 0 m/s for radon and radon progeny; and ingrowth of the radon progeny over the transport distance. The final outdoor radon progeny concentration is the sum of the contributions from both contamination sources:

$$C_{out,offsite}^{n} = C_{out,second}^{n} + \overline{C_{a,Rn\ progeny\ n,offsite}} \tag{D.23}$$

The restrictions Equations (D.12) and (D.13) imposed on the onsite outdoor Pb-212 and Bi-212 concentrations, respectively, do not apply to limit their concentrations at offsite locations.

D.2.4 Indoor Radon Concentration

The indoor radon concentration attributed to the water-independent component of the radon exposure pathway at an offsite dwelling is calculated in the same manner as that at an onsite dwelling, by using Equation (D.16), in which J_{in} refers to $J_{in,offsite}$ and C_{out}^{Rn} refers to the final outdoor radon concentration, $C_{out,offsite}^{Rn}$, calculated with Equation (D.22). Because $C_{out,offsite}^{Rn}$ is used to calculate the indoor radon concentration, the contribution of radon exhalation from the primary contamination source is implicitly included.

D.2.5 Indoor Radon Progeny Concentrations

The indoor radon progeny concentration attributed to the water-independent component of the radon exposure pathway at an offsite dwelling is also calculated in the same manner as that at an onsite dwelling, by using Equation (D.18), in which C_{in}^1 (i.e., C_{in}^{Rn}) refers to the indoor radon concentration discussed in Section D.2.4 and C_{out}^n refers to the final outdoor radon progeny concentration, $C_{out,offsite}^n$, calculated with Equation (D. 23). The inclusion of these two terms implies the influence of radon exhalation from the primary contamination source on the offsite indoor radon progeny concentration.

D.3 <u>Intermediate Results for Radon Flux</u>

The radon flux from the accumulation at offsite locations (i.e., the secondary contaminations) is proportional to the activity concentration at each offsite location because the thickness of the accumulation layer does not change over time. RESRAD-OFFSITE calculates and lists the proportionality factor covering each offsite area for each radon precursor present at the primary contamination. These are given in pCi of the radon isotope per square meter per second, regardless of the units chosen in the interface for the input file. The proportionality factors are listed in the first 6 to 12 lines of the output file, RadonFlux.OUT, depending on whether precursors of one or both radon isotopes are present. The radon flux at each offsite area can be obtained by multiplying the proportionality factor by the concentration of the radon isotope at that same offsite location.

After the listing of the proportionality factors for offsite locations, there is a listing of the temporal onsite outdoor and indoor radon fluxes. A temporal listing is necessary because the thicknesses of the cover and the primary contamination can change over time due to erosion. The temporal flux is listed for each transformation thread of each radon precursor.

Figure D-1 shows a sample of the RadonFlux.OUT file. In the listing, area 1 refers to a fruit, grain, and nonleafy vegetable field, area 2 refers to a leafy vegetable field, area 3 refers to a pasture and silage-growing field for livestock, area 4 refers to a grain-growing field for livestock, and area 5 refers to a dwelling area.

Figure D-1   Sample Radon Flux Output in RadonFlux.OUT

D.4   <u>Dosimetry for Radon Exposures</u>

Radon that is breathed into the lungs as a noble gas is mostly breathed out before it can decay. The hazard from radon arises from its progeny, which are not gaseous. When they are inhaled, they deposit on the interior surfaces of the lung. Figures D.2 and D.3 show the primary decay schemes of Rn-222 and Rn-220, respectively. The physical properties of Rn-220 and its progeny, and consequently their behavior in the atmosphere, are almost the same as those of Rn-222 and its progeny. The first four decay progeny of Rn-222—Po-218, Pb-214, Bi-214, and Po-214 (or RaA, RaB, RaC, and RaC′, respectively)—have half-lives that are very short compared with the 22 years of Pb-210 (RaD). Under most circumstances, only these short-lived alpha-emitting nuclides have health consequences. The half-life of Rn-220 is 55.6 seconds; it decays via Po-216 with a half-life of 0.15 seconds to Pb-212 with a half-life of 10.64 hours. Thus, in general, levels of Pb-212 will reflect concentrations of Rn-220 in the air. Once radon decays, the decay products become solids with electrical charges because of the decay process. In the air, most of the charged atoms rapidly attach to aerosol particles. Because the fraction of ions that do not attach is particularly important to the radon dosimetry, it has been given a special designation, that is, the unattached fraction *f*.
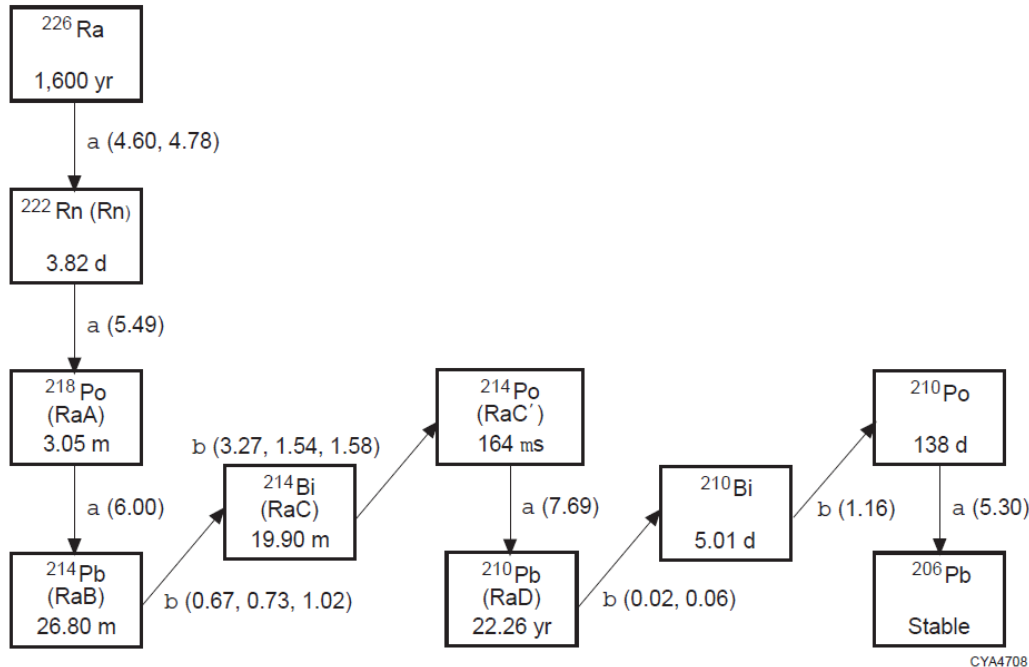
Figure D-2 Decay Scheme of Rn-222 (including its long-lived parent Ra-226) (Source: Kocher 1981)

The radiation dose from inhalation of radon and its progeny depends on the emitted alpha energies and radioactivities, the various lung tissues in which they are retained, and the period of time they are retained. Inhalation of radon, or more specifically radon progeny, leads to the retention of radioactive atoms on the mucus layer covering the respiratory system, especially in the bronchial region of the lung. The short-lived radon progeny, which consist of various isotopes of polonium, lead, and bismuth, emit high-energy alpha particles and irradiate the cells of the lung tissue. These irradiated cells may become cancerous. The rate of lung cancer induction depends on the rate of retention of the radon progeny atoms in various parts of the lungs. This, in turn, depends on many factors, including the concentrations of radon and its progeny in the air, the fraction of the progeny that attach to dust particles, the sizes of the dust particles, and the breathing rate. Given data for these factors and an adequate model of the lungs' dynamics, it is possible to calculate the radiation dose. A number of complicated lung models have been developed to calculate the dose from inhalation of radon and its progeny (ICRP 1979, 1980, 1981, 1982; Jacobi and Eisfeld 1980; James et al. 1980; Harley and Pasternack 1982). Although calculated results from these models are not in complete agreement, they are close enough to permit reasonably good estimates of the radiation dose to the lung from radon and its progeny (National Research Council 1988).
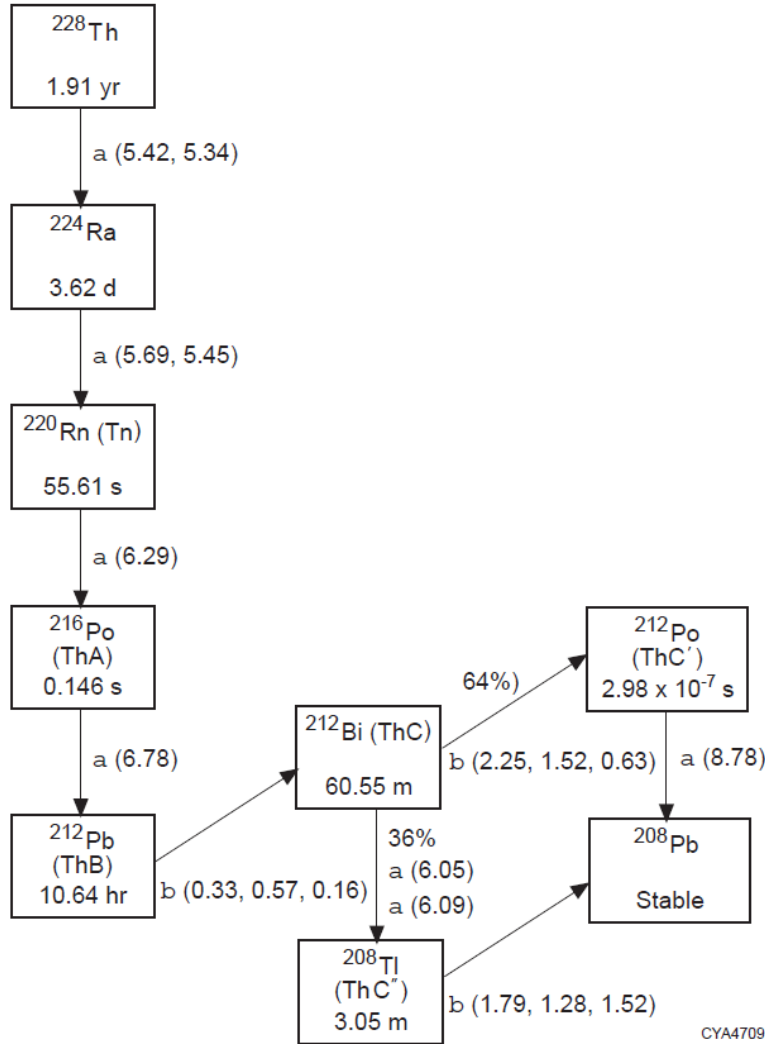
Figure D-3   Decay Scheme of Rn-220 (including its long-lived parent Th-228) (Source: Kocher 1981)

D.4.1   Working Levels

The working level (WL) was first introduced in 1957 (Holaday et al. 1957) as a convenient one-parameter measure of the concentration of radon decay products in uranium mine air that can be used as a measure of exposure. Since then, WL has become a convention for measuring the concentration of radon progeny. The WL is defined as any combination of short-lived radon progeny in 1 L of air that results in the ultimate release of 1.3×10^5 MeV of potential alpha energy. Only the short-lived progeny are included in the definition of the WL because they contribute most of the dose to the lungs. The dose due to radon itself is minimal. For the same amount of activity inhaled, the Rn-222 progeny mixture would result in a dose about 40 to 100 times higher than the dose from Rn-222 alone, and the Rn-220 progeny mixture (Pb-212 and Bi-212) would result in a dose about 60 to 400 times higher than that from Rn-220 alone (ICRP 1981). Based on the definition of WL and when alpha energy is used for the different Rn-222 progeny, the WL value for an atmosphere containing a mixture of radon progeny can be evaluated as follows:

$$WL_{Rn-222} = 1.03 \times 10^{-6}A + 5.07 \times 10^{-6}B + 3.73 \times 10^{-6}C \tag{D.24}$$

where *A*, *B*, and *C* represent the individual concentrations of Po-218, Pb-214, and Bi-214, respectively, in units of pCi/m^3. Similarly, for Rn-220 progeny, the WL value can be evaluated as follows:

$$WL_{Rn-220} = 9.48 \times 10^{-10}A' + 1.23 \times 10^{-4}B' + 1.17 \times 10^{-5}C' \tag{D.25}$$

where *A'*, *B'*, and *C'* represent the individual concentrations of Po-216, Pb-212, and Bi-212, respectively, in units of pCi/m^3.

RESRAD-OFFSITE uses Equations (D.24) and (D.25) to calculate the WL for Rn-222 and Rn-220, respectively. To calculate WLs using these equations, the radon progeny concentrations in the air must be determined first.

D.4.2 Working Level Months

In RESRAD-OFFSITE, the radiation dose from radon and its progeny is calculated using the accumulated exposure in terms of working level month (WLM). WLM is a cumulative exposure unit historically applied to uranium miners and now defined as the product of WL and the duration of exposure, normalized to a 170-hour working month exposure (ICRP 1981, 1986). This unit was introduced so that both the duration and level of exposure could be taken into account.

D.4.3 WLM to Radiation Dose Conversion

To convert WLM or the total cumulative potential alpha energy of radon progeny deposited in the lungs to the CEDE, the ICRP recommendation was adopted in RESRAD-OFFSITE. According to ICRP Publications 32 and 47 (ICRP 1981, 1986), for workers in uranium and other mines, the recommended dosimetric conversion factors are 10 mSv/WLM (1,000 mrem/WLM) for Rn-222 progeny and 3.5 mSv/WLM (350 mrem/WLM) for Rn-220 progeny. Because the exposure for the general population is continuous and this group's breathing rate is lower and shallower than that of miners, the conversion factors for workers must be adjusted for the general population. For the adjustment, the National Research Council introduced a proportional factor *K* in its Biological Effects of Ionizing Radiations (BEIR) IV report (National Research Council 1988) and derived its value for different bronchial cells and different sex and age groups in a later study (National Research Council 1991). Table D-1 presents the *K* factors derived by the National Research Council. For the range of exposure scenarios as well as sex and age groups considered, most values of *K* were less than unity. Thus, it can be concluded that the delivered bronchial dose per WLM exposure is less for the general population in a home than for workers in a mine.

The conversion of WLM to radiation dose in RESRAD-OFFSITE depends on the internal dose conversion factors selected for use in calculations, as shown in Table D-2. The following considerations determine the conversion factors used when the ICRP Publication 26 methodology-based DCFs are selected: (1) To be consistent with the ICRP dosimetric model for the reference man approach, a *K* factor of 0.76 is used for Rn-222 progeny indoors. (2) Ventilation in an outdoor environment is higher than in an indoor environment (i.e., the effect of wind); the unattached fraction is higher (15% outdoors versus 8% indoors); the particle size is larger (0.25 µm in activity median aerodynamic diameter (AMAD) outdoors versus 0.15 µm AMAD indoors), and the breathing rate is higher (21 L/min outdoors versus 12.5 L/min indoors),

and thereby a *K* factor of 0.57 is used for Rn-222 progeny outdoors. (3) The ratio of the inhalation rate for miners to the inhalation rate for an average person in a home (30 versus 12.5 L/min) is more appropriate for converting indoor Rn-220 exposure, because the dose from Rn-220 progeny is determined principally by the behavior of Pb-212; for Pb-212 that is inhaled, a considerable fraction is transferred to blood and other organs or tissues, which renders the *K* factor (derived solely for the lung dose) inappropriate for use to estimate the radiation dose. (4) The ratio of the inhalation rate for miners to the inhalation rate for an average person outdoors (30 versus 21 L/min) is used to approximate the outdoor Rn-220 exposure to a radiation dose.

Table D-1   Summary of K Factors for Bronchial Dose Calculated for the General Public Relative to Underground Miners

	K Factor	
Subject Category	Basal Cells	Secretory Cells
Infant, age 1 mo.	0.64	0.74
Child, age 1 yr	0.87	1.00
Child, age 5–10 yr	0.72	0.83
Female	0.62	0.72
Male	0.69	0.76

Source: National Research Council (1991).

Table D-2   Radiation Dose Conversion Factors Used for Radon Exposures in RESRAD-OFFSITE

Radon Isotope	ICRP-26-Based DCFs		ICRP-60-Based DCFs
	Indoor (mrem/WLM)	Outdoor (mrem/WLM)	Indoor and Outdoor (mrem/WLM)
Rn-222	760	570	388
Rn-220	150	250	188

When the ICRP Publication 60 methodology-based DCFs are selected for use in RESRAD-OFFSITE calculations, the conversion factors are 388 mrem/WLM for Rn-222 exposures and 188 mrem/WLM for Rn-220 exposures. The conversion of Rn-222 exposure is based on epidemiological determinations, by dividing the nominal mortality probability coefficient of 8×10^{-5}/(mJ/m^3 ×h) where the denominator refers to the equilibrium equivalent concentration (EEC) of the radon progeny, by the coefficient of 7.3×10^{-5}/mSv relating the detriment per unit effective dose for the public (ICRP 1991), which results in 1.10 mSv/(mJ/m^3 × h) or 388 mrem/WLM

(ICRP 1993). This conversion factor corresponds to 6 nSv/(Bq/m^3 × h) and is different by a factor of 2.5 from the central value [15 nSv/(Bq/m^3 × h)] derived using the dosimetric approach (UNSCEAR 2000). According to UNSCEAR (2000), Annex B, updated and additional epidemiological studies performed after the calculations made in ICRP (1993) suggest an increased radon risk per unit exposure. Therefore, an increase in the epidemiologically based dose conversion factor is anticipated. As such, UNSCEAR (2000) believes that the dose conversion factor of 9 nSv/(Bq/m^3 × h), equivalent to 582 mrem/WLM), which was calculated in previous reports (UNSCEAR 1988, 1993), is still appropriate.

There are no epidemiological data for lung cancer risk from Rn-220 exposures; therefore, it is impossible to derive an epidemiologically based dose conversion factor. UNSCEAR (2000) believes that the value of 40 nSv/(Bq/m^3 × h), based on the equilibrium equivalent concentration of thoron, is appropriate for evaluating the exposures to Rn-220 both indoors and outdoors; this corresponds to 188 mrem/WLM as used in RESRAD-OFFSITE calculations.

D.5   **Cancer Risk for Radon Exposures**

Potential cancer risk associated with the radon exposure pathway is evaluated by RESRAD-OFFSITE in the same way as that associated with the inhalation exposure pathway: by using the indoor and outdoor radon and radon progeny concentrations, the time spent indoors and outdoors, the exposure duration, and the slope factors for radon and radon progeny.

D.6   **References**

Bodansky, D., M.A. Robinson, and D.R. Stadler, 1987, *Indoor Radon and Its Hazards*, University of Washington Press, Seattle, Washington.

Cohen, B.L., 1991, "Variation of Radon Levels in U.S. Homes Correlated with House Characteristics, Location, and Socioeconomic Factors," *Health Physics* 60:631–642.

EPA (U.S. Environmental Protection Agency), 1984, *Risk Analysis of TCDD Contaminated Soil*, EPA 60018-84-03, Office of Health and the Environmental Assessment, Washington, D.C.

Harley, N.H., and B.S. Pasternack, 1982, "Environmental Radon Daughter Alpha Factors in Five-Lobed Human Lung," *Health Physics* 42:789–799.

Holaday, D.A., D.E. Rushing, R.D. Coleman, P.F. Woolrich, H.L. Kusnetz, W.F. Bale, 1957, *Control of Radon and Daughters in Uranium Mines and Calculations of Biological Effects*, U.S. Public Health Service Publication No. 494, U.S. Government Printing Office, Washington, D.C.

ICRP (International Commission on Radiological Protection), 1979, *Limits for Intakes of Radionuclides by Workers*, ICRP Publication 30, Part 1, a report of Committee 2 of the International Commission on Radiological Protection, adopted by the Commission in July 1978, Annals of the ICRP, Pergamon Press, New York, N.Y.

ICRP, 1980, *Limits for Intakes of Radionuclides by Workers*, ICRP Publication 30, Part 2, a report of Committee 2 of the International Commission on Radiological Protection, adopted by the Commission in July 1978, Annals of the ICRP, Pergamon Press, New York, N.Y.

ICRP, 1981, *Limits for Intakes of Radionuclides by Workers*, ICRP Publication 30, Part 3, a report of Committee 2 of the International Commission on Radiological Protection, adopted by the Commission in July 1978, Annals of the ICRP, Pergamon Press, New York, N.Y.

ICRP, 1982, *Limits for Intakes of Radionuclides by Workers*, ICRP Publication 30, Index, Annals of the ICRP, Pergamon Press, New York, N.Y.

ICRP, 1981, *Limits for Inhalation of Radon Daughters by Workers*, Publication 32, Annals of the ICRP, Vol. 6, No. 1, Pergamon Press, New York, N.Y.

ICRP, 1986, *Radiation Protection of Workers in Mines*, Annals of the ICRP, Publication 47, Vol. 16, No. 1, Pergamon Press, New York, N.Y.

ICRP, 1991, *1990 Recommendations of the International Commission on Radiological Protection.* Annals of the ICRP 21(1-3). Publication 60. Pergamon Press, Oxford.

ICRP, 1993, *Protection against Radon-222 at Home and at Work.* Annals of the ICRP 22(2). Publication 65. Pergamon Press, Oxford.

Jacobi, W., and K. Eisfeld, 1980, *Dose to Tissue and Effective Dose Equivalent by Inhalations of Radon-222 and Their Short-Lived Daughters*, GSF Report S-626, Geschelscheft Fur Strahlen and Umwelfforschung, Neurherberg, Germany.

James, A.C., J.R. Greenhalgh, and A. Birchall, 1980, "A Domestic Model for Tissues of the Human Respiratory Tract at Risk from Inhaled Radon and Thoron Daughters," pp. 1045–1048 in *Radiation Protection. A Systematic Approach to Safety*, in Proc. 5th Congress of the International Radiation Protection Association (IRPA), Vol. 2, Jerusalem, Pergamon Press, New York, N.Y.

Knutson, E.O., A.C. George, J.J. Frey, and B.R. Koh, 1983, "Radon Daughter Plateout-II, Prediction Model," *Health Physics* 45:445.

Kocher, D.C., 1981, *Radioactive Decay Data Tables: A Handbook of Decay Data for Application to Radiation Dosimetry and Radiological Assessments*, DOE/TIC-11026, U.S. Department of Energy, Washington, D.C.

Lawrence, E.P., R.B. Wanty, and P. Nyberg, 1992, "Contribution of ^{222}Rn in Domestic Water Supplies to 222Rn in Indoor Air in Colorado Homes," *Health Physics* 62:171–177.

Mueller Associates, Inc., 1986, *Indoor Air Quality Environmental Information Handbook: Radon,* DOE/PE/72013-2, prepared by Mueller Associates, Inc., Baltimore, Maryland, for U.S. Department of Energy, Washington, D.C.

National Research Council, 1988, *Health Risks of Radon and Other Internally Deposited Alpha-Emitters*, BEIR IV, Committee on the Biological Effects of Ionizing Radiations, National Academy Press, Washington, D.C.

National Research Council, 1991, *Comparative Dosimetry of Radon in Mines and Homes*, National Academy Press, Washington, D.C.

Nazaroff, W.W., and A.V. Nero (eds.), 1988, *Radon and Its Decay Products in Indoor Air*, John Wiley & Sons, New York, N.Y.

Rogers, V.C., and K.K. Nielson, 1991, "Correlations for Predicting Air Permeabilities and Rn-222 Diffusion Coefficients of Soils," *Health Physics* 61:225–2300.

UNSCEAR (United Nations Scientific Committee on the Effects of Atomic Radiation), 1988, *UNSCEAR 1988 Report to the General Assembly*, with annexes, United Nations sales publication E.88.IX.7, United Nations, New York.

UNSCEAR, 1993, *UNSCEAR 1993 Report to the General Assembly*, with scientific annexes, United Nations sales publication E.94.IX.2, United Nations, New York.

UNSCEAR, 2000, *UNSCEAR 2000 Report to the General Assembly*, with annexes, United Nations sales publication E.88.IX.7, United Nations, New York.

U.S. Nuclear Regulatory Commission, 1980, *Final Generic Environmental Impact Statement on Uranium Milling*, NUREG-0706, Washington, D.C.

Yu, C., A.J. Zielen, J.-J. Cheng, D.J. LePoire, E. Gnanapragasam, S. Kamboj, J. Arnish, A. Wallo III, W.A. Williams, and H. Peterson, 2001, *User's Manual for RESRAD Version 6*, ANL/EAD-4, Environmental Assessment Division, Argonne National Laboratory, Lemont, Illinois.

Yu, C., S. Kamboj, C. Wang, and J.-J. Cheng, 2015, *Data Collection Handbook to Support Modeling Impacts of Radioactive Material in Soil and Building Structures*, ANL/EVS/TM-14/4, Environmental Science Division, Argonne National Laboratory, Lemont, Illinois.

Yuan, Y.C., and C.J. Roberts, 1981, "Numerical Investigation of Radon Transport through a Porous Medium," *Transactions of the American Nuclear Society* 38:108–110.

APPENDIX E:
EXPOSURE FROM INGESTION

The releases from and the concentrations in the primary contamination, the transfers across the boundaries between environmental media and between different zones within a medium, the concentrations in the media, the radiological dose and the excess cancer risk are all computed at a sequence of times distributed over the time horizon. These times are referred to as the calculation times. The dose and the risk output from the code are time-integrated values, not instantaneous rates. The relationships between these times are discussed in Section E.1. The time integration is described in Section E.2.

The instantaneous rate of dose or risk from internal exposure is the product of the rate of intake of radionuclides and the dose coefficient or the slope factor (Section E.5). The rate of intake of the radionuclide from ingesting a contaminated food or drink is the product of the rate of ingestion of the food or drink and the concentration of the radionuclide in the food or drink at the time of ingestion. The food or drink are not always consumed immediately upon harvest or extraction. They are typically stored for a period before they are ingested. The code models the radiological transformations that take place during the period of storage, as described in Section E.3.

The dose coefficients and the slope factors (for risk) for each radionuclide are obtained from the specified library. As mentioned in Section A.1, to reduce the computation time, the code generates all the transformation threads of a radionuclide and condenses the threads with the same sequence of principal radionuclides into a single condensed thread. The internal exposure dose coefficients and the internal exposure slope factors of the associated progeny radionuclides are added to those of their principal parent radionuclide after applying the appropriate branching factors. Section E.4 describes condensing the thread and adding the appropriate fractions of the internal exposure dose coefficients or internal exposure slope factors of the associated progeny to those of their principal parent radionuclide.

The time integrated dose and the time integrated risk due to the progeny that grew from the radiological transformations of a radionuclide that was initially present in the primary contamination are attributed to that parent radionuclide in the deterministic and probabilistic plots. This is described in Section E.6. The time integrated dose and the time integrated risk are reported in two ways in the text report: attributed to the initially present parent as in the case of the plots, or attributed to the progeny that was ingested regardless of progeny's origin.

E.1   Evaluation Time Horizon, Exposure Durations, Calculation Times and Reporting Times

The dose computed by the code is a time integrated quantity and not an instantaneous rate; it is the committed dose due to intake of or the dose from exposure to radionuclides over a period of 1 year.

$$D_{TI}(t) = \int_{t}^{t+1} D_{rate}(\tau)d\tau \qquad\qquad (E.1)$$

where

$D_{TI}(t)$ = time integrated dose due to intake or exposure between time t to $t + 1$, Dose in a year,

$D_{rate}(\tau)$ = instantaneous dose rate due to intake or exposure at time τ, Dose/year.

The risk computed by the code is a time integrated quantity and not an instantaneous rate; it is the risk over a user-specified exposure duration.

$$R_{TI}(t) = \int_{t}^{t+T_{edr}} R_{rate}(\tau)d\tau \tag{E.2}$$

where

$R_{TI}(t)$ = time integrated risk due to intake or exposure between time t to $t + T_{edr}$,

$R_{rate}(\tau)$ = instantaneous risk rate due to intake or exposure at time t,

T_{edr} = time period over which the rate of risk is to be integrated (year).

The code performs all its calculations at a sequence of time points over the evaluation time horizon. The evaluation time horizon is the time period over which the code is to perform calculations.

$$T_{horizon} = T_{report}^{max} + T_{edr} \tag{E.3}$$

where

$T_{horizon}$ = time horizon over which the code is to perform calculations (year),

T_{report}^{max} = largest of the times at which the dose or risk is to be reported in the text report (year),

$T_{edr} \geq 1$ = time period over which the instantaneous rate of risk is to be integrated to determine the time integrated risk (year).

As mentioned in most of the appendices, the code assumes that the releases, the transfers across boundaries, and the concentrations vary linearly between the values computed at the calculation time points. The instantaneous dose rates and risk rates are also assumed to vary linearly between the calculation time points. The number of time points specified must be sufficient to capture the temporal variation, under this assumption of linear variation, of the releases, transfers, and concentrations in order to compute the dose or risk to the desired precision. While the code provides choices of the powers of 2 ranging from 32 to 16384 and also 22000, the user can type in any desired number. The sequence of calculation time points under the linear spacing option, the efficient and strongly suggested spacing option for RESRAD-OFFSITE, is:

$$t_{cl}(l) = \frac{T_{horizon}}{N_{times}} l \tag{E.4}$$

where,

$t_{cl}(l)$ = l^{th} non-zero calculation time (year),

N_{times} = number of calculation time points, excluding 0 year.

E.2   Time Integration

The integration over time is performed numerically utilizing the trapezoidal formula on the rates at the beginning of the time period, at the end of the time period, and the rates at any calculation times that fall between those two times. If the end of the time period does not coincide with a calculation time point, the rate at that time is found by linear interpolation using the rates at the two adjacent calculation time points surrounding that time. If the exposure duration extends beyond the time horizon, the rate at the time horizon is assumed to apply until the end of the exposure duration. This is expressed mathematically by the following equations.

$$Q_{TI}(t) = \sum_{t < t_{cl}(l) < t + t_{ed}} \frac{\{Q_{rate}[t_{cl}(l-1)] + Q_{rate}[t_{cl}(l)]\}[t_{cl}(l) - t_{cl}(l-1)]}{2}$$
$$+ \frac{\{Q_{rate}[t_{cl}(l_{last})] + Q_{rate}(t + t_{ed})\}[t + t_{ed} - t_{cl}(l_{last})]}{2}$$

(E.5)

where,

$\quad Q_{TI}(t)$ = time integrated dose or risk at calculation time t (year),

$\quad Q_{rate}[t_{cl}(l)]$ = instantaneous dose or risk rate at $t_{cl}(l)$,

$\quad t_{ed}$ = time period over which the instantaneous rate is to be integrated (year),

$\quad t_{ed}$ = 1, if the dose rate is being integrated,

$\quad t_{ed}$ = T_{edr}, if the risk rate is being integrated,

$\quad l_{last}$ = largest value of l that satisfies $t_{cl}(l) < t + t_{ed}$,

$\quad Q_{rate}(t + t_{ed})$ = instantaneous rate at the end of the time integration period,

$\quad Q_{rate}(t + t_{ed}) = \frac{Q_{rate}[t_{cl}(l_{last})][t_{cl}(l_{last}+1) - t - t_{ed}] + Q_{rate}[t_{cl}(l_{last}+1)][t + t_{ed} - t_{cl}(l_{last})]}{[t_{cl}(l_{last}+1) - t_{cl}(l_{last})]}$

$\quad\quad$ if $t_{cl}(N_{times}) \geq t + t_{ed}$,

$\quad Q_{rate}(t + t_{ed}) = Q_{rate}[t_{cl}(N_{times})]$, if $t_{cl}(N_{times}) < t + t_{ed}$.

E.3   Concentration in the Media at the Time of Use

The food products including milk, water, and livestock feed are not always consumed immediately upon harvest or extraction. They are typically stored for a period of time before they are ingested. Water extracted for irrigation is assumed to be stored for the same duration as the water extracted for use in the house and to water livestock.

$$t_{harvest}(l) = t_{cl}(l) - t_{storage}$$

(E.6)

where,

$\quad t_{harvest}(l)$ = time of harvest or extraction of the product that is to be consumed at the lth calculation time (year),

$\quad t_{cl}(l)$ = lth calculation time, the time of consumption or use (year),

$\quad t_{storage}$ = time period for which the product is stored after harvest or extraction before it is consumed or used (year).

The code models the radiological transformations that take place in the food during the time period of storage. The harvest time will not necessarily coincide with any of the calculation time points. The concentration in the consumable at the time of harvest is needed to compute the ingrowth and decay over the storage time. In general, in a departure from its assumption of

linear variation of the calculated quantities between calculation time points, the code uses the concentrations at the three calculation times closest to the time of harvest to perform a quadratic interpolation for the concentration at the time of harvest. The first of the three exceptions to the quadratic interpolation is that the concentration at time 0 is used as the harvest time concentration when the harvest time is before 0 years. The other two exceptions are when the harvest time falls either in first half of the time interval from 0 years to the first calculation time or and in the second half of the time interval between the last two calculation times; a linear interpolation is used in both cases.

The ingrowth and decay over the storage time is then computed using the Bateman equations,

$$c_i^{stor}(t) = \sum_{k=1}^{i} B_i^k e^{-\lambda_k t} \tag{E.7}$$

with $B_1^1 = c_1^{harvest}$, $B_j^k = \lambda_j \frac{B_{j-1}^k}{\lambda_j - \lambda_k}$ for all $0 < k < j \le i$, and $B_j^j = c_j^{harvest} - \sum_{k=1}^{j-1} B_j^k$ for all $1 < j \le i$, which is the solution to the equation $\frac{dc_i^{stor}(t)}{dt} + \lambda_i c_i^{stor}(t) = \lambda_i c_{i-1}^{stor}(t)$ with initial conditions of $c_i^{stor}(0) = c_i^{harvest}$.

where

$c_i^{stor}(t)$ = concentration of radionuclide i in the food at time t since harvest or extraction (Activity/kg or Activity/L),

λ_i = transformation constant for radionuclide i (1/year),

B_i^k = represents the dimensionless coefficients,

$c_i^{harvest}$ = concentration of radionuclide i at the time of harvest or extraction (Activity/kg or Activity/L),

i, j, k = radionuclide indices that satisfy the relevant conditions specified above.

E.4   Internal Dose Coefficients and Slope Factors for Principal Radionuclides

As mentioned in Section A.1, the code has two radiological transformations databases, one based on ICRP 107 and the other based on ICRP 38. Regardless of which transformation database is chosen, the code does the following for each radionuclide chosen for analysis:

1. Generates a list of all the transformation threads with the fraction of the chosen radionuclide that transforms according to each thread, termed the thread fraction, and the radionuclides in each transformation thread in order;

2. Uses the specified cutoff half-life to represent each transformation thread using only those radionuclides with half-lives greater than the specified cutoff, termed principal radionuclides in RESRAD-OFFSITE;

3. Combines the threads that are identical in their principal radionuclide representation to form a condensed thread;

4. Assigns the radionuclides with half-lives less than or equal to the cutoff, termed associated radionuclides in RESRAD-OFFSITE, to the principal radionuclide that immediately preceded them, at the appropriate fraction;

5. Computes the dose coefficients and the slope factors for internal exposure for each representation of the principal radionuclide, adding the dose coefficients and slope factors of the associated progeny at the appropriate fraction.

This process is illustrated for three of four progressively more complex examples. The most complex of the four examples is outlined with directions on where to find the information that is not presented here. The file *inputfilename*.CHN contains the information on steps 1 through 4; the dose coefficients and slope factors for the individual radionuclides for step 5 can be viewed in the dose conversion factor Editor (DCF Editor), while the results of step 5 are in the parent dose report and in the risk report.

E.4.1 ^{210}Pb under the ICRP-38 Transformation Database

The ^{210}Pb(22.3y) transforms to ^{210}Bi(0.01372y) which transforms to ^{210}Po(0.3789y) which transforms to the stable isotope ^{206}Pb. When using a 30-day (0.082136y) cutoff half-life with the ICRP-72 (adult) internal exposure library and the FGR-13 morbidity risk library, the five steps above yield:

1. thread 1, fraction = 1.0000, thread ^{210}Pb, ^{210}Bi, ^{210}Po;
2. thread 1, fraction = 1.0000, thread ^{210}Pb, ^{210}Po;
3. condensed thread 1, fraction = 1.0000, condensed thread ^{210}Pb+D, ^{210}Po;
4. ^{210}Pb+D = ^{210}Pb + 1.0000 ^{210}Bi;
5. Dose coefficient, in mSv/Bq, for:
   ingestion 210Pb +D = $6.9\ 10^{-4} + 1.0 \times 1.3\ 10^{-6} = 6.913\ 10^{-4}$,
   inhalation 210Pb +D = $5.6\ 10^{-3} + 1.0 \times 9.3\ 10^{-5} = 5.693\ 10^{-3}$.
   Slope factor, in risk/Bq, for:
   ingestion of food 210Pb +D = $3.189\ 10^{-8} + 1.0 \times 3.514\ 10^{-10} = 3.22\ 10^{-8}$,
   ingestion of water 210Pb +D = $2.381\ 10^{-8} + 1.0 \times 2.411\ 10^{-10} = 2.41\ 10^{-8}$,
   ingestion of soil 210Pb +D = $3.189\ 10^{-8} + 1.0 \times 3.514\ 10^{-10} = 3.22\ 10^{-8}$,
   inhalation ^{210}Pb +D = $4.27\ 10^{-7} + 1.0 \times 1.23\ 10^{-8} = 4.393\ 10^{-7}$.

The dose coefficients and slope factors of the individual radionuclides were read from the dose factor editor. The composite dose coefficients and slope factors for the principal radionuclides with the associated progeny are from the text reports. The dose factor editor displays the data to a lower precision than to which it transfers the data to the interface. This accounts for the difference in the least significant digits that are computed from the expression above and the results shown, which are from the text reports.

E.4.2 ^{210}Pb under the ICRP-107 Transformation Database

1.9 10^{-8} of the ^{210}Pb(22.2y) transforms to ^{206}Hg(1.55 10^{-5} y) while the remainder transforms to ^{210}Bi(0.01372y). 1.32 10^{-6} of the ^{210}Bi transforms to ^{206}Tl(7.985 10^{-6} y) while the remainder transforms to ^{210}Po(0.3789y). All of the ^{206}Hg transforms to ^{206}Tl. All of the ^{206}Tl transforms to stable isotope ^{206}Pb. All of the ^{210}Po transforms to the stable isotope ^{206}Pb. When using a 30-day (0.082136y) cutoff half-life with the DCFPAK3.02 (adult) internal exposure library and the DCFPAK3.02 morbidity risk library, the five steps above yield:

1. thread 1, fraction = 1.0000, ^{210}Pb, ^{210}Bi, ^{210}Po,
   thread 2, fraction = 1.32 10^{-6}, ^{210}Pb, ^{210}Bi, ^{206}Tl,
   thread 3, fraction = 1.9 10^{-8}, ^{210}Pb, ^{206}Hg, ^{206}Tl;

2. thread 1, fraction = 1.0000, ^{210}Pb, ^{210}Po,
   thread 2, fraction = 1.32 10^{-6}, ^{210}Pb,
   thread 3, fraction = 1.9 10^{-8}, ^{210}Pb;

3. condensed thread 1, fraction = 1.0000, ^{210}Pb+D, ^{210}Po,
   condensed thread 2, fraction = 1.339 10^{-6}, ^{210}Pb+D1;

4. ^{210}Pb+D = ^{210}Pb + 1.0000 ^{210}Bi,
   ^{210}Pb+D1 = ^{210}Pb + 1.32/1.339 ^{210}Bi + 0.019/1.339 ^{206}Hg + 1.0000 ^{206}Tl;

5. Dose coefficient, in mSv/Bq, for:
   ingestion ^{210}Pb +D = 6.96 10^{-4} + 1.0 × 1.31 10^{-6} = 6.973 10^{-4},
   ingestion ^{210}Pb +D1 = 6.96 10^{-4} + 0.98581 × 1.31 10^{-6} + 0.01419 × 0 + 1.0 × 0 = 6.972 10^{-4},
   inhalation ^{210}Pb +D = 5.614 10^{-3} + 1.0 × 1.33 10^{-4} = 5.746 10^{-3},
   inhalation ^{210}Pb +D1 = 5.614 10^{-3} + 0.98581 × 1.33 10^{-4} + 0.01419 × 0 + 1.0 × 0 = 5.745 10^{-3}.
   Slope factor, in risk/Bq, for:
   ingestion of food ^{210}Pb +D = 3.178 10^{-8} + 1.0 × 3.519 10^{-10} = 3.21 10^{-8},
   ingestion of food ^{210}Pb +D1 = 3.178 10^{-8} + 0.98581 × 3.519 10^{-10} + 0.01419 × 0 + 1.0 × 0 = 3.21 10^{-8};
   ingestion of water ^{210}Pb +D = 2.39 10^{-8} + 1.0 × 2.41 10^{-10} = 2.41 10^{-8},
   ingestion of water ^{210}Pb +D1 = 2.39 10^{-8} + 0.98581 × 2.41 10^{-10} + 0.01419 × 0 + 1.0 × 0 = 2.41 10^{-8};
   ingestion of soil ^{210}Pb +D = 3.178 10^{-8} + 1.0 × 3.519 10^{-10} = 3.21 10^{-8},
   ingestion of soil ^{210}Pb +D1 = 3.178 10^{-8} + 0.98581 × 3.519 10^{-10} + 0.01419 × 0 + 1.0 × 0 = 3.21 10^{-8};
   inhalation ^{210}Pb +D = 4.289 10^{-7} + 1.0 × 1.23 10^{-8} = 4.41 10^{-7};
   inhalation ^{210}Pb +D1 = 4.289 10^{-7} + 0.98581 × 1.23 10^{-8} + 0.01419 × 0 + 1.0 × 0 = 4.41 10^{-7}.

The dose coefficients and slope factors of the individual radionuclides were read from the dose factor editor. The composite dose coefficients and slope factors for the principal radionuclides with the associated progeny are from the text reports. The dose factor editor displays the data to a lower precision than at which it transfers the data to the interface. This accounts for the difference in the least significant figures that are computed from the expression above and the results shown, which are from the text reports.

While the preceding two examples illustrate the process of condensing the threads and determining the appropriate fractions of the progeny associated with their principal radionuclide, they do not illustrate the significant reduction in the number of threads and the consequent reduction in the run time due to the condensing of the threads; the next two example do.

E.4.3 ^{227}Ac under the ICRP-107 Transformation Database

The transformation scheme for ^{227}Ac is shown in Figure E-1. When using a 30-day (0.082136y) cutoff half-life with the DCFPAK3.02 (adult) internal exposure library and the DCFPAK3.02 morbidity risk library, the five steps above condense the six thread to one. As seen in step 5, the short-lived progeny make an appreciable contribution to the dose and risk from ^{227}Ac.

1. T# 1, f = 9.8348 10^{-1} ^{227}Ac, ^{227}Th, ^{223}Ra, ^{219}Rn, ^{215}Po, ^{211}Pb, ^{211}Bi, ^{207}Tl,
   T# 2, f = 2.7219 10^{-3} ^{227}Ac, ^{227}Th, ^{223}Ra, ^{219}Rn, ^{215}Po, ^{211}Pb, ^{211}Bi, ^{211}Po,
   T# 3, f = 1.3761 10^{-2} ^{227}Ac, ^{223}Fr, ^{223}Ra, ^{219}Rn, ^{215}Po, ^{211}Pb, ^{211}Bi, ^{207}Tl,
   T# 4, f = 3.8086 10^{-5} ^{227}Ac, ^{223}Fr, ^{223}Ra, ^{219}Rn, ^{215}Po, ^{211}Pb, ^{211}Bi, ^{211}Po,
   T# 5, f = 8.2571 10^{-7} ^{227}Ac, ^{223}Fr, ^{219}At, ^{215}Bi, ^{215}Po, ^{211}Pb, ^{211}Bi, ^{207}Tl,
   T# 6, f = 2.2853 10^{-9} ^{227}Ac, ^{223}Fr, ^{219}At, ^{215}Bi, ^{215}Po, ^{211}Pb, ^{211}Bi, ^{211}Po;

2. T# 1, f = 9.8348 10^{-1} ^{227}Ac,
   T# 2, f = 2.7219 10^{-3} ^{227}Ac,
   T# 3, f = 1.3761 10^{-2} ^{227}Ac,
   T# 4, f = 3.8086 10^{-5} ^{227}Ac,
   T# 5, f = 8.2571 10^{-7} ^{227}Ac,
   T# 6, f = 2.2853 10^{-9} ^{227}Ac;

3. condensed thread 1, fraction = 1.0000, ^{227}Ac+D;

4. ^{227}Ac+D = ^{227}Ac + 9.8620 10^{-1} ^{227}Th + ^{223}Ra + ^{219}Rn + ^{215}Po + ^{211}Pb + ^{211}Bi + 9.9724 10^{-1} ^{207}Tl + 2.7600 10^{-3} ^{211}Po + 1.3800 10^{-2} ^{223}Fr + 8.2800 10^{-7} ^{219}At + 8.2800 10^{-7} ^{215}Bi;

5. Dose coefficient, in mSv/Bq, for:
   ingestion ^{227}Ac+D = $3.22\ 10^{-4} + 9.8620\ 10^{-1} \times 9.11\ 10^{-6} + 1.03\ 10^{-4} + 0 + 0 + 1.78\ 10^{-7} + 0 + 9.9724\ 10^{-1} \times 0 + 2.76\ 10^{-3} \times 0 + 1.38\ 10^{-2} \times 2.38\ 10^{-6} + 8.28\ 10^{-7} \times 0 + 8.28\ 10^{-7} \times 0 = 4.341\ 10^{-4}$,
   inhalation ^{227}Ac+D $1.557\ 10^{-1} + 9.8620\ 10^{-1} \times 1.036\ 10^{-2} + 8.662\ 10^{-3} + 0 + 0 + 1.202\ 10^{-5} + 0 + 9.9724\ 10^{-1} \times 0 + 2.76\ 10^{-3} \times 0 + 1.38\ 10^{-2} \times 1.214\ 10^{-5} + 8.28\ 10^{-7} \times 0 + 8.28\ 10^{-7} \times 0 = 1.746\ 10^{-1}$.
   Slope factor, in risk/Bq for:
   ingestion of food ^{227}Ac+D = $6.63\ 10^{-9} + 9.8620\ 10^{-1} \times 1.9\ 10^{-9} + 9.149\ 10^{-9} + 0 + 0 + 1.57\ 10^{-11} + 0 + 9.9724\ 10^{-1} \times 0 + 2.76\ 10^{-3} \times 0 + 1.38\ 10^{-2} \times 2.73\ 10^{-10} + 8.28\ 10^{-7} \times 0 + 8.28\ 10^{-7} \times 0 = 1.77\ 10^{-8}$,
   ingestion of water $5.43\ 10^{-9} + 9.8620\ 10^{-1} \times 1.3\ 10^{-9} + 6.441\ 10^{-9} + 0 + 0 + 1.11\ 10^{-11} + 0 + 9.9724\ 10^{-1} \times 0 + 2.76\ 10^{-3} \times 0 + 1.38\ 10^{-2} \times 1.99\ 10^{-10} + 8.28\ 10^{-7} \times 0 + 8.28\ 10^{-7} \times 0 = 1.32\ 10^{-8}$,
   ingestion of soil ^{227}Ac+D = $6.63\ 10^{-9} + 9.8620\ 10^{-1} \times 1.9\ 10^{-9} + 9.149\ 10^{-9} + 0 + 0 + 1.57\ 10^{-11} + 0 + 9.9724\ 10^{-1} \times 0 + 2.76\ 10^{-3} \times 0 + 1.38\ 10^{-2} \times 2.73\ 10^{-10} + 8.28\ 10^{-7} \times 0 + 8.28\ 10^{-7} \times 0 = 1.77\ 10^{-8}$,
   inhalation ^{227}Ac+D = $4.041\ 10^{-6} + 9.8620\ 10^{-1} \times 9.459\ 10^{-7} + 7.889\ 10^{-7} + 0 + 0 + 1.09\ 10^{-9} + 0 + 9.9724\ 10^{-1} \times 0 + 2.76\ 10^{-3} \times 0 + 1.38\ 10^{-2} \times 1.1\ 10^{-9} + 8.28\ 10^{-7} \times 0 + 8.28\ 10^{-7} \times 0 = 5.76\ 10^{-6}$.
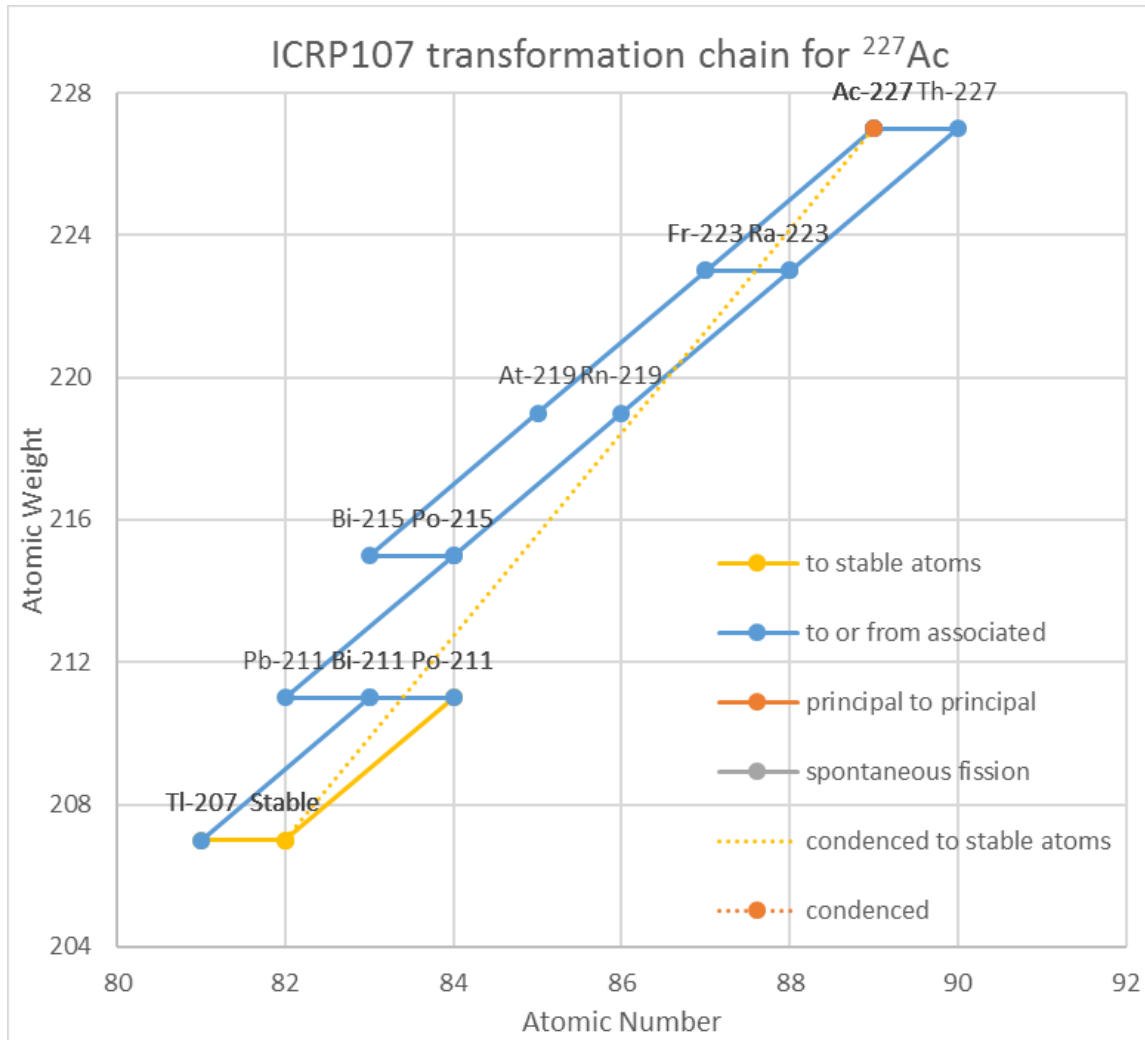
Figure E-1   ICRP-107 Transformation Chain for ^{227}Ac for Cutoff Half-Life of 30 Days

E.4.4 ^{226}Ra under the ICRP-107 Transformation Database

The transformation scheme for ^{226}Ra is shown in Figure E-2. The *inputfilename*.CHN file that is produced by the code in the same directory as the input file, *inputfilename*.ROF, has 15 threads for ^{226}Ra when using a 30-day (0.082136y) cutoff half-life with the ICRP-107 transformation data. That file also shows that these 15 threads are condensed to two (2) threads. The two threads are ^{226}Ra+D, ^{210}Pb+D, ^{210}Po, with a thread fraction of 1 and ^{226}Ra+D, ^{210}Pb+D1 with a thread fraction of 1.339 10^{-6}. The dose coefficients and slope factors for the individual radionuclides for step 5 can be viewed in the dose Conversion Factor Editor (DCF Editor), while the results of step 5 are in the parent dose report and the risk report.
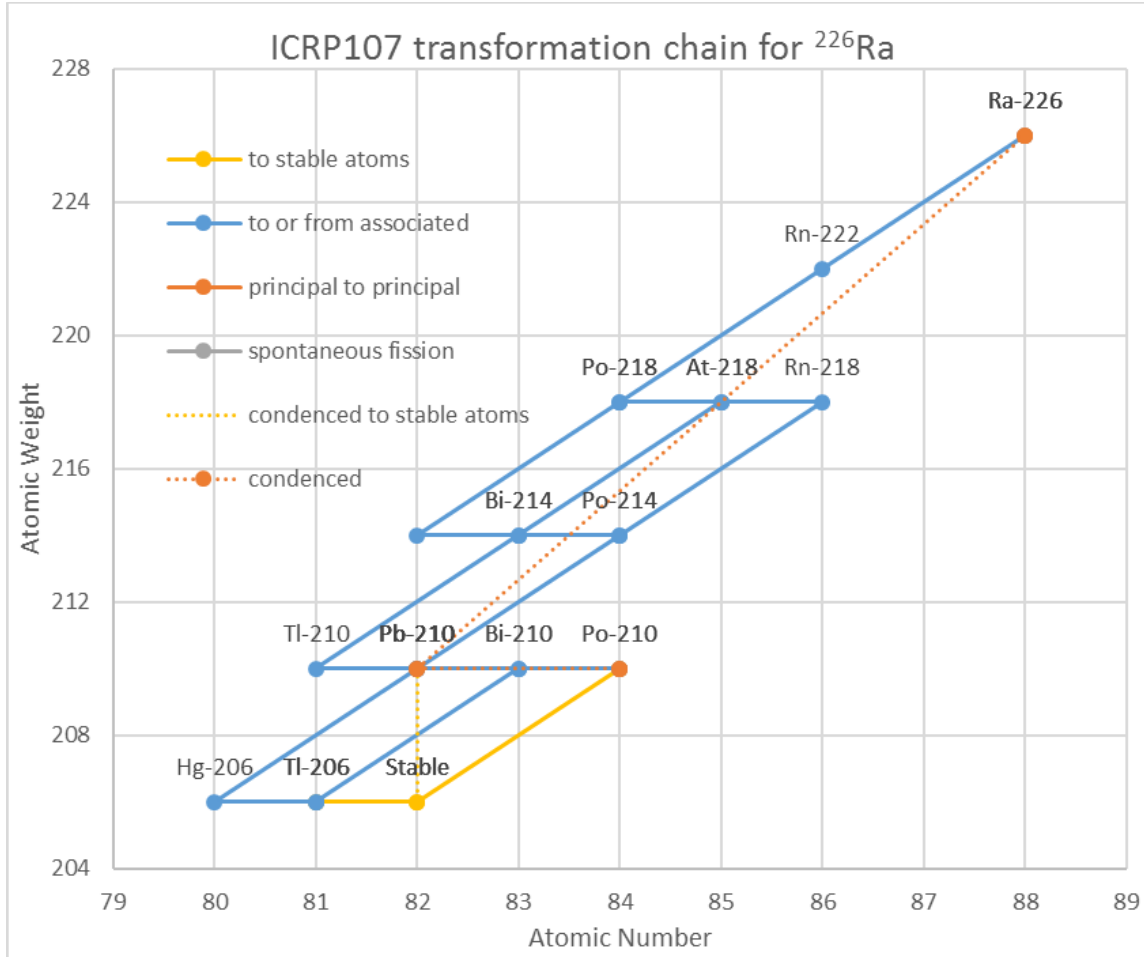
Figure E-2   ICRP-107 Transformation Chain for ^{226}Ra for Cutoff Half-Life of 30 Days

E.5   Instantaneous Dose Rate and the Instantaneous Excess Cancer Risk Rate

The instantaneous dose rate due to the ingestion of food and drink are the product of the dose factor for ingestion and the rate of intake of the radionuclide.

The instantaneous dose rate from the ingestion of vegetables is computed using the expression

$$D_{rate_{i,m}}^{p}(t) = DC_{i,m}^{ing} \sum_{vegetables} f_p R_{ing}^p p_{i,m}(t)$$

(E.8)

where

$D_{rate_{i,m}}^{p}(t)$ = instantaneous dose rate due to ingestion of vegetables containing radionuclide i in thread m of initially present radionuclide pa at time t (Dose/year),

$DC_{i,m}^{ing}$ = dose coefficient for ingestion, of the principal radionuclide i in thread m of initially present radionuclide pa and the appropriate fractions of the dose coefficients of the associated progeny (Dose/Activity),

$$f_p \quad = \quad \text{fraction of vegetables from the site that are consumed by the individual,}$$

R^p_{ing} = rate of ingestion of vegetables consumed by the individual (kg/year),

$p_{i,m}(t)$ = concentration of radionuclide i, in thread m of initially present radionuclide pa, in the vegetables from the site consumed at time t (Activity/kg).

The instantaneous excess cancer risk rate from the ingestion of vegetables is computed using the expression

$$R^p_{rate\,i,m}(t) = SF^{i,f}_{i,m} \sum_{vegetables} f_p R^p_{ing} p_{i,m}(t) \tag{E.9}$$

where

$R^p_{rate\,i,m}(t)$ = instantaneous excess cancer risk rate due to ingestion of vegetables containing radionuclide i, in thread m of initially present radionuclide pa, at time t (1/year),

$SF^{i,f}_{i,m}$ = excess cancer slope factor for the ingestion of food, of the principal radionuclide i, in thread m of initially present radionuclide pa, and the appropriate fractions of the slope factors of the associated progeny (1/Activity).

Similarly, the instantaneous dose rate from the ingestion of meat or milk is computed using the expression

$$D^m_{rate\,i,m}(t) = DC^{ing}_{i,m} f_m R^m_{ing} m_{i,m}(t) \tag{E.10}$$

where

$D^m_{rate\,i,m}(t)$ = instantaneous dose rate due to ingestion of meat or milk containing radionuclide i, in thread m of initially present radionuclide pa, at time t (Dose/year),

f_m = fraction of meat or milk from the site that is consumed by the individual,

R^m_{ing} = rate of ingestion of meat or milk by the individual (kg/year or L/year),

$m_{i,m}(t)$ = concentration of radionuclide i, in thread m of initially present radionuclide pa, in the meat or in the milk from the site consumed at time t (Activity/kg or Activity/L).

Similarly, the instantaneous excess cancer risk rate from the ingestion of meat and milk is computed using the expression

$$R^m_{rate\,i,m}(t) = SF^{i,f}_{i,m} f_m R^m_{ing} m_{i,m}(t) \tag{E.11}$$

where

$R^m_{rate\,i,m}(t)$ = instantaneous excess cancer risk rate due to ingestion of meat or milk containing radionuclide i, in thread m of initially present radionuclide pa, at time t (1/year).

Likewise, the instantaneous dose rate from the ingestion of aquatic food is computed using the expression

$$D^{aqf}_{rate\,i,m}(t) = DC^{ing}_{i,m} \sum_{aquatic\,foods} f_{aqf} R^{aqf}_{ing} aqf_{i,m}(t)$$

(E.12)

where

$D^{aqf}_{rate\,i,m}(t)$ = instantaneous dose rate due to ingestion of aquatic food containing radionuclide i, in thread m of initially present radionuclide pa, at time t (Dose/year),

f_{aqf} = fraction of aquatic food from the site that is consumed by the individual,

R^{aqf}_{ing} = rate of ingestion of aquatic food by the individual (kg/year),

$aqf_{i,m}(t)$ = concentration of radionuclide i, in thread m of initially present radionuclide pa, in the aquatic food from the site consumed at time t (Activity/kg).

Likewise, the instantaneous excess cancer risk rate from the ingestion of aquatic food is computed using the expression

$$R^{aqf}_{rate\,i,m}(t) = SF^{i,f}_{i,m} \sum_{aquatic\,foods} f_{aqf} R^{aqf}_{ing} aqf_{i,m}(t)$$

E.13

where

$R^{aqf}_{rate\,i,m}(t)$ = instantaneous excess cancer risk rate due to ingestion of aquatic food containing radionuclide i, in thread m of initially present radionuclide pa, at time t (1/year).

The instantaneous dose rate from the ingestion of water is computed using the expression,

$$D^{w}_{rate\,i,m}(t) = DC^{ing}_{i,m} R^{w}_{ing} \left[f^{w}_{w} ww_{i,m}(t) + f^{s}_{w} sw_{i,m}(t) \right]$$

(E.14)

where

$D^{w}_{rate\,i,m}(t)$ = instantaneous dose rate due to ingestion of water containing radionuclide i, in thread m of initially present radionuclide pa, at time t (Dose/year),

R^{w}_{ing} = rate of ingestion of water by the individual (L/year),

f^{w}_{w} = fraction of water consumed by the individual that is from the well at the site,

$ww_{i,m}(t)$ = concentration of radionuclide i, in thread m of initially present radionuclide pa, in the water from the well at the site consumed at time t (Activity/L),

f^{s}_{w} = fraction of water consumed by the individual that is from the surface water body at the site,

$sw_{i,m}(t)$ = concentration of radionuclide i, in thread m of initially present radionuclide pa, in the water from the surface water body at the site consumed at time t (Activity/L).

The instantaneous excess cancer risk rate from the ingestion of water is computed using the expression

$$R^w_{rate\,i,m}(t) = SF^{i,w}_{i,m} R^w_{ing} \left[f^w_w ww_{i,m}(t) + f^s_w sw_{i,m}(t) \right] \tag{E.15}$$

where

$R^w_{rate\,i,m}(t)$ = instantaneous excess cancer risk rate due to ingestion of water containing radionuclide i, in thread m of initially present radionuclide pa, at time t (1/year),

$SF^{i,w}_{i,m}$ = excess cancer slope factor for the ingestion of water, of the principal radionuclide i, in thread m of initially present radionuclide pa, and the appropriate fractions of the slope factors of the associated progeny (1/Activity).

The instantaneous dose rate from the incidental ingestion of soil is computed using the expression

$$D^s_{rate\,i,m}(t) = DC^{ing}_{i,m} R^s_{ing} \sum_{receptor\ locations} f_{area} f_{oc} s_{i,m}(t) \tag{E.16}$$

where

$D^s_{rate\,i,m}(t)$ = instantaneous dose rate due to the incidental ingestion of surface soil containing radionuclide i, in thread m of initially present radionuclide pa, at time t (Dose/year),

R^s_{ing} = rate of incidental ingestion of soil by the individual (g/year),

f_{area} = area factor to account for the size of the primary contamination for onsite exposure (Yu et al. 2001). The area factor for offsite locations is 1

f_{oc} = occupancy factor at each receptor location,

$s_{i,m}(t)$ = concentration of radionuclide i, in thread m of initially present radionuclide pa, in the surface soil at the receptor location at time t (Activity/g).

Likewise, the instantaneous excess cancer risk rate from the incidental ingestion of soil is computed using the expression

$$R^s_{rate\,i,m}(t) = SF^{i,s}_{i,m} R^s_{ing} \sum_{receptor\ locations} f_{area} f_{oc} s_{i,m}(t) \tag{E.17}$$

where

$R^{aqf}_{rate\,i,m}(t)$ = instantaneous excess cancer risk rate due to ingestion of aquatic food containing radionuclide i, in thread m of initially present radionuclide pa, at time t (1/year),

$SF^{i,s}_{i,m}$ = excess cancer slope factor for the incidental ingestion of soil, of the principal radionuclide i, in thread m of initially present radionuclide pa, and the appropriate fractions of the slope factors of the associated progeny (1/Activity).

E.6 Dose or Risk Attributed to the Parent Radionuclide that Was Initially Present in the Primary Contamination

The time integrated dose and the time integrated risk due to the progeny that grew from the radiological transformations of a radionuclide that was initially present in the primary contamination are attributed to that parent radionuclide in the deterministic and probabilistic plots. These quantities are determined by summing the time-integrated dose or the time-integrated risk of the radionuclides in all of the threads of the radionuclide that was initially present in the primary contamination:

$$Q_{TI}^{pa}(t) = \sum_{m=1}^{threads_{pa}} \sum_{i=1}^{nuclides_m} Q_{rate_{i,m}}(t) \qquad (E.18)$$

where

$\quad Q_{TI}^{pa}(t)$ = time-integrated dose or risk due to intake between time t and time $t + T_{ed}$ of the initially present radionuclide pa and all of the progeny radionuclides that grew from it (Dose in a year or Risk over the exposure duration),

$\quad T_{ed}$ = time period over which the dose rate or risk rate is integrated (year),

$\quad threads_{pa}$ = number of transformation threads for initially present radionuclide pa,

$\quad nuclides_m$ = number of radionuclides in thread m of initially present radionuclide pa,

$\quad Q_{rate_{i,m}}(t)$ = instantaneous dose rate of radionuclide i, in thread m of initially present radionuclide pa, due to intake or exposure at time t (Dose/year).

It should be noted that there is the option in the deterministic graphics program to view the contribution of each progeny radionuclide to the dose or risk attributed to the parent.

The main text report (the summary report or the parent dose report) has tables of dose, attributed to the initially present parent, at time 0 and at up to nine reporting times. The intake and risk report (risk report) has tables that report risk attributed to the initially present parent, at time 0 and at up to nine reporting times. It also has tables listing the risk attributed to the principal progeny nuclides whose intake led to the risk. The progeny text report has tables of dose, at time 0 and at up to nine reporting times, attributed to the principal progeny whose intake lead to the dose. The next section describes the computation of the dose or risk attributed to the progeny.

E.7 Dose or Risk Attributed to the Principal Progeny Radionuclides

The dose or risk attributed to the principal progeny radionuclide is determined by summing the time integrated dose or the time integrated risk of due to that radionuclide in all of the threads of all the radionuclides that were initially present in the primary contamination:

$$Q_{TI}^{pp}(t) = \sum_{i=1}^{n_{pa}} \sum_{m=1}^{threads_{pa}} Q_{rate_{pp,m}}(t) \qquad (E.19)$$

where

$\quad Q_{TI}^{pp}(t)$ = time-integrated dose or risk due to intake between time t and time $t + T_{ed}$ of the principal radionuclide pp that was derived from all the

radionuclides that were initially present in the primary contamination (Dose in a year or Risk over the exposure duration),

T_{ed} = time period over which the dose rate or risk rate is integrated (year),

n_{pa} = number of radionuclides that were initially present in the primary contamination,

$Q_{rate_{pp,m}}(t)$ = instantaneous dose rate of the principal progeny radionuclide pp, in thread m of initially present radionuclide pa, due to intake or exposure at time t (Dose/year).

E.8   Waterborne Doses and Direct and Airborne Doses

In addition to providing graphical and text output of the grand total dose and the grand total risk as a function of time, the code also outputs the contribution of the initially present radionuclides and the different exposure pathways to these grand totals. The nine exposure pathways modeled by the code are discussed in Section 3.1. Rather than apportioning the grand total between the nine exposure pathways, the code has been apportioning it between fifteen exposure sub-pathways after dividing some of the exposure pathways into two categories.

The components that resulted from the leaching release to infiltration and the erosion release to runoff are eventually carried by water from the well or the surface water body and were reported as waterborne doses or risks in the graphics. These were reported as doses or risks "From releases to ground water and to surface water" in the text report.

The direct exposure from the primary contamination and those components from the release to the air were reported together as direct and airborne doses or risks in the graphics. These were reported as doses or risks "directly from primary contamination and from release to atmosphere" in the text report.

The distinction between these two components of each exposure pathway is blurring as compound transport pathways are added to the code. All inhalation doses (excluding radon) belonged in the airborne category until the code was updated, in Version 3.2, to model the inhalation of resuspended particulates from the secondary contamination. But the accumulation at the offsite locations following irrigation with contaminated water is a mode of secondary contamination. The question then arose as to which category the component from the inhalation of particulates that were resuspended from the secondary contamination resulting from contaminated irrigation belonged. Was it airborne because the resuspended particulates were in air prior to inhalation? Or was it waterborne because it was carried by water? A decision was made to include this in airborne and to avoid creating a new waterborne category for inhalation.

Version 4 of the code includes even more complex transport pathways. Radionuclides can be released to the air and be transported by the atmosphere to the catchment of the surface water body, where they can be deposited as particulates from the air (dry deposition) or washed out of the air (wet deposition); part of the deposited material can be transported to the surface water body by the runoff. Water from the surface water body can then be used to irrigate an agricultural area where the plant can be contaminated by root uptake. It could be airborne because of the atmospheric transport segment; it could be waterborne because of the transport by water from the catchment to the surface water body and then to the agricultural area. This is currently being reported as waterborne to avoid having to create an airborne category during the modeling of the radionuclide concentration in the surface water body.

APPENDIX F:
TRITIUM AND CARBON-14 PATHWAY MODELS

This appendix describes the submodels developed for RESRAD-OFFSITE to estimate the environmental media concentrations of carbon-14 (C-14) and tritium (H-3) in soil, soil water, and air, as well as their concentrations in food products (i.e., plants, meat, milk, and aquatic foods). RESRAD-OFFSITE estimates C-14 and H-3 concentrations in groundwater and surface water using the transport models described in Appendix H; therefore, this appendix does not include the water pathway-related submodel. The special models are necessary because in the environment, C-14 and H-3 could easily convert to $^{14}CO_2$ and ^3HHO, respectively, and be released from soil to the air as gases. The distributions of their stable isotopes, C-12 and H-1, in the environment are referenced in the special model to predict the transfer of C-14 and H-3; due to chemical similarity; the transfer of C-14 and H-3 are expected to follow that of a stable isotope.

In general, the special H-3 and C-14 pathway models used in RESRAD-OFFSITE are the same as those implemented in RESRAD-ONSITE. The models are applied with C-14 and H-3 concentrations in the primary contaminated zone as the source for the onsite location. They are applied with the cumulative C-14 and H-3 concentrations in the secondary contaminated zone as the source for an offsite location, where in addition to the H-3 and C-14 from the secondary source, the C-14 and H-3 released to the air from the primary source and then blown to the offsite location are also modeled.

As in RESRAD-ONSITE, RESRAD-OFFSITE assumes H-3 is present as ^3HHO in the environment. ^3HHO in soil could vaporize. Those molecules that do not vaporize could attach to soil particles and resuspend to the air. The inhalation exposure reported for H-3 covers inhalation of vapor and particulates, as well as a 50% increase to account for the absorption of ^3HHO vapor through the skin at a rate equal to 50% of the breathing rate (ICRP 1979, 1980, 1981, 1982). In addition to being converted to $^{14}CO_2$ and released as a gas, C-14 could also exist in other organic or inorganic forms, which are solids. Thus, the inhalation exposure for C-14 also includes exposure to its particulate form and its gaseous form. Different dose coefficients can be used for the two different forms of C-14. The submodel for H-3 and C-14 in Section F.1.2 and F.2.1, respectively, concerns the gaseous form. The modeling for the inhalation of solid form is presented in Appendix C.

F.1   Tritium Submodels

Tritium, which has an atomic mass number of 3 and a decay half-life of about 12.3 years, is a naturally occurring isotope of hydrogen produced when cosmic-ray protons and neutrons interact with nitrogen and oxygen atoms. H-3 is also a product of ternary fission of uranium and plutonium and can be produced by activation of deuterium in the coolant ($^2H(n,\gamma)^3H$) of heavy-water reactors. Because H-3 decays to helium-3 by emitting a low-energy beta particle ($E_{max} = 0.0186$ MeV), it does not pose an external hazard. However, it can pose an internal radiological hazard once inhaled or ingested. Because H-3 has essentially the same chemical behavior as the stable isotope of hydrogen (i.e., H-1), it will occur in organisms throughout ecosystems in concentrations that depend on the ratio of H-3 to stable hydrogen in the environment.

F.1.1 Tritium in Soil Water

The H-3 concentration in soil water in the form of ^{3}HHO in the onsite primary contaminated zone or offsite secondary contaminated zone under equilibrium conditions can be expressed as follows:

$$^3H_{soil\ moisture} = \frac{\rho_b \times\ ^3H_{soil}}{\theta \times R_d}$$

(F.1)

where

$^3H_{soil\ moisture}$ = concentration of H-3 in soil water in the primary or secondary contaminated zone (Bq/cm^3 or pCi/cm^3),

ρ_b = bulk density of the contaminated zone (g/cm^3),

$^3H_{soil}$ = concentration of H-3 in contaminated soil (Bq/g or pCi/g),

θ = volumetric water content of the contaminated zone (dimensionless), and

R_d = retardation factor of H-3 in the contaminated zone (dimensionless).

The retardation factor, R_d, is expressed as

$$R_d = 1 + \frac{\rho_b \times K_d}{\theta}$$

(F.2)

where K_d = soil/water distribution coefficient of H-3 (0 cm^3/g).

Substituting Equation (F.2) into Equation (F.1), $^3H_{soil\ moisture}$ can be written as follows:

$$^3H_{soil\ moisture} = \left(\frac{\rho_b}{\theta + \rho_b K_d}\right) \times\ ^3H_{soil}$$

(F.3)

F.1.2 Tritium in Air

If H-3 closely follows the transport of stable hydrogen in the environment, the relationship of H-3 in air compared to H-3 in the ground will be analogous to that of stable hydrogen in these media. In the case of ^{3}HHO, this relationship implies that H-3 concentrations in air and soil will depend on the ratio of water vapor in the air to the water content in soil. The primary environmental parameter that describes the concentration of water vapor in air is site-specific absolute humidity. Although other factors such as wind speed and temperature can temporarily affect the humidity in a localized area, the long-term average water concentration in air can be represented by the average humidity measured at the site.

The equilibrium H-3 concentration in air resulting from an infinitely large contaminated area can be related to the stable hydrogen content in air and soil water in proportion to the H-3 concentration in soil water as follows:

$$^3H_{air}^{eqm} = \frac{^3H_{soil\ moisture} \times H_{air}^{eqm}}{H_{soil\ moisture}}$$

(F.4)

where

$^{3}H_{air}^{eqm}$ = average equilibrium concentration of H-3 in air (Bq/m^3 or pCi/m^3),

H_{air}^{eqm} = average equilibrium concentration of hydrogen in air (g/m^3), and

$H_{soil\ moisture}$ = average concentration of hydrogen in soil moisture (1/9 ρ_w = 1/9 g/cm^3, on the basis of assumption that the density of water, ρ_w, is 1 g/cm^3, which is not an input).

The average equilibrium concentration of hydrogen in air can be expressed as follows:

$$H_{air}^{eqm} = \frac{1}{9} \times Humidity \tag{F.5}$$

where

1/9 = mass fraction of hydrogen in the water (dimensionless) and

Humidity = average absolute humidity in the air (8 g/m^3).

Then Equation (F.4) can be rewritten as follows:

$$^{3}H_{air}^{eqm} = {^{3}H_{soil\ moisture}} \times 1/\rho_w \times Humidity \tag{F.6}$$

$^{3}H_{air}^{eqm}$ is the upper limit of H-3 concentration in the air ($^{3}H_{air,evap}$). When $^{3}H_{air,evap}$ exceeds $^{3}H_{air}^{eqm}$, it is replaced by the equilibrium concentration.

A site-specific value of absolute humidity is required as input to determine the equilibrium concentration of H-3 in air. Because atmospheric humidity varies widely from one location to another within the United States, a contour map of absolute humidity values is provided for user reference (Figure F-1).
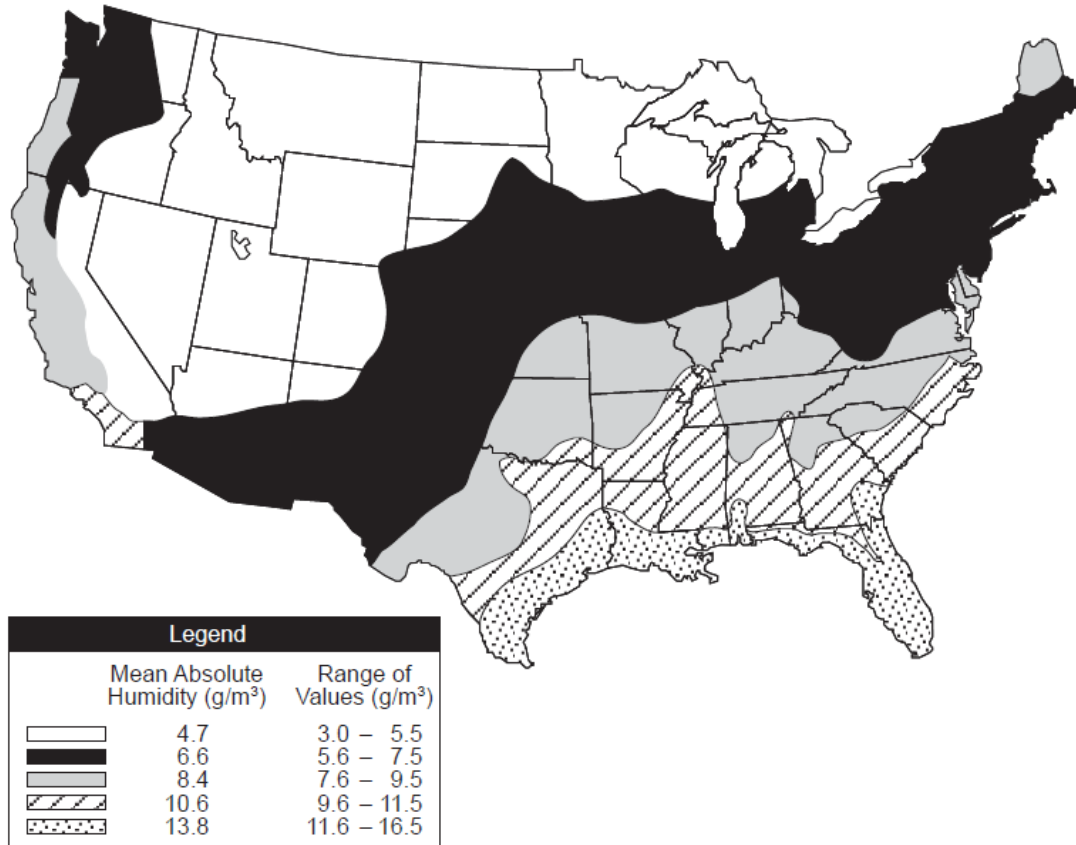
Figure F-1 Absolute Humidity by Geographical Region (Source: Etnier 1980)

For the primary or secondary contamination source with a finite area, the H-3 concentration in the air due to evaporation of soil moisture, $^3H_{air,evap}$, can be estimated using the following approximation, which neglects the small amount of water retained in plants relative to the amount released from the soil:

$$^3H_{air,evap}(t) = \frac{3.17 \times 10^{-8} \times {}^3H_{release}(t) \times \sqrt{A}}{2 \times H_{mix} \times V_{wind}}$$ (F.7)

where

$^3H_{air,evap}(t)$ = H-3 concentration in air over the contaminated area (Bq/m^3 or pCi/m^3),

$^3H_{release}(t)$ = H-3 flux (evasion rate) from the contaminated area [Bq/(m^2×yr) or pCi/(m^2×yr)],

3.17×10^{-8} = unit conversion factor (yr/s),

A = area of the contaminated zone (m^2),

H_{mix} = height at which ^{3}HHO vapor is uniformly mixed (two inputs can be specified, one used for the human inhalation pathway, and the other used for the plant, meat, and milk ingestion pathways), and

V_{wind} = annual average wind speed (m/s; computed in the RESRAD-OFFSITE code using the input joint frequency data).

F-4

For ^{3}HHO, the H-3 flux $^3H_{release}$ can be calculated based on the water balance equation for the contaminated site:

$$^3H_{release}(t) = 10^6 \times \ ^3H_{soil\ moisture} \times E_t \ \times CF_{evasion,H-3}\ (t) \tag{F.8}$$

$$\text{and } E_t = C_e \times [(1 - C_r) \times P_r + I_{rr}] \tag{F.9}$$

where

$^3H_{release}$ = evasion flux of H-3 (pCi/m²/yr or Bq/m²/yr),
10^6 = unit conversion factor (cm³/m³),
E_t = evapotranspiration rate (m/yr),
C_e = evapotranspiration coefficient,
C_r = runoff coefficient,
P_r = annual precipitation rate (m/yr),
I_{rr} = annual irrigation rate (m/yr), and
$CF_{evasion,H-3}(t)$ = cover and depth correction factor for evasion of H-3.

The H-3 special model assumes that only the soil moisture within the reference evasion depth (d_{ref}) from the ground surface would evaporate to the air. The calculation of the release rate of H-3, $^3H_{release}$, factors this into account via the use of $CF_{evasion}$ as follows:

$$CF_{evasion,H-3}(t) = \begin{cases} 0, \text{when } d_{ref,H-3} \ - \ T_{CV}\ (t) \le 0 \\ \dfrac{d_{ref,H-3} - T_{CV}(t)}{d_{ref,H-3}}, \text{when } 0 \ < d_{ref,H-3} - T_{CV}(t) \le T_{CZ}(t) \\ \dfrac{T_{CZ}}{d_{ref,H-3}}, \text{when } d_{ref,H-3} - T_{CV}\ (t) > T_{CZ}(t) \end{cases} \tag{F.10}$$

where

$CF_{evasion,H-3}$ = cover and depth correction factor for evasion of H-3,
$d_{ref,H-3}$ = reference evasion depth for H-3 (0.3 m is assumed in RESRAD-OFFITE, which is not an input),
$T_{CV}(t)$ = cover thickness (m), and
$T_{CZ}(t)$ = thickness of the contaminated zone (m).

The H-3 flux to the atmosphere results in a fractional loss of H-3 from soil in addition to the loss of H-3 because of radioactive decay and leaching. The code accounts for H-3 loss to the atmosphere and subtracts it from the inventory in the primary contaminated zone (see Appendix G). When the RESRAD-ONSITE exponential release model is implemented for the primary contamination, to account for the H-3 lost to air from the contaminated zone, it includes an evasion source factor for H-3 in addition to the source factor for radioactive decay and leaching. (Note: The source factor is the ratio of the radioactivity inventory at time t to the initial radioactivity inventory at time 0.) The evasion source factor $SF_E(t)$ can be calculated as follows:

$$SF_{E,H-3}(t) = e^{-(E_{c,H-3} \times t)} \tag{F.11}$$

$$E_{c,H-3} = \frac{10^{-6} \times \ ^3H_{release}(t)}{\rho_b \times \ ^3H_{soil} \times T_{cz}(t)} \tag{F.12}$$

where

> $SF_{E,H-3}$ = source factor for H-3 due to evasion,
> $E_{c,H-3}$ = evasion rate constant (1/yr), and
> 10^{-6} = unit conversion factor (m³/cm³).

At an offsite location, H-3 concentration in the air is contributed by the H-3 released from the primary contamination and then blown to the offsite location. When evaluating the contribution from the primary contamination, the average H-3 concentration over the offsite area of concern, $\overline{C_{H-3,onsite \rightarrow offsite}^{air}}$, is obtained by multiplying the release rate of H-3 from the primary contaminated area (i.e., $^3H_{release} \times A$), with the χ/Q value determined using the Gaussian plume dispersion model, as shown in Equation F.13. Because H-3 is considered to be released as ^{3}HHO vapor, a deposition velocity of 0 m/s is used to determine the χ/Q value. The integration scheme used to obtain $\overline{C_{H-3,onsite \rightarrow offsite}^{air}}(t)$ is discussed and detailed in Appendix I.

$$^3H_{air,offfsite}(t) = \overline{C_{H-3,onsite \rightarrow offsite}^{air}}(t) = \ ^3H_{release}(t) \times A \times \overline{(\chi/Q)_{gas}} \qquad \text{(F.13)}$$

F.1.3 Tritium in Food

F.1.3.1 Plant Food/Soil Concentration Ratio for Root Uptake

RESRAD-OFFSITE calculates the transfer of H-3 to foods such as produce, meat, milk, and fish by using the general equations derived in Appendix J, Sections J.3 through J.6, via food transfer factors. This section details the derivation of the food transfer factors for H-3 by taking into account water content in foods, animal diets, and intake rates, which correlates with the concentrations and intake of stable hydrogen.

Tritium concentrations in plants grown in contaminated soil can be modeled by assuming that the transfer of H-3 from soil to plants follows the path of stable hydrogen from soil to plants as follows:

$$^3H_{plant} = \frac{^3H_{soil\ moisture} \times H_{plant}}{H_{soil\ moisture}} \qquad \text{(F.14)}$$

$$^3H_{plant} = \ ^3H_{soil\ moisture} \times H_2O_{plant} \times 1/\rho_w \qquad \text{(F.15)}$$

where

> $^3H_{plant}$ = H-3 concentration in plants (pCi/g),
> H_{plant} = mass concentration (or mass fraction) of hydrogen in plants (g/g), and
> H_2O_{plant} = mass fraction of water in plants.

Therefore, the soil-to-plant transfer factor (i.e., the plant-food/soil concentration ratio for root uptake, RTF) for H-3 can be derived as follows:

$$RTF = \frac{^3H_{plant}}{^3H_{soil}} = \frac{^3H_{soil\ moisture} \times 1/\rho_w \times H_2O_{plant}}{^3H_{soil}}$$
$$= \left(\frac{\rho_b}{\theta + \rho_b K_d}\right) \times 1/\rho_w \times H_2O_{plant} \qquad \text{(F.16)}$$

Depending on the type of plants considered (i.e., leafy vegetables, fruit, grain, nonleafy vegetables, pasture and silage, or grain for livestock), the ρ_b, θ, or K_d of the corresponding

agricultural field where the plants grow and the mass fraction of water in representative plants should be used to derive the RTF. Table F-1 provides default mass fractions of water (i.e., water content) in fresh fruits, vegetables, and fodder, and in grain and store feed used in RESRAD-OFFSITE.

Table F-1   Water Content of Food Types

Food Type	Water Fraction (kg/kg)
Fruit, grain, nonleafy vegetables	0.8
Leafy vegetables	0.8
Pasture and silage	0.8
Livestock feed grain	0.8
Meat	0.6
Milk	0.88

Source: Based on Napier et al. (1988).

After the RTF has been determined with Equation (F.16), the concentration of H-3 in plants due to root uptake can be calculated as the product of the concentration of H-3 in soil, the RTF, and the fraction of root depth within the thickness of contaminated soil. In addition to root uptake, foliar deposition of irrigation water can also contribute to the radionuclide concentration in plants. However, for H-3, the contribution from water irrigation is implicitly considered in the derivation of RTF; therefore, this contribution is not modeled in the RESRAD-OFFSITE code. The contribution to H-3 in plants due to foliar deposition of airborne H-3 would be zero, because the deposition velocity of ^3HHO vapor is 0 m/s. Section J.4 provides the mathematical formulations used to calculate radionuclide concentrations in plants.

F.1.3.2   Transfer Factor for Meat and Milk

The transfer of H-3 to meat and milk can be calculated via the correlation with the transfer of stable hydrogen to meat and milk from the intake rate of hydrogen in the animal diet. The transfer of stable hydrogen can be evaluated by considering the mass fraction of water in meat and milk, which results from intake of water in the animal diet. Following this reasoning, the intake-to-meat (or milk) transfer factor, *IMTF*, for H-3 can be expressed as follows:

$$IMTF = \frac{^3H_{animal\ product}}{Intake_{water}^{livstock} \times \,^3H_{water} + \sum_{feed} Intake_{feed}^{livestock} \times \,^3H_{feed} + \sum_{agri} Intake_{soil}^{livestock} \times \,^3H_{soil} \times 1000\ (g/kg)}$$

$$= \frac{^3H_{animal\ product}}{Intake_{water}^{livstock} \times \,^3H_{water} + \sum_{feed} Intake_{feed}^{livestock} \times \,^3H_{feed} + \sum_{agri} Intake_{soil}^{livestock} \times (\theta/\rho_b + K_d) \times \,^3H_{soil\ moisture} \times 1000\ (g/kg)}$$

$$= \frac{H_{animal\ product}}{Intake_{water}^{livstock} \times H_{water} + \sum_{feed} Intake_{feed}^{livestock} \times H_{feed} + \sum_{agri} Intake_{soil}^{livestock} \times (\theta/\rho_b + K_d) \times H_{soil\ moisture} \times 1000\ (g/kg)}$$

$$= \frac{H_2O_{animal\ product}}{Intake_{water}^{livstock} \times \rho_w + \sum_{feed} Intake_{feed}^{livestock} \times H_2O_{feed} + \sum_{agri} Intake_{soil}^{livestock} \times (\theta/\rho_b + K_d) \times \rho_w} \quad (F.17)$$

where

$$IMTF = \text{intake-to-meat or milk transfer factor for H-3 (d/kg or d/L),}$$

$^3H_{animal\ product}$ = H-3 concentration in animal product (meat or milk) (pCi/kg or pCi/L),

$Intake_{water}^{livestock}$ = daily intake rate of water by livestock (50 L/d for meat, 160 L/d for milk),

$^3H_{water}$ = H-3 concentration in livestock water (pCi/L),

feed = (1) pasture and silage, and (2) grain,

$Intake_{feed}^{livestock}$ = daily intake rate of pasture and silage or grain by livestock (kg/d),

$^3H_{feed} = {}^3H_{plant} \times 1000 \text{ (g/kg)}$ = H-3 concentration in pasture and silage or grain (pCi/kg),

agri = agricultural field for (1) pasture and silage, and (2) grain,

$Intake_{soil}^{livestock}$ = daily intake rate of soil by livestock at the agricultural field (kg/d),

$^3H_{soil}$ = H-3 concentration in soil at the agricultural field (pCi/g),

θ, ρ_b, K_d = moisture content, bulk density, and distribution coefficient of H-3 for soil at the agricultural field (dimensionless, g/cm³, and cm³/g),

$^3H_{soil\ moisture}$ = H-3 concentration in soil moisture at the agricultural field (pCi/cm³),

$H_{animal\ product}$ = stable hydrogen concentration in animal product (meat or milk) (g/kg or g/L),

H_{water} = stable hydrogen concentration in livestock water (g/L),

H_{feed} = stable hydrogen concentration in pasture and silage or in grain (g/kg),

$H_{soil\ moisture}$ = stable hydrogen concentration in soil moisture at the agricultural field (g/cm³),

$H_2O_{animal\ product}$ = mass fraction of water in animal product (meat or milk),

ρ_w = density of water (1 kg/L or 1 cm/g), and

H_2O_{feed} = mass fraction of water in pasture and silage or in grain.

Table F-1 provides the default mass fraction of water (i.e., water content) in meat, milk, and livestock feed used in RESRAD-OFFSITE. These mass fractions are needed in the last expression of Equation (F.17) to calculate the *IMTF* for H-3. After the value of *IMTF* has been determined, it can be multiplied by the livestock daily intake rate of H-3 to determine the concentration of H-3 in meat or milk. The livestock daily intake rate of H-3 can be calculated using the denominator of the first expression in Equation (F.17), which requires knowledge of $^3H_{feed}$ or $^3H_{plant}$. The calculation of $^3H_{plant}$ is discussed in the previous section.

F.1.3.3   Transfer Factor for Aquatic Food

Tritium transfer from contaminated water to fish or other aquatic foods is calculated by using aquatic bioaccumulation factors, *ABFs*, as described in Appendix J, Section J.6:

$$^3H_{seafood} = ABF \times {}^3H_{surface\ water} \tag{F.18}$$

where

$^3H_{seafood}$ = H-3 concentration in seafood (fish or crustaceans/mollusks) (Bq/kg or pCi/kg),

ABF = aquatic bioaccumulation factor for H-3 (L/kg), and

$^3H_{surface\ water}$ = H-3 concentration in surface water (Bq/L or pCi/L).

The RESRAD-OFFSITE code uses a fish/water and crustacean-mollusk/water transfer factor of 1.0 L/kg for H-3.

F.1.4   Tritium Dermal Absorption Dose

Water vapor is absorbed through the skin at approximately 50% of the inhalation rate of water vapor (ICRP 1979, 1980, 1981, 1982; Hamby 1992). To account for dermal absorption of ^3HHO vapor in air, RESRAD-OFFSITE multiplies the dose from inhalation alone by a factor of 1.5 and reports the resulting dose under the inhalation pathway.

F.2   Carbon-14 Submodels

C-14, with a radiological half-life of about 5,730 years, is a naturally occurring isotope of carbon produced in the stratosphere by the interaction of cosmic-ray neutrons with nitrogen atoms. C-14 is also produced in appreciable quantities in atmospheric and underground testing of nuclear and thermonuclear devices, as well as in nuclear power operations (primarily the result of fission and neutron activation). C-14 decays to stable nitrogen by emitting a beta particle (E_{max} = 0.156 MeV) and does not pose an external hazard. Because C-14 emits a higher-energy beta particle, it poses a more severe internal radiological hazard than H-3. The ingestion dose conversion factor is approximately 30 times that of H-3. One of the most important pathways involving the radiological dose to humans from soil contaminated with C-14 is plant ingestion. In addition to direct root uptake from soil and foliar deposition of dust particles contaminated with C-14, carbon in gases volatilized from the soil are directly incorporated into the plant through the process of photosynthesis.

Models that calculate the dose from C-14 in air usually assume a steady-state relationship among carbon isotopes, from the point of photosynthetic fixation through the food chain to humans. In the natural environment, the ratio of C-14 to C-12 (the common form of stable carbon) in the body, as well as in plants and animals, is the same as it is in the atmosphere. At a site contaminated with C-14, the amount of C-14 in air (and hence in all living organisms) would increase over the natural background.

F.2.1   Carbon-14 in Air

Inorganic and organic reactions convert most forms of soil carbon into carbon dioxide (CO_2). Because CO_2 is volatile, soil carbon is usually lost to the air, where plants absorb it through photosynthesis. The concentration of C-14 in air above a contaminated zone depends on the volatilization (evasion) rate of carbon from the soil, the size and location of the source area, and meteorological dispersion conditions.

Sheppard et al. (1991) measured the rate of C-14 loss from soils in outdoor lysimeter experiments. They found that the evasion rate, E, was not a strong function of soil properties. For clay and loam soils, the evasion rate was estimated to be 3.8×10^{-7}/s; for sand and organic soils, the evasion rate was estimated to be 6.7×10^{-7}/s. However, Amiro et al. (1991) observed evasion rates from as low as 1.0×10^{-10}/s from native carbonates and humified soils.

For a local contaminated source of area *A*, the C-14 concentration in air can be estimated in a manner similar to Equation (F.7) used for H-3:

$$^{14}C_{air,vol} = \frac{3.17 \times 10^{-8} \times {}^{14}C_{release} \times \sqrt{A}}{2 \times H_{mix} \times V_{wind}} \tag{F.19}$$

where

$^{14}C_{air,vol}$ = C-14 concentration in air over the contaminated area due to volatilization (Bq/m^3 or pCi/m^3),

$^{14}C_{release}$ = C-14 flux (evasion rate) from the contaminated area [Bq/(m^2×yr) or pCi/(m^2×yr)], and

H_{mix} = height at which CO_2 gas is uniformly mixed (2 m for the human inhalation pathway; 1 m for the plant, meat, and milk ingestion pathways).

The flux of gaseous C-14 to the atmosphere from soil, considering the evasion loss rate proposed by Sheppard et al. (1991) for a reference depth of 30 cm and the cover thickness, can be calculated as follows:

$$^{14}C_{release} = 10^6 \times {}^{14}C_{soil} \times 3.156 \times 10^7 \times E_{c,C-14} \times \rho_b \times d_{ref,C-14} \times CF_{evasion,C-14} \tag{F.20}$$

where

10^6 = unit conversion factor (cm^3/m^3),

$^{14}C_{soil}$ = concentration of C-14 in contaminated soil (Bq/g or pCi/g),

3.156×10^7 = unit conversion factor (s/yr),

$E_{c,C-14}$ = evasion loss rate constant of C-14 in soil (1/s),

ρ_b = bulk density of contaminated soil (g/cm^3),

$d_{ref,C-14}$ = reference evasion depth (m; unlike the evasion depth for H-3, the evasion depth for C-14 is an input parameter), and

$CF_{evasion,C-14}$ = cover and depth correction factor for evasion of C-14.

The reference evasion depth, $d_{ref,C-14}$, and evasion loss rate constant, E_{C-14}, are input parameters. The evasion loss rate constant of C-14 describes the fraction of the soil inventory of C-14 within the reference evasion depth that is lost to the atmosphere per unit time. This rate can usually be obtained by measuring the C-14 inventory as a function of time in the contaminated zone. Table F-2 lists the measured evasion rates for C-14 from lysimeter experiments. The cover and depth correction factor for evasion, $CF_{evasion,C-14}$, corrects the evasion rate of C-14 associated with the reference depth; its value can be determined using Equation (F.10), in which $CF_{evasion,H-3}$ is replaced with $CF_{evasion,C-14}$ and $d_{ref,H-3}$ is replaced with $d_{ref,C-14}$.

Table F-2 Carbon-14 Evasion Rate Factor

Soil Type	Evasion Rate (yr^{-1})
Clay	12
Loamy soils	12
Sandy soils	22
Organic soils	22
Stable carbon in carbonate soils	0.0032
Water	0.91

Sources: Sheppard et al. (1991), Amiro and
Davis (1991).

The transport of C-14 is assumed to follow that of stable carbon in the environment. For an infinitely large source area, the ratio of C-14 in air to C-14 in soil is analogous to that of stable carbon in air and soil:

$$^{14}C_{air}^{eqm} = \,^{12}C_{air}^{eqm} \times \frac{E_{c,C-14} \times \,^{14}C_{soil}}{E_{c,C-12} \times \,^{12}C_{soil}} \tag{F.21}$$

where
$^{14}C_{air}^{eqm}$ = equilibrium concentration of C-14 in air (Bq/m3 or pCi/m³),
$^{12}C_{air}^{eqm}$ = equilibrium concentration of stable carbon in air (0.18 g/m³),
$E_{c,C-12}$ = evasion loss rate constant of stable carbon in soil (0.0032 yr^{-1}), and
$^{12}C_{soil}$ = concentration of stable carbon in soil, the fraction of soil that is stable carbon (0.03 g/g or dimensionless). This parameter varies with soil type and would be considerably higher for soils rich in organic content (e.g., peat).

For a finite source contaminated with C-14, the concentration of C-14 in air due to volatilization, $^{14}C_{air,vol}$, should always be less than the concentration of C-14 from an infinitely large contaminated source area, $^{14}C_{air}^{eqm}$. If the calculated value of $^{14}C_{air,vol}$ exceeds the value of $^{14}C_{air}^{eqm}$, it is set to the value of $^{14}C_{air}^{eqm}$.

The loss of C-14 (as CO_2 gas) to air is subtracted from the inventory of the contaminated zone. To account for the C-14 lost to air, an evasion source factor for C-14 is needed in addition to the source factor for radioactive decay and leaching, when the RESRAD-ONSITE exponential release model is implemented for the primary contamination (see Appendix G). The evasion source factor $SF_{E,C-14}(t)$ can be calculated as follows:

$$SF_{E,C-14}(t) = e^{-(E_{c,C-14} \times CF_{evasion,C-14} \times t)}. \tag{F.22}$$

At an offsite location, the C-14 (as CO_2) concentration in the air is contributed by the C-14 released from the primary contamination and then blown to the offsite location. When evaluating the contribution from the primary contamination, the average C-14 concentration over the offsite area of concern, $\overline{C_{C-14,onsite \rightarrow offsite}^{air}}$, is obtained by multiplying the release rate of C-14 from the primary contaminated area (i.e., $^{14}C_{release} \times A$), with the χ/Q value determined using the Gaussian plume dispersion model. For C-14 being released as CO_2 gas, a deposition velocity of 0 m/s is used to determine the χ/Q value. The integration scheme used to obtain $\overline{C_{C-14,onsite \rightarrow offsite}^{air}}(t)$ is the same as that discussed in Appendix I:

$$^{14}C_{air,offsite} \;=\; \overline{C^{air}_{C-14,onsite \rightarrow offsite}} \tag{F.23}$$

Equation (F.23) concerns air concentration of C-14 due to volatilization as CO_2. The air concentration of C-14 attaching to dust particles (i.e., in solid form) is calculated in the same manner as other solid radionuclides (see discussions in Appendix C). The radiation dose associated with the inhalation pathway as listed in the text report and shown in graphics include contributions from inhalation of dust particles contaminated with C-14 and inhalation of $^{14}CO_2$ gas.

F.2.2   Carbon-14 in Food

The main pathway for C-14 intake by humans from a C-14-contaminated site is usually food ingestion. The transfer of C-14 to foods such as produce, meat, milk, and fish is calculated using the general equations derived in Appendix J, Sections J.3 through J.6. However, the food transfer factors for C-14 must be derived by accounting for site-specific parameters such as the carbon content in foods, animal diets, and intake rates. Derivation of the food transfer factors is discussed in Sections F.2.2.1 through F.2.2.3.

F.2.2.1   Transfer Factors for Plants

Sheppard et al. (1991) indicates that a new pathway exists for the incorporation of carbon to vegetation: uptake by foliage of gases volatilized from the soil and absorbed from the atmosphere. Therefore, in addition to the root uptake and foliar deposition of airborne particulates pathways considered for all radionuclides, an additional pathway involving the contribution from photosynthesis is considered when evaluating C-14 concentration in plants. (Note that foliar deposition through irrigation is not modeled for both C-14 and H-3.)

The contribution to the C-14 concentration in plants from the root uptake pathway depends on the C-14 level in the soil source, the RTF, and the fraction of the root depth within the soil source (see discussions in Sections J.4.1 and J.4.2). The contribution from the foliar deposition of particulates pathway depends on the particulate concentration in the air, C-14 concentration in particulates, deposition velocity of particulates, interception and translocation fraction, weathering removal constant, growth period, and yield of the plant (see discussion in Section J.4.4). This section evaluates the contribution from the photosynthesis pathway, as well as the derivation of RTF for use to evaluate the root uptake pathway.

RESRAD-OFFSITE assumes that C-14 in plants due to photosynthesis will follow the path of stable carbon in the foliar absorption pathway:

$$^{14}C_{plant,ps} = {}^{14}C_{air} \times AP_{C-14} = {}^{14}C_{air} \times \frac{{}^{12}C_{plant,ps}}{{}^{12}C_{air}} = {}^{14}C_{air} \times \frac{F_a \times {}^{12}C_{plant}}{{}^{12}C_{air}} \tag{F.25}$$

$$AP_{C-14} = \frac{F_a \times {}^{12}C_{plant}}{{}^{12}C_{air}} \tag{F.26}$$

where

$^{14}C_{plant,ps}$ = concentration of C-14 in plants derived from photosynthesis (Bq/kg or pCi/kg),

$^{14}C_{air}$ = concentration of C-14 (as CO_2) in the air (pCi/m^3),

AP_{C-14} = $^{14}C_{plant,ps}/^{14}C_{air}$ = air to plant transfer factor for photosynthesis for C-14 (m^3/kg),

$^{12}C_{plant,ps}$ = stable carbon concentration in plant (i.e., fraction of plant mass that is carbon), derived from photosynthesis (kg/kg or dimensionless),

$^{12}C_{air} = {}^{12}C_{air}^{eqm}$ = concentration of stable carbon in air (kg/m^3),

F_a = fraction of stable carbon in plants derived from carbon in air, and

$^{12}C_{plant}$ = stable carbon concentration in plant (i.e., fraction of plant mass that is carbon) (kg/kg or dimensionless; 0.4 for fruit, grain, and nonleafy vegetables; 0.09 for leafy vegetables and pasture and silage).

To derive RTF, the assumption that C-14 follows the path of stable carbon is applied as follows:

$$^{14}C_{plant,ru} = {}^{14}C_{soil} \times 1000 \times RTF_{C-14}$$

$$= {}^{14}C_{soil} \times 1000 \times \frac{{}^{12}C_{plant,ru}}{{}^{12}C_{soil}} = {}^{14}C_{soil} \times 1000 \times \frac{F_s \times {}^{12}C_{plant}}{{}^{12}C_{soil}} \qquad (F.27)$$

$$RTF_{C-14} = \frac{F_s \times {}^{12}C_{plant}}{{}^{12}C_{soil}} \qquad (F.28)$$

where

$^{14}C_{plant,ru}$ = concentration of C-14 in plants derived from root uptake (Bq/kg or pCi/kg),

1,000 = unit conversion factor (g/kg),

$^{12}C_{plant,up}$ = stable carbon concentration in plant (i.e., fraction of plant mass that is carbon, derived from root uptake) (kg/kg or dimensionless), and

F_s = fraction of stable carbon in plants derived from carbon in soil ($F_s = 0$, if $^{12}C_{soil} = 0$).

It has been shown that most (~98%) of plant carbon is assimilated from the atmosphere through photosynthesis. Only 1 to 2% is absorbed directly through the roots (Sheppard et al. 1991). In RESRAD-OFFSITE, the default values of Fa and Fs are assumed to be 0.98 and 0.02, respectively. RESRAD-OFFSITE uses Equation (F.28) to calculate RTF for C-14, which is then used to calculate C-14 concentration due to root uptake in various plants consumed by either human or livestock, following the methodology described in J.4.1 and J.4.2. Equation (F.26) is used to calculate AP for C-14, which is then used to calculate C-14 concentration due to photosynthesis in various plants following the methodology described in J.4.5. The calculation of C-14 concentration due to foliar deposition of particulates follows the methodology described in J.4.4. The C-14 concentrations due to root uptake, photosynthesis, and foliar deposition of particulates are added to obtain the total C-14 concentration in plants, which is shown in the RESRAD-OFFSITE graphic output.

F.2.2.2 Transfer Factors for Meat and Milk

The C-14 concentrations in meat and milk are assumed to be derived totally from livestock diets. The transfer of C-14 from livestock diets to meat and milk is assumed to follow the same route as that of stable carbon. The C-14 content in meat and milk is related to the intake rates of stable carbon and C-14 by livestock as follows:

$$IMTF = \frac{{}^{14}C_{animal\,product}}{Intake_{water}^{livstock} \times {}^{14}C_{water} + \sum_{feed} Intake_{feed}^{livestock} \times {}^{14}C_{feed} + \sum_{agri} Intake_{soil}^{livestock} \times {}^{14}C_{soil} \times 1000\,(g/kg)}$$

$$= \frac{^{12}C_{animal\,product}}{Intake_{water}^{livstock}\times ^{12}C_{water}+\sum_{feed} Intake_{feed}^{livestock}\times ^{12}C_{feed}+\sum_{agri} Intake_{soil}^{livestock}\times ^{12}C_{soil}} \quad \text{(F.29)}$$

where

$IMTF$	=	intake-to-meat or milk transfer factor for C-14 (d/kg or d/L),
$^{14}C_{animal\,product}$	=	C-14 concentration in animal product (meat or milk) (pCi/kg or pCi/L),
$^{14}C_{water}$	=	C-14 concentration in livestock water (pCi/L),
feed	=	(1) pasture and silage, and (2) grain,
$Intake_{feed}^{livestock}$	=	daily intake rate of pasture and silage or grain by livestock (kg/d),
$^{14}C_{feed} = {}^{14}C_{plant}$	=	C-14 concentration in pasture and silage or grain (pCi/kg),
agri	=	agricultural field for (1) pasture and silage, and (2) grain,
$Intake_{soil}^{livestock}$	=	daily intake rate of soil by livestock at the agricultural field (kg/d),
$^{14}C_{soil}$	=	C-14 concentration in soil at the agricultural field (pCi/g),
$^{12}C_{animal\,product}$	=	concentration of stable carbon, equivalent to fraction of stable carbon (assuming density of milk is 1 kg/L), in animal product (meat or milk) (0.24 kg/kg for meat, or 0.070 kg/L for milk),
$^{12}C_{water}$	=	concentration of stable carbon, equivalent to fraction of stable carbon (assuming density of water is 1 kg/L), in livestock water (2.0 × 10⁻⁵ kg/L),
$^{12}C_{feed} = {}^{12}C_{plant}$	=	stable carbon concentration (i.e., mass fraction of stable carbon) in pasture and silage or in grain (kg/kg; 0.4 for grain and 0.09 for pasture and silage), and
$^{12}C_{soil}$	=	concentration of stable carbon in soil, i.e., fraction of soil that is stable carbon (0.03 kg/kg or dimensionless).

Table F-3 provides the default mass fraction of stable carbon in different plants, food types, and water that are used in RESRAD-OFFSITE. These mass fractions are needed in the second expression of Equation (F.29) to calculate the IMTF for C-14. After the value of IMTF has been determined, it can be multiplied by the livestock daily intake rate of C-14 to determine the concentration of C-14 in meat or milk. The livestock daily intake rate of C-14 can be calculated using the denominator of the first expression in Equation (F.29), which requires knowledge of $^{14}C_{feed}$, or $^{14}C_{plant}$. The calculation of $^{14}C_{plant}$ is discussed in Section F.2.2.1.

Table F-3   Carbon Content of Plants, Food Types, and Water

Food Type	Carbon Fraction (kg/kg)
Fruit, grain, nonleafy vegetables	0.4
Leafy vegetables	0.09
Pasture and silage	0.09
Livestock feed grain	0.4
Meat	0.24
Milk	0.07
Water	2 × 10⁻⁵

Source: Based on Napier et al. (1988).

F.2.2.3   Transfer Factor for Aquatic Food

C-14 in fish or other aquatic food is calculated by using aquatic bioaccumulation factors, ABFs, as described in J.6:

$$^{14}C_{seafood} = ABF \times 10^{-3} \times {}^{14}C_{surface\,water} \qquad (F.30)$$

where

$^{14}C_{seafood}$ = C-14 concentration in seafood (fish or crustaceans/mollusks) (Bq/kg or pCi/kg),
ABF = aquatic bioaccumulation factor for C-14 (L/kg),
10^{-3} = unit conversion factor (m^3/L), and
$^{14}C_{surface\,water}$ = C-14 concentration in surface water (Bq/m^3 or pCi/m^3.

The values RESRAD-OFFSITE uses for the fish/water and crustacean-mollusk/water bioaccumulation factor for C-14 are 5×10^4 and 9.1×10^3 L/kg, respectively.

F.3   References

Amiro, B.D., Y. Zhuang, and S.C. Sheppard, 1991, "Relative Importance of Atmospheric and Root Uptake Pathways for $_{14}CO_2$, Transfer from Contaminated Soil to Plants," *Health Physics* 61:825–829.

Etnier, E.L., 1980, "Regional and Site-Specific Absolute Humidity Data for Use in Tritium Dose Calculations," *Health Physics* 39:318–320.

Hamby, D.M., 1992, "A Methodology for Estimating the Radiological Consequence of an Acute Aqueous Release," *Health Physics* 62:567–570.

ICRP (International Commission on Radiological Protection), 1979, *Limits for Intakes of Radionuclides by Workers*, ICRP Publication 30, Part 1, a report of Committee 2 of the International Commission on Radiological Protection, adopted by the Commission in July 1978, Annals of the ICRP, Pergamon Press, New York, N.Y.

ICRP, 1980, *Limits for Intakes of Radionuclides by Workers*, ICRP Publication 30, Part 2, a report of Committee 2 of the International Commission on Radiological Protection, adopted by the Commission in July 1978, Annals of the ICRP, Pergamon Press, New York, N.Y.

ICRP, 1981, *Limits for Intakes of Radionuclides by Workers*, ICRP Publication 30, Part 3, a report of Committee 2 of the International Commission on Radiological Protection, adopted by the Commission in July 1978, Annals of the ICRP, Pergamon Press, New York, N.Y.

ICRP, 1982, *Limits for Intakes of Radionuclides by Workers*, ICRP Publication 30, Index, Annals of the ICRP, Pergamon Press, New York, N.Y.

Napier, B.A., D.L. Strenge, R.A. Peloquin, and J.V. Ramsdell, 1988, *GENII—The Hanford Environmental Radiation Software Dosimetry System*, PNL-6584/UC-600, Pacific Northwest Laboratory, Hanford, Wash., Dec.

Sheppard, M.I., S.C. Sheppard, and B.D. Amiro, 1991, "Mobility and Plant Uptake of Inorganic C-14 and C-14-Labelled PCB in Soils of High and Low Retention," *Health Physics* 61:481–492.

APPENDIX G:
PRIMARY CONTAMINATION

Chapter 2 presents the conceptualization of the primary contamination. This appendix describes the mathematical expression used to model the primary contamination as conceptualized in Chapter 2.

G.1   Physical Properties of the Primary Contamination

As described in Sections 2.1 and 2.2 of the main report, the RESRAD-OFFSITE code models a primary contamination of uniform thickness, a clean cover if one is present, and mixing within a specified depth at the surface. RESRAD-OFFSITE uses two conceptualizations of the vertical dimensions of the cover and contamination (Figure G-1). The first (Sections G.1.1 through G.1.4), which assumes no mixing, is shown on the left half of each diagram in Figure G-1. It is used to model direct external exposure from the primary contamination, the diffusion of radon isotopes from the primary contamination, the evasion of carbon-14 (C-14) and hydrogen-3 (H-3) from the primary contamination, and the erosion of the cover and of the primary contamination. The other (Section G.1.5), shown on the right half of each of the two diagrams in Figure G-1, is used to compute the other releases from the primary contamination and to model exposure from the other pathways.
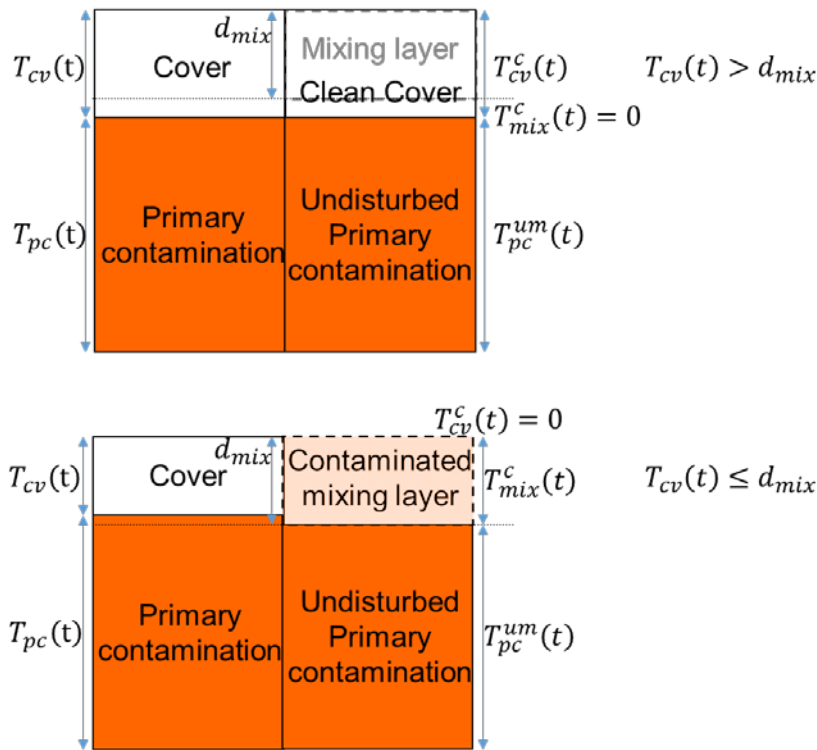
Figure G-1   Alternative Conceptualizations of Cover and Contamination

G.1.1 Erosion Rate

The erosion rates of any cover above the primary contamination, the primary contamination, and the surface soil at the offsite locations are computed using the Universal Soil-Loss Equation. Section 12.10 of the *Handbook of Hydrology* (Shen and Julien 1993) has figures and tables for the first five factors in the following expression for the erosion rate:

$$\mathcal{E}_{sl} = 224 \times R \times K_{sl} \times LS_l \times C_l \times P_l / (\rho_b^{sl} \times 10^6) \tag{G.1}$$

where

$\mathcal{E}_{sl}$ = erosion rate of the soil layer (m/year),

sl = soil layer, which can be the cover, *cv*, primary contamination, *pc*, or the offsite farmed lands, *o*,

224 = to convert tons per acre to gram per square meter [(g/m^2)/(tons/acre)],

R = annual rainfall erosion index, the rainfall erosivity factor, or the rainfall and runoff factor (1/year),

K_{sl} = soil erodibility factor of the soil layer *sl* (tons/acre),

LS_l = slope length-steepness factor at location *l*,

l = location of the soil layer, which can be at the primary contamination, *pc*, or at one of the offsite farmed lands, *o*,

C_l = cropping-management factor or the cover and management factor at location *l*,

P_l = conservation practice factor or the support practice factor at location l,

ρ_b^{sl} = dry bulk density of the soil layer *sl* (g/[cm]^3), and

10^6 = to convert per cubic centimeter to per cubic meter ([m/cm]^3).

G.1.2 Time for the Cover and the Primary Contamination to Erode

If there is a cover above the primary contamination, the time at which the cover will be completely eroded away, assuming no mixing at the location of the primary contamination, is given by:

$$t_{cv} = T_{cv}(0)/\mathcal{E}_{cv} \tag{G.2a}$$

where

t_{cv} = time at which the cover is completely eroded (yr),

$T_{cv}(0)$ = initial thickness of the cover (m), and

$\mathcal{E}_{cv}$ = erosion rate of the cover (m/yr).

The time at which the primary contamination will be completely eroded away, assuming no mixing at the location of the primary contamination, is given by:

$$t_{pc} = T_{pc}(0)/\mathcal{E}_{pc} + t_{cv} \tag{G.2b}$$

where

t_{pc} = time at which the primary contamination is completely eroded (yr),
$T_{pc}(0)$ = initial thickness of the primary contamination (m), and
$\mathcal{E}_{pc}$ = erosion rate of the primary contamination (m/yr).

G.1.3 Thickness of Cover

The thickness of the cover at any time is given by the following equations:

$$T_{cv}(t) = T_{cv}(0) - \mathcal{E}_{cv}t \text{ when } t < t_{cv}$$
$$T_{cv}(t) = 0 \text{ when } t \geq t_{cv}$$

(G.3)

where $T_{cv}(t)$ = thickness of the cover at time t (m).

G.1.4 Thickness of Primary Contamination

The thickness of the primary contamination at any time is given by the following equations:

$$T_{pc}(t) = T_{pc}(0) \text{ when } (t \leq t_{cv})$$
$$T_{pc}(t) = T_{pc}(0) - \mathcal{E}_{pc}(t - t_{cv}) \text{ when } (t_{pc} > t > t_{cv})$$
$$T_{pc}(t) = 0 \text{ when } (t \geq t_{cv})$$

(G.4)

where

$T_{pc}(t)$ = thickness of the primary contamination at time t (m), and
$\mathcal{E}_{pc}$ = erosion rate of the primary contamination (m/yr).

G.1.5 Thickness of Layers with Mixing Model

As shown in Figure G-1, this conceptualization considers three layers: a clean cover/clean mixing layer, a contaminated mixing layer and a physically undisturbed primary contamination. When the cover is thicker than the mixing layer, the cover will be clean, there will be no contaminated mixing layer and the primary contamination will be physically undisturbed. The expressions for the thickness of the three layers are as follows:

$$T_{cv}^{c}(t) = T_{cv}(t)$$
$$T_{mix}^{c}(t) = 0 \quad \text{when } T_{cv}(t) \geq d_{mix}$$
$$T_{pc}^{um}(t) = T_{pc}(0)$$

(G.5)

where

$T_{cv}^{c}(t)$ = thickness of the clean cover at time t (m),
$T_{mix}^{c}(t)$ = thickness of the contaminated mixing layer at time t, (m),
$T_{pc}^{um}(t)$ = thickness of the physically undisturbed primary contamination at time t (m),
d_{mix} = depth of the mixing layer at the primary contamination (m).

When the mixing layer is thicker than the cover, there will be no clean cover, there will be a contaminated mixing layer, and there will be a physically undisturbed primary contamination

provided the mixing layer is thinner than the sum of the thicknesses of the cover and the primary contamination. The expressions for the thickness of the three layers are as follows:

$$
\begin{aligned}
T_{cv}^c(t) &= 0 \\
T_{mix}^c(t) &= d_{mix}
\end{aligned} \quad \text{when } T_{cv}(t) < d_{mix}
$$

$$
T_{pc}^{um}(t) = T_{cv}(t) + T_{pc}(t) - d_{mix} \quad \text{when } T_{cv}(t) < d_{mix} < T_{cv}(t) + T_{pc}(t)
$$

$$
T_{pc}^{um}(t) = 0 \quad \text{when } d_{mix} \geq T_{cv}(t) + T_{pc}(t)
$$

$\qquad$ (G.6)

G.1.6 Dry Bulk Density of the Mixing Layer

The density of the mixing zone is computed by assuming that mixing occurs continuously (over time) over the specified mixing depth. The initial density of the mixing layer depends on the extent to which the mixing layer penetrates the primary contamination at time 0:

If the mixing layer is initially within the cover, $T_{cv}(0) \geq d_{mix}$,

$$
\rho_b^{mix}(t = 0) = \rho_b^{cv} \qquad (G.7)
$$

where
$\qquad \rho_b^{mix}(t = 0) \quad$ = dry bulk density of the mixing layer at time 0 (g/[cm]³), and
$\qquad \qquad \rho_b^{cv} \quad$ = dry bulk density of the cover (g/[cm]³).

If the mixing layer is initially within the primary contamination, $T_{cv}(0) < d_{mix} < T_{cv}(0) + T_{pc}(0)$:

$$
\rho_b^{mix}(t = 0) = \rho_b^{pc} + \frac{T_{cv}(0)}{d_{mix}} \left(\rho_b^{cv} - \rho_b^{pc} \right) \qquad (G.8)
$$

where ρ_b^{pc} = dry bulk density of the primary contamination (g/[cm]³).

If the mixing layer penetrates through the entire primary contamination at time 0, $d_{mix} \geq T_{cv}(0) + T_{pc}(0)$, the effect of the densities of the fraction of the mixing layer in each layer is considered by the code:

$$
\rho_b^{mix}(t = 0) = \rho_b^{pc} + \frac{T_{cv}(0)}{d_{mix}} \left(\rho_b^{cv} - \rho_b^{pc} \right) + \sum_{z=uz}^{sz} \frac{d_{mix}^z(t = 0)}{d_{mix}} \left(\rho_b^z - \rho_b^{pc} \right) \qquad (G.9)
$$

where
$\qquad \sum_{z=uz}^{sz} \quad$ = the summation over the unsaturated and saturated zones,
$\qquad d_{mix}^z(t = 0) \quad$ = the depth of the mixing layer that is within zone z (m), and
$\qquad \qquad \rho_b^z \quad$ = dry bulk density of zone z (g/[cm]³).

It is easier to compute and to understand the expression for the density of the mixing layer as a function of the depth to which the mixing layer penetrates beyond the boundary between the cover and the primary contamination. The initial conditions in terms of time can be translated to be in terms of the depth of penetration:

$$
\rho_b^{mix} \left(d_{mix}^{pc} = d_{mix}^{pc\ ini} \right) = \rho_b^{mix}(t = 0) \qquad (G.10)
$$

where

$$d_{mix}^{pc} = \text{depth of penetration of the mixing layer below the top of the primary contamination (m), and}$$

$$d_{mix}^{pc\ ini} = \text{initial penetration of the mixing layer below the top of the primary contamination at time 0 (m).}$$

When the mixing layer is within the primary contamination, the mass balance of the mixing layer is obtained by equating the rate at which the density of the mixing layer changes with the depth of penetration, to the difference between the densities of the material entering and exiting the mixing layer, distributed over the depth of the mixing layer:

$$\frac{d\rho_b^{mix}\left(d_{mix}^{pc}\right)}{dd_{mix}^{pc}} = \frac{\rho_b^{pc} - \rho_b^{mix}\left(d_{mix}^{pc}\right)}{d_{mix}} \tag{G.11}$$

The density of the mixing layer is determined by solving the mass balance equation with the appropriate initial condition as follows:

$$\frac{d\rho_b^{mix}\left(d_{mix}^{pc}\right)e^{\frac{d_{mix}^{pc}}{d_{mix}}}}{dd_{mix}^{pc}} = \frac{\rho_b^{pc}}{d_{mix}}e^{\frac{d_{mix}^{pc}}{d_{mix}}}$$

$$\rho_b^{mix}\left(d_{mix}^{pc}\right)e^{\frac{d_{mix}^{pc}}{d_{mix}}} - \rho_b^{mix}\left(d_{mix}^{pc\ ini}\right)e^{\frac{d_{mix}^{pc\ ini}}{d_{mix}}} = \rho_b^{pc}e^{\frac{d_{mix}^{pc}}{d_{mix}}} - \rho_b^{pc}e^{\frac{d_{mix}^{pc\ ini}}{d_{mix}}}$$

$$\rho_b^{mix}\left(d_{mix}^{pc}\right) = \rho_b^{pc} - \left[\rho_b^{pc} - \rho_b^{mix}\left(d_{mix}^{pc\ ini}\right)\right]e^{-\frac{d_{mix}^{pc} - d_{mix}^{pc\ ini}}{d_{mix}}}$$

$$\frac{\rho_b^{mix}\left(d_{mix}^{pc}\right)}{\rho_b^{pc}} = 1 - \left[1 - \frac{\rho_b^{mix}\left(d_{mix}^{pc\ ini}\right)}{\rho_b^{pc}}\right]e^{-\frac{d_{mix}^{pc} - d_{mix}^{pc\ ini}}{d_{mix}}} \tag{G.12}$$

Eventually, the cover and primary contamination will erode so that their combined thickness will be equal to the depth of the mixing zone. Then the soil underlying the primary contamination will enter the mixing zone. Because it is too cumbersome to track the layers (any unsaturated zones first and then the saturated zone) that can enter the mixing zone over time, density changes are not modeled beyond that point.

G.1.7 Volume Fraction of Primary Contamination in Mixing Layer

The quantity of radionuclides in the mixing layer is directly proportional to the volume of the material from the primary contamination in the mixing layer. The mixing layer is uncontaminated as long as its depth is less than the thickness of the clean cover. The volume fraction of the material from the primary contamination in the mixing layer is evaluated when the depth of the mixing layer exceeds the thickness of the clean cover. It is evaluated by assuming that mixing occurs continuously (over time) over the specified mixing depth and that the volume fraction in the eroded soil is the same as the volume fraction in surface soil.

The initial volume fraction of the material from the primary contamination in the mixing layer depends on extent to which the mixing layer penetrates the primary contamination at time 0:

If the mixing layer is initially within the cover, $T_{cv}(0) \geq d_{mix}$,

$$f_{vm}(t = 0) = 0 \tag{G.13}$$

where $f_{vm}(t = 0)$ = volume fraction of the material from the primary contamination in the mixing layer at time 0.

If the mixing layer is initially within the primary contamination, $T_{cv}(0) < d_{mix} < T_{cv}(0) + T_{pc}(0)$:

$$f_{vm}(t = 0) = 1 - \frac{T_{cv}(0)}{d_{mix}} \tag{G.14}$$

If the mixing layer penetrates through the entire primary contamination at time 0, $d_{mix} \geq T_{cv}(0) + T_{pc}(0)$:

$$f_{vm}(t = 0) = \frac{T_{pc}(0)}{d_{mix}} \tag{G.15}$$

It is easier to compute and to understand the expression for the volume fraction of the material from the primary contamination in the mixing layer as a function of the depth to which the mixing layer penetrates beyond the boundary between the cover and the primary contamination. The initial conditions in terms of time can be translated to be in terms of the depth of penetration:

$$f_{vm}\left(d_{mix}^{pc} = d_{mix}^{pc\ ini}\right) = f_{vm}(t = 0) \tag{G.16}$$

where

d_{mix}^{pc} = depth of penetration of the mixing layer below the top of the primary contamination (m), and

$d_{mix}^{pc\ ini}$ = initial penetration of the mixing layer below the top of the primary contamination (m).

When the mixing layer is within the primary contamination, the expression for the conservation of volume fraction of material from the primary contamination in the mixing layer is obtained by equating the rate at which that volume fraction changes with the depth of penetration, to the difference between the volume fractions entering and exiting the mixing layer, distributed over the depth of the mixing layer:

$$\frac{df_{vm}\left(d_{mix}^{pc}\right)}{dd_{mix}^{pc}} = \frac{1 - f_{vm}\left(d_{mix}^{pc}\right)}{d_{mix}} \tag{G.17}$$

The volume fraction of the material from the primary contamination in the mixing layer is determined by solving the conservation equation with the appropriate initial condition as follows:

$$\frac{df_{vm}\left(d_{mix}^{pc}\right)e^{\frac{d_{mix}^{pc}}{d_{mix}}}}{dd_{mix}^{pc}} = \frac{e^{\frac{d_{mix}^{pc}}{d_{mix}}}}{d_{mix}}$$

$$f_{vm}(d_{mix}^{pc})e^{\frac{d_{mix}^{pc}}{d_{mix}}} - f_{vm}\left(d_{mix}^{pc\ ini}\right)e^{\frac{d_{mix}^{pc\ ini}}{d_{mix}}} = e^{\frac{d_{mix}^{pc}}{d_{mix}}} - e^{\frac{d_{mix}^{pc\ ini}}{d_{mix}}}$$

$$f_{vm}(d_{mix}^{pc}) = 1 - \left[1 - f_{vm}\left(d_{mix}^{pc\ ini}\right)\right]e^{-\frac{d_{mix}^{pc}-d_{mix}^{pc\ ini}}{d_{mix}}} \tag{G.18}$$

As the cover erodes, the mixing layer penetrates deeper into the primary contamination, and the volume fraction increases asymptotically toward unity as long as the bottom of the mixing zone stays within the primary contamination. Eventually, the cover and primary contamination will erode so that their combined thickness will be equal to the depth of the mixing zone. Thereafter, the bottom of the mixing zone moves out of the primary contamination and into the underlying layers and the volume fraction will decrease. The volume fraction is then computed under the assumption that the underlying soil is uncontaminated. This assumption is necessary because the code currently does not calculate the concentration profile in the layers of soil that underlie the primary contamination. Under this assumption, the peak value of the volume fraction of the primary contamination in the mixing layer will occur when the sum of the thicknesses of the cover and primary contamination equals the depth of mixing. The peak value of the volume fraction of the primary contamination in the mixing layer and the depth of penetration at which this occurs are given below.

If the mixing layer is initially within the cover, $T_{cv}(0) \geq d_{mix}$:

$$f_{vm}^{peak}\left(d_{mix}^{pc\ peak} = T_{pc}(0)\right) = 1 - e^{-\frac{T_{pc}(0)}{d_{mix}}} \tag{G.19}$$

If the mixing layer is initially within the primary contamination, $T_{cv}(0) < d_{mix} < T_{cv}(0) + T_{pc}(0)$:

$$f_{vm}^{peak}\left(d_{mix}^{pc\ peak} = T_{pc}(0)\right) = 1 - \frac{T_{cv}(0)}{d_{mix}}e^{-\frac{T_{cv}(0)+T_{pc}(0)-d_{mix}}{d_{mix}}} \tag{G.20}$$

If the mixing layer penetrates through the entire primary contamination at time 0, $d_{mix} \geq T_{cv}(0) + T_{pc}(0)$:

$$f_{vm}^{peak}\left(d_{mix}^{pc\ peak} = d_{mix} - T_{cv}(0)\right) = \frac{T_{pc}(0)}{d_{mix}} \tag{G.21}$$

where

f_{vm}^{peak} = peak volume fraction of the material from the primary contamination in the mixing layer, and

$d_{mix}^{pc\ peak}$ = depth of penetration of the mixing layer below the top of the primary contamination when the peak volume fraction occurs (m).

The expression for the conservation of volume fraction of material from the primary contamination in the mixing layer after the occurrence of the peak is obtained by equating the rate at which that volume fraction changes with the depth of penetration, to the difference between the volume fractions entering and exiting the mixing layer, distributed over the depth of the mixing layer:

$$\frac{df_{vm}(d_{mix}^{pc})}{dd_{mix}^{pc}} = \frac{0 - f_{vm}(d_{mix}^{pc})}{d_{mix}} \tag{G.22}$$

The volume fraction of the material from the primary contamination in the mixing layer is determined by solving the conservation equation with the appropriate initial condition as follows:

$$\frac{df_{vm}(d_{mix}^{pc})e^{\frac{d_{mix}^{pc}}{d_{mix}}}}{dd_{mix}^{pc}} = 0$$

$$f_{vm}(d_{mix}^{pc})e^{\frac{d_{mix}^{pc}}{d_{mix}}} = f_{vm}\left(d_{mix}^{pc\ peak}\right)e^{\frac{d_{mix}^{pc\ peak}}{d_{mix}}}$$

$$f_{vm}(d_{mix}^{pc}) = f_{vm}\left(d_{mix}^{pc\ peak}\right)e^{-\frac{d_{mix}^{pc}-d_{mix}^{pc\ peak}}{d_{mix}}} \tag{G.23}$$

G.1.8 Mass of Material Eroded from the Location of Primary Contamination

The rate at which the material is eroded from the mixing layer at the location of the primary contamination is computed using the following expression:

$$m_{ro}^{ss}(t) = \frac{\rho_b^{mix}(t)}{\rho_b^{pc}}\mathcal{E}(t)A10^6\rho_b^{pc} \tag{G.24}$$

where

$m_{ro}^{ss}(t)$ = rate at which material is eroded from the surface soil at the location of the primary contamination by runoff at time t (g/yr),

$\frac{\rho_b^{mix}(t)}{\rho_b^{pc}}$ = ratio of the dry bulk densities of the mixing layer and the primary contamination,

$\mathcal{E}(t)$ = rate of erosion at the location of the primary contamination at time t (m/yr),

$\mathcal{E}(t) = \mathcal{E}_{cv}$ when $t < t_{cv}$,

$\mathcal{E}(t) = \mathcal{E}_{pc}$ when $t \geq t_{cv}$,

t_{cv} = time at which the cover is completely eroded (yr),

$\mathcal{E}_{cv}$ = erosion rate of the cover (m/yr),

$\mathcal{E}_{pc}$ = erosion rate of the primary contamination (m/yr),

A = horizontal area of the primary contamination (m²),

10^6 = to convert m³ to (cm)³, and

ρ_b^{pc} = dry bulk density of the primary contamination (g/[cm]³).

The rate at which the material is eroded from the primary contamination is computed using the following expression:

$$m_{ro}^{pc}(t) = f_{vm}(t)\mathcal{E}(t)A10^6\rho_b^{pc} \tag{G.25}$$

where

$m_{ro}^{pc}(t)$ = rate at which material is eroded from the primary contamination by runoff at time t (g/yr), and

$f_{vm}(t)$ = volume fraction of the material from the primary contamination in the mixing layer at time t.

G.1.9 Computation of Physical Properties at Calculation Times

The expressions for the thickness of the cover (Section G.1.3), of the primary contamination (Section G.1.4), and of the three layers of the mixing model (Section G.1.5) for the dry bulk density of the mixing layer (Section G.1.6), for the volume fraction from the primary contamination in the mixing layer (Section G.1.7), and the rates at which material is eroded from the mixing layer and the primary contamination (Section G.1.8) are evaluated analytically at each calculation time (Section E.1). The intermediate output file, CZTHICK3.DAT, contains some of these calculated values. This file has five columns of data:

- The first column lists the calculation times in years. The next four columns contains information about four of the computed quantities at these calculation times.

- The second column lists the concentration of the radionuclides in the surface mixing layer of the soil as a fraction of the concentration in the physically undisturbed primary contamination.

- The third column lists the thickness of the clean cover in meters.

- The fourth column lists the thickness of the contaminated mixing layer in meters.

- The fifth column lists the thickness of the physically undisturbed (unmixed) thickness of the primary contamination.

The other intermediate files described in Section G.16, contain some of the other values described in the previous sections.

G.1.10 Horizontal Dimensions of the Primary Contamination

The horizontal dimensions of the primary contamination are used in the calculations of atmospheric transport (Appendix I.10), groundwater transport (Appendix H), and external exposure from the primary contamination (Appendix B). The area calculated from the horizontal dimensions is used in the calculation of all exposure pathways. The conceptualization of the primary contamination is different for different calculations:

- It is conceptualized as a rectangle; the dimensions and orientation, with respect to the north, are specified in the inputs for atmospheric transport calculations. The sides of this rectangle must be parallel to the sides of the rectangles defining the offsite farmed lands, the catchment, and the surface water body (Figure I-4).

- It is also conceptualized as being a rectangle for groundwater transport calculations (Figure H-1). This rectangle must have one pair of sides parallel to the direction of groundwater flow. If the direction of groundwater flow is not parallel to either pair of sides used to define the rectangular shape for air

transport, then the shapes used for groundwater transport will be different from the one used for air transport. The code uses the area computed using the dimensions specified for the air transport calculations and the specified length parallel to the aquifer flow to determine the width perpendicular to the aquifer flow.

- The rectangular shape specified for the air transport calculations are used for external exposure calculations unless the user chooses to specify a circular shape or a polygonal shape. If a circular shape is specified, the code will calculate the radius of the circle based on the area computed using the dimension specified for the air transport conceptualizations. If a polygonal shape is defined in the interface, the interface will estimate the area of the polygon. The polygon can have as many sides as necessary to approximate the shape of the actual contamination. The area of the polygon defined in the interface should be as close as possible to the area implied by the dimensions specified for air transport.

Unless the primary contamination is circular and the receptor is concentric, the code will calculate the shape factor for external exposure in the interface by finding the fractions of the areas of a set of 16 annular regions, concentric with the receptor, that are covered by the primary contamination. It does this by counting the pixels in each annular ring that is in the figure defining the primary contamination.

If the primary contamination is not circular or if the receptor is not at the center of that circular region when probabilistic analysis is performed on the dimensions of the primary contamination, the code will assume a rectangular primary contamination and will calculate the shape factors analytically. If probabilistic analysis is performed on the dimensions of the primary contamination when the primary contamination is circular and the receptor is concentric, the code will recalculate the radius of a circular primary contamination to correspond to the area computed using the dimension of the primary contamination, and it will perform calculations assuming that the receptor is concentric.

G.2   Modeling Radionuclide-Bearing Material Surrounded by Initially Clean Soil

Version 4 of the code allows explicit specification of the properties of a radionuclide-bearing material and the initially clean soil that surrounds it in the primary contamination. The code computes the properties of the combined media in the primary contamination as follows.

Dry bulk density of the combined medium:

$$\rho_b^{eq} = \rho_b^{pc} + \left[M_{bm} 10^3 - \rho_b^{pc} V_{bm} 10^6 \right] / \left[A\, T_{pc}(0) 10^6 \right] \tag{G.26}$$

where

ρ_b^{eq} = dry bulk density of the combined medium in the primary contamination (g/[cm]^3),

ρ_b^{pc} = dry bulk density of the initially clean soil in the primary contamination surrounding the radionuclide-bearing material (g/[cm]^3),

M_{bm} = mass of the radionuclide-bearing material (kg),

10^3 = to convert kg to g,

V_{bm} = volume of the radionuclide-bearing material (m^3),

$$10^6 \quad = \quad \text{to convert m}^3 \text{ to (cm)}^3,$$
$$A \quad = \quad \text{area (horizontal footprint) of the primary contamination (m}^2\text{), and}$$
$$T_{pc}(0) \quad = \quad \text{thickness of the primary contamination at time 0 (m).}$$

Mass of initially clean soil in the primary contamination:

$$M_{ic} = \rho_b^{pc} 10^3 \left[A\, T_{pc}(0) - V_{bm} \right] \tag{G.27}$$

where

M_{ic} = mass of the initially clean soil in the primary contamination (kg) and
10^3 = to convert g/(cm)^3 to kg/m^3.

Linear distribution coefficient of the combined medium:

$$K_{d_i}^{eq} = \frac{K_{d_i}^{pc} M_{ic} + K_{d_i}^{bm} M_{bm}}{M_{ic} + M_{bm}} \tag{G.28}$$

where

$K_{d_i}^{eq}$ = linear distribution coefficient of radionuclide i in the combined medium in the primary contamination ([cm]^3/g),

$K_{d_i}^{pc}$ = linear distribution coefficient of radionuclide i, in the initially clean soil in the primary contamination surrounding the radionuclide-bearing medium ([cm]^3/g), and

$K_{d_i}^{bm}$ = linear distribution coefficient of radionuclide i, in the radionuclide-bearing medium ([cm]^3/g).

The linear distribution coefficient and the dry bulk density of the combined medium in the primary contamination are used to model the transfer to the aqueous phase and the transport in the primary contamination.

Activity concentration of the radionuclide in the primary contamination:

$$s_i = \frac{s_i^{bm} M_{bm} 10^3}{\rho_b^{pc} A\, T_{pc}(0) 10^6} \tag{G.29}$$

where

s_i = activity concentration expressed in terms of the primary contamination (Activity/g) and

s_i^{bm} = activity concentration expressed in terms of the radionuclide-bearing material in the primary contamination (Activity/g).

G.3   <u>Concentration in Primary Contamination</u>

In order to model releases that are delayed and distributed over time (Section 2.5), and the advective-dispersive transport in the primary contamination, the code conceptualizes the inventory of each radionuclide in four categories or phases. The part of the inventory that is protected from release by engineered barriers is termed "release immune." As the engineered barriers deteriorate over time, some or all of the radionuclides can change from release immune

to "release susceptible." The change from release immune to release susceptible can occur either instantaneously, or gradually over time. Depending on the transfer mechanism specified for the radionuclide, a fraction of the release susceptible inventory will transfer to the aqueous phase over part or all of the transport length of the primary contamination. Thus, part of the inventory will be in the aqueous phase. If the primary contamination is a mixture of a contaminated medium and initially clean medium, the radionuclides in the aqueous phase can be adsorbed on the initially clean medium according to the distribution coefficient specified for the primary contamination. Thus, part of the inventory can be in the adsorbed phase.

Both the activity concentration of the release immune form (Section G.4) and the activity concentration of the release susceptible form (Section G.10) are dependent on radiological transformations and on the fraction of radionuclide-bearing material that is susceptible to release (Section G.9). The concentration of the release-susceptible form also depends on the transfer to the aqueous phase (Section G.11). The three transfer mechanisms available in the code are described and represented mathematically in Sections G.6, G.7, and G.8. Diffusive transport out of the radionuclide-bearing material into the surrounding soil in the primary contamination is developed in Section G.12. The release out of the primary contamination is the result of the transport of the radionuclides from where they are transferred to the aqueous phase to the down gradient edge of the primary contamination. The expressions for the release out of the primary contamination are outlined in Section G.13. These expressions are dependent on the extent to which the primary contamination is submerged (Section G.5).The expressions that can be used to compute the adsorbed concentration profile in the primary contamination are described in Section G.14. The releases from the surface soil to the atmosphere and to runoff are described in Section G.15. The intermediate output of the source module are discussed in Section G.16. Section G.17 describes methods to verify that the code maintains activity balance of radionuclides. Section G.18 outlines the procedure for overriding the source module.

G.4   Release-Immune Concentration

The inventory of the radionuclides in the release immune category is affected by the radiological transformations and by changes from the release immune form to the release-susceptible form. The code expresses the activity concentration in terms of the mass of the primary contamination. The activity concentration of the radionuclides in the release-immune form in the primary contamination is obtained by considering the loss of the radionuclides by radiological transformations (decay), the gain due to radiological transformations of the parent radionuclide (ingrowth), and then adjusting for change to the release-susceptible form. The activity concentration balance of the radionuclide in the primary contamination assuming no changes to release susceptible form is as follows:

$$\frac{ds_{i,m}(t)}{dt} + \lambda_i s_{i,m}(t) = \lambda_i s_{i-1,m}(t) \tag{G.30}$$

where

$\quad s_{i,m}(t)$ = activity concentration of radionuclide i of transformation thread m at time t in the primary contamination if it were all release immune (Activity/g) and

$\quad\quad \lambda_i$ = radiological transformation constant of radionuclide i (1/yr).

The activity concentration of the first radionuclide of the transformation thread m in the primary contamination assuming no changes to release susceptible form is obtained by integrating the activity balance equation:

$$\frac{ds_{1,m}(t)}{dt} + \lambda_1 s_{1,m}(t) = 0 \tag{G.31}$$

with the initial condition of $s_{1,m}(0) = f_m^t s_1(0)$,

where

f_m^t = thread fraction (Section E.4) of thread m of the initially present radionuclide 1 and

$s_1(0)$ = initial concentration of the initially present radionuclide 1 (Activity/g).

This can be integrated as follows,

$$\frac{de^{\lambda_1 t} s_{1,m}(t)}{dt} = 0$$

$$s_{1,m}(t) = f_m^t s_1(0)e^{-\lambda_1 t} \tag{G.32}$$

The activity concentration of the second radionuclide in the transformation thread m in the primary contamination assuming no changes to release susceptible form is obtained by integrating the activity balance equation:

$$\frac{ds_{2,m}(t)}{dt} + \lambda_2 s_{2,m}(t) = \lambda_2 s_{1,m}(t) \tag{G.33}$$

with the initial condition of $s_{2,m}(0) = 0$, and with $s_{1,m}(t) = f_m^t s_1(0)e^{-\lambda_1 t}$.

$$\frac{de^{\lambda_2 t} s_{2,m}(t)}{dt} = \lambda_2 f_m^t s_1(0)e^{(\lambda_2 - \lambda_1)t}$$

$$e^{\lambda_2 t} s_{2,m}(t) = \frac{\lambda_2}{\lambda_2 - \lambda_1} f_m^t s_1(0)\left[e^{(\lambda_2 - \lambda_1)t} - 1\right]$$

$$s_{2,m}(t) = \frac{\lambda_2}{\lambda_2 - \lambda_1} f_m^t s_1(0)\left[e^{-\lambda_1 t} - e^{-\lambda_2 t}\right]$$

$$s_{2,m}(t) = \sum_{k=1}^{2} B_2^k e^{-\lambda_k t} \tag{G.34}$$

with $B_1^1 = f_m^t s_1(0)$, $B_2^1 = \frac{\lambda_2 B_1^1}{\lambda_2 - \lambda_1}$ and $B_2^2 = -B_2^1$.

The activity concentration of the radionuclide i in the transformation thread m in the primary contamination assuming no changes to release susceptible form is obtained by integrating the activity balance equation:

$$\frac{ds_{i,m}(t)}{dt} + \lambda_i s_{i,m}(t) = \lambda_i s_{i-1,m}(t)$$

with the initial condition of $s_{i,m}(0) = 0$, and with $s_{i-1,m}(t) = \sum_{k=1}^{i-1} B_{i-1}^k e^{-\lambda_k t}$, where $B_1^1 = f_m^t s_1(0)$, $B_j^k = \frac{\lambda_j B_{j-1}^k}{\lambda_j - \lambda_k}$ for $k < j \le i - 1$, and $B_j^j = -\sum_{k=1}^{j-1} B_j^k$ for $1 < j \le i - 1$.

$$\frac{de^{\lambda_i t} s_{i,m}(t)}{dt} = \lambda_i \sum_{k=1}^{i-1} B_{i-1}^k e^{(\lambda_i - \lambda_k)t}$$

$$e^{\lambda_i t} s_{i,m}(t) = \lambda_i \sum_{k=1}^{i-1} \frac{B_{i-1}^k}{\lambda_i - \lambda_k} \left[e^{(\lambda_i - \lambda_k)t} - 1 \right]$$

$$s_{i,m}(t) = \lambda_i \sum_{k=1}^{i-1} \frac{B_{i-1}^k}{\lambda_i - \lambda_k} \left[e^{-\lambda_k t} - e^{-\lambda_i t} \right]$$

$$s_{i,m}(t) = \sum_{k=1}^{i-1} \frac{\lambda_i B_{i-1}^k}{\lambda_i - \lambda_k} e^{-\lambda_k t} - e^{-\lambda_i t} \sum_{k=1}^{i-1} \frac{\lambda_i B_{i-1}^k}{\lambda_i - \lambda_k}$$

$$s_{i,m}(t) = \sum_{k=1}^{i} B_i^k e^{-\lambda_k t} \tag{G.35}$$

with $B_1^1 = f_m^t s_1(0)$, $B_j^k = \frac{\lambda_j B_{j-1}^k}{\lambda_j - \lambda_k}$ for $0 < k < j \le i$ and $B_j^j = -\sum_{k=1}^{j-1} B_j^k$ for $1 < j \le i$.

The activity concentration of the radionuclides in the release-immune form averaged over the primary contamination is obtained by multiplying the activity concentration of the radionuclides in the primary contamination assuming no changes to release-susceptible form as computed above and the release-immune fraction of the inventory at time t. The expression is of the same form as above but starts with a different initial coefficient, B_1^1:

$$s_{i,m}^{im}(t) = \sum_{k=1}^{i} B_i^k e^{-\lambda_k t} \tag{G.36}$$

with
$$B_1^1 = [1 - f_1^{su}(t)] f_m^t s_1(0),$$
if $0 < k < j \le i$, $B_j^k = \frac{\lambda_j B_{j-1}^k}{\lambda_j - \lambda_k}$
if $1 < j \le i$, $B_j^j = -\sum_{k=1}^{j-1} B_j^k$

where
$s_{i,m}^{im}(t)$ = release-immune activity concentration of radionuclide i of transformation thread m at time t in the primary contamination (Activity/g), and
$f_1^{su}(t)$ = fraction of material bearing radionuclide 1 that is release susceptible at time t.

G.5 Submerged Source

As illustrated in Chapter 2, the code can model a primary contamination that is entirely above the water table, one that straddles the water table, or one that is submerged with the top of the primary contamination at the water table. The release from the primary contamination depends on the flow of water through the primary contamination. The schematic for a contamination that straddles the water table in Figure G-2; the schematics for the other two cases can be inferred by using submerged fractions, f_{sub}, of 0 and 1.
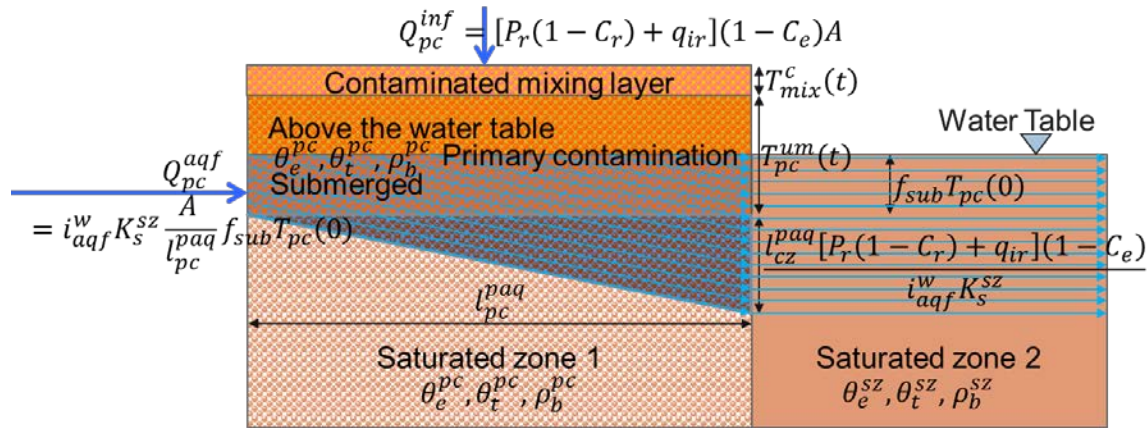
Figure G-2 Schematic of a Primary Contamination that Straddles the Water Table

The flow that enters through the top of the primary contamination is as follows:

$$Q_{pc}^{inf} = IA \qquad (G.37)$$

where

Q_{pc}^{inf} = rate at which water enters the primary contamination from the top (m³/yr) and
I = rate at which water infiltrates the primary contamination (m/yr).

The rate at which the water infiltrates from the top is determined by considering an annual average water balance which yields the expression,

$$I = [P_r(1 - C_r) + q_{ir}](1 - C_e) \qquad (G.38)$$

where

P_r = annual precipitation rate (m/yr),
C_r = runoff coefficient,
q_{ir} = amount of irrigation applied annually to the primary contamination (m/yr),
C_e = evapotranspiration coefficient, and
A = area (horizontal footprint) of the primary contamination (m²).

The flow that enters through the side of the submerged portion of the primary contamination is as follows:

$$Q_{pc}^{aqf} = i_{aqf}^w K_s^{sz} f_{sub} T_{pc}(0) \, A/l_{pc}^{paq} \qquad (G.39)$$

where

Q_{pc}^{aqf} = rate at which water enters the submerged portion of the primary contamination from the side (m³/yr),

i_{aqf}^{w} = hydraulic gradient in the aquifer from the primary contamination to the well (m/m),

K_s^{sz} = saturated hydraulic conductivity of the saturated zone/aquifer (m/yr),

f_{sub} = fraction of the primary contamination that is below the water table,

$T_{pc}(0)$ = initial thickness of the primary contamination (m),

A = area (horizontal footprint) of the primary contamination (m²), and

l_{pc}^{paq} = length of the primary contamination parallel to the aquifer flow (m).

The total flow rate through the primary contamination, in m³/yr, is as follows:

$$Q_{pc} = Q_{pc}^{inf} + Q_{pc}^{aqf} \tag{G.40}$$

The code computes the releases from both portions—the submerged portion and the part above the water table—of the primary contamination. The equivalent thickness of the primary contamination and the equivalent thickness of the part of the primary contamination above the water tables are given by:

$$T_{pc}^{eq}(t) = f_{vm}(t)T_{mix}^{c}(t) + T_{pc}^{um}(t)$$
$$T_{pc}^{eq,awt}(t) = T_{pc}^{eq}(t) - f_{sub}T_{pc}(0) \geq 0 \tag{G.41}$$

where

$T_{pc}^{eq}(t)$ = equivalent thickness of the contaminated mixing layer and the undisturbed primary contamination (m),

$T_{pc}^{eq,awt}(t)$ = equivalent thickness of the contaminated mixing layer and the undisturbed primary contamination above the water table (m),

$f_{vm}(t)$ = volume fraction of the material from the primary contamination in the mixing layer at time t,

$T_{mix}^{c}(t)$ = thickness of the contaminated mixing layer at time t (m),

$T_{pc}^{um}(t)$ = the thickness of the physically undisturbed primary contamination at time t (m),

f_{sub} = fraction of the primary contamination that is submerged, and

$T_{pc}(0)$ = initial thickness of the primary contamination.

The mass of the solids in the part of the primary contamination that is above the water table is as follows:

$$M_{pc}^{awt}(t) = 10^6\, AT_{pc}^{eq,awt}(t)\rho_b^{pc} \tag{G.42}$$

where

$M_{pc}^{awt}(t)$ = mass of the solids in the primary contamination that is above the water table at time t (g),

10^6 = to convert from m³ to (cm)³, and

ρ_b^{pc} = dry bulk density of the primary contamination (g/[cm]³).

The mass of the solids in the part of the primary contamination that is submerged is as follows:

$$M_{pc}^{sub} = 10^6 \, A f_{sub} T_{pc}(0) \rho_b^{pc} \tag{G.43}$$

where

M_{pc}^{sub} = mass of the solids in the primary contamination that is submerged (g),
10^6 = to convert from m³ to (cm)³,
ρ_b^{pc} = dry bulk density of the primary contamination (g/[cm]³).

The total mass of the primary contamination at time t in grams is as follows:

$$M_{pc}(t) = M_{pc}^{awt}(t) + M_{pc}^{sub} \tag{G.44}$$

G.6   Equilibrium Desorption Transfer to the Aqueous Phase

The equilibrium desorption is characterized in RESRAD-OFFSITE by a linear distribution coefficient of the radioisotope. At equilibrium, the concentrations in the aqueous phase and in the release susceptible form are related to the linear distribution coefficient as follows:

$$K_{d_i}^{pc} = s_{i,m}^{su}(t)/s_{i,m}^{aq}(t) \tag{G.45}$$

where

$s_{i,m}^{su}(t)$ = release-susceptible activity concentration of radionuclide i of transformation thread m at time t in the primary contamination (Activity/g),
$s_{i,m}^{aq}(t)$ = aqueous activity concentration of radionuclide i of transformation thread m at time t in the primary contamination (Activity/[cm]³), and
$K_{d_i}^{pc}$ = the linear distribution coefficient of radionuclide i, in the primary contamination ([cm]³/g).

As the water enters the primary contamination at the up gradient edge, the radionuclides in the radionuclide-bearing material will desorb into the infiltrating water. If the desorption is rapid, the infiltrating water will attain the equilibrium concentration, $s_{i,m}^{aq}(t) = s_{i,m}^{su}(t)/K_{d_i}^{pc}$, before it travels far into the primary contamination. Although there can be no net transfer of radionuclides from the radionuclide-bearing materials into the infiltrating water that is already at the equilibrium concentration, equal quantities of radionuclides can be exchanged between the infiltrating water already at the equilibrium concentration and the radionuclide-bearing material through which it continues to flow.

The rate of transfer from the release susceptible form to the infiltrating water is as follows:

$$T_{i,m}^{su \to aq}(t) = 10^6 Q_{pc} \, s_{i,m}^{aq}(t) = 10^6 Q_{pc} \, s_{i,m}^{su}(t)/K_{d_i}^{pc} \tag{G.46}$$

where

$T_{i,m}^{su \to aq}(t)$ = rate of transfer of radionuclide i of transformation thread m from the release-susceptible form to the aqueous phase (Activity/yr),
Q_{pc} = rate at which water enters the primary contamination (m³/yr), and
10^6 = to convert from m³ to (cm)³.

The code assumes that the adsorption-desorption equilibrium is attained instantaneously; thus the assumption is that the infiltrating water will attain the equilibrium concentration as soon as it enters the up-gradient edge of the primary contamination. The concentration profiles of the release-susceptible form and the aqueous phase, of the radionuclide that follows an equilibrium desorption transfer, will not be uniform over the transport length of the primary contamination, the depth in the case of a primary contamination that is above the water table. There will be a "clean" region at the up-gradient part from which the radionuclide have been desorbed and the depth of contamination will decrease with time. The concentration of the radionuclide in the water and in the release-susceptible form will be uniform over most of the depth that is contaminated at that time. There will a zone of transition at the up-gradient edge of the contamination due to dispersion. The transition zone will be wider if the equilibrium is not attained instantaneously. A schematic of the change in the concentration profile with time is shown in Figure G-3.
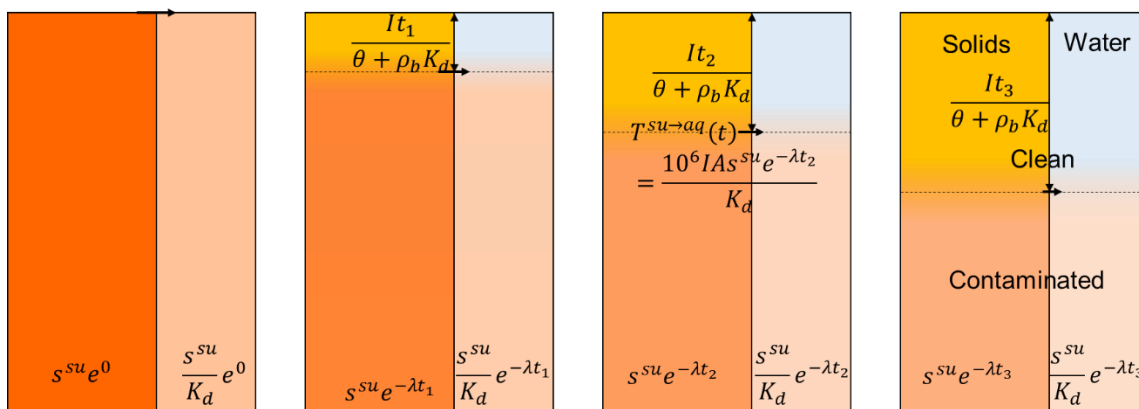
Figure G-3 Equilibrium Desorption Transfer and Release

Analytically modeling this release as described above would not have been possible if not for the realization that the initial state and the subsequent release from that state as described above could be achieved by starting with a different scenario that can be modeled analytically. Imagine an instantaneous injection of the total release susceptible inventory of the radionuclide through an infinite number of injection points distributed uniformly over the primary contamination as shown in Figure G-4. Because of the assumption that equilibrium is attained instantaneously, the radionuclide will be distributed between the solids and water in the primary contamination in the same manner it would have if the radionuclide had initially been in the radionuclide-bearing material.

Figure G-4 shows three panels labeled $t = t_{rel} - \delta t$, $t = t_{rel}$, and $t = t_{rel} + \delta t$. The middle panel contains the annotation:

$$Injection = \rho_b V s^{su} + \theta V \frac{s^{su}}{K_d}$$

The right panel shows s^{su} and $\frac{s^{su}}{K_d}$.
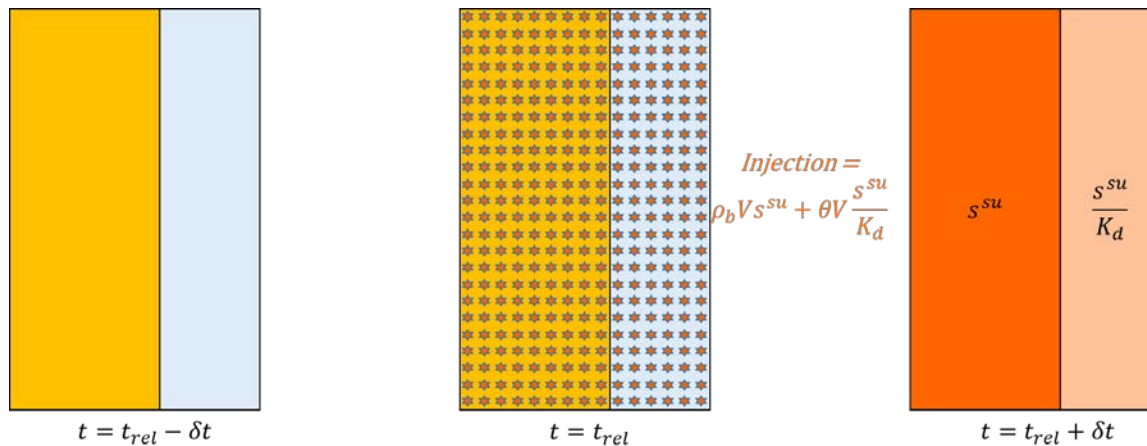
Figure G-4 Instantaneous, Uniform Injection of Releasable Inventory over the Primary Contamination

The temporal variation of the release-susceptible concentration of any radionuclide undergoing equilibrium desorption transfer is not currently computed by the code because (a) it is not necessary to compute the release of that radionuclide to infiltration when using the imaginary instantaneous injection scenario to model the release and (b) the release-susceptible concentration in the primary contamination is not uniform over the primary contamination. Therefore, the code cannot compute the releases to the atmosphere and to erosion of the release-susceptible form of radionuclides that are undergoing equilibrium desorption transfer.

One other consequence of not calculating the profile of the release-susceptible concentration when using the imaginary instantaneous injection scenario to model the release of a radionuclide undergoing equilibrium desorption transfer is that the concentration profiles of the progeny that grow from the release-susceptible form of that radionuclide are also not computed. They are instead modeled as ingrowing while the parent radionuclide is in transit through the primary contamination. In effect, the progeny that would have ingrown from the release-susceptible form of a parent being transferred under equilibrium desorption are also transferred according their equilibrium desorption characteristics.

Section G.14 discusses the expressions that can be used to compute the sum of the release-susceptible concentration, the adsorbed concentration, and the aqueous concentration. These would need to be computed at different locations along the transport length because the concentration is not uniform. Because these three concentrations are modeled as being related by linear distributions coefficients, their profiles along the direction of transport will be identical.

G.7   First-Order Rate-Controlled Transfer to the Aqueous Phase

When the transfer is first-order rate controlled, the rate of transfer of the radionuclide from the release immune phase to the soil moisture is proportional to the release-susceptible inventory. The specified leach rate coefficient is the proportionality constant:

$$T_{i,m}^{su \to aq}(t) = \mu_i M_{pc}(t) s_{i,m}^{su}(t) \tag{G.47}$$

where

$T_{i,m}^{su \rightarrow aq}(t)$ = rate of transfer of radionuclide i of transformation thread m from the release-susceptible form to the aqueous phase at time t (Activity/yr),

μ_i = leach rate coefficient of the radionuclide i (1/yr), and

$M_{pc}(t)$ = mass of the primary contamination at time t (g).

The radionuclide transfers uniformly over the transport length of the primary contamination. Therefore, the release-susceptible concentration remains uniform over the length of transport, the depth for a primary contamination that is above the water table (Figure G-5). The aqueous concentration will not be uniform along the length of transport because more radionuclides are transferred to the infiltrating water while it moves through the primary contamination. If the primary contamination is a mixture of contaminated media and initially clean soil, the concentration profile of the adsorbed concentration will be identical to that of the aqueous concentration; it too will not be uniform.
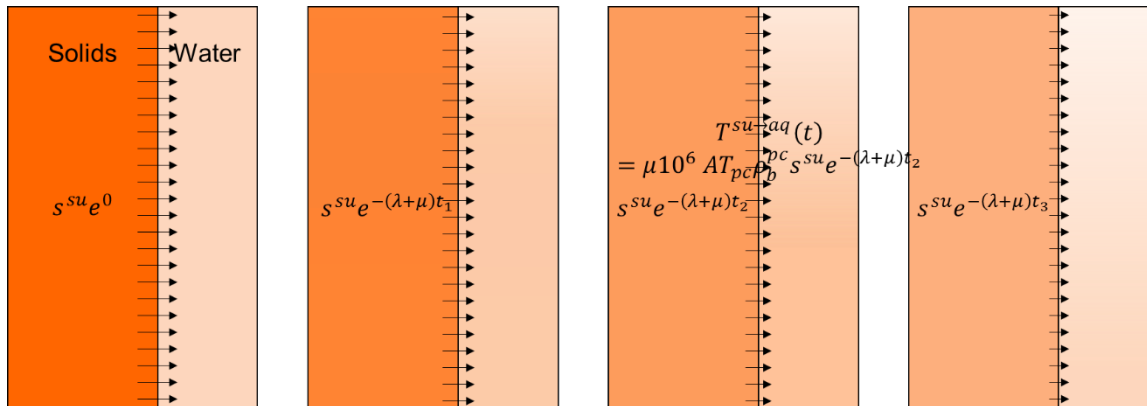
Figure G-5   First-Order Rate-Controlled Transfer and Release

G.8   Equilibrium Solubility Transfer to the Aqueous Phase

The equilibrium dissolution is characterized in RESRAD-OFFSITE by the soluble concentration of the element. Although the soluble concentration applies to the sum of all isotopes of the element, both stable and radioactive, the code does not model stable isotopes. The code apportions the soluble concentration specified for the element between each radioisotope of the element in every transformation thread in proportion to the releasable concentration of the radioisotope in that thread as follows:

$$s_{i,m}^{aq}(t) = SA_i \frac{\dfrac{s_{i,m}^{su}(t)}{SA_i}}{\sum_{istopes\ of\ the\ element_i} \dfrac{s_{i,m}^{su}(t)}{SA_i}} c_{element_i}^{soluble}(t) \qquad (G.48)$$

$$= SA_i f_{i,m}^{su}(t) c_{element_i}^{soluble}(t)$$

where

$s_{i,m}^{aq}(t)$ = activity concentration of radionuclide i of transformation thread m at time t in the aqueous phase of the primary contamination (Activity/L),

$$SA_i \quad = \quad \text{specific activity of radioisotope } i \text{ (Activity/g atomic weight),}$$

$s_{i,m}^{su}(t) \quad = \quad$ release-susceptible activity concentration of radionuclide i of transformation thread m at time t in the primary contamination (Activity/g),

$\Sigma_{istopes\ of\ the\ element_i} \quad = \quad$ summation over all isotopes of the element of radionuclide i,

$c_{element_i}^{soluble}(t) \quad = \quad$ soluble concentration specified for the element of radioisotope i, at time t (g atomic weight/L),

$f_{i,m}^{su}(t) \quad = \quad$ releasable isotopic fraction of radionuclide i of transformation thread m at time t, on a g atomic weight basis, and

$$f_{i,m}^{su}(t) = \frac{s_{i,m}^{su}(t)}{SA_i} \bigg/ \Sigma_{istopes\ of\ the\ element_i} \frac{s_{i,m}^{su}(t)}{SA_i}.$$

If there is only one isotope of the element at the site, the concentrations in the aqueous phase are independent of the concentration of the release-susceptible phase.

As the water enters the primary contamination at the up-gradient edge, the radionuclides in the radionuclide-bearing material will dissolve into the infiltrating water. The concentration in the water increases as it travels along the primary contamination. As the concentration in the water increases, the rate at which the radionuclide precipitates out of the water and back onto the solid phase increases. When the concentration in the water reaches the soluble concentration apportioned to that isotope, the rates of dissolutions and precipitation will be equal. From that point onward, any reduction in the aqueous concentration of the radionuclide due to radiological transformations as it flows through the primary contamination is made up by dissolution along the transport length. The radionuclides will be removed primarily from the up-gradient edge of the primary contamination and the depth of contamination will decrease with time. If the solubility equilibrium is assumed to occur instantaneously, the concentration of the radionuclide in the water will be uniform over most of the depth that is contaminated at that time. There will a zone of transition at the up-gradient edge of the contamination due to dispersion (Figure G-6). The transition zone will be wider if equilibrium is not attained instantaneously. The rate of transfer from the release susceptible form to the infiltrating water at the up gradient edge is as follows:

$$T_{i,m}^{su \to aq}(t) = 10^3 Q_{pc}\, s_{i,m}^{aq}(t) = 10^3 Q_{pc} SA_i f_{i,m}^{su}(t) c_{element_i}^{soluble}(t) \qquad (G.49)$$

where

$T_{i,m}^{su \to aq}(t) \quad = \quad$ rate of transfer of radionuclide i of transformation thread m at time t from the release-susceptible form to the aqueous phase (Activity/yr),

$Q_{pc} \quad = \quad$ rate at which water flows into the primary contamination (m³/yr), and

$10^3 \quad = \quad$ to convert from m³ to L.
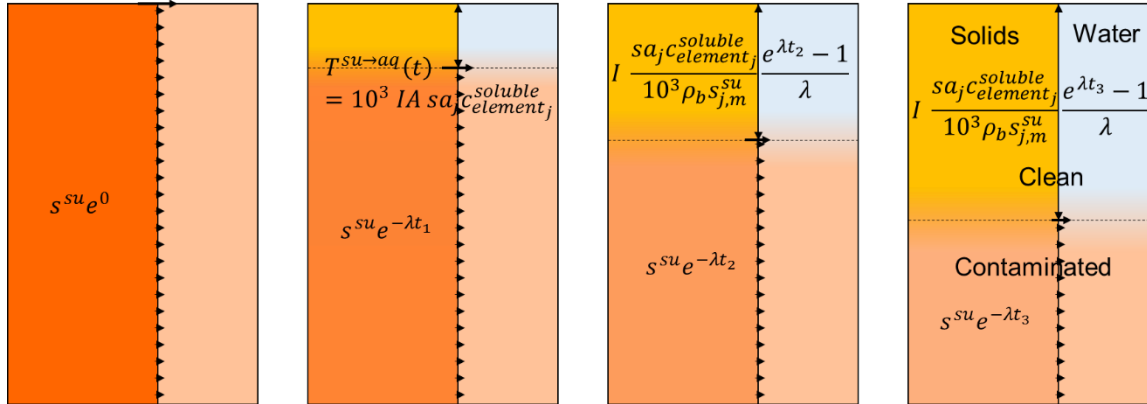
Figure G-6   Equilibrium Dissolution Transfer and Release

The RESRAD-OFFSITE code cannot model either of the situations described above, instantaneous or non-instantaneous equilibrium, analytically. In order to model the equilibrium solubility release analytically, RESRAD-OFFSITE assumes that the radionuclide is released uniformly over the transport length, and that the dissolution equilibrium is attained when the infiltrating water reaches the down gradient edge of the primary contamination. A schematic of the change in the concentration profile with time under these assumptions is shown in Figure G-7. This conceptualization can be modeled using the first-order rate-controlled release formulations with a leach rate coefficient that varies with time. The expression for estimating the leach rate coefficient to yield the soluble concentration at the down gradient edge of the primary contamination is given by the following equation:

$$\mu_{i,m}(t) = \frac{10^3 \, Q_{pc} SA_i c^{soluble}_{element_i}(t)}{10^6 A T^{eq}_{pc}(t) \rho^{pc}_b s^{su}_{i,m}(t)} \frac{\dfrac{s^{su}_{i,m}(t)}{SA_i}}{\sum_{isotopes \, of \, the \, element_i} \dfrac{s^{su}_{i,m}(t)}{SA_i}} \tag{G.50}$$

where $\mu_{i,m}(t)$ = the leach rate coefficient to be used for the radionuclide i of transformation thread m at time t to produce the releasable concentration at the down-gradient edge of the primary contamination (1/yr).

This estimate does not account for the effects of the travel time from where they are transferred to the aqueous phase, to the down-gradient edge of the primary contamination for two reasons. First, the travel time is likely to be small for radionuclides undergoing equilibrium dissolution transfer as a distribution coefficient of zero is used to model water transport of these radionuclides in the primary contamination. Second, this conceptualization does not apportion the soluble concentration of the element to the progeny produced during the transport of a parent radionuclide.

The leach rate coefficient to be used at each calculation time to produce the soluble concentration at the down-gradient edge of the primary contamination is determined iteratively because the releasable concentration of all the isotopes of an element at a calculation time depend on their leach rate coefficients at that time. RESRAD-OFFSITE uses the expression below to estimate the leach rate coefficient. Notice that the expression for the leach rate coefficient is the same for all isotopes of an element, a result that is to be expected because the

rate coefficient of a chemical reaction is the same for all isotopes. The code iterates five times when the equilibrium solubility options is selected for any radionuclide. The number of iterations is fixed in the code because it was found to be sufficient in the test runs:

$$\mu_{i,m}(t_2) = \frac{10^3 Q_{pc} c^{soluble}_{element_i}(t_2)}{10^6 \, T^{eq}_{pc}(t_2) A \rho^{pc}_b \left(\sum_{istopes \ of \ the \ element_i} \frac{s^{su}_{i,m}(t_2)}{SA_i} \right)^{previous \ iteration}} \qquad (G.51)$$

where $\mu_{i,m}(t_2)$ = the leach rate coefficient to be used for of the radionuclide i of transformation thread m at time t_2 to produce the releasable concentration at the down-gradient edge of the primary contamination (1/yr).
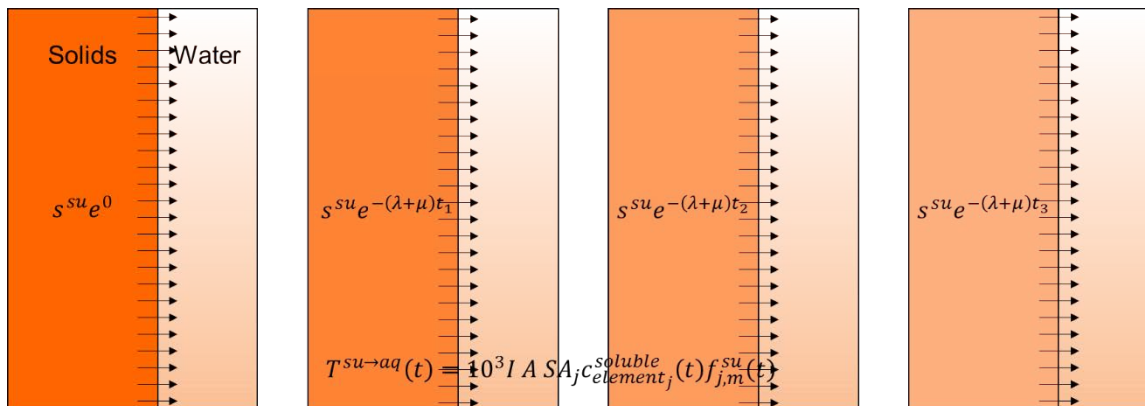
Figure G-7   Equilibrium Dissolution Transfer and Release Modeled by RESRAD-OFFSITE

G.9   Temporal Variation in Release Properties

The code models releases that are delayed and distributed over time using the releasable fractions specified at up to nine times. The releasable fraction is assumed to be zero before the first time; the releasable fraction is modeled as changing in a stepwise manner to the value specified at that time. The code accepts input on how the releasable fraction varies over the eight time intervals between those nine times. The releasable fraction can be specified to increase uniformly over a time interval, or it can be specified to change in a stepwise manner at the end of the time interval. The leach rate coefficient of a radionuclide and the soluble concentration of an element can be varied over time by specifying their values at the same nine times and the manner in which they change, stepwise or uniformly over time. The distribution coefficient and the diffusion coefficient cannot be changed over time.

The times at which the release properties are specified apply for all the radionuclides in the input file. Different sets of nine times for different radionuclides could not be accommodated, mainly because all radionuclides in a chain need to have properties that change at the same time and because soluble concentrations specified for an element apply to all isotopes of that element; which requires that all isotopes of an element undergoing equilibrium dissolution transfer have properties that change at the same times. If any of the nine times do not coincide with a calculation time, then the specified values are applied at the calculation time that immediately precedes it.

If the releasable fraction is specified to change in a stepwise fashion, this is modeled in the code as follows:

$$\Delta f_1^{su}(t_a) = f_1^{su}(t_l^r) - f_1^{su}(t_{l-1}^r)$$ (G.52)

where

$t_a \leq t_{l-1}^r < t_{a+1}$ and $t_b \leq t_l^r < t_{b+1}$

$\dot{f}_1^{su}(t_a, t_b)$ = rate at which the release-susceptible fraction of material bearing radionuclide 1 changes from calculation time t_a to calculation time t_b,

t_a = a^{th} calculation time that immediately precedes t_{l-1}^r (yr),

t_b = b^{th} calculation time that immediately precedes t_l^r (yr),

$f_1^{su}(t_l^r)$ = fraction of material bearing radionuclide 1 that is release-susceptible at time t_l^r, and

t_l^r = l^{th} time at which releasable fractions are specified (yr).

If the releasable fraction is specified to change uniformly over time, this is modeled in the code as follows:

$$\dot{f}_1^{su}(t_a, t_b) = \frac{f_1^{su}(t_l^r) - f_1^{su}(t_{l-1}^r)}{t_b - t_a} \text{ when } t_a < t_b$$ (G.53)

where

$t_a \leq t_{l-1}^r < t_{a+1}$ and $t_b \leq t_l^r < t_{b+1}$

$\dot{f}_1^{su}(t_a, t_b)$ = rate at which the release-susceptible fraction of material bearing radionuclide 1 changes from calculation time t_a to calculation time t_b,

t_a = a^{th} calculation time that immediately precedes t_{l-1}^r (yr),

t_b = b^{th} calculation time that immediately precedes t_l^r (yr),

$f_1^{su}(t_l^r)$ = fraction of material bearing radionuclide 1 that is release-susceptible at time t_l^r, and

t_l^r = l^{th} time at which releasable fractions are specified (yr).

If $t_a = t_b$, this is modeled as a stepwise change in the releasable fraction at t_a.

G.10   Concentration of Release-Susceptible Form

The inventory of the radionuclides in the release-susceptible category is affected by the radiological transformations, by changes from the release-immune form to the release-susceptible form, the transfer of radionuclides to the aqueous phase including the imaginary injections used to model the equilibrium desorption transfer and transport. The release susceptible concentrations of hydrogen-3 (H-3) and carbon-14 (C-14) are also affected by evasion of carbon dioxide and water vapor. Because the releasable fraction, the leach rate coefficient specified for the rate controlled release, and the leach rate coefficient used to produce the specified soluble concentration at the down-gradient edge of the primary contamination can each vary with time, the analytical expression for the release susceptible concentration is derived assuming either a linear variation of those quantities between the calculation times or a step change at a calculation time point as specified. Thus, these expressions are used from one calculation time to the next to calculate the concentration at each calculation time.

The change in the activity concentration of the radionuclides in the release susceptible form in the primary contamination at any time between two adjacent calculation times is obtained by considering the loss of the radionuclides by radiological transformations (decay), the gain due to radiological transformations of the parent radionuclide (ingrowth), the gain due to the gradual change from the release immune form to the release susceptible form and the loss due to transfer to the aqueous phase and in the case of radionuclides transferring to the aqueous phase under equilibrium desorption, the loss to the virtual injection that is used to model the equilibrium desorption transfer and transport:

$$\frac{ds_{i,m}^{su}(t)}{dt} = -\lambda_i s_{i,m}^{su}(t) - \mu_i s_{i,m}^{su}(t) + \lambda_i s_{i-1,m}^{su}(t) + \dot{f}_{1,m}^{su}(t_a, t_b) s_{i,m}(t) \tag{G.54}$$

where

$s_{i,m}^{su}(t)$ = release-susceptible activity concentration of radionuclide i of transformation thread m at time t in the primary contamination (Activity/g),

λ_i = radiological transformation constant of radionuclide i (1/yr),

μ_i = leach rate coefficient of radionuclide i, for the time interval between two consecutive calculation times (1/yr),

$\dot{f}_{1,m}^{su}(t_a, t_b)$ = rate at which the release-susceptible fraction of material bearing radionuclide 1 of transformation thread m changes from calculation time t_a calculation time t_b, and

$s_{i,m}(t)$ = activity concentration of radionuclide i of transformation thread m at time t in the primary contamination, if it were all release-immune (Activity/g).

This can be integrated over the time interval between two consecutive calculation time points t_1 and t_2, which satisfy $t_a \le t_1, t_2 \le t_b$, to obtain the concentration at t_2:

$$\frac{ds_{i,m}^{su}(t)}{dt} + \lambda_i s_{i,m}^{su}(t) + \mu_i s_{i,m}^{su}(t) = \dot{f}_{1,m}^{su}(t_a, t_b) s_{i,m}(t) + \lambda_i s_{i-1,m}^{su}(t)$$

$$\int_{t_1}^{t_1+t \le t_2} \left[\frac{de^{(\lambda_i+\mu_i)\tau} s_{i,m}^{su}(\tau)}{d\tau} = \dot{f}_{1,m}^{su}(t_a, t_b) s_{i,m}(\tau) e^{(\lambda_i+\mu_i)\tau} + \lambda_i s_{i-1,m}^{su}(\tau) e^{(\lambda_i+\mu_i)\tau} \right] d\tau$$

$$e^{(\lambda_i+\mu_i)(t_1+t)} s_{i,m}^{su}(t+t_1) - e^{(\lambda_i+\mu_i)t_1} s_{i,m}^{su}(t_1)$$

$$= \int_0^t \dot{f}_{1,m}^{su}(t_a, t_b) \left\{ s_{i,m}(t_1) + \frac{s_{i,m}(t_2) - s_{i,m}(t_1)}{t_2 - t_1} \tau \right\} e^{(\lambda_i+\mu_i)(t_1+\tau)} d\tau$$

$$+ \int_0^t \lambda_i s_{i-1,m}^{su}(t_1+\tau) e^{(\lambda_i+\mu_i)(t_1+\tau)} d\tau$$

$$e^{(\lambda_i+\mu_i)t}s_{i,m}^{su}(t+t_1) - s_{i,m}^{su}(t_1)$$

$$= \dot{f}_{1,m}^{su}(t_a,t_b)s_{i,m}(t_1)\frac{e^{(\lambda_i+\mu_i)t}-1}{(\lambda_i+\mu_i)}$$

$$+ \dot{f}_{1,m}^{su}(t_a,t_b)\frac{s_{i,m}(t_2)-s_{i,m}(t_1)}{t_2-t_1}\left[\frac{te^{(\lambda_i+\mu_i)t}-0}{(\lambda_i+\mu_i)}-\frac{e^{(\lambda_i+\mu_i)t}-1}{(\lambda_i+\mu_i)^2}\right]$$

$$+ \int_0^t \lambda_i s_{i-1,m}^{su}(t_1+\tau)e^{(\lambda_i+\mu_i)\tau}d\tau$$

$$s_{i,m}^{su}(t+t_1) = e^{-(\lambda_i+\mu_i)t}s_{i,m}^{su}(t_1) + e^{-(\lambda_i+\mu_i)t}\int_0^t \lambda_i s_{i-1,m}^{su}(\tau+t_1)e^{(\lambda_i+\mu_i)\tau}d\tau$$

$$+ \dot{f}_{1,m}^{su}(t_a,t_b)$$

$$\times \frac{\left[s_{i,m}(t_1)-\frac{s_{i,m}(t_2)-s_{i,m}(t_1)}{(t_2-t_1)(\lambda_i+\mu_i)}\right]\left[1-e^{-(\lambda_i+\mu_i)t}\right]+\frac{s_{i,m}(t_2)-s_{i,m}(t_1)}{(t_2-t_1)}t}{(\lambda_i+\mu_i)} \qquad (G.55)$$

The release-susceptible activity concentration of the first radionuclide of the transformation thread *m* in the primary contamination is obtained directly from the previous equation:

$$s_{1,m}^{su}(t+t_1) = e^{-(\lambda_1+\mu_1)t}s_{1,m}^{su}(t_1)$$

$$+ \dot{f}_{1,m}^{su}(t_a,t_b)\frac{\left[s_{1,m}(t_1)-\frac{s_{1,m}(t_2)-s_{1,m}(t_1)}{(t_2-t_1)(\lambda_1+\mu_1)}\right]\left[1-e^{-(\lambda_1+\mu_1)t}\right]+\frac{s_{1,m}(t_2)-s_{1,m}(t_1)}{(t_2-t_1)}t}{(\lambda_1+\mu_1)}$$

Collecting terms to obtain a compact and computationally efficient expression:

$$s_{1,m}^{su}(t+t_1) = A_1^0 + A_1^1 t + B_1^1 e^{-(\lambda_1+\mu_1)t}$$

where

(a) if radionuclide 1 transfers to the infiltration water under equilibrium dissolution or under first-order rate control,

$$A_1^1 = \dot{f}_{1,m}^{su}(t_a,t_b)\frac{s_{1,m}(t_2)-s_{1,m}(t_1)}{(t_2-t_1)(\lambda_1+\mu_1)},$$

$$A_1^0 = \dot{f}_{1,m}^{su}(t_a,t_b)\frac{s_{1,m}(t_1)-\frac{s_{1,m}(t_2)-s_{1,m}(t_1)}{(t_2-t_1)(\lambda_1+\mu_1)}}{\lambda_1+\mu_1} = \frac{\dot{f}_{1,m}^{su}(t_a,t_b)s_{1,m}(t_1)}{\lambda_1+\mu_1}-\frac{A_1^1}{\lambda_1+\mu_1}, \text{ and}$$

$$B_1^1 = s_{1,m}^{su}(t_1) - \dot{f}_{1,m}^{su}(t_a,t_b)\frac{s_{1,m}(t_1)-\frac{s_{1,m}(t_2)-s_{1,m}(t_1)}{(t_2-t_1)(\lambda_1+\mu_1)}}{\lambda_1+\mu_1} = s_{1,m}^{su}(t_1) - A_1^0;$$

(b) if radionuclide 1 transfers to the infiltration water under equilibrium desorption, $A_1^0 = 0$, $A_1^1 = 0$ and $B_1^1 = 0$, as the release-susceptible concentration is not computed in this case, only the release at the down-gradient edge of the primary contamination is.

The concentration of the two radionuclides that can escape from the primary contamination by evasion, H-3 and C-14 ,are computed using the following expression:

$$s_{1,m}^{su}(t+t_1) = A_1^0 + A_1^1 t + B_1^1 e^{-(\lambda_1+\mu_1+\varepsilon_v)t} \qquad (G.56)$$

where

ε_v = evasion rate coefficient of the radionuclide (1/yr),

$\varepsilon_v = E_{c,H-3}(t_1)$, which is discussed in Equation (F.12) of Appendix F, and

$\varepsilon_v = E_{c,C-14} \, CF_{evasion,C-14}(t_1)$, which is discussed in Section F.2.1.

The release-susceptible activity concentration of the second radionuclide in the transformation thread m in the primary contamination is obtained by integrating the general equation for the ith radionuclide of the chain using the expression derived for the first member of the chain:

$$s_{2,m}^{su}(t + t_1) = e^{-(\lambda_2+\mu_2)t} s_{2,m}^{su}(t_1) + e^{-(\lambda_2+\mu_2)t} \int_0^t \lambda_2 \big(A_1^0 + A_1^1\tau + B_1^1 e^{-(\lambda_1+\mu_1)\tau}\big) e^{(\lambda_2+\mu_2)\tau} d\tau$$

$$+ \dot{f}_{1,m}^{su}(t_a,t_b) \frac{\left[s_{2,m}(t_1) - \frac{s_{2,m}(t_2) - s_{2,m}(t_1)}{(t_2 - t_1)(\lambda_2 + \mu_2)}\right]\left[1 - e^{-(\lambda_2+\mu_2)t}\right] + \frac{s_{2,m}(t_2) - s_{2,m}(t_1)}{(t_2 - t_1)}t}{(\lambda_2 + \mu_2)}$$

$$s_{2,m}^{su}(t + t_1) = e^{-(\lambda_2+\mu_2)t} s_{2,m}^{su}(t_1)$$

$$+ \lambda_2 e^{-(\lambda_2+\mu_2)t} \left\{ \frac{A_1^0\big(e^{(\lambda_2+\mu_2)t} - 1\big)}{\lambda_2 + \mu_2} + A_1^1 \left[\frac{te^{(\lambda_2+\mu_2)t} - 0}{(\lambda_2 + \mu_2)} - \frac{e^{(\lambda_2+\mu_2)t} - 1}{(\lambda_2 + \mu_2)^2}\right] \right.$$

$$+ \frac{B_1^1}{(\lambda_2 + \mu_2) - (\lambda_1 + \mu_1)} \left[e^{[(\lambda_2+\mu_2)-(\lambda_1+\mu_1)]t} - 1\right] \Bigg\}$$

$$+ \dot{f}_{1,m}^{su}(t_a,t_b) \frac{\left[s_{2,m}(t_1) - \frac{s_{2,m}(t_2) - s_{2,m}(t_1)}{(t_2 - t_1)(\lambda_2 + \mu_2)}\right]\left[1 - e^{-(\lambda_2+\mu_2)t}\right] + \frac{s_{2,m}(t_2) - s_{2,m}(t_1)}{(t_2 - t_1)}t}{(\lambda_2 + \mu_2)}$$

$$s_{2,m}^{su}(t + t_1) = e^{-(\lambda_2+\mu_2)t} s_{2,m}^{su}(t_1)$$

$$+ \left\{ \frac{\lambda_2 A_1^0\big(1 - e^{-(\lambda_2+\mu_2)t}\big)}{\lambda_2 + \mu_2} + \lambda_2 A_1^1 \left[\frac{t}{(\lambda_2 + \mu_2)} - \frac{1 - e^{-(\lambda_2+\mu_2)t}}{(\lambda_2 + \mu_2)^2}\right] \right.$$

$$+ \frac{\lambda_2 B_1^1}{(\lambda_2 + \mu_2) - (\lambda_1 + \mu_1)} \left[e^{-(\lambda_1+\mu_1)t} - e^{-(\lambda_2+\mu_2)t}\right] \Bigg\}$$

$$+ \dot{f}_{1,m}^{su}(t_a,t_b) \frac{\left[s_{2,m}(t_1) - \frac{s_{2,m}(t_2) - s_{2,m}(t_1)}{(t_2 - t_1)(\lambda_2 + \mu_2)}\right]\left[1 - e^{-(\lambda_2+\mu_2)t}\right] + \frac{s_{2,m}(t_2) - s_{2,m}(t_1)}{(t_2 - t_1)}t}{(\lambda_2 + \mu_2)}$$

Collecting terms to obtain a compact and computationally efficient expression,

$$s_{2,m}^{su}(t + t_1) = A_2^0 + A_2^1 t + B_2^1 e^{-(\lambda_1+\mu_1)t} + B_2^2 e^{-(\lambda_2+\mu_2)t}$$

where

(a) if radionuclide 2 transfers to the infiltration water under equilibrium dissolution or under first-order rate control,

$$A_2^1 = \dot{f}_{1,m}^{su}(t_a,t_b) \frac{s_{2,m}(t_2) - s_{2,m}(t_1)}{(t_2 - t_1)(\lambda_2 + \mu_2)} + \frac{\lambda_2 A_1^1}{\lambda_2 + \mu_2},$$

$$A_2^0 = \frac{\dot{f}_{1,m}^{su}(t_a,t_b) s_{2,m}(t_1)}{\lambda_2 + \mu_2} - \frac{A_2^1}{\lambda_2 + \mu_2} + \frac{\lambda_2 A_1^0}{\lambda_2 + \mu_2},$$

If $(\lambda_2 + \mu_2) - (\lambda_1 + \mu_1) \neq 0$,

$$B_2^1 = \frac{\lambda_2 B_1^1}{(\lambda_2 + \mu_2) - (\lambda_1 + \mu_1)},$$

If $(\lambda_2 + \mu_2) - (\lambda_1 + \mu_1) = 0$,

$$B_2^1 = 0, \text{ and } A_2^1 = A_2^1 + \lambda_2 B_1^1,$$
$$B_2^2 = s_{2,m}^{su}(t_1) - A_2^0 - B_2^1.$$

(b) if radionuclide 2 transfers to the infiltration water under equilibrium desorption, $A_2^0 = 0$, $A_2^1 = 0$, $B_2^1 = 0$ and $B_2^2 = 0$, because the release-susceptible concentration is not computed in this case, only the release at the down-gradient edge of the primary contamination is.

The form of the expressions for the first and second members of the chain are used to obtain the expression for the ith member of the chain by induction. Assume that the release susceptible activity concentration of the $(i-1)^{\text{th}}$ member of the transformation chain is of the following form:

$$s_{i-1,m}^{su}(t + t_1) = A_{i-1}^0 + A_{i-1}^1 t + \sum_{k=1}^{i-1} B_{i-1}^k e^{-(\lambda_k + \mu_k)t}$$

Then the release susceptible concentration of the next member, i, of the transformation chain is given by:

$$s_{i,m}^{su}(t + t_1) = e^{-(\lambda_i + \mu_i)t} s_{i,m}^{su}(t_1) + e^{-(\lambda_i + \mu_i)t} \int_0^t \lambda_i \left[A_{i-1}^0 + A_{i-1}^1 \tau + \sum_{k=1}^{i-1} B_{i-1}^k e^{-(\lambda_k + \mu_k)\tau} \right] e^{(\lambda_i + \mu_i)\tau} d\tau$$

$$+ \dot{f}_{1,m}^{su}(t_a, t_b) \frac{\left[s_{i,m}(t_1) - \frac{s_{i,m}(t_2) - s_{i,m}(t_1)}{(t_2 - t_1)(\lambda_i + \mu_i)} \right] \left[1 - e^{-(\lambda_i + \mu_i)t} \right] + \frac{s_{i,m}(t_2) - s_{i,m}(t_1)}{(t_2 - t_1)} t}{(\lambda_i + \mu_i)}$$

$$s_{i,m}^{su}(t + t_1) = e^{-(\lambda_i + \mu_i)t} s_{i,m}^{su}(t_1)$$

$$+ \lambda_i e^{-(\lambda_i + \mu_i)t} \left\{ A_{i-1}^0 \frac{e^{(\lambda_i + \mu_i)t} - 1}{\lambda_i + \mu_i} + A_{i-1}^1 \left[\frac{t e^{(\lambda_i + \mu_i)t} - 0}{\lambda_i + \mu_i} - \frac{e^{(\lambda_i + \mu_i)t} - 1}{(\lambda_i + \mu_i)^2} \right] \right.$$

$$\left. + \sum_{k=1}^{i-1} B_{i-1}^k \frac{e^{[(\lambda_i + \mu_i) - (\lambda_k + \mu_k)]t} - 1}{(\lambda_i + \mu_i) - (\lambda_k + \mu_k)} \right\}$$

$$+ \dot{f}_{1,m}^{su}(t_a, t_b) \frac{\left[s_{i,m}(t_1) - \frac{s_{i,m}(t_2) - s_{i,m}(t_1)}{(t_2 - t_1)(\lambda_i + \mu_i)} \right] \left[1 - e^{-(\lambda_i + \mu_i)t} \right] + \frac{s_{i,m}(t_2) - s_{i,m}(t_1)}{(t_2 - t_1)} t}{(\lambda_i + \mu_i)}$$

$$s_{i,m}^{su}(t+t_1) = e^{-(\lambda_i+\mu_i)t}s_{i,m}^{su}(t_1) + \lambda_i A_{i-1}^0 \frac{1-e^{-(\lambda_i+\mu_i)t}}{\lambda_i+\mu_i} + \lambda_i A_{i-1}^1 \left[\frac{t}{\lambda_i+\mu_i} - \frac{1-e^{-(\lambda_i+\mu_i)t}}{(\lambda_i+\mu_i)^2}\right]$$

$$+ \sum_{k=1}^{i-1} \frac{\lambda_i B_{i-1}^k}{(\lambda_i+\mu_i)-(\lambda_k+\mu_k)} e^{-(\lambda_k+\mu_k)t} - e^{-(\lambda_i+\mu_i)t} \sum_{k=1}^{i-1} \frac{\lambda_i B_{i-1}^k}{(\lambda_i+\mu_i)-(\lambda_k+\mu_k)}$$

$$+ \dot{f}_{1,m}^{su}(t_a,t_b) \frac{\left[s_{i,m}(t_1) - \frac{s_{i,m}(t_2)-s_{i,m}(t_1)}{(t_2-t_1)(\lambda_i+\mu_i)}\right]\left[1-e^{-(\lambda_i+\mu_i)t}\right] + \frac{s_{i,m}(t_2)-s_{i,m}(t_1)}{(t_2-t_1)}t}{(\lambda_i+\mu_i)}$$

Collecting terms to obtain a compact and computationally efficient expression,

$$s_{i,m}^{su}(t+t_1) = A_i^0 + A_i^1 t + \sum_{k=1}^{j} B_i^k e^{-(\lambda_k+\mu_k)t} \tag{G.571}$$

where

(a) for $j = 1$,

(1) if radionuclide j transfers to the infiltration water under equilibrium dissolution or under first-order rate control,

$$A_1^1 = \dot{f}_{1,m}^{su}(t_a,t_b) \frac{s_{1,m}(t_2)-s_{1,m}(t_1)}{(t_2-t_1)(\lambda_1+\mu_1)},$$

$$A_1^0 = \frac{\dot{f}_{1,m}^{su}(t_a,t_b)s_{1,m}(t_1)}{\lambda_1+\mu_1} - \frac{A_1^1}{\lambda_1+\mu_1}, \text{ and}$$

$$B_1^1 = s_{1,m}^{su}(t_1) - A_1^0;$$

(2) if radionuclide j transfers to the infiltration water under equilibrium desorption, the release-susceptible concentration is not computed in this case, only the release at the down-gradient edge of the primary contamination is. Thus,

$$A_1^1 = 0,$$

$$A_1^0 = 0, \text{ and}$$

$$B_1^1 = 0;$$

(b) for all j satisfying $1 < j \leq i$,

(1) if radionuclide j transfers to the infiltration water under equilibrium dissolution or under first-order rate control,

$$A_j^1 = \dot{f}_{1,m}^{su}(t_a,t_b) \frac{s_{j,m}(t_2)-s_{j,m}(t_1)}{(t_2-t_1)(\lambda_j+\mu_j)} + \frac{\lambda_j A_{j-1}^1}{\lambda_j+\mu_j},$$

$$A_j^0 = \dot{f}_{1,m}^{su}(t_a,t_b) \frac{s_{j,m}(t_1)}{\lambda_j+\mu_j} - \frac{A_j^1}{\lambda_j+\mu_j} + \frac{\lambda_j A_{j-1}^0}{\lambda_j+\mu_j},$$

for all k satisfying $0 < k < j$,

if $(\lambda_j+\mu_j)-(\lambda_k+\mu_k) \neq 0$,

$$B_j^k = \lambda_j \frac{B_{j-1}^k}{(\lambda_j+\mu_j)-(\lambda_k+\mu_k)},$$

if $(\lambda_j+\mu_j)-(\lambda_k+\mu_k) = 0$,

$$B_j^k = 0 \text{ and } A_j^1 = A_j^1 + \lambda_j B_{j-1}^k$$

$$B_j^j = s_{j,m}^{su}(t_1) - A_j^0 - \sum_{k=1}^{j-1} B_j^k.$$

(2) if radionuclide j transfers to the infiltration water under equilibrium desorption, the release-susceptible concentration is not computed, only the release at the down-gradient edge of the primary contamination is. Thus,

$$A_j^1 = 0,$$
$$A_j^0 = 0,$$
$$B_j^j = 0$$

for all k satisfying $0 < k < j$,

$$B_j^k = 0.$$

Any stepwise change in the releasable fraction is modeled as occurring at the calculation time immediately preceding it (Section G.9). The release susceptible concentration of radionuclide i at each calculation time is computed by combining the expression obtained by considering the gradual changes over the preceding time interval with any stepwise change occurring at that calculation time:

$$s_{i,m}^{su}(t_2) = A_i^0 + A_i^1(t_2 - t_1) + \sum_{k=1}^{j} B_i^k e^{-(\lambda_k + \mu_k)(t_2 - t_1)} + \Delta s_{i,m}^{step}(t_2) \qquad \text{(G.58)}$$

where

$\Delta s_{i,m}^{step}(t_2)$ = stepwise change from release-immune to release-susceptible form (Activity/g),

If $t_2 \leq t_l^r < t_3$, $\Delta s_{j,m}^{step}(t_2) = \Delta f_1^{su}(t_a) s_{j,m}(t_2)$ for all j satisfying $1 \leq j \leq i$, and $\Delta s_{j,m}^{step}(t_2) = 0$ otherwise.

The sum of the release immune and release susceptible concentration computed by the code are output to SFSIN.DAT. The format of this file is described in Section G.16.

G.11 Transfer to Aqueous Phase

The primary contamination may be above the water table, it may straddle the water table, or it may be submerged with the top of the primary contamination at the water table. Depending on the extent to which the primary contamination is submerged, the code will compute one or both of the components of transfer described below.

If radionuclide i transfers to the infiltration water under equilibrium dissolution or under first order rate control, the transfer from the release susceptible form is computed using the following expression(s):

$$T_{i,m}^{su \to aq}{}_{awt}(t) = \mu_{i,m} M_{pc}^{awt}(t) s_{i,m}^{su}(t)$$
$$T_{i,m}^{su \to aq}{}_{sub}(t) = \mu_{i,m} M_{pc}^{sub} s_{i,m}^{su}(t) \qquad \text{(G.59)}$$

where

$T_{i,m}^{su \to aq}{}_{awt}(t)$ = rate of transfer of radionuclide i of transformation thread m from the release-susceptible form in the part of the primary contamination that is above the water table to the aqueous phase (Activity/yr),

$T_{i,m}^{su \to aq}{}_{sub}(t)$ = rate of transfer of radionuclide i of transformation thread m from the release-susceptible form in the part of the primary contamination that is below the water table to the aqueous phase (Activity/yr),

$\mu_{i,m}$ = leach rate coefficient of the radionuclide i for a first-order rate-controlled release or the leach rate coefficient used to produce the specified soluble concentration at the down-gradient edge of the primary contamination for equilibrium dissolution release (1/yr),

M_{pc}^{awt} = mass of the solids in the primary contamination that is above the water table (g),

M_{pc}^{sub} = mass of the solids in the primary contamination that is submerged (g), and

$s_{i,m}^{su}(t)$ = release-susceptible concentration of radionuclide i of transformation thread m at time t in the primary contamination (Activity/g).

If radionuclide i transfers to the infiltration water under equilibrium desorption, the release from the bottom of the primary contamination is modeled using an imaginary injection into the primary contamination. The rate of gradual injection, in Activity/yr, is computed using the following expression(s):

$$In_{i,m}^{su \to aq\,gdl}{}_{awt}(t_2: t_a \le t_2 < t_b) = \left[\dot{f}_{1,m}^{su}(t_a, t_b)s_{i,m}(t_2) + \lambda_i s_{i-1,m}^{su}(t_2)\right]M_{pc}^{awt}(t_2)$$
$$In_{i,m}^{su \to aq\,gdl}{}_{sub}(t_2: t_a \le t_2 < t_b) = \left[\dot{f}_{1,m}^{su}(t_a, t_b)s_{i,m}(t_2) + \lambda_i s_{i-1,m}^{su}(t_2)\right]M_{pc}^{sub} \qquad (G.60)$$

The first term in each expression is the rate at which radionuclide i becomes releasable because of the gradual change in the releasable fraction over time; the second term is the rate at which radionuclide i becomes releasable because of ingrowth from the releasable parent radionuclide.

Up to nine instantaneous imaginary injections would be necessary to model the release from the primary contamination if the releasable fraction of the radionuclide i changes in a stepwise manner at all nine of the times at which the releasable fraction is specified. These instantaneous injections, in activity, are given by the following expressions:

$$In_{i,m}^{su \to aq\,ins}{}_{awt}(t_1: t_1 \le t_l^r < t_2) = \Delta f_1^{su}(t_1)s_{i,m}(t_1)M_{pc}^{awt}(t_1)$$
$$In_{i,m}^{su \to aq\,ins}{}_{sub}(t_1: t_1 \le t_l^r < t_2) = \Delta f_1^{su}(t_1)s_{i,m}(t_1)M_{pc}^{sub} \qquad (G.61)$$

The code computes these rates of transfer and of gradual injections at each calculation time; the rates are assumed to vary linearly between calculation times. The rates at the calculation times are written to AQTRANIN.DAT. Any instantaneous injections that are computed are also listed in this file. The structure of this file is described in Section G.16.

G.12 Diffusive Transport in Non-Conducting Media

This option is available to model situations where transport out of the radionuclide-bearing material is by diffusion and not by advection. The representative fragments of the radionuclide-bearing material are assumed to be rectangular prisms of dimensions L_x, L_y, L_z.

The equation to be solved is obtained by considering the changes in an elemental volume of dimensions δx, δy, and δz over time δt.

The difference in diffusive transfer into the elemental volume from the pair of faces in the *x* direction is:

$$D \frac{\partial^2 c_{aq}}{\partial x^2} \delta x 10^6 \delta t \theta_c \delta y \delta z$$

where

D = diffusion coefficient of the radionuclide (m²/yr),

c_{aq} = concentration of the radionuclide in the water in the pores of the radionuclide-bearing material (activity/[cm]³),

10^6 = to convert per (cm)³ to per m³,

θ_c = moisture content of the radionuclide-bearing material,

$\delta x, \delta y, \delta z$ = dimensions of the elemental volume in the shape of a rectangular prism (m), and

δt = increment in time (yr).

The differences in the diffusive transfer into the elemental volume from other two pairs of faces are as follows:

$$D \frac{\partial^2 c_{aq}}{\partial y^2} \delta y 10^6 \delta t \theta_c \delta z \delta x$$

and

$$D \frac{\partial^2 c_{aq}}{\partial z^2} \delta z 10^6 \delta t \theta_c \delta x \delta y$$

The change in the quantity within the elemental volume due to radiological transformations is as follows:

$$-\lambda \left(\theta_c c_{aq} + \rho_b c_{ad} \right) \delta t \delta x 10^6 \delta y \delta z$$

where

λ = transformation rate of the radionuclide (1/yr),

ρ_b = dry bulk density of the radionuclide-bearing material (g/[cm]³), and

c_{ad} = concentration of the radionuclide adsorbed to the solids in the radionuclide-bearing material (Activity/g).

The net change in the elemental volume is:

$$\left(\theta_c \frac{\partial c_{aq}}{\partial t} + \rho_b \frac{\partial c_{ad}}{\partial t} \right) \delta t \delta x 10^6 \delta y \delta z$$

Equating the net change to the combined effects,

$$\theta_c \frac{\partial c_{aq}}{\partial t} + \rho_b \frac{\partial c_{ad}}{\partial t} = -\lambda(\theta_c c_{aq} + \rho_b c_{ad}) + D\theta_c \frac{\partial^2 c_{aq}}{\partial x^2} + D\theta_c \frac{\partial^2 c_{aq}}{\partial y^2} + D\theta_c \frac{\partial^2 c_{aq}}{\partial z^2}$$

Under the assumption of a linear reversible adsorption-desorption isotherm, the aqueous and adsorbed concentrations are related by the linear distribution coefficient:

$$c_{ad} = K_d c_{aq}$$

Substituting for the concentration in the adsorbed phase in the mass balance equation gives the following:

$$(\theta_c + K_d \rho_b) \frac{\partial c_{aq}}{\partial t} = -\lambda(\theta_c + K_d \rho_b) c_{aq} + D\theta_c \frac{\partial^2 c_{aq}}{\partial x^2} + D\theta_c \frac{\partial^2 c_{aq}}{\partial y^2} + D\theta_c \frac{\partial^2 c_{aq}}{\partial z^2}$$

This can be condensed to the governing equation:

$$\frac{\partial c_{aq}}{\partial t} = -\lambda c_{aq} + D_c \frac{\partial^2 c_{aq}}{\partial x^2} + D_c \frac{\partial^2 c_{aq}}{\partial y^2} + D_c \frac{\partial^2 c_{aq}}{\partial z^2} \tag{G.62}$$

where D_c = effective diffusion coefficient in the radionuclide-bearing material (m²/yr):

$$D_c = \frac{D\theta_c}{\theta_c + K_d \rho_b} \tag{G.63}$$

While the interface accepts input of the diffusion coefficient and the distribution coefficient of the radionuclide in the radionuclide-bearing material, the effective diffusion coefficient can be input in place of the diffusion coefficient together with a zero value for the distribution coefficient. Then the value computed by the code would be the effective diffusion coefficient that was input as the $K_d \rho_b$ term will be zero and the θ_c in the denominator and the numerator will cancel each other.

The solution to the governing equation (Equation [G.62]) for a unit point pulse input at the origin, $(0,0,0, t = 0)$ for an unbounded transport zone is:

$$
\begin{aligned}
c_{aq}(x, y, z, t) &= \frac{e^{-\lambda t}}{\theta_c + K_d \rho_b} \sqrt{\frac{1}{4\pi D_c t}} e^{\frac{-x^2}{4D_c t}} \sqrt{\frac{1}{4\pi D_c t}} e^{\frac{-y^2}{4D_c t}} \sqrt{\frac{1}{4\pi D_c t}} e^{\frac{-z^2}{4D_c t}} \\
&= \frac{e^{-\lambda t - \frac{x^2+y^2+z^2}{4D_c t}}}{\theta_c + K_d \rho_b} \left(\frac{1}{4\pi D_c t}\right)^{\frac{3}{2}}
\end{aligned}
\tag{G.64}
$$

Verification of the solution:

$$\frac{\partial c_{aq}}{\partial t} = -\lambda c_{aq} - \frac{x^2 + y^2 + z^2}{4D_c}\left(\frac{-1}{t^2}\right)c_{aq} - \frac{3}{2t}c_{aq}$$

$$\frac{\partial c_{aq}}{\partial x} = \frac{-2x}{4D_c t}c_{aq}$$

$$\frac{\partial^2 c_{aq}}{\partial x^2} = -\frac{2}{4D_c t}c_{aq} + \left(\frac{-2x}{4D_c t}\right)^2 c_{aq}$$

$$D_c \frac{\partial^2 c_{aq}}{\partial x^2} = -\frac{1}{2t}c_{aq} + \frac{1}{4D_c}\left(\frac{x}{t}\right)^2 c_{aq}$$

$$D_c \frac{\partial^2 c_{aq}}{\partial x^2} + D_c \frac{\partial^2 c_{aq}}{\partial y^2} + D_c \frac{\partial^2 c_{aq}}{\partial z^2} = -\frac{3}{2t}c_{aq} + \frac{x^2+y^2+z^2}{4D_c t^2}c_{aq} = \frac{\partial c_{aq}}{\partial t} + \lambda c_{aq}$$

Thus, the solution satisfies the governing equation.

The mass balance over the infinite extent is also satisfied as seen from the integral over the region:

$$\iiint\limits_{-\infty}^{\infty} (\theta_c + K_d \rho_b)c_{aq}(x,y,z,t)dxdydz$$

$$= e^{-\lambda t} \int_{-\infty}^{\infty} \frac{1}{\sqrt{\pi}} e^{\frac{-x^2}{4D_c t}} d\left(\frac{x}{\sqrt{4D_c t}}\right) \int_{-\infty}^{\infty} \frac{1}{\sqrt{\pi}} e^{\frac{-y^2}{4D_c t}} d\left(\frac{y}{\sqrt{4D_c t}}\right) \int_{-\infty}^{\infty} \frac{1}{\sqrt{\pi}} e^{\frac{-z^2}{4D_c t}} d\left(\frac{z}{\sqrt{4D_c t}}\right)$$

$$= e^{-\lambda t}$$

The initial condition is also satisfied as follows:

$$(\theta_c + K_d \rho_b)c_{aq}(x,y,z,0) = \lim_{t\to 0} \sqrt{\frac{1}{4\pi D_c t}} e^{\frac{-x^2}{4D_c t}} \sqrt{\frac{1}{4\pi D_c t}} e^{\frac{-y^2}{4D_c t}} \sqrt{\frac{1}{4\pi D_c t}} e^{\frac{-z^2}{4D_c t}}$$

$$= \lim_{t\to 0} \sqrt{\frac{1}{4\pi D_c t}} e^{\frac{-x^2}{4D_c t}} \lim_{t\to 0} \sqrt{\frac{1}{4\pi D_c t}} e^{\frac{-y^2}{4D_c t}} \lim_{t\to 0} \sqrt{\frac{1}{4\pi D_c t}} e^{\frac{-z^2}{4D_c t}} = \delta(x,y,z)$$

The solution to the governing equation:

$$\frac{\partial c_{aq}}{\partial t} = -\lambda c_{aq} + D_c \frac{\partial^2 c_{aq}}{\partial x^2} + D_c \frac{\partial^2 c_{aq}}{\partial y^2} + D_c \frac{\partial^2 c_{aq}}{\partial z^2}$$

for a unit pulse input over a rectangular prism of dimensions, L_x, L_y, L_z centered on the orgin, for an unbounded transport zone is:

$$c_{aq}(x,y,z,t)$$

$$= \frac{e^{-\lambda t}}{\theta_c + K_d \rho_b} \int_{x-L_x/2}^{x+L_x/2} \frac{1}{L_x}\sqrt{\frac{1}{4\pi D_c t}} e^{\frac{-x^2}{4D_c t}} dx \int_{y-L_y/2}^{y+L_y/2} \frac{1}{L_y}\sqrt{\frac{1}{4\pi D_c t}} e^{\frac{-y^2}{4D_c t}} dy \int_{z-L_z/2}^{z+L_z/2} \frac{1}{L_z}\sqrt{\frac{1}{4\pi D_c t}} e^{\frac{-z^2}{4D_c t}} dz$$

$$= \frac{e^{-\lambda t}}{\theta_c + K_d \rho_b} \frac{1}{L_x L_y L_z} \frac{erf\left(\frac{x+L_x/2}{\sqrt{4D_c t}}\right) - erf\left(\frac{x-L_x/2}{\sqrt{4D_c t}}\right)}{2} \times \frac{erf\left(\frac{y+L_y/2}{\sqrt{4D_c t}}\right) - erf\left(\frac{y-L_y/2}{\sqrt{4D_c t}}\right)}{2}$$

$$\times \frac{erf\left(\frac{z+L_z/2}{\sqrt{4D_c t}}\right) - erf\left(\frac{z-L_z/2}{\sqrt{4D_c t}}\right)}{2}$$

The transfer out of the two opposite faces at $x = L_x/2$ and at $x = -L_x/2$ into the surrounding soil in the primary contamination from a unit pulse distributed over the rectangular prism of dimensions, L_x, L_y, L_z is:

$$T_x^{cm \to aqpc}(t) = -2D\theta_c \int_{-L_y/2}^{L_y/2} \int_{-L_z/2}^{L_z/2} \left. \frac{\partial c_{aq}(x,y,z,t)}{\partial x} \right|_{x=L_x/2} dzdy$$

$$= \frac{-2D\theta_c e^{-\lambda t}}{\theta_c + K_d\rho_b} \frac{1}{L_xL_yL_z} \sqrt{\frac{1}{4\pi D_c t}} \left[e^{-\left(\frac{x+L_x/2}{\sqrt{4D_c t}}\right)^2} - e^{-\left(\frac{x-L_x/2}{\sqrt{4D_c t}}\right)^2} \right]_{x=L_x/2}$$

$$\times \int_{-L_y/2}^{L_y/2} \frac{erf\left(\frac{y+L_y/2}{\sqrt{4D_c t}}\right) - erf\left(\frac{y-L_y/2}{\sqrt{4D_c t}}\right)}{2} dy$$

$$\times \int_{-L_z/2}^{L_z/2} \frac{erf\left(\frac{z+L_z/2}{\sqrt{4D_c t}}\right) - erf\left(\frac{z-L_z/2}{\sqrt{4D_c t}}\right)}{2} dz$$

$$T_x^{cm \to aqpc}(t) = \frac{2e^{-\lambda t}}{L_xL_yL_z} \sqrt{\frac{D_c}{4\pi t}} \left[1 - e^{-\left(\frac{L_x}{\sqrt{4D_c t}}\right)^2} \right]$$

$$\times \frac{1}{2} \left[\int_{-L_y/2}^{L_y/2} erf\left(\frac{y+L_y/2}{\sqrt{4D_c t}}\right) dy - \int_{-L_y/2}^{L_y/2} erf\left(\frac{y-L_y/2}{\sqrt{4D_c t}}\right) dy \right]$$

$$\times \frac{1}{2} \left[\int_{-L_z/2}^{L_z/2} erf\left(\frac{z+L_z/2}{\sqrt{4D_c t}}\right) dz - \int_{-L_z/2}^{L_z/2} erf\left(\frac{z-L_z/2}{\sqrt{4D_c t}}\right) dz \right]$$

$$T_x^{cm \to aqpc}(t) = \frac{2e^{-\lambda t}}{L_xL_yL_z} \sqrt{\frac{D_c}{4\pi t}} \left[1 - e^{-\left(\frac{L_x}{\sqrt{4D_c t}}\right)^2} \right] \sqrt{D_c t} \sqrt{D_c t}$$

$$\times \left[\int_{0}^{\frac{L_y}{\sqrt{4D_c t}}} erf\left(\frac{y+\frac{L_y}{2}}{\sqrt{4D_c t}}\right) d\left(\frac{y+\frac{L_y}{2}}{\sqrt{4D_c t}}\right) - \int_{\frac{-L_y}{\sqrt{4D_c t}}}^{0} erf\left(\frac{y-\frac{L_y}{2}}{\sqrt{4D_c t}}\right) d\left(\frac{y-\frac{L_y}{2}}{\sqrt{4D_c t}}\right) \right]$$

$$\times \left[\int_{0}^{\frac{L_z}{\sqrt{4D_c t}}} erf\left(\frac{z+\frac{L_z}{2}}{\sqrt{4D_c t}}\right) d\left(\frac{z+\frac{L_z}{2}}{\sqrt{4D_c t}}\right) - \int_{\frac{-L_z}{\sqrt{4D_c t}}}^{0} erf\left(\frac{z-\frac{L_z}{2}}{\sqrt{4D_c t}}\right) d\left(\frac{z-\frac{L_z}{2}}{\sqrt{4D_c t}}\right) \right]$$

$$T_x^{cm \to aqpc}(t) = \frac{2e^{-\lambda t}}{L_x L_y L_z} \sqrt{\frac{D_c}{4\pi t}} \left[1 - e^{-\left(\frac{L_x}{\sqrt{4D_c t}}\right)^2} \right] \sqrt{D_c t} \sqrt{D_c t}$$

$$\times \left[\int_0^{\frac{L_y}{\sqrt{4D_c t}}} erf\left(\frac{y + \frac{L_y}{2}}{\sqrt{4D_c t}}\right) d\left(\frac{y + \frac{L_y}{2}}{\sqrt{4D_c t}}\right) + \int_0^{\frac{L_y}{\sqrt{4D_c t}}} erf\left(\frac{y - \frac{L_y}{2}}{\sqrt{4D_c t}}\right) d\left(\frac{y - \frac{L_y}{2}}{\sqrt{4D_c t}}\right) \right]$$

$$\times \left[\int_0^{\frac{L_z}{\sqrt{4D_c t}}} erf\left(\frac{z + \frac{L_z}{2}}{\sqrt{4D_c t}}\right) d\left(\frac{z + \frac{L_z}{2}}{\sqrt{4D_c t}}\right) + \int_0^{\frac{L_z}{\sqrt{4D_c t}}} erf\left(\frac{z - \frac{L_z}{2}}{\sqrt{4D_c t}}\right) d\left(\frac{z - \frac{L_z}{2}}{\sqrt{4D_c t}}\right) \right]$$

$$T_x^{cm \to aqpc}(t) = \frac{2e^{-\lambda t}}{L_x L_y L_z} \sqrt{\frac{D_c}{4\pi t}} \left[1 - e^{-\left(\frac{L_x}{\sqrt{4D_c t}}\right)^2} \right] \times \sqrt{D_c t}\sqrt{D_c t}\, 2\, interf\left(\frac{L_y}{\sqrt{4D_c t}}\right) 2\, interf\left(\frac{L_z}{\sqrt{4D_c t}}\right)$$

$$T_x^{cm \to aqpc}(t) = \frac{2e^{-\lambda t}}{L_x} \sqrt{\frac{D_c}{4\pi t}} \left[1 - e^{-\left(\frac{L_x}{\sqrt{4D_c t}}\right)^2} \right] \times \frac{interf\left(\frac{L_y}{\sqrt{4D_c t}}\right)}{\frac{L_y}{\sqrt{4D_c t}}} \frac{interf\left(\frac{L_z}{\sqrt{4D_c t}}\right)}{\frac{L_z}{\sqrt{4D_c t}}} \qquad \text{(G.65)}$$

Combining the transfers out of the two pairs of opposite faces at $y = \pm L_y/2$ and at $z = \pm L_z/2$, and the Bateman equation in Section G.4, the total transfer of radionuclide i of thread m into the surrounding soil in the primary contamination from a unit pulse of radionuclide 1, distributed over the rectangular prism of dimensions, L_x, L_y, L_z is:

$$T_{i,m}^{cm \to aqpc}(t) = \frac{\sum_{k=1}^i B_i^k e^{-\lambda_k t}}{2\sqrt{\pi t}} \frac{1 - e^{-\left(\frac{L_x}{\sqrt{4D_c t}}\right)^2}}{\frac{L_x}{\sqrt{4D_c t}}} \frac{interf\left(\frac{L_y}{\sqrt{4D_c t}}\right)}{\frac{L_y}{\sqrt{4D_c t}}} \frac{interf\left(\frac{L_z}{\sqrt{4D_c t}}\right)}{\frac{L_z}{\sqrt{4D_c t}}}$$

$$+ \frac{\sum_{k=1}^i B_i^k e^{-\lambda_k t}}{2\sqrt{\pi t}} \frac{interf\left(\frac{L_x}{\sqrt{4D_c t}}\right)}{\frac{L_x}{\sqrt{4D_c t}}} \frac{1 - e^{-\left(\frac{L_y}{\sqrt{4D_c t}}\right)^2}}{\frac{L_y}{\sqrt{4D_c t}}} \frac{interf\left(\frac{L_z}{\sqrt{4D_c t}}\right)}{\frac{L_z}{\sqrt{4D_c t}}} \qquad \text{(G.66)}$$

$$+ \frac{\sum_{k=1}^i B_i^k e^{-\lambda_k t}}{2\sqrt{\pi t}} \frac{interf\left(\frac{L_x}{\sqrt{4D_c t}}\right)}{\frac{L_x}{\sqrt{4D_c t}}} \frac{interf\left(\frac{L_y}{\sqrt{4D_c t}}\right)}{\frac{L_y}{\sqrt{4D_c t}}} \frac{1 - e^{-\left(\frac{L_z}{\sqrt{4D_c t}}\right)^2}}{\frac{L_z}{\sqrt{4D_c t}}}$$

with $B_1^1 = 1$, $B_j^k = \frac{\lambda_j B_{j-1}^k}{\lambda_j - \lambda_k}$ for $0 < k < j \le i$ and $B_j^j = -\sum_{k=1}^{j-1} B_j^k$ for $1 < j \le i$.

The imaginary injections used to model the equilibrium desorption transfer described in Section G.11 occur uniformly over the transport length of the contaminated medium. The transfer from the contaminated medium by diffusion into the surrounding soil is obtained by multiplying the expression for a unit distributed pulse by the magnitude of the instantaneous injections and by convolving the expressions for the unit distributed pulse with the gradual injections.

For a primary contamination that is above the water table, the transfer of radionuclide i of thread m from the contaminated medium by diffusion into the surrounding soil from the gradual transfer of radionuclide 1, $T_{i,m}^{aqpc \to aq\,gdl}{}_{awt}(t)$, is of the following form:

$$T_{i,m}^{aqpc \to aq\,gdl}{}_{awt}(t_m) = \int_{t_0=0}^{t_m} In_{1,m}^{su \to aq\,gdl}{}_{awt}(t_m - \tau)\, T_{i,m}^{cm \to aqpc}(\tau)\, d\tau$$

The evaluation of this convolution is faster if the calculation time points are linearly spaced (see Section E.1).

For a primary contamination that is above the water table, the transfer of radionuclide i of thread m from the contaminated medium by diffusion into the surrounding soil from the instantaneous injection of radionuclide 1, $T_{i,m}^{aqpc \to aq\,ins}{}_{awt}(t)$, is of the following form:

$$T_{i,m}^{aqpc \to aq\,ins}{}_{awt}(t_m) = In_{1,m}^{su \to aq\,ins}{}_{awt}(t_l)\, T_{i,m}^{cm \to aqpc}(t_m - t_l)$$

For a primary contamination that is above the water table, the total transfer of radionuclide i of thread m from the contaminated medium by diffusion into the surrounding soil due to the transfer of radionuclide 1 from the contaminated medium into the moisture in the contaminated medium, $T_{i,m}^{aqpc \to aq}{}_{awt}(t)$, is the sum of the transfers from the gradual and instantaneous injections:

$$T_{i,m}^{aqpc \to aq}{}_{awt}(t_m) = T_{i,m}^{aqpc \to aq\,gdl}{}_{awt}(t_m) + T_{i,m}^{aqpc \to aq\,ins}{}_{awt}(t_m)$$

For a primary contamination that is submerged, the transfer of radionuclide i of thread m from the contaminated medium by diffusion into the surrounding soil from the gradual transfer of radionuclide 1, $T_{i,m}^{aqpc \to aq\,gdl}{}_{sub}(t)$, is of the following form:

$$T_{i,m}^{aqpc \to aq\,gdl}{}_{sub}(t_m) = \int_{t_0}^{t_m} In_{1,m}^{su \to aq\,gdl}{}_{sub}(t_m - \tau)\, T_{i,m}^{cm \to aqpc}(\tau)\, d\tau$$

The evaluation of this convolution is faster if the calculation time points are linearly spaced (see Section E.1).

For a primary contamination that is submerged, the transfer of radionuclide i of thread m from the contaminated medium by diffusion into the surrounding soil from the instantaneous injection of radionuclide 1, $T_{i,m}^{aqpc \to aq\,ins}{}_{sub}(t)$, is of the following form:

$$T_{i,m}^{aqpc \to aq}{}_{sub}^{ins}(t_m) = In_{1,m}^{su \to aq}{}_{sub}^{ins}(t_l)T_{i,m}^{cm \to aqpc}(t_m - t_l)$$

For a primary contamination that is submerged, the total transfer of radionuclide i of thread m from the contaminated medium by diffusion into the surrounding soil due to the transfer of radionuclide 1 from the contaminated medium into the moisture in the contaminated medium, $T_{i,m}^{aqpc \to aq}{}_{sub}(t)$, is the sum of the transfers from the gradual and instantaneous injections:

$$T_{i,m}^{aqpc \to aq}{}_{sub}(t_m) = T_{i,m}^{aqpc \to aq}{}_{sub}^{gdl}(t_m) + T_{i,m}^{aqpc \to aq}{}_{sub}^{ins}(t_m)$$

G.13 Release to Infiltration and Groundwater

The transfers and imaginary injections described in Section G.11 occur uniformly over the transport length of the primary contamination. The release at the down gradient edge of the primary contamination is obtained by convolving the transfer or gradual injection with the appropriate transfer function developed in Appendix H and by multiplying the instantaneous injections by the appropriate transfer function.

The release from gradual transfers and injections over time is obtained by convolving with the transfer function described in Section H.3.4. For a primary contamination that is above the water table, the release of radionuclide i at the bottom from the gradual transfer of radionuclide i, $R_b^g\left(\frac{T_{pc}^{eq,awt}}{2}, t\right)$, is of the following form:

$$
\begin{aligned}
R_b^g&\left(\frac{T_{pc}^{eq,awt}}{2}, t_m\right) \\
&= \int_{t_0=0}^{t_m} In_{awt}^{gdl}(t_m - \tau)\left\{\frac{V_C}{2}\left[erf\left(\frac{T_{pc}^{eq,awt} - V_C\tau}{\sqrt{4D_x^c\tau}}\right) - erf\left(\frac{0 - V_C\tau}{\sqrt{4D_x^c\tau}}\right)\right]\right. \\
&\quad \left. - \sqrt{\frac{D_x^c}{4\pi\tau}}\left[e^{-\left(\frac{T_{pc}^{eq,awt} - V_C\tau}{\sqrt{4D_x^c\tau}}\right)^2} - e^{-\left(\frac{0 - V_C\tau}{\sqrt{4D_x^c\tau}}\right)^2}\right]\right\}\frac{e^{-\lambda\tau}}{T_{pc}^{eq,awt}}\, d\tau
\end{aligned}
$$

where
$In_{awt}^{gdl}(t) = T_{i,m}^{su \to aq}{}_{awt}(t)$ for first-order rate-controlled or equilibrium dissolution transfers,

$In_{awt}^{gdl}(t) = In_{i,m}^{su \to aq\,gra}{}_{awt}(t)$ for gradual injections to model equilibrium desorption, and

$In_{awt}^{gdl}(t) = T_{i,m}^{aqpc \to aq}{}_{awt}(t)$ for diffusive transport in the moisture from the radionuclide-bearing material to the primary contamination.

The other symbols are described in Appendix H and represent the values that apply to the part of the primary contamination that is above the water table. The distribution coefficient is set to zero for any radionuclide for which equilibrium solubility transfer is specified. As described in Section H.3.1, the evaluation of this convolution is faster if the calculation time points are linearly spaced (see Section E.1).

The release from the instantaneous injections is obtained by multiplying the magnitude of the injection by the transfer function described in Section H.3.4. For a primary contamination that is above the water table, the release of radionuclide i at the bottom from the instantaneous injection of radionuclide i, $R_b^i\left(\frac{T_{pc}^{eq,awt}}{2}, t\right)$, is of the following form:

$$R_b^i\left(\frac{T_{pc}^{eq,awt}}{2}, t_m\right)$$

$$= In_{i,m}^{su\to aq} {}_{awt}^{ins}(t_l) \frac{e^{-\lambda(t_m-t_l)}}{T_{pc}^{eq,awt}}$$

$$\times \left\{ \frac{V_C}{2}\left[erf\left(\frac{T_{pc}^{eq,awt} - V_C(t_m - t_l)}{\sqrt{4D_x^c(t_m - t_l)}}\right) - erf\left(\frac{-V_C(t_m - t_l)}{\sqrt{4D_x^c(t_m - t_l)}}\right)\right] \right.$$

$$\left. - \sqrt{\frac{D_x^c}{4\pi(t_m - t_l)}}\left[e^{-\left(\frac{T_{pc}^{eq,awt} - V_C(t_m-t_l)}{\sqrt{4D_x^c(t_m-t_l)}}\right)^2} - e^{-\left(\frac{V_C(t_m-t_l)}{\sqrt{4D_x^c(t_m-t_l)}}\right)^2} \right] \right\}$$

The total release of radionuclide i at the bottom from the gradual and instantaneous injections used to model the equilibrium desorption transfer of radionuclide i, $R_b\left(\frac{T_{pc}^{eq,awt}}{2}, t_m\right)$, is the sum of the releases from the gradual and instantaneous injections:

$$R_b\left(\frac{T_{pc}^{eq,awt}}{2}, t_m\right) = R_b^g\left(\frac{T_{pc}^{eq,awt}}{2}, t_m\right) + R_b^i\left(\frac{T_{pc}^{eq,awt}}{2}, t_m\right)$$

A schematic of modeling the equilibrium release at the bottom of the portion of the primary contamination that is above the water table is shown in Figure G-8.
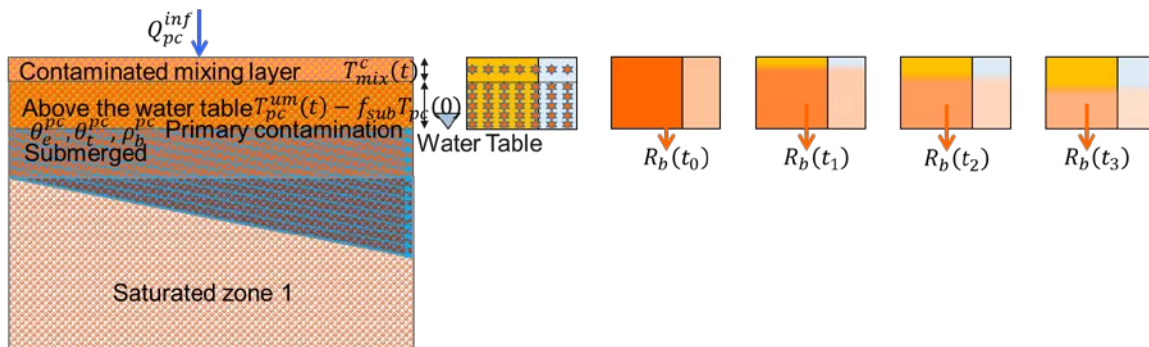
Figure G-8   Equilibrium Release at the Bottom of the Portion of the Primary Contamination that Is above the Water Table

The release from the down-gradient edge of the submerged portion of the primary contamination is due to both the releases entering the submerged portion from the portion that is above the water table and the transfers or injections that occur in the submerged portion (Figure G-9).
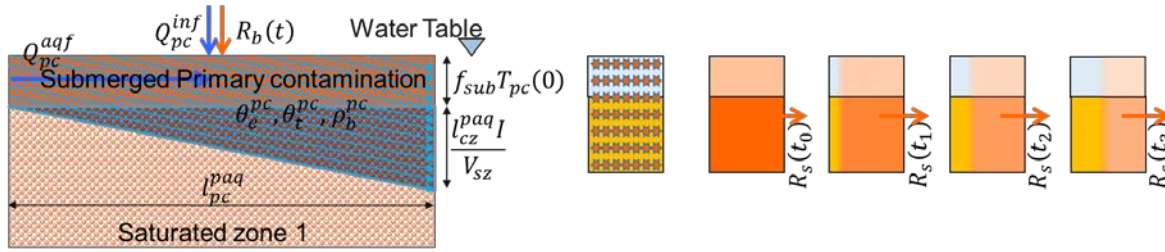
Figure G-9   Release at the Down-Gradient Edge of the Primary Contamination that Is Submerged

The release from a gradual transfers and injections over time is obtained by convolving the transfer function described in Section H.3.4. For a primary contamination that is submerged, the release of radionuclide i at the down-gradient edge from the gradual transfer of radionuclide i, $R_s^g \left(\frac{l_{pc}^{paq}}{2}, t \right)$, is of the following form:

$$R_s^g \left(\frac{l_{pc}^{paq}}{2}, t_m \right) = \int_{t_0=0}^{t_m} In_{sub}^{gdl}(t_m - \tau) \frac{e^{-\lambda \tau}}{l_{pc}^{paq}} \left\{ \frac{V_C}{2} \left[erf \left(\frac{l_{pc}^{paq} - V_C \tau}{\sqrt{4 D_x^c \tau}} \right) - erf \left(\frac{0 - V_C \tau}{\sqrt{4 D_x^c \tau}} \right) \right] \right.$$
$$\left. - \sqrt{\frac{D_x^c}{4 \pi \tau}} \left[e^{-\left(\frac{l_{pc}^{paq} - V_C \tau}{\sqrt{4 D_x^c \tau}} \right)^2} - e^{-\left(\frac{0 - V_C \tau}{\sqrt{4 D_x^c \tau}} \right)^2} \right] d\tau \right\}$$

where

$In_{sub}^{gdl}(t) = T_{i,m}^{su \to aq}{}_{sub}(t) + R_b \left(\frac{T_{pc}^{eq,awt}}{2}, t \right)$ for first-order rate-controlled or equilibrium dissolution transfers,

$In_{sub}^{gdl}(t) = In_{i,m}^{su \to aq}{}_{sub}^{gdl}(t) + R_b \left(\frac{T_{pc}^{eq,awt}}{2}, t \right)$ for gradual injections to model equilibrium desorption, and

$In_{sub}^{gdl}(t) = T_{i,m}^{aqpc \to aq}{}_{sub}(t)$ for diffusive transport in the moisture from the radionuclide-bearing material to the primary contamination.

The other symbols are described in Appendix H and represent the values that apply to the part of the primary contamination that is submerged. As described in Section H.3.1, the evaluation of this convolution is faster if the calculation time points are linearly spaced (see Section E.1).

The release from the instantaneous injection is obtained by multiplying the magnitude of the injection by the transfer function described in Section H.3.4. For a primary contamination that is submerged, the release of radionuclide i at the down-gradient edge from the instantaneous injection of radionuclide i, $R_s^i \left(\frac{l_{pc}^{paq}}{2}, t \right)$, is of the following form:

$$R_s^i\left(\frac{l_{pc}^{paq}}{2}, t_m\right) = In_{i,m}^{su \to aq\,ins}{}_{sub}(t_l)\frac{e^{-\lambda(t_m - t_l)}}{l_{pc}^{paq}}$$

$$\times \left\{ \frac{V_C}{2}\left[erf\left(\frac{l_{pc}^{paq} - V_C(t_m - t_l)}{\sqrt{4D_x^c(t_m - t_l)}}\right) - erf\left(\frac{-V_C(t_m - t_l)}{\sqrt{4D_x^c(t_m - t_l)}}\right)\right] \right.$$

$$\left. - \sqrt{\frac{D_x^c}{4\pi(t_m - t_l)}}\left[e^{-\left(\frac{l_{pc}^{paq} - V_C(t_m - t_l)}{\sqrt{4D_x^c(t_m - t_l)}}\right)^2} - e^{-\left(\frac{V_C(t_m - t_l)}{\sqrt{4D_x^c(t_m - t_l)}}\right)^2}\right]\right\}$$

The total release of radionuclide i at the down-gradient edge from the gradual and instantaneous injections used to model the equilibrium desorption transfer of radionuclide i, $R_s\left(\frac{l_{pc}^{paq}}{2}, t_m\right)$, is the sum of the releases from the gradual and instantaneous injections:

$$R_s\left(\frac{l_{pc}^{paq}}{2}, t_m\right) = R_s^g\left(\frac{l_{pc}^{paq}}{2}, t_m\right) + R_s^i\left(\frac{l_{pc}^{paq}}{2}, t_m\right)$$

The effective porosity of the primary contamination should be set to the total porosity when using the default choice of retardation factor described in Section H.2.1.11. If different values are specified for the effective and total porosities of the primary contamination, the other choice of the retardation factor must be used to obtain the release with the expected magnitude and duration for an equilibrium desorption-based release.

The release of the progeny of radionuclide i due to the transfer of radionuclide i is computed in a similar manner using one of the two choices of transfer factors described in Section H.2.5.

G.14 Concentration Profile in Adsorbed and Aqueous Phases

The transfers and imaginary injections described in Section G.11 occur uniformly over the transport length of the primary contamination. The concentration at any point within the primary contamination can be obtained by convolving the transfer or the gradual injection with the appropriate transfer function developed in Appendix H and by multiplying the instantaneous injection by the transfer function. The code currently does not compute the concentrations along the transport distance. The following is a description of how they might be computed in a future version of the code.

The aqueous concentration from a gradual transfers and injections over time is obtained by convolving the transfer function described in Section H.2.4. For a primary contamination that is above the water table, the aqueous concentration of radionuclide i, at a distance x from the center of the primary contamination, from the gradual transfer of radionuclide i, $c_{awt}^{g,aq}(x, t)$, is of the following form:

$$c_{awt}^{g,aq}(x, t_m) = \int_{t_0=0}^{t_m} In_{awt}^{gdl}(t_m - \tau)\frac{e^{-\lambda\tau}}{2AT_{pc}^{eq,awt}\theta_m R_d}$$

$$\times \left[erf\left(\frac{x + T_{pc}^{eq,awt}/2 - V_C\tau}{\sqrt{4D_x^c\tau}}\right) - erf\left(\frac{x - T_{pc}^{eq,awt}/2 - V_C\tau}{\sqrt{4D_x^c\tau}}\right)\right]d\tau$$

where

$$In_{awt}^{gdl}(t) = T_{i,mawt}^{su \to aq}(t) \text{ for first-order rate-controlled or equilibrium dissolution transfers,}$$

$$In_{awt}^{gdl}(t) = In_{i,mawt}^{su \to aq\,gra}(t) \text{ for gradual injections to model equilibrium desorption, and}$$

$$In_{awt}^{gdl}(t) = T_{i,mawt}^{aqpc \to aq}(t) \text{ for diffusive transport in the moisture from the radionuclide-bearing material to the primary contamination.}$$

The other symbols are described in Appendix H and represent the values that apply to the part of the primary contamination that is above the water table. As described in Section H.3.1, the evaluation of this convolution is faster if the calculation time points are linearly spaced (see Section E.1).

The aqueous concentration from the instantaneous injections is obtained by multiplying the magnitude of the injection by the transfer function described in Section H.2.4. For a primary contamination that is above the water table, the aqueous concentration of radionuclide i, at a distance x from the center of the primary contamination, from the instantaneous injection of radionuclide i, $c_{awt}^{i,aq}(x, t_m)$, is of the following form:

$$c_{awt}^{i,aq}(x, t_m) = In_{i,mawt}^{su \to aq\,ins}(t_l) \frac{e^{-\lambda(t_m - t_l)}}{2AT_{pc}^{eq,awt}\theta_m R_d}\left[erf\left(\frac{x + T_{pc}^{eq,awt}/2 - V_C(t_m - t_l)}{\sqrt{4D_x^c(t_m - t_l)}} \right) \right.$$
$$\left. - erf\left(\frac{x - T_{pc}^{eq,awt}/2 - V_C(t_m - t_l)}{\sqrt{4D_x^c(t_m - t_l)}} \right) \right]$$

The total aqueous concentration of radionuclide i, at a distance x from the center of the primary contamination that is above the water table, from the gradual and instantaneous injections used to model the equilibrium desorption transfer of radionuclide i, $c_{awt}^{aq}(x, t_m)$, is the sum of the concentrations from the gradual and instantaneous injections:

$$c_{awt}^{aq}(x, t_m) = c_{awt}^{g,aq}(x, t_m) + c_{awt}^{i,aq}(x, t_m)$$

The concentration in the submerged portion of the primary contamination is due to both the releases entering the submerged portion from the portion that is above the water table and the transfers or injections that occur in the submerged portion. The aqueous concentration from transfers and gradual injections over time is obtained by convolving the transfer function described in Section H.2.4. For a primary contamination that is submerged, the aqueous concentration of radionuclide i, at a distance x from the center of the primary contamination, from the gradual transfer of radionuclide i, $c_{sub}^{g,aq}(x, t)$, is of the following form:

$$c_{sub}^{g,aq}(x, t_m) = \int_{t_0=0}^{t_m} In_{sub}^{gdl}(t_m - \tau) \frac{e^{-\lambda\tau}}{2Af_{sub}T_{pc}\theta_m R_d}$$
$$\times \left[erf\left(\frac{x + l_{pc}^{paq}/2 - V_C\tau}{\sqrt{4D_x^c\tau}} \right) - erf\left(\frac{x - l_{pc}^{paq}/2 - V_C\tau}{\sqrt{4D_x^c\tau}} \right) \right] d\tau$$

where

$$In_{sub}^{gdl}(t) = T_{i,m}^{su \to aq}{}_{sub}(t) + R_b\left(\frac{T_{pc}}{2}, t\right) \text{ for first-order rate-controlled or equilibrium}$$
dissolution transfers,

$$In_{sub}^{gdl}(t) = In_{i,m}^{su \to aq\,gdl}{}_{sub}(t) + R_b\left(\frac{T_{pc}}{2}, t\right) \text{ for gradual injections to model equilibrium}$$
desorption, and

$$In_{sub}^{gdl}(t) = T_{i,m}^{aqpc \to aq}{}_{sub}(t) \text{ for diffusive transport in the moisture from the radionuclide-}$$
bearing material to the primary contamination.

The other symbols are described in Appendix H and represent the values that are applicable to the part of the primary contamination that is submerged. As described in Section H.3.1, the evaluation of this convolution is faster if the calculation time points are linearly spaced (see Section E.1).

The aqueous concentration from the instantaneous injection is obtained by multiplying the magnitude of the injection by the transfer function described in Section H.2.4. For a primary contamination that is submerged, the aqueous concentration of radionuclide i, at a distance x from the center of the primary contamination, from the instantaneous injection of radionuclide i, $c_{sub}^{i,aq}(x,t)$, is of the following form:

$$c_{sub}^{i,aq}(x,t_m) = In_{i,m}^{su \to aq\,ins}{}_{sub}(t_l) \frac{e^{-\lambda(t_m - t_l)}}{2Af_{sub}T_{pc}\theta_m R_d}\left[erf\left(\frac{x + l_{pc}^{paq}/2 - V_C(t_m - t_l)}{\sqrt{4D_x^c \tau}}\right)\right.$$
$$\left. - erf\left(\frac{x - l_{pc}^{paq}/2 - V_C(t_m - t_l)}{\sqrt{4D_x^c \tau}}\right)\right]$$

The total aqueous concentration of radionuclide i, at a distance x from the center of the primary contamination that is submerged, from the gradual and instantaneous injections used to model the equilibrium desorption transfer of radionuclide i, $c_{sub}^{aq}(x,t_m)$, is the sum of the concentrations from the gradual and instantaneous injections:

$$c_{sub}^{aq}(x,t_m) = c_{sub}^{g,aq}(x,t_m) + c_{sub}^{i,aq}(x,t_m)$$

The aqueous concentration of the progeny of radionuclide i due to the transfer of radionuclide i, can be computed in a manner similar to the computation of the release of the progeny.

G.15 Releases from the Surface Layer

The concentration of the radionuclides in the surface mixing layer at the location of the primary contamination is computed using the following expression:

$$s_{i,m}^{ss}(t) = f_{vm}(t)\rho_b^{pc}s_{i,m}^{pc}(t)/\rho_b^{mix}(t) \tag{G.67}$$

where

$s_{i,m}^{ss}(t)$ = concentration of radionuclide i of transformation thread m in the surface mixing layer at time t (Activity/g),

$s_{i,m}^{pc}(t)$ = concentration of radionuclide i of transformation thread m in primary contamination at time t (Activity/g),

$f_{vm}(t)$ = volume fraction of the primary contamination in the mixing layer,
ρ_b^{pc} = dry bulk density of the primary contamination at time t (g/[cm]³), and
$\rho_b^{mix}(t)$ = dry bulk density of the surface mixing layer at time t (g/[cm]³).

The release of radionuclide i of transformation thread m with eroded material to surface runoff at time t is given by:

$$ER_{i,m}(t) = s_{i,m}^{ss}(t)m_{ro}^{ss}(t) = m_{ro}^{pc}(t)s_{i,m}^{pc}(t) \qquad (G.68)$$

where

$ER_{i,m}(t)$ = rate of release of radionuclide i of transformation thread m in the eroded material in runoff at time t (Activity/yr),

$m_{ro}^{pc}(t)$ = rate at which material is eroded from the primary contamination by runoff at time t (g/yr),

$s_{i,m}^{pc}(t)$ = concentration of radionuclide i of transformation thread m in primary contamination at time t (Activity/g),

$s_{i,m}^{pc}(t) = s_{i,m}^{su}(t)$; by default, only the release-susceptible concentration is used to compute the release from the surface layer, and

$s_{i,m}^{pc}(t) = s_{i,m}^{su}(t) + s_{i,m}^{im}(t)$; the user can choose to use the sum of the release-susceptible and release-immune-concentrations to compute the release from the surface layer. This can be useful when a radionuclide transfers under equilibrium desorption.

The release of radionuclide i of transformation thread m, attached to particulates, to the atmosphere at time t is given by:

$$AR_{i,m}^{tl}(t) = s_{i,m}^{ss}(t)ML\,A\,V_{d_i}^{tl} = f_{vm}(t)\rho_b^{pc}s_{i,m}^{pc}(t)ML\,A\,V_{d_i}^{tl}/\rho_b^{mix}(t) \qquad (G.69)$$

where

$AR_{i,m}^{tl}(t)$ = rate at which radionuclide i of transformation thread m, attached to particulates, is released to the atmosphere at time t (Activity/yr),

ML = mass loading of particulates in air above the primary contamination (g/m³),

$V_{d_i}^{tl}$ = deposition velocity of particulates containing radionuclide i (m/yr),

$s_{i,m}^{pc}(t)$ = concentration of radionuclide i of transformation thread m in primary contamination at time t (Activity/g),

$s_{i,m}^{pc}(t) = s_{i,m}^{su}(t)$ by default, only the release-susceptible concentration is used to compute the release from the surface layer, and

$s_{i,m}^{pc}(t) = s_{i,m}^{su}(t) + s_{i,m}^{im}(t)$; the user can choose to use the sum of the release-susceptible and release-immune concentrations to compute the release from the surface layer. This can be useful when a radionuclide transfers under equilibrium desorption.

The release of radionuclide i of transformation thread m, attached to respirable particulates, to the atmosphere at time t is given by the following:

$$AR_{i,m}^{rp}(t) = s_{i,m}^{ss}(t) f_{rp} ML \, A \, V_{d_i}^{rp} = f_{vm}(t) \rho_b^{pc} s_{i,m}^{pc}(t) f_{rp} ML \, A \, V_{d_i}^{rp} / \rho_b^{mix}(t) = f_{rp} \frac{V_{d_i}^{rp}}{V_{d_i}^{tl}} AR_{i,m}^{tl}(t) \quad \text{(G.70)}$$

where

$AR_{i,m}^{rp}(t)$ = rate at which radionuclide i of transformation thread m, attached to respirable particulates, is released to the atmosphere at time t (Activity/yr),

f_{rp} = respirable fraction of particulates at the primary contamination, and

$V_{d_i}^{rp}$ = deposition velocity of respirable particulates containing radionuclide i (m/yr).

Thus, the temporal release of radionuclides attached to the respirable particulates can be obtained by multiplying the temporal release of radionuclides attached to (all) particulates, described in Section G.16, by $f_{rp} V_{d_i}^{rp} / V_{d_i}^{tl}$.

G.16 Description of Intermediate Output

Sample intermediate output files for a run with radionuclides Ac-227 and Ra-226 using a 30-day cutoff half-life and the ICRP-107 transformation data (Appendix A) are shown in Figure G-16. The determination of the transformation threads for these radionuclides are described in Appendix E, Section E.4. Ac-227 has a single transformation thread with Ac-227 as the only principal radionuclide. Ra-226 has two transformation threads, Ra-226, Pb-210, Po-210, with a thread fraction of 1 and Ra-226, Pb-210 with a thread fraction of 1.339 10^{-6}. Thus each of the intermediate output files, AIFLUXIN.DAT, AQFLUXIN.DAT, GWtoSWBFLUX.DAT, SFSIN.DAT, and WTFLUXIN.DAT have seven columns of data for the example run. The first column lists the calculation times in ascending order. The second through seventh columns contain information about the radionuclides Ac-227, Ra-226 (thread 1), Pb-210 (thread 1), Po-210 (thread 1), Ra-226 (thread 2), and Pb-210 (thread 2) at each of the calculation time. In general, these files will have the calculation time in the first column and a column of data for each of the principal radionuclides in each transformation thread in the order in which the threads are listed in the chain file corresponding to the input file, *inputfilename*.CHN.

Figure G-10 Sample Intermediate Output

The information contained in each file corresponds to the file name, as shown in Table G-1. The file AQTRANIN.DAT has additional rows of data in two columns. The file SWFLUXIN.DAT has four more columns in addition to the ones in the other files. These additional rows and columns are illustrated in Figures G-11 and G-12 and are described in the next two paragraphs.

Table G-1 Information in Intermediate Output File

Intermediate File	Information in File
AIFLUXIN.DAT	Release, attached to particulates, to atmosphere from the surface layer in pCi/yr.[a]
AQFLUXIN.DAT	Release, in aqueous phase, to water at the down gradient edge of the primary contamination in pCi/year.
GWtoSWBFLUX.DAT	Transfer, in aqueous phase, from the aquifer to the surface water body in pCi/year.
SFSIN.DAT	The concentration in the primary contamination in pCi/g, averaged over the primary contamination. Currently includes the release immune form for all transfer options and the release susceptible form for the rate controlled and the equilibrium dissolution transfer mechanisms, but not the aqueous or adsorbed phases.
WTFLUXIN.DAT	Transfer, in aqueous phase, across the water table to the aquifer in pCi/yr.
AQTRANIN.DAT	Transfer to infiltration or gradual injection in the part of the primary contamination that is above the water table in pCi/yr. Instantaneous injection in the part of the primary contamination that is above the water table in pCi.
SWFLUXIN.DAT	Release, in eroded material, to surface runoff from the surface layer in pCi/yr. Mass of material eroded from the primary contamination and the surface layer in g/yr. Mass of suspended sediment in the surface water body in g and mass of bottom sediment on which the radionuclides are in adsorption-desorption equilibrium with water in the surface water body.

[a] The computations are performed in pCi and mrem regardless of units specified in the input file. The intermediate output are in these units. The final output, both graphical and the textural, is converted to the units specified in the input file.

There are four additional columns in SWFLUXIN.DAT Figure G-11. The first of the additional columns lists the rate at which the material from the primary contamination is released in the runoff in g/yr. The second additional column lists the rate at which material from the surface layer of the primary contamination is released in the runoff in g/yr. The last two columns list the mass of suspended sediments in the surface water body and the mass of the bottom sediments on which the radionuclides are in adsorption-desorption equilibrium with the water in the surface water body, both in grams.
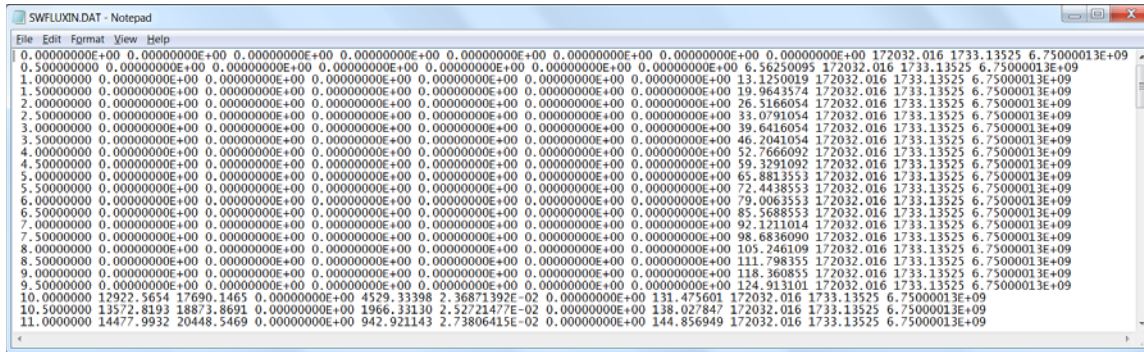
Figure G-11 Sample of SWFLUXIN.DAT

The file AQTRANIN.DAT has additional rows of data in two columns (Figure G-12). The first column has the time, in years, of an instantaneous injection used to model the release of radionuclides out of the primary contamination when they transfer under equilibrium desorption. The second column has the activity of the injection in pCi. The file has a row for each time at which the release properties change and for each of the principal radionuclides in each transformation thread in the order in which the threads are listed in the chain file corresponding to the input file, *inputfilename*.CHN.
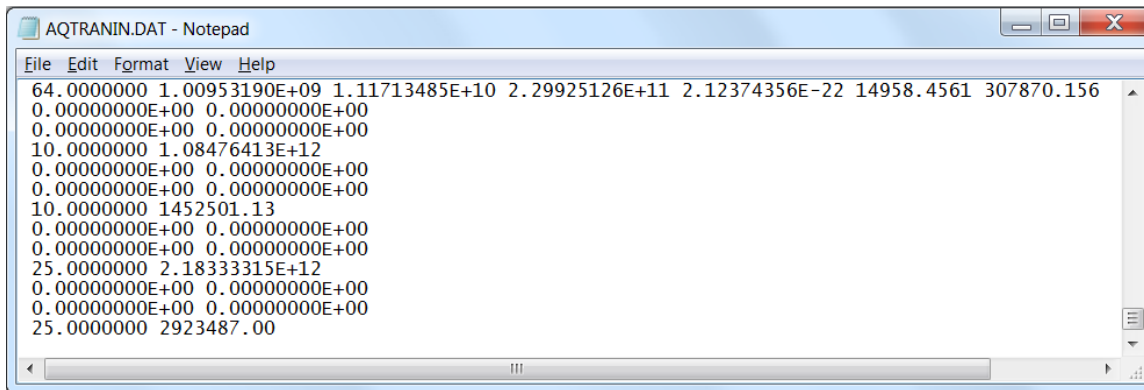
Figure G-12   Sample of Additional Rows of Data in AQTRANIN.DAT

G.17 Radionuclide Balance

The code maintains a balance of the radionuclide inventory taking into account the loss and gain from radiological transformation within the primary contamination, the releases to infiltrating water and to runoff. The evasion losses are also included in the mass balance considerations of H-3 and of C-14.

For the radionuclides with half-lives that are very long relative to the duration of the releases, this balance can be checked by integrating over time, the temporal releases in AQFLUXIN.DAT and in SWFLUXIN.DAT and by verifying that the sum of the time integrated releases is equal to the initial inventory of the radionuclide. The time integration of the data in AIFLUXIN.DAT, of the release of radionuclides attached to particulates, to the atmosphere, will give an indication of the inventory that the code does not consider in maintaining mass balance; this will be negligible in almost all cases.

The mass balance of radionuclides with half-lives that are comparable or smaller in than the duration of the releases can be verified by first converting the releases at each time back to the rate at time 0 by adjusting for the loss due to radiological transformations during time t. This is done using the following expression:

$$R_0(t) = R(t)e^{\lambda t}$$

where

$R_0(t)$ = release at time t expressed in terms of Activity at time 0 (Activity/yr),
$R(t)$ = release at time t expressed in terms of Activity at time t (Activity/yr) and,
λ = transformation constant of the radionuclide (1/yr).

These release rates expressed in terms of the activity at time 0 can be integrated over time and the sum of these integrals can be compared with the initial inventory to verify that they are equal.

Verifying the mass balance of progeny produced from initially present parent radionuclides is more difficult. One way is to compare the difference between the number of atoms in the initial inventory of parent radionuclide and the number of atoms of the parent that were released over time with the number of atoms of all the progeny that were released over time.

G.18 Overriding the Source Term

For scenarios for which the primary contamination is entirely above the water table, the code can be flagged to suppress the source concentration and release models and read information on the source concentrations, releases and dimensions. The intermediate files AIFLUXIN.DAT, AQFLUXIN.DAT, SFSIN.DAT and SWFLUXIN.DAT (described in Section G.16) and the file CZTHICK3.DAT (described in Section G.1.9) can be used to input this information. These files must be in the format described in those sections. The RESRAD-OFFSITE input file must be modified in a text editor to specify the number of times at which the data is to be read; these must be specified in both the locations shown in Figure G-13:

- NAIFLXT is the number of times at which the release to the atmosphere is being specified in file AIFLUXIN.DAT.

- NAQFLXT is the number of times at which the release to the infiltrating water is being specified in file AQFLUXIN.DAT.

- NSFST is the number of times at which the concentration in the primary contamination is being specified in file SFSIN.DAT. It is also the number of times at which the thicknesses are specified in CZTHICK3.DAT.

- NSWFLXT is the number of times at which the release to the infiltrating water is being specified in file SWFLUXIN.DAT.

The five files containing the data in the specified number of rows must be placed in the RESRAD-OFFSITE directory and to be read by the code. The code will overwrite them after they are read. The procedure for overriding the source module is illustrated in detail in Appendix A to NUREG/CR-7189.


```
SAMPLE OUTOPUT AC227 RA226 ICRP107.ROF - Notepad

File  Edit  Format  View  Help

&DB
CODENAME = 'RESRAD-OFFSITE',
ICRPTRANS = 'ICRP107',
HAFTIM = '30 days',
EDFFILE = 'DCFPAK3.02',
DFFILE = 'DCFPAK3.02 (Adult)',
SFFILE = 'DCFPAK3.02 Morbidity',
TFFILE = 'RESRAD Default Transfer factors',
EXTDLIB= 'DCFPAK3.02',
DOSELIB= 'DCFPAK3.02 (Adult)',
RISKLIB= 'DCFPAK3.02 Morbidity',
NAIFLXT = 0 ,
NAQFLXT = 0 ,
NSFST = 0 ,
NSWFLXT = 0 ,
NSWCONC = 0 ,
NWWCONC = 0 ,
NANUC =  6 ,
NIY =  7 ,
NPD =  6 ,
NPTS =  128 ,
NS =  1 ,
NPDS =  10 ,
```

```
SAMPLE OUTOPUT AC227 RA226 ICRP107.ROF - Notepad

File  Edit  Format  View  Help

RLEACH = .0001, .001, 7*0, .0001, 8*0, .0001, 8*0,
SOLUB = 1E-12, 35*0, 1E-12, 1E-11, 7*0, 1E-12, 1E-
RELFRAC = .5, 8*1, .5, 8*1, .5, 8*1, .5, 8*1, .5,
RELTIMEOPT = 1, 8*0, 1, 8*0, 1, 8*0, 1, 8*0, 2*1,
RELTIMEOPTP = 1, 8*0, 1, 8*0, 1, 8*0, 1, 8*0, 1, 8
RELOPT = 0, 2*1, 0, 2*2,
RELAIRTIMEOPT = 6*0,
DEPVEL = 6*.001,
DEPVELT = 6*.001,
NSENA = 0,
NUM_SAMPS = 0, NUMVAR = 0, NUMRELVAR = 0,
SELPATH = 255,
NAIFLXT = 0 ,
NAQFLXT = 0 ,
NSFST = 0 ,
NSWFLXT = 0 ,
NSWCONC = 0 ,
NWWCONC = 0 ,
STARFILEREAD = 0 ,
STARFILELOCATION = '',
SAVEGTDATA = 0 ,
&END
&DCSF
```

Figure G-13 The Two Locations in the Input File where the Code must be Flagged to Suppress Source Term Calculations and to Read in the Releases from and the Concentration in the Primary Contamination

G.19 <u>References</u>

Gnanapragasam, E.K., and C. Yu, 2015, *User's Guide for RESRAD-OFFSITE*, ANL/EVS/TM/14/2, NUREG/CR-7189, prepared by Argonne National Laboratory for U.S. Nuclear Regulatory Commission, April.

Shen, H.W., and P.Y. Julien, 1993, "Erosion and Sediment Transport" in *Handbook of Hydrology*, D.R. Maidment (ed.), McGraw-Hill Inc.

APPENDIX H:
GROUNDWATER TRANSPORT MODEL

Section 5.2.2 presents an overview of the groundwater transport modeled in RESRAD-OFFSITE. This appendix expands on the conceptualization, develops the mathematical expression, and describes how the expressions are implemented in RESRAD-OFFSITE. Section H.1 describes the manner in which RESRAD-OFFSITE conceptualizes the groundwater transport pathway, specifically the unsaturated or partially saturated zones, including the primary contamination that is above the water table, and the saturated zone, including the primary contamination that is below the water table and the transport through these zones. Section H.2 discusses derivation of the mathematical expressions that result from the conceptualization. Section H.3 deals with the implementation of the mathematical expressions and the evaluation of these expressions in the computational code.

H.1   Conceptualization of Groundwater Transport

The conceptual model for the groundwater pathway consists of the primary contamination, zero to five horizontal layers of partially saturated zones, and one unconfined, initially uncontaminated, saturated zone; Figure H-1 illustrates a situation in which a primary contamination is above the water table with two partially saturated zones. The flow in the partially saturated zones, including in the primary contamination that is above the water table, is in the downward vertical direction; advective and dispersive transport in the vertical direction are modeled in these zones. The flow in the saturated zone, including the primary contamination that is below the water table, is in the horizontal direction; advective and dispersive transport in the direction of flow and dispersive transport in the two directions perpendicular to the flow are modeled.

The plan view of the primary contamination (its shape in the horizontal plane) is assumed to be rectangular, with one pair of sides parallel to the direction of groundwater flow. The contaminant plume in the partially saturated zone maintains this rectangular shape because transport in the partially saturated zone is assumed to occur only in the vertical direction.

The transport zones are treated as homogenous layers; the specified properties (density, porosities, hydraulic conductivity, dispersivities, and hydraulic gradient) are assumed to be constant over a transport zone. Only the pores that are interconnected are of concern in modeling the transport of radionuclides in groundwater, because isolated pores do not affect the movement of the radionuclides. The conceptual model differentiates between two kinds of interconnected pores: mobile pores and immobile pores (Figure H-2). The water in mobile pores is free to move and contributes to the advective transport of radionuclides. The moisture in the immobile pores is held in place either because it is in dead-end pores or because it is tightly bound to the solid phase and does not contribute to the advective transport of radionuclides. The total porosity is the measure of all the moisture-filled connected pores (both mobile and immobile) into which the radionuclide can enter by either advection or diffusion. The effective porosity is the measure of the moisture-filled pores that are effective in the advective transport of the radionuclide. Moisture in pores that lead to dead ends and moisture that is tightly bound to the solid phase of the soil and is thus immobile are two factors that can cause the total porosity to be greater than the effective porosity. The derivation in Section H.2.1 assumes that immobile pores are due to dead ends.
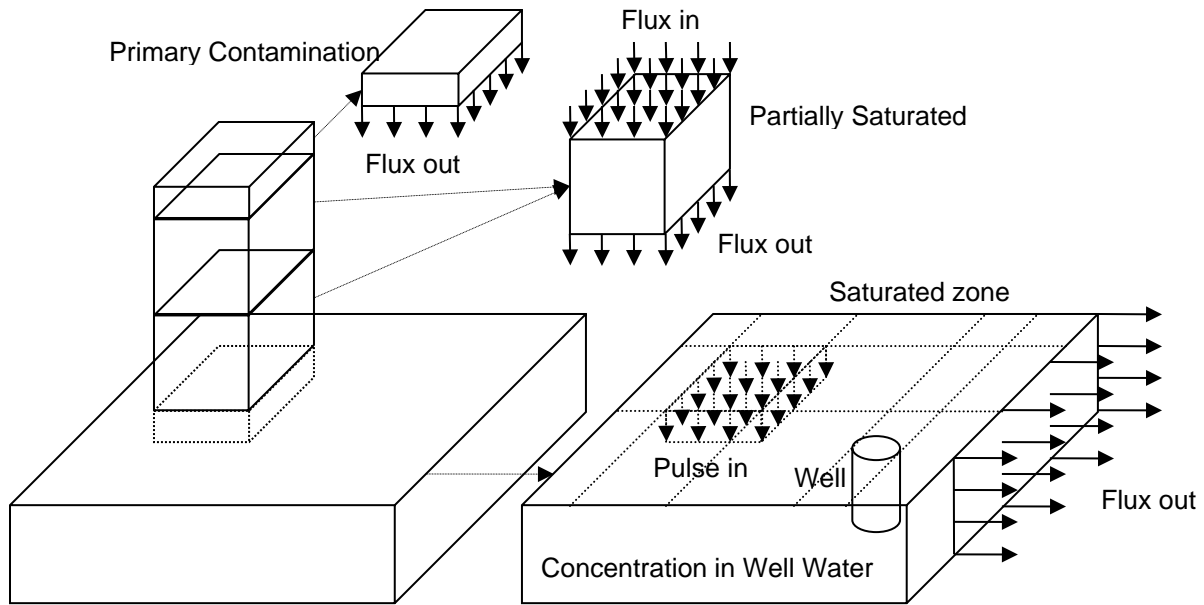
Figure H-1   Conceptualization of Groundwater Transport in RESRAD-OFFSITE
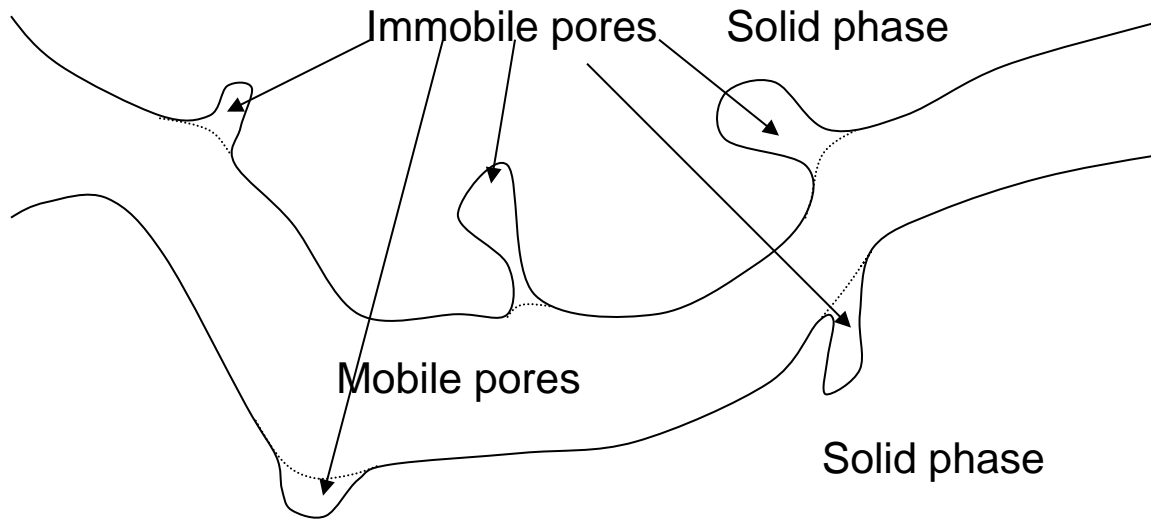
Figure H-2   Conceptualization of Mobile and Immobile Pores

H.2   Derivation of Mathematical Expressions for the Conceptual Groundwater Transport Model

The conceptual model must be translated into mathematical expressions that can be implemented in the computational code. The idealized descriptions of Section H.1 are expressed in mathematical terms in this section.

Each partially saturated zone is idealized in the conceptual model as a rectangular prism. The rate at which the radionuclide exits the contaminated zone is known at each of the calculation times, as discussed in Section G.13. If the primary contamination is above the water table, this is also the rate at which the radionuclide enters across the upper boundary of the uppermost partially saturated zone, a flux input. The groundwater transport model computes the rates at which the radionuclide and its progeny, if any, exit the lower boundary of each partially saturated layer.

When a large number of atoms of a radionuclide travel across a transport layer, some of them will undergo radiological transformations and will exit the layer as one of the progeny of the radionuclide that entered the layer. The remainder, which did not transform, will exit the layer in the same form as when they entered. If a radionuclide travels through an entire transport layer in the same form, the equations developed in this section for the rate of exit as a function of the rate of entry consider the effects of longitudinal dispersion on the transport of that radionuclide. Two solutions are developed for the transport of a progeny radionuclide that enters the layer as one of its parents and then transforms within the layer. One considers the effects of radionuclide-specific distribution coefficients of the radionuclides in the transformation chain from the parent to the progeny and ignores the effects of longitudinal dispersion; the other considers the effects of longitudinal dispersion and ignores the effects of radionuclide-specific distribution coefficients. A method for modeling both processes is discussed in Section H.3.13.

The idealized saturated zone that is conceptualized by the code is depicted in Figure H-3. The rate at which the radionuclide transfers out of the last unsaturated zone, or in the absence of any unsaturated zone, out of the primary contamination, is treated as a pulse input distributed over a rectangular prism within the saturated zone. The length and width of this rectangular prism are the same as those of the primary contamination. The depth is determined by the depth of advective penetration (Section H.2.4).
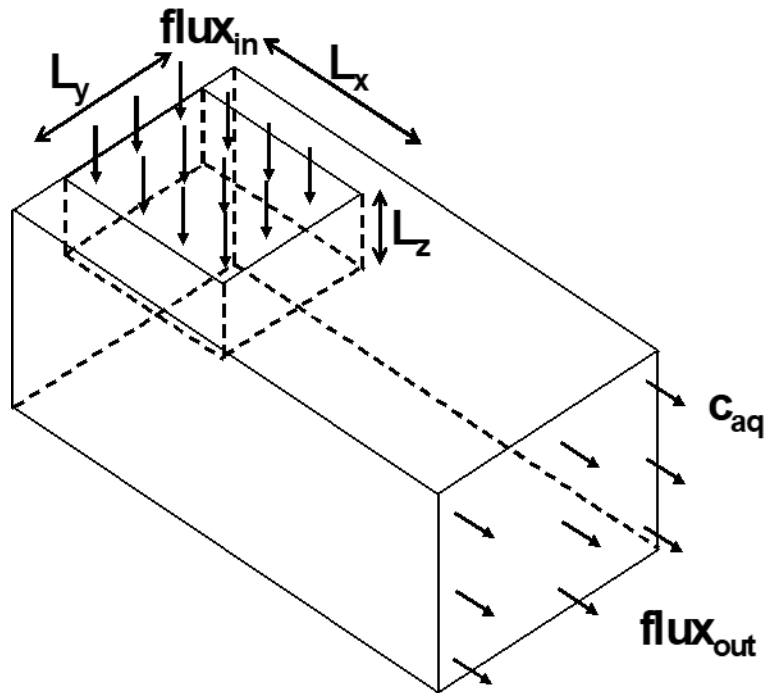
Figure H-3   Idealized Saturated Zone Modeled by RESRAD-OFFSITE

The groundwater transport model computes the spatial profile of the transfer across a vertical plane in the aquifer or the spatial profile of the concentration in water over a vertical plane in the aquifer. Consideration of transverse and lateral dispersion is separated from the consideration of longitudinal dispersion for ease of computation. Two expressions are developed to model the transport of those atoms that transformed within the transport zone following a pulse input; one considers longitudinal dispersion while the other considers the radionuclide-specific distribution coefficients, just as they were considered for a flux input.

H.2.1   Governing Equation for the Transport of Radionuclides in Soil

The equation governing the transport of radionuclides in porous media is obtained by expressing each of the processes being modeled in mathematical form. The processes considered are the losses and gains resulting from radiological transformations, advective transport by water as it flows through the porous medium, and dispersive transport caused by concentration gradients. The net result of these processes is a change in storage in the surface of the solid phase and in the aqueous phase of the soil. The mathematical representations of the process are written considering an elemental volume (Figure H-4) of dimensions $δx$ (m), $δy$ (m), and $δz$ (m) over a time period of $δt$ (yr).
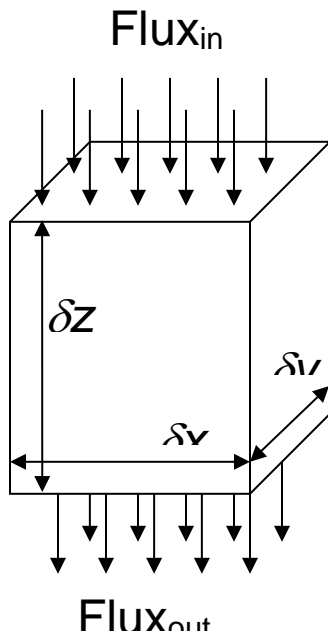
Figure H-4   Elemental Volume of Soil

H.2.1.1   Volume of Connected Moisture-Filled Pores and the Soil in Contact with the Pores

The porosities of the two types of pores (Figure H-2) are related by the following expression:

$$\theta_m + \theta_{im} = \theta_t \; , \tag{H.1}$$

where

θ_m = mobile porosity, the porosity that allows or contributes to the movement of water;

θ_{im} = immobile porosity, the porosity that does not contribute to the movement of water; and

θ_t = sum of the two porosities; i.e., the total connected porosity.

Although the radionuclides are adsorbed to the surface of the solids in the soil, their concentration in soil is expressed in terms of the mass of the solids. The volume fraction of the soil associated with the mobile (υ_m) and the volume fraction of the soil associated with the immobile pores (υ_{im}) are assumed to be in the same ratio as the porosities of those two phases:

$$\upsilon_m : \upsilon_{im} :: \theta_m : \theta_{im} \; . \tag{H.2}$$

H.2.1.2   Partitioning of Radionuclides between the Aqueous and Solid Phases of Soil

The partitioning of radionuclides between the aqueous phase in the pores and the solid phase adsorbed to the surface is dynamic. The radionuclides are adsorbed at a rate that depends on the concentration of the radionuclides in the aqueous phase. Conversely, the radionuclides that were adsorbed on the surface desorb at a rate that depends on the concentration of radionuclides in the solid (adsorbed) phase. Over time, the two phases achieve equilibrium, and the partitioning of radionuclides between the aqueous and solid phases is characterized by a linear equilibrium distribution coefficient in RESRAD-OFFSITE:

$$K_d = \frac{s_m}{c_m}10^6 = \frac{s_{im}}{c_{im}}10^6, \tag{H.3}$$

where

K_d = distribution coefficient (cm³/g);

s_m, s_{im} = concentrations of the radionuclides in soil associated with the mobile and immobile pores, respectively (Activity/g);

c_m, c_{im} = concentrations of the radionuclides in the mobile and immobile pores, respectively (Activity/m³); and

10^6 = unit conversion factor (cm³/m³).

H.2.1.3   Quantity of Radionuclides in a Unit Volume of Soil

The quantity of radionuclides in a unit volume of soil is the sum of the quantities in the mobile and immobile pores and in the solid phase associated with these pores:

$$\theta_m c_m + \theta_{im} c_{im} + \upsilon_m \rho_b 10^6 s_m + \upsilon_{im} \rho_b 10^6 s_{im}$$

$$= \theta_m c_m + \theta_{im} c_{im} + \frac{\upsilon_m}{\upsilon_m + \upsilon_{im}} \rho_b 10^6 s_m + \frac{\upsilon_{im}}{\upsilon_m + \upsilon_{im}} \rho_b 10^6 s_{im}$$

$$= \theta_m c_m + \theta_{im} c_{im} + \frac{\theta_m}{\theta_m + \theta_{im}} \rho_b K_d c_m + \frac{\theta_{im}}{\theta_m + \theta_{im}} \rho_b K_d c_{im}$$

$$= \theta_m c_m + \frac{\rho_b K_d}{\theta_t} \theta_m c_m + \theta_{im} c_{im} + \frac{\rho_b K_d}{\theta_t} \theta_{im} c_{im} \tag{H.4}$$

$$= \left(1 + \frac{\rho_b K_d}{\theta_t}\right)\theta_m c_m + \left(1 + \frac{\rho_b K_d}{\theta_t}\right)\theta_{im} c_{im}$$

$$= \frac{\theta_m c_m + \theta_{im} c_{im}}{\theta_t}\left(\theta_t + \rho_b K_d\right)$$

$$= c_{av}\left(\theta_t + \rho_b K_d\right)$$

where C_{av} = average concentration of the radionuclide in the connected pores (pCi/m³).

H.2.1.4 Change in Quantity of Radionuclides Stored in the Elemental Volume Due to Radiological Transformations

This change in the quantity of radionuclides in the elemental volume of soil over time as a result of radiological transformations follows from the expression for the quantity of radionuclides in a unit volume of soil derived in Section H.2.1.3:

$$\text{change} = -\lambda c_{av}\left(\theta_t + \rho_b K_d\right)\delta x \delta y \delta z \; . \tag{H.5}$$

H.2.1.5 Change in Quantity of Radionuclides Stored in the Elemental Volume Due to Advective Transport

This change is the difference between the amount of radionuclides carried in by water flowing in through the mobile pores at the up-gradient face of the elemental volume and the amount of radionuclides carried out by water flowing out through the mobile pores at the down-gradient face of the elemental volume:

$$\text{change} = -V_m \theta_m \delta x \delta y \frac{\partial c_m}{\partial z}\delta z \; , \tag{H.6}$$

where V_m = average velocity of the water flowing through the mobile pores (m/yr).

H.2.1.6 Change in Quantity of Radionuclides Stored in the Elemental Volume Due to Longitudinal Dispersion

This change is the difference between the amount of radionuclides dispersing through the mobile pores across the up-gradient face of the elemental volume and the amount of radionuclides dispersing out through the mobile pores across the down-gradient face of the elemental volume:

$$\text{change} = \theta_m \delta x \delta y D_z^m \frac{\partial^2 c_m}{\partial z^2}\delta z \; , \tag{H.7}$$

where D_z^m = dispersion coefficient of the radionuclides in the mobile pores (m²/yr).

H.2.1.7 Net Change in Quantity of Radionuclides Stored in the Elemental Volume

This net change in the quantity of radionuclides in the elemental volume of soil over time follows from the expression for the quantity of radionuclides in a unit volume of soil derived in Section H.2.1.3:

$$\text{net change} = \left(\theta_t + \rho_b K_d\right)\frac{\partial c_{av}}{\partial t}\delta x \delta y \delta z \; . \tag{H.8}$$

H.2.1.8 Mass Balance Equation

Mass balance requires that the sum of changes represented by Equations (H.5), (H.6), and (H.7) be equal to the net change represented by Equation (H.8):

$$\left(\theta_t + \rho_b K_d\right)\frac{\partial c_{av}}{\partial t} = -\lambda\left(\theta_t + \rho_b K_d\right)c_{av} - V_m\theta_m\frac{\partial c_m}{\partial z} + D_z^m\theta_m\frac{\partial^2 c_m}{\partial z^2} \,. \tag{H.9}$$

Rearranging the above equation gives

$$\frac{\partial c_{av}}{\partial t} = -\lambda c_{av} + \frac{\theta_m}{\left(\theta_t + \rho_b K_d\right)}\left(-V_m\frac{\partial c_m}{\partial z} + D_z^m\frac{\partial^2 c_m}{\partial z^2}\right). \tag{H.10}$$

This equation must be solved with appropriate initial and boundary conditions to model the transport of the radionuclides in the unsaturated and saturated zones. Some of these conditions (e.g., the boundary condition for transport in the unsaturated zone, Equation [H.25]) are expressed in terms of the concentration in the mobile pores, c_m. Other conditions (e.g., the initial condition for transport in the saturated zone, Equation [H.34]) are expressed in terms of the average concentration in the connected pores, c_{av}. A relationship between these two concentrations is therefore necessary to model the transport.

H.2.1.9 Concentration of Radionuclides in the Mobile Pores and Immobile Pores

As the contaminant plume moves, the water entering the mobile pores contains radionuclides. The radionuclides in the mobile pores are transferred into the immobile pores at a rate that depends on the concentration of the radionuclides in the mobile pores. Conversely, the radionuclides in the immobile pores are transferred to the mobile pores at a rate that depends on the concentration of radionuclides in the immobile pores. Over time, the concentration in the immobile pores increases to a level that achieves equilibrium between the two (mobile and immobile pores). Two limiting assumptions are used to obtain the relationships among the concentrations in the mobile, immobile, and total pores. If the time needed to travel through a region of soil is much shorter than the time needed for the mobile and immobile pores to achieve equilibrium, then the concentration in the immobile pores will be negligible compared to the concentration in the mobile pores. Under these conditions, the average concentration in the total pores is given by the following equation:

$$c_{av} = \frac{\theta_m c_m + \theta_{im} c_{im}}{\theta_t} \approx \frac{\theta_m}{\theta_t}c_m \,. \tag{H.11}$$

If the time needed to travel through a region of soil is much greater than the time needed by the mobile and immobile pores to achieve equilibrium, then the concentration in the immobile pores will be equal to the concentration in the mobile pores. Under these conditions, the average concentration in the total pores is given by the following equation:

$$c_{av} = \frac{\theta_m c_m + \theta_{im} c_{im}}{\theta_t} \approx \frac{\theta_t}{\theta_t}c_m = c_m \,. \tag{H.12}$$

H.2.1.10 Governing Equation for Transport

Combining Equations (H.10) and (H.11) produces the following:

$$\frac{\theta_m}{\theta_t}\frac{\partial c_m}{\partial t} = -\lambda\frac{\theta_m}{\theta_t}c_m + \frac{\theta_m}{(\theta_t + \rho_b K_d)}\left(-V_m\frac{\partial c_m}{\partial z} + D_z^m\frac{\partial^2 c_m}{\partial z^2}\right)$$

$$\frac{\partial c_m}{\partial t} = -\lambda c_m + \frac{\theta_t}{(\theta_t + \rho_b K_d)}\left(-V_m\frac{\partial c_m}{\partial z} + D_z^m\frac{\partial^2 c_m}{\partial z^2}\right) \tag{H.13}$$

$$= -\lambda c_m - V_c\frac{\partial c_m}{\partial z} + D_z^c\frac{\partial^2 c_m}{\partial z^2} \, ,$$

where

$$V_c = V_m\frac{\theta_t}{\theta_t + \rho_b K_d}$$ = average velocity of contaminants in the soil (m/yr) and

$$D_z^c = D_z^m\frac{\theta_t}{\theta_t + \rho_b K_d}$$ = dispersion coefficient of contaminants in the soil (m² /yr).

Combining Equations (H.10) and (H.12) produces the following:

$$\frac{\partial c_m}{\partial t} = -\lambda c_m + \frac{\theta_m}{(\theta_t + \rho_b K_d)}\left(-V_m\frac{\partial c_m}{\partial z} + D_z^m\frac{\partial^2 c_m}{\partial z^2}\right)$$

$$\tag{H.14}$$

$$= -\lambda c_m - V_c\frac{\partial c_m}{\partial z} + D_z^c\frac{\partial^2 c_m}{\partial z^2} \, ,$$

where

$$V_c = V_m\frac{\theta_m}{\theta_t + \rho_b K_d}$$ = average velocity of contaminants in the soil (m/yr) and

$$D_z^c = D_z^m\frac{\theta_m}{\theta_t + \rho_b K_d}$$ = dispersion coefficient of contaminant in the soil (m²/yr).

H.2.1.11 Retardation Factor

The ratio between the average velocity of water in the mobile pores and the average velocity of the contaminants is called the retardation factor:

$$R_d = \frac{V_m}{V_c} \tag{H.15}$$

When the travel time through a region of soil is much shorter than the time needed for the mobile and immobile pores to achieve equilibrium, the governing equation (H.13) contains a retardation factor of

$$R_d = \frac{\theta_t + \rho_b K_d}{\theta_t} = 1 + \frac{\rho_b K_d}{\theta_t} \ . \tag{H.16}$$

When the travel time through a region of soil is much longer than the time needed for the mobile and immobile pores to achieve equilibrium, the governing equation (H.14) contains a retardation factor of

$$R_d = \frac{\theta_t + \rho_b K_d}{\theta_m} = \frac{\theta_t}{\theta_m} + \frac{\rho_b K_d}{\theta_m} \ . \tag{H.17}$$

Equation (H.16) is used as the default retardation factor in RESRAD-OFFSITE code because it gives a faster breakthrough time and higher radionuclide concentrations than Equation (H.17) does. See further discussion at the end of Section H.2.1.12.

H.2.1.12   Pore Water Velocity

The volumetric flow rate through a unit cross section is called the Darcy velocity or apparent velocity of flow. The Darcy velocity of flow in the partially saturated zone is the infiltration rate, which is computed by using the following expression:

$$V_d^{ps} = I = [P_r(1 - C_r) + q_{ir}](1 - C_e), \tag{H.18}$$

where
$\quad V_d^{ps}$ = Darcy velocity in the partially saturated zone (m/yr),
$\quad\quad I$ = infiltration rate (m/yr),
$\quad\quad C_e$ = evapotranspiration coefficient,
$\quad\quad C_r$ = runoff coefficient,
$\quad\quad P_r$ = precipitation rate (m/yr), and
$\quad\quad q_{ir}$ = annual irrigation applied over the primary contamination (m/yr).

The Darcy velocity of flow in the saturated zone is the groundwater flow rate, which is computed by using the following expression:

$$V_d^s = K_s^{aqf} i_{aqf}, \tag{H.19}$$

where
$\quad\quad V_d^s$ = Darcy velocity in the saturated zone (m/yr),
$\quad K_s^{aqf}$ = saturated hydraulic conductivity (m/yr) and
$\quad\quad i_{aqf}$ = hydraulic gradient.

The pore water velocity through the mobile pores is V_m, which is related to the Darcy velocity, V_d, by the following expression:

$$V_d = \theta_m V_m \ . \tag{H.20}$$

Equation (H.20) combines with Equations (H.18) and (H.19), respectively, to compute the pore water velocities in the unsaturated and saturated zones.

The code computes the average velocity of the radionuclides in soil using the following expression:

$$V_c = \frac{V_d}{\theta_m R_d} .$$

(H.21)

Equation (H.21) combines with the equation for the retardation factor (H.16 or H.17) and with Equations (H.18) and (H.19), respectively, to compute the radionuclide transport velocities in the unsaturated and saturated zones.

Using Equation (H.16) with Equation (H.21) instead of Equation (H.17) with Equation (H.21) gives a faster average radionuclide velocity and hence an earlier breakthrough time for radionuclides. Because Equation (H.16) predicts a shorter breakthrough time and consequently a higher concentration in water, it is used as the default retardation factor definition in the RESRAD-OFFSITE code. For derivation of cleanup criteria and for dose/risk assessment, the default retardation factor (i.e., Equation [H.16]) provides more conservative results. The use of Equation (H.16) also is consistent with the retardation factor definition used in the RESRAD-ONSITE code. Equation (H.17) was used in beta versions of RESRAD-OFFSITE.

H.2.1.13 Dispersivity

Dispersivity is the ratio between the dispersion coefficient of the radionuclide in soil and the velocity of the radionuclide in soil:

$$d = \frac{D_z^c}{V_c} = \frac{D_z^m}{V_m} ,$$

(H.22)

where d = dispersivity of the radionuclide (m).

The dispersion coefficient of the radionuclide in soil is computed in the code using the following expression:

$$D_z^c = \frac{dV_d}{\theta_m R_d} .$$

(H.23)

H.2.2 Output Flux and Concentration Resulting from an Input Flux for Parent Radionuclides that Enter and Exit the Transport Layer in the Same Form

The governing equation is solved for an instantaneous unit flux across the upper boundary, assuming a layer of unbounded thickness. The governing equation to be solved is as follows:

$$\frac{\partial c_m(z,t)}{\partial t} + \lambda c_m(z,t) + V_c \frac{\partial c_m(z,t)}{\partial z} - D_z^c \frac{\partial^2 c_m(z,t)}{\partial z^2} = 0 .$$

(H.24)

The instantaneous unit flux across the upper boundary can be expressed by the equation:

$$V_m \theta_m c_m(z,t) - \theta_m D_z^m \frac{\partial c_m(z,t)}{\partial z} = V_c R_d \theta_m c_m(z,t) - D_z^c R_d \theta_m \frac{\partial c_m(z,t)}{\partial z} = \delta(z,t), \qquad \text{(H.25)}$$

where $\delta(z,t)$ = a delta function.

The assumption of a layer of unbounded thickness allows the global mass balance equation to be written as $\int_{z=0}^{z=\infty} (\theta_t + \rho_b K_d) c_{av}(z,t) dz = R_d \theta_m \int_{z=0}^{z=\infty} c_m(z,t) dz = e^{-\lambda t}$.

Starting with the solution of Lindstrom et al. (1967) for a "flux-plug type of input at the surface" and considering the limit where the duration of the flux plug tends to zero while the total flux goes to unity, and then modifying for a transforming solute, we obtain (after fixing a typo in the reference):

$$c_m(z,t) = \frac{e^{-\lambda t}}{\theta_m R_d} \left[\frac{2}{\sqrt{4\pi D_z^c t}} \exp\left(-\frac{(z - V_c t)^2}{4 D_z^c t} \right) - \frac{V_c}{2 D_z^c} \exp\left(\frac{z V_c}{D_z^c} \right) erfc\left(\frac{z + V_c t}{\sqrt{4 D_z^c t}} \right) \right]. \qquad \text{(H.26)}$$

The flux at a distance z at time t is given by

$$f(z,t) = \frac{z}{t} \sqrt{\frac{1}{4\pi D_z^c t}} \exp\left(-\frac{(z - V_c t)^2}{4 D_z^c t} - \lambda t \right). \qquad \text{(H.27)}$$

If the flux entering a partially saturated layer is known as a function of time, it can be convolved with the above expression (for output flux from an instantaneous unit input flux) to obtain the flux exiting the layer:

$$f(z,t) = \int_0^t f(0, t - \tau) \frac{z}{\tau} \sqrt{\frac{1}{4\pi D_z^c \tau}} \exp\left(-\frac{(z - V_c \tau)^2}{4 D_z^c \tau} - \lambda \tau \right) d\tau . \qquad \text{(H.28)}$$

H.2.3 Output Flux and Concentration Resulting from an Input Flux of Parent Radionuclide for Radionuclides that Are Produced by Radiological Transformations within the Transport Layer

Ingrowth from the parent radionuclides needs to be considered in addition to the processes discussed in Section H.2.2 when modeling the transport of progeny that are produced in transit. The governing equation then becomes

$$\lambda c_m(z,t) + \frac{\partial c_m(z,t)}{\partial t} + V_c \frac{\partial c_m(z,t)}{\partial z} - D_z^c \frac{\partial^2 c_m(z,t)}{\partial z^2} = \lambda c_m^p(z,t) \frac{\theta_t + K_d^p \rho_b}{\theta_t + K_d \rho_b}, \qquad \text{(H.29)}$$

where

c_m^p = concentration of the parent radionuclide in water (pCi/m³), and

$K_d^{\,p}$ = soil-water distribution coefficient of the parent radionuclide (cm³/g).

An exact solution involves solving this equation for each radionuclide of the chain using the solution for the previous member of the chain and is complex, especially for the later members of a transport chain. RESRAD-OFFSITE provides two simpler solutions; one that is applicable when longitudinal dispersion is dominant and the other for cases where the differences in the distribution coefficients of the parent and progeny are significant. Situations where both processes are of comparable importance can be modeled by subdividing the transport layer as discussed in Section H.3.13.

H.2.3.1 Concentration and Flux for Radionuclides That Are Produced by Radiological Transformations When Dispersion Is Dominant

The solutions in this case are obtained under the assumption that the radionuclides in the transformation chain, from the parent that enters the zone to the progeny that exit the zone, all travel at the same velocity and partition to the same extent between the solid and aqueous phases of the soil. The transport can then be separated out from the ingrowth and the flux of the kth progeny resulting from an instantaneous unit flux of the parent is given by

$$f_k(z,t) = \sum_{i=1}^{k} a_{k,i} \frac{z}{t} \sqrt{\frac{1}{4\pi D_z^c t}} \exp\left(-\frac{(z - V_c t)^2}{4 D_z^c t} - \lambda_i t \right),$$ (H.30)

where

$f_k(z,t)$ = flux of the kth radionuclide of the transformation chain (pCi/yr) and $a_{k,i}$

is a set of coefficients defined by $a_{1,1} = 1$,

$a_{k,i} = \dfrac{\lambda_k a_{k-1,i}}{\lambda_k - \lambda_i}$ for all $1 \leq i < k$, and

$a_{k,k} = -\displaystyle\sum_{i=1}^{k-1} a_{k,i}$.

The concentration is given by

$$c_k(z,t) = \frac{\dfrac{2}{\sqrt{4\pi D_z^C t}}\exp\left(-\dfrac{(z - V_C t)^2}{4 D_z^C t}\right) - \dfrac{V_C}{2 D_Z^C}\exp\left(\dfrac{z V_C}{D_Z^C}\right) erfc\left(\dfrac{z + V_C t}{\sqrt{4 D_Z^C t}}\right)}{\theta_m R_d} \sum_{i=1}^{k} a_{k,i}\exp(-\lambda_i t).$$ (H.31)

H.2.3.2 Concentration and Flux for Radionuclides that Are Produced by Radiological Transformations When Differences in Distribution Coefficients Are Dominant

The solution in this case is obtained by ignoring longitudinal dispersion. The derivation of the solution for the first three members of a transport chain is discussed in Appendix I of the *User's Manual for RESRAD*, Version 6 (Yu et al. 2001). The solutions are expressed in terms of the contaminant travel times, $T_i = z/v_i$. Subscripts i, j, k, l, and m are used to describe the

radionuclides of the transport chain in the order in which they occur in the transformation chain, while subscripts 1, 2, 3, 4, and 5 are used to describe the radionuclides sorted in ascending order of the travel time. The transfer functions for advective flux are all of the form

$$f_k(z,t) = \frac{\lambda_k}{\lambda_i} \sum \gamma \exp(\alpha_{l,m}t + \beta_{l,m}T_1),$$

(H.32)

where

γ, $\alpha_{l,m}$, $\beta_{l,m}$ = all functions of the radiological transformation constants, the ratios of the travel times of the radionuclides, and the travel time of the fastest radionuclide of the transport chain, and

T_1 = travel time of the fastest radionuclide of the transport chain.

The concentration is obtained by dividing the advective flux by the volumetric flow rate in this case.

H.2.4   Concentration and Flux Resulting from a Pulse Input for Radionuclides that Traverse the Transport Layer in the Same Form

The governing equation for longitudinal transport is the same as the one for the flux input. The boundary condition, however, is different. For the flux input boundary condition in Section H.2.2, the radionuclides transferred across the up-gradient face of the transport zone. In the pulse input condition, the radionuclides are either transferred uniformly over a region of the transport zone, as in the case of the transport in the primary contamination, or enter from the top side over a length of the horizontal transport zone, as in the case of transfer across the water table into the saturated zone (Figure H-3). The radionuclides from a pulse input can, under the appropriate conditions, disperse out of the up-gradient face of the transport zone.

The solution for a volume source is obtained by integrating the solution for a plane source along the longitudinal axis. The governing evaluation for transport in the saturated zone is

$$\lambda c_{aq} + \frac{\partial c_{aq}}{\partial t} + V_c \frac{\partial c_{aq}}{\partial x} - D_x^c \frac{\partial^2 c_{aq}}{\partial^2 x} = 0,$$

(H.33)

The boundary condition of a unit pulse over a transverse plane can be written as

$$L_y L_z (\theta_t + \rho_b K_d) c_{av}(x,t=0) = L_y L_z \theta_m R_d c_m(x,t=0) = \delta(x),$$

(H.34)

where

L_y = width of the transport zone, equal to the width of the primary contamination (m),

L_z = breadth of the transport zone, (m),

L_z = equal to the breadth of the primary contamination when modeling transport in the primary contamination that is above the water table,

$L_z = L_x \frac{V_d^{ps}}{V_d^s} + f_{sub}T_{pc}(0)$ = depth of advective penetration of the contamination into the saturated zone when modeling transport in the aquifer (m),

L_x = length of the primary contamination in the direction of groundwater flow (m),

H-14

$V_d^{ps} = I$ = the Darcy velocity or the infiltration rate through the primary contamination (m/yr),

V_d^s = the Darcy velocity in the saturated zone (m/yr),

f_{sub} = the submerged fraction of the primary contamination, and

$T_{pc}(0)$ = the initial thickness of the primary contamination.

Assuming that the transport zone is infinite in length, the global mass balance equation can be written as $L_y L_z \left(\theta_t + \rho_b K_d\right) \int\limits_{x=0}^{x=\infty} c_{av}(x,t)dx = L_y L_z R_d \theta_m \int\limits_{x=0}^{x=\infty} c_m(x,t)dx = e^{-\lambda t}$.

The solution to the governing equation (Equation [H.33]) under the mass balance and boundary conditions is

$$c_m(x,t) = \frac{1}{L_y L_z \theta_m R_d} \sqrt{\frac{1}{4\pi D_x^c t}} \exp\left(-\frac{(x - V_c t)^2}{4 D_x^c t} - \lambda t\right). \tag{H.35}$$

The flux is given by[1]

$$f(x,t) = \frac{1}{2 L_y L_z}\left(V_c + \frac{x}{t}\right)\sqrt{\frac{1}{4\pi D_x^c t}} \exp\left(-\frac{(x - V_c t)^2}{4 D_x^c t} - \lambda t\right). \tag{H.36}$$

The solution for an instantaneous unit release over the rectangular prism is obtained by integrating over the appropriate length of the transport zone. The concentration at a distance *x* from the center of the rectangular prism is

$$C_m(x,t) = \frac{1}{L_x L_y L_z (\theta_m R_d)} \sqrt{\frac{1}{4\pi D_x^c t}} \int_{x - L_x/2}^{x + L_x/2} \exp\left(-\frac{(\hat{x} - V_c t)^2}{4 D_x^c t} - \lambda t\right) d\hat{x} \tag{H.37}$$

which, upon integration, yields[2]

---

[1] $f(x,t) = \theta_m V_m c_m - \theta_m D_m \dfrac{\partial c_m}{\partial x}$, substituting for the concentration gives

$$f(x,t) = \frac{1}{L_y L_z}\left[\frac{V_m}{R_d} - \frac{D_m}{R_d}\left(\frac{V_c t - x}{2 D_x^c t}\right)\right]\sqrt{\frac{1}{4\pi D_x^c t}} e^{\left(-\frac{(x - V_c t)^2}{4 D_x^c t} - \lambda t\right)}.$$

[2] Transforming the variable to recognize the error function yields

$$c_m(x,t) = \frac{1}{L_x L_y L_z (\theta_m R_d)} \frac{e^{-\lambda t}}{2} \frac{2}{\sqrt{\pi}} \int\limits_{\frac{x - \frac{L_x}{2} - V_c t}{\sqrt{4 D_x^c t}}}^{\frac{x + \frac{L_x}{2} - V_c t}{\sqrt{4 D_x^c t}}} \exp\left[-\left(\frac{\hat{x} - V_c t}{\sqrt{4 D_x^c t}}\right)^2\right] d\left(\frac{\hat{x} - V_c t}{\sqrt{4 D_x^c t}}\right).$$

$$c_m(x,t) = \frac{\exp(-\lambda t)}{L_x L_y L_z (\theta_m R_d)} \frac{erf\left(\frac{x + L_x/2 - V_c t}{\sqrt{4D_x^c t}}\right) - erf\left(\frac{x - L_x/2 - V_c t}{\sqrt{4D_x^c t}}\right)}{2} \quad \text{.(H.38)}$$

The flux at distance x from the center of the rectangular prism is

$$f(x,t) = \frac{V_c e^{-\lambda t}}{2L_x L_y L_z}\left[erf\left(\frac{x + \frac{L_x}{2} - V_c t}{\sqrt{4D_x^c t}}\right) - erf\left(\frac{x - \frac{L_x}{2} - V_c t}{\sqrt{4D_x^c t}}\right)\right] \quad \text{(H.39)}$$

$$- \sqrt{\frac{D_x^c}{4\pi t}} \frac{e^{-\lambda t}}{L_x L_y L_z}\left[e^{-\frac{\left(x + \frac{L_x}{2} - V_c t\right)^2}{4D_x^c t}} - e^{-\frac{\left(x - \frac{L_x}{2} - V_c t\right)^2}{4D_x^c t}}\right].$$

Now include the effect of lateral dispersion. The simplified equations to be solved are

$$\frac{\partial c_{aq}}{\partial t} - \frac{\partial^2 c_{aq}}{\partial y^2} = 0 \text{ and } \frac{\partial c_{aq}}{\partial t} - \frac{\partial^2 c_{aq}}{\partial z^2} = 0 \text{ .(H.40)}$$

By using the analogy between these equations and the equation for longitudinal transport,

$$c_m(x,y,z,t) = \frac{\exp(-\lambda t)}{8L_x L_y L_z (\theta_m R_d)}\left[erf\left(\frac{x + L_x/2 - V_c t}{\sqrt{4D_x^c t}}\right) - erf\left(\frac{x - L_x/2 - V_c t}{\sqrt{4D_x^c t}}\right)\right]$$
$$\times \left[erf\left(\frac{y + L_y/2}{\sqrt{4D_y^c t}}\right) - erf\left(\frac{y - L_y/2}{\sqrt{4D_y^c t}}\right)\right]\left[erf\left(\frac{z + L_z}{\sqrt{4D_z^c t}}\right) - erf\left(\frac{z - L_z}{\sqrt{4D_z^c t}}\right)\right]. \quad \text{(H.41)}$$

A reflection will occur when the vertical concentration profile reaches the boundary of the impermeable layer underlying the aquifer. This is modeled by including a mirror source at twice the depth of the aquifer, $2H_{aq}$. Additional mirror sources are introduced each time the reflected profile reaches the water table or the lower impermeable boundary:

$$-2H_{aq}, 4H_{aq}, -4H_{aq}, 6H_{aq}, \ldots \quad \text{(H.42)}$$

Now consider a well that obtains water from a depth d_W of the aquifer over a pumping diameter of $\phi_W = U_W/(d_W V_d)$ and is situated at a distance x_W along the plume centerline and a distance y_W perpendicular to the plume centerline from the center of the prism.

The concentration in the water extracted from the well is obtained by integrating over the region of the aquifer defined by the depth d_W and width ϕ_W:

$$c_w(x_w, y_w, t) = \frac{1}{d_w} \int_0^{d_w} \frac{1}{\varphi_w} \int_{y_w - \frac{\varphi_w}{2}}^{y_w + \frac{\varphi_w}{2}} c_{aq}(x_w, y, z, t) dy dz , \qquad (H.43)$$

$$c_w(x_w, y_w, t) = \frac{\exp(-\lambda t)}{2 L_x L_y L_z (\theta_m R_d)} \frac{\sqrt{D_y^c t}}{\phi_w} \frac{\sqrt{D_z^c t}}{d_w} \left[erf\left(\frac{x_w + L_x/2 - V_c t}{\sqrt{4 D_x^c t}} \right) - erf\left(\frac{x_w - L_x/2 - V_c t}{\sqrt{4 D_x^c t}} \right) \right] \qquad (H.44)$$

$$\times \int_{y_w - \frac{\phi_w}{2}}^{y_w + \frac{\phi_w}{2}} \left[erf\left(\frac{y + L_y/2}{\sqrt{4 D_y^c t}} \right) - erf\left(\frac{y - L_y/2}{\sqrt{4 D_y^c t}} \right) \right] \frac{dy}{\sqrt{4 D_y^c t}} \int_0^{d_w} \left[erf\left(\frac{z + L_z}{\sqrt{4 D_z^c t}} \right) - erf\left(\frac{z - L_z}{\sqrt{4 D_z^c t}} \right) \right] \frac{dz}{\sqrt{4 D_z^c t}} .$$

The integral of the error function is evaluated by using the following series for the error function, which is useful for arguments in the range −4.0 to +4.0:

$$erf(x) = \frac{2}{\sqrt{\pi}} \sum_{n=0}^{\infty} (-1)^n \frac{x^{2n+1}}{(2n+1)n!} . \qquad (H.45)$$

Thus, $Interf(x) = \int_0^x erf(\hat{x}) d\hat{x} = \frac{2}{\sqrt{\pi}} \sum_{n=0}^{\infty} \frac{x^{2n+2}}{(2n+2)(2n+1)n!} .$

The concentration in well water may be written as the product of three factors:

$$c_w(x_w, y_w, t) = c_{w,x}(x_w, t) \, c_{w,y}(y_w, t) \, c_{w,z}(t) , \qquad (H.46)$$

where

$$c_{w,x}(x_w, t) = \frac{\exp(-\lambda t)}{2 L_z} \frac{V_c}{V_d L_x L_y} \left[- erf\left(\frac{x_w + L_x/2 - V_c t}{\sqrt{4 D_x^c t}} \right) - erf\left(\frac{x_w + L_x/2 - V_c t}{\sqrt{4 D_x^c t}} \right) \right],$$

$$C_{w,y}(y_w, t) = \frac{\sqrt{D_y^c t}}{\varphi_w} \left(Interf \frac{2 y_w + \varphi_w + L_y}{\sqrt{16 D_y^c t}} - Interf \frac{2 y_w + \varphi_w - L_y}{\sqrt{16 D_y^c t}} - Interf \frac{2 y_w - \varphi_w + L_y}{\sqrt{16 D_y^c t}} \right.$$
$$\left. + Interf \frac{2 y_w - \varphi_w - L_y}{\sqrt{16 D_y^c t}} \right), \text{and}$$

$$C_{w,z}(t) = \frac{\sqrt{D_z^c t}}{d_w} \left(Interf \frac{d_w + L_z}{\sqrt{4 D_z^c t}} - Interf \frac{d_w - L_z}{\sqrt{4 D_z^c t}} - Interf \frac{L_z}{\sqrt{4 D_z^c t}} + Interf \frac{-L_z}{\sqrt{4 D_z^c t}} \right)$$

with additional terms in $c_{w,z}(t)$ for reflections off the impermeable layer and the water table, if necessary.

The concentration in well water can be computed by convolving the above expression for the concentration in well water due to a unit pulse input into the saturated zone with the time-dependent input pulse obtained from the unsaturated zone transport calculations. RESRAD-OFFSITE, however, uses a further approximation to simplify the calculations in order to (1) reduce run time, (2) generate the transverse cross-sectional concentration profile in the

aquifer at the location of the well without excessive demand on memory, and (3) implement the subdivision of the saturated zone to better predict the transport of the progeny.

The previous expressions pertained to an instantaneous source in the shape of a rectangular prism; we now consider a point source. The concentration due to an instantaneous point source is

$$c_p(x,y,z,t) = \frac{\exp\left[-\lambda t - \dfrac{(x-V_c t)^2}{4D_x^c t} - \dfrac{y^2}{4D_y^c t} - \dfrac{z^2}{4D_y^c t}\right]}{(\theta_m R_d)\sqrt{4\pi D_x^c t}\sqrt{4\pi D_y^c t}\sqrt{4\pi D_z^c t}}.$$

(H.47)

The peak concentration at any location occurs at a time given by[3]

$$t_p = \left[-\frac{3}{2} + \sqrt{\left(\frac{3}{2}\right)^2 + \left(\lambda + \frac{V_c^2}{4D_x^c}\right)\left(\frac{x^2}{D_x^c} + \frac{y^2}{D_y^c} + \frac{z^2}{D_z^c}\right)}\right] \div \left[2\left(\lambda + \frac{V_c^2}{4D_x^c}\right)\right].$$

(H.48)

More generally, the peak concentration at the centerline occurs at

$$t_p = \frac{-nD_x^c + \sqrt{\left(nD_x^c\right)^2 + \left(4\lambda D_x^c + V_c^2\right)x^2}}{\left(4\lambda D_x^c + V_c^2\right)},$$

(H.49)

where n is the number of directions in which dispersion is active. Dispersion is considered to be inactive in the vertical direction, if the concentration profile in the vertical direction becomes essentially uniform because of repeated reflection of the plume by the lower impermeable layer and the water table. It is also inactive if a zero value is specified for the vertical-lateral dispersivity.

If there were no dispersion in the longitudinal direction, contaminants would show up at a point x distance away along the plume centerline at a time x/V_c following an instantaneous point release. Longitudinal dispersion spreads out the contaminants and they arrive over a period of time, with the peak occurring at time t_p. The transverse profile of the concentration will vary somewhat over this period of time. In RESRAD-OFFSITE, the transverse concentration profile at time t_p is used in place of the range of profiles. The expression used by RESRAD-OFFSITE for concentration in water extracted from the well due to an instantaneous pulse input over a region in the shape of a rectangular prism is

$$c_w(x_w, y_w, t) = c_{w,x}(x_w, t)c_{w,y}(y_w)c_{w,z},$$

(H.50)

---

[3] $\left.\dfrac{\partial c_p(x,y,z,t)}{\partial t}\right|_{t=t_p} = 0$

$\left[-\dfrac{3}{2t} - \lambda - \dfrac{V_c^2}{4D_x^c} + \dfrac{x^2}{4D_x^c t^2} + \dfrac{y^2}{4D_y^c t^2} + \dfrac{z^2}{4D_z^c t^2}\right]c_p(x,y,z,t)\Bigg|_{t=t_p} = 0.$

where

$$c_{w,x}(x_w, t) = \frac{\exp(-\lambda t)}{2L_x} \frac{V_c}{V_d L_y L_z} \left[erf\left(\frac{x_w + L_x/2 - V_c t}{\sqrt{4D_x^c t}} \right) - erf\left(\frac{x_w - L_x/2 - V_c t}{\sqrt{4D_x^c t}} \right) \right],$$

$$c_{w,y}(y_w) = \frac{\sqrt{D_y^c t_p}}{\phi_w} \left(Interf \frac{2y_w + \phi_w + L_y}{\sqrt{16 D_y^c t_p}} - Interf \frac{2y_w + \phi_w - L_y}{\sqrt{16 D_y^c t_p}} - Interf \frac{2y_w - \phi_w + L_y}{\sqrt{16 D_y^c t_p}} + Interf \frac{2y_w - \phi_w - L_y}{\sqrt{16 D_y^c t_p}} \right), \text{ and}$$

$$C_{w,z} = \frac{\sqrt{D_z^c t_p}}{d_w} \left(Interf \frac{d_w + L_z}{\sqrt{4 D_z^c t_p}} - Interf \frac{d_w - L_z}{\sqrt{4 D_z^c t_p}} - Interf \frac{L_z}{\sqrt{4 D_z^c t_p}} + Interf \frac{-L_z}{\sqrt{4 D_z^c t_p}} \right).$$

The above expression for concentration due to a unit pulse input into the saturated zone is convolved numerically with the time-dependent input pulse obtained from the unsaturated zone transport calculations to compute the concentration in the well water. Under the peak time approximation, the shapes of the lateral profiles are independent of time; $c_{w,y}(y_w)$ and $c_{w,z}$ are computed once outside the convolution. The analytical model in the code does not consider the effects of any clean infiltration along the length of offsite transport.

Dispersion is not modeled in RESRAD-ONSITE. In order to preproduce what the RESRAD-ONSITE code simulates for an onsite exposure scenario, the RESRAD-OFFSITE code can model a situation with no vertical dispersion using the following expression which is equivalent to the first expression in Equation (E.27) of the *User's Manual for RESRAD(-ONSITE)* Version 6 (Yu et al. 2001):

$$c_{w,z} = \min(d_w, L_z) / d_w \tag{H.51}$$

This model is retained in RESRAD-OFFSITE solely in order to simulate the RESRAD-ONSITE code and is not intended for use in any other case in RESRAD-OFFSITE.

The effect of lateral dispersion on the radionuclide flux entering the surface water body is modeled in a similar manner. The flux into a surface water body is

$$f_s(x_s, y_n, y_f, t) = f_{s,x}(x_s, t) f_{s,y}(y_n, y_f) f_{s,z}, \tag{H.52}$$

where

$$f_{s,x}(x_s, t) = \frac{V_c e^{-\lambda t}}{2 L_x L_y L_z} \left[erf\left(\frac{x_s + \frac{L_x}{2} - V_c t}{\sqrt{4 D_x^c t}} \right) - erf\left(\frac{x_s - \frac{L_x}{2} - V_c t}{\sqrt{4 D_x^c t}} \right) \right] - \sqrt{\frac{D_x^c}{4\pi t}} \frac{e^{-\lambda t}}{L_x L_y L_z} \left[e^{-\frac{\left(x_s + \frac{L_x}{2} - V_c t\right)^2}{4 D_x^c t}} - e^{-\frac{\left(x_s - \frac{L_x}{2} - V_c t\right)^2}{4 D_x^c t}} \right],$$

$$f_{s,y}(y_n, y_f) = \sqrt{D_y^c t_p} \left(Interf \frac{2y_f + L_y}{\sqrt{16 D_y^c t_p}} - Interf \frac{2y_f - L_y}{\sqrt{16 D_y^c t_p}} - Interf \frac{2y_n + L_y}{\sqrt{16 D_y^c t_p}} + Interf \frac{2y_n - L_y}{\sqrt{16 D_y^c t_p}} \right),$$

$$f_{s,z} = \sqrt{D_z^c t_p} \left(Interf \frac{d_s + L_z}{\sqrt{4 D_z^c t_p}} - Interf \frac{d_s - L_z}{\sqrt{4 D_z^c t_p}} - Interf \frac{L_z}{\sqrt{4 D_z^c t_p}} + Interf \frac{-L_z}{\sqrt{4 D_z^c t_p}} \right),$$

x_S = distance along the plume centerline from the center of the rectangular prism source to the center of the surface water body (m),

y_n = distance from the plume centerline to the near edge of the surface
   water body (m),

y_f = distance from the plume centerline to the far edge of the surface water
   body (m), and

d_s = depth of the aquifer contributing to the surface water body (m).

The above expression for flux due to a unit pulse input into the saturated zone is convolved numerically with the time-dependent input pulse obtained from the unsaturated zone transport calculations to compute the flux to the surface water body. Under the peak time approximation, the shapes of the lateral profiles are independent of time; $f_{s,y}(y_n, y_f)$ and $f_{s,z}$ are computed once outside the convolution.

H.2.5 Concentration and Flux from a Pulse Input of Parent Radionuclide for Radionuclides that Are Produced by Radiological Transformations and Traverse the Transport Layer

As in the case of the flux input (Section H.2.3), RESRAD-OFFSITE contains two solutions for the transport of progeny produced in transit. One is applicable when longitudinal dispersion is dominant, and the other is for cases where the differences in the distribution coefficients of the parent and progeny are significant. Situations where both processes are comparably important can be modeled by subdividing the transport layer as discussed in Section H.3.13.

H.2.5.1 Concentration and Flux for Radionuclides that Are Produced by Radiological Transformations When Dispersion Is Dominant

The solution in this case is obtained under the assumption that the radionuclides in the transformation chain from the parent that enters the zone to the progeny that exits the zone all travel at the same velocity and partition between the aqueous and solid phases of the soil in the same proportion. The transport can then be separated out from the ingrowth, and the concentration of the kth progeny in well water, resulting from an instantaneous unit flux of the parent is given by

$$c_w^k(x_w, y_w, t) = c_{w,x}^k(x_w, t) c_{w,y}(y_w) c_{w,z} , \qquad (H.53)$$

where

$$c_{w,x}^k(x_w, t) = \sum_{i=1}^{k} a_{k,i} \frac{e^{-\lambda_i t}}{2 L_x} \frac{V_c}{V_d L_y L_z} \left[erf\left(\frac{x_w + L_x/2 - V_c t}{\sqrt{4 D_x^c t}} \right) - erf\left(\frac{x_w - L_x/2 - V_c t}{\sqrt{4 D_x^c t}} \right) \right]$$

$c_{w,y}(y_w)$, $c_{w,z}$ = same as in Equation (H.50),

$a_{k,i}$ = a set of coefficients defined by $a_{1,1} = 1$,

$$a_{k,i} = \frac{\lambda_k a_{k-1,i}}{\lambda_k - \lambda_i} \text{ for all } 1 \le i < k \text{ , and}$$

$$a_{k,k} = -\sum_{i=1}^{k-1} a_{k,i} \text{ .}$$

The flux of the kth progeny to the surface water body is given by

$$f_s^k\left(x_s, y_n, y_f, t\right) = f_{s,x}^k(x_s, t) f_{s,y}\left(y_n, y_f\right) f_{s,z},$$ (H.54)

where

$$f_{s,x}^k(x_s, t) = \sum_{i=1}^{k} \frac{a_{k,i} e^{-\lambda_i t}}{L_x L_y L_z} \left\{ \frac{V_c}{2} \left[\mathrm{erf}\left(\frac{x_s + \frac{L_x}{2} - V_c t}{\sqrt{4 D_x^c t}} \right) - \mathrm{erf}\left(\frac{x_s - \frac{L_x}{2} - V_c t}{\sqrt{4 D_x^c t}} \right) \right] \right.$$
$$\left. - \sqrt{\frac{D_x^c}{4\pi t}} \left[e^{-\frac{\left(x_s + \frac{L_x}{2} - V_c t\right)^2}{4 D_x^c t}} - e^{-\frac{\left(x_s - \frac{L_x}{2} - V_c t\right)^2}{4 D_x^c t}} \right] \right\},$$

$f_{s,y}$ (y_n, y_f), $f_{s,z}$ = same as in Equation (H.52).

The above expressions for concentration and flux due to a unit pulse input into the saturated zone are convolved numerically with the time-dependent input pulse obtained from the unsaturated zone transport calculations to compute the concentration in well water and the flux to the surface water body. Under the peak time approximation, the shapes of the lateral profiles are independent of time; the expressions for the effects of lateral dispersion are computed once outside the convolution.

H.2.5.2 Concentration and Flux for Radionuclides that Are Produced by Radiological Transformations When Differences in Distribution Coefficients Are Dominant

The solution in this case is obtained by ignoring longitudinal dispersion. The derivation of the solution for the first three members of a transport chain is discussed in Appendix I of the *User's Manual for RESRAD* Version 6 (Yu et al. 2001). The solutions are expressed in terms of the onsite and offsite contaminant travel times, $T_{i,on}$ and $T_{i,off}$. Subscripts *i, j, k, l, m* are used to describe the radionuclides of the transport chain in the order in which they occur in the transformation chain, while subscripts 1, 2, 3, 4, 5 are used to describe the radionuclides sorted in ascending order of the travel time. The transfer functions are all of the form

$$f_k(z, t) = \frac{\lambda_k}{\lambda_i} \sum \gamma \exp\left[\alpha_{l,m} t + \beta_{l,m} T_{1,off} + \beta_{l,m} T_{1,on} y(t)\right],$$ (H.55)

where
$\gamma, \alpha_{l,m}, \beta_{l,m}$ = all functions of the radiological transformation constants and the ratios of the travel times of the radionuclides and the travel time of the fastest radionuclide of the transport chain,
$T_{1,off}$ = offsite travel time of the fastest radionuclide of the transport chain,
$T_{1,off}$ = onsite travel time of the fastest radionuclide of the transport chain, and
$y(t)$ = onsite travel distance.

The above expression for flux due to a unit pulse input into the saturated zone is convolved numerically with the time-dependent input pulse obtained from the unsaturated zone transport calculations to compute the advective flux. The concentration, in this case, is obtained by dividing the advective flux by the volumetric flow rate.

H.3   Implementation of the Groundwater Transport Models

This section describes how the expressions derived from the conceptual model (Section H.2) are implemented in the computational code. As shown in Figure H-1, modeling the transport in the partially saturated zone involves predicting the flux out of the zone that is a result of the known flux into the zone. The implementation of the expressions for output flux resulting from an input flux is discussed in Sections H.3.1 through H.3.3. Section H.3.1 deals with those atoms that travel across the transport zone without undergoing any radioactive transformations, while Sections H.3.2 and H.3.3 give the two alternative formulations for those atoms that undergo radioactive transformations during their travel across the transport zone. Sections H.3.4 through H.3.9 deal with the implementation of the expressions for the output flux or the concentration in well water resulting from a pulse input. Sections H.3.10, H.3.11, and H.3.12 deal with the implementation of the expressions for the concentration in well water that results from an input flux. Although the concentration from a flux input is not necessary for the conceptual model depicted in Figure H-1, it is utilized in Section H.3.13, where a method for improving the modeling of progeny produced in transit is discussed.

H.3.1   Output Flux Resulting from an Input Flux for Parent Radionuclides that Transport the Layer in the Same Form

In RESRAD-OFFSITE, the fluxes entering a layer are known at each of a sequence of times. Assuming that the fluxes entering a layer vary linearly between those times, an analytical solution for the flux exiting the layer can be obtained as follows.

Let the input fluxes at times t_1 and t_2 be $f(0,t_1)$ and $f(0,t_2)$, respectively.

Applying the expression developed in Section H.2.2, the output flux at a distance z at time $t_n > t_2 > t_1$ due to the input flux entering between times t_1 and t_2 is obtained by the convolution:

$$f_{t_1}^{t_2}(z,t_n) = \int_{t_n - t_2}^{t_n - t_1} f(0, t_n - \tau) \frac{z}{\tau} \sqrt{\frac{1}{4\pi D_z^c \tau}} \exp\left(-\frac{(z - V_c \tau)^2}{4 D_z^c \tau} - \lambda \tau\right) d\tau \ . \tag{H.56}$$

Approximate the input flux during that time interval by linear interpolation:

$$f(0, t_1 \le t_n - \tau \le t_2) = f(0,t_1) \frac{t_2 - (t_n - \tau)}{t_2 - t_1} + f(0,t_2) \frac{(t_n - \tau) - t_1}{t_2 - t_1} \ . \tag{H.57}$$

By rearranging in terms of τ,

$$f(0, t_1 \le t_n - \tau \le t_2) = a + b\tau \ ,$$

where

$$a = f(0,t_1) \frac{t_2 - t_n}{t_2 - t_1} + f(0,t_2) \frac{t_n - t_1}{t_2 - t_1} \ , \text{ and}$$

$$b = \frac{f(0,t_1) - f(0,t_2)}{t_2 - t_1} \ .$$

Substituting the linear interpolation in the convolution gives

$$f_{t_1}^{t_2}(z,t_n) = \int_{t_n-t_2}^{t_n-t_1} (a+b\tau)\frac{z}{\tau}\sqrt{\frac{1}{4\pi D_z^c\tau}}\exp\left(-\frac{(z-V_c\tau)^2}{4D_z^c\tau}-\lambda\tau\right)d\tau .$$ (H.58)

The convolution can be performed analytically[4] to give

$$f_{t_1}^{t_2}(z,t_n) = \frac{1}{2}\left(a+\frac{bz}{\sqrt{V_c^2+4D_z^c\lambda}}\right)\exp\left(\frac{z\left(V_c-\sqrt{V_c^2+4D_z^c\lambda}\right)}{2D_z^c}\right)\left[erf\left(\frac{z-\sqrt{V_c^2+4D_z^c\lambda}(t_n-t_2)}{\sqrt{4D_z^c(t_n-t_2)}}\right)-erf\left(\frac{z-\sqrt{V_c^2+4D_z^c\lambda}(t_n-t_1)}{\sqrt{4D_z^c(t_n-t_1)}}\right)\right]$$

$$+\frac{1}{2}\left(a-\frac{bz}{\sqrt{V_c^2+4D_z^c\lambda}}\right)\exp\left(\frac{z\left(V_c+\sqrt{V_c^2+4D_z^c\lambda}\right)}{2D_z^c}\right)\left[erf\left(\frac{z+\sqrt{V_c^2+4D_z^c\lambda}(t_n-t_2)}{\sqrt{4D_z^c(t_n-t_2)}}\right)-erf\left(\frac{z+\sqrt{V_c^2+4D_z^c\lambda}(t_n-t_1)}{\sqrt{4D_z^c(t_n-t_1)}}\right)\right].$$ (H.59)

The flux exiting the layer at the nth time point is obtained by summing the contributions of the input fluxes over the preceding n–1 time intervals.

---

[4] First recognize that the exponent of the exponential part of the integrand can be written as

$$\frac{(z-V_c\tau)^2}{4D_z^c\tau}+\lambda\tau = \frac{\left(z-\sqrt{V_c^2+4D_z^c\lambda}\,\tau\right)^2}{4D_z^c\tau}-\frac{zV_c}{2D_z^c}+\frac{z\sqrt{V_c^2+4D_z^c\lambda}}{2D_z^c} = \frac{\left(z+\sqrt{V_c^2+4D_z^c\lambda}\,\tau\right)^2}{4D_z^c\tau}-\frac{zV_c}{2D_z^c}-\frac{z\sqrt{V_c^2+4D_z^c\lambda}}{2D_z^c} ,$$

and write the non-exponential part of the integrand as

$$(a+b\tau)\frac{z}{\tau}\sqrt{\frac{1}{4\pi D_z^c\tau}} = \frac{-1}{\sqrt{\pi}}\left(a+\frac{bz}{\sqrt{V_c^2+4D_z^c\lambda}}\right)\left(\frac{z}{\sqrt{4D_z^c\tau}}\frac{-1}{2\tau}-\sqrt{\frac{(V_c^2+4D_z^c\lambda)\tau}{4D_z^c}}\frac{1}{2\tau}\right)$$

$$+\frac{-1}{\sqrt{\pi}}\left(a-\frac{bz}{\sqrt{V_c^2+4D_z^c\lambda}}\right)\left(\frac{z}{\sqrt{4D_z^c\tau}}\frac{-1}{2\tau}+\sqrt{\frac{(V_c^2+4D_z^c\lambda)\tau}{4D_z^c}}\frac{1}{2\tau}\right)$$

in order to transform the variables to $\dfrac{z\pm\sqrt{V_c^2+4D_z^c\lambda}\,\tau}{\sqrt{4D_z^c\tau}}$ for the two components. Then the convolution can be expressed as the sum of two integrals that are recognizable as error functions, namely,

$$\frac{1}{2}\left(a+\frac{bz}{\sqrt{V_c^2+4D_z^c\lambda}}\right)\exp\frac{z\left(V_c-\sqrt{V_c^2+4D_z^c\lambda}\right)}{2D_z^c}\int\frac{2}{\sqrt{\pi}}\exp\left[-\left(\frac{z-\sqrt{V_c^2+4D_z^c\lambda}\,\tau}{\sqrt{4D_z^c\tau}}\right)^2\right]d\left(\frac{z-\sqrt{V_c^2+4D_z^c\lambda}\,\tau}{\sqrt{4D_z^c\tau}}\right)$$

and

$$\frac{1}{2}\left(a-\frac{bz}{\sqrt{V_c^2+4D_z^c\lambda}}\right)\exp\frac{z\left(V_c+\sqrt{V_c^2+4D_z^c\lambda}\right)}{2D_z^c}\int\frac{2}{\sqrt{\pi}}\exp\left[-\left(\frac{z+\sqrt{V_c^2+4D_z^c\lambda}\,\tau}{\sqrt{4D_z^c\tau}}\right)^2\right]d\left(\frac{z+\sqrt{V_c^2+4D_z^c\lambda}\,\tau}{\sqrt{4D_z^c\tau}}\right).$$

$$f(z,t_n) = \sum_{m=1}^{n-1} \frac{1}{2}\left(a_m + \frac{b_m z}{\sqrt{V_c^2 + 4D_z^c\lambda}}\right) exp \frac{z\left(V_c - \sqrt{V_c^2 + 4D_z^c\lambda}\right)}{2D_z^c}\left[erf\left(\frac{z - \sqrt{V_c^2 + 4D_z^c\lambda}(t_n - t_{m+1})}{\sqrt{4D_z^c(t_n - t_{m+1})}}\right) - erf\left(\frac{z - \sqrt{V_c^2 + 4D_z^c\lambda}(t_n - t_m)}{\sqrt{4D_z^c(t_n - t_m)}}\right)\right]$$

(H.60)

$$+ \sum_{m=1}^{n-1} \frac{1}{2}\left(a_m - \frac{b_m z}{\sqrt{V_c^2 + 4D_z^c\lambda}}\right) exp \frac{z\left(V_c + \sqrt{V_c^2 + 4D_z^c\lambda}\right)}{2D_z^c}\left[erf\left(\frac{z + \sqrt{V_c^2 + 4D_z^c\lambda}(t_n - t_{m+1})}{\sqrt{4D_z^c(t_n - t_{m+1})}}\right) - erf\left(\frac{z + \sqrt{V_c^2 + 4D_z^c\lambda}(t_n - t_m)}{\sqrt{4D_z^c(t_n - t_m)}}\right)\right],$$

with

$$a_m = f(0,t_m)\frac{t_{m+1} - t_n}{t_{m+1} - t_m} + f(0,t_{m+1})\frac{t_n - t_m}{t_{m+1} - t_m} \text{ and } b_m = \frac{f(0,t_m) - f(0,t_{m+1})}{t_{m+1} - t_m}.$$

This expression is semi-analytical; in other words, part of this analytical expression, specifically the error function, must be evaluated numerically. The error functions in this expression depend only on the length of the transport zone, the contaminant transport velocity, contaminant dispersion coefficient, radiological transformation rate, and time intervals between the calculation times; they are independent of the (time-dependent) flux coefficients a_m and b_m. If the calculation time points are spaced linearly, then the time interval $(t_n - t_m)$ depends only on the difference $n - m$ and not on the value of n. For example, the time interval between the first and the 20th calculation time point will be same as the time interval between the 21st and 40th calculation time points. Thus, when the linear spacing option is chosen, the error function for all the appropriate time intervals can be computed once and stored in memory for subsequent use, thus reducing the run time.

H.3.2 Output Flux Resulting from an Input Flux of Parent Radionuclide for Radionuclides that Are Produced by Radiological Transformations within the Transport Layer when Dispersion Is Dominant

Let the input fluxes of the parent radionuclide entering the transport layer be $f_1(0, t_1)$ and $f_1(0, t_2)$, respectively, at times t_1 and t_2.

Applying the expression developed in Section H.2.3.1, the output flux of the kth progeny at a distance z at time $t_n > t_2 > t_1$, due to the input flux of the parent radionuclide between times t_1 and t_2, is obtained by the convolution:

$$f_k{}_{t_1}^{t_2}(z,t_n) = \sum_{i=1}^{k} a_{k,i} \int_{t_n - t_2}^{t_n - t_1} f_1(0,t_n - \tau)\frac{z}{\tau}\sqrt{\frac{1}{4\pi D_z^c\tau}} exp\left(-\frac{(z - V_c\tau)^2}{4D_z^c\tau} - \lambda_i\tau\right)d\tau.$$

(H.61)

The flux of the kth radionuclide of the transformation chain exiting the layer at the end of the nth time point is obtained by summing the contributions of the input fluxes over the preceding n–1 time intervals as in Section H.3.1:

$$f_k(z,t_n) = \sum_{m=1}^{n-1}\sum_{i=1}^{k} \frac{a_{k,i}}{2}\left(a_m + \frac{b_m z}{\sqrt{V_c^2 + 4D_z^c\lambda_i}}\right) exp \frac{z\left(V_c - \sqrt{V_c^2 + 4D_z^c\lambda_i}\right)}{2D_z^c}\left[erf\left(\frac{z - \sqrt{V_c^2 + 4D_z^c\lambda_i}(t_n - t_{m+1})}{\sqrt{4D_z^c(t_n - t_{m+1})}}\right) - erf\left(\frac{z - \sqrt{V_c^2 + 4D_z^c\lambda_i}(t_n - t_m)}{\sqrt{4D_z^c(t_n - t_m)}}\right)\right]$$

(H.62)

$$+ \sum_{m=1}^{n-1}\sum_{i=1}^{k} \frac{a_{k,i}}{2}\left(a_m - \frac{b_m z}{\sqrt{V_c^2 + 4D_z^c\lambda_i}}\right) exp \frac{z\left(V_c + \sqrt{V_c^2 + 4D_z^c\lambda_i}\right)}{2D_z^c}\left[erf\left(\frac{z + \sqrt{V_c^2 + 4D_z^c\lambda_i}(t_n - t_{m+1})}{\sqrt{4D_z^c(t_n - t_{m+1})}}\right) - erf\left(\frac{z + \sqrt{V_c^2 + 4D_z^c\lambda_i}(t_n - t_m)}{\sqrt{4D_z^c(t_n - t_m)}}\right)\right].$$

The code uses this solution if all the radionuclides in the transformation chain from the parent entering the transport zone to the progeny exiting the zone have the same distribution coefficient. In this case, all these radionuclides under consideration will have the same transport velocity and the same dispersion coefficient. Even in cases where these radionuclides have different distribution coefficients, it is possible to instruct the code to use this equation to model the transport of the progeny produced in transit. When this choice is made, it is also necessary to make a choice of whether to use the distribution coefficient of the parent or the distribution coefficient of the progeny to calculate the transport velocity and the dispersion coefficient of these radionuclides. When the linear spacing option is chosen for the calculation time points, the error function for all the appropriate time intervals is computed once and stored in memory for subsequent use for the reasons mentioned previously.

H.3.3 Output Flux Resulting from an Input Flux of Parent Radionuclide for Radionuclides that Are Produced by Radiological Transformations within the Transport Layer When Differences in Distribution Coefficients Are Dominant

In RESRAD-OFFSITE, the fluxes entering a layer are known at each of a sequence of times. Assuming that the fluxes entering a layer vary linearly between the fluxes at the calculation times and applying the expression developed in Section H.2.3.2, an analytical solution for the output flux of the kth progeny at a distance z at time $t_n > t_2 > t_1$, due to the input flux of the parent radionuclide between times t_1 and t_2, is obtained by the convolution:

$$f_{kt_1}^{t_2}(z,t_n) = \int_{t_n-t_2}^{t_n-t_1}(a+b\tau)\frac{\lambda_k}{\lambda_1}\sum_{i,j}\gamma\exp(\alpha_{i,j}\tau+\beta_{i,j}T_1)d\tau . \tag{H.63}$$

The convolution can be performed analytically[5] to give

$$f_{kt_1}^{t_2}(z,t_n) = \frac{\lambda_k}{\lambda_1}\sum_{i,j}\gamma\left[\frac{\alpha_{i,j}a-b}{\alpha_{i,j}^2}\left(e^{\alpha_{i,j}(t_n-t_1)+\beta_{i,j}T_1}-e^{\alpha_{i,j}(t_n-t_2)+\beta_{i,j}T_1}\right)\right.$$

$$\left.+\frac{b(t_n-t_1)}{\alpha_{i,j}}e^{\alpha_{i,j}(t_n-t_1)+\beta_{i,j}T_1}-\frac{b(t_n-t_2)}{\alpha_{i,j}}e^{\alpha_{i,j}(t_n-t_2)+\beta_{i,j}T_1}\right] . \tag{H.64}$$

The flux exiting the layer at the end of the nth time point is obtained by summing the contributions of the input fluxes over the preceding n–1 time intervals.

$$f_k(z,t_n) = \frac{\lambda_k}{\lambda_1}\sum_{m=1}^{n-1}\sum_{i,j}\gamma\left[\frac{\alpha_{i,j}a_m-b_m}{\alpha_{i,j}^2}\left(e^{\alpha_{i,j}(t_n-t_m)+\beta_{i,j}T_1}-e^{\alpha_{i,j}(t_n-t_{m+1})+\beta_{i,j}T_1}\right)\right. \tag{H.65}$$

---

[5] $f_{kt_1}^{t_2}(z,t_n) = \frac{\lambda_k}{\lambda_1}\sum_{i,j}\gamma\int_{t_n-t_2}^{t_n-t_1}(a+b\tau)\exp(\alpha_{i,j}\tau+\beta_{i,j}T_1)\,d\tau$ and

$$f_{kt_1}^{t_2}(z,t_n) = \frac{\lambda_k}{\lambda_1}\sum_{i,j}\gamma\left[\frac{a+b\tau}{\alpha_{i,j}}\exp(\alpha_{i,j}\tau+\beta_{i,j}T_1)-\frac{b}{\alpha_{i,j}^2}\exp(\alpha_{i,j}\tau+\beta_{i,j}T_1)\right]_{t_n-t_2}^{t_n-t_1} .$$

$$+\frac{b_m\left(t_n-t_m\right)}{\alpha_{i,j}}e^{\alpha_{i,j}\left(t_n-t_m\right)+\beta_{i,j}T_1}-\frac{b_m\left(t_n-t_{m+1}\right)}{\alpha_{i,j}}e^{\alpha_{i,j}\left(t_n-t_{m+1}\right)+\beta_{i,j}T_1}\Bigg].$$

This expression is a linear function of: (1) the time-dependent flux coefficients a_m and b_m; (2) the advective travel times, T_i, of the radionuclides in the transformation chain; (3) the coefficients $\alpha_{i,j}$, $\beta_{i,j}$, which are functions of the ratios of the advective travel times and the radiological transformation constants of the radionuclides in the transformation chain; and (4) the time intervals between the calculation times. If the calculation time points are spaced linearly, then the time interval $(t_n - t_m)$ depends only on the difference $n - m$ and not on the value of n. Thus, when the linear spacing option is chosen, the output flux from a unit input flux can be computed once for all the appropriate time intervals and stored in memory for subsequent use with the appropriate flux, thus reducing the run time.

H.3.4 Output Flux Resulting from a Pulse Input for Parent Radionuclides That Traverse the Transport Layer in the Same Form

In RESRAD-OFFSITE, the fluxes entering the water table across the footprint of the primary contamination are known at each of a sequence of times. The spatially integrated flux across a vertical plane in the saturated zone, at a distance x down-gradient of the center of the primary contamination, is obtained as follows.

Let the spatially integrated flux at the water table at time t be $F_{wt}(t)$.

By applying the expression developed in Section H.2.4, the spatially integrated output flux at time t_n is obtained by the convolution:

$$F(x,t_n)=L_yL_z\int_0^{t_n}F_{wt}\left(t_n-\tau\right)\left\{\begin{array}{c}\dfrac{V_ce^{-\lambda\tau}}{2L_xL_yL_z}\left[erf\left(\dfrac{x+\dfrac{L_x}{2}-V_c\tau}{\sqrt{4D_x^c\tau}}\right)-erf\left(\dfrac{x-\dfrac{L_x}{2}-V_c\tau}{\sqrt{4D_x^c\tau}}\right)\right]\\[20pt]-\sqrt{\dfrac{D_x^c}{4\pi t}}\dfrac{e^{-\lambda\tau}}{L_xL_yL_z}\left[e^{-\frac{\left(x+\frac{L_x}{2}-V_c\tau\right)^2}{4D_x^c\tau}}-e^{-\frac{\left(x-\frac{L_x}{2}-V_c\tau\right)^2}{4D_x^c\tau}}\right]\end{array}\right\}d\tau\quad(H.66)$$

This is evaluated numerically by using either Simpson's (parabolic) formula or Romberg's method (Section H.3.14), assuming that the flux to the water table varies linearly between the values at the calculation times.

As in the previous cases, substantial savings in computation time can be achieved if the calculation times are in a linear sequence. Two transfer functions are computed for each time interval. The first is for a flux that increases linearly from zero at time t_{m-1} to one at time t_m, and the second is for a flux that decreases linearly from one at time t_{m-1} to zero at time t_m.

$$f_1(x, t_n - t_m) = \int_{t_n - t_m}^{t_n - t_{m-1}} \left(\frac{t_n - t_{m-1} - \tau}{t_m - t_{m-1}}\right) \left\{ \begin{array}{l} \dfrac{V_c e^{-\lambda \tau}}{2L_x}\left[erf\left(\dfrac{x + \dfrac{L_x}{2} - V_c \tau}{\sqrt{4D_x^c \tau}}\right) - erf\left(\dfrac{x - \dfrac{L_x}{2} - V_c \tau}{\sqrt{4D_x^c \tau}}\right)\right] \\[3em] - \sqrt{\dfrac{D_x^c}{4\pi t}} \dfrac{e^{-\lambda \tau}}{L_x}\left[e^{-\frac{\left(x + \frac{L_x}{2} - V_c \tau\right)^2}{4D_x^c \tau}} - e^{-\frac{\left(x - \frac{L_x}{2} - V_c \tau\right)^2}{4D_x^c \tau}} \right] \end{array} \right\} d\tau .$$ (H.67)

$$f_2(x, t_n - t_{m-1}) = \int_{t_n - t_m}^{t_n - t_{m-1}} \left(\frac{\tau - t_n + t_m}{t_m - t_{m-1}}\right) \left\{ \begin{array}{l} \dfrac{V_c e^{-\lambda \tau}}{2L_x}\left[erf\left(\dfrac{x + \dfrac{L_x}{2} - V_c \tau}{\sqrt{4D_x^c \tau}}\right) - erf\left(\dfrac{x - \dfrac{L_x}{2} - V_c \tau}{\sqrt{4D_x^c \tau}}\right)\right] \\[3em] - \sqrt{\dfrac{D_x^c}{4\pi t}} \dfrac{e^{-\lambda \tau}}{L_x}\left[e^{-\frac{\left(x + \frac{L_x}{2} - V_c \tau\right)^2}{4D_x^c \tau}} - e^{-\frac{\left(x - \frac{L_x}{2} - V_c \tau\right)^2}{4D_x^c \tau}} \right] \end{array} \right\} d\tau .$$ (H.68)

Both of these are evaluated numerically by using either Simpson's (parabolic) formula or Romberg's method (Section H.3.14) and stored in memory for subsequent use with the appropriate flux.

Then the spatially integrated flux across the vertical plane is obtained by summing the contributions of all the relevant time intervals,

$$F(x, t_n) = \sum_{m=1}^{n-1} F_{wt}(t_m)\left(f_1(x, t_n - t_m) + f_2(x, t_n - t_m)\right).$$ (H.69)

The radionuclide enters the surface water body through a rectangle of finite dimensions, a subsection of the vertical plane. This is accounted for by using the expressions derived in Section H.2.4, as follows:

$$F_{sw}(x_s, t_n) = F(x_s, t_n)\frac{f_{s,y}(y_n, y_f)}{L_y}\frac{f_{s,z}}{L_z} ,$$ (H.70)

where

$$f_{s,y}(y_n, y_f) = \sqrt{D_y^c t_p}\left(Interf \frac{2y_f + L_y}{\sqrt{16D_y^c t_p}} - Interf \frac{2y_f - L_y}{\sqrt{16D_y^c t_p}} - Interf \frac{2y_n + L_y}{\sqrt{16D_y^c t_p}} + Interf \frac{2y_n - L_y}{\sqrt{16D_y^c t_p}}\right) ,$$

and

$$f_{s,z} = \sqrt{D_z^c t_p} \left(Interf \frac{d_s + L_z}{\sqrt{4D_z^c t_p}} - Interf \frac{d_s - L_z}{\sqrt{4D_z^c t_p}} - Interf \frac{L_z}{\sqrt{4D_z^c t_p}} + Interf \frac{-L_z}{\sqrt{4D_z^c t_p}} \right),$$

or

$$f_{s,z} = \max\left[0, \min\left(d_s, \frac{(x_s + L_x)I}{V_d} \right) - \frac{xI}{V_d} \right],$$

depending on whether the dispersivity in the vertical direction is nonzero or not. The expression for $f_{s,z}$ will contain additional terms for every reflection of the dispersion plume at the lower impervious boundary and at the water table.

H.3.5 Concentration in Well Water Resulting from a Pulse Input for Parent Radionuclides that Traverse the Transport Layer in the Same Form

In RESRAD-OFFSITE, the fluxes entering the water table across the footprint of the primary contamination are known at each of a sequence of times. The concentration in well water is obtained as follows.

Let the spatially integrated flux at the water table at time t be $F_{wt}(t)$.

By applying the expression developed in Section H.2.4, the concentration in well water at time t_n is obtained by the convolution:

$$c_{well}(x_w, y_w, t_n) = c_{w,z} c_{w,y}(y_w) \frac{V_c}{2V_d L_y L_z L_x} \int_0^{t_n} F_{wt}(t_n - \tau) e^{-\lambda\tau} \left[erf\left(\frac{x_w + L_x/2 - V_c\tau}{\sqrt{4D_x^c\tau}} \right) - erf\left(\frac{x_w - L_x/2 - V_c\tau}{\sqrt{4D_x^c\tau}} \right) \right] d\tau, \quad (H.71)$$

where

$$c_{w,y}(y_w) = \frac{\sqrt{D_y^c t_p}}{\varphi_w} \left(Interf \frac{2y_w + \varphi_w + L_y}{\sqrt{16D_y^c t_p}} - Interf \frac{2y_w + \varphi_w - L_y}{\sqrt{16D_y^c t_p}} - Interf \frac{2y_w - \varphi_w + L_y}{\sqrt{16D_y^c t_p}} + Interf \frac{2y_w - \varphi_w - L_y}{\sqrt{16D_y^c t_p}} \right),$$

and

$$c_{w,z} = \frac{\sqrt{D_z^c t_p}}{d_w} \left(\begin{array}{c} Interf \dfrac{d_w + L_z}{\sqrt{4D_z^c t_p}} - Interf \dfrac{d_w - L_z}{\sqrt{4D_z^c t_p}} \\[3ex] - Interf \dfrac{L_z}{\sqrt{4D_z^c t_p}} + Interf \dfrac{-L_z}{\sqrt{4D_z^c t_p}} \end{array} \right).$$

with additional terms in $c_{w,z}$ for reflections off the lower impermeable layer and the water table, if necessary.

This is evaluated numerically using either Simpson's (parabolic) formula or Romberg's method (Section H.3.14), assuming that the flux to the water table varies linearly between the values at the calculation times.

As in the previous cases, substantial savings in computational time can be achieved if the calculation times are in a linear sequence. Two transfer functions are computed for each time interval. The first is for a flux that increases linearly from zero at time t_{m-1} to one at time t_m, and the second is for a flux that decreases linearly from one at time t_{m-1} to zero at time t_m:

$$f_1(x, t_n - t_m) = \int_{t_n - t_m}^{t_n - t_{m-1}} \left(\frac{t_n - t_{m-1} - \tau}{t_m - t_{m-1}} \right) \frac{V_c e^{-\lambda \tau}}{2 L_x V_d L_y L_z} \left[erf\left(\frac{x + L_x/2 - V_c \tau}{\sqrt{4 D_x^c \tau}} \right) - erf\left(\frac{x - L_x/2 - V_c \tau}{\sqrt{4 D_x^c \tau}} \right) \right] d\tau \qquad \text{(H.72)}$$

$$f_2(x, t_n - t_{m-1}) = \int_{t_n - t_m}^{t_n - t_{m-1}} \left(\frac{\tau - t_n + t_m}{t_m - t_{m-1}} \right) \frac{V_c e^{-\lambda \tau}}{2 L_x V_d L_y L_z} \left[erf\left(\frac{x + L_x/2 - V_c \tau}{\sqrt{4 D_x^c \tau}} \right) - erf\left(\frac{x - L_x/2 - V_c \tau}{\sqrt{4 D_x^c \tau}} \right) \right] d\tau. \qquad \text{(H.73)}$$

Both of these are evaluated numerically using either Simpson's (parabolic) formula or Romberg's method (Section H.3.14) and stored in memory for subsequent use with the appropriate flux.

Then the concentration in well water is obtained by summing the contributions of all the relevant time intervals:

$$c_{well}(x_w, y_w, t_n) = c_{w,z} c_{w,y}(y_w) \sum_{m=1}^{n-1} F_{wt}(t_m) \left[f_1(x_w, t_n - t_m) + f_2(x_w, t_n - t_m) \right]. \text{(H.74)} \qquad \text{(H.74)}$$

H.3.6 Output Flux Resulting from a Pulse Input of Parent Radionuclide for Radionuclides that Are Produced by Radiological Transformations and Traverse the Transport Layer When Dispersion Is Dominant

In RESRAD-OFFSITE, the fluxes entering the water table across the footprint of the primary contamination are known at each of a sequence of times. The spatially integrated flux of the kth progeny across a vertical plane in the saturated zone, at a distance x down-gradient of the center of the primary contamination, is obtained as follows.

Let the spatially integrated flux of the parent radionuclide across the water table at time t be $F_{wt}(t)$. By applying the expression developed in Section H.2.5.1, the spatially integrated output flux at time t_n is obtained by the convolution:

$$
F_k(x, t_n) = L_y L_z \sum_{j=1}^{k} a_{k,j} \int_0^{t_n} F_{wt}(t_n - \tau) \left\{ \frac{V_c e^{-\lambda_j \tau}}{2 L_x L_y L_z} \left[\mathrm{erf}\left(\frac{x + \frac{L_x}{2} - V_c \tau}{\sqrt{4 D_x^c t}} \right) - \mathrm{erf}\left(\frac{x - \frac{L_x}{2} - V_c \tau}{\sqrt{4 D_x^c t}} \right) \right] \right.
$$
$$
\left. - \sqrt{\frac{D_x^c}{4\pi\tau}} \frac{e^{-\lambda_j \tau}}{L_x L_y L_z} \left[e^{-\frac{\left(x + \frac{L_x}{2} - V_c \tau\right)^2}{4 D_x^c \tau}} - e^{-\frac{\left(x - \frac{L_x}{2} - V_c \tau\right)^2}{4 D_x^c \tau}} \right] \right\} d\tau .
\tag{H. 75}
$$

This is evaluated numerically using either Simpson's (parabolic) formula or Romberg's method (Section H.3.14), assuming that the flux to the water table varies linearly between the values at the calculation times.

As in the previous cases, substantial savings in computational time can be achieved if the calculation times are in a linear sequence. Two transfer functions are computed for each time interval. The first is for a flux that increases linearly from zero at time t_{m-1} to one at time t_m, and the second is for a flux that decreases linearly from one at time t_{m-1} to zero at time t_m:

$$
f_1^{1 \to k}(x, t_n - t_m) = \int_{t_n - t_m}^{t_n - t_{m-1}} \left(\frac{t_n - t_{m-1} - \tau}{t_m - t_{m-1}} \right) \sum_{j=1}^{k} a_{k,j} e^{-\lambda_j \tau} \frac{1}{L_x} \left\{ \frac{V_c}{2} \left[\mathrm{erf}\left(\frac{x + \frac{L_x}{2} - V_c \tau}{\sqrt{4 D_x^c \tau}} \right) - \mathrm{erf}\left(\frac{x - \frac{L_x}{2} - V_c \tau}{\sqrt{4 D_x^c \tau}} \right) \right] \right.
$$
$$
\left. - \sqrt{\frac{D_x^c}{4\pi t}} \left[e^{-\frac{\left(x + \frac{L_x}{2} - V_c \tau\right)^2}{4 D_x^c \tau}} - e^{-\frac{\left(x - \frac{L_x}{2} - V_c \tau\right)^2}{4 D_x^c \tau}} \right] \right\} d\tau .
\tag{H.76}
$$

$$f_2^{1 \to k}(x, t_n - t_{m-1}) = \int_{t_n - t_m}^{t_n - t_{m-1}} \left(\frac{\tau - t_n + t_m}{t_m - t_{m-1}} \right) \sum_{j=1}^{k} a_{k,j} e^{-\lambda_j \tau} \frac{1}{L_x} \left\{ \begin{array}{l} \left| \frac{V_c}{2} \left[erf\left(\frac{x + \frac{L_x}{2} - V_c \tau}{\sqrt{4D_x^c \tau}} \right) - erf\left(\frac{x - \frac{L_x}{2} - V_c \tau}{\sqrt{4D_x^c \tau}} \right) \right] \right. \\ \left. - \sqrt{\frac{D_x^c}{4\pi t}} \left[e^{-\frac{\left(x + \frac{L_x}{2} - V_c \tau\right)^2}{4D_x^c \tau}} - e^{-\frac{\left(x - \frac{L_x}{2} - V_c \tau\right)^2}{4D_x^c \tau}} \right] \right| \end{array} \right\} d\tau \qquad (H.77)$$

Both of these are evaluated numerically using either Simpson's (parabolic) formula or Romberg's method (Section H.3.14) and stored in memory for subsequent use with the appropriate flux.

Then the spatially integrated flux of the kth progeny across the vertical plane is obtained by summing the contributions of all the relevant time intervals:

$$F_k(x, t_n) = \sum_{m=1}^{n-1} F_{wt}(t_m) \left(f_1^{1 \to k}(x, t_n - t_m) + f_2^{1 \to k}(x, t_n - t_m) \right) . \qquad (H.78)$$

As in Section H.3.4, the lateral dispersion factors $f_{s,y}(y_n, y_f)$ and $f_{s,z}$ are used to account for the size and location of the rectangular subsection of the plane through which the flux must pass to enter the surface water body.

$$F_{sw,k}(x_s, t_n) = F_k(x_s, t_n) \frac{f_{s,y}(y_n, y_f) f_{s,z}}{L_y \ L_z} , \qquad (H.79)$$

where

$$f_{s,y}(y_n, y_f) = \sqrt{D_y^c t_p} \left(\begin{array}{l} Interf \frac{2y_f + L_y}{\sqrt{16 D_y^c t_p}} - Interf \frac{2y_f - L_y}{\sqrt{16 D_y^c t_p}} \\ \\ - Interf \frac{2y_n + L_y}{\sqrt{16 D_y^c t_p}} + Interf \frac{2y_n - L_y}{\sqrt{16 D_y^c t_p}} \end{array} \right) ,$$

and

$$f_{s,z} = \sqrt{D_z^c t_p} \left(\begin{array}{l} Interf \frac{d_s + L_z}{\sqrt{4 D_z^c t_p}} - Interf \frac{d_s - L_z}{\sqrt{4 D_z^c t_p}} - Interf \frac{L_z}{\sqrt{4 D_z^c t_p}} \\ \\ + Interf \frac{-L_z}{\sqrt{4 D_z^c t_p}} \end{array} \right) .$$

The expression for $f_{s,z}$ will contain additional terms for every reflection of the dispersion plume at the lower impervious boundary and at the water table.

The code uses this solution if all the radionuclides in the transformation chain from the parent entering the transport zone to the progeny exiting the zone have the same distribution coefficient. In this case, all these radionuclides under consideration will have the same transport velocity and the same dispersion coefficient. Even in cases where these radionuclides have different distribution coefficients, it is possible to instruct the code to use this equation to model the transport of the progeny produced in transit. When this choice is made, it is also necessary to make a choice of whether to use the distribution coefficient of the parent or the distribution coefficient of the progeny to calculate the transport velocity and the dispersion coefficient of these radionuclides.

H.3.7 Concentration in Well Water Resulting from a Pulse Input of Parent Radionuclide for Radionuclides that Are Produced by Radiological Transformations and Traverse the Transport Layer When Dispersion Is Dominant

In RESRAD-OFFSITE, the fluxes entering the water table across the footprint of the primary contamination are known at each of a sequence of times. The concentration of the kth progeny in well water is obtained as follows.

Let the spatially integrated flux of the parent radionuclide across the water table at time t be $F_{wt}(t)$. By applying the expression developed in Section H.2.5.1, the concentration of the kth progeny in well water at time t_n is obtained by the convolution:

$$c_{well,k}(x_w, y_w, t_n) = c_{w,z} c_{w,y}(y_w) \frac{V_c}{2V_d L_y L_z L_x} \int_0^{t_0} F_{wt}(t_n - \tau) \sum_{j=1}^{k} a_{k,j} e^{-\lambda_j \tau} \left[\begin{array}{c} erf\left(\dfrac{x_w + L_x/2 - V_c \tau}{\sqrt{4D_x^c \tau}} \right) \\[2ex] - erf\left(\dfrac{x_w - L_x/2 - V_c \tau}{\sqrt{4D_x^c \tau}} \right) \end{array} \right] d\tau , \qquad (H.80)$$

where

$$c_{w,y}(y_w) = \frac{\sqrt{D_y^c t_p}}{\varphi_w} \left(\begin{array}{c} Interf \dfrac{2y_w + \varphi_w + L_y}{\sqrt{16D_y^c t_p}} - Interf \dfrac{2y_w + \varphi_w - L_y}{\sqrt{16D_y^c t_p}} - Interf \dfrac{2y_w - \varphi_w + L_y}{\sqrt{16D_y^c t_p}} \\[3ex] + Interf \dfrac{2y_w - \varphi_w - L_y}{\sqrt{16D_y^c t_p}} \end{array} \right) ,$$

and

$$c_{w,z} = \frac{\sqrt{D_z^c t_p}}{d_w} \left(Interf \dfrac{d_w + L_z}{\sqrt{4D_z^c t_p}} - Interf \dfrac{d_w - L_z}{\sqrt{4D_z^c t_p}} - Interf \dfrac{L_z}{\sqrt{4D_z^c t_p}} + Interf \dfrac{-L_z}{\sqrt{4D_z^c t_p}} \right) .$$

with additional terms in $c_{w,z}$ for reflections off the lower impermeable layer and the water table, if necessary.

This is evaluated numerically using either Simpson's (parabolic) formula or Romberg's method (Section H.3.14), assuming that the flux to the water table varies linearly between the values at the calculation times.

As in the previous cases, substantial savings in computational time can be achieved if the calculation times are in a linear sequence. Two transfer functions are computed for each time interval. The first is for a flux that increases linearly from zero at time t_{m-1} to one at time t_m, and the second is for a flux that decreases linearly from one at time t_{m-1} to zero at time t_m:

$$f_1^{1 \to k}(x, t_n - t_m) = \int_{t_n - t_m}^{t_n - t_{m-1}} \left(\frac{t_n - t_{m-1} - \tau}{t_m - t_{m-1}}\right) \sum_{j=1}^{k} a_{k,j} e^{-\lambda_j \tau} \frac{V_c}{2 L_x V_d L_y L_z} \left[erf\left(\frac{x + L_x/2 - V_c \tau}{\sqrt{4 D_x^c \tau}}\right) - erf\left(\frac{x - L_x/2 - V_c \tau}{\sqrt{4 D_x^c \tau}}\right) \right] d\tau \quad \text{(H.81)}$$

$$f_2^{1 \to k}(x, t_n - t_{m-1}) = \int_{t_n - t_m}^{t_n - t_{m-1}} \left(\frac{\tau - t_n + t_m}{t_m - t_{m-1}}\right) \sum_{j=1}^{k} a_{k,j} e^{-\lambda_j \tau} \frac{V_c}{2 L_x V_d L_y L_z} \left[erf\left(\frac{x + L_x/2 - V_c \tau}{\sqrt{4 D_x^c \tau}}\right) - erf\left(\frac{x - L_x/2 - V_c \tau}{\sqrt{4 D_x^c \tau}}\right) \right] d\tau \quad \text{(H.82)}$$

Both of these are evaluated numerically by using either Simpson's (parabolic) formula or Romberg's method (Section H.3.14) and stored in memory for subsequent use with the appropriate flux.

Then the concentration in well water is obtained by summing the contributions of all the relevant time intervals:

$$c_{well,k}(x_w, y_w, t_n) = c_{w,z} c_{w,y}(y_w) \sum_{m=1}^{n-1} F_{wt}(t_m)(f_1^{1 \to k}(x_w, t_n - t_m) + f_2^{1 \to k}(x_w, t_n - t_m). \quad \text{(H.83)}$$

H.3.8 Output Flux Resulting from a Pulse Input of Parent Radionuclide for Radionuclides that Are Produced by Radiological Transformations and Traverse the Transport Layer When Differences in Distribution Coefficients Are Dominant

In RESRAD-OFFSITE, the fluxes entering the water table across the footprint of the primary contamination are known at each of a sequence of times. The spatially integrated flux of the kth progeny across a vertical plane in the saturated zone, at a distance x down-gradient of the center of the primary contamination, is obtained as follows.

Let the spatially integrated flux of the parent radionuclide across the water table at time t be $F_{wt}(t)$. By applying the expression developed in Section H.2.5.2, the spatially integrated output flux at time t_n is obtained by the convolution:

$$F_k(x, t_n) = \int_0^{t_n} F_{wt}(t_n - \tau) \frac{\lambda_k}{\lambda_1} \sum_{i,j} \gamma \exp\left(\alpha_{i,j} \tau + \beta_{i,j} T_{1,off} + \beta_{i,j} T_{1,on} y(\tau)\right) d\tau . \quad \text{(H.84)}$$

This is evaluated numerically by using either Simpson's (parabolic) formula or Romberg's method (Section H.3.14), assuming that the flux to the water table varies linearly between the values at the calculation times.

As in the previous cases, substantial savings in computational time can be achieved if the calculation times are in a linear sequence. Two transfer functions are computed for each time interval. The first is for a flux that increases linearly from zero at time t_{m-1} to one at time t_m, and the second is for a flux that decreases linearly from one at time t_{m-1} to zero at time t_m.

$$f_1^{1 \to k}(x, t_n - t_m) = \frac{\lambda_k}{\lambda_1} \int_{t_n - t_m}^{t_n - t_{m-1}} \left(\frac{t_n - t_{m-1} - \tau}{t_m - t_{m-1}} \right) \sum_{i,j} \gamma \exp\left(\alpha_{i,j}\tau + \beta_{i,j}T_{1,off} + \beta_{i,j}T_{1,on} y(\tau)\right) d\tau \quad . \quad \text{(H.85)}$$

$$f_2^{1 \to k}(x, t_n - t_{m-1}) = \frac{\lambda_k}{\lambda_1} \int_{t_n - t_m}^{t_n - t_{m-1}} \left(\frac{\tau - t_n + t_m}{t_m - t_{m-1}} \right) \sum_{i,j} \gamma \exp\left(\alpha_{i,j}\tau + \beta_{i,j}T_{1,off} + \beta_{i,j}T_{1,on} y(\tau)\right) d\tau \quad . \quad \text{(H.86)}$$

Both of these are evaluated numerically by using either Simpson's (parabolic) formula or Romberg's method (Section H.3.14) and stored in memory for subsequent use with the appropriate flux.

Then the spatially integrated flux of the kth progeny across the vertical plane is obtained by summing the contributions of all the relevant time intervals:

$$F_k(x, t_n) = \sum_{m=1}^{n-1} F_{wt}(t_m)\left(f_1^{1 \to k}(x, t_n - t_m) + f_2^{1 \to k}(x, t_n - t_m)\right) . \quad \text{(H.87)}$$

As in Section H.3.4, the lateral dispersion factors $f_{s,y}(y_n, y_f)$ and $f_{s,z}$ are used to account for the size and location of the rectangular subsection of the plane through which the radionuclide must pass to enter the surface water body.

$$F_{sw,k}(x_s, t_n) = F_k(x_s, t_n) \frac{f_{s,y}(y_n, y_f)}{L_y} \frac{f_{s,z}}{L_z}, \quad \text{(H.88)}$$

where

$$f_{s,y}(y_n, y_f) = \sqrt{D_y^c t_p} \left(Interf \frac{2y_f + L_y}{\sqrt{16 D_y^c t_p}} - Interf \frac{2y_f - L_y}{\sqrt{16 D_y^c t_p}} - Interf \frac{2y_n + L_y}{\sqrt{16 D_y^c t_p}} + Interf \frac{2y_n - L_y}{\sqrt{16 D_y^c t_p}} \right) ,$$

and

$$f_{s,z} = \sqrt{D_z^c t_p} \left(Interf \frac{d_s + L_z}{\sqrt{4 D_z^c t_p}} - Interf \frac{d_s - L_z}{\sqrt{4 D_z^c t_p}} - Interf \frac{L_z}{\sqrt{4 D_z^c t_p}} + Interf \frac{-L_z}{\sqrt{4 D_z^c t_p}} \right) .$$

The expression for $f_{s,z}$ will contain additional terms for every reflection of the dispersion plume at the lower impervious boundary and at the water table.

H.3.9   Concentration in Well Water Resulting from a Pulse Input of Parent Radionuclide for Radionuclides that Are Produced by Radiological Transformations and Traverse the Transport Layer When Differences in Distribution Coefficients Are Dominant

In RESRAD-OFFSITE, the fluxes entering the water table across the footprint of the primary contamination are known at each of a sequence of times. The concentration of the kth progeny in well water is obtained as follows.

Let the spatially integrated flux of the parent radionuclide across the water table at time t be $F_{wt}(t)$. By applying the expression developed in Section H.2.5.2, the concentration of the kth progeny in well water at time t_n is obtained by the convolution:

$$c_{well,k}(x_w, y_w, t_n) = c_{w,z} c_{w,y}(y_w) \frac{1}{V_d L_y L_z} \int_0^{t_n} F_{wt}(t_n - \tau) \frac{\lambda_k}{\lambda_1} \sum_{i,j} \gamma \, exp\!\left(\alpha_{i,j}\tau + \beta_{i,j}T_{1,off} + \beta_{i,j}T_{1,on}\, y(\tau) \right) d\tau, \quad \text{(H.89)}$$

where

$$c_{w,y}(y_w) = \frac{\sqrt{D_y^c t_p}}{\varphi_w} \left(\begin{array}{c} Interf\,\dfrac{2y_w + \varphi_w + L_y}{\sqrt{16 D_y^c t_p}} - Interf\,\dfrac{2y_w + \varphi_w - L_y}{\sqrt{16 D_y^c t_p}} - Interf\,\dfrac{2y_w - \varphi_w + L_y}{\sqrt{16 D_y^c t_p}} \\[3mm] + Interf\,\dfrac{2y_w - \varphi_w - L_y}{\sqrt{16 D_y^c t_p}} \end{array} \right),$$

and

$$c_{w,z} = \frac{\sqrt{D_z^c t_p}}{d_w} \left(Interf\,\frac{d_w + L_z}{\sqrt{4 D_z^c t_p}} - Interf\,\frac{d_w - L_z}{\sqrt{4 D_z^c t_p}} - Interf\,\frac{L_z}{\sqrt{4 D_z^c t_p}} + Interf\,\frac{-L_z}{\sqrt{4 D_z^c t_p}} \right).$$

with additional terms in $c_{w,z}$ for reflections off the lower impermeable layer and the water table, if necessary.

This is evaluated numerically by using either Simpson's (parabolic) formula or Romberg's method (Section H.3.14), assuming that the flux to the water table varies linearly between the values at the calculation times.

As in the previous cases, substantial savings in computational time can be achieved if the calculation times are in a linear sequence. Two transfer functions are computed for each time interval. The first is for a flux that increases linearly from zero at time t_{m-1} to one at time t_m, and the second is for a flux that decreases linearly from one at time t_{m-1} to zero at time t_m:

$$f_1^{1 \to k}(x, t_n - t_m) = \frac{1}{V_d L_y L_z} \frac{\lambda_k}{\lambda_1} \int_{t_n - t_m}^{t_n - t_{m-1}} \left(\frac{t_n - t_{m-1} - \tau}{t_m - t_{m-1}} \right) \sum_{i,j} \gamma \, exp\!\left(\alpha_{i,j}\tau + \beta_{i,j}T_{1,off} + \beta_{i,j}T_{1,on}\, y(\tau) \right) d\tau. \quad \text{(H.90)}$$

$$f_2^{1 \to k}(x, t_n - t_{m-1}) = \frac{1}{V_d L_y L_z} \frac{\lambda_k}{\lambda_1} \int\limits_{t_n - t_{m+1}}^{t_n - t_m} \left(\frac{\tau - t_n + t_m}{t_m - t_{m-1}} \right) \sum_{i,j} \gamma \exp\left(\alpha_{i,j} \tau + \beta_{i,j} T_{1,off} + \beta_{i,j} T_{1,on} y(\tau) \right) d\tau \ . \quad \text{(H.91)}$$

Both of these are evaluated numerically using either Simpson's (parabolic) formula or Romberg's method (Section H.3.14) and stored in memory for subsequent use with the appropriate flux.

Then the concentration in well water is obtained by summing the contributions of all the relevant time intervals:

$$c_{well,k}(x_w, y_w, t_n) = c_{w,z} c_{w,y}(y_w) \sum_{m=1}^{n-1} F_{wt}(t_m)(f_1^{1 \to k}(x_w, t_n - t_m) + f_2^{1 \to k}(x_w, t_n - t_m). \quad \text{(H.92)}$$

H.3.10 Concentration in Well Water Resulting from a Flux Input for Parent Radionuclides that Traverse the Transport Layer in the Same Form

In RESRAD-OFFSITE, the fluxes entering a transport layer are known at each of a sequence of times. Assuming that the fluxes entering a layer vary linearly between those times, the concentration in well water can be obtained as follows.

Let the spatially integrated input fluxes at times t_1 and t_2 be $F(0,t_1)$ and $F(0,t_2)$, respectively. Let the length of the layer be x. By applying the expression developed in Section H.2.2, the concentration in well water at time t_n is obtained by the convolution:

$$c_{well}(x_w, y_w, t_n) = c_{w,z} c_{w,y}(y_w) \frac{V_c}{V_d L_y L_z} \int\limits_0^{t_n} F(0, t_n - \tau) e^{-\lambda t} \left[\begin{array}{l} \frac{2}{\sqrt{4\pi D_x^c \tau}} \exp\left(-\frac{(x_w - V_c \tau)^2}{4 D_x^c \tau} \right) \\ -\frac{V_c}{2 D_x^c} \exp\left(\frac{x_w V_c}{D_x^c} \right) erfc\left(\frac{x_w + V_c \tau}{\sqrt{4 D_x^c \tau}} \right) \end{array} \right] d\tau \ , \text{(H.93)}$$

where

$$c_{w,y}(y_w) = \frac{\sqrt{D_y^c t_p}}{\varphi_w} \left(\begin{array}{l} Interf \dfrac{2 y_w + \varphi_w + L_y}{\sqrt{16 D_y^c t_p}} - Interf \dfrac{2 y_w + \varphi_w - L_y}{\sqrt{16 D_y^c t_p}} - Interf \dfrac{2 y_w - \varphi_w + L_y}{\sqrt{16 D_y^c t_p}} \\ \\ + Interf \dfrac{2 y_w - \varphi_w - L_y}{\sqrt{16 D_y^c t_p}} \end{array} \right) ,$$

and

$$c_{w,z} = \frac{\sqrt{D_z^c t_p}}{d_w} \left(Interf \frac{d_w + L_z}{\sqrt{4 D_z^c t_p}} - Interf \frac{d_w - L_z}{\sqrt{4 D_z^c t_p}} - Interf \frac{L_z}{\sqrt{4 D_z^c t_p}} + Interf \frac{-L_z}{\sqrt{4 D_z^c t_p}} \right) .$$

With additional terms in $c_{w,z}$ for reflections off the lower impermeable layer and the water table, if necessary.

This is evaluated numerically by using either Simpson's (parabolic) formula or Romberg's method (Section H.3.14), assuming that the flux to the water table varies linearly between the values at the calculation times.

As in the previous cases, substantial savings in computational time can be achieved if the calculation times are in a linear sequence. Two transfer functions are computed for each time interval. The first is for a flux that increases linearly from zero at time t_{m-1} to one at time t_m, and the second is for a flux that decreases linearly from one at time t_{m-1} to zero at time t_m:

$$f_1(x, t_n - t_m) = \int_{t_n - t_m}^{t_n - t_{m-1}} \left(\frac{t_n - t_{m-1} - \tau}{t_m - t_{m-1}}\right) \frac{V_c e^{-\lambda t}}{V_d L_y L_z} \left[\begin{array}{c} \frac{2}{\sqrt{4\pi D_x^c \tau}} \exp\left(-\frac{(x - V_c\tau)^2}{4D_x^c \tau}\right) \\ -\frac{V_c}{2D_x^c} \exp\left(\frac{xV_c}{D_x^c}\right) erfc\left(\frac{x + V_c\tau}{\sqrt{4D_x^c \tau}}\right) \end{array}\right] d\tau \qquad \text{(H.94)}$$

$$f_2(x, t_n - t_{m-1}) = \int_{t_n - t_m}^{t_n - t_{m-1}} \left(\frac{\tau - t_n + t_m}{t_m - t_{m-1}}\right) \frac{V_c e^{-\lambda t}}{V_d L_y L_z} \left[\begin{array}{c} \frac{2}{\sqrt{4\pi D_x^c \tau}} \exp\left(-\frac{(x - V_c\tau)^2}{4D_x^c \tau}\right) \\ -\frac{V_c}{2D_x^c} \exp\left(\frac{xV_c}{D_x^c}\right) erfc\left(\frac{x + V_c\tau}{\sqrt{4D_x^c \tau}}\right) \end{array}\right] d\tau \qquad \text{(H.95)}$$

Both of these are evaluated numerically by using either Simpson's (parabolic) formula or Romberg's method (Section H.3.14) and stored in memory for subsequent use with the appropriate flux.

Then the concentration in well water is obtained by summing the contributions of all the relevant time intervals:

$$c_{well}(x_w, y_w, t_n) = c_{w,z} c_{w,y}(y_w) \sum_{m=1}^{n-1} F(t_m) \left[f_1(x_w, t_n - t_m) + f_2(x_w, t_n - t_m)\right]. \qquad \text{(H.96)}$$

H.3.11 Concentration in Well Water Resulting from a Flux Input of Parent Radionuclide for Radionuclides that Are Produced by Radiological Transformations and Traverse the Transport Layer When Dispersion Is Dominant

In RESRAD-OFFSITE, the fluxes entering a transport layer are known at each of a sequence of times. Assuming that the fluxes entering a layer vary linearly between those times, the concentration in well water for the kth progeny that is produced by radiological transformation within the transport layer can be obtained as follows.

Let the spatially integrated input fluxes of the parent radionuclide at times t_1 and t_2 be $F_1(0,t_1)$ and $F_1(0,t_2)$, respectively. Let the length of the layer be x. By applying the expression developed in Section H.2.3.1, the concentration in well water at time t_n is obtained by the convolution:

$$c_{well,k}(x_w, y_w, t_n) = c_{w,z} c_{w,y}(y_w) \frac{V_c}{V_d L_y L_z} \int_0^{t_n} F_1(0, t_n - \tau) \sum_{i=1}^{k} a_{k,i} e^{-\lambda_i t} \left[\begin{array}{c} \frac{2}{\sqrt{4\pi D_x^c \tau}} \exp\left(-\frac{(x_w - V_c\tau)^2}{4D_x^c \tau}\right) \\ -\frac{V_c}{2D_x^c} \exp\left(\frac{x_w V_c}{D_x^c}\right) erfc\left(\frac{x_w + V_c\tau}{\sqrt{4D_x^c \tau}}\right) \end{array}\right] d\tau, \qquad \text{(H.97)}$$

where

$$c_{w,y}(y_w) = \frac{\sqrt{D_y^c t_p}}{\varphi_w} \left[\begin{array}{l} Interf \dfrac{2y_w + \varphi_w + L_y}{\sqrt{16D_y^c t_p}} - Interf \dfrac{2y_w + \varphi_w - L_y}{\sqrt{16D_y^c t_p}} - Interf \dfrac{2y_w - \varphi_w + L_y}{\sqrt{16D_y^c t_p}} \\[3mm] + Interf \dfrac{2y_w - \varphi_w - L_y}{\sqrt{16D_y^c t_p}} \end{array} \right],$$

and

$$c_{w,z} = \frac{\sqrt{D_z^c t_p}}{d_w} \left(Interf \dfrac{d_w + L_z}{\sqrt{4D_z^c t_p}} - Interf \dfrac{d_w - L_z}{\sqrt{4D_z^c t_p}} - Interf \dfrac{L_z}{\sqrt{4D_z^c t_p}} + Interf \dfrac{-L_z}{\sqrt{4D_z^c t_p}} \right).$$

With additional terms in $c_{w,z}$ for reflections off the lower impermeable layer and the water table, if necessary.

This is evaluated numerically by using either Simpson's (parabolic) formula or Romberg's method (Section H.3.14), assuming that the flux to the water table varies linearly between the values at the calculation times.

As in the previous cases, substantial savings in computational time can be achieved if the calculation times are in a linear sequence. Two transfer functions are computed for each time interval. The first is for a flux that increases linearly from zero at time t_{m-1} to one at time t_m, and the second is for a flux that decreases linearly from one at time t_{m-1} to zero at time t_m:

$$f_1^{1 \to k}(x, t_n - t_m) = \int_{t_n - t_m}^{t_n - t_{m-1}} \left(\frac{t_n - t_{m-1} - \tau}{t_m - t_{m-1}} \right) \sum_{i=1}^{k} a_{k,i} \, e^{-\lambda_i t} \frac{V_c}{V_d L_y L_z} \left[\begin{array}{l} \dfrac{2}{\sqrt{4\pi D_x^c \tau}} \exp\left(-\dfrac{(x - V_c \tau)^2}{4D_x^c \tau} \right) \\[3mm] - \dfrac{V_c}{2D_x^c} \exp\left(\dfrac{xV_c}{D_x^c} \right) erfc\left(\dfrac{x + V_c \tau}{\sqrt{4D_x^c \tau}} \right) \end{array} \right] d\tau. \quad \text{(H.98)}$$

$$f_2^{1 \to k}(x, t_n - t_{m-1}) = \int_{t_n - t_m}^{t_n - t_{m-1}} \left(\frac{\tau - t_n + t_m}{t_m - t_{m-1}} \right) \sum_{i=1}^{k} a_{k,i} \, e^{-\lambda_i t} \frac{V_c}{V_d L_y L_z} \left[\begin{array}{l} \dfrac{2}{\sqrt{4\pi D_x^c \tau}} \exp\left(-\dfrac{(x - V_c \tau)^2}{4D_x^c \tau} \right) \\[3mm] - \dfrac{V_c}{2D_x^c} \exp\left(\dfrac{xV_c}{D_x^c} \right) erfc\left(\dfrac{x + V_c \tau}{\sqrt{4D_x^c \tau}} \right) \end{array} \right] d\tau. \quad \text{(H.99)}$$

Both of these are evaluated numerically by using either Simpson's (parabolic) formula or Romberg's method (Section H.3.14) and stored in memory for subsequent use with the appropriate flux.

Then the concentration in well water is obtained by summing the contributions of all the relevant time intervals:

$$c_{well,k}(x_w, y_w, t_n) = c_{w,z} c_{w,y}(y_w) \sum_{m=1}^{n-1} F_1(t_m) \left[f_1^{1 \to k}(x_w, t_n - t_m) + f_2^{1 \to k}(x_w, t_n - t_m) \right]. \quad \text{(H.100)}$$

H.3.12 Concentration in Well Water Resulting from a Flux Input of Parent Radionuclide for Radionuclides that Are Produced by Radiological Transformations and Traverse the Transport Layer When Differences in Distribution Coefficients Are Dominant

In RESRAD-OFFSITE, the fluxes entering a transport layer are known at each of a sequence of times. Assuming that the fluxes entering a layer vary linearly between those times, the concentration in well water for the kth progeny that is produced by radiological transformation within the transport layer can be obtained as follows.

Let the spatially integrated input fluxes of the parent radionuclide at times t_1 and t_2 be $F_1(0, t_1)$ and $F_1(0, t_2)$, respectively. Let the length of the layer be x. By applying the expression developed in Section H.2.3.2, the concentration in well water at time t_n is obtained by the convolution:

$$c_{well,k}(x_w, y_w, t_n) = c_{w,z}c_{w,y}(y_w)\frac{1}{V_d L_y L_z} \int_0^{t_n} F_1(0, t_n - \tau)\frac{\lambda_k}{\lambda_1} \sum_{i,j} \gamma \exp(\alpha_{i,j}\tau + \beta_{i,j}T_1)\, d\tau , \quad \text{(H.101)}$$

where

$$c_{w,y}(y_w) = \frac{\sqrt{D_y^c t_p}}{\varphi_w}\left(\begin{array}{l} Interf\, \dfrac{2y_w + \varphi_w + L_y}{\sqrt{16D_y^c t_p}} - Interf\, \dfrac{2y_w + \varphi_w - L_y}{\sqrt{16D_y^c t_p}} - Interf\, \dfrac{2y_w - \varphi_w + L_y}{\sqrt{16D_y^c t_p}} \\[3mm] + Interf\, \dfrac{2y_w - \varphi_w - L_y}{\sqrt{16D_y^c t_p}} \end{array} \right),$$

and

$$c_{w,z} = \frac{\sqrt{D_z^c t_p}}{d_w}\left(Interf\, \frac{d_w + L_z}{\sqrt{4D_z^c t_p}} - Interf\, \frac{d_w - L_z}{\sqrt{4D_z^c t_p}} - Interf\, \frac{L_z}{\sqrt{4D_z^c t_p}} + Interf\, \frac{- L_z}{\sqrt{4D_z^c t_p}} \right),$$

With additional terms in $c_{w,z}$ for reflections off the lower impermeable layer and the water table, if necessary.

This is evaluated numerically by using either Simpson's (parabolic) formula or Romberg's method (Section H.3.14), assuming that the flux to the water table varies linearly between the values at the calculation times.

As in the previous cases, substantial savings in computational time can be achieved if the calculation times are in a linear sequence. Two transfer functions are computed for each time interval. The first is for a flux that increases linearly from zero at time t_{m-1} to one at time t_m, and the second is for a flux that decreases linearly from one at time t_{m-1} to zero at time t_m:

$$f_1^{1 \to k}(x, t_n - t_m) = \frac{1}{V_d L_y L_z} \frac{\lambda_k}{\lambda_1} \int_{t_n - t_m}^{t_n - t_{m-1}} \left(\frac{t_n - t_{m-1} - \tau}{t_m - t_{m-1}} \right) \sum_{i,j} \gamma \exp\left(\alpha_{i,j} \tau + \beta_{i,j} T_1 \right) d\tau .$$ (H.102)

$$f_2^{1 \to k}(x, t_n - t_{m-1}) = \frac{1}{V_d L_y L_z} \frac{\lambda_k}{\lambda_1} \int_{t_n - t_m}^{t_n - t_{m-1}} \left(\frac{\tau - t_n + t_m}{t_m - t_{m-1}} \right) \sum_{i,j} \gamma \exp\left(\alpha_{i,j} \tau + \beta_{i,j} T_1 \right) d\tau .$$ (H.103)

Both of these are evaluated numerically by using either Simpson's (parabolic) formula or Romberg's method (Section H.3.14) and stored in memory for subsequent use with the appropriate flux.

Then the concentration in well water is obtained by summing the contributions of all the relevant time intervals:

$$c_{well,k}(x_w, y_w, t_n) = c_{w,z} c_{w,y}(y_w) \sum_{m=1}^{n-1} F_1(t_m) \left[f_1^{1 \to k}(x_w, t_n - t_m) + f_2^{1 \to k}(x_w, t_n - t_m) \right].$$ (H.104)

H.3.13 Improving the Modeling of the Transport of Radionuclides Produced by Radiological Transformations in Transit by Subdividing the Transport Layer

Consider a situation that requires the modeling of the flux or concentration in the aquifer of a progeny of a radionuclide that is initially present in the primary contamination. Assume that there is an unsaturated layer between the primary contamination and the aquifer. The progeny atoms in the saturated zone can be classified into three groups on the basis of the zone in which the radiological transformation of the parent atom produces that atom of the progeny, as shown in Figure H-5. Some of the atoms would have transformed in the primary contamination and traveled both the unsaturated zone and the saturated zone as a progeny. The second group consists of those atoms that exited the primary contamination and traveled part of the unsaturated zone in the form of parent atoms, transformed to the progeny in the unsaturated zone, and traveled the rest of the unsaturated zone and the saturated zone as progeny atoms. The last group consists of those atoms that exited and traveled the unsaturated zone and part of the saturated zone in the form of the parent, transformed to the progeny in the saturated zone, and traveled the rest of the saturated zone as a progeny.
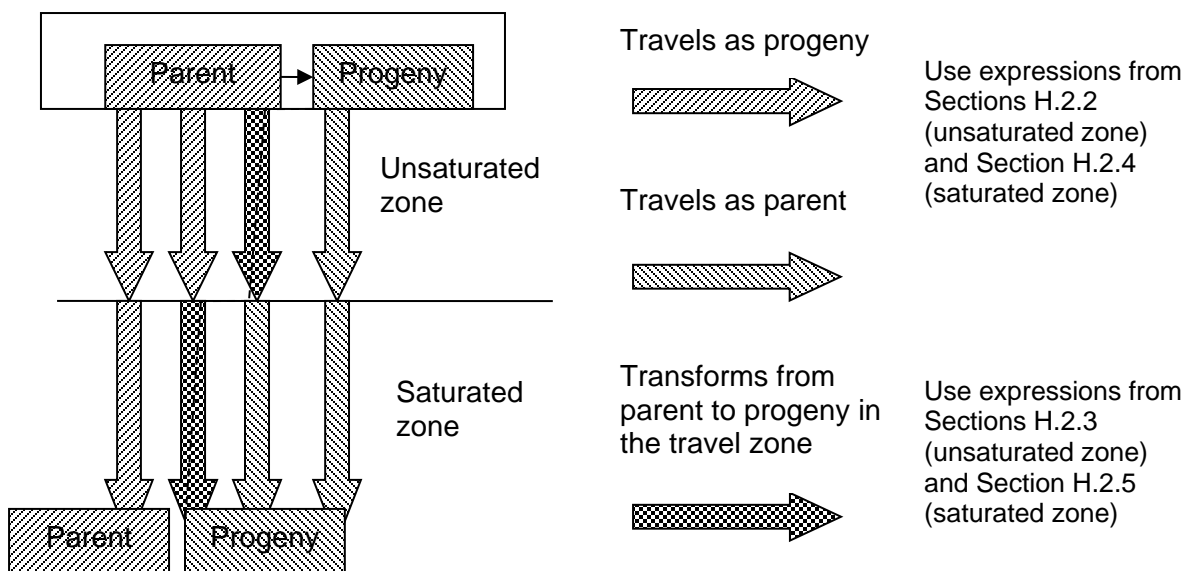
**Figure H-5   Progeny in the Aquifer Due to a Parent Radionuclide in Primary
Contamination**

RESRAD-OFFSITE uses the expressions in Sections H.2.2 and H.2.4 to model the transport of the first group of radionuclides that traverse the unsaturated and saturated zones as progeny atoms without transformation. The transport of the second group of atoms is modeled by using one of the expressions in Sections H.2.3.1 or H.2.3.2 for the unsaturated zone and the expression in Section H.2.4 for the saturated zone. Modeling the transport of the third group of atoms involves the expression in Section H.2.2 for the unsaturated zone and one of the expressions in Section H.2.5.1 or Section H.2.5.2 for the saturated zone. The code will model the effects of longitudinal dispersion and will ignore the differences in the distribution coefficients of the radionuclides in the zone in which the transformation occurs by using the first of the pair of expressions, or it will model the effects of the differences in the distribution coefficients of the radionuclides and ignore the effects of longitudinal dispersion by using the second expression according to the user's preference specified in the input interface. Such a choice may not be acceptable when both processes are of comparable importance. Both processes can be modeled over a greater part of the transport zone by dividing the transport zone into a number of smaller subzones. This is illustrated in Figure H-6, where the unsaturated and saturated zones are divided into two subzones for groundwater transport calculations. Now one of the processes (longitudinal dispersion or radionuclide-specific distribution coefficient) will have to be ignored over either half the length of the unsaturated zone or half the length of the saturated zone when modeling the transport of any progeny radionuclide produced in transit.

The diagram shows transport zones with the following legend:

Travels as progeny
Use expressions from Sections H.2.2 (unsaturated zone) and Section H.2.4 (saturated zone)

Travels as parent

Transforms from parent to progeny in the travel zone
Use expressions from Sections H.2.3 (unsaturated zone) and Section H.2.5 (saturated zone)
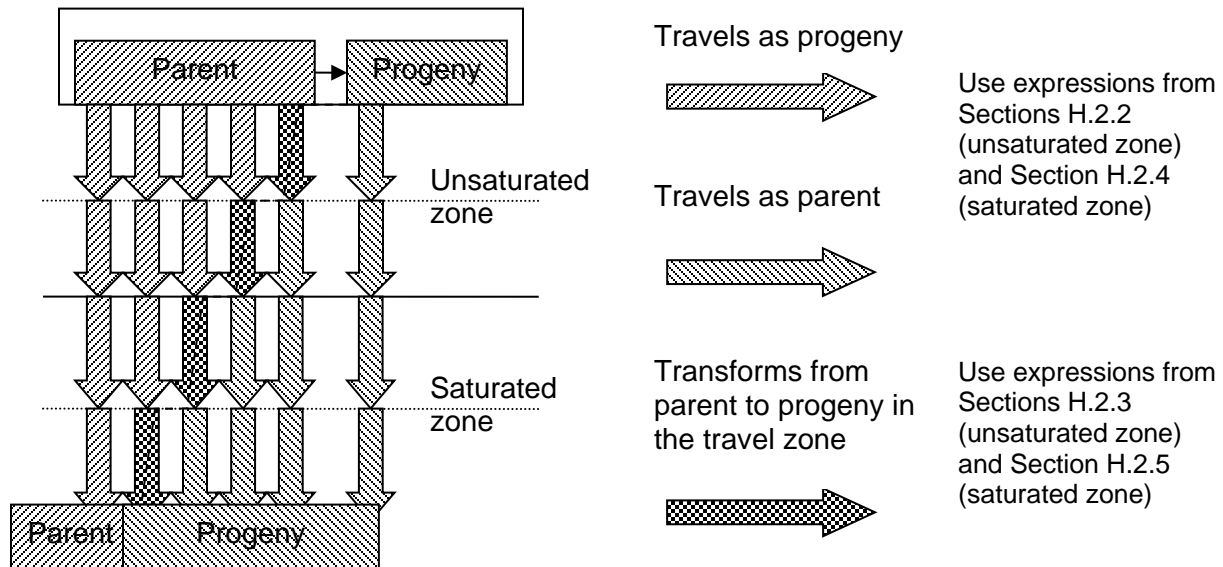
Figure H-6   Progeny in Aquifer Due to Parent Radionuclide in Primary Contamination, with Subdivided Transport Zones

The code-suggested default is to model the radionuclide-specific distribution coefficients in the subzones in which each atom undergoes radiological transformations and to ignore longitudinal dispersion in those subzones. This choice is appropriate in most cases for the following reasons:

1. If the subzones are small enough, longitudinal dispersion in a subzone will be small and ignoring it for that subzone would not cause a significant change in the result.

2. The distribution coefficient affects both the partitioning of the radionuclide between the water and the solid phases of soil and the radionuclide's transport velocity. The differences in the partitioning are not affected by the size of the subzone and will still be significant even in a small subzone.

However, in situations where longitudinal dispersion overwhelms longitudinal transport, it would be better to ignore the effects of differences in the distribution coefficients and to model the effects of longitudinal dispersion in the zones of transformations and to use the distribution coefficient of the progeny for all radionuclides.

The input and output for the subdivided zones in the partially saturated layers are the flux entering the up-gradient face and the flux exiting the down-gradient face, the same as for the undivided partially saturated zone. The formulations in Sections H.3.1 through H.3.3 are repeatedly applied for each subzone. Furthermore, because the subzones are identical the transfer factors computed for the first subzone can be saved and used for all the subsequent subzones, thereby reducing the computation time, this is practical only when the calculation time points are spaced uniformly (Section E.1).

Only the part of the saturated transport zone that is outside the footprint of the primary contamination, called the offsite transport distance, can be subdivided. The first subzone of the saturated zone consists of the saturated zone within the footprint of the primary contamination and the first subdivision of the offsite transport distance. The input for this first subzone is the pulse flux at the water table, and the output is the flux at the down-gradient face of the subzone. Thus, the formulations discussed in Sections H.3.4, H.3.6, and H.3.8 for the flux output are used for the first subzone of the saturated zone. The input for each of the remaining subzones is the flux entering at the up-gradient face. The output for all but the last subzone is the flux exiting the down-gradient face. The formulations in Sections H.3.1 through H.3.3 are used for all but the first and last subzones of the saturated zone. The output of the last subzone depends on the water source; it is the flux exiting the down-gradient face for the surface water body, and the concentration for the well. The formulations for flux discussed in Sections H.3.1 through H.3.3 are applicable for the last subzone to the surface water body. The expressions for concentration discussed in Sections H.3.10 through H.3.12 are applicable for the last subzone to the well.

H.3.14 Simpson's and Romberg Numerical Integration

The computational code uses the numerical integration method described in Press et al. (1989) to evaluate the integral $\int_a^b f(x)dx$ when the analytical solution is not known.

A sequence of trapezoidal integrals is first computed as follows:

$$T_1 = (b-a)\frac{f(a)+f(b)}{2} \tag{H.105}$$

is the first trapezoidal estimate using only the endpoints;

$$T_2 = \frac{b-a}{2}\frac{f(a)+f\left(\frac{a+b}{2}\right)}{2}+\frac{b-a}{2}\frac{f\left(\frac{a+b}{2}\right)+f(b)}{2}$$

$$T_2 = \frac{b-a}{2}\left[\frac{f(a)}{2}+\frac{f(b)}{2}+f\left(\frac{a+b}{2}\right)\right]=\frac{T_1}{2}+\frac{b-a}{2}f\left(\frac{a+b}{2}\right) \tag{H.106}$$

is the second trapezoidal estimate using the endpoints and the midpoint; and

$$T_3 = \frac{b-a}{4}\left[\frac{f(a)+f\left(\frac{3a+b}{4}\right)}{2}+\frac{f\left(\frac{3a+b}{4}\right)+f\left(\frac{a+b}{2}\right)}{2}+\frac{f\left(\frac{a+b}{2}\right)+f\left(\frac{a+3b}{4}\right)}{2}+\frac{f\left(\frac{a+3b}{4}\right)+f(b)}{2}\right] \tag{H.107}$$

$$T_3 = \frac{b-a}{4}\left[\frac{f(a)}{2}+\frac{f(b)}{2}+f\left(\frac{a+b}{2}\right)+f\left(\frac{3a+b}{4}\right)+f\left(\frac{a+3b}{4}\right)\right]=\frac{T_2}{2}+\frac{b-a}{4}\left[f\left(\frac{3a+b}{4}\right)+f\left(\frac{a+3b}{4}\right)\right]$$

is the third trapezoidal estimate using the endpoints and the quarter points.

The succeeding trapezoidal estimates using values of the function at 1/8 of the interval, at 1/16 of the interval, etc., are computed in a similar fashion. Then a sequence of parabolic estimates (Simpson's method) can be obtained from the successive trapezoidal estimates as follows:

$$S_1 = \frac{b-a}{6}\left[f(a)+4f\left(\frac{a+b}{2}\right)+f(b)\right] = \frac{4T_2-T_1}{3} \qquad \text{(H.108)}$$

is the 3-point parabolic integral.

$$S_2 = \frac{b-a}{12}\left[f(a)+4f\left(\frac{3a+b}{4}\right)+f\left(\frac{a+b}{2}\right)\right]+\frac{b-a}{12}\left[f\left(\frac{a+b}{2}\right)+4f\left(\frac{a+3b}{4}\right)+f(b)\right]$$

$$S_2 = \frac{b-a}{12}\left[f(a)+f(b)+2f\left(\frac{a+b}{2}\right)+4f\left(\frac{3a+b}{4}\right)+4f\left(\frac{a+3b}{4}\right)\right] = \frac{4T_3-T_2}{3} \qquad \text{(H.109)}$$

is the 5-point parabolic integral.

In a similar fashion, the 9-point (1/8 interval) parabolic estimate is $S_3 = \frac{4T_4-T_3}{3}$, the 17-point (1/16 interval) parabolic estimate is $S_4 = \frac{4T_5-T_4}{3}$, and the 33-point (1/32 interval) parabolic estimate is $S_5 = \frac{4T_6-T_5}{3}$.

If the 17-point and 33-point parabolic estimates agree within the user-specified criterion, the 33-point parabolic estimate is used. Otherwise, successive fourth-order interpolations of the trapezoidal estimates (Romberg integration) are obtained until they agree within the user-specified criterion. If the fourth-order Romberg estimates with 16,385 points and 32,769 points do not agree within the criterion, the 32,769-point estimate is used.

H.4   <u>References</u>

Lindstrom, F.T., R. Haque, V.H. Freed, and L. Boersma, 1967, "Theory on the Movement of Some Herbicides in Soils: Linear Diffusion and Convection of Chemicals in Soils," *Environmental Science and Technology* 1(7):561−565.

Press, W.H., B.P. Flannery, S.A. Teukolsky, and W.T. Vetterling, 1989, *Numerical Recipes, the Art of Scientific Computing (Fortran Version)*, Cambridge University Press, New York, N.Y.

Yu, C., A.J. Zielen, J.-J. Cheng, D.J. LePoire, E. Gnanapragasam, S. Kamboj, J. Arnish, A. Wallo III, W.A. Williams, and H. Peterson, 2001, User's Manual for RESRAD Version 6, ANL/EAD-4, Environmental Assessment Division, Argonne National Laboratory, Lemont, Illinois.

APPENDIX I:
ATMOSPHERIC TRANSPORT

The atmospheric transport model used in RESRAD-OFFSITE is a Gaussian plume dispersion model based on an area source release. Radionuclides released from a contaminated area are transported by the wind and are dispersed as a result of atmospheric turbulence. The area source is characterized as a rectangular area with a time-dependent emission rate and is located upwind of a receptor location. A plume-rise model developed by Briggs (1969) is used to estimate the buoyancy-induced rise of the release, if applicable. Depending on the circumstances, either the standard Pasquill-Gifford dispersion coefficients (Slade 1968; Eimutis and Konicek 1972) or the Briggs (1974) dispersion coefficients can be used. The former are suitable for ground-level releases; the latter are better for elevated releases. The code considers deposition of radionuclides from the plume, by dry and wet deposition, both for radionuclides attached to particulates and for radionuclides in gas form. The code calculates the concentrations of radionuclides in air and the rate of deposition of radionuclides on the catchment.

The primary contamination and the offsite receptor locations are all treated as rectangles oriented parallel to a set of common Cartesian axes. The code performs a spatial integration of the atmospheric transport in one of two ways. It computes the concentration in the air above the receptor locations by subdividing the primary contamination and the receptor regions into small rectangles based on the grid spacing. The model computes the transport from each subdivision of the primary contamination to each subdivision of the receptor region and combines these results to obtain the spatially integrated value. The model performs atmospheric transport calculations to a receptor region (agricultural or farmed land and the surface water body) only if that region and the primary contamination do not overlap. This restriction does not apply to the calculation of atmospheric transport from the primary contamination to the catchment of the surface water body. In this case, the code calculates the deposition on the catchment from an increasing number of points from the primary contamination until a specified convergence criterion is met.

The code models transport of the radionuclides in particulate form, transport of carbon-12 (C-12) and hydrogen-3 (H-3) in vapor or gaseous form, and the transport of the radon isotopes Rn-220 and Rn-222 and their short-lived progeny. The decay and ingrowth of the radon isotopes and the three short-lived progeny of each of those radon isotopes during the transport are also modeled.

I.1   Effective Release Height

Material released from a contaminated area may rise above the release point as a result of thermal buoyancy. The thermal buoyancy could be related to solar heating of the ground or a local heat source, such as underground steam lines. An effective release height, H, is used in the atmospheric dispersion equations to account for the additional height of the release. The effective release height is the sum of the actual physical release height, h, and the thermally induced plume rise, Δh, with an adjustment for terrain height:

$$H = h + \Delta h - (1 - P_c)\,min\big(h + \Delta h, E_r - E_p\big),\tag{I.1}$$

where

H = effective release height (m),

h = physical release height (m),

Δh = plume rise (m),

P_c = plume-path coefficient,

E_r = receptor elevation (m), and

E_p = release elevation, the reference point for the release height (m).

I.2 Plume Rise

To estimate plume rise, RESRAD-OFFSITE uses the formulas derived by Briggs (1969) for buoyant plumes. The rise from thermal buoyancy depends on stability class, wind speed, and receptor distance.

For stability classes A, B, C, and D, plume rise is given by:

$$\Delta h = \frac{1.6F^{1/3}x^{2/3}}{u_H}, \text{ for } x \leq 10h,$$
$$\Delta h = \frac{1.6F^{1/3}(10h)^{2/3}}{u_H}, \text{ for } x > 10h,$$

(I.2)

where

F = $3.7 \times 10^{-5}\ Q_h$ (m^4/s^3),

Q_h = heat flux from radionuclide release area (cal/s),

x = downwind receptor distance from the release area (m), and

u_H = wind speed at effective release height (m/s).

For stability classes E and F, the plume rise is calculated according to:

$$\Delta h = \frac{1.6F^{1/3}x^{2/3}}{u_H}, \text{ for } x \leq 2.4\frac{u_H}{\sqrt{s}},$$
$$\Delta h = 2.9\left(\frac{F}{u_H s}\right)^{1/3}, \text{ for } x > 2.4\frac{u_H}{\sqrt{s}},$$

(I.3)

except when the wind is so light that the plume rises vertically. Under such conditions, the final plume rise is given by Briggs (1969) as follows:

$$\Delta h = \frac{5.0F^{1/4}}{s^{3/8}}, \text{ when } u_H \leq u_{test},$$

(I.4)

where

$s = \frac{g}{T_a}\left(\frac{\partial T_a}{\partial z} + l\right)$ = stability parameter (1/s^2),

u_{test} = $0.195F^{1/4}s^{1/8}$ (m/s),

$g = 9.80665$ = gravitational acceleration (m/s^2),

T_a = ambient air temperature (K),

$l = 0.0098$ = normal adiabatic lapse rate of the atmosphere (K/m),

$\frac{\partial T_a}{\partial z} + l$ = potential temperature lapse rate (0.002 and 0.035 for stability classes E and F, respectively), and

z = vertical distance above the release point (m).

As recommended by Briggs (1969), the first four equations for plume rise (Equations [I.2] and [I.3]) contain wind speed in the denominator, which would produce unrealistically high values for very low wind speeds. Because the Briggs equations apply only to windy conditions, a minimum wind speed of 0.1 m/s is imposed in the plume-rise calculations.

I.3   Terrain Height Adjustment

The presence of rising terrain downwind from an area emission source requires that the release height derived for flat terrain be adjusted accordingly. RESRAD-OFFSITE uses stability-dependent plume-path coefficients to estimate the effects of terrain elevation on the height of the plume centerline. The third term in the equation for the release height (Equation [I.1]) is the adjustment for downwind elevations, as given in Ross et al. (1985).

An increase in receptor elevation downwind effectively reduces the release height if the release height is greater than zero. This condition is embodied in the $(1 - P_c)$ min $(h + \Delta h, E_r - E_p)$ portion of the equation for the release height (Equation [I.1]). On the other hand, the plume will not travel straight into a hillside; it will follow air currents partway up the hill on its approach. The portion of the equation with the plume-path coefficient $(1 - P_c)$ partially defines the amount of effective reduction in release height and ensures that the terrain height adjustment is not too extreme. For neutral and unstable conditions (stability classes A, B, C, and D), P_c is set to 0.5 so that the plume height remains at least one-half the distance aboveground as it would be if no adjustment was made. Similarly, for stable conditions (stability classes E and F), P_c is set to 0.3 so that the plume height remains at least one-third the height above the ground as it would be if no adjustments were made. A plume-path coefficient of 1 represents a non-terrain-lifted plume.

I.4   Wind Power Law Adjustment

For atmospheric dispersion calculations, the measured average wind speed at the effective release height, u_H, is not always available. RESRAD-OFFSITE uses a power-law function with the following form to estimate the wind speed at the desired height:

$$\frac{u_H}{u_a} = \left(\frac{H}{z_a}\right)^p \qquad (I.5)$$

where
  u_a = wind speed at measurement height (m/s),
  z_a = height of anemometer for wind speed measurement (m), and
  p = power to which height ratio is raised.

The wind speed of u_a from the measurement height z_a is adjusted to the effective release height H of the plume for the dispersion calculations. Values for the exponent p as presented in Table I-1 were taken from Irwin (1979), as modified by Hanna et al. (1982) for the different population zones and stability classes.

Table I-1   Estimates of the Power (*p*) for the Wind Power Law for
Population Zones as a Function of Stability Class

		Stability Class				
Population Zone	A	B	C	D	E	F
Rural	00.07	00.07	00.10	00.15	00.35	00.55
Suburban/urban	00.15	00.15	00.20	00.25	00.40	00.60

I.5   Atmospheric Dispersion

RESRAD-OFFSITE uses a Gaussian plume atmospheric dispersion model to evaluate the downwind transport of radionuclide contaminants released to the atmosphere from a continuous (chronic) area source. The model preserves mass balance and accounts for depletion of the plume from dry and wet deposition processes. The effects of radiological transformations (decay and ingrowth) are not modeled except in the case of radon because transport times are relatively short, on the order of minutes.

I.5.1   Gaussian Plume

The Gaussian time-dependent dispersion equation for a discrete puff generated from a point source with an effective release height H above ground level can be written, assuming Gaussian symmetry, that is, $\sigma_x = \sigma_y$, as (Pasquill 1974):

$$C_a(i,x,y,z,t) = \frac{Q_{x_i}}{(2\pi)^{3/2}\sigma_y^2\sigma_z} e^{-\frac{r^2}{2\sigma_y^2}} \left[e^{-\frac{(z-H)^2}{2\sigma_z^2}} + e^{-\frac{(z+H)^2}{2\sigma_z^2}} \right] \tag{I.6}$$

where

$\quad C_a(i, x, y, z, t)$ = is the concentration of radionuclide i at (x, y, z) at time t after release, from a release at $(0, 0, H)$ (Activity/m³),

$\quad x$ = downwind distance from the release point (m),

$\quad y$ = crosswind distance from the plume centerline (m),

$\quad z$ = vertical distance above the ground level (m),

$\quad t$ = time since the release (s),

$\quad H$ = effective release height (see Section I.1) (m),

$\quad Q_{xi}$ = depleted source strength of radionuclide i at a distance of x from the release (see Section I.6) (Activity),

$\quad \sigma_y$ = horizontal dispersion coefficient discussed in Sections I.8 and I.9 (m),

$\quad \sigma_z$ = vertical dispersion coefficient discussed in Sections I.8 and I.9 (m),

$\quad r^2 = (x - u_Ht)^2 + y^2$ = square of the distance from the center of the puff to the receptor location, and

$\quad u_H$ = wind speed at effective release height (see Section I.4) (m/s).

The ground-level air concentration for a discrete puff is obtained by setting $z = 0$ in the preceding expression:

$$C_a(i, x, y, z = 0, t) = \frac{2Q_{x_i}}{(2\pi)^{3/2}\sigma_y^2\sigma_z} e^{-\frac{r^2}{2\sigma_y^2} - \frac{H^2}{2\sigma_z^2}}.$$

A continuous point source can be considered to be a series of overlapping puff emissions (Figure I-1). Thus, integration over time yields the downwind air concentration due to a continuous point release:

$$\bar{C}_a(i, x, y, z = 0) = \int_0^\infty C_a(i, x, y, z = 0, t)dt,$$

which can be shown to be (Slade 1968)[1]:

$$\bar{C}_a(i, x, y, z = 0) = \frac{Q_{x_i}}{\pi\sigma_y\sigma_z u_H} e^{-\frac{y^2}{2\sigma_y^2} - \frac{H^2}{2\sigma_z^2}} \tag{I.7}$$

where Q_{xi} is the source term for radionuclide i, now in units of Activity/s for a continuous source, corrected for wet and dry deposition from the plume (Equation [I.18]), as shown in Section I.6.
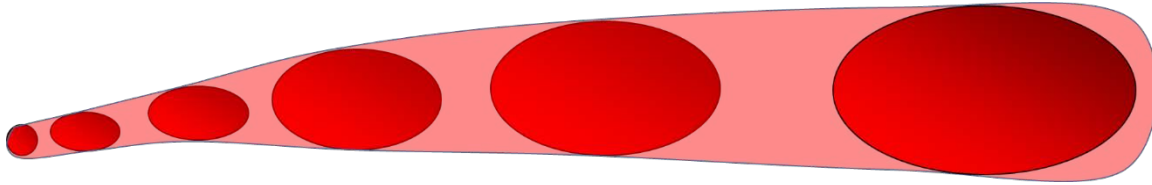
Figure I-1   From Discrete Puffs to a Continuous Point Source

I.5.2   Plume Reflection

The existence of a stable air layer at higher altitudes under unstable and neutral atmospheric conditions affects atmospheric dispersion at great distances from the release point. The upward dispersion of the plume is eventually restricted when the plume encounters an elevated stable layer (or lid) or a mixing layer at some height L (Figure I-2). RESRAD-OFFSITE assumes this stable layer reflects the plume at these distances. When the vertical distribution becomes uniform because of reflection, the integration of the Gaussian time-dependent dispersion (Equation [I.6]) for a discrete puff release over z and t yields[2]:

---

[1] $\bar{C}_a(i, x, y, z = 0) = \frac{2Q_{x_i}}{(2\pi)^{3/2}\sigma_y^2\sigma_z} e^{-\frac{H^2}{2\sigma_z^2}} \int_0^\infty e^{-\frac{(x - u_H t)^2 + y^2}{2\sigma_y^2}} dt = \frac{Q_{x_i}}{\pi\sigma_y\sigma_z} e^{-\frac{y^2}{2\sigma_y^2} - \frac{H^2}{2\sigma_z^2}} \frac{\sqrt{2}}{\sqrt{\pi}\sigma_y} \int_0^\infty e^{-\left(\frac{u_H t - x}{\sqrt{2}\sigma_y}\right)^2} dt =$

$\frac{Q_{x_i}}{\pi\sigma_y\sigma_z} e^{-\frac{y^2}{2\sigma_y^2} - \frac{H^2}{2\sigma_z^2}} \frac{\sqrt{2}}{\sqrt{\pi}\sigma_y} \frac{\sqrt{2}\sigma_y}{u_H} \int_0^\infty e^{-\left(\frac{u_H t - x}{\sqrt{2}\sigma_y}\right)^2} d\left(\frac{u_H t - x}{\sqrt{2}\sigma_y}\right) = \frac{Q_{x_i}}{\pi\sigma_y\sigma_z} e^{-\frac{y^2}{2\sigma_y^2} - \frac{H^2}{2\sigma_z^2}} \frac{\sqrt{2}}{\sqrt{\pi}\sigma_y} \frac{\sqrt{2}\sigma_y}{u_H} \frac{\sqrt{\pi}}{2}$

[2] $\frac{1}{L}\int_{-\infty}^\infty \int_0^\infty C_a(i, x, y, z, t)dt\,dz = \frac{1}{L}\int_{-\infty}^\infty \int_0^\infty \frac{Q_{x_i}}{(2\pi)^{3/2}\sigma_y^2\sigma_z L} e^{-\frac{r^2}{2\sigma_y^2}} \left[e^{-\frac{(z-H)^2}{2\sigma_z^2}} + e^{-\frac{(z+H)^2}{2\sigma_z^2}}\right] dt\,dz =$

$\frac{Q_{x_i}}{(2\pi)^{3/2}\sigma_y^2\sigma_z L} \int_0^\infty e^{-\frac{(x - u_H t)^2 + y^2}{2\sigma_y^2}} dt \int_{-\infty}^\infty \left[e^{-\frac{(z-H)^2}{2\sigma_z^2}} + e^{-\frac{(z+H)^2}{2\sigma_z^2}}\right] dz =$

$$\bar{C}_a^{mixed}(i,x,y) = \frac{Q_{x_i}}{\sqrt{2\pi}\sigma_y u_H L} e^{-\frac{y^2}{2\sigma_y^2}} \qquad (I.8)$$

where L is the height of the mixing layer (in m), sometimes referred to as the lid height.
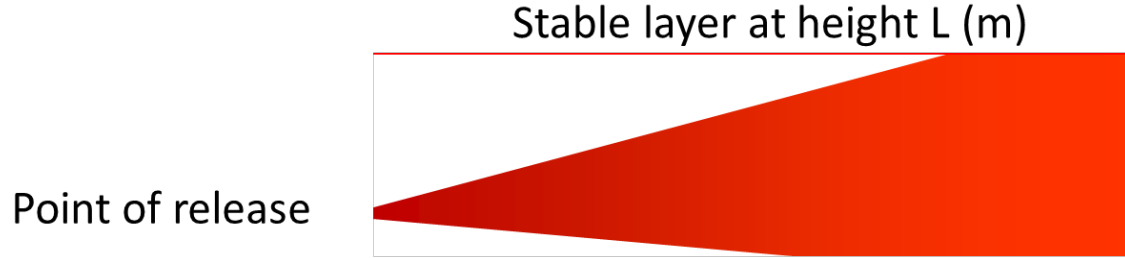
Stable layer at height L (m)

Figure I-2   Mixing in the Vertical Direction of a Plume Constrained by a Mixing Layer

The following conditions (Powell et al. 1979) are used to determine which of the two preceding equations, Equation (I.7) or Equation (I.8), is used for the dispersion calculation.

The "no-mixing" equation, Equation (I.7), which includes the vertical distribution, is used at distances where the vertical dispersion coefficient is small compared to the lid height:

$$\frac{\sigma_z}{L} \leq \frac{\sqrt{1-\frac{H}{L}}}{1.2} \qquad (I.9)$$

The "total mixing" equation, Equation (I.8), is used at distances where the vertical dispersion coefficient is of the same order as the lid height and a uniform distribution can be assumed. This is the case when either of the following conditions is satisfied:

$$0 \leq H/L < 0.5 \text{ and } \frac{\sigma_z}{L} \geq -2.37\left(\frac{H}{L}\right)^2 + 0.489\left(\frac{H}{L}\right) + 0.756, \qquad (I.10)$$

or

$$0.5 \leq H/L < 1.0 \text{ and } \frac{\sigma_z}{L} \geq -2.37\left(\frac{H}{L}\right)^2 + 4.25\left(\frac{H}{L}\right) - 1.13. \qquad (I.11)$$

At downwind distances between the "no-mixing" conditions (Equation [I.9]) and the "total mixing" conditions (Equation [I.10] or Equation [I.11]), the concentration is determined by linear interpolation between Equations (I.7) and (I.8).

$$\frac{Q_{x_i}}{4\sqrt{2\pi}\sigma_y L} e^{-\frac{y^2}{2\sigma_y^2}} \frac{\sqrt{2}}{\sqrt{\pi}\sigma_y} \frac{\sqrt{2}\sigma_y}{u_H} \int_0^\infty e^{-\left(\frac{u_H t - x}{\sqrt{2}\sigma_y}\right)^2} d\left(\frac{u_H t - x}{\sqrt{2}\sigma_y}\right) \times \frac{\sqrt{2}}{\sqrt{\pi}\sigma_z}\sqrt{2}\sigma_z \left[\int_{-\infty}^\infty e^{-\left(\frac{z-H}{\sqrt{2}\sigma_z}\right)^2} d\left(\frac{z-H}{\sqrt{2}\sigma_z}\right) + \right.$$

$$\left.\int_{-\infty}^\infty e^{-\left(\frac{z+H}{\sqrt{2}\sigma_z}\right)^2} d\left(\frac{z+H}{\sqrt{2}\sigma_z}\right)\right] = \frac{Q_{x_i}}{4\sqrt{2\pi}\sigma_y L} e^{-\frac{y^2}{2\sigma_y^2}} \frac{\sqrt{2}}{\sqrt{\pi}\sigma_y} \frac{\sqrt{2}\sigma_y}{u_H} \frac{\sqrt{\pi}}{2} \times \frac{\sqrt{2}}{\sqrt{\pi}\sigma_z}\sqrt{2}\sigma_z[\sqrt{\pi} + \sqrt{\pi}]$$

I.5.3   Chronic Release

Equation (I.7), which is the "no-mixing" equation in Section I.5.1, and Equation (I.8), which is the "total mixing" equation in Section I.5.2, are both valid for unchanging weather conditions when the period of release exceeds the time necessary for the airborne material to travel downwind from the release point to the receptor location. However, weather conditions will fluctuate with time (generally on the order of minutes or longer), causing the plume to meander within a sector when the wind blows in a particular direction. Thus, it is more appropriate to evaluate the sector-average air concentration to estimate human health impacts under such conditions.

The air dispersion model in RESRAD-OFFSITE uses a polar grid with 16 sectors to specify wind direction. The sector-average air concentration at a receptor location that is a distance of x meters from the release point (see Figure I-3) can be estimated as the integral of Equation (I.7), and Equation (I.8), over y, from minus infinity to plus infinity, divided by the width of the sector, $2y_{sec}$, at that distance. Because the Gaussian equation is symmetrical, this sector-average concentration at ground level for the case where there is no plume reflection can be written as follows:

$$\bar{C}_{sec}^{no\ mixing}(i,x,z=0) = \frac{\int_0^\infty \bar{C}_a(i,x,y,z=0)dy}{y_{sec}} = \int_0^\infty \frac{Q_{x_i}}{\pi y_{sec}\sigma_y\sigma_z u_H} e^{-\frac{y^2}{2\sigma_y^2}-\frac{H^2}{2\sigma_z^2}} dy$$

where $y_{sec} = x\tan 11.25°$.
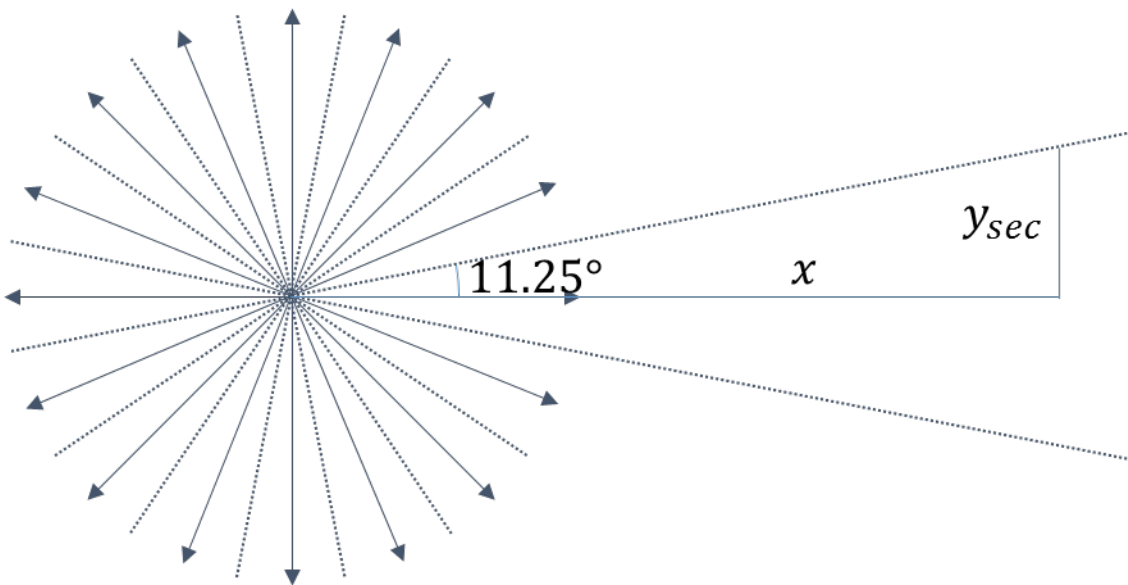
Figure I-3   Relationships Used in Sector-Average Air Concentration Calculations

Evaluating the integral using the identity $\int_0^\infty e^{-(ay)^2} dy = \frac{\sqrt{\pi}}{2a}$ produces the following expression:

$$\bar{C}_{sec}^{no\ mixing}(i, x, z = 0) = \frac{Q_{x_i}}{\pi y_{sec} \sigma_z u_H} e^{-\frac{H^2}{2\sigma_z^2}} \frac{1}{\sigma_y} \int_0^\infty e^{-\left(\frac{y}{\sqrt{2}\sigma_y}\right)^2} dy = \frac{Q_{x_i}}{\pi y_{sec} \sigma_z u_H} e^{-\frac{H^2}{2\sigma_z^2}} \frac{1}{\sigma_y} \sqrt{2}\sigma_y \frac{\sqrt{\pi}}{2}$$

This gives the sector-averaged air concentration at ground level at a distance of x meters from the source when there is no plume reflection:

$$\bar{C}_{sec}^{no\ mixing}(i, x, z = 0) = \frac{Q_{x_i}}{\sqrt{2\pi} y_{sec} \sigma_z u_H} e^{-\frac{H^2}{2\sigma_z^2}} \tag{I.12}$$

where

Q_{xi} = depleted source strength of radionuclide i at a distance of x from the release (Activity/s),
H = effective release height (see Section I.1) (m),
σ_z = vertical dispersion coefficient discussed in Sections I.8 and I.9 (m),
y_{sec} = x tan 11.25°, and
u_H = wind speed at effective release height (see Section I.4) (m/s).

In the case of total mixing in the vertical direction because of plume reflection, the sector-average air concentration at a distance x meters from the source is given as follows:

$$\bar{C}_{sec}^{total\ mixing}(i, x) = \frac{\int_0^\infty \bar{C}_a^{mixed}(i, x, y) dy}{y_{sec}} = \int_0^\infty \frac{Q_{x_i}}{y_{sec}\sqrt{2\pi}\sigma_y u_H L} e^{-\frac{y^2}{2\sigma_y^2}} dy = \frac{Q_{x_i}}{2 y_{sec} u_H L} \tag{I.13}$$

where

Q_{xi} = depleted source strength of radionuclide i at a distance of x from the release (Activity/s),
y_{sec} = x tan 11.25°,
u_H = wind speed at effective release height (see Section I.4) (m/s), and
L = height of the mixing layer, sometimes referred to as the lid height (m).

In both Equation (I.13) and Equation (I.12), with and without plume reflection, the integration of y to infinity and averaging using the sector width result in the compression of the plume to within the sector boundaries.

I.6 Depletion Correction

As a radioactive plume travels downwind, its radionuclide content decreases due to deposition on the ground. Two deposition mechanisms, dry and wet, account for this radionuclide depletion from the plume. This section describes the methods RESRAD-OFFSITE uses to calculate plume depletion from radionuclide deposition.

I.6.1 Dry Deposition

With the exception of inert gases, most radioactive material emitted from area sources will be in particulate form. Those particulates with dimensions on the order of a few micrometers or less have vertical movements that largely depend on the vertical turbulence and mean motion of the air; particle settling due to gravity is minimal. Deposition of such small particles on the ground surface is the result of turbulent diffusion and Brownian motion. Chemical absorption, impaction, and other physical and chemical processes cause the material to be retained at the surface. Such a deposition mechanism depletes the amount of radioactivity in the plume, causing ground contamination, and thus affects potential radiological hazards as the plume travels farther downwind. Radiological hazards to individuals occur by way of either direct exposure from the ground or indirect exposure via the ingestion of contaminated foodstuff.

Calculation of the dry deposition rate involves the concept of deposition velocity, that is, the ratio of the deposition rate to the air concentration expressed in units of velocity. The deposition velocity is determined from either field measurements or laboratory measurements of air and ground concentrations. The code employs user-specified deposition velocities to model the transport of radionuclides attached to particulates. Velocities of zero are used to model the transport of C-12 and H-3 in vapor or gaseous form, and the transport of the radon isotopes Rn-220 and Rn-222 and their short-lived progeny are modeled by the code. When plume depletion by dry deposition is considered, the initial source term, Q_{0i}, at the release point can be replaced by a depleted source term, $Q_{x_i}^{dry}$, along the downwind sector. This approach, known as the source depletion model, assumes that depletion reduces only the effective source strength and that the vertical Gaussian profile remains unchanged. In this derivation, total activity is conserved.

The reduced source strength Q_{xi} as the result of deposition is calculated from the following equation (Slade 1968):

$$Q_{x_i}^{dry} = Q_{0_i} \exp\left[-\frac{V_{d_i}}{\sqrt{\frac{\pi}{2}} u_H} \int_0^x F(x)dx \right] \tag{I.14}$$

where

$\quad Q_{x_i}^{dry}$ = depleted source strength of radionuclide i at a distance of x from the release (Activity/s),

$\quad Q_{0i}$ = source strength of radionuclide i at the point of release (Activity/s),

$\quad V_{di}$ = deposition velocity of radionuclide i (m/s),

$\quad u_H$ = wind speed at effective release height (see Section I.4) (m/s),

$\quad F(x)$ depends on the degree of mixing in the vertical direction,

$\quad F(x) = \dfrac{e^{-\frac{H^2}{2\sigma_z^2}}}{\sigma_z}$ at downwind distances not affected by the presence of a mixing layer,

$\quad F(x) = \dfrac{1}{L}$ at downwind distances where total mixing by the presence of a mixing layer can be assumed (Powell et al. 1979),

I-9

At downwind distances between the no-mixing (Equation [I.9]) and total-mixing conditions (Equation [I.10] or Equation [I.11]), $F(x)$ is determined by a linear combination the function under the two conditions,

H = effective release height (see Section I.1) (m), and

σ_z = vertical dispersion coefficient discussed in Sections I.8 and I.9 (m).

I.6.2 Wet Deposition

Radionuclides can also be removed from a plume by rain or snowfall. In wet deposition, radionuclides are depleted from the plume by "washing out" due to rain or snow. Thus, the wet deposition rate depends on the total amount of radioactivity contained in the plume. This is different from dry deposition, where depletion is closely related to the air concentration at ground level. The fraction of material removed per unit time by wet deposition is known as the "washout coefficient," V_w, and is defined as follows:

$$V_w = -\frac{1}{C_a}\frac{dC_a}{dt} \tag{I.15}$$

where

V_w = washout coefficient (1/s), and

C_a = local concentration of the radionuclide in air (Activity/m^3).

Calculated and measured values of the washout coefficient range from about 1.0×10^{-5} to 1.0×10^{-2} per second (Ritchie et al. 1978; McMahon and Dennison 1979). The value of the washout coefficient increases with an increasing rainfall rate and depends linearly on the rainfall rate, as follows:

$$V_w = W_c R \tag{I.16}$$

where

W_c depends on the atmospheric stability class ([1/s]/[mm/hr]),

W_c = 10^{-3} for stability classes A to D,

W_c = 10^{-4} for stability classes E and F (Ritchie et al. 1978),

R = 1,000 P_r/8,766 = rainfall rate (mm/hr), and

P_r = precipitation rate (m/year).

The depleted source strength from wet deposition, assuming a steady rainfall rate and wind speed, is given by the following equation:

$$Q_{WET_{x_i}} = Q_{0_i} \exp\left(-\frac{V_w x}{u_H}\right). \tag{I.17}$$

I.6.3 Dry and Wet Deposition

The depleted source strength at a distance x downwind becomes a function of both dry and wet deposition. The composite depleted source strength is calculated using the following equation:

$$Q_{x_i} = Q_{0_i} \exp\left[-\frac{V_w x}{u_H} - \frac{V_{d_i}}{\sqrt{\frac{\pi}{2}} u_H} \int_0^x F(x)dx\right] \qquad (\text{I.18})$$

This is a combination of Equations (I.14) and (I.17), all the terms of which are defined in Sections I.6.1 and I.6.2.

I.7   Mixing Height

The value of the mixing height (L) is estimated from the annual average input values for morning and afternoon (Holzworth 1972). It depends on the stability class of the atmosphere. The mixing height is estimated from the following:

  $L = 1.5L_{pm}$ for an extremely unstable atmosphere (stability class A) (m),
  $L = L_{pm}$ for the other unstable situations (stability class B and C) (m),
  $L = 0.5(L_{am} + L_{pm})$ for a neutral atmosphere (stability class D) (m), and
  the mixing height does not apply for stable atmospheric conditions.

I.8   Meteorological Conditions

As presented in the previous sections, the dispersion model in RESRAD-OFFSITE requires the following meteorological data:

1. Stability class (A through F),
2. Wind speed (m/s),
3. Mixing height (m) (for stability classes A through D),
4. Ambient temperature (K), and
5. Rainfall rate (mm/hr).

Joint frequency data on weather conditions over a period of time (e.g., annual data) can be input manually or read from a STability ARray (STAR) format data file. If a STAR file has any class G frequencies, they are added to the corresponding class F frequencies when the code reads that STAR file.

Atmospheric stabilities are classified into six categories (A, B, C, D, E, and F) in order of increasing stability based on criteria established by Pasquill (1974). The dispersion equations in the models used are generic to all stability categories and empirical in nature. For each stability category, a set of dispersion coefficients, σ_y and σ_z, are initially calculated on the basis of the Pasquill-Gifford curves (Eimutis and Konicek 1972) and later adjusted for buoyancy-induced dispersion, as discussed in Section I.9. The Pasquill-Gifford dispersion coefficients are calculated according to the following expression:

$$\sigma'_y = (0.000246\sigma_\theta{}^2 + 0.00576\sigma_\theta + 0.066)x^{0.9031} \qquad (\text{I.19})$$

and

$$\sigma'_z = ax^b + c \qquad (\text{I.20})$$

where

$$\sigma'_y \quad = \quad \text{horizontal Pasquill-Gifford dispersion coefficient (m),}$$
$$\sigma'_z \quad = \quad \text{vertical Pasquill-Gifford dispersion coefficient (m),}$$
$$\sigma_\theta, a, b, c \quad = \quad \text{unitless dispersion parameters in Table I-2, and}$$
$$x \quad = \quad \text{downwind distance from the release point (m).}$$

Briggs (1974) developed formulas for the dispersion coefficients on the basis of data collected from elevated releases. In addition, Briggs coefficients have been derived for rural and urban population zones. The urban values are also used in suburban zone calculations in RESRAD-OFFSITE. The Briggs dispersion coefficients are calculated according to the following equation:

$$\sigma'_y \ or \ \sigma'_z = ax(1 + bx)^c \qquad (I.21)$$

where

$$\sigma'_y \quad = \quad \text{horizontal Briggs dispersion coefficient (m),}$$
$$\sigma'_z \quad = \quad \text{vertical Briggs dispersion coefficient (m),}$$
$$a, b, c \quad = \quad \text{unitless dispersion parameters in Table I-3, and}$$
$$x \quad = \quad \text{downwind distance from the release point (m).}$$

Table I-2 Pasquill-Gifford Dispersion Parameters for Ground-Level Releases

Applicable Range (downwind distance, m)	Stability Class	Coefficients			
		σ_θ	a	b	c
$x > 1{,}000$	A	25	0.00024	2.094	9.6
	B	20	0.055	1.098	2.0
	C	15	0.133	0.911	0.0
	D	10	1.26	0.516	−13.0
	E	5	6.73	0.305	−34.0
	F	1.5	18.05	0.18	−48.6
$100 \le x \le 1{,}000$	A	25	0.00066	1.941	9.27
	B	20	0.0382	1.149	3.3
	C	15	0.113	0.911	0.0
	D	10	0.222	0.725	−1.7
	E	5	0.211	0.678	−1.3
	F	1.5	0.086	0.74	−0.35
$x < 100$	A	25	0.192	0.936	0.0
	B	20	0.156	0.922	0.0
	C	15	0.116	0.905	0.0
	D	10	0.079	0.881	0.0
	E	5	0.063	0.871	0.0
	F	1.5	0.053	0.814	0.0

Source: Data from Eimutis and Konicek (1972).

Table I-3   Briggs Dispersion Coefficients for Elevated Releases

Weather Conditions	Stability Class	Rural			Urban		
		a	b	c	a	b	c
			σ'_y				
Extremely unstable	A	0.22	0.0001	−0.5	0.32	0.0004	−0.5
Moderately unstable	B	0.16	0.0001	−0.5	0.32	0.0004	−0.5
Slightly unstable	C	0.11	0.0001	−0.5	0.22	0.0004	−0.5
Neutral	D	0.08	0.0001	−0.5	0.16	0.0004	−0.5
Moderately stable	E	0.06	0.0001	−0.5	0.11	0.0004	−0.5
Very stable	F	0.04	0.0001	−0.5	0.11	0.0004	−0.5
			σ'_z				
Extremely unstable	A	0.20	0.0	0.0	0.24	0.001	0.5
Moderately unstable	B	0.12	0.0	0.0	0.24	0.001	0.5
Slightly unstable	C	0.08	0.0002	−0.5	0.20	0.0	0.0
Neutral	D	0.06	0.0015	−0.5	0.14	0.0003	−0.5
Moderately stable	E	0.03	0.0003	−1.0	0.08	0.00015	−0.5
Very stable	F	0.016	0.0003	−1.0	0.08	0.00015	−0.5

Source: Briggs (1974).

I.9   Buoyancy-Induced Dispersion

RESRAD-OFFSITE considers buoyancy-induced dispersion because emitted plumes undergo a certain amount of growth during the plume-rise phase as a result of turbulent motions associated with plume release conditions and turbulent entrainment of ambient air. Pasquill (1976) suggests that this induced dispersion, σ_{zb}, can be approximated by the following equation:

$$\sigma_{zb} = \Delta h / 3.5 \tag{I.22}$$

where

σ_{zb} = buoyancy-induced vertical dispersion (m), and
Δh = plume rise (m).

The effective dispersion coefficient used in RESRAD-OFFSITE calculations can then be determined by adding variances, such as:

$$\sigma_z = \sqrt{\sigma_{zb}^2 + \sigma'_z{}^2} \tag{I.23}$$

The plume rise is a function of the downwind distance to the receptor location (see Section I.2). At the distance of final plume rise and beyond, σ_{zb} becomes constant.

Because the plume can be assumed to be symmetrical about its centerline in the initial growth phases of release, the calculation assumes that buoyancy-induced dispersion in the horizontal direction is equal to that in the vertical direction:

$$\sigma_{yb} = \Delta h / 3.5 \qquad\qquad\qquad (I.24)$$

where

σ_{yb} = buoyancy-induced vertical dispersion (m).

This expression is combined with that for dispersion resulting from ambient turbulence, either Equation I.20 or I.21, in the same manner described above for the vertical direction, to give the horizontal dispersion coefficient used in the RESRAD-OFFSITE calculations for estimating air and ground concentrations:

$$\sigma_y = \sqrt{\sigma_{yb}{}^2 + \sigma'_y{}^2} \qquad\qquad\qquad (I.25)$$

I.10   Area Source Models

RESRAD-OFFSITE assumes rectangular source and receptor areas. The atmospheric transport calculations from an area source to an area receptor are implemented in one of two ways. The formulations present in the code since the initial release version were designed to compute the concentration in the air above the offsite receptor and accumulation locations that did not overlap with the primary contamination. A formulation to compute the deposition on a catchment that could potentially overlap the primary contamination was added to Version 4.

I.10.1 Concentration in Air at a Non-Overlapping Receptor or Exposure Location

RESRAD-OFFSITE does not use any area source approximations. Instead, it performs a series of point-to-point calculations using the no-mixing and/or total-mixing forms of the expressions for the sector averaged concentration (Section I.5.3), depending on the downwind distance from the source to the receptor.

The source and receptor areas are each partitioned into rectangles with dimensions no greater than the user-specified grid spacing. This is done by dividing each side of the source area and of the receptor area by the grid spacing; if any of the quotients are non-integers, the code chooses the next largest integer. Each side is divided into that many congruent segments. Thus, the source is partitioned into congruent rectangles and each receptor area is also partitioned into congruent rectangles, but the rectangles used to partition any one of the areas does not necessarily need to be congruent to the rectangle used to partition any of the other areas (Figure I-4).

The center point of each grid rectangle is used as the source or receptor point representing that small area. Air concentration calculations are performed for each receptor grid rectangle for emissions from every source grid rectangle, and an average chronic air concentration is then calculated for each receptor grid rectangle. The average air concentration over the entire receptor area is then taken to be the average value over all receptor grid rectangles.

Each point-to-point (or grid rectangle–to–grid rectangle) calculation uses the appropriate wind direction, joint frequency, and distance for the specific points involved. Although the accuracy of the calculations increases as grid size decreases, computation time increases rapidly as grid size decreases. Sensitivity analysis on the grid size can guide the optimal choice of grid size for a particular scenario.

The code outputs the intermediate results of the atmospheric transport calculations of concentrations in air to a file named CHIOVERQ.OUT. The ratio of the concentration in air at a receptor location to the rate of release is denoted by the symbol χ/Q:

$$\frac{\chi}{Q} = \frac{\bar{C}_{sec}(i, x, z = 0)}{Q_{0_i}} \tag{I.26}$$

where

$\bar{C}_{sec}(i, x, z = 0)$ = concentration of the radionuclide i in air at ground level at a downwind distance x from a continuous release (Activity/m³), and

Q_{0i} = source strength of radionuclide i at the point of release (Activity/s).

Primary contamination
21m x 16m
4.2m x 4m grid

Grain field
23m x 10m
4.6m x 5m grid

grid spacing ≤ 5m

Example of transport from every source grid rectangle to a receptor grid rectangle

Pasture
27m x 19m
4.5m x 4.75m grid
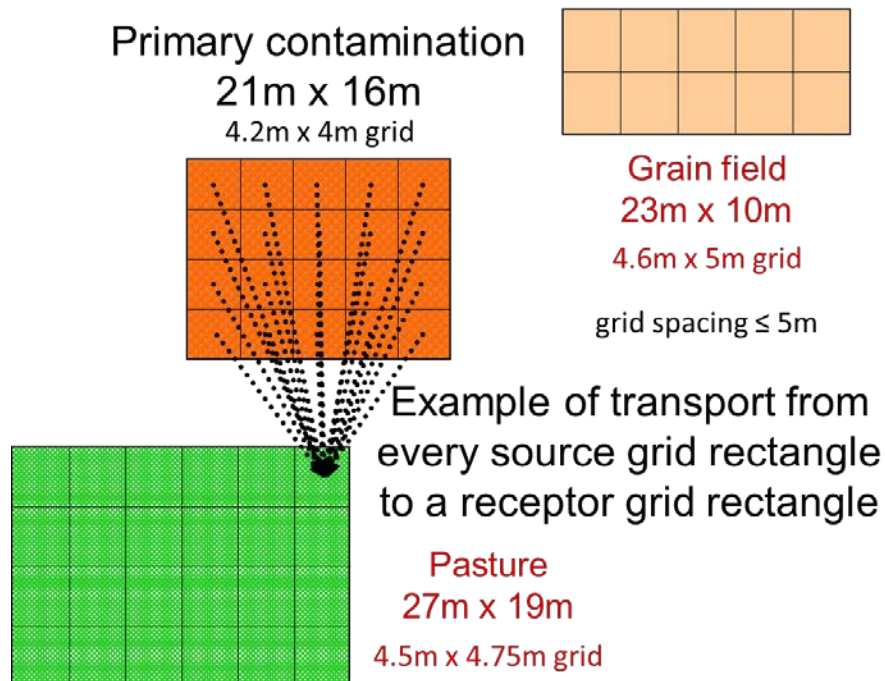
Figure I-4   Example of Grids for Atmospheric Transport from Area Source to Area Receptor Location

This text file contains a listing of the chi over Q, χ/Q, values computed by the code for each receptor area, for each radionuclide associated with total particulates and with respirable particulates, and, where relevant, for C-14 in the form of carbon dioxide, for H-3 in the form of water vapor, for the two radon isotopes, Rn-220 and Rn-222, and for the three short-lived progeny of each of the two radon isotopes.

I.10.2 Wet and Dry Deposition over the Catchment

This method uses an increasing number of points within the primary contamination from which the calculations of deposition on the catchment are performed (Figure I-5), until a specified precision is achieved. The code starts with a single source point at the center of the primary contamination. It then performs calculations from four points at the corners of the primary contamination to obtain a four-point estimate of the deposition over the catchment. If the

difference between the results of these two computations is not within a user-specified limit, the code performs calculations from four additional points at the midpoints of the sides of the primary contamination to obtain a nine-point estimate of the deposition over the catchment. If the four-point estimate and the nine-point estimate do not agree within the user-specified limit, the code continues to add source points in the Cartesian direction with the larger interval between source points, by bisecting that interval, until two consecutive estimates of the deposition over the catchment converge to within the specified limit. The first set of such additional points is shown by 5 × 3 points in Figure I-5. The limit on the number of source points in each of the two Cartesian directions is 512, and potentially 262,144 points total.

| 1 point | 2 x 2 points | 3 x 3 points | 5 x 3 points |
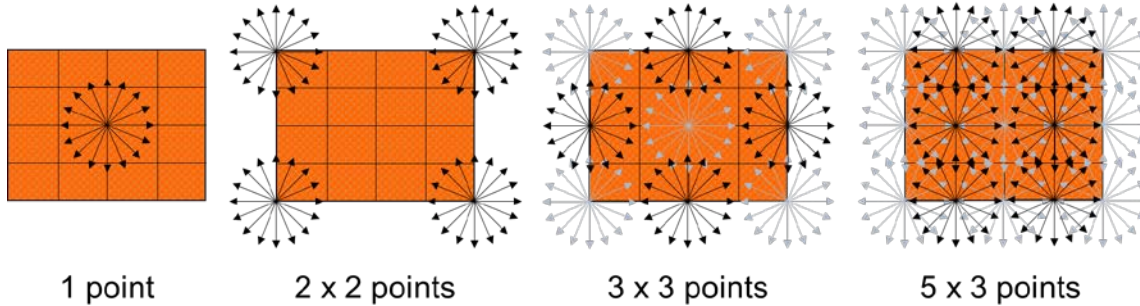
Figure I-5   Increasing the Number of Source Points

If the source point is within the catchment (Figure I-6), the code computes the sum of the average depleted source strength crossing out of the boundary of the catchment across each sector, for a unit source strength from the source point. The deposition rate due to the release associated with the source point is computed using the following expression:

$$D^{ca}(t) = \left(1 - \sum_{j=1}^{16} Q_j^{out} \right) f_p AR^{tl}(t) \tag{I.27}$$

where

$D^{ca}(t)$ = rate at which the radionuclide deposited on the catchment (Activity/yr),

Q_j^{out} = depleted source strength out of the boundary of the catchment across sector j for a unit source strength at the release point ([Activity/s]/[Activity/s]),

f_p = fraction of the primary contamination represented by the source point, and

$AR^{tl}(t)$ = rate of release to the atmosphere of radionuclide attached to particulates (Activity/yr).
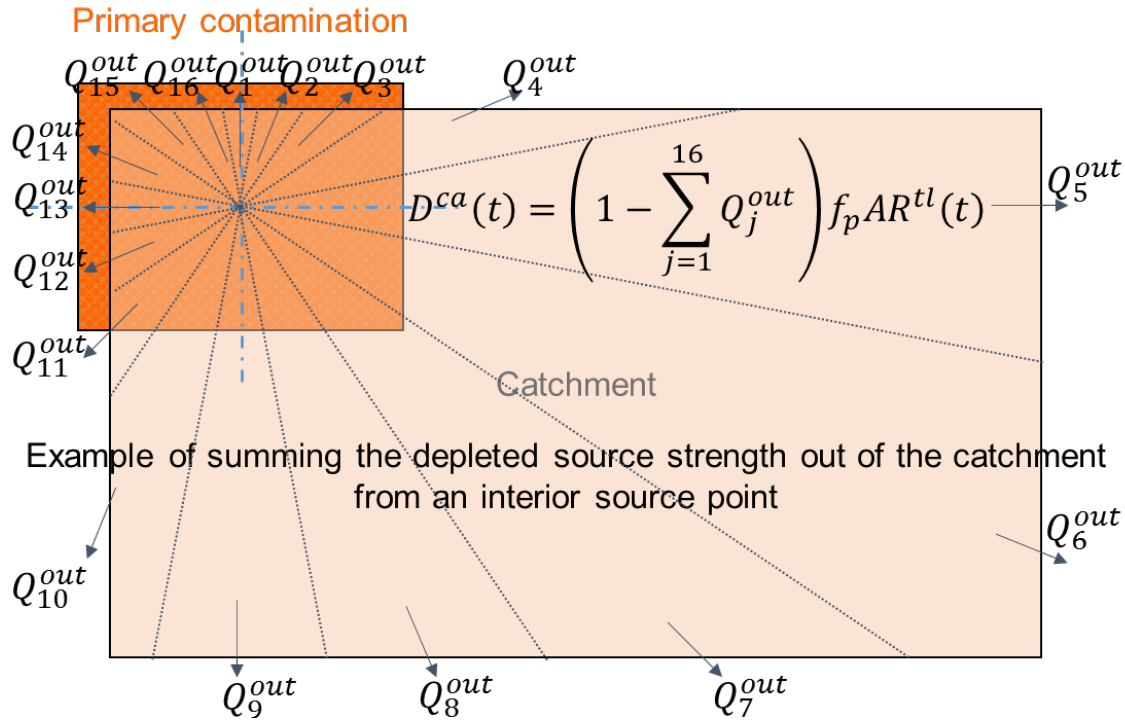
Figure I-6   Summing Deposition over the Catchment from an Interior Source

If the source point is outside the catchment (Figure I-7), the code computes the difference between the sum of the average depleted source strength crossing in to the boundary of the catchment across each sector and the sum of the average depleted source strength crossing out of the boundary of the catchment across each sector, both for a unit source strength from the source point. The deposition rate due to the release associated with the source point is computed using the following expression:

$$D^{ca}(t) = \left(\sum_{j=1}^{16} Q_j^{in} - \sum_{j=1}^{16} Q_j^{out} \right) f_p AR^{tl}(t) \tag{I.28}$$

where

$D^{ca}(t)$ = rate at which the radionuclide deposited on the catchment (Activity/yr),

Q_j^{in} = depleted source strength out of the boundary of the catchment across sector j for a unit source strength at the release point ([Activity/s]/[Activity/s]),

Q_j^{out} = depleted source strength out of the boundary of the catchment across sector j for a unit source strength at the release point ([Activity/s]/[Activity/s]),

f_p = fraction of the primary contamination represented by the source point, and

$AR^{tl}(t)$ = rate of release to the atmosphere of radionuclides attached to particulates (Activity/yr).
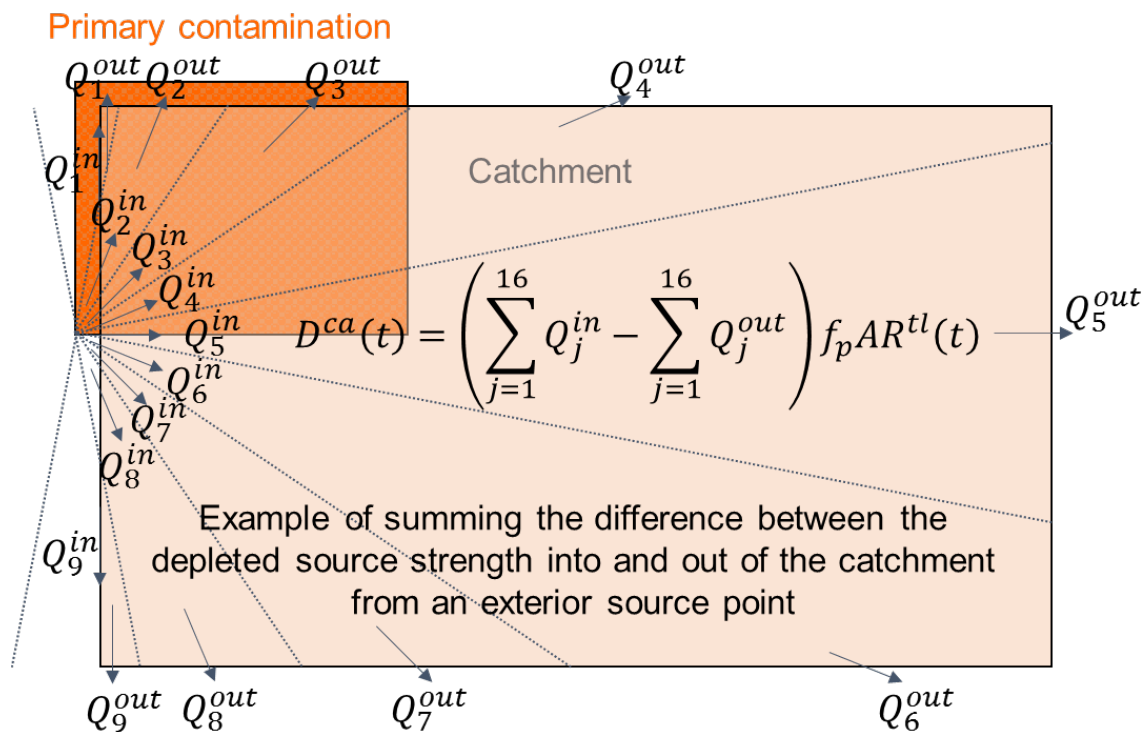
Figure I-7   Summing Deposition over the Catchment from an Exterior Source

The code outputs the intermediate results of the atmospheric transport calculations of deposition in the catchment to SectorDepletedFraction.OUT. The file has 17 columns of data; the first is the distance from the point release, and the next 16 contain the depleted source strength in the 16 sectors at the distance in the first column, expressed as fraction of the release. The 16 columns are in the order N, NNE, NE, ENE, E, ESE, SE, SSE, S, SSW, SW, WSW, W, WNW, NW, NNW.

I.11   References

Briggs, G.A., 1969, *Plume Rise*, U.S. Atomic Energy Commission Critical Review Series, prepared for Nuclear Safety Information Center, Oak Ridge National Laboratory, reprinted by the National Technical Information Service, Springfield, Va.

Briggs, G.A., 1974, *Diffusion Estimation for Small Emissions*, Environmental Research Laboratories Atmospheric Turbulence and Diffusion Laboratory 1973 Annual Report, Report No. ATDL-106, National Oceanic and Atmospheric Administration, Washington, D.C.

Eimutis, E.C., and M.G. Konicek, 1972, "Derivation of Continuous Functions for the Lateral and Vertical Dispersion Coefficients," *Atmospheric Environment* 6:859–863.

Hanna, S.R., et al., 1982, *Handbook on Atmospheric Diffusion*, DOE/TIC-11223, Technical Information Center, U.S. Department of Energy, Washington, D.C.

Holzworth, G., 1972, *Mixing Heights, Wind Speeds, and Potential for Urban and Air Pollution throughout the Contiguous United States*, AP-101, U.S. Environmental Protection Agency, Washington, D.C.

Irwin, J.S., 1979, "A Theoretical Variation of the Wind Profile Power-Law Exponent as a Function of Surface Roughness and Stability," *Atmospheric Environment* 13:191–194.

McMahon, T.A., and P.J. Dennison, 1979, "Empirical Atmospheric Deposition Parameters— A Survey," *Atmospheric Environment* 13:571–585.

Pasquill, F., 1974, *Atmospheric Diffusion*, 2nd ed., John Wiley & Sons, New York, N.Y.

Pasquill, F., 1976, *Atmospheric Dispersion Parameters in Gaussian Plume Modeling. Part II. Possible Requirements for Change in the Turner Workbook Values*, EPA-600/4-76-03b, U.S. Environmental Protection Agency, Washington, D.C.

Powell, D.C., et al., 1979, *MESODIF-II: A Variable Trajectory Plume Segment Model to Assess Ground-Level Air Concentrations and Deposition of Effluent Releases from Nuclear Power Facilities*, NUREG/CR-0523, U.S. Nuclear Regulatory Commission, Washington, D.C.

Ritchie, L.T., et al., 1978, "Effects of Rainstorms and Runoff on Consequences of Atmospheric Releases from Nuclear Reactor Accidents," *Nuclear Safety* 19:200–238.

Ross, D.G., et al., 1985, *CITPUFF: A Gaussian Puff Model for Estimating Pollutant Concentrations in Complex Terrain*, RM-261, U.S. Department of Agriculture, Rocky Mountain Forest and Range Experimentation Station, Ft. Collins, Colo., July.

Slade, D.H. (ed.), 1968, *Meteorology and Atomic Energy*, NTIS TID-24190, prepared by the Air Resources Laboratories, Research Laboratories, Environmental Science Service Administration, U.S. Department of Commerce, for Division of Reactor Development and Technology, U.S. Atomic Energy Commission, July.

APPENDIX J:
CONCENTRATION IN ENVIRONMENTAL MEDIA

Chapter 5 describes the manner in which RESRAD-OFFSITE conceptualizes the accumulation of contaminants in offsite agricultural areas, in a surface water body, and in the plants and animals that live off those areas. That chapter also presents conceptualizations of releases from the primary contamination and the transport from the primary contamination to the locations of accumulation. This appendix presents the mathematical expressions for the concentrations of radionuclides in water in a surface water body, in surface soil in agricultural or farmed lands, in particulate and gaseous forms in the air above agricultural or farmed lands, in plants, in meat and milk, and in aquatic organisms, that follow from those conceptualizations. The code computes the concentrations of the radionuclides in the surface water body before computing the concentrations of the radionuclides in the agricultural and farmed lands because irrigation water from the surface water body can be a source of contamination for these lands. The formulations for the accumulation in the agricultural and farmed lands are discussed in Section J.1, before those for the accumulation in the surface water body in Section J.2, because the latter are more complex and are derived by building upon the former.

The concentrations computed at each of the calculation times (Section E.1) and displayed in the deterministic graphical output are the concentrations in the media (especially in water from the well and the surface water body, plant, meat, milk and aquatic food) at that time. This will not necessarily be the concentrations in the consumable media when they are ingested. Section E.3 describes changes in the concentrations in the consumable media between the time they are harvested or extracted and the time when they are consumed. The concentrations in the consumable media at the time of consumption are used to compute the dose and are not saved for output. Note that the code computes the concentrations of radionuclides in two ways. The concentration of a radionuclide that is output by the code is the concentration of that radionuclide in the medium at that time regardless of which parent radionuclide it was derived from; it is the sum of the concentration of the radionuclide derived from all the parents. The code also computes the concentration of each radionuclide, keeping track of which parent radionuclide it was derived from and to which transformation thread of that parent radionuclide it belongs. This later concentration is used to compute the dose (and risk) so that the dose may be attributed back to the parent radionuclide (Section E.6).

J.1   Concentration in Offsite Surface Soils

RESRAD-OFFSITE models the concentration of a radionuclide in the offsite surface soil by considering the radionuclide balance in the surface mixing layer at that location. The surface layer is modeled as being mixed continuously, which allows the use of uniform radionuclide concentrations over the entire mixing layer. The expression for the radionuclide balance is integrated from one calculation time to the next to obtain the concentrations at each calculation time.

J.1.1   Influx of Radionuclide into the Mixing Layer at Agricultural or Farmed Areas

The code models the influx of radionuclides from the primary contamination by three mechanisms: irrigation with contaminated water from the well or from the surface water body, deposition of contaminated particulates following atmospheric transport, and deposition of eroded material transported by runoff. The values of these three influxes are known at each

calculation time. The values of the influxes as a function of time are described in the following subsections.

J.1.1.1 Influx Due to Contaminated Irrigation Water

Depending on the distribution of the potential evapotranspiration and rainfall over the year, it will be necessary to irrigate the land only during part of the year. It is possible to model the influx as occurring only during the part of the year when irrigation is applied. However, given the assumption of uniform mixing throughout the year rather than the once or twice a year mixing that occurs during plowing, it is appropriate to model the accumulation by assuming that the specified quantity of irrigation water is applied uniformly over the year. The rate at which the contaminant is added to the mixing layer is then given by the following equation:

$$I_i^{ir}(t) = q_{ir}w_i^{ir}(t)\left[1 - f_{int}^{ir}\frac{1 - e^{-\lambda_w t_g}}{\lambda_w t_g}\right]$$
(J.1)

where

$I_i^{ir}(t)$ = rate of addition of radionuclide i due to irrigation (Activity/m²/yr),

q_{ir} = quantity of irrigation water applied to a unit area of the agricultural or farmed land during a year (m/yr),

$w_i^{ir}(t)$ = concentration of radionuclide i in irrigation water (Activity/m³),

f_{int}^{ir} = fraction of irrigation water intercepted and retained on foliage of the plant,

λ_w = weathering removal constant of the plant (1/yr), and

t_g = growing period of the plant (yr).

The last term in the expression adjusts for the fraction of deposition intercepted and retained by the plant as described in Section J.4.3. The activity concentration of the radionuclide in irrigation water is known at a series of times and is assumed to vary linearly between them. Thus, the influx of the radionuclide by irrigation water is approximated by a linear function of time.

J.1.1.2 Influx Due to Deposition of Particulates from the Atmosphere

The rate at which the contaminant is deposited on the ground from the atmosphere is given by the following equation:

$$I_i^{at}(t) = V_{d_i}^{tl}\left(\frac{\chi}{Q}\right)_{o_i}^{tl} AR_i^{tl}(t)\left[1 - f_{int}^{p}\frac{1 - e^{-\lambda_w t_g}}{\lambda_w}\right]$$
(J.2)

where

$I_i^{at}(t)$ = rate of addition of radionuclide i due to deposition of particulates from the atmosphere (Activity/m²/yr),

$V_{d_i}^{tl}$ = deposition velocity of particulates containing radionuclide (m/s),

$\left(\frac{\chi}{Q}\right)_{o_i}^{tl}$ = ratio of the concentration of radionuclide i attached to particulates in the air above the offsite receptor location to the release of radionuclide i attached to particulates from the primary contamination (see Section I.10.1) (s/m³),

$AR_i^{tl}(t)$ = release rate of radionuclide i in the particulates released to air from the primary contamination (see Section G.15) (Activity/yr), and

f_{int}^{p} = fraction of particulates intercepted and retained on the foliage of the plant.

The last term adjusts for the fraction of deposition intercepted and retained by the plant as described in Section J.4.4. The release rate of the radionuclide in the particulates released to air from the primary contamination is assumed to vary linearly between the calculation times. Thus, deposition of the radionuclide associated with particulates is approximated by a linear function of time.

J.1.1.3 Influx Due to Deposition of Eroded Material from the Runoff from the Primary Contamination

The rate at which the radionuclide is deposited on the ground from the runoff from the primary contamination is given by the following equation:

$$I_i^{ro}(t) = SDR^o \, ER_i(t)/A^o \tag{J.3}$$

where

$$\begin{aligned}
I_i^{ro}(t) &= \text{rate of addition of radionuclide } i, \text{ due to deposition of eroded material from the} \\
&\quad \text{runoff from the primary contamination (Activity/m}^2\text{/yr),} \\
SDR^o &= \text{fraction of sediment from the primary contamination that is deposited at the} \\
&\quad \text{offsite agricultural or farmed land,} \\
ER_i(t) &= \text{release rate of radionuclide } i \text{ in the eroded material from the primary} \\
&\quad \text{contamination (see Section G.15) (Activity/yr), and} \\
A^o &= \text{area of the offsite agricultural or farmed land (m}^2\text{).}
\end{aligned}$$

The release of the radionuclide in the eroded material is known at a series of times and is assumed to vary linearly between them. Thus, deposition of the radionuclide associated with particulates is approximated by a linear function of time.

J.1.1.4 Combined Influx to Mixing Layer

The sums of the three influxes are also known at each of the calculation times and are assumed to vary linearly between each pair of successive times. The combined influx is represented by $I_i(t)$.

J.1.2 Radionuclide Balance in the Mixing Layer

The processes that are considered in modeling the accumulation of a radionuclide are represented mathematically in the following subsections. These are then combined to obtain the expression for the radionuclide balance, Figure J-1.
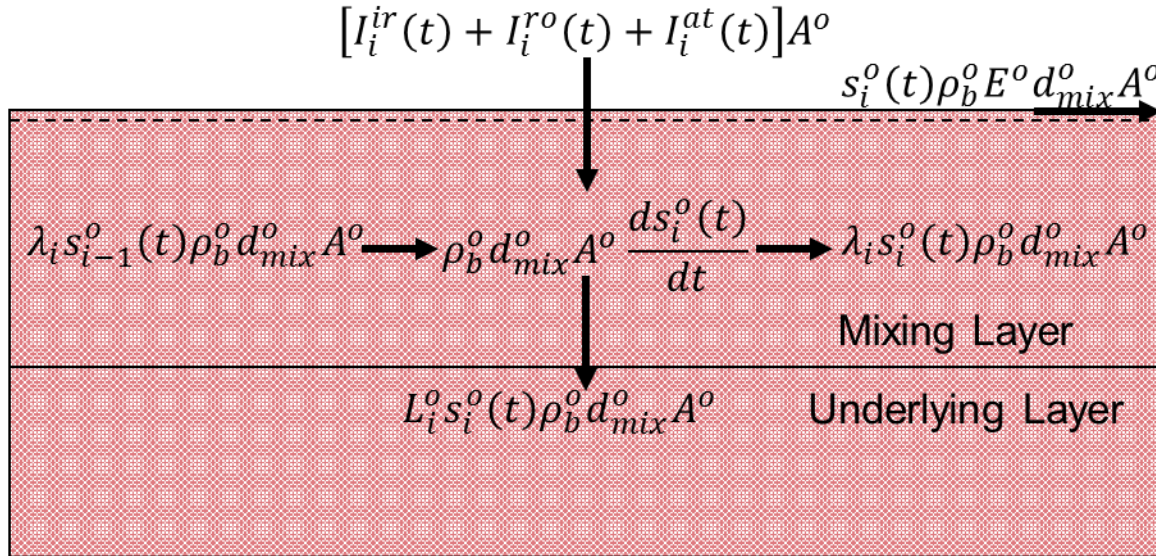
Figure J-1   Radionuclide Balance in Mixing Layer

The expression for the radionuclide balance is integrated between each pair of successive calculation times to obtain the Activity concentration of the radionuclide in the mixing layer of the offsite receptor location at each time.

J.1.2.1   Radioactive Transformations

The rate at which radionuclide i is added by ingrowth from its parent radionuclide i–1 within the mixing zone is given by:

$$\lambda_i s_{i-1}^o(t)\rho_b^o 10^6 d_{mix}^o A^o$$

where

$$
\begin{aligned}
\lambda_i &= \text{transformation constant for radionuclide } i \text{ (1/yr)}, \\
s_{i-1}^o(t) &= \text{concentration of the parent radionuclide } i\text{–1 in offsite soil (Activity/g)}, \\
\rho_b^o &= \text{dry bulk density of soil at the offsite location (g/[cm]}^3), \\
10^6 &= \text{converts per (cm)}^3 \text{ to per m}^3, \\
d_{mix}^o &= \text{depth of the mixing layer at the offsite location (m), and} \\
A^o &= \text{area of the offsite receptor location (m}^2).
\end{aligned}
$$

The rate at which radionuclide i is lost by decay within the mixing layer is given by the following expression:

$$\lambda_i s_i^o(t)\rho_b^o 10^6 d_{mix}^o A^o$$

where $s_i^o(t)$ is the concentration of the radionuclide i in offsite soil (Activity/g).

J.1.2.2   Surface Erosion

The rate of removal of radionuclide i with soil that is eroded from the mixing layer is given by the following equation:

$$s_i^o(t)\rho_b^o 10^6 \varepsilon^o A^o = s_i^o(t)\rho_b^o 10^6 E^o d_{mix}^o A^o$$

where

$\varepsilon^o =$ erosion rate of soil at the offsite location (m/yr), and
$E^o =$ fraction of the mixing layer that erodes each year (1/yr).

J.1.2.3   *Adsorption-Desorption Equilibrium Leaching*

Let $c_i^o(t)$ and $s_i'(t)$ denote the activity concentrations of nuclide i in the aqueous and solid phases of the mixing layer at time t. These are related to the Activity concentration in the soil, $s_i^o(t)$, by the following expression:

$$\rho_b^o s_i^o(t) = \rho_b^o s_i'(t) + \theta_c^o c_i^o(t)$$

where

$s_i'(t) =$ concentration of radionuclide i adsorbed on the solid phase of the soil in the mixing layer at the offsite location (Activity/g),
$c_i^o(t) =$ concentration of radionuclide i in the aqueous phase of the soil in the mixing layer at the offsite location (Activity/[cm]^3), and
$\theta_c^o =$ contaminated porosity, assumed to be equal to the volumetric water content, at the offsite location.

They are also related by the linear distribution coefficient, $K_{d_i}^o$, which is used to characterize the adsorption desorption equilibrium between the concentration in the two phases:

$$s_i'(t) = K_{d_i}^o c_i^o(t)$$

Combining these two expressions for the relationships between the concentrations in the two phases produces the following equation:

$$c_i^o(t) = \frac{\rho_b^o s_i^o(t)}{\rho_b^o K_{d_i}^o + \theta_c^o}$$

The rate of removal of the radionuclide by the water that infiltrates through the mixing layer at the offsite location is given by the following equation:

$$c_i^o(t)10^6 I^o A^o = \frac{\rho_b^o s_i^o(t)}{\rho_b^o K_{d_i}^o + \theta_c^o}10^6 I^o A^o = \frac{I^o/d_{mix}^o}{\rho_b^o K_{d_i}^o + \theta_c^o} s_i^o(t)10^6 \rho_b^o d_{mix}^o A^o = L_i^o s_i^o(t)10^6 \rho_b^o d_{mix}^o A^o$$

where

$I^o =$ infiltration rate at the offsite location (m/yr),
$K_{d_i}^o =$ linear distribution coefficient of radionuclide i in the mixing layer at the offsite location ([cm]^3/g), and
$L_i^o =$ rate at which the radionuclide leaches from the mixing layer (1/yr).

J.1.2.4   *Change in the Activity in the Mixing Layer*

The rate of change in the activity concentration in the mixing layer due to the processes listed above is:

$$\rho_b^o 10^6 d_{mix}^o A^o \frac{ds_i^o(t)}{dt}$$

Equating this to the net effect of those process give the expression for radionuclide balance,

$$\rho_b^o 10^6 d_{mix}^o A^o \frac{ds_i^o(t)}{dt}$$
$$= \lambda_i s_{i-1}^o(t)\rho_b^o 10^6 d_{mix}^o A^o - \lambda_i s_i^o(t)\rho_b^o 10^6 d_{mix}^o A^o - s_i^o(t)\rho_b^o 10^6 E^o d_{mix}^o A^o$$
$$- L_i^o s_i^o(t)\rho_b^o 10^6 d_{mix}^o A^o + I_i(t)A^o$$

This simplifies to:

$$\frac{ds_i^o(t)}{dt} + (\lambda_i + E^o + L_i^o)s_i^o(t) = \frac{I_i(t)}{10^6 \rho_b^o d_{mix}^o} + \lambda_i s_{i-1}^o(t) \tag{J.4}$$

This can be integrated over the time interval between two consecutive calculation times to obtain the concentrations at each calculation time:

$$\int_{t_1}^{t_1+t\le t_2} \left[\frac{de^{(\lambda_i+E^o+L_i^o)\tau}s_i^o(\tau)}{d\tau} = \frac{I_i(\tau)}{10^6 \rho_b^o d_{mix}^o}e^{(\lambda_i+E^o+L_i^o)\tau} + \lambda_i s_{i-1}^o(\tau)e^{(\lambda_i+E^o+L_i^o)\tau} \right] d\tau$$

$$e^{(\lambda_i+E^o+L_i^o)(t_1+t)}s_i^o(t+t_1) - e^{(\lambda_i+E^o+L_i^o)t_1}s_i^o(t_1)$$
$$= \int_0^t \frac{I_i(t_1) + \dfrac{[I_i(t_2)-I_i(t_1)]}{t_2-t_1}\tau}{10^6 \rho_b^o d_{mix}^o}e^{(\lambda_i+E^o+L_i^o)(t_1+\tau)}d\tau$$
$$+ \int_0^t \lambda_i s_{i-1}^o(t_1+\tau)e^{(\lambda_i+E^o+L_i^o)(t_1+\tau)}d\tau$$

$$e^{(\lambda_i+E^o+L_i^o)t}s_i^o(t+t_1) - s_i^o(t_1)$$
$$= \frac{I_i(t_1)}{10^6 \rho_b^o d_{mix}^o}\frac{e^{(\lambda_i+E^o+L_i^o)t}-1}{(\lambda_i+E^o+L_i^o)}$$
$$+ \frac{[I_i(t_2)-I_i(t_1)]}{(t_2-t_1)10^6 \rho_b^o d_{mix}^o}\left[\frac{te^{(\lambda_i+E^o+L_i^o)t}-0}{(\lambda_i+E^o+L_i^o)} - \frac{e^{(\lambda_i+E^o+L_i^o)t}-1}{(\lambda_i+E^o+L_i^o)^2} \right]$$
$$+ \int_0^t \lambda_i s_{i-1}^o(t_1+\tau)e^{(\lambda_i+E^o+L_i^o)\tau}d\tau$$

$$s_i^o(t+t_1) = e^{-(\lambda_i+E^o+L_i^o)t}s_i^o(t_1) + e^{-(\lambda_i+E^o+L_i^o)t}\int_0^t \lambda_i s_{i-1}^o(\tau+t_1)e^{(\lambda_i+E^o+L_i^o)\tau}d\tau$$
$$+ \frac{\left[I_i(t_1) - \dfrac{I_i(t_2)-I_i(t_1)}{(t_2-t_1)(\lambda_i+E^o+L_i^o)}\right]\left[1 - e^{-(\lambda_i+E^o+L_i^o)t}\right] + \dfrac{I_i(t_2)-I_i(t_1)}{(t_2-t_1)}t}{10^6 \rho_b^o d_{mix}^o(\lambda_i+E^o+L_i^o)} \tag{J.5}$$

J.1.3 Concentration of the First Member of a Transformation Chain in the Mixing Layer

The ingrowth term does not apply to the first member of the transformation chain; it has no parent radionuclide. The concentration of the first member is given by the following equation:

$$s_1^o(t + t_1) = e^{-(\lambda_1 + E^o + L_1^o)t} s_1^o(t_1)$$
$$+ \frac{\left[I_1(t_1) - \frac{I_1(t_2) - I_1(t_1)}{(t_2 - t_1)(\lambda_1 + E^o + L_1^o)}\right]\left[1 - e^{-(\lambda_1 + E^o + L_1^o)t}\right] + \frac{I_1(t_2) - I_1(t_1)}{(t_2 - t_1)}t}{10^6 \rho_b^o d_{mix}^o(\lambda_1 + E^o + L_1^o)}$$

Collecting terms to obtain a compact and computationally efficient expression,

$$s_1^o(t + t_1) = A_1^0 + A_1^1 t + B_1^1 e^{-(\lambda_1 + E^o + L_1^o)t}$$

where

$$A_1^1 = \frac{\frac{I_1(t_2) - I_1(t_1)}{(t_2 - t_1)}}{10^6 \rho_b^o d_{mix}^o(\lambda_1 + E^o + L_1^o)},$$

$$A_1^0 = \frac{\left[I_1(t_1) - \frac{I_1(t_2) - I_1(t_1)}{(t_2 - t_1)(\lambda_1 + E^o + L_1^o)}\right]}{10^6 \rho_b^o d_{mix}^o(\lambda_1 + E^o + L_1^o)} = \frac{I_1(t_1)}{10^6 \rho_b^o d_{mix}^o(\lambda_1 + E^o + L_1^o)} - \frac{A_1^1}{\lambda_1 + E^o + L_1^o}, \text{ and}$$

$$B_1^1 = s_1^o(t_1) - \frac{\left[I_1(t_1) - \frac{I_1(t_2) - I_1(t_1)}{(t_2 - t_1)(\lambda_1 + E^o + L_1^o)}\right]}{10^6 \rho_b^o d_{mix}^o(\lambda_1 + E^o + L_1^o)} = s_1^o(t_1) - A_1^0.$$

J.1.4 Concentration of the Second Member of a Transformation Chain in the Mixing Layer

The expressions for the contributions of the influx and of the concentration at the previous calculation time of the second member are the same as for the first member. There are additional terms to account for the ingrowth from the first member of the transformation chain. The concentration of the second member is as follows:

$$s_2^o(t + t_1) = e^{-(\lambda_2 + E^o + L_2^o)t} s_2^o(t_1)$$
$$+ \frac{\left[I_2(t_1) - \frac{I_2(t_2) - I_2(t_1)}{(t_2 - t_1)(\lambda_2 + E^o + L_2^o)}\right]\left[1 - e^{-(\lambda_2 + E^o + L_2^o)t}\right] + \frac{I_2(t_2) - I_2(t_1)}{(t_2 - t_1)}t}{10^6 \rho_b^o d_{mix}^o(\lambda_2 + E^o + L_2^o)}$$
$$+ \lambda_2 e^{-(\lambda_2 + E^o + L_2^o)t} \int_0^t \left(A_1^0 + A_1^1 \tau + B_1^1 e^{-(\lambda_1 + E^o + L_1^o)\tau}\right)e^{(\lambda_2 + E^o + L_2^o)\tau} d\tau$$

Integrating the contribution of the ingrowth from the first member gives:

$$s_2^o(t + t_1) = e^{-(\lambda_2 + E^o + L_2^o)t}s_2^o(t_1)$$

$$+ \frac{\left[I_2(t_1) - \frac{I_2(t_2) - I_2(t_1)}{(t_2 - t_1)(\lambda_2 + E^o + L_2^o)}\right]\left[1 - e^{-(\lambda_2 + E^o + L_2^o)t}\right] + \frac{I_2(t_2) - I_2(t_1)}{(t_2 - t_1)}t}{10^6 \rho_b^o d_{mix}^o(\lambda_2 + E^o + L_2^o)}$$

$$+ \lambda_2 \frac{A_1^0\left[1 - e^{-(\lambda_2 + E^o + L_2^o)t}\right]}{\lambda_2 + E^o + L_2^o} + \lambda_2 \frac{A_1^1}{\lambda_2 + E^o + L_2^o}t - \lambda_2 \frac{A_1^1\left[1 - e^{-(\lambda_2 + E^o + L_2^o)t}\right]}{(\lambda_2 + E^o + L_2^o)^2}$$

$$+ \lambda_2 \frac{B_1^1}{\lambda_2 - \lambda_1 + L_2^o - L_1^o}\left(e^{-(\lambda_1 + E^o + L_1^o)t} - e^{-(\lambda_2 + E^o + L_2^o)t}\right)$$

Collecting terms to obtain a compact and computationally efficient expression:

$$s_2^o(t + t_1) = A_2^0 + A_2^1 t + B_2^1 e^{-(\lambda_1 + E^o + L_1^o)t} + B_2^2 e^{-(\lambda_2 + E^o + L_2^o)t}$$

where

$$A_2^1 = \frac{\frac{I_2(t_2) - I_2(t_1)}{(t_2 - t_1)}}{10^6 \rho_b^o d_{mix}^o(\lambda_2 + E^o + L_2^o)} + \frac{\lambda_2 A_1^1}{\lambda_2 + E^o + L_2^o},$$

$$A_2^0 = \frac{I_2(t_1)}{10^6 \rho_b^o d_{mix}^o(\lambda_2 + E^o + L_2^o)} - \frac{A_2^1}{\lambda_2 + E^o + L_2^o} + \frac{\lambda_2 A_1^0}{\lambda_2 + E^o + L_2^o},$$

If $\lambda_2 - \lambda_1 + L_2^o - L_1^o \neq 0$,

$$B_2^1 = \lambda_2 \frac{B_1^1}{\lambda_2 - \lambda_1 + L_2^o - L_1^o},$$

If $\lambda_2 - \lambda_1 + L_2^o - L_1^o = 0$,
$B_2^1 = 0$ and $A_2^1 = A_2^1 + \lambda_2 B_1^1$, and
$B_2^2 = s_2^o(t_1) - A_2^0 - B_2^1$.

J.1.5 Concentration of the ith Member of a Transformation Chain in the Mixing Layer

Using the form of the expressions for the first and second members of the chains, the expression for the ith member of the chain is obtained by induction. Assume that the concentration of the $(i-1)^{th}$ member of the transformation chain in offsite soil has the following form:

$$s_{i-1}^o(t + t_1) = A_{i-1}^0 + A_{i-1}^1 t + \sum_{k=1}^{i-1} B_{i-1}^k e^{-(\lambda_k + E^o + L_k^o)t}$$

Then the concentration of the next member, i, of the transformation chain is given by the following equation:

$$s_i^o(t + t_1) = e^{-(\lambda_i + E^o + L_i^o)t}s_j^o(t_1)$$

$$+ \frac{\left[I_i(t_1) - \frac{I_i(t_2) - I_i(t_1)}{(t_2 - t_1)(\lambda_i + E^o + L_i^o)}\right]\left[1 - e^{-(\lambda_i + E^o + L_i^o)t}\right] + \frac{I_i(t_2) - I_i(t_1)}{(t_2 - t_1)}t}{10^6 \rho_b^o d_{mix}^o(\lambda_i + E^o + L_i^o)}$$

$$+ \lambda_i e^{-(\lambda_i + E^o + L_i^o)t} \int_0^t \left(A_{i-1}^0 + A_{i-1}^1 \tau + \sum_{k=1}^{i-1} B_{i-1}^k e^{-(\lambda_k + E^o + L_k^o)\tau}\right)e^{(\lambda_i + E^o + L_i^o)\tau}d\tau$$

Integrating the contribution of the ingrowth from the parent radionuclide gives the following:

$$
\begin{aligned}
s_i^o(t + t_1) &= e^{-(\lambda_i + E^o + L_i^o)t} s_i^o(t_1) \\
&+ \frac{\left[I_i(t_1) - \dfrac{I_i(t_2) - I_i(t_1)}{(t_2 - t_1)(\lambda_i + E^o + L_i^o)}\right]\left[1 - e^{-(\lambda_i + E^o + L_i^o)t}\right] + \dfrac{I_i(t_2) - I_i(t_1)}{(t_2 - t_1)}t}{10^6 \rho_b^o d_{mix}^o (\lambda_i + E^o + L_i^o)} \\
&+ \lambda_i \frac{A_{i-1}^0 \left[1 - e^{-(\lambda_i + E^o + L_i^o)t}\right]}{\lambda_i + E^o + L_i^o} + \lambda_i \frac{A_{i-1}^1}{\lambda_i + E^o + L_i^o} t - \lambda_i \frac{A_{i-1}^1 \left[1 - e^{-(\lambda_i + E^o + L_i^o)t}\right]}{(\lambda_i + E^o + L_i^o)^2} \\
&+ \lambda_i \sum_{k=1}^{i-1} \frac{B_{i-1}^k}{\lambda_i - \lambda_k + L_i^o - L_k^o} e^{-(\lambda_k + E^o + L_k^o)t} - \lambda_i e^{-(\lambda_i + E^o + L_i^o)t} \sum_{k=1}^{j-1} \frac{B_i^k}{\lambda_i - \lambda_k + L_i^o - L_k^o}
\end{aligned}
$$

Collecting terms to obtain a compact and computationally efficient expression,

$$
s_i^o(t + t_1) = A_i^0 + A_i^1 t + \sum_{k=1}^{j} B_i^k e^{-(\lambda_k + E^o + L_k^o)t} \tag{J.6}
$$

where

$$
A_1^1 = \frac{\frac{I_1(t_2) - I_1(t_1)}{(t_2 - t_1)}}{10^6 \rho_b^o d_{mix}^o (\lambda_1 + E^o + L_1^o)},
$$

$$
A_1^0 = \frac{I_1(t_1)}{10^6 \rho_b^o d_{mix}^o (\lambda_1 + E^o + L_1^o)} - \frac{A_1^1}{\lambda_1 + E^o + L_1^o},
$$

$$
B_1^1 = s_1^o(t_1) - A_1^0,
$$

if $1 < j \le i$

$$
A_j^1 = \frac{\frac{I_j(t_2) - I_j(t_1)}{(t_2 - t_1)}}{10^6 \rho_b^o d_{mix}^o (\lambda_j + E^o + L_j^o)} + \frac{\lambda_j A_{j-1}^1}{\lambda_j + E^o + L_j^o},
$$

$$
A_j^0 = \frac{I_j(t_1)}{10^6 \rho_b^o d_{mix}^o (\lambda_j + E^o + L_j^o)} - \frac{A_j^1}{\lambda_j + E^o + L_j^o} + \frac{\lambda_j A_{j-1}^0}{\lambda_j + E^o + L_j^o},
$$

if $0 < k < j$ and $\lambda_j - \lambda_k + L_j^o - L_k^o \ne 0$,

$$
B_j^k = \lambda_j \frac{B_{j-1}^k}{\lambda_j - \lambda_k + L_j^o - L_k^o},
$$

if $0 < k < j \le i$ and $\lambda_i - \lambda_k + L_i^o - L_k^o = 0$,

$$
B_j^k = 0 \text{ and } A_j^1 = A_j^1 + \lambda_j B_{j-1}^k
$$

$$
B_j^j = s_j^o(t_1) - A_j^0 - \sum_{k=1}^{j-1} B_j^k.
$$

J.2   <u>Concentration in the Water in the Surface Water Body</u>

The movement of water is the principal passageway for the movement of radionuclides in to and out of the surface water body. The radionuclides enter and exit the surface water body in soluble form or attached to particulates. Thus, the code considers the water balance, sediment balance, and radionuclide balance of the surface water body in order to compute the aqueous concentrations of the radionuclides in the surface water body.

J.2.1 Water Balance

Three inflows and three outflow are considered in the water balance of the surface water body (Figure J-2). This section describes how these inflows and outflows are computed by the code. The surface water body is modeled as having a constant volume over time.

J.2.1.1 *Interception of Groundwater by the Surface Water Body*

The rate at which the groundwater is intercepted by the surface water body, Q_{aqf}^{sw}, is computed using the following expression:

$$Q_{aqf}^{sw} = V_d^{sw} d_{aqf}^{sw} w_{aqf}^{sw} = K_s^{sz} i_{aqf}^{sw} d_{aqf}^{sw} \left(d_{right}^{sw} - d_{left}^{sw} \right) \tag{J.7}$$

where

$$V_d^{sw} = K_s^{aqf} i_{aqf}^{sw} =$$ average groundwater flow rate per unit cross section, also known as Darcy velocity or apparent velocity, from the primary contamination to the surface water body (m/yr),

$K_s^{aqf} =$ saturated hydraulic conductivity of the aquifer (m/yr),

$i_{aqf}^{sw} =$ hydraulic gradient of the aquifer from primary contamination to the surface water body (m/m),

$d_{aqf}^{sw} =$ average depth of the aquifer intercepted by the surface water body (m),

$w_{aqf}^{sw} = d_{right}^{sw} - d_{left}^{sw} =$ width of the aquifer intercepted by the surface water body (m), and

d_{right}^{sw} and $d_{left}^{sw} =$ distances from the flow line through the center of the primary contamination to the flow lines through the right and left edges of the surface water body (m).

J.2.1.2 *Stream Flow or Runoff from the Catchment into the Surface Water Body*

The rate at which the runoff from the catchment enters the surface water body, Q_{ro}^{sw}, is computed using the following expression:

$$Q_{ro}^{sw} = P_r \sum_{i=1}^{N_{ca}} C_r^{ca}(i) A^{ca}(i) = P_r \sum_{i=1}^{N_{ca}} C_r^{ca}(i) \left(x_{large}^{ca}(i) - x_{small}^{ca}(i) \right) \left(y_{large}^{ca}(i) - y_{small}^{ca}(i) \right) \tag{J.8}$$

where

$P_r =$ annual average precipitation rate at the site (m/yr),

$N_{ca} =$ number of rectangular regions used to define the catchment,

$i =$ index of the rectangular region used to define the catchment,

$C_r^{ca}(i) =$ runoff coefficient for the ith rectangle used to define the catchment,

$A^{ca}(i) =$ area of the ith rectangle used to define the catchment (m²),

$x_{large}^{ca}(i) =$ larger *x* coordinate of the ith rectangle used to define the catchment (m),

$x_{small}^{ca}(i) =$ smaller *x* coordinate of the ith rectangle used to define the catchment (m),

$y_{large}^{ca}(i) =$ larger *y* coordinate of the ith rectangle used to define the catchment (m), and

$y_{small}^{ca}(i) =$ smaller *y* coordinate of the ith rectangle used to define the catchment (m).

J.2.1.3   Precipitation over a Surface Water Body

The rate at which water precipitates directly on the surface of the surface water body, Q_{pr}^{sw}, is computed using the following expression:

$$Q_{pr}^{sw} = P_r A^{sw} = P_r\left(x_{large}^{sw} - x_{small}^{sw}\right)\left(y_{large}^{sw} - y_{small}^{sw}\right) \tag{J.9}$$

where

$$
\begin{aligned}
P_r &= \text{precipitation rate at the site (m/yr),} \\
A^{sw} &= \text{area of the top of the surface water body (m}^2\text{),} \\
x_{large}^{sw} &= \text{larger } x \text{ coordinate of the surface water body (m),} \\
x_{small}^{sw} &= \text{smaller } x \text{ coordinate of the surface water body (m),} \\
y_{large}^{sw} &= \text{larger } y \text{ coordinate of the surface water body (m), and} \\
y_{small}^{sw} &= \text{smaller } y \text{ coordinate of the surface water body (m).}
\end{aligned}
$$

J.2.1.4   Evaporation from the Surface Water Body

The rate at which water evaporates from the surface of the surface water body, Q_{sw}^{ev}, is computed using the following expression:

$$Q_{sw}^{ev} = E_p A^{sw} = E_p\left(x_{large}^{sw} - x_{small}^{sw}\right)\left(y_{large}^{sw} - y_{small}^{sw}\right) \tag{J.10}$$

where E_p is the potential evaporation for the site (m/yr).

J.2.1.5   Outflow and Extraction from the Surface Water Body

The annual water balance (Figure J-2) gives the sum of the stream outflow, Q_{sw}^{st}, the water extracted for use by the receptor, Q_{sw}^{us}, and the seepage to the aquifer, Q_{sw}^{aqf}. The code models a perennial surface water body and therefore ensures that the outflow, Q_{sw}^{out}, can satisfy the specified water uses, Q_{sw}^{us}. If the inputs indicate a situation where the potential evaporation exceeds the inflows to the surface water body, which indicates that the water body is ephemeral, the code will limit the other outflows to zero and will caution the user, in the message log, to review the surface water body inputs:

$$Q_{sw}^{out} = Q_{sw}^{st} + Q_{sw}^{us} + Q_{sw}^{aqf} = Q_{aqf}^{sw} + Q_{ro}^{sw} + Q_{pr}^{sw} - Q_{sw}^{ev} \geq Q_{sw}^{us} \tag{J.11}$$
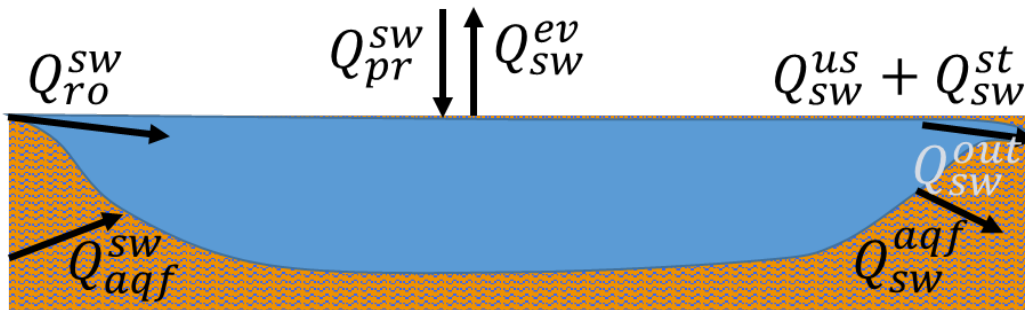
Figure J-2   Water Balance over the Surface Water Body

The sum of the rate at which water is extracted for use by the receptor, Q_{sw}^{us}, and the streamflow out of the surface water body, Q_{sw}^{st}, is computed using the following expression:

$$Q_{sw}^{st} + Q_{sw}^{us} = f_{out}^{st} \, Q_{sw}^{out}$$

(J.12)

where f_{out}^{st} is the fraction of outflow that goes to the stream or is extracted.

This fraction can be input to the code or, in the absence of site-specific data, the code can be flagged to set it to the fraction of the inflows:

$$f_{out}^{st} = Q_{ro}^{sw} / \left(Q_{ro}^{sw} + Q_{aqf}^{sw} \right)$$

(J.13)

J.2.1.7   *Seepage from the Surface Water Body to the Aquifer*

The flow out of the surface water body due to seepage into the aquifer, Q_{sw}^{aqf}, is computed using the following expression:

$$Q_{sw}^{aqf} = Q_{sw}^{out} - Q_{sw}^{st} - Q_{sw}^{us}$$

(J.14)

J.2.2   Sediment Balance

The code considers the influx of eroded material from the catchment. The catchment can include part or all of the primary contamination. It models removal of suspended sediments with the streamflow and with the extraction of water out of the surface water body and the settling of suspended sediment to the bottom of the surface water body. The change in the amount of suspended sediment and the rate at which the suspended sediments settle on the bed of the surface water body are computed by considering the sediment (Figure J-3). This section describes how these quantities are computed.

J.2.2.1   *Influx of Eroded Material from the Catchment*

The rate at which the eroded material from the catchment enters the surface water body at time zero, $m_{ro}^{ca}(t = 0)$, in g/yr, is computed using the following expression:

$$m_{ro}^{ca}(0) = 224R \sum_{i=1}^{N_{ca}} SDR^{ca}(i) A^{ca}(i) K^{ca}(i) LS^{ca}(i) C^{ca}(i) P^{ca}(i)$$

(J.15)

where

224	=	a factor to convert tons/acre to g/m²,
R	=	annual rainfall erosion index, the rainfall erosivity factor, or the rainfall and runoff factor for the site,
N_{ca}	=	number of rectangular regions used to define the catchment,
i	=	index of the rectangular region used to define the catchment,
$SDR^{ca}(i)$	=	sediment delivery ratio from the ith rectangle used to define the catchment,
$A^{ca}(i)$	=	area of the ith rectangle used to define the catchment (m²),
$K^{ca}(i)$	=	soil erodibility factor of the ith rectangle used to define the catchment (tons/acre),

$LS^{ca}(i)$ = slope length-steepness factor of the ith rectangle used to define the catchment,

$C^{ca}(i)$ = cropping-management factor or cover and management factor of the ith rectangle used to define the catchment, and

$P^{ca}(i)$ = conservation factor or the support practice factor of the ith rectangle used to define the catchment.

If the rate at which the eroded material from the catchment enters the surface water body at time zero, $m_{ro}^{ca}(0)$, exceeds the rate at which the material from the mixing layer at the location of the primary contamination enters the surface water body, $SDR\ m_{ro}^{ss}(0)$, then the rate at which the eroded material from the catchment enters the surface water body at any subsequent time, $m_{ro}^{ca}(t)$ is computed using the following expression to account for any temporal changes in the rate of erosion from the primary contamination:

$$m_{ro}^{ca}(t) = m_{ro}^{ca}(0) + SDR[m_{ro}^{ss}(t) - m_{ro}^{ss}(0)] \tag{J.16}$$

Where

SDR = sediment delivery ratio from the primary contamination,

$m_{ro}^{ss}(t)$ = rate at which material is eroded from the primary contamination, section G.1.8, g/year.

As discussed in Appendix G, the rate at which material is eroded from the primary contamination can vary with time if the scenario involves a cover with erosion related properties that differ from those of the primary contamination. If the rate at which the eroded material from the catchment enters the surface water body at time zero, $m_{ro}^{ca}(0)$, calculated using the specified inputs, is less than the rate at which the material from the primary contamination enters the surface water body, $SDR\ m_{ro}^{ss}(0)$, calculated using the specified inputs, a physically impossible situation, then the rate at which the eroded material from the catchment enters the surface water body at any subsequent time, $m_{ru}^{ca}(t)$, is computed using the following expression:

$$m_{ro}^{ca}(t) = m_{ro}^{ca}(0) \tag{J.17}$$

The above expression, J.17, is used to avoid the negative values that could result when the effect of any temporal changes in the rate of erosion from the primary contamination is accounted for using equation J.16.

J.2.2.2 Removal of Suspended Sediment by Stream Outflow and with Water Extracted for Use

The rate at which the suspended sediment is removed from the surface water body by stream outflow and with water extracted for use, $m_{sw}^{st+us}(t)$, is computed using the following expression:

$$m_{sw}^{st+us}(t) = (Q_{sw}^{st} + Q_{sw}^{us})c^{ss}(t) = \frac{(Q_{sw}^{st} + Q_{sw}^{us})M^{ss}(t)}{V^{sw}} \tag{J.18}$$

where

Q_{sw}^{st} = stream outflow from the surface water body (m³/yr),

Q_{sw}^{us} = water extracted for use from the surface water body (m³/yr),

$c^{ss}(t)$ = concentration of suspended sediment in the water in the surface water body (g/m³),

$M^{ss}(t)$ = mass of the suspended sediment in the surface water body (g), and
V^{sw} = volume of the surface water body (m³).

J.2.2.3   Removal of Suspended Sediment by Settling

The rate at which the suspended sediment is removed from the surface water body by settling, $m_{sw}^{settle}(t)$, is computed using the following expression:

$$m_{sw}^{settle}(t) = v_{settle}^{ss} A^{sw} c^{ss}(t) = \frac{v_{settle}^{ss} A^{sw} M^{ss}(t)}{V^{sw}}$$ (J.19)

where
v_{settle}^{ss} = settling velocity of the sediments in the surface water body (m/yr),
A^{sw} = surface area of the top of the surface water body (m²), and
$c^{ss}(t)$ = concentration of suspended sediment in water in the surface water body (g/m³).

J.2.2.4   Transfer of Sediment from the Recent Layer to the Deep Layer

Because the recently deposited layer of sediment is defined by constant thickness and density in the code, the sediments that settled recently will displace an equal quantity of previously settled sediments into the deep layer. The rate at which sediments transfer to the deep layer, $m_{sw}^{burial}(t)$, will be equal to the rate at which the suspended sediment is removed from the surface water body by settling, $m_{sw}^{settle}(t)$:

$$m_{sw}^{burial}(t) = m_{sw}^{settle}(t)$$ (J.20)
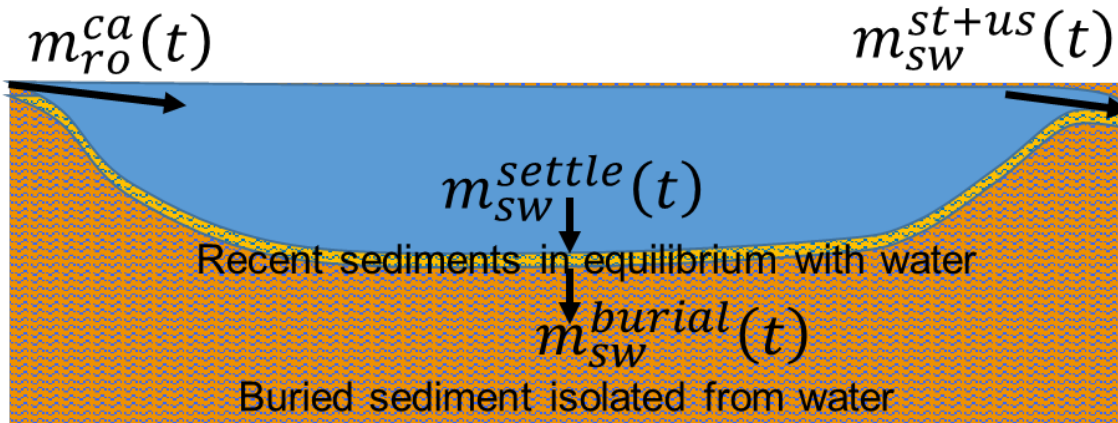
Figure J-3   Sediment Balance over the Surface Water Body

J.2.2.5   Mass of Suspended Sediment in the Surface Water Body

The mass of the suspended sediment in the surface water body, $M^{ss}(t)$, is determined by the sediment balance over surface water body. The rate of change of the quantity of the suspended sediment in the surface water body is equal to the difference between the rate at which the eroded material enters the surface water body, $m_{ro}^{ca}(t)$, and the rates at which the suspended

sediments are removed by stream outflow, by water extracted for use by the receptor, $m_{sw}^{st+us}(t)$, and by settling, $m_{sw}^{settle}(t)$:

$$\frac{dM^{ss}(t)}{dt} = m_{ro}^{ca}(t) - m_{sw}^{st+us}(t) - m_{sw}^{settle}(t)$$

$$\frac{dM^{ss}(t)}{dt} = m_{ro}^{ca}(t) - \frac{(Q_{sw}^{st} + Q_{sw}^{us})M^{ss}(t)}{V^{sw}} - \frac{v_{settle}^{ss}A^{sw}M^{ss}(t)}{V^{sw}}$$

$$\frac{dM^{ss}(t)}{dt} = m_{ro}^{ca}(t) - \frac{Q_{sw}^{st} + Q_{sw}^{us} + v_{settle}^{ss}A^{sw}}{V^{sw}}M^{ss}(t) \tag{J.21}$$

Assume that the mass of the suspended sediment was at a steady state at time zero. Then the mass of suspended sediment at time zero, $M^{ss}(0)$, is given by the following expression:

$$0 = m_{ro}^{ca}(0) - \frac{Q_{sw}^{st} + Q_{sw}^{us} + v_{settle}^{ss}A^{sw}}{V^{sw}}M^{ss}(0)$$

$$M^{ss}(0) = V^{sw}m_{ro}^{ca}(0)/(Q_{sw}^{st} + Q_{sw}^{us} + v_{settle}^{ss}A^{sw}) \tag{J.22}$$

The mass of the suspended sediment at each subsequent calculation time is computed by integrating the sediment balance equation, assuming that the influx of sediments varies linearly between the known values at the calculation times:

$$\frac{dM^{ss}(t)}{dt} + \frac{Q_{sw}^{st} + Q_{sw}^{us} + v_{settle}^{ss}A^{sw}}{V^{sw}}M^{ss}(t) = m_{ro}^{ca}(t) \tag{J.23}$$

Multiplying the sediment balance equation by $e^{\gamma t}$, with $\gamma = \frac{Q_{sw}^{st} + Q_{sw}^{us} + v_{settle}^{ss}A^{sw}}{V^{sw}}$, and integrating from one calculation time to the next after changing the variable to $\tau = t - t_1$ and assuming a linear variation of the influx of sediments:

$$\int_0^{t_2-t_1} \frac{de^{\gamma(\tau+t_1)}M^{ss}(\tau+t_1)}{d\tau}d\tau = m_{ro}^{ca}(t_1)e^{\gamma t_1}\int_0^{t_2-t_1}e^{\gamma \tau}d\tau + \frac{m_{ro}^{ca}(t_2) - m_{ro}^{ca}(t_1)}{t_2 - t_1}e^{\gamma t_1}\int_0^{t_2-t_1}\tau e^{\gamma \tau}d\tau$$

$$e^{\gamma t_2}M^{ss}(t_2) - e^{\gamma t_1}M^{ss}(t_1)$$
$$= m_{ro}^{ca}(t_1)\frac{e^{\gamma t_2} - e^{\gamma t_1}}{\gamma} + \frac{m_{ro}^{ca}(t_2) - m_{ro}^{ca}(t_1)}{t_2 - t_1}e^{\gamma t_1}\frac{(t_2 - t_1)e^{\gamma(t_2-t_1)} - 0}{\gamma}$$
$$- \frac{m_{ro}^{ca}(t_2) - m_{ro}^{ca}(t_1)}{t_2 - t_1}\frac{e^{\gamma t_2} - e^{\gamma t_1}}{\gamma^2}$$

$$e^{\gamma t_2}M^{ss}(t_2) - e^{\gamma t_1}M^{ss}(t_1) = \frac{m_{ro}^{ca}(t_2)e^{\gamma t_2} - m_{ro}^{ca}(t_1)e^{\gamma t_1}}{\gamma} - \frac{m_{ro}^{ca}(t_2) - m_{ro}^{ca}(t_1)}{t_2 - t_1}\frac{e^{\gamma t_2} - e^{\gamma t_1}}{\gamma^2}$$

$$M^{ss}(t_2) = e^{\gamma(t_1-t_2)}M^{ss}(t_1) + \frac{m_{ro}^{ca}(t_2) - m_{ro}^{ca}(t_1)e^{\gamma(t_1-t_2)}}{\gamma} - \frac{m_{ro}^{ca}(t_2) - m_{ro}^{ca}(t_1)}{t_2 - t_1}\frac{1 - e^{\gamma(t_1-t_2)}}{\gamma^2}$$

$$M^{ss}(t_2) = \frac{m_{ro}^{ca}(t_2)}{\gamma} - \frac{m_{ro}^{ca}(t_2) - m_{ro}^{ca}(t_1)}{(t_2 - t_1)\gamma^2}$$
$$+ e^{-\gamma(t_2-t_1)}\left[M^{ss}(t_1) - \frac{m_{ro}^{ca}(t_1)}{\gamma} + \frac{m_{ro}^{ca}(t_2) - m_{ro}^{ca}(t_1)}{(t_2 - t_1)\gamma^2}\right] \tag{J.24}$$

J.2.3   Radionuclide Balance in the Surface Water Body

Four modes of entry of radionuclides into the surface water body are modeled: (1) influx of dissolved radionuclides in the water intercepted from the aquifer; (2) influx of radionuclides adsorbed on soil eroded from the primary contamination; (3) influx of radionuclides transported by air, then deposited on the catchment, and ultimately washed out into the surface water body; and (4) influx of radionuclides transported by air and deposited on the surface water body. The code considers four ways of removal of radionuclide from the surface water body: (1) loss of radionuclides, both dissolved in the water and adsorbed on the suspended sediments, in the stream outflow; (2) loss of radionuclides, both dissolved in the water and adsorbed on the suspended sediments, in the water extracted for use; (3) loss of radionuclides dissolved in the water that seeps into the aquifer; and (4) loss of radionuclides adsorbed on the deeper layers of the sediments that are assumed to be isolated from the water by the recently buried sediments. The surface water body is modeled as being continuously mixed throughout the year. The radionuclides dissolved in the water are modeled as being in adsorption-desorption equilibrium with the radionuclides in the suspended sediment and the radionuclides in the recent bottom sediments.

J.2.3.1   Influx Due to Interception of Aquifer

The rate at which radionuclide i enters the surface water body with the water that is intercepted from the aquifer, $I_i^{aq}(t) = f_s(t)$, is obtained by integrating the flux across a vertical plane of the aquifer defined by the depth and width of interception, as described in Appendix H. The rate is known at a series of times and is assumed to vary linearly between them.

J.2.3.2   Influx Due to Delivery of Eroded Material in Runoff from the Primary Contamination

The rate at which radionuclide i is delivered to the surface water body by the runoff from the primary contamination is given by the following equation:

$$I_i^{ro}(t) = SDR \; ER_i(t) \tag{J.25}$$

where
$\quad I_i^{ro}(t)$ = rate of addition of radionuclide i due to delivery of eroded material by the runoff from the primary contamination (Activity/yr),
$\quad SDR$ = fraction of sediment from the primary contamination that is delivered to the surface water body, and
$\quad ER_i(t)$ = release rate of radionuclide i in the eroded material from the primary contamination (see Section G.15) (Activity/yr).

The rate of release of radionuclide i in the eroded material is known at a series of times and is assumed to vary linearly between them. Thus, the delivery of the radionuclide associated with particulates is approximated by a linear function of time.

J.2.3.3   Influx Due to Washout and Deposition over the Catchment

Radionuclide i is transported by air, then deposited on the catchment, and ultimately washed out into the surface water body. The rate at which it enters the surface water body with the runoff from the catchment, $I_i^{ca}(t)$, is given by the following equation:

$$I_i^{ca}(t) = DDR^{ca} D_i^{ca}(t) \tag{J.26}$$

where

$I_i^{ca}(t)$ = rate of addition of radionuclide i due to the delivery of radionuclides that are deposited from air over the catchment (Activity/yr),

DDR^{ca} = fraction of radionuclides deposited over the catchment and delivered to the surface water body, and

$D_i^{ca}(t)$ = rate at which radionuclide i is deposited over the catchment (Activity/yr). (This is described in Section I.10.2.)

The rate is known at a series of times and is assumed to vary linearly between them.

J.2.3.4 Influx Due to Deposition of Particulates from the Atmosphere

The rate at which the radionuclide is deposited on the surface water body from the atmosphere is given by the following equation:

$$I_i^{at}(t) = V_{d_i}^{tl} \left(\frac{\chi}{Q}\right)_{sw_i}^{tl} AR_i^{tl}(t) A^{sw} \tag{J.27}$$

where

$I_i^{at}(t)$ = rate of addition of radionuclide i due to deposition of particulates from the atmosphere (Activity/yr),

$V_{d_i}^{tl}$ = deposition velocity of particulates containing radionuclide i (m/s),

$\left(\dfrac{\chi}{Q}\right)_{sw_i}^{tl}$ = ratio of the concentration of radionuclide i attached to particulates in the air above the surface water body to the rate of release of radionuclide i from the primary contamination (see Section I.10.1) (s/m^3),

$AR_i^{tl}(t)$ = release rate of radionuclide i in the particulates released to air from the primary contamination (see Section G.15) (Activity/yr), and

A^{sw} = area of the top of the surface water body (m^2).

The rate of release of radionuclide i in the particulates released to air from the primary contamination is known at a series of times and is assumed to vary linearly between them. Thus, deposition of the radionuclide associated with particulates is approximated by a linear function of time.

J.2.3.5 Combined Influx of Radionuclides into the Surface Water Body

The sum of the four influxes is also known at each of the calculation times and is assumed to vary linearly between each pair of successive times. The combined influx of radionuclide i is represented by $I_i(t)$:

$$I_i(t) = I_i^{aq}(t) + I_i^{ca}(t) + I_i^{ro}(t) + I_i^{at}(t) \tag{J.28}$$

J.2.3.6 Removal of the Radionuclide with Seepage to the Aquifer

The rate at which radionuclide i is removed from the surface water body by seepage to the aquifer is given by the following expression:

$$Q_{sw}^{aqf} w_i^{sw}(t)$$

where

Q_{sw}^{aqf} = seepage from the surface water body to the aquifer (m³/yr), and

$w_i^{sw}(t)$ = concentration of radionuclide i in the water in the surface water body (Activity/m³).

J.2.3.7 Removal of the Radionuclide with Stream Outflow and Extraction for Use

The rate at which radionuclide i is removed from the surface water body by stream outflow and with water extracted for use is given by the following expression:

$$(Q_{sw}^{st} + Q_{sw}^{us})w_i^{sw}(t) + (Q_{sw}^{st} + Q_{sw}^{us})\frac{M^{ss}(t)}{V^{sw}}10^{-6}K_{d_i}^{ss}w_i^{sw}(t)$$

where

Q_{sw}^{st} = stream outflow from the surface water body (m³/yr),

Q_{sw}^{us} = water extracted for use by the receptor from the surface water body (m³/yr),

$M^{ss}(t)$ = mass of suspended sediments in the water in the surface water body (g),

V^{sw} = volume of the surface water body (m³),

10^{-6} = converts per m³ to per (cm)³,

$K_{d_i}^{ss}$ = linear distribution coefficient of the radionuclide i between the suspended sediments and the water ([cm]³/g).

J.2.3.8 Removal of the Radionuclide Due to the Burial of the Older Bed Sediment by the Recently Settled Sediment

As the suspended sediments settle out of the water, the thickness of the sediment layer at the bottom of the surface water body increases. Only the radionuclides adsorbed on the bottom sediment within a specific depth from the water are assumed to be in equilibrium with the radionuclides in the water in the surface water body. The radionuclides adsorbed on sediment at a greater depth are assumed to be isolated from the water and take with them the Activity they had when they became isolated. The following expression gives the rate at which radionuclide i is removed from the surface water body by the burial of sediments below the specified depth:

$$\frac{315576 \, v_{settle}^{ss} A^{sw} M^{ss}(t)}{V^{sw}}10^{-6}K_{d_i}^{bs}w_i^{sw}(t)$$

where

315,576 = converts cm/s to m/yr,

v_{settle}^{ss} = settling velocity of the suspended sediments in the surface water body (cm/s),

A^{sw} = surface area of the top of the surface water body (m²),

$K_{d_i}^{bs}$ = linear distribution coefficient of the radionuclide i between the bottom sediments and the water ([cm]³/g).

J.2.3.9 Loss of the Radionuclide Due to Radiological Transformation

The expression for the rate at which radionuclide i is lost from the surface water body due to radiological transformations has three terms, one each for the radionuclides dissolved in water, adsorbed on suspended sediments, and adsorbed on the recent bottom sediments:

$$\lambda_i V^{sw} w_i^{sw}(t) + \lambda_i M^{ss}(t) 10^{-6} K_{d_i}^{ss} w_i^{sw}(t) + \lambda_i \rho_b^{bs} d^{bs} A^{sw} K_{d_i}^{bs} w_i^{sw}(t) = \lambda_i V_i^{sw}(t) w_i^{sw}(t)$$

where

λ_i = radiological transformation constant for radionuclide i (1/yr),

ρ_b^{bs} = dry bulk density of bottom sediments $(g/[cm])^3$,

d^{bs} = depth of the upper layer of the bottom sediment within which the radionuclides are in adsorption-desorption equilibrium with the radionuclides in the water (m), and

$V_i^{sw}(t) = V^{sw} + M^{ss}(t) 10^{-6} K_{d_i}^{ss} + \rho_b^{bs} d^{bs} A^{sw} K_{d_i}^{bs}$ = equivalent volume of the surface water body for radionuclide i, where the mass of the sediments is replaced by an equivalent volume of water based on the equilibrium radionuclide concentrations (m^3).

J.2.3.10 Gain of the Radionuclide Due to Radiological Transformation

The expression for the rate at which radionuclide i is added to the surface water body due to radiological transformations has three terms, one each for the radionuclides dissolved in water, adsorbed on suspended sediments, and adsorbed on the recent bottom sediments:

$$\lambda_i V^{sw} w_{i-1}^{sw}(t) + \lambda_i M^{ss}(t) 10^{-6} K_{d_{i-1}}^{ss} w_{i-1}^{sw}(t) + \lambda_i \rho_b^{bs} d^{bs} A^{sw} K_{d_{i-1}}^{bs} w_{i-1}^{sw}(t) = \lambda_i V_{i-1}^{sw}(t) w_{i-1}^{sw}(t)$$

where $w_{i-1}^{sw}(t)$ is the soluble concentration of the parent of radionuclide i in the surface water body (Activity/m^3).

J.2.3.11 Change in the Radionuclide Inventory in the Surface Water Body

The net rate of change in the inventory of radionuclide i caused by the gains and losses listed in Sections J.2.3.1 through J.2.3.10 results in a change to the concentration of radionuclide i in the water in the surface water body over time. The expression for the change in inventory is as follows:

$$V^{sw} \frac{dw_i^{sw}(t)}{dt} + 10^{-6} K_{d_i}^{ss} \frac{dM^{ss}(t) w_i^{sw}(t)}{dt} + \rho_b^{bs} d^{bs} A^{sw} K_{d_i}^{bs} \frac{dw_i^{sw}(t)}{dt}$$
$$= [V^{sw} + 10^{-6} K_{d_i}^{ss} M^{ss}(t) + \rho_b^{bs} d^{bs} A^{sw} K_{d_i}^{bs}] \frac{dw_i^{sw}(t)}{dt} + 10^{-6} K_{d_i}^{ss} w_i^{sw}(t) \frac{dM^{ss}(t)}{dt}$$
$$= V_i^{sw}(t) \frac{dw_i^{sw}(t)}{dt} + 10^{-6} K_{d_i}^{ss} w_i^{sw}(t) \frac{dM^{ss}(t)}{dt}$$

J.2.3.12 Radionuclide Balance Equation

Equating the change in inventory over time in Section J.2.3.11 to the net rate of change from the processes listed in Sections J.2.3.1 through J.2.3.10 gives the expression for radionuclide balance in the surface water body (Figure J-4):

$$V_i^{sw}(t)\frac{dw_i^{sw}(t)}{dt} + 10^{-6}K_{d_i}^{ss}w_i^{sw}(t)\frac{dM^{ss}(t)}{dt}$$
$$= -\lambda_i V_i^{sw}(t)w_i^{sw}(t) - Q_{sw}^{aqf}w_i^{sw}(t) - (Q_{sw}^{st}+Q_{sw}^{us})w_i^{sw}(t)$$
$$- (Q_{sw}^{st}+Q_{sw}^{us})\frac{M^{ss}(t)}{V^{sw}}10^{-6}K_{d_i}^{ss}w_i^{sw}(t) - \frac{315576\, v_{settle}^{ss}A^{sw}M^{ss}(t)}{V^{sw}}10^{-6}K_{d_i}^{bs}w_i^{sw}(t)$$
$$+ I_i(t) + \lambda_i V_{i-1}^{sw}(t)w_{i-1}^{sw}(t)$$
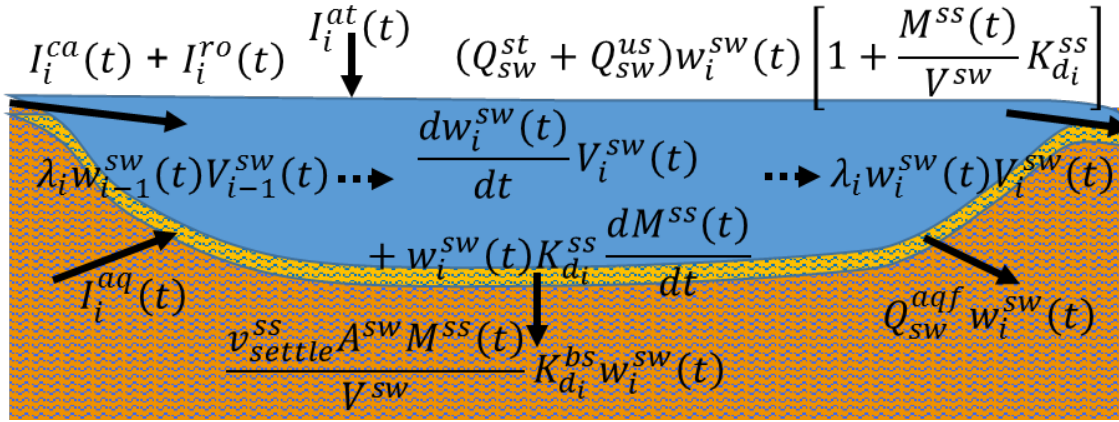
Figure J-4   Radionuclide Balance in the Surface Water Body

$$\frac{dw_i^{sw}(t)}{dt} + \left\{\lambda_i + \frac{Q_{sw}^{st}+Q_{sw}^{us}+Q_{sw}^{aqf}}{V_i^{sw}(t)} + \left(\frac{Q_{sw}^{st}+Q_{sw}^{us}}{V^{sw}}K_{d_i}^{ss} + \frac{315576 v_{settle}^{ss}A^{sw}}{V^{sw}}K_{d_i}^{bs}\right)10^{-6}\frac{M^{ss}(t)}{V_i^{sw}(t)}\right.$$
$$\left. + \frac{K_{d_i}^{ss}}{V_i^{sw}(t)}10^{-6}\frac{dM^{ss}(t)}{dt}\right\}w_i^{sw}(t) = \frac{I_i(t)}{V_i^{sw}(t)} + \lambda_i\frac{V_{i-1}^{sw}(t)}{V_i^{sw}(t)}w_{i-1}^{sw}(t)$$

The terms within the braces in the expression above combine to give the effective removal coefficient of radionuclide i from the surface water body at time t. When the terms within the braces are replaced by the effective removal coefficient, $\gamma_i(t)$, the radionuclide balance expression takes the following compact form:

$$\frac{dw_i^{sw}(t)}{dt} + \gamma_i(t)w_i^{sw}(t) = \frac{I_i(t)}{V_i^{sw}(t)} + \lambda_i\frac{V_{i-1}^{sw}(t)}{V_i^{sw}(t)}w_{i-1}^{sw}(t) \tag{J.29}$$

where,

$$\gamma_i(t) = \lambda_i + \frac{Q_{sw}^{st}+Q_{sw}^{us}+Q_{sw}^{aqf}+10^{-6}\left[\frac{(Q_{sw}^{st}+Q_{sw}^{us})K_{d_i}^{ss}+315576 v_{settle}^{ss}A^{sw}K_{d_i}^{bs}}{V^{sw}}M^{ss}(t)+K_{d_i}^{ss}\frac{dM^{ss}(t)}{dt}\right]}{V_i^{sw}(t)}, \tag{J.30}$$

The radionuclide balance expression can be integrated between consecutive calculation times by assuming the following:

1. The effective removal coefficient can be represented by a constant over each time interval between consecutive calculation times:

$$\gamma_i(t_1) = \lambda_i + \frac{Q_{sw}^{out}}{V_i^{sw}(t_1)} + 10^{-6} \frac{\frac{\left(Q_{sw}^{st}+Q_{sw}^{us}\right)K_{d_i}^{ss}+315576v_{settle}^{ss}A^{sw}K_{d_i}^{bs}}{V^{sw}}M^{ss}(t_1)+K_{d_i}^{ss}\frac{M^{ss}(t_2)-M^{ss}(t_1)}{t_2-t_1}}{V_i^{sw}(t_1)},$$ (J.31)

2. The ratio of the equivalent volumes of the surface water body for parent radionuclide, i–1, and the progeny radionuclide i can be represented by constant over the time interval between consecutive calculation times:

$$\frac{V_{i-1}^{sw}(t)}{V_i^{sw}(t)} = \frac{V_{i-1}^{sw}(t_1)}{V_i^{sw}(t_1)}$$ (J.32)

The integration is as follows:

$$\int_{t_1}^{t_1+t\le t_2} \left[\frac{dw_i^{sw}(\tau)}{d\tau} + \gamma_i(t_1)w_i^{sw}(\tau) = \frac{I_i(\tau)}{V_i^{sw}(\tau)} + \lambda_i \frac{V_{i-1}^{sw}(t_1)}{V_i^{sw}(t_1)} w_{i-1}^{sw}(\tau) \right] d\tau$$

$$\int_{t_1}^{t_1+t\le t_2} \left[\frac{de^{\gamma_i(t_1)\tau}w_i^{sw}(\tau)}{d\tau} = e^{\gamma_i(t_1)\tau} \left\{ \frac{I_i(\tau)}{V_i^{sw}(\tau)} + \lambda_i \frac{V_{i-1}^{sw}(t_1)}{V_i^{sw}(t_1)} w_{i-1}^{sw}(\tau) \right\} \right] d\tau$$

$$e^{\gamma_i(t_1)(t_1+t)}w_i^{sw}(t+t_1) - e^{\gamma_i(t_1)t_1}w_i^{sw}(t_1)$$

$$= \int_0^t \left[\frac{I_i(t_1)}{V_i^{sw}(t_1)} + \frac{\frac{I_i(t_2)}{V_i^{sw}(t_2)} - \frac{I_i(t_1)}{V_i^{sw}(t_1)}}{t_2 - t_1} \tau \right] e^{\gamma_i(t_1)(t_1+\tau)} d\tau$$

$$+ \int_0^t \lambda_i \frac{V_{i-1}^{sw}(t_1)}{V_i^{sw}(t_1)} w_{i-1}^{sw}(\tau) e^{\gamma_j(t_1)(t_1+\tau)} d\tau$$

$$e^{\gamma_i(t_1)t}w_i^{sw}(t+t_1) - w_i^{sw}(t_1)$$

$$= \frac{I_i(t_1)}{V_i^{sw}(t_1)} \frac{e^{\gamma_i(t_1)t} - 1}{\gamma_i(t_1)} + \frac{\frac{I_i(t_2)}{V_i^{sw}(t_2)} - \frac{I_i(t_1)}{V_i^{sw}(t_1)}}{(t_2-t_1)} \left[\frac{te^{\gamma_i(t_1)t} - 0}{\gamma_i(t_1)} - \frac{e^{\gamma_i(t_1)t} - 1}{[\gamma_i(t_1)]^2} \right]$$

$$+ \lambda_i \frac{V_{i-1}^{sw}(t_1)}{V_i^{sw}(t_1)} \int_0^t w_{i-1}^{sw}(\tau) e^{\gamma_i(t_1)\tau} d\tau$$

$$w_i^{sw}(t + t_1) = e^{-\gamma_i(t_1)\,t}w_i^{sw}(t_1) + \frac{\dfrac{I_i(t_2)}{V_i^{sw}(t_2)} - \dfrac{I_i(t_1)}{V_i^{sw}(t_1)}}{(t_2 - t_1)\,\gamma_i(t_1)}\,t$$

$$+ \left[\frac{I_i(t_1)}{V_i^{sw}(t_1)} - \frac{\dfrac{I_i(t_2)}{V_i^{sw}(t_2)} - \dfrac{I_i(t_1)}{V_i^{sw}(t_1)}}{(t_2 - t_1)\gamma_i(t_1)}\right]\frac{1 - e^{-\gamma_i(t_1)\,t}}{\gamma_i(t_1)}$$

$$+ \lambda_i\frac{V_{i-1}^{sw}(t_1)}{V_i^{sw}(t_1)}e^{-\gamma_i(t_1)\,t}\int_0^t w_{i-1}^{sw}(\tau)e^{\gamma_i(t_1)\,\tau}d\tau$$

(J.33)

J.2.4 Concentration of the First Member of a Transformation Chain in the Water in the Surface Water Body

The ingrowth term does not apply to the first member of the transformation chain because it does not have a parent radionuclide. The concentration of the first member is given by the following equation:

$$w_1^{sw}(t + t_1) = e^{-\gamma_1(t_1)\,t}w_1^{sw}(t_1) + \frac{\dfrac{I_1(t_2)}{V_1^{sw}(t_2)} - \dfrac{I_1(t_1)}{V_1^{sw}(t_1)}}{(t_2 - t_1)\,\gamma_1(t_1)}\,t$$

$$+ \left[\frac{I_1(t_1)}{V_1^{sw}(t_1)} - \frac{\dfrac{I_1(t_2)}{V_1^{sw}(t_2)} - \dfrac{I_1(t_1)}{V_1^{sw}(t_1)}}{(t_2 - t_1)\,\gamma_1(t_1)}\right]\frac{1 - e^{-\gamma_1(t_1)\,t}}{\gamma_1(t_1)}$$

Collecting terms to obtain a compact and computationally efficient expression produces the following equation:

$$w_1^{sw}(t + t_1) = A_1^0 + A_1^1 t + B_1^1 e^{-\gamma_1(t_1)\,t}$$

where

$$A_1^1 = \frac{\dfrac{I_1(t_2)}{V_1^{sw}(t_2)} - \dfrac{I_1(t_1)}{V_1^{sw}(t_1)}}{(t_2 - t_1)\,\gamma_1(t_1)},$$

$$A_1^0 = \frac{\dfrac{I_1(t_1)}{V_1^{sw}(t_1)}}{\gamma_1(t_1)} - \frac{\dfrac{I_1(t_2)}{V_1^{sw}(t_2)} - \dfrac{I_1(t_1)}{V_1^{sw}(t_1)}}{(t_2 - t_1)[\gamma_1(t_1)]^2} = \frac{I_1(t_1)}{V_1^{sw}(t_1)\gamma_1(t_1)} - \frac{A_1^1}{\gamma_1(t_1)}, \text{ and}$$

$$B_1^1 = w_1^{sw}(t_1) - \frac{\dfrac{I_1(t_1)}{V_1^{sw}(t_1)}}{\gamma_1(t_1)} + \frac{\dfrac{I_1(t_2)}{V_1^{sw}(t_2)} - \dfrac{I_1(t_1)}{V_1^{sw}(t_1)}}{(t_2 - t_1)[\gamma_1(t_1)]^2} = w_1^{sw}(t_1) - A_1^0.$$

J.2.5 Aqueous Concentration of the Second Member of a Transformation Chain in the Surface Water Body

The expressions for the contributions of the influx of the second member and of the concentration at the previous calculation time of the second member are the same as for the first member. There are additional terms to account for the ingrowth from the first member of the transformation chain. The concentration of the second member is given by the following equation:

$$w_2^{sw}(t+t_1) = e^{-\gamma_2(t_1)\,t}w_2^{sw}(t_1) + \frac{\dfrac{I_2(t_2)}{V_2^{sw}(t_2)} - \dfrac{I_2(t_1)}{V_2^{sw}(t_1)}}{(t_2 - t_1)\,\gamma_2(t_1)}t$$

$$+ \left[\frac{I_2(t_1)}{V_2^{sw}(t_1)} - \frac{\dfrac{I_2(t_2)}{V_2^{sw}(t_2)} - \dfrac{I_2(t_1)}{V_2^{sw}(t_1)}}{(t_2 - t_1)\,\gamma_2(t_1)}\right]\frac{1 - e^{-\gamma_2(t_1)\,t}}{\gamma_2(t_1)}$$

$$+ \lambda_2 \frac{V_1^{sw}(t_1)}{V_2^{sw}(t_1)}e^{-\gamma_2(t_1)\,t}\int_0^t \left(A_1^0 + A_1^1\tau + B_1^1 e^{-\gamma_1(t_1)\tau}\right)e^{\gamma_2(t_1)\,\tau}d\tau$$

Integrating the contribution of the ingrowth from the first member gives the following equation:

$$w_2^{sw}(t+t_1) = e^{-\gamma_2(t_1)\,t}w_2^{sw}(t_1) + \frac{\dfrac{I_2(t_2)}{V_2^{sw}(t_2)} - \dfrac{I_2(t_1)}{V_2^{sw}(t_1)}}{(t_2 - t_1)\,\gamma_2(t_1)}t$$

$$+ \left[\frac{I_2(t_1)}{V_2^{sw}(t_1)} - \frac{\dfrac{I_2(t_2)}{V_2^{sw}(t_2)} - \dfrac{I_2(t_1)}{V_2^{sw}(t_1)}}{(t_2 - t_1)\,\gamma_2(t_1)}\right]\frac{1 - e^{-\gamma_2(t_1)\,t}}{\gamma_2(t_1)} + \lambda_2 \frac{V_1^{sw}(t_1)}{V_2^{sw}(t_1)}A_1^0\frac{1 - e^{-\gamma_2(t_1)\,t}}{\gamma_2(t_1)}$$

$$+ \lambda_2 \frac{V_1^{sw}(t_1)}{V_2^{sw}(t_1)}\frac{A_1^1}{\gamma_2(t_1)}t - \lambda_2 \frac{V_1^{sw}(t_1)}{V_2^{sw}(t_1)}\frac{A_1^1}{\gamma_2(t_1)}\frac{1 - e^{-\gamma_2(t_1)\,t}}{\gamma_2(t_1)}$$

$$+ \lambda_2 \frac{V_1^{sw}(t_1)}{V_2^{sw}(t_1)}B_1^1\frac{e^{-\gamma_1(t_1)\,t} - e^{-\gamma_2(t_1)\,t}}{\gamma_2(t_1) - \gamma_1(t_1)}$$

Collecting terms to obtain a compact and computationally efficient expression produces the following:

$$w_2^{sw}(t+t_1) = A_2^0 + A_2^1 t + B_2^1 e^{-\gamma_1(t_1)\,t} + B_2^2 e^{-\gamma_2(t_1)\,t}$$

where

$$A_2^1 = \frac{\dfrac{I_2(t_2)}{V_2^{sw}(t_2)} - \dfrac{I_2(t_1)}{V_2^{sw}(t_1)}}{(t_2 - t_1)\,\gamma_2(t_1)} + \frac{V_1^{sw}(t_1)}{V_2^{sw}(t_1)}\frac{\lambda_2 A_1^1}{\gamma_2(t_1)},$$

$$A_2^0 = \frac{I_2(t_1)}{V_2^{sw}(t_1)\gamma_2(t_1)} - \frac{A_2^1}{\gamma_2(t_1)} + \frac{V_1^{sw}(t_1)}{V_2^{sw}(t_1)}\frac{\lambda_2 A_1^0}{\gamma_2(t_1)},$$

$$B_2^1 = \lambda_2 \frac{B_1^1}{\gamma_2(t_1) - \gamma_1(t_1)}, \text{ and}$$

$$B_2^2 = w_2^{sw}(t_1) - B_2^1 \cdot A_2^0$$

J.2.6 Aqueous Concentration of the i th Member of a Transformation Chain in the Surface Water Body

Using the form of the expressions for the first and second members of the chain, the expression for the ith member of the chain is obtained by induction. Assume that the concentration of the (i–1)th member of the transformation chain in offsite soil is of the following form:

$$w_{i-1}^{sw}(t+t_1) = A_{i-1}^0 + A_{i-1}^1 t + \sum_{k=1}^{i-1} B_{i-1}^k e^{-\gamma_k(t_1)\,t}$$

Then the concentration of the next member, *I*, of the transformation chain is given by the following equation:

$$
w_i^{sw}(t + t_1) = e^{-\gamma_i(t_1)\,t} w_i^{sw}(t_1) + \frac{\dfrac{I_i(t_2)}{V_i^{sw}(t_2)} - \dfrac{I_i(t_1)}{V_i^{sw}(t_1)}}{(t_2 - t_1)\,\gamma_i(t_1)}\, t
$$

$$
+ \left[\frac{I_i(t_1)}{V_i^{sw}(t_1)} - \frac{\dfrac{I_i(t_2)}{V_i^{sw}(t_2)} - \dfrac{I_i(t_1)}{V_i^{sw}(t_1)}}{(t_2 - t_1)\gamma_i(t_1)} \right] \frac{1 - e^{-\gamma_i(t_1)\,t}}{\gamma_i(t_1)}
$$

$$
+ \lambda_i \frac{V_{i-1}^{sw}(t_1)}{V_i^{sw}(t_1)} e^{-\gamma_i(t_1)\,t} \int_0^t \left(A_{i-1}^0 + A_{i-1}^1 \tau + \sum_{k=1}^{i-1} B_{i-1}^k e^{-\gamma_k(t_1)\,\tau} \right) e^{\gamma_i(t_1)\,\tau} d\tau
$$

Integrating the contribution of the ingrowth from the parent radionuclide gives the following equation:

$$
w_i^{sw}(t + t_1) = e^{-\gamma_i(t_1)\,t} w_i^{sw}(t_1) + \frac{\dfrac{I_i(t_2)}{V_i^{sw}(t_2)} - \dfrac{I_i(t_1)}{V_i^{sw}(t_1)}}{(t_2 - t_1)\,\gamma_i(t_1)}\, t
$$

$$
+ \left[\frac{I_i(t_1)}{V_i^{sw}(t_1)} - \frac{\dfrac{I_i(t_2)}{V_i^{sw}(t_2)} - \dfrac{I_i(t_1)}{V_i^{sw}(t_1)}}{(t_2 - t_1)\gamma_i(t_1)} \right] \frac{1 - e^{-\gamma_i(t_1)\,t}}{\gamma_i(t_1)} + \frac{V_{i-1}^{sw}(t_1)}{V_i^{sw}(t_1)} \frac{\lambda_i A_i^1}{\gamma_i(t_1)}\, t
$$

$$
+ \left[\lambda_i A_i^0 \frac{V_{i-1}^{sw}(t_1)}{V_i^{sw}(t_1)} - \frac{V_{i-1}^{sw}(t_1)}{V_i^{sw}(t_1)} \frac{\lambda_i A_i^1}{\gamma_i(t_1)} \right] \frac{1 - e^{-\gamma_i(t_1)\,t}}{\gamma_i(t_1)}
$$

$$
+ \lambda_i \frac{V_{i-1}^{sw}(t_1)}{V_i^{sw}(t_1)} \sum_{k=1}^{i-1} \frac{B_{i-1}^k}{\gamma_i(t_1) - \gamma_k(t_1)} e^{-\gamma_k(t_1)\,t} - \lambda_i \frac{V_{i-1}^{sw}(t_1)}{V_i^{sw}(t_1)} e^{-\gamma_i(t_1)\,t} \sum_{k=1}^{i-1} \frac{B_{i-1}^k}{\gamma_i(t_1) - \gamma_k(t_1)}
$$

Collecting terms to obtain a compact and computationally efficient expression:

$$
w_i^{sw}(t + t_1) = A_i^0 + A_i^1 t + \sum_{k=1}^{i} B_i^k e^{-\gamma_k(t_1)\,t} \tag{J.34}
$$

where

$$
A_1^1 = \frac{\dfrac{I_1(t_2)}{V_1^{sw}(t_2)} - \dfrac{I_1(t_1)}{V_1^{sw}(t_1)}}{(t_2 - t_1)\,\gamma_1(t_1)},
$$

$$
A_1^0 = \frac{\dfrac{I_1(t_1)}{V_1^{sw}(t_1)}}{\gamma_1(t_1)} - \frac{\dfrac{I_1(t_2)}{V_1^{sw}(t_2)} - \dfrac{I_1(t_1)}{V_1^{sw}(t_1)}}{(t_2 - t_1)[\gamma_1(t_1)]^2} = \frac{I_1(t_1)}{V_1^{sw}(t_1)\gamma_j(t_1)} - \frac{A_1^1}{\gamma_j(t_1)},
$$

$$
B_1^1 = w_1^{sw}(t_1) - \frac{\dfrac{I_1(t_1)}{V_1^{sw}(t_1)}}{\gamma_1(t_1)} + \frac{\dfrac{I_1(t_2)}{V_1^{sw}(t_2)} - \dfrac{I_1(t_1)}{V_1^{sw}(t_1)}}{(t_2 - t_1)[\gamma_1(t_1)]^2} = w_1^{sw}(t_1) - A_1^0,
$$

if $1 < j \le i$

$$
A_j^1 = \frac{\dfrac{I_j(t_2)}{V_j^{sw}(t_2)} - \dfrac{I_j(t_1)}{V_j^{sw}(t_1)}}{(t_2 - t_1)\,\gamma_j(t_1)} + \frac{V_{j-1}^{sw}(t_1)}{V_j^{sw}(t_1)} \frac{\lambda_j A_{j-1}^1}{\gamma_j(t_1)},
$$

$$A_j^0 = \frac{I_j(t_1)}{V_j^{sw}(t_1)\gamma_j(t_1)} - \frac{A_j^1}{\gamma_j(t_1)} + \frac{V_{j-1}^{sw}(t_1)}{V_j^{sw}(t_1)}\frac{\lambda_j A_{j-1}^0}{\gamma_j(t_1)},$$

if $0 < k < j$ and $\gamma_j(t_1) - \gamma_k(t_1) \neq 0$,
$$B_j^k = \lambda_j \frac{V_{j-1}^{sw}(t_1)}{V_j^{sw}(t_1)}\frac{B_{j-1}^k}{\gamma_j(t_1) - \gamma_k(t_1)},$$

if $0 < k < j \leq i$ and $\gamma_j(t_1) - \gamma_k(t_1) = 0$,
$$B_j^k = 0 \text{ and } A_j^1 = A_j^1 + \lambda_j \frac{V_{j-1}^{sw}(t_1)}{V_j^{sw}(t_1)}B_{j-1}^k,$$
$$B_j^j = w_j^{sw}(t_1) - A_j^0 - \sum_{k=1}^{j-1} B_j^k.$$

J.3　Concentration in Air

The code computes and outputs the concentration of radionuclides attached to particulates, both total and respirable, in air at a number of locations. The code also computes the gaseous concentrations of carbon-14 (C-14) and hydrogen-3 (H-3) at these locations. The expressions used are described in Sections J.3.1–J.3.3.

J.3.1　Concentration in Air above Primary Contamination

The concentration of radionuclides attached to particles in the air above the primary contamination is computed using the following expression:

$$a_i^{tl}(t) = f_{area}\, ML\, s_i^{ss}(t) \tag{J.35}$$

where

$a_i^{tl}(t)$ = concentration of radionuclide i in the air above the primary contamination (Activity/m³),

f_{area} = area factor to account for uncontaminated dust from outside the primary contamination and blown by wind into the air above the primary contamination (see discussion in Argonne [1998]),

ML = mass loading of particulates in the air above the primary contamination (g/m³), and

$s_i^{ss}(t)$ = concentration of radionuclide i in the surface soil at the location of the primary contamination (see Section G.15) (Activity/g).

The concentration of radionuclides attached to respirable particles in the air above the primary contamination is computed using the following expression:

$$a_i^{rp}(t) = f_{rp}\, a_i^{tl}(t) \tag{J.36}$$

where

$a_i^{rp}(t)$ = concentration of radionuclide i in the air above the primary contamination (Activity/m³), and

f_{rp} = respirable fraction of particulates at the offsite location.

The concentration of C-14 in the form of carbon dioxide in air above the primary contamination is computed as part of the calculations for inhalation exposure, but the value of the

concentration is not saved. This calculation is performed using the expression below, which is a combination of Equations (F.10), (F.19), and (F.20), subject to the limits described in Appendix F:

$$a_{14_C}^{gas}(t) = f_{cd}^{ec_{on}^C}(t) d_{evasion}^C 10^6 \rho_b^{pc} \epsilon_v^C s_{14_C}(t) \frac{0.5\sqrt{A}}{h_{mix}\, u_{wind}} \tag{J.37}$$

where

$a_{14_C}^{gas}(t)$ = concentration of ^{14}C in the form of carbon dioxide in the air above the primary contamination (Activity/m³),

$f_{cd}^{ec_{on}^C}(t)$ = onsite cover and depth factor, which accounts for the depth of soil from which carbon dioxide can escape,

$d_{evasion}^C$ = depth of evasion of carbon dioxide (m),

10^6 = converts from per (cm)³ to per m³,

ρ_b^{pc} = dry bulk density of the soil in the primary contamination (g/[cm]³),

$\epsilon_v^{14_C}$ = evasion rate of ^{14}C (1/s),

$s_{14_C}(t)$ = concentration of ^{14}C in the primary contamination (Activity/g),

A = area of the primary contamination (m²),

h_{mix} = height of the rectangular space above the primary contamination within which the carbon dioxide is assumed to be mixed when calculating inhalation exposure (m), and

u_{wind} = average wind speed (m/s).

The onsite cover and depth factor for evasion of carbon dioxide or water vapor is given by,

$$f_{cd}^{ec_{on}^C}(t) = 0 \text{ when } T_{cv}(t) \geq d_{evasion}^C,$$

$$f_{cd}^{ec_{on}^C}(t) = [d_{evasion}^C - T_{cv}(t)]/d_{evasion}^C \text{ when } T_{cv}(t) + T_{pc}(t) \geq d_{evasion}^C > T_{cv}(t) \tag{J.38}$$

$$f_{cd}^{ec_{on}^C}(t) = T_{pc}(t)/d_{evasion}^C \text{ when } T_{cv}(t) + T_{pc}(t) < d_{evasion}^C$$

where

$f_{cd}^{ec_{on}}(t)$ = onsite cover and depth factor, which accounts for the depth of soil from which carbon dioxide or water vapor can escape,

$T_{cv}(t)$ = thickness of cover (m),

$T_{pc}(t)$ = thickness of the primary contamination (m), and

$d_{evasion}$ = depth of evasion of water vapor (not an input) or carbon dioxide (m).

The concentration of H-3 in the form of water vapor in air above the primary contamination is computed as part of the calculations for inhalation exposure, but the value of the concentration is not saved. This calculation is performed using the expression below, which is a combination of Equations (F.3), (F.7), (F.8), (F.9), and (F.10), subject to the limits described in Appendix F:

$$a_{3_H}^{gas}(t) = f_{cd}^{ec_{on}^H}(t)[P_r(1 - C_r) + q_{ir}]C_e \times \frac{\rho_b^{pc}}{\theta_{mc} + K_{d_{3_H}}\rho_b^{pc}} \frac{10^6}{31557600} s_{3_H}(t) \frac{0.5\sqrt{A}}{h_{mix}\, u_{wind}} \tag{J.39}$$

J-26

where

$a_{3_H}^{gas}(t)$ = concentration of ³H in the form of water vapor in the air above the primary contamination (Activity/m³),

$f_{cd}^{ec_{on}^H}(t)$ = onsite cover and depth factor, which accounts for the depth of soil from which water vapor can escape out of the soil,

P_r = annual precipitation rate (m/yr),

C_r = runoff coefficient,

q_{ir} = amount of irrigation applied annually to the primary contamination (m/yr),

C_e = evapotranspiration coefficient,

θ_{mc} = moisture content of the soil in the primary contamination,

ρ_b^{pc} = dry bulk density of the soil in the primary contamination (g/[cm]³),

$K_{d_{3_H}}$ = distribution coefficient of ³H in the primary contamination (g/[cm³]),

10^6 = converts from per (cm)³ to per m³,

31,557,600 = factor to convert per second to per year,

$s_{3_H}(t)$ = concentration of ³H in the primary contamination (Activity/g),

A = area of the primary contamination (m²),

h_{mix} = height of the rectangular space above the primary contamination within which the water vapor is assumed to be mixed when calculating inhalation exposure (m), and

u_{wind} = average wind speed (m/s).

J.3.2   Concentration in Air above the Surface Water Body

The concentration in the air above the surface water body is computed using the expression:

$$a_i^{sw}(t) = \left(\frac{\chi}{Q}\right)_{sw_i}^{tl} \frac{AR_i^{tl}(t)}{31557600} \tag{J.40}$$

where

$a_i^{sw}(t)$ = concentration of radionuclide i attached to particulates in the air above the surface water body (Activity/m³),

$\left(\frac{\chi}{Q}\right)_{sw_i}^{tl}$ = ratio of the concentration of radionuclide i attached to particulates in the air above the surface water body to the rate of release of radionuclide i from the primary contamination (see Section I.10.1) (s/m³),

$AR_i^{tl}(t)$ = release rate of radionuclide i, in the particulates released to air from the primary contamination (Section G.15) (Activity/yr), and

31,557,600 = factor to convert years to seconds.

J.3.3   Concentration in Air at the Offsite Receptor Location

The expression for the concentration of radionuclides attached to particulates in air at the offsite location has two components. The first is the concentration of radionuclides attached to particulates released from the primary contamination and transported by air to the offsite location. The second is the concentration of radionuclides attached to particulates that are re-suspended from the accumulation at the offsite location:

$$a_{o_i}^{tl}(t) = \left(\frac{\chi}{Q}\right)_{o_i}^{tl} \frac{AR_i^{tl}(t)}{31557600} + s_i^o(t)ML_o \tag{J.41}$$

where

$a_{o_i}^{tl}(t)$ = concentration of radionuclide i attached to particulates in the air above the offsite receptor location (Activity/m³),

$\left(\frac{\chi}{Q}\right)_{o_i}^{tl}$ = ratio of the concentration of radionuclide i attached to particulates in the air above the offsite receptor location to the release of radionuclide i attached to particulates from the primary contamination (see Section I.10.1) (s/m³),

$AR_i^{tl}(t)$ = release rate of radionuclide i in the particulates released to air from the primary contamination (see Section G.15) (Activity/yr),

31,557,600 = factor to convert years to seconds,

$s_i^o(t)$ = concentration of the radionuclide i in offsite soil (Section J.1.5) (Activity/g), and

ML_o = mass loading of particulates from the offsite location (g/m³).

The expression for the concentration of radionuclides attached to respirable particulates in air at the offsite location has two components. The first is the concentration of radionuclides attached to particulates released from the primary contamination and transported by air to the offsite location. The second is the concentration of radionuclides attached to particulates that are re-suspended from the accumulation at the offsite location:

$$a_{o_i}^{rp}(t) = \left(\frac{\chi}{Q}\right)_{o_i}^{rp} \frac{AR_i^{tl}(t)}{31557600} \frac{f_{rp}V_{d_i}^{rp}}{V_{d_i}^{tl}} + s_i^o(t)ML_o f_{rp}^o \tag{J.42}$$

where

$a_{o_i}^{rp}(t)$ = concentration of radionuclide i attached to respirable particulates in the air above the offsite receptor location (Activity/m³),

$\left(\frac{\chi}{Q}\right)_{o_i}^{rp}$ = ratio of the concentration of radionuclide i attached to respirable particulates in the air above the offsite receptor location to the release of radionuclide i attached to respirable particulates from the primary contamination (see Section I.10.1) (s/m³),

f_{rp} = respirable fraction of particulates above the primary contamination,

$V_{d_i}^{tl}$ = deposition velocity of particulates containing radionuclide i (m/yr),

$V_{d_i}^{rp}$ = deposition velocity of respirable particulates containing radionuclide i (m/yr), and

f_{rp}^o = respirable fraction of particulates at the offsite location.

The concentration of C-14 in the form of carbon dioxide and of H-3 in the form of water vapor in air at the offsite location is computed as part of the calculations for inhalation exposure, but the value of the concentration is not saved. This calculation is performed using the expression below, subject to the limits described in Appendix F:

$$a_{o_i}^{gas}(t) = f_{cd}^{econ}(t)d_{evasion}A10^6\rho_b^{pc}\epsilon_v\left(\frac{\chi}{Q}\right)_{o_i}^{g}s_i(t) \tag{J.43}$$

where

$a_{o_i}^{gas}(t)$ = concentration of ^{14}C in the form of carbon dioxide and ^3H in the form of water vapor, in air above the offsite receptor location (Activity/m³),

$f_{cd}^{ec_{on}}(t)$ = onsite cover and depth factor, which accounts for the depth of soil from which carbon dioxide or water vapor can escape out of the soil,

$d_{evasion}$ = depth of evasion of ^{14}C or ^3H (not an input) (m),

A = area of the primary contamination (m²),

10^6 = converts from m³ to (cm)³,

ρ_b^{pc} = dry bulk density of the soil in the primary contamination (g/[cm]³),

ϵ_v = evasion rate of ^{14}C or ^3H (1/s),

$$\epsilon_v^{^3H} = \frac{[P_r(1 - C_r) + q_{ir}]C_e}{31557600 \, d_{evasion}} \frac{1}{\theta_{mc} + K_{d_{3H}}\rho_b^{pc}}$$

$\left(\frac{\chi}{Q}\right)_{o_i}^g$ = ratio of the concentration of ^{14}C in the form of carbon dioxide or of ^3H in the form of water vapor in the air above the offsite receptor location to the release of ^{14}C in the form of carbon dioxide or ^3H in the form of water vapor from the primary contamination respectively (s/m³), and

$s_i(t)$ = concentration of ^{14}C or ^3H in the primary contamination (Activity/g).

J.4   Concentration in Plant

The code computes and uses the concentration of radionuclides in plants to compute the dose and risk from the ingestion of vegetables and the concentration in meat and milk. The code models two modes of contamination of the plants, root uptake and foliar interception followed by translocation. The expressions for these are discussed in Sections J.4.1–J.4.5. The concentration in plant has multiple components:

$$p_i(t) = p_{on_i}^{ru}(t) + p_{ag_i}^{ru}(t) + p_i^{fi}(t) + p_{of_i}^{fp}(t) \tag{J.44}$$

where

$p_i(t)$ = concentration of radionuclide i in the part of the plant that is consumed by livestock or by humans (Activity/kg),

$p_{on_i}^{ru}(t)$ = contribution of root uptake directly from the primary contamination to the concentration of radionuclide i in the part of the plant that is consumed by livestock or by humans (Activity/kg),

$p_{ag_i}^{ru}(t)$ = contribution of root uptake from the accumulation in the surface soil in agricultural land to the concentration of radionuclide i in the part of the plant that is consumed by livestock or by humans (Activity/kg),

$p_i^{fi}(t)$ = contribution of foliar interception of irrigation water to the concentration of radionuclide $i \neq {}^{14}C \, or \, {}^3H$, in the part of the plant that is consumed by livestock or by humans (Activity/kg),

$p_{of_i}^{fp}(t)$ = contribution of foliar interception of particulates to the concentration of radionuclide i in the part of the plant, grown offsite, that is consumed by livestock or by humans (Activity/kg).

J.4.1 Contribution of Root Uptake from the Primary Contamination

If part (or all) of the agricultural land lies above the primary contamination, the roots of the plants could penetrate the primary contamination and take up the radionuclides directly from the primary contamination:

$$p_{on_i}^{ru}(t) = 10^3 f_a f_{cd}^{root}(t) rtf_i s_i(t) \tag{J.45}$$

where

$\quad p_{on_i}^{ru}(t)$ = contribution of root uptake directly from the primary contamination to the concentration of radionuclide i in the part of the plant that is consumed by livestock or by humans (Activity/kg),

$\quad 10^3$ = converts from per g to per kg,

$\quad f_a$ = fraction of the agricultural land that lies directly above the primary contamination,

$\quad f_{cd}^{root}(t)$ = cover and depth factor, which accounts for the length of the roots that are exposed to different concentrations of the radionuclide in the various layers of the primary contamination,

$\quad rtf_i$ rtf_i = root uptake factor of radionuclide $i$radionuclide i for the plant, which is the ratio of the concentration in the edible part of the plant to the concentration in soil ([Activity/g of plant]/[Activity/g of soil]), and

$\quad s_i(t)$ $s_i(t)$ = concentration of radionuclide $i$radionuclide i in the primary contamination (Activity/g).

The cover and depth which accounts for the length of the roots that are exposed to different concentrations of the radionuclide in the various layers of the primary contamination is given by,

$$f_{cd}^{root}(t) = 0 \text{ when } T_{cv}^c(t) \geq d_{root},$$

$$f_{cd}^{root}(t) = f_{vm}(t)\rho_{pc}/\rho_{mix} \text{ when } T_{mix}^c(t) \geq d_{root}$$

$$f_{cd}^{root}(t) = \frac{f_{vm}(t)\dfrac{\rho_{pc}}{\rho_{mix}}T_{mix}^c(t) + d_{root} - T_{cv}^c(t) - T_{mix}^c(t)}{d_{root}} \tag{J.46}$$
$$\text{when } T_{cv}^c(t) + T_{mix}^c(t) + T_{pc}^{um}(t) \geq d_{root} > T_{cv}^c(t) + T_{mix}^c(t)$$

$$f_{cd}^{root}(t) = \frac{f_{vm}(t)\frac{\rho_{pc}}{\rho_{mix}}T_{mix}^c(t) + T_{pc}^{um}(t)}{d_{root}} \text{ when } T_{cv}^c(t) + T_{mix}^c(t) + T_{pc}^{um}(t) < d_{root}$$

where

$\quad f_{cd}^{root}(t)$ = cover and depth factor, which accounts for the length of the roots that are exposed to different concentrations of the radionuclide in the various layers of the primary contamination,

$\quad d_{root}$ = length of the root (m).

The other terms are defined and discussed in Appendix G:

J.4.2 Contribution of Root Uptake from the Accumulation in Surface Soil

The expression for the contribution of root uptake from accumulation in the surface soil is similar to the expression in Section J.4.1 except that adjustments are not made for the situation where the depth of root might exceed the thickness of the mixing layer, because the code only models the concentration of radionuclides in the mixing zone, not in the soil below. The soil below can be contaminated to a similar extent due to leaching:

$$p_{ag_i}^{ru}(t) = 10^3 rtf_i s_i^o(t) \tag{J.47}$$

where

$p_{ag_i}^{ru}(t)$ = contribution of root uptake from the accumulation in the mixing layer to the concentration of radionuclide i in the part of the plant that is consumed by livestock or by humans (Activity/kg), and

$s_i^o(t)$ = concentration of radionuclide i due to accumulation at the agricultural land (Activity/g).

J.4.3 Contribution of Foliar Interception of Irrigation

This contamination pathway is active for all radionuclides other than C-14 and H-3. The following expression is for the contribution of the foliar interception of irrigation:

$$p_i^{fi}(t) = \frac{f_{int}^{ir} f_{tl}}{Y} \frac{1 - e^{-\lambda_w t_g}}{\lambda_w} \frac{q_{ir}}{t_g} w_i^{ir}(t) \tag{J.48}$$

where

$p_i^{fi}(t)$ = contribution of foliar interception of irrigation water to the concentration of radionuclide i, other than ^{14}C or ^{3}H, in the part of the plant that is consumed by livestock or by humans (Activity/kg),

f_{int}^{ir} = fraction of irrigation water intercepted and retained on the foliage of the plant,

f_{tl} = fraction of the radionuclide intercepted by the foliage and translocated to the edible portion of the plant,

Y = yield of the edible portion of the plant (kg/m^2),

λ_w = weathering removal constant of the plant (1/yr),

t_g = growing period of the plant (yr),

q_{ir} = quantity of irrigation water applied to a unit area of agricultural or farmed land during a year (m/yr), and

$w_j^{ir}(t)$ = concentration of radionuclide j in irrigation water (Activity/m^3).

The expression above, for the contribution of foliar interception of irrigation, $p_i^{fi}(t)$, is derived by considering the quantity of the radionuclide retained in the plant foliage per unit area of land, $pf_i^{fi}(t)$.

The rate at which the radionuclide is intercepted by the foliage of the plant:

$$f_{int}^{ir} \frac{q_{ir}}{t_g} w_i^{ir}(t)$$

The rate at which the radionuclide is lost from the foliage due to weathering:

$$\lambda_w p f_i^{fi}(t)$$

The rate of change of the quantity of the radionuclide in the foliage of the plant:

$$\frac{d p f_i^{fi}(t)}{dt}$$

Equating the change to the net change gives the mass balance equation:

$$\frac{d p f_i^{fi}(t)}{dt} = f_{int}^{ir} \frac{q_{ir}}{t_g} w_i^{ir}(t) - \lambda_w p f_i^{fi}(t)$$

Integrating over the growing period after assuming that the concentration in the irrigation water is constant over the growing period gives the following:

$$\int_0^{t_g} \frac{d e^{\lambda_w t} p f_i^{fi}(t)}{dt} dt = f_{int}^{ir} \frac{q_{ir}}{t_g} w_i^{ir}(t) \int_0^{t_g} e^{\lambda_w t} dt$$

$$e^{\lambda_w t_g} p f_i^{fi}(t_g) = f_{int}^{ir} \frac{q_{ir}}{t_g} w_i^{ir}(t) \frac{e^{\lambda_w t_g} - 1}{\lambda_w}$$

$$p f_i^{fi}(t_g) = f_{int}^{ir} \frac{1 - e^{-\lambda_w t_g}}{\lambda_w} \frac{q_{ir}}{t_g} w_i^{ir}(t)$$

This is the factor applied in Section J.1.1 to account for the quantity of the radionuclide retained by the plant when quantifying the influx of the radionuclide to the mixing layer of the agricultural land from irrigation.

The concentration in the edible portion of the plant is obtained by applying the translocation factor and the yield:

$$p_i^{fi}(t) = \frac{f_{tl}}{Y} p f_i^{fi}(t_g) = \frac{f_{int}^{ir} f_{tl}}{Y} \frac{1 - e^{-\lambda_w t_g}}{\lambda_w} \frac{q_{ir}}{t_g} w_i^{ir}(t)$$

J.4.4   Contribution of Foliar Interception of Particulates by Plants at Offsite Locations

The expression for the contribution of the foliar interception of particulates is as follows:

$$p_{of_i}^{fp}(t) = \frac{f_{int}^p f_{tl}}{Y} \frac{1 - e^{-\lambda_w t_g}}{\lambda_w} V_{d_i}^{tl} \left(\frac{\chi}{Q}\right)_{o_i}^{tl} A R_i^{tl}(t) \tag{J.49}$$

where

$p_{of_i}^{fp}(t)$ = contribution of foliar interception of particulates to the concentration of radionuclide i in the part of the plant, grown offsite, that is consumed by livestock or by humans (Activity/kg),

f_{int}^{p} = fraction of particulates that are intercepted and retained on the foliage of the plant,

$V_{d_i}^{tl}$ = deposition velocity of particulates containing radionuclide i (m/s),

$\left(\dfrac{\chi}{Q}\right)_{o_i}^{tl}$ = ratio of the concentration of radionuclide i attached to particulates in the air above the offsite receptor location to the release of radionuclide i attached to particulates from the primary contamination (see Section I.10.1) (s/m³),

$AR_i^{tl}(t)$ = release rate of radionuclide i in the particulates released to air from the primary contamination (see Section G.15) (Activity/yr).

The expression above, for the contribution of foliar interception of particulates, $p_{of_i}^{fp}(t)(t)$, is derived by considering the quantity of the radionuclide retained in the plant foliage per unit area of land, $pf_i^{fp}(t)$.

The rate at which the radionuclide is intercepted by the foliage of the plant:

$$f_{int}^{p} V_{d_i}^{tl} \left(\frac{\chi}{Q}\right)_{o_i}^{tl} AR_i^{tl}(t)$$

The rate at which the radionuclide is lost from the foliage due to weathering:

$$\lambda_w pf_i^{fp}(t)$$

The rate of change of the quantity of the radionuclide in the foliage of the plant:

$$\frac{dpf_i^{fp}(t)}{dt}$$

Equating the change to the net change gives the mass balance equation:

$$\frac{dpf_i^{fp}(t)}{dt} = f_{int}^{p} V_{d_i}^{tl} \left(\frac{\chi}{Q}\right)_{o_i}^{tl} AR_i^{tl}(t) - \lambda_w pf_i^{fp}(t)$$

Integrating over the growing period after assuming that the concentration in the irrigation water is constant over the growing period gives the following:

$$\int_0^{t_g} \frac{de^{\lambda_w t} pf_i^{fp}(t)}{dt} dt = f_{int}^{p} V_{d_i}^{tl} \left(\frac{\chi}{Q}\right)_{o_i}^{tl} AR_i^{tl}(t) \int_0^{t_g} e^{\lambda_w t} dt$$

$$e^{\lambda_w t_g} pf_i^{fp}(t_g) = f_{int}^{p} V_{d_i}^{tl} \left(\frac{\chi}{Q}\right)_{o_i}^{tl} AR_i^{tl}(t) \frac{e^{\lambda_w t_g} - 1}{\lambda_w}$$

$$pf_i^{fi}(t_g) = f_{int}^p \frac{1 - e^{-\lambda_w t_g}}{\lambda_w} V_{d_i}^{tl} \left(\frac{\chi}{Q}\right)_{o_i}^{tl} AR_i^{tl}(t)$$

This is the factor applied in Section J.1.1 to account for the quantity of the radionuclide that is retained by the plant when quantifying the influx of the radionuclide to the mixing layer of the agricultural land from the particulates in the atmosphere.

The concentration in the edible portion of the plant is obtained by applying the translocation factor and the yield:

$$p_{of_i}^{fp}(t) = \frac{f_{tl}}{Y} pf_i^{fp}(t_g) = \frac{f_{int}^p f_{tl}}{Y} \frac{1 - e^{-\lambda_w t_g}}{\lambda_w} V_{d_i}^{tl} \left(\frac{\chi}{Q}\right)_{o_i}^{tl} AR_i^{tl}(t)$$

J.4.5 Contribution of Photosynthesis

The concentration of C-14 in plants has two additional components to account for photosynthesis, but does not have any contribution from the foliar interception of irrigation:

$$p_c(t) = p_{on_c}^{ru}(t) + p_{ag_c}^{ru}(t) + p_{of_c}^{fp}(t) + p_{on}^{ps}(t) + p_{of}^{ps}(t) \tag{J.50}$$

where

$p_c(t)$ = concentration of ^{14}C in the part of the plant consumed by livestock or by humans (Activity/kg),

$p_{on_c}^{ru}(t)$ = contribution of root uptake directly from the primary contamination to the concentration of ^{14}C in the part of the plant that is consumed by livestock or by humans (Activity/kg),

$p_{ag_c}^{ru}(t)$ = contribution of root uptake from the accumulation in the surface soil in the agricultural land to the concentration of ^{14}C in the part of the plant that is consumed by livestock or by humans (Activity/kg),

$p_{of_c}^{fp}(t)$ = contribution of foliar interception of particulates to the concentration of ^{14}C in the part of the plant, grown offsite, that is consumed by livestock or by humans (Activity/kg),

$p_{on}^{ps}(t)$ = contribution of photosynthesis of ^{14}CO$_2$ to the concentration of ^{14}C in the part of the plant, grown above the primary contamination, that is consumed by livestock or by humans (Activity/kg), and

$p_{of}^{ps}(t)$ = contribution of photosynthesis of ^{14}CO$_2$ to the concentration of ^{14}C in the part of the plant, grown offsite, that is consumed by livestock or by humans (Activity/kg).

The contribution of photosynthesis to plants grown above the primary contamination is computed using the following expression:

$$p_{on}^{ps}(t) = 10^3 f_a f_{cd}^{ec}(t) \, sap_{14_C} s_{14_C}(t) \tag{J.51}$$

where

$p_{on}^{ps}(t)$ = contribution of photosynthesis of ^{14}CO$_2$ to the concentration of ^{14}C in the part of the plant, grown above the primary contamination, that is consumed by livestock or by humans (Activity/kg),

10^3 = converts from per g to per kg,

f_a = fraction of the agricultural land that lies directly above the primary contamination,

$f_{cd}^{ec}(t)$ = cover and depth factor, which accounts for the depth of soil from which carbon dioxide can escape out of the soil,

sap_{14_C} = soil to air to plant transfer factor of ^{14}C, which is the ratio of the concentration in the edible part of the plant to the concentration in soil for uptake by evasion followed by photosynthesis ([Activity/g of plant]/[Activity/g of soil]),

$sap_{14_C} = \frac{0.5 d_{evasion}^C 10^6 \rho_b^{pc} \epsilon_v \sqrt{A}}{h_{mix}^v u_{wind}} ap_{14_C}$ subject to limits discussed in Appendix F,

ρ_b^{pc} = dry bulk density of the soil in the primary contamination (g/[cm]³),

ϵ_v = evasion rate of ^{14}C (1/s),

h_{mix}^v = height of the rectangular space above the primary contamination within which the $^{14}CO_2$ is assumed to be mixed in for calculation of photosynthesis by plants (m),

u_{wind} = average wind speed (m/s),

$s_{14_C}(t)$ = concentration of ^{14}C in the primary contamination (Activity/g).

The contribution of photosynthesis to plants grown offsite is computed using the expression:

$$p_{off}^{ps}(t) = 10^3 f_{cd}^{ec_{on}}(t) d_{evasion}^C A 10^6 \rho_b^{pc} \epsilon_v \left(\frac{\chi}{Q}\right)_{o_i}^g ap_{14_C} s_{14_C}(t)$$
$$+ 10^3 minimum\left(\frac{d_{mix}^o}{d_{evasion}^C}, 1\right) sap_{14_C} s_{14_C}^o(t)$$

(J.52)

where

$p_{off}^{ps}(t)$ = contribution of photosynthesis of $^{14}CO_2$ to the concentration of ^{14}C in the part of the plant, grown offsite, that is consumed by livestock or by humans (Activity/kg),

10^3 = converts from per g to per kg,

$f_{cd}^{ec_{on}}(t)$ = onsite cover and depth factor, which accounts for the depth of soil from which carbon dioxide can escape out of the soil,

$d_{evasion}^C$ = depth of evasion of ^{14}C (m),

A = the area of the primary contamination (m²),

10^6 = converts from m³ to (cm)³,

ρ_b^{pc} = dry bulk density of the soil in the primary contamination, g/(cm)³,

ϵ_v = evasion rate of ^{14}C (1/s),

$\left(\frac{\chi}{Q}\right)_{o_i}^g$ = ratio of the concentration of ^{14}C in the form of carbon dioxide in the air above the offsite receptor location to the release of ^{14}C in the form of carbon dioxide from the primary contamination (see Section I.10.1) (s/m³),

$ap_{14_C} = mf_{12_C} f_C^a / a_{12_C}$ = air to plant transfer factor of ^{14}C for the plant, which is the ratio of the concentration in the edible part of the plant to the concentration in air ([Activity/g of plant]/[Activity/m³]),

$mf_{12_C}^p$ = mass fraction of ^{12}C in plants,

f_C^a = fraction of ^{12}C in plant obtained from air,

a_{12_C} = (mass) concentration of ^{12}C in air, g/m³,

$s_{14_C}(t)$ = concentration of ^{14}C in the primary contamination (Activity/g),

d^o_{mix} = depth of the mixing layer at the offsite location (m),

sap_{14_C} = soil to air to plant transfer factor of ^{14}C for the plant, which is the ratio of the concentration in the edible part of the plant to the concentration in soil ([Activity/g of plant]/[Activity/g of soil]),

$sap_{14_C} = \frac{0.5 d^C_{evasion} 10^6 \rho^{pc}_b \epsilon_v \sqrt{A}}{h^v_{mix} u_{wind}} ap_{14_C}$ subject to limits discussed in Appendix F,

h^v_{mix} = height of the rectangular space above the primary contamination within which the ^{14}CO$_2$ is assumed to be mixed in for calculation of photosynthesis by plants (m),

u_{wind} = average wind speed (m/s), and

$s^o_{14_C}(t)$ = concentration of ^{14}C in the offsite location (Activity/g).

J.5   Concentration in Meat and Milk

The code models the accumulation of the radionuclide in meat and the transfer of the radionuclide to milk resulting from the ingestion of contaminated plant material, the incidental ingestion of soil with plant feed, and the consumption of contaminated livestock water. The concentration of the radionuclide in meat and in milk are computed using the following expression:

$$m_i(t) = imf_i \left[q^p_{ing} p^f_i(t) + q^s_{ing} \left\{ s^o_i(t) + f_a f_{vm}(t) \frac{\rho^{pc}_b}{\rho^{mix}_b} s_i(t) \right\} 10^3 + q^w_{ing} w^{ls}_i(t) 10^{-3} \right] \qquad \text{(J.53)}$$

where

$m_i(t)$ = concentration of radionuclide i in meat (Activity/kg) or milk (Activity/L),

imf_i = intake to meat accumulation factor, the concentration in meat at the time of slaughter due to a uniform daily intake of unit Activity ([Activity/kg]/[Activity/day]), or is the intake to milk transfer factor, the concentration in milk at the time of milking due to a uniform daily intake of unit Activity ([Activity/L]/[Activity/day]),

q^p_{ing} = rate of ingestion of plant feed by livestock (kg/day),

$p^f_i(t)$ = concentration of radionuclide i in the plant feed at the time of consumption (Activity/kg),

q^s_{ing} = rate of ingestion of soil with plant feed by livestock (kg/day),

$s^o_i(t)$ = concentration of radionuclide i in the offsite soil associated with plant feed (Activity/g),

$s_i(t)$ = concentration of radionuclide i in soil in the primary contamination (Activity/g),

f_a = fraction of the agricultural land that lies directly above the primary contamination,

$f_{vm}(t)$ = volume fraction of soil from the primary contamination in the mixing zone,

ρ^{pc}_b = dry bulk density of the soil in the primary contamination (g/[cm]^3),

ρ^{mix}_b = dry bulk density of the mixing layer at the primary contamination (g/[cm]^3),

10^3 = converts from kg to g,

q^w_{ing} = rate of ingestion of water by livestock (L/day),

$w^{ls}_i(t)$ = concentration of radionuclide i in the livestock water (Activity/m^3), and

10^{-3} = converts from L to m^3.

J.6 Concentration in Aquatic Food

The code models bioaccumulation of the radionuclide in the aquatic organisms living in a surface water body containing radionuclides. An equilibrium transfer is used. The concentration in aquatic food is computed using the following equation:

$$aqf_i(t) = baf_i \, w_i^{sw}(t) 10^{-3} \qquad\qquad (J.54)$$

where

$aqf_i(t)$ = concentration of radionuclide i in the aquatic food (Activity/kg),

baf_i = bioaccumulation factor or the equilibrium concentration ratio between the aquatic food and the water in the surface water body ([Activity/kg]/[Activity/L]),

$w_i^{sw}(t)$ = concentration of radionuclide i in the water in the surface water body (Activity/m³), and

10^{-3} = converts from L to m³.

J.7 Reference

Argonne (Argonne National Laboratory), 1998, *Evaluation of the Area Factors Used in the RESRAD Code for Estimation of Airborne Contaminant Concentrations of Finite Area Sources*, ANL/EAD/TM-82, July.

APPENDIX K:
SIMULATING THE RESRAD-ONSITE CODE

The RESRAD-OFFSITE code has a feature to simulate the RESRAD-ONSITE code when modeling a wholly onsite exposure scenario. When this feature is activated, the interface does the following in order to mimic RESRAD-ONSITE to the extent possible:

- The exposure locations are placed above the primary contamination. The water sources, the well, and the surface water body are placed at the down-gradient edge of the primary contamination.

- The input boxes for the properties of the exposure locations are disabled, and the values in the disabled input boxes are related to the properties specified for the primary contamination in the corresponding input boxes, as illustrated in the example in Section K.1.

- The input boxes relating to **offsite transport** by air, groundwater, and surface water are disabled.

- The input boxes corresponding to processes not modeled in RESRAD-ONSITE are disabled.

The relationships between the properties of the exposure locations and the properties of the primary contamination are also specified in the computational code to simulate the RESRAD-ONSITE single-parameter sensitivity analysis and RERAD-ONSITE probabilistic analysis. These are described in Section K.2.

The implementation of this feature in the code is illustrated in Section K.1 using an example onsite exposure scenario with five radionuclides selected to test all aspects of the codes.

RESRAD-OFFSITE also has a feature to model an onsite exposure scenario without suppressing its additional capabilities. This is described in Appendix L.

K.1 Example Onsite Exposure Scenario Showing RESRAD-ONSITE Simulated in RESRAD-OFFSITE

A 40,000-square-meter parcel of land is contaminated over a depth of 2 meters with 0.06 Bq/g of carbon-14, 4 Bq/g of hydrogen-3, 0.005 Bq/g of radium-226, 0.09 Bq/g of technetium-99, and 0.04 Bq/g of thorium-228. Technetium-99 is selected as a representative radionuclide with no transformation progeny; radium-226 is selected to represent a transformation chain and also to compare the radon-222 modeling; thorium-228 is selected to compare the radon-220 modeling; carbon-14 is selected to compare the additional components to model carbon, and tritium to compare the additional components with model hydrogen.

The scenario is modeled in two parts: first with all the radionuclides over a time horizon of 1,000 years, and then, based on the results of the first run, with all but radium-226 over a time horizon of 16 years. The latter run uses 4,096 calculation time points; an exposure duration for risk of one year, because this comparison is not looking at risk; and a maximum reporting time of 15 years. The output is compared with the corresponding output from two runs using RESRAD-ONSITE Version 7.2 to model the same scenarios.

K.1.1   Input Interface for Simulating RESRAD-ONSITE

1. Use either the File menu command or the RESRAD-ONSITE icon on the toolbar to simulate the RESRAD-ONSITE code, as illustrated in Figure K-1.
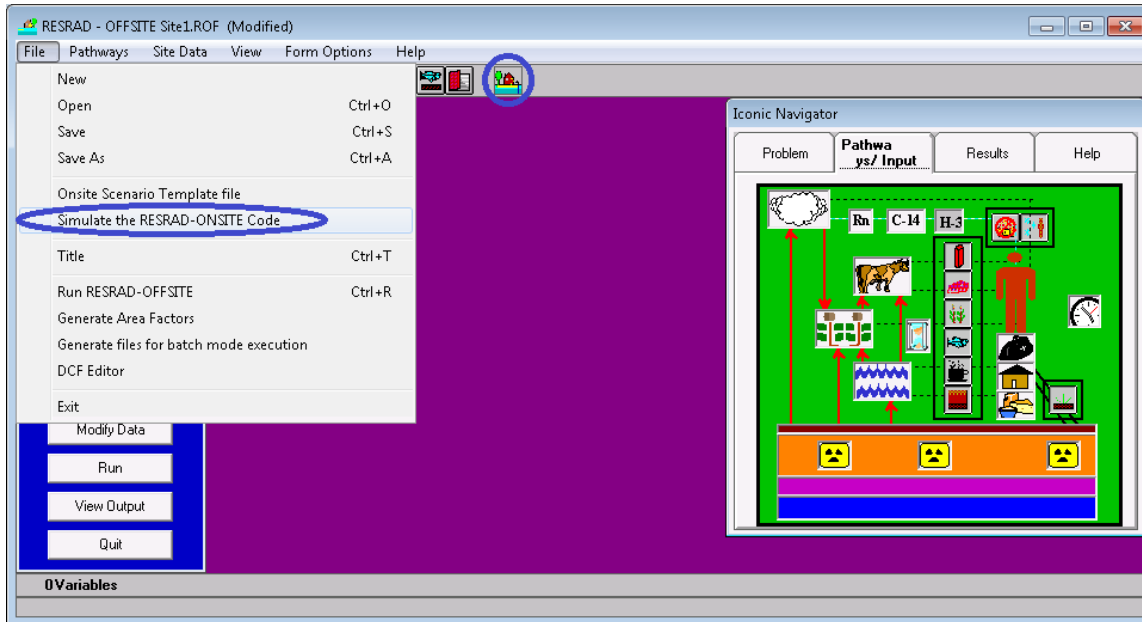
Figure K-1   Activating the "Simulate RESRAD-ONSITE" Feature

2. The Title form will pop up as shown in Figure K-2. All inputs there are active for simulating the RESRAD-ONSITE code. The Title text box has the text "Simulating the RESRAD-ONSITE code"; this can be changed to describe the scenario being modeled.
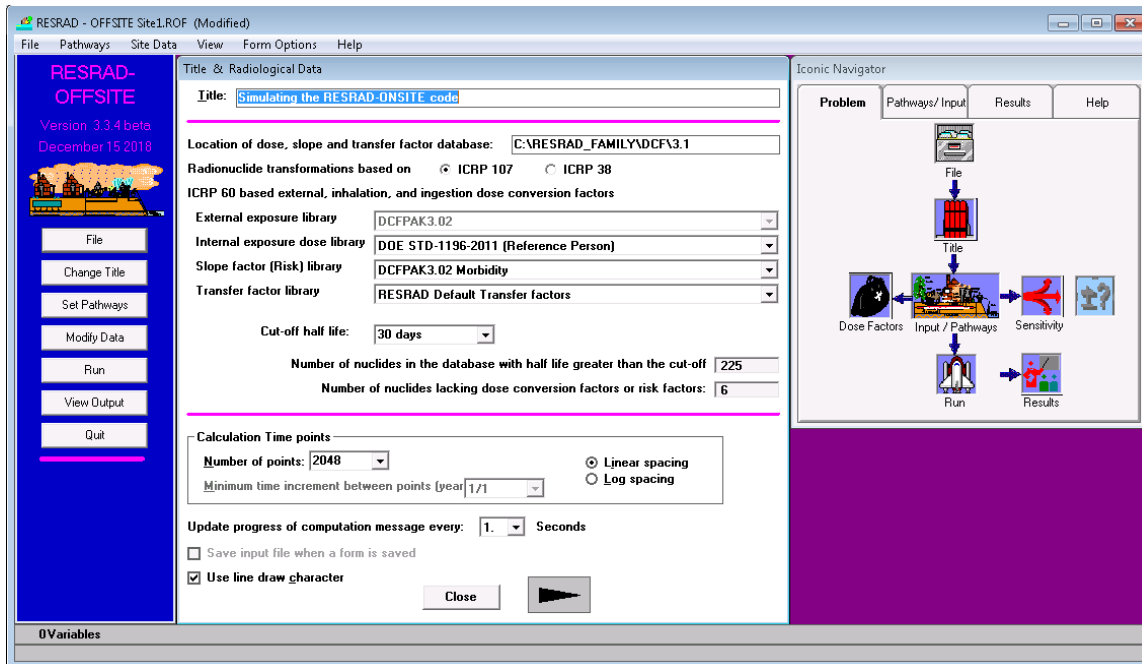
Figure K-2   Title and Radiological Data Form when Simulating RESRAD-ONSITE

3. Only the RESRAD-ONSITE exponential release model conceptualization is active when simulating the RESRAD-ONSITE code as depicted in Figure K-3.
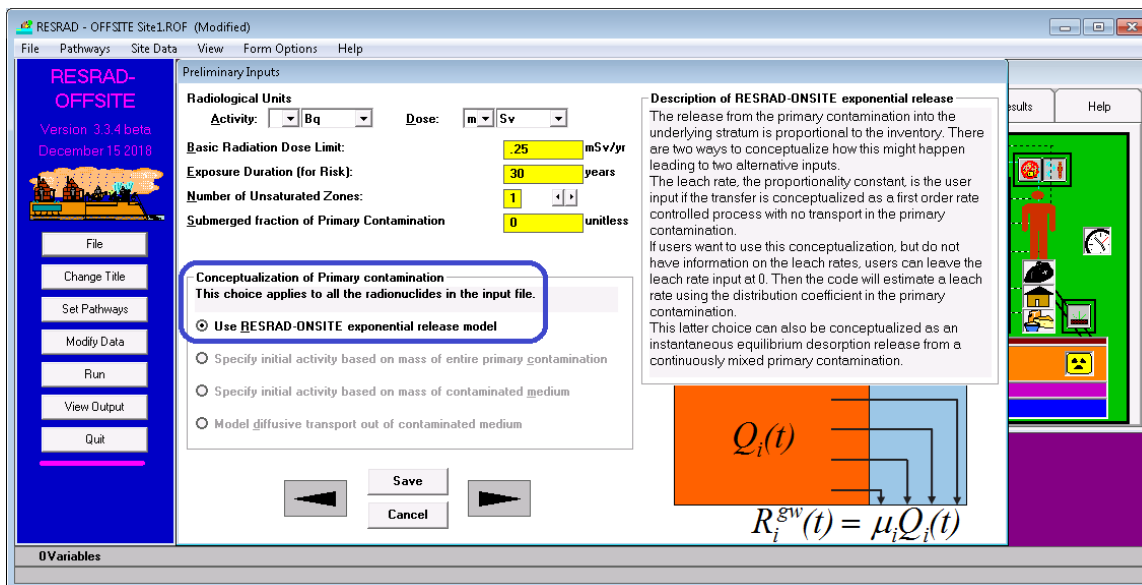
Figure K-3   Preliminary Inputs Form when Simulating RESRAD-ONSITE

4. Select carbon-14 at a concentration of 0.06 Bq/g; hydrogen-3 at 4 Bq/g; radon-226 at 0.005 Bq/g; technetium-99 at 0.09 Bq/g, and thorium-228 at 0.037 Bq/g. Turn on the radon exposure pathway for a complete comparison of the two codes. These are highlighted in Figure K-4.
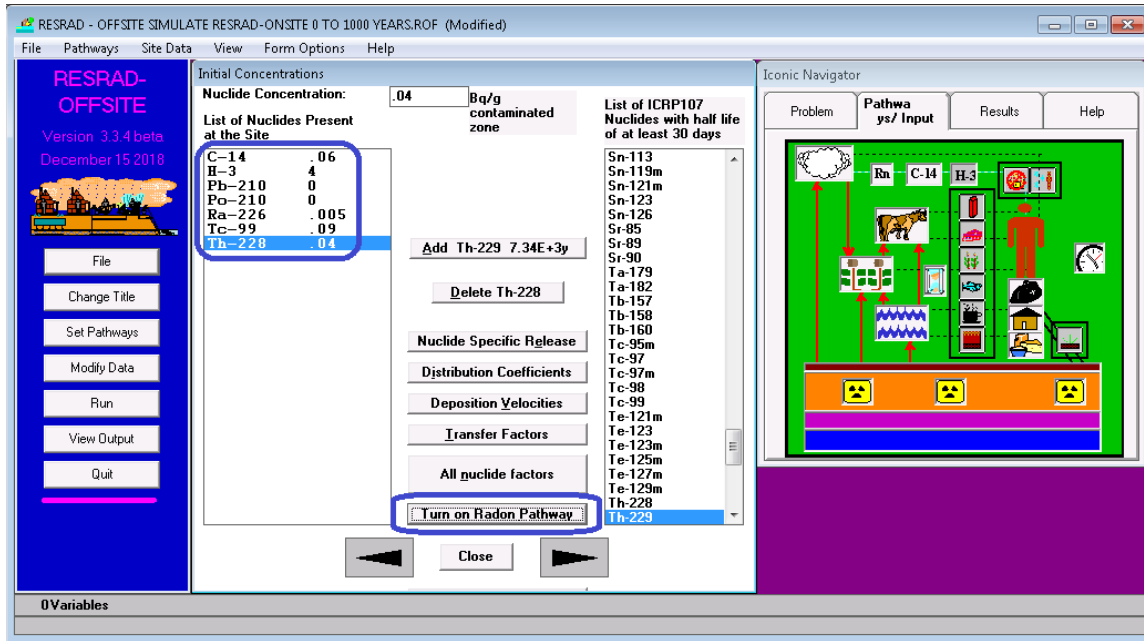
Figure K-4   Example-Specific Inputs to Illustrate the "Simulate RESRAD-ONSITE" Feature

5. The deposition velocities used to model atmospheric transport and foliar deposition are disabled. So are the distribution coefficients, on the right half of the form, which are used to model accumulation at offsite locations. The distribution coefficients for the farmed areas are set to the value entered for the contaminated zone, as shown in Figure K-5.
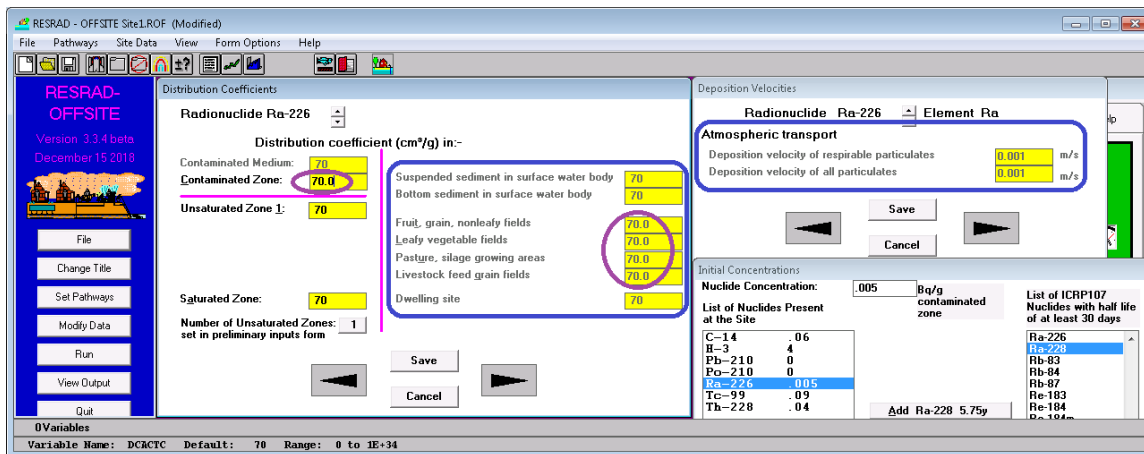
Figure K-5   The Distribution Coefficients and Deposition Velocities Forms when Simulating RESRAD-ONSITE

6. The dispersivity in the contaminated zone and the deposition velocities of particulates are disabled and set to zero because RESRAD-ONSITE models neither dispersive transport in groundwater nor atmospheric transport. The code adjusts some of the inputs so that the erosion rate is equal to the default value in RESRAD-ONSITE, Figure K-6; these can be changed if a different erosion rate is to be specified.

Figure K-6   The Physical and Hydrological Form and the Primary Contamination Form when Simulating RESRAD-ONSITE

For this example, set the area of the contaminated zone to 40,000 m^2. Change the length of contamination parallel to aquifer flow to 200 m.

7. All inputs characterizing farmed lands, except for their areas and the fractions of their areas overlapping the primary contamination, are disabled and related to the properties specified for the primary contamination, as shown in Figure K-7. The irrigation applied per year for each type of plant is the product of the growing period of that plant type and the irrigation applied per year on the primary contamination. The other properties are the average values over the soil-mixing layer or the values for either the cover or the contaminated zone. The sediment delivery ratio at each farmed area is disabled and set to zero because it does not apply to onsite farmed areas.
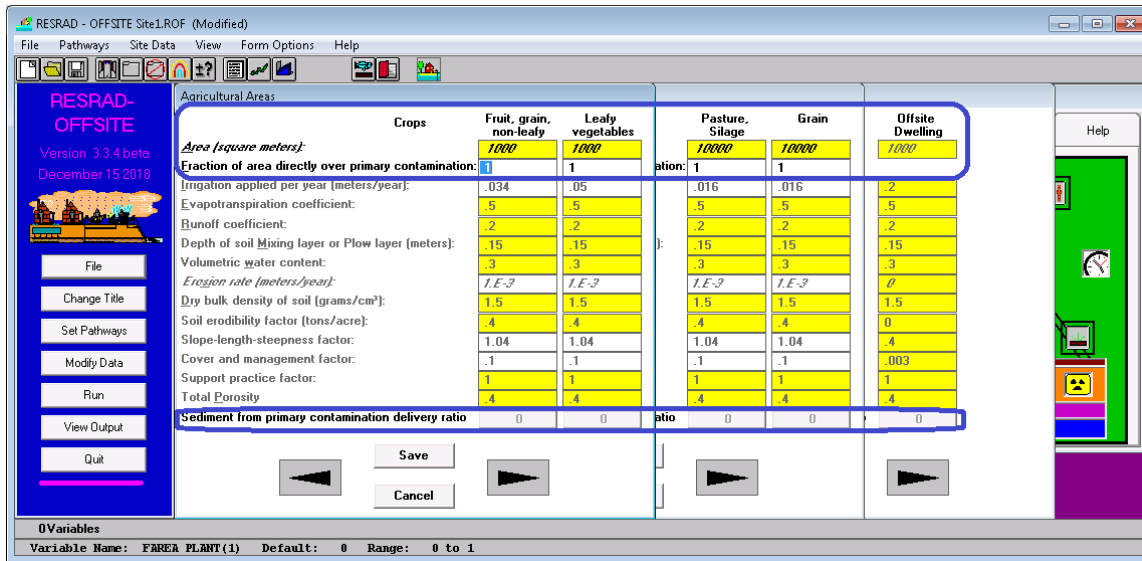
Figure K-7   Physical and Hydrological Properties of Farmed Areas when Simulating RESRAD-ONSITE

8. The only items enabled in the Atmospheric Transport form are the average wind speed and the command button to read a STAR format file (containing joint frequency data of wind speed, wind direction, and atmosphere stability class), as highlighted in Figure K-8. When a STAR file is read, the code computes the average wind speed for that file and shows it in the corresponding input box. The user can enter an average wind speed or change the calculated value.
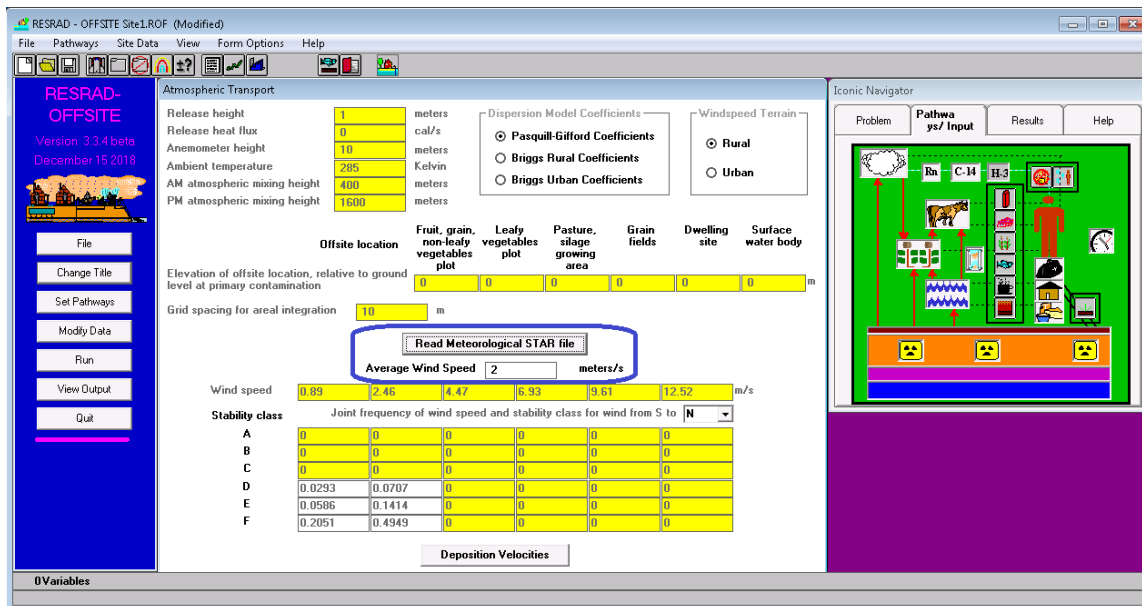
Figure K-8   Atmospheric Transport Form for Simulating RESRAD-ONSITE

9. The dispersivities in the unsaturated and the saturated zones are disabled and set to zero, as shown in Figure K-9, because dispersive transport is not modeled in RESRAD-ONSITE. The well and the surface water body are both at the down-gradient edge of the primary contamination in RESRAD-ONSITE. The input boxes for the hydraulic gradient of the saturated zone to the surface water body and the depth of aquifer contributing to the surface water body are disabled and are set to reflect the values specified for the saturated zone to the well because RESRAD-ONSITE uses the same values for both sources of water.

Figure K-9   Unsaturated and Saturated Zone Hydrology Forms when Simulating RESRAD-ONSITE

10. The convergence criterion is the only input enabled in the Groundwater Transport form. The code places the well and the surface water body at the down-gradient edge of the primary contamination and disables those inputs. The distances to the two edges of the surface water body from the plume centerline are set by the code based on the area of the surface water body. These are shown in Figure K-10.
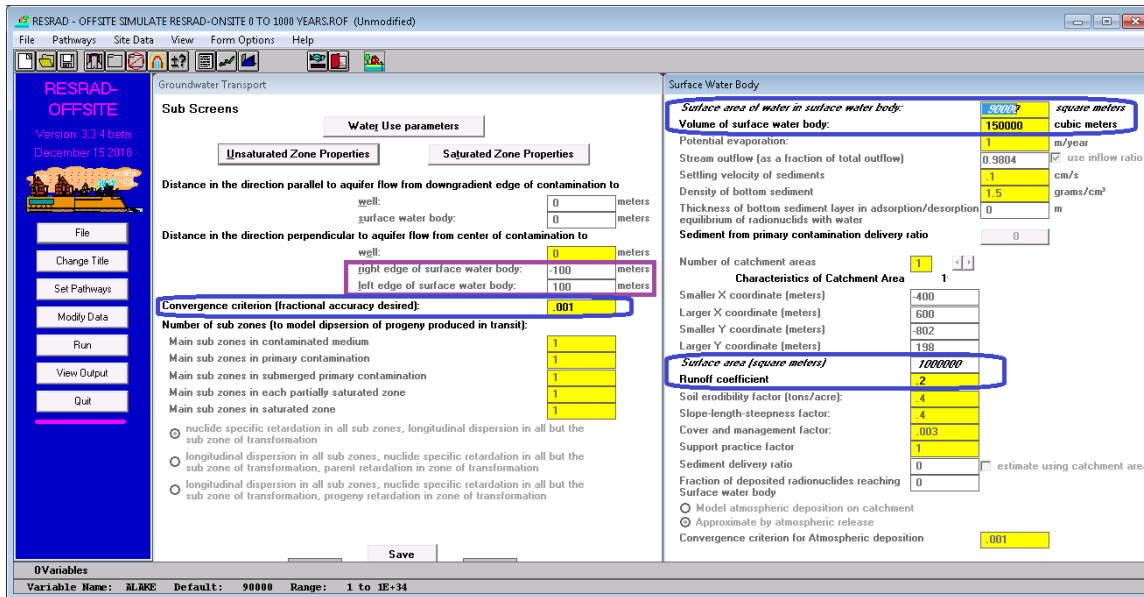
Figure K-10 Groundwater Transport and Surface Water Body Forms when Simulating RESRAD-ONSITE

The surface area and the volume of the surface water body, the surface area of the catchment from which runoff flows into the surface water body, and the runoff coefficient from the catchment are the only inputs that are enabled in the surface Water Body form, Figure K-10. The stream flow as a fraction of total outflow is set to the ratio of the corresponding inflows, and the computational code is flagged to compute this ratio and use it. The delivery ratios of the eroded material from the primary contamination and from the catchment and the material deposited in the catchment are each set to zero because RESRAD-ONSITE does not model the fate of the eroded material nor the atmospheric transport of particulates from the primary contamination to the catchment.

11. As shown in Figure K-11, the input boxes in the Site Layout form are disabled, as is the ability it make changes to the dimensions and locations in the map. However, the ability to move the primary contamination is enabled in the map interface. The code determines the dimensions and locations based on the area values input in the Primary Contamination, Agricultural Areas, Livestock Feed Areas, and Surface Water Accumulation forms.
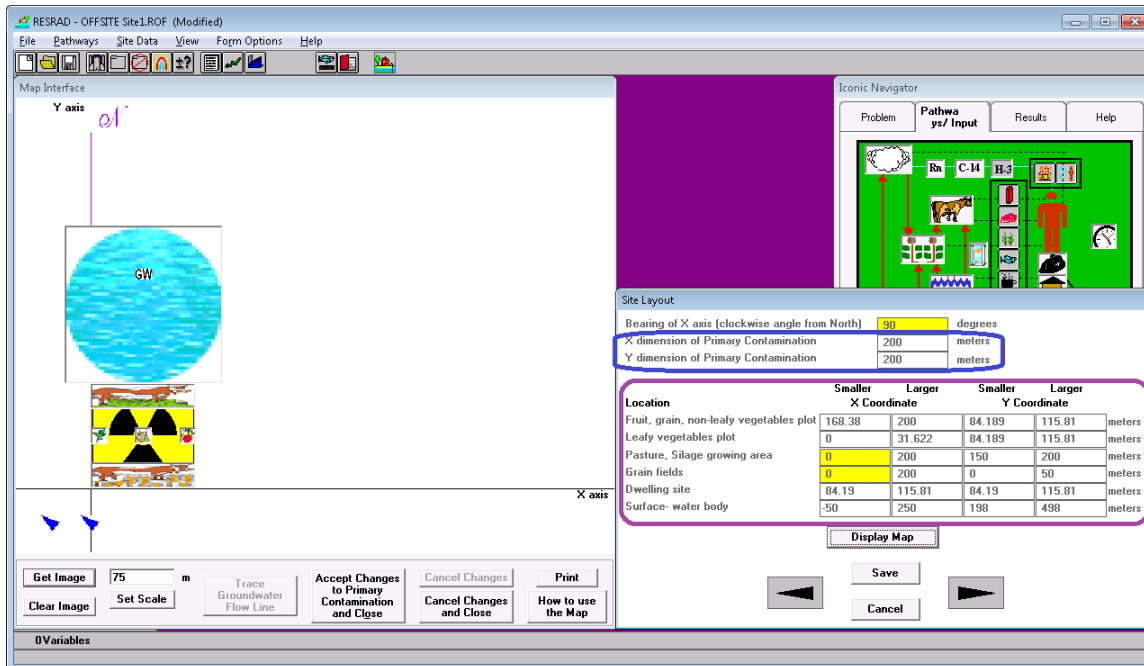
Figure K-11 Site Layout Form and Map Interface when Simulating RESRAD-ONSITE

12. Some of the inputs in the Plant Factors and Livestock Feed Factors forms are disabled to reflect the inputs available in RESRAD-ONSITE. The values input for fruit, grain, and nonleafy vegetables for the weathering removal constant and for the root depth are use for all plant types. The input boxes for the other three categories of plants are disabled and reflect the input in the enabled boxes. The properties of the livestock feed grain are disabled and set to the value for pasture and silage because RESRAD-ONSITE uses the same values for both types of feed. This is shown in Figure K-12.
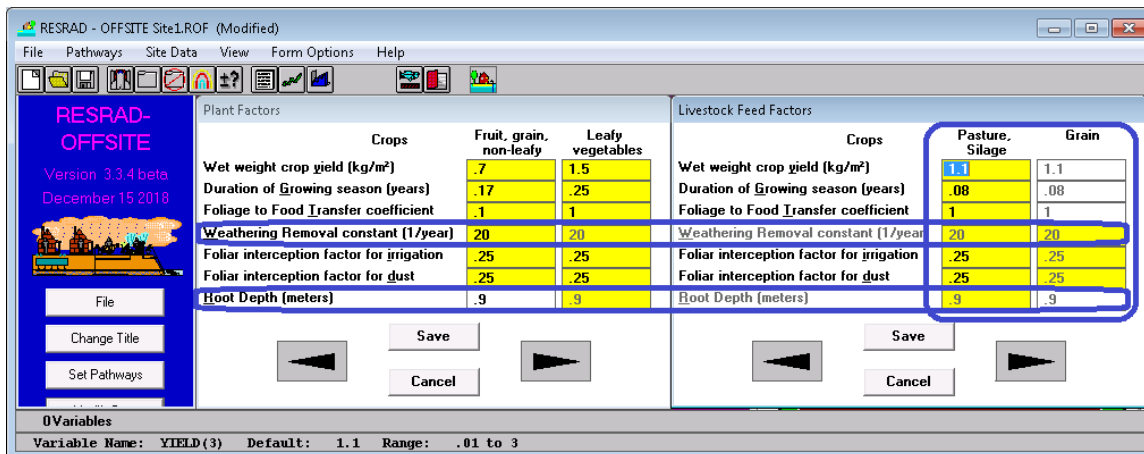

Figure K-12 Plant and Livestock Feed Factor Forms when Simulating RESRAD-ONSITE

13. The option to input the mass loadings and respirable fractions for each offsite exposure location is disabled in the Inhalation and External Gamma form. The input boxes for the fractions of times spent at each of the offsite exposure locations are disabled and set to zero in the Occupancy form. This suppresses the calculation of resuspension of particulates and the emanation of radon from the farmed locations. This is illustrated in Figure K-13.

Figure K-13 Inhalation and External Gamma Form and Occupancy Form when Simulating RESRAD-ONSITE

14. The shape of the primary contamination is set to circular, and the onsite receptor is placed at the center of the circle in the interface. The computational code is flagged to use a circular primary contamination with the receptor at the center, allowing probabilistic and sensitivity analysis on the area. The receptor location can be moved away from the center of the circular; this is not advisable if sensitivity or probabilistic analysis is to be performed on the area of the primary contamination. Neither code can currently determine the shape factors for the sensitivity and probabilistic runs of a nonconcentric receptor when a circular shape is specified for the primary contamination.

The offsite occupancies are disabled and set to zero and the onsite occupancies are set to the RESRAD-ONSITE defaults, as shown in Figure K-14. This suppresses calculation of external exposure from accumulation in the farmed areas.
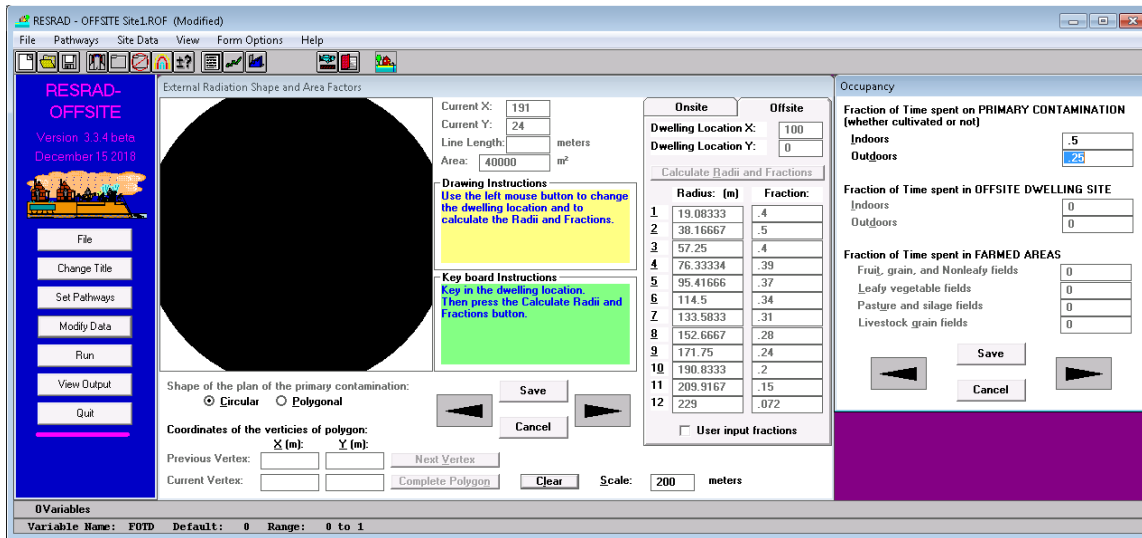
Figure K-14 External Radiation Shape and Area Factor Form when Simulating RESRAD-ONSITE

15. As shown in Figure K-15, the effective radon diffusion coefficients in the offsite locations are disabled because the emanation from accumulation is not modeled in RESRAD-ONSITE.
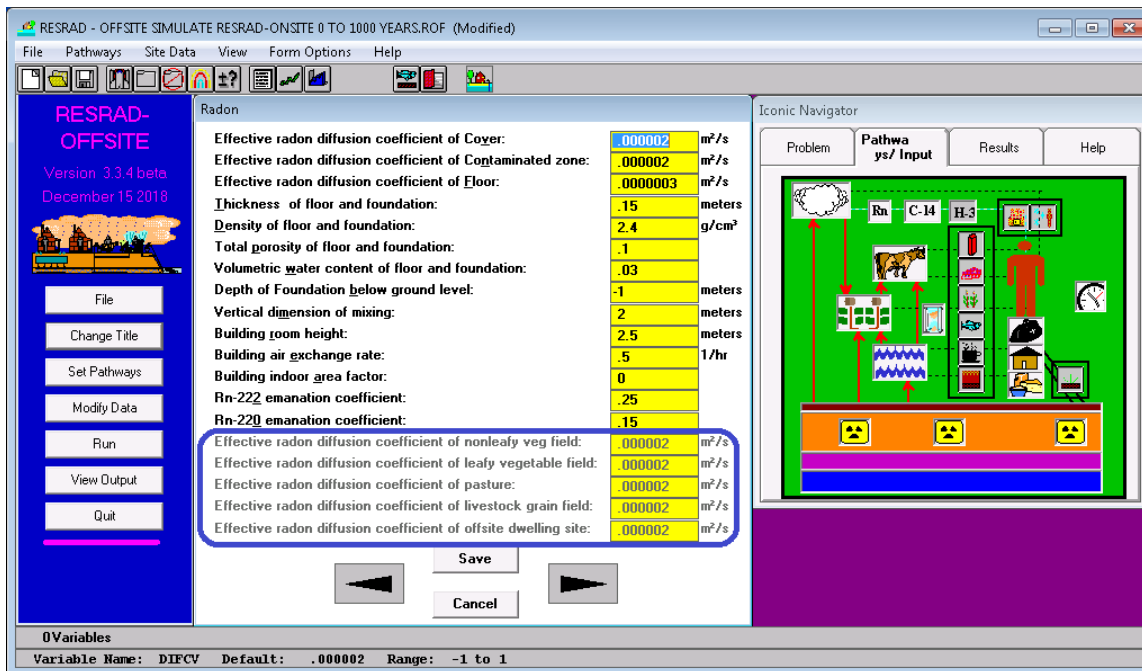

Figure K-15 Radon Form when Simulating RESRAD-ONSITE

K.1.2 Modeling the Same Scenario on RESRAD-ONSITE Version 7.2

1. Select the same radionuclide transformation database, dose factor libraries, and cutoff half-life that were used in the RESRAD-OFFSITE run. Select 1,024 linearly spaced points for the graphics to produce smooth temporal dose plots for comparison with the plots obtained by simulating RESRAD-ONSITE in RESRAD-OFFSITE. Change the maximum number of time integration points for risk to 1 because risk is not being compared in this example. These are shown in Figure K-16.
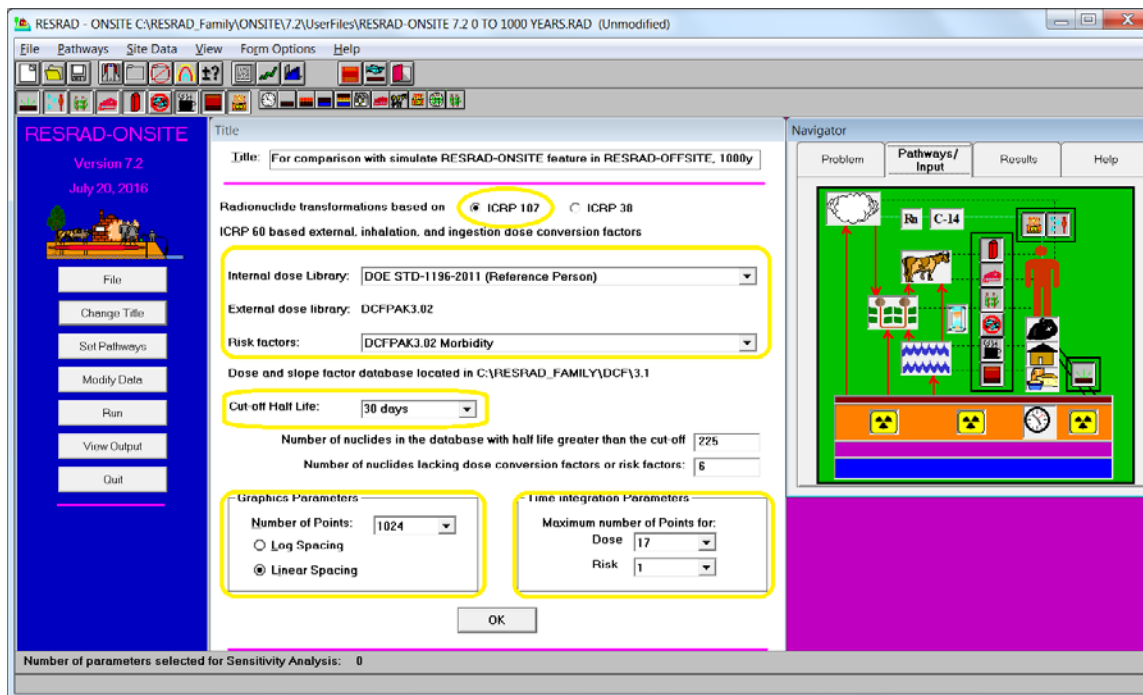

Figure K-16 Setting the Radionuclide Transformation Database and Dose Factor Libraries

2. Specify the concentrations of the radionuclides and turn on the radon exposure pathway, as shown in Figure K-17.

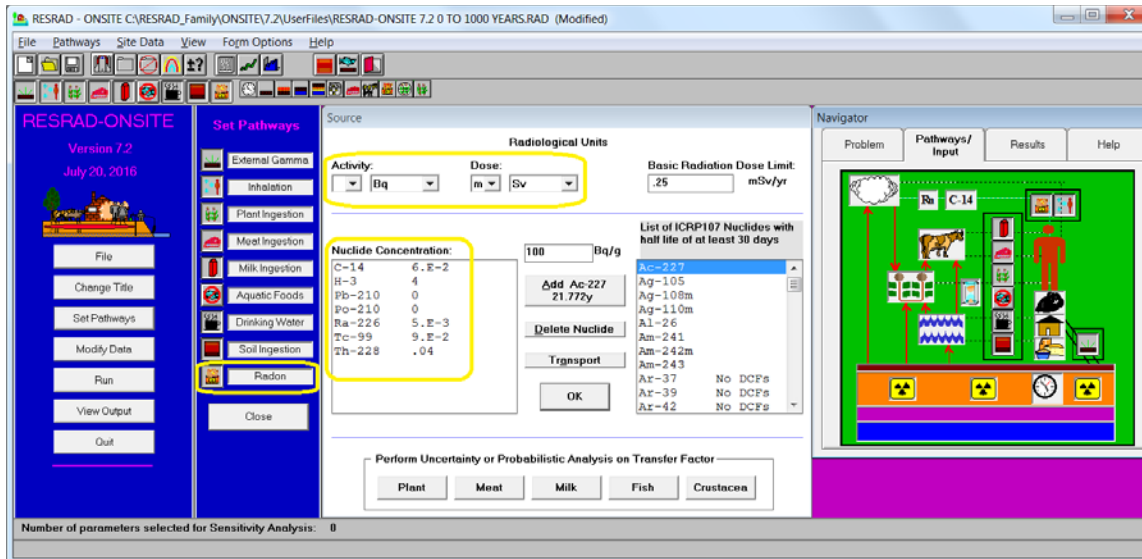**Figure K-17 Specifying the Radionuclide Concentrations and Turning on the Radon Exposure Pathway**

3.   Specify the area and length parallel to aquifer flow of the contaminated zone, as shown in Figure K-18.
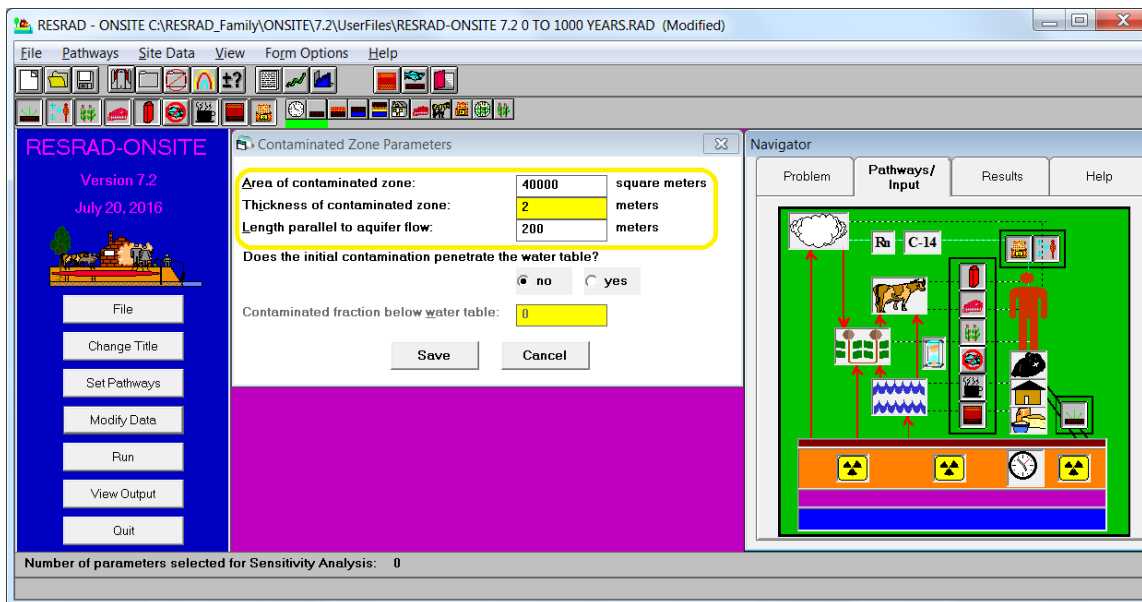

Figure K-18 Specifying the Dimensions of the Contaminated Zone

4.   Set the water table drop rate to 0 because RESRAD-OFFSITE does not model changes to the water table, as shown in Figure K-19.
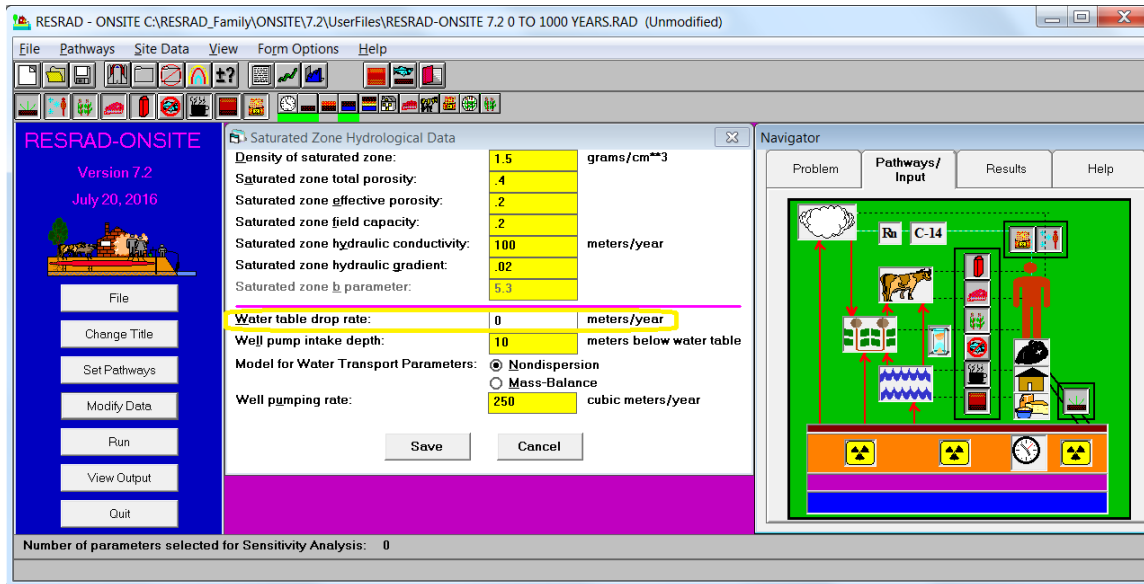
Figure K-19 Zeroing the Water Table Drop Rate to Match the Scenario in RESRAD-OFFSITE

K.1.3   Comparison of the Outputs of RESRAD-ONSITE Version 7.2 and the "Simulate RESRAD-ONSITE" Feature in RESRAD-OFFSITE

The temporal plots of dose from the two codes are compared subpathway-by-subpathway in this section. Each figure has a pair of plots for a radionuclide: the plots on the left are from RESRAD-OFFSITE, while the plots on the right are from RESRAD-ONSITE. The reasons for the differences in the outputs of the two codes are discussed.

The comparisons indicated the need for a second set of runs over a shorter time horizon to properly compare the temporal dose plots of the radionuclides that produce a dose in the first few years. The second set of runs used a 16-year time horizon with 4,096 calculation time points. These temporal plots are also compared in this section.

1. For this scenario, no differences are observed between the outputs of the two codes in dose from external exposure from the primary contamination (Figure K-20). This will be the case provided sufficient computational time points are used in RESRAD-OFFSITE to capture the temporal variation in radionuclide concentration in the contaminated zone, especially radionuclides that leach out or escape rapidly as a gas or vapor.

Figure K-20 External Exposure

2. For this scenario, no differences were observed between the outputs of the two codes for the dose from the inhalation of particulates from the primary contamination (Figure K-21). This will be the case provided there is no clean cover above the primary contamination and the condition in Item 1 is satisfied. The outputs will differ when a cover is present because of the differences in how the codes model the concentration in the mixing layer.

K-15
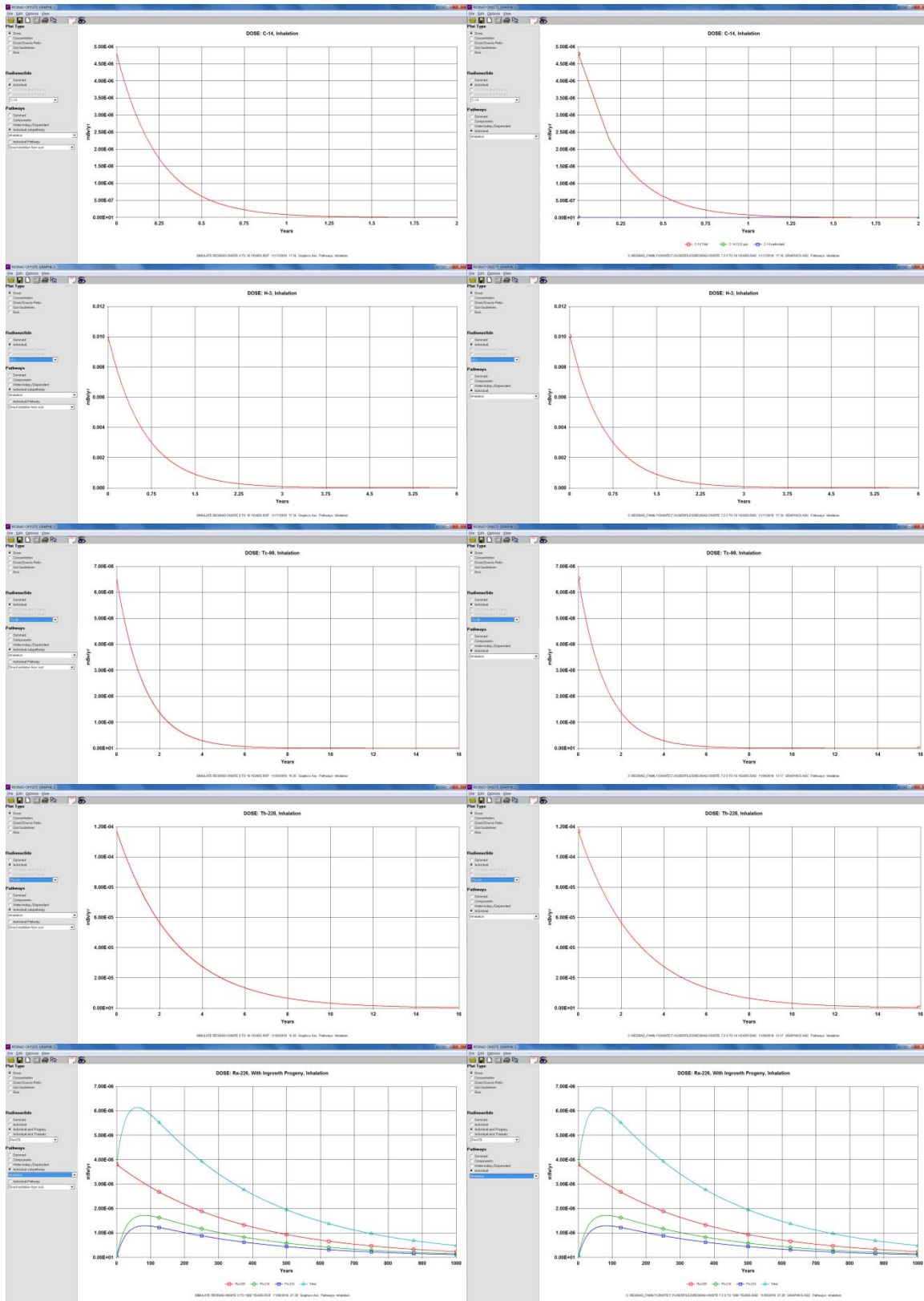
Figure K-21   Dose from the Inhalation of Particulates
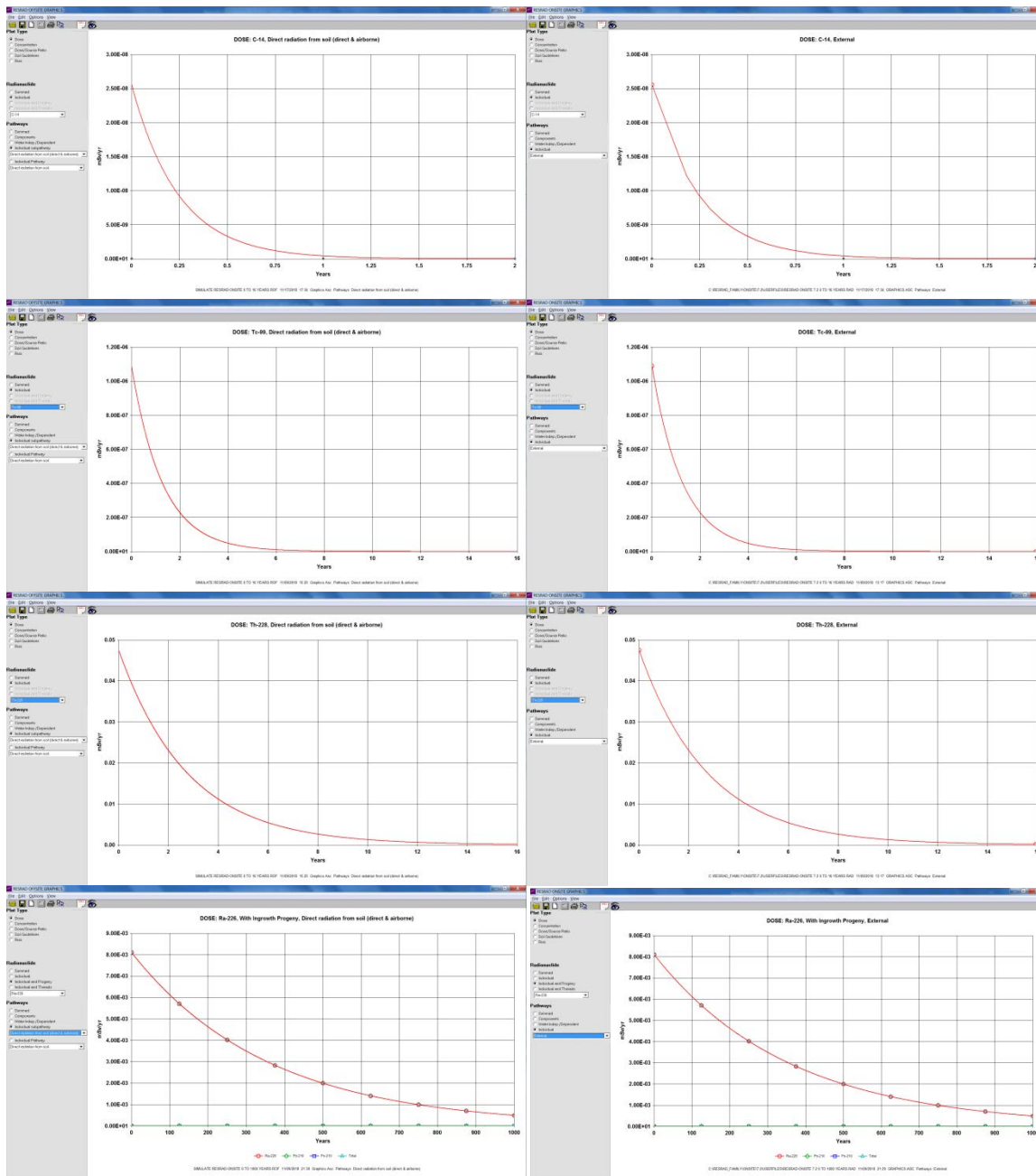
3. For this scenario, no differences were observed between the outputs of the two codes for dose from the inhalation of the short-lived progeny that formed from radon emanating from the primary contamination (Figure K-22). This will be the case provided the condition in Item 1 is satisfied.
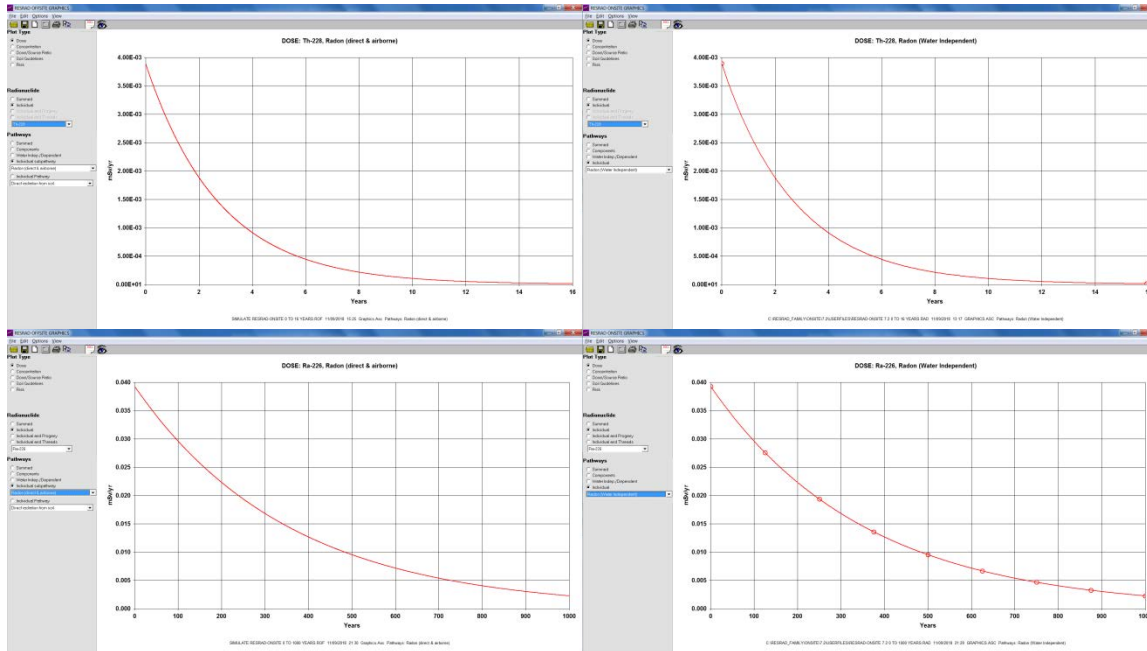
Figure K-22 Dose from Inhalation of Radon Progeny, Water Independent

4. In this scenario, no differences of consequence were observed between the outputs of the two codes in dose from the ingestion of vegetables contaminated by root uptake from the primary contamination and by translocation of particulates deposited on the leaves (Figure K-23). This will be the case provided the contribution of the foliar deposition and translocation contamination pathway is very small compared with the contribution of root uptake contamination pathway and the condition in Item 1 is satisfied. If the farmed land overlaps the primary contamination, foliar deposition is not modeled by RESRAD-OFFSITE because the current formulations of atmospheric transport apply only to receptor locations that do not overlap with the primary contamination.
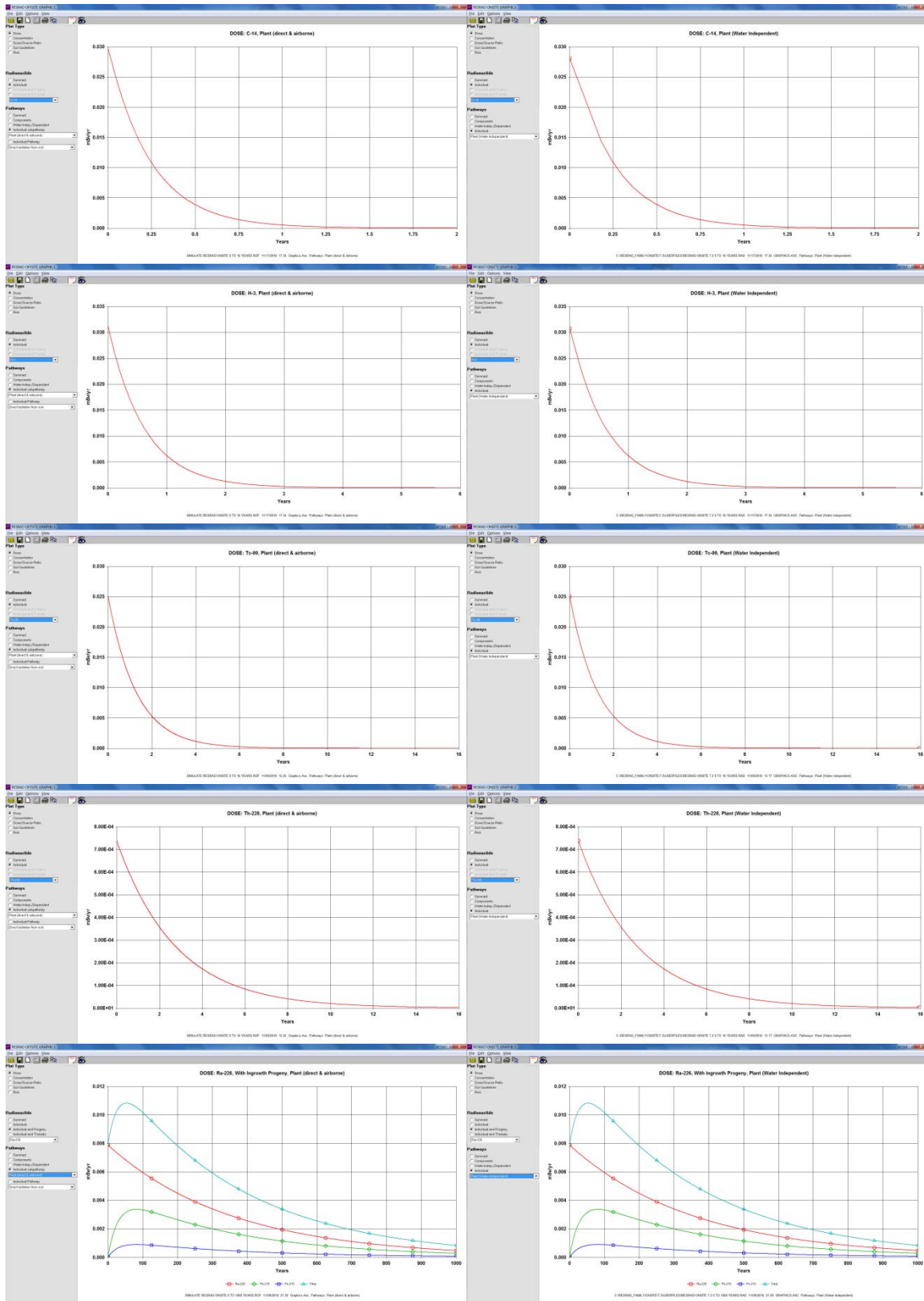
Figure K-23 Dose from Ingestion of Vegetables, Water Independent

5. In this scenario, no differences of consequence were observed between the outputs of the two codes in dose from the consumption of meat (Figure K-24) and milk (Figure K-25) from livestock that ingested feed contaminated by root uptake from the primary contamination and by translocation of particulates deposited on the leaves and ingested soil from the primary contamination. This will be the case provided the contribution of the foliar deposition and translocation contamination pathway is very small compared with the contribution of root uptake contamination pathway and the contribution of the soil ingestion contamination pathway, and the condition in Item 1 is satisfied. If the farmed land overlaps the primary contamination, foliar deposition is not modeled by RESRAD-OFFSITE because the current formulations of atmospheric transport apply only to receptor locations that do not overlap with the primary contamination.

6. In this scenario, no differences were observed between the outputs of the two codes in dose from the incidental ingestion of soil from the primary contamination (Figure K-26). This will be the case provided there is no cover and the condition in Item 1 is satisfied. The outputs will differ when a cover is present because of the differences in how the codes model the concentration in the mixing layer.

    In the subpathways termed "water independent" in RESRAD-ONSITE (Figures K-22 through K-26), exposure occurs without the nuclides having to pass through the well or the surface water body. The exposure subpathways termed "water dependent" in RESRAD-ONSITE (Figures K-28 through K-31) are so termed because the radionuclides pass through either the well or the surface water body before impacting the receptor.
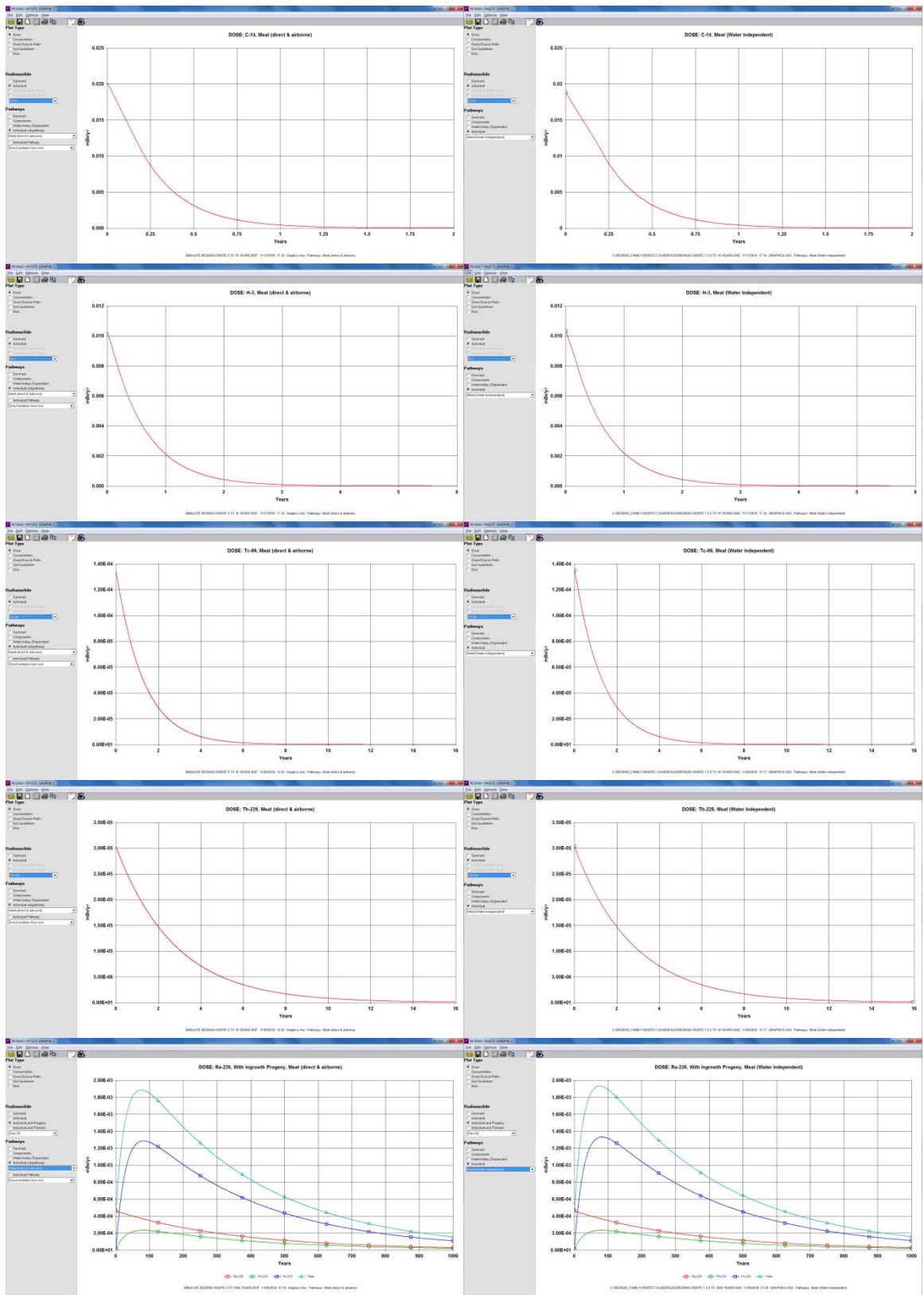
Figure K-24 Dose from Ingestion of Meat, Water Independent
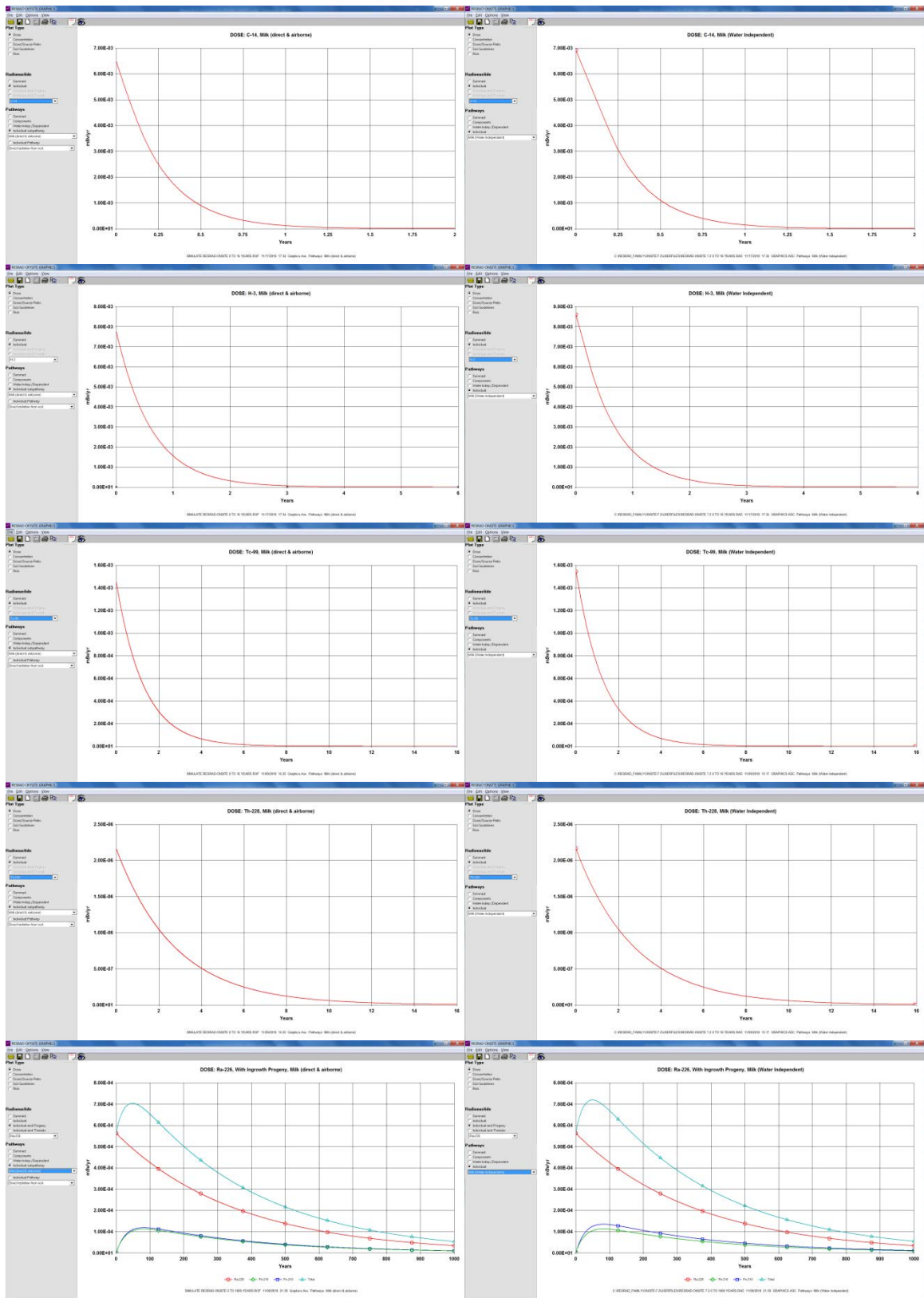
Figure K-25 Dose from Ingestion of Milk, Water Independent
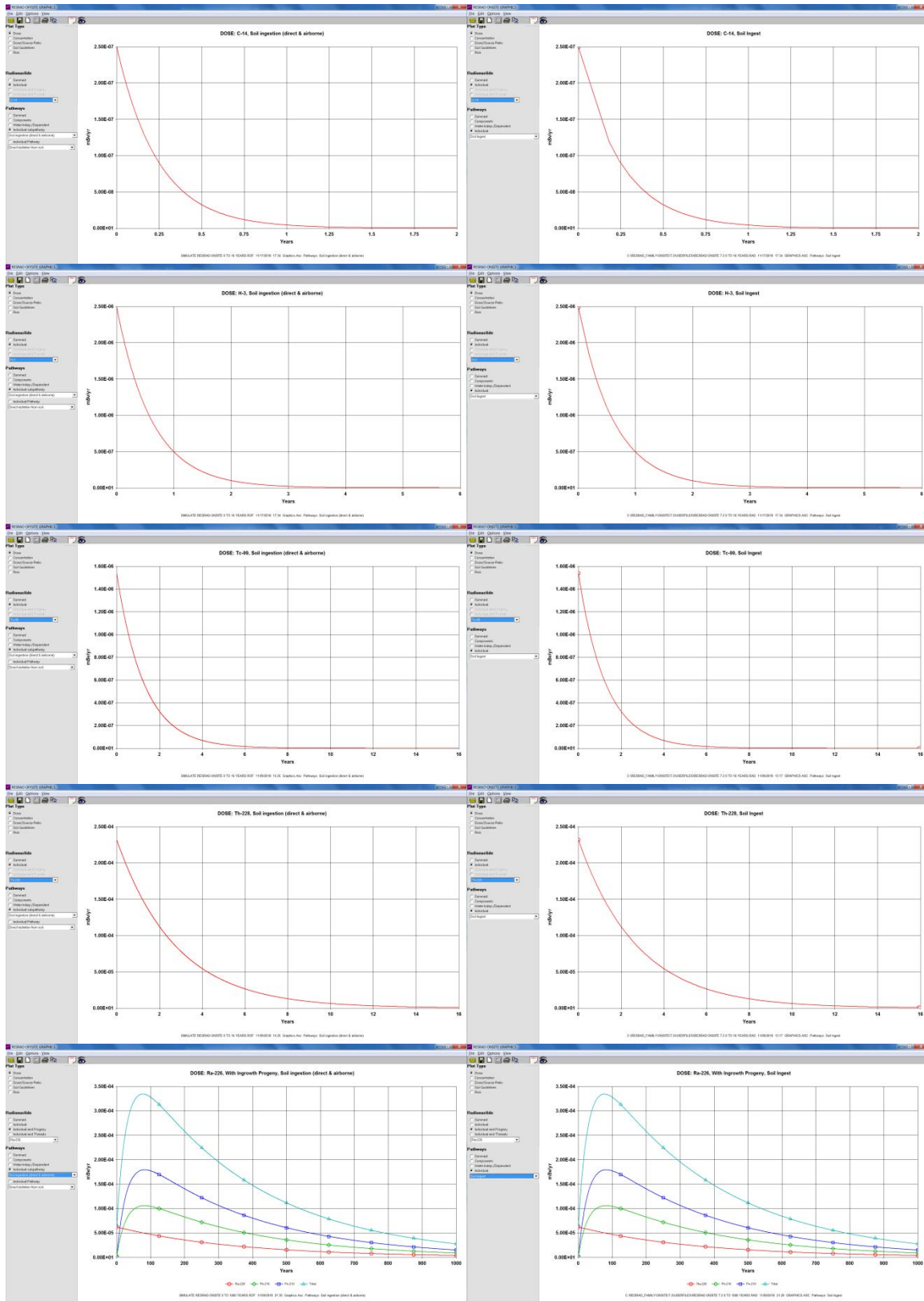
Figure K-26 Dose from Ingestion of Soil, Water Independent

7. For this scenario, no differences of consequence are observed in the outputs of the two codes from the ingestion of well water (Figure K-27). This will be the case provided sufficient computational time points are used to capture the variation of the leaching release from the primary contamination and the conditions in Item 11 regarding progeny transport are satisfied. A total of 4,096 computational time points were used over the 16-year time horizon for the radionuclides whose release changes rapidly, especially for carbon-14, which was completely released from the contaminated zone within a year in this example.

Figure K-27   Dose from Ingestion of Well Water

8. For this scenario, no differences are observed in the outputs of the two codes from the inhalation of the short-lived progeny of radon that was released in the dwelling from well water used for household purposes, mainly showering (Figure K-28). This will be the case provided sufficient computational time points are used to capture the variation of the leaching release from the primary contamination.
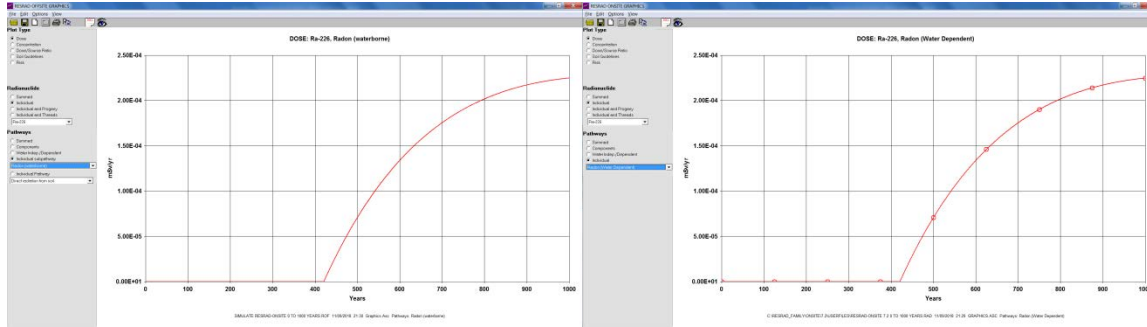
Figure K-28 Dose from Inhalation of Radon Progeny, Water Dependent

9. For three of the radionuclides in this scenario, there are significant differences between the outputs of the two codes in dose from ingestion of vegetables (Figure K-29), meat (Figure K-30), and milk (Figure K-31) contaminated by radionuclides that passed through well water. There are no differences of consequence in the case of one radionuclide in this scenario. The vegetables were contaminated by irrigation water from the well, while the meat and milk were contaminated by the livestock ingesting well water and feed that was irrigated with well water.

    The vegetables and the livestock feed are contaminated in two ways if irrigation is applied by sprinklers. The contaminated irrigation water can be intercepted by the foliage, then the radionuclides in the intercepted water can be translocated to the edible part of the plant. The remainder of the irrigation water falls to the ground and the radionuclides accumulate in the soil; these can be taken up through the roots.

    Accumulation in soil is modeled differently in the two codes. RESRAD-ONSITE uses the leach rate estimated with the entire thickness of the primary contamination (2 m in this example scenario), while RESRAD-OFFSITE uses the leach rate corresponding to the thickness of the mixing layer (0.15 m in this example). RESRAD-ONSITE models the accumulation over a layer of surface density 225 kg/m^2, while RESRAD-OFFSITE models the accumulation over a mixing layer of the specified thickness and density. RESRAD-OFFSITE also models ingrowth and decay during accumulation and losses due to erosion. RESRAD-ONSITE models the accumulation over a single growing season, while RESRAD-OFFSITE models the accumulation from time zero over multiple growing seasons. RESRAD-OFFSITE spreads out the input of radionuclides in the irrigation over the entire year rather than modeling it as a periodic, shorter- term input over the growing season. Because of these differences, the outputs from both codes are expected to agree only when the contribution of the root uptake pathway is insignificant compared with the contribution of the foliar interception contamination pathway.
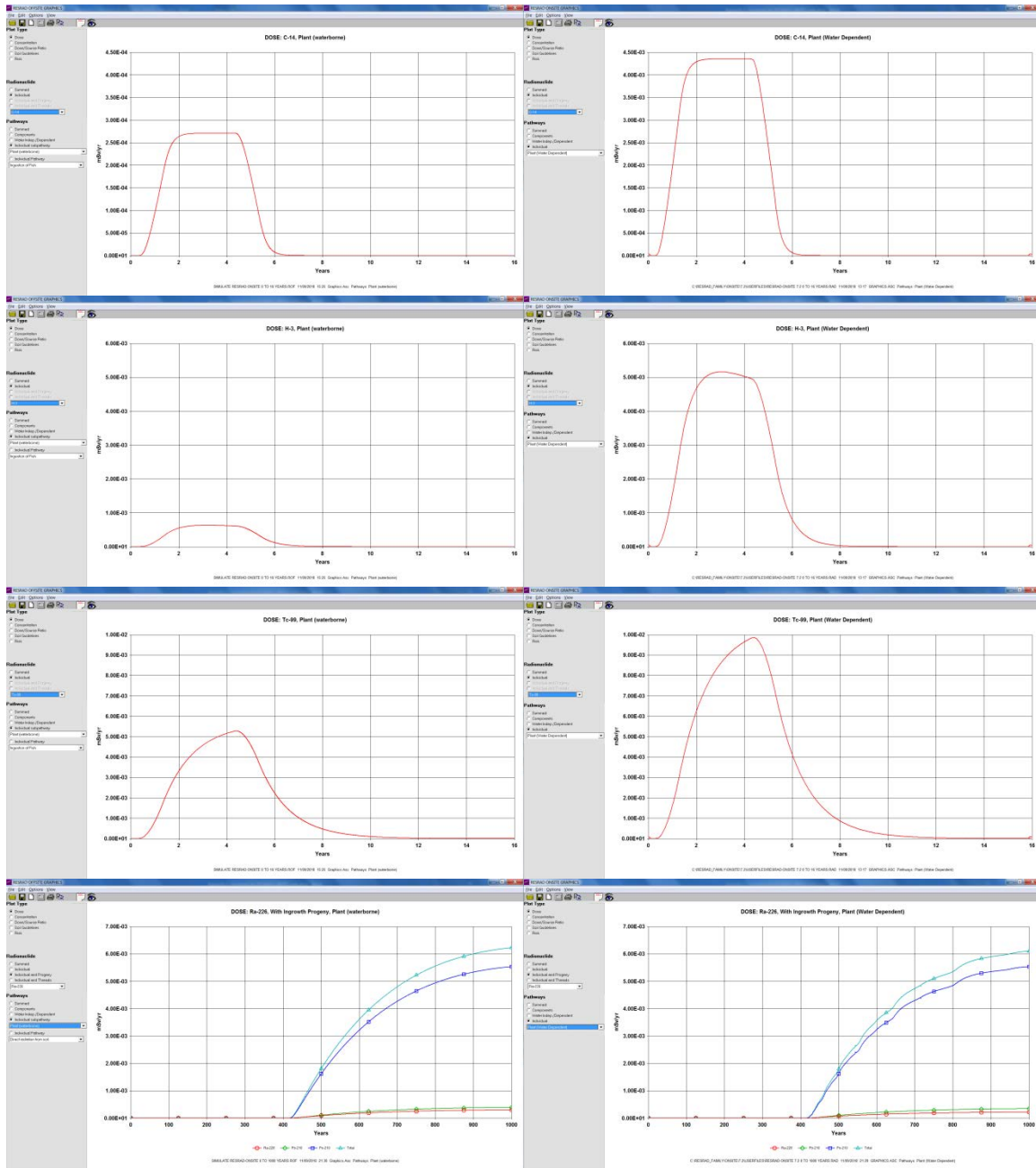
Figure K-29 Dose from Ingestion of Vegetables, Water Dependent

K-25

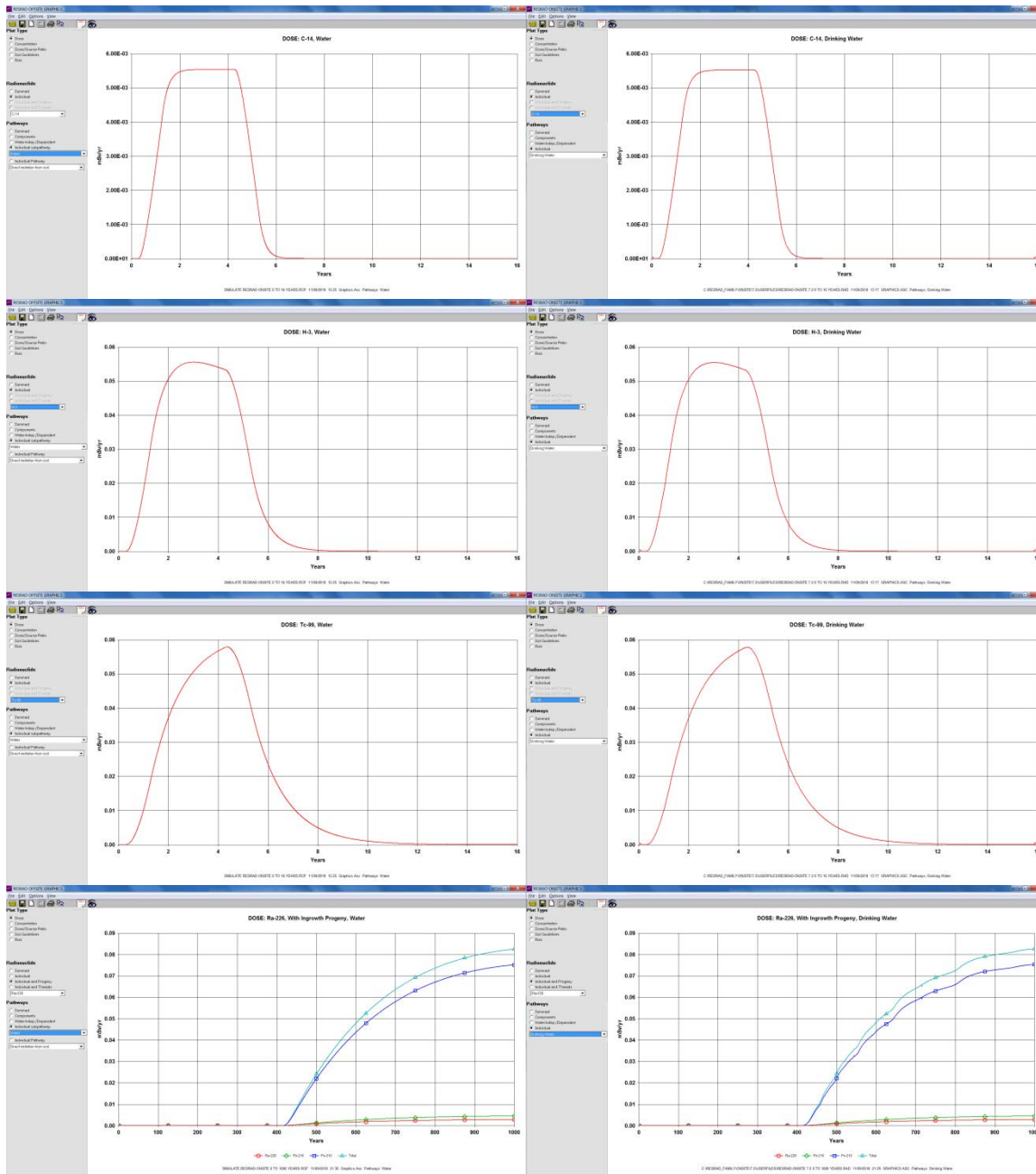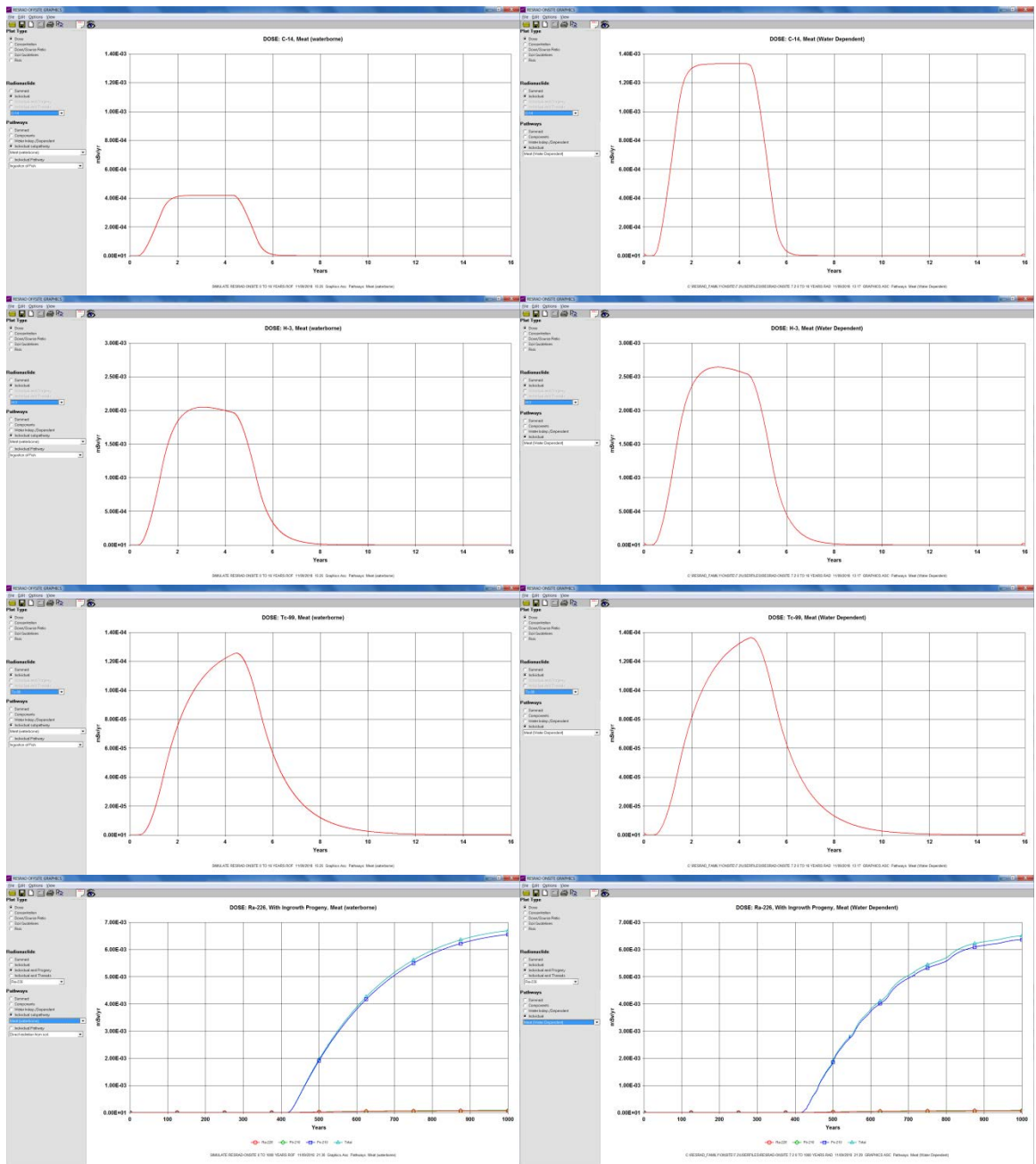**Figure K-30 Dose from Ingestion of Meat, Water Dependent**
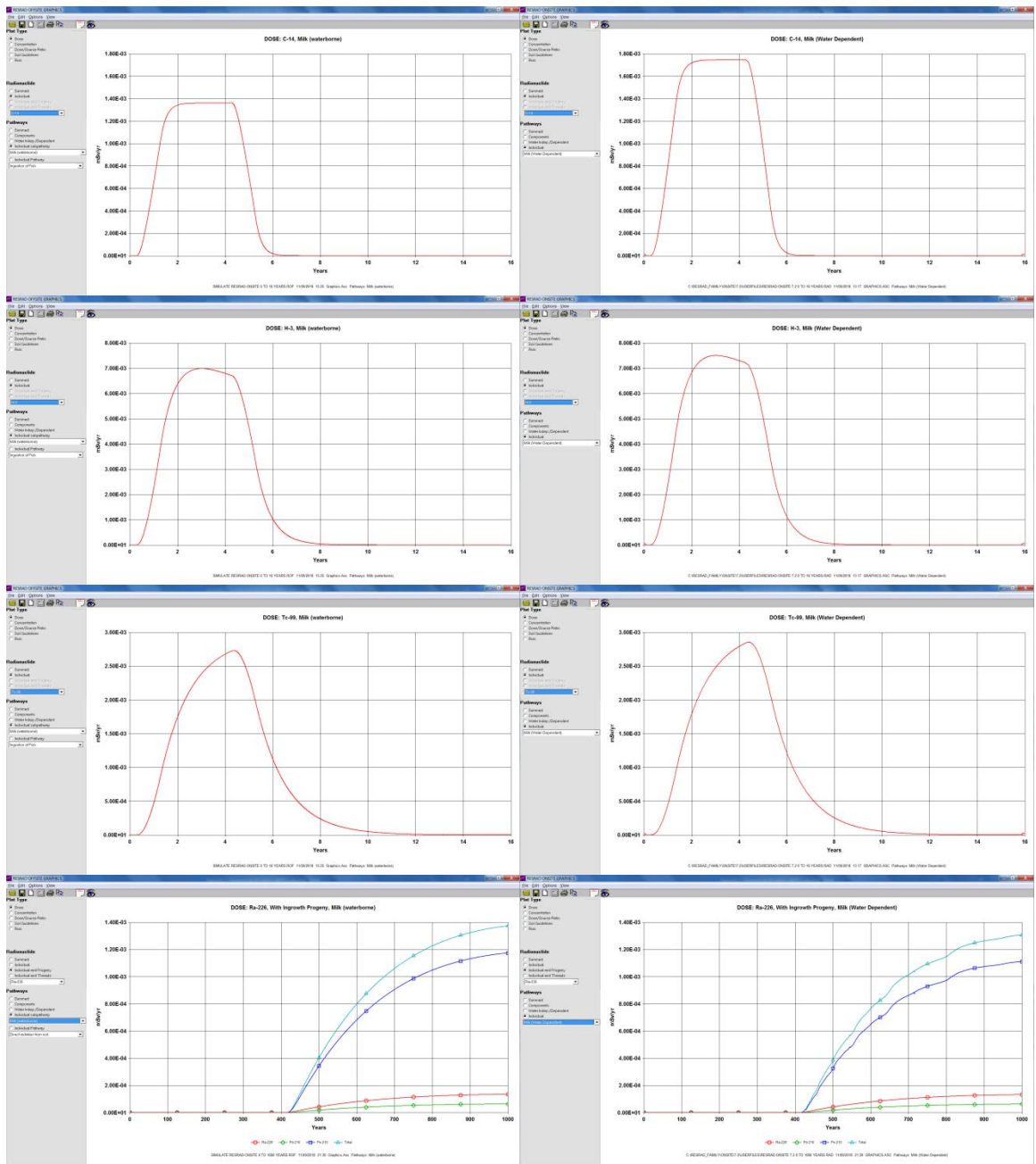
Figure K-31 Dose from Ingestion of Milk, Water Dependent

10. There are significant differences in the outputs of the two codes for all of the radionuclides in this scenario for the doses from the ingestion of aquatic food (Figure K-32). Two classes of aquatic organisms are considered: fish and mollusks and crustaceans. The concentration of radionuclides in each class of aquatic organisms is modeled as being in proportion to the concentration of the radionuclide in the surface water body. The two codes model the concentration in the surface water body differently (Section J.2 of this manual and Section E.3.2.3 of the User's Manual for RESRAD Version 6), leading to the difference in the doses from the ingestion of aquatic organisms.
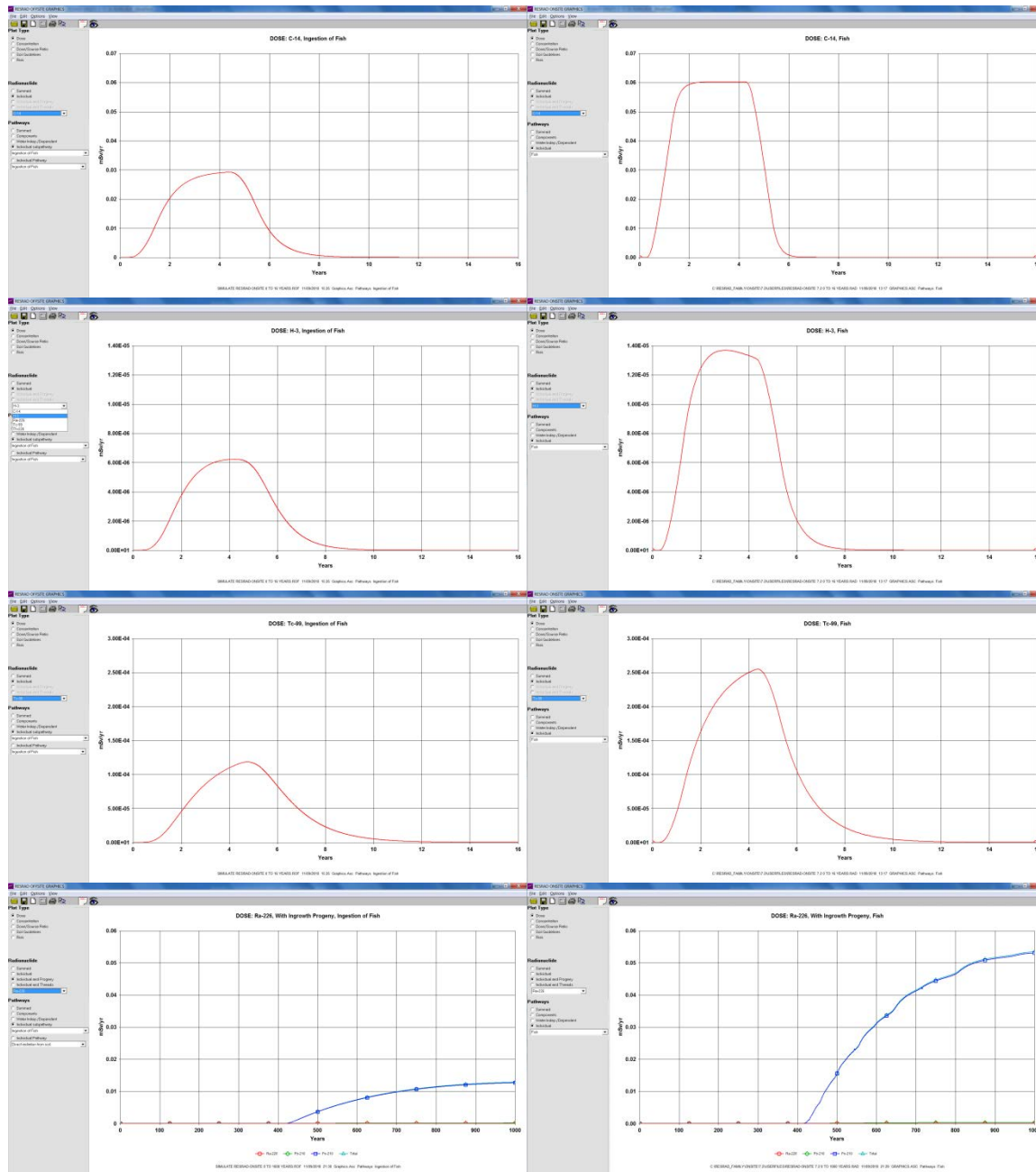
Figure K-32 Dose from Ingestion of Aquatic Food

11. In addition to the reasons discussed in items 1 through 10, the outputs of the two codes can differ for the following reasons:

a.) Transport of progeny produced during the transport of a parent radionuclide. When simulating RESRAD-ONSITE, the RESRAD-OFFSITE code solves the same set of equations for advective transport with solute soil interaction as RESRAD-ONSITE does, but the solutions are arrived at differently in the two codes.

In RESRAD-ONSITE, the explicit analytic expressions for the concentration in water in either the well or the surface water body are derived with the assumption that the ratio of the transport velocities of parent and progeny radionuclides are the same in all the layers of soil through which they travel from the primary contamination to the source of water. The concentrations are computed by evaluating (convolving) the expressions numerically. The advantage of this solution is that the concentration in water at any time can be evaluated without having to evaluate the fluxes through the intervening layers in the preceding times.

RESRAD-OFFSITE models the transport of radionuclides layer by layer. The temporal variation of the flux across each layer must be determined in order to compute the concentration in well water. The accuracy of this computation depends on the number of time points used to calculate the temporal flux across each layer. The advantage of this approach is that it is not necessary to assume that the ratio of the transport velocities of the parent and progeny remains the same in each layer through which they travel. When computing the concentration of the radionuclides in the surface water body, the RESRAD-OFFSITE code considers both dilution and accumulation. The dilution is modeled differently in the two codes.

The well water-related output of the two codes will agree provided the ratio of the transport velocities of the parent and progeny radionuclides are the same or are almost the same in each transport layer and sufficient computational time points are used in RESRAD-OFFSITE. The surface water-related output of the two codes are not expected to agree.

b.) Time-integrated dose. Both codes output the dose rate integrated over a period of a year, but the time integration is performed differently in the two codes.

RESRAD-ONSITE begins by evaluating the dose rates at the beginning, middle, and end of the one-year time period to obtain the first estimate of time-integrated dose over that year. It then evaluates the dose rate at the midpoints of the two half-year intervals (i.e., at the quarter points) to get a better estimate. If the first two estimates do not agree within a specified limit, it then uses the dose rates at the eighth points to get an even better estimate of the time-integrated dose. It can use up to 17 points at 1/16th-year intervals, if necessary, to evaluate the time-integrated dose.

As stated in Chapter 4, RESRAD-OFFSITE will first evaluate the dose rate at each of the computational time points. It will then use the dose rates at all the time points that fall within a one-year interval of a time point, including the dose rate at the end of the one-year interval, to evaluate the time-integrated dose over the year. If a time point does not occur at the end of the one-year interval, it will estimate the dose rate at that end of the one-year interval using the dose rates at the two times surrounding it.

The outputs of the two codes will differ if an insufficient number of computational time points are used in RESRAD-OFFSITE to model the variation of the dose rate over time or if dose is to be evaluated within the longest cumulative storage time in RESRAD-ONSITE (see Section 4.15 of the RESRAD-ONSITE User's Guide).

c.) Contaminated fraction of vegetables, meat, and milk. The fraction of food produced at the contaminated site can either be input into RESRAD-ONSITE or the code can be flagged to compute this fraction based on the area of the primary contamination. The fraction of food produced at the site must be input into RESRAD-OFFSITE. The values to be input can be obtained using equations in Section D.2.1.2 of the User's Manual for RESRAD Version 6. A better alternative would be to input the appropriate values for the fractions of the agricultural areas and the livestock feed growing areas that are directly above the primary contamination in the corresponding forms in RESRAD-OFFSITE, taking into account whether the farmed areas overlap with each other. Then the RESRAD-OFFSITE code will limit the modeling of root uptake from the primary contamination to those fractions of the vegetables and animal feed grown on the land that is directly above the primary contamination, while modeling contaminated irrigation to the all the vegetables and animal feed grown at the site. These differences in modeling the vegetable, meat, and milk can cause the outputs to be different if the area of contamination is small.

d.) Resetting distribution coefficients when a leach rate is specified. The RESRAD-ONSITE code will reset the distribution coefficients in the transport zones and in the contaminated zone if it accepts the user input leach rate. The RESRAD-OFFSITE code uses the user-specified values of distribution coefficient and does not reset them. This can lead to differences in the output of the two codes.

e.) Modeling a falling water table. RESRAD-OFFSITE does not model a falling water table, while RESRAD-ONSITE does. The water table drop rate is set to zero in RESRAD-ONSITE in the example. If the scenario requires modeling a falling water table, the output from the two codes is likely to differ.

K.2   Relationships between Inputs Specified in the Computational Code When Simulating RESRAD-ONSITE

The properties of the offsite receptor locations are related to the properties of the primary contamination in both the interface and the computational code. The latter is necessary to perform sensitivity and probabilistic analysis. The relationships specified in the computational code are described in this section.

1.   The distribution coefficients of each radionuclide in the four farmed areas (the fruit, grain, and nonleafy vegetable growing area; the leafy vegetable growing area; the pasture and the silage growing area; and the livestock feed grain growing area) are set to the value specified for the primary contamination.

2.   The irrigation applied over a year to each farmed area is obtained by multiplying the irrigation applied over a year at the primary contamination and the duration of the growing season in the farmed area.

3. The evapotranspiration coefficient, the runoff coefficient, the depth of the soil- mixing layer or the plow layer, the slope length steepness factor, the cover and management factor, and the support factor for the farmed areas are set to the values for the primary contamination.

4. The dry bulk density, the soil erodibility factor, the volumetric water content, and the total porosity of the farmed areas are set to the values for the cover if the non-zero initial thickness of the cover is at least as large as the depth of mixing layer. Otherwise, the first two properties are set to the average value of those properties over the mixing layer, while the remaining three properties are set to the values for the contaminated zone.

5. The depth of aquifer flowing into the surface water body is set to the value of the depth of aquifer intercepted by the well. The hydraulic gradient from the primary contamination to the surface water body is set to the hydraulic gradient from the primary contamination to the well.

6. The potential evaporation from the surface water body is set to the value of precipitation.

7. The weathering removal constant and the root depths of the leafy vegetables, pasture and silage crops, and the livestock feed grain are all set to the values for the fruit, grain, and nonleafy vegetables. The wet-weight crop yield, duration of the growing season, foliage to food transfer coefficient, foliar interception factor for irrigation, and foliar interception factor for dust for livestock feed grain are set to the values for pasture and the silage crops.

K.3   Reference

Kamboj, S., E. Gnanapragasam, and C. Yu, 2018, *User's Guide for RESRAD-ONSITE Code*, ANL/EVS/TM-18/1, March.

APPENDIX L:
THE ONSITE SCENARIO TEMPLATE

This menu option in RESRAD-OFFSITE facilitates modeling of onsite exposure scenarios using all the applicable release, transport, accumulation, and exposure models in the code. When this menu option is selected, the code queries the user for the dimensions of the primary contamination and does the following to maximize the overlap between the farmed lands and the primary contamination:

- If the sum of the areas of the farmed lands is less than or equal to the area of the primary contamination, the farmed lands are placed centrally over the primary contamination.

- If the sum of the areas of the farmed land is greater than the area of the primary contamination, the farmed lands are placed so that each farmed land overlaps the primary contamination to the same extent.

- The well and the surface water body are placed at the down-gradient edge of the primary contamination.

- The occupancies are set to reflect onsite exposure.

The implementation of this menu option is illustrated in Section L.1. The exposure sub-pathways and processes that are modeled when using this menu option are discussed in Section L.2.

L.1   Illustration of the Onsite Scenario Template

A 150-m by 175-m parcel of land is contaminated. The receptor spends half of the time indoors in a dwelling on the primary contamination area and a quarter of the time outdoors on the primary contamination area tending to the farmed lands.

L.1.1   Onsite Scenario Specific Input Forms

1.   The File menu command is used to activate the onsite scenario template. The Onsite Scenario Primary Contamination form (Figure L-1) will pop up to solicit the user input of the horizontal dimensions of the primary contamination. When this form is saved, the code uses the dimensions to initialize the inputs related to the locations of farmed lands and the sources of water.
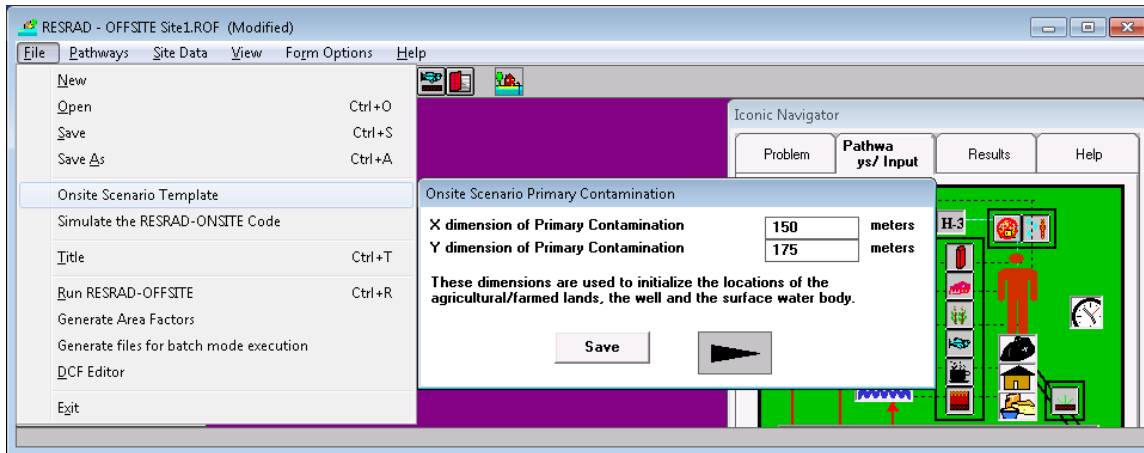
Figure L-1   Activating the Onsite Scenario Template

2.   The code uses the dimensions entered in the Onsite Scenario Primary Contamination form to initialize the placement of the farmed lands, the surface water body, and the well (Figure L-2). These initial placements will be overridden by any changes that are made in any of the input forms.
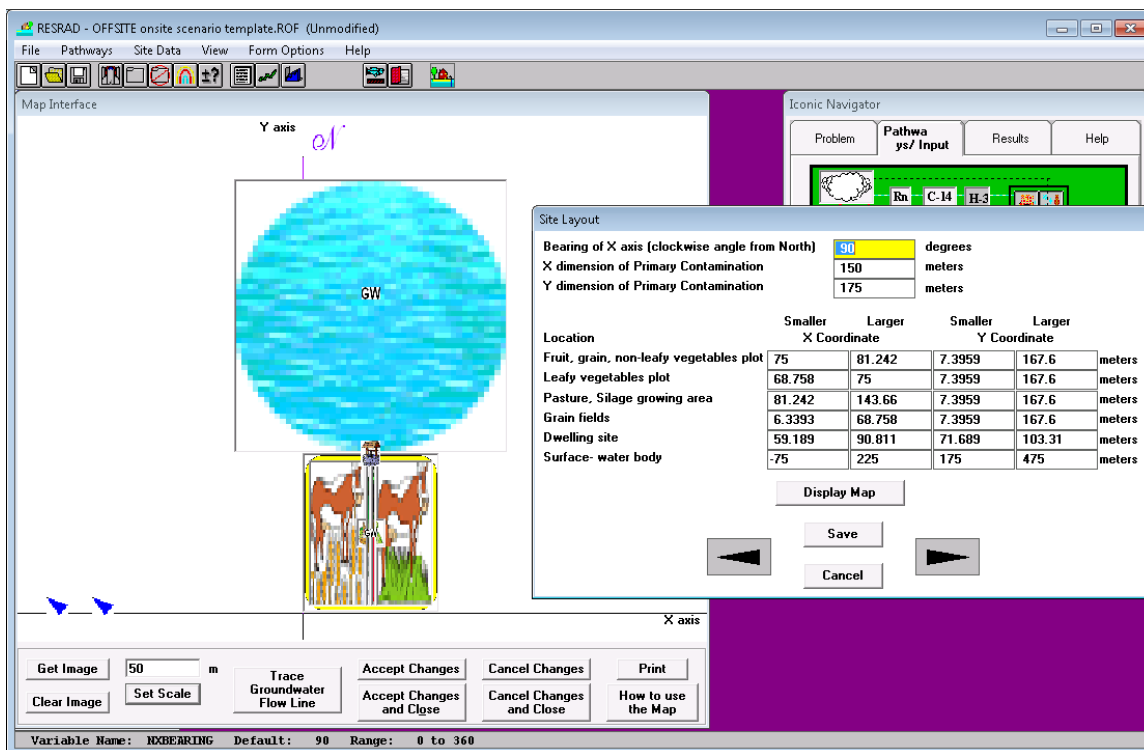
Figure L-2   Site Layout Form and the Map Interface Initialized by the Onsite Scenario Template

L-2

The area of the primary contamination in this example, 26,250 square meters, is larger than the sum of the default areas of the farmed lands, 22,000 square meters. In this case, the code initializes the farmed lands centrally within the primary contamination; with the farmed lands having the same Y dimension and with the smaller vegetable growing areas located closest to the center of the primary contamination (Figure L-2) for reasons discussed in Item 1 of Section L.2. The user can change the locations and sizes of the farmed lands.

If the area of the primary contamination were to be less than the sum of the default areas of the farmed lands as in the figure below (Figure L-3), the code will initially place the farmed lands such that they all extend out of the primary contamination to the same extent, away from the water sources.
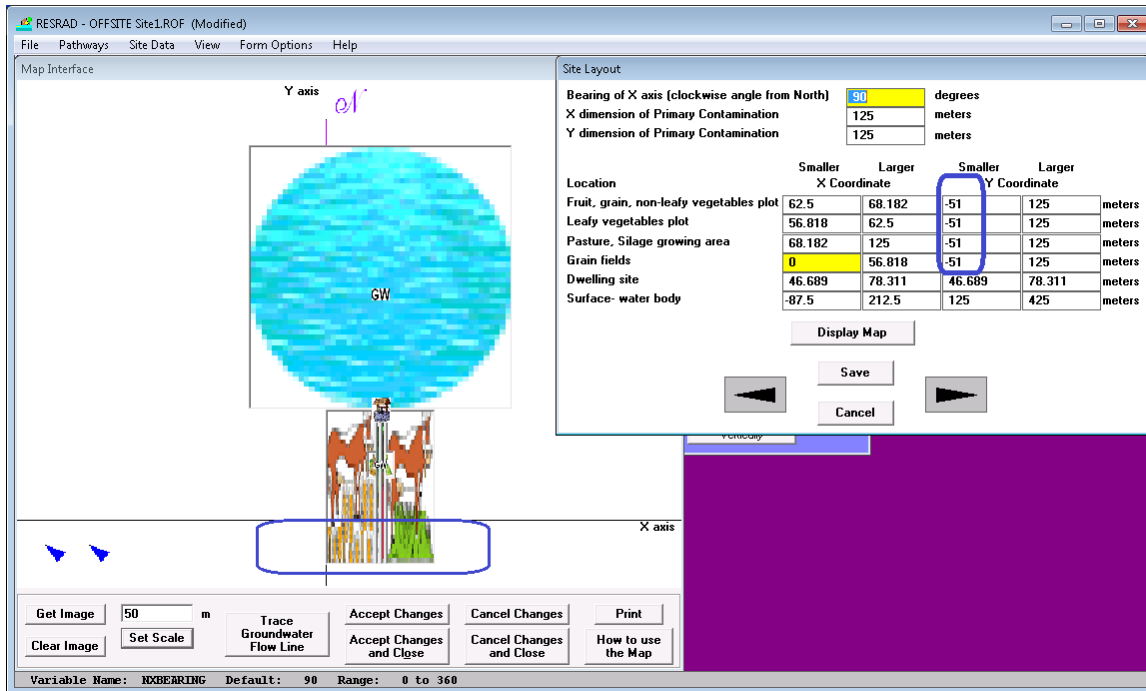
Figure L-3   Placement of Farmed Lands When Larger than the Primary Contamination

3.   The code initializes the "length of contamination parallel to the aquifer flow" to the Y dimension as the default groundwater flow is to the North (Figure L-4). It also initializes the area of the primary contamination. The area may be shown to two significant digits as the External Radiation Shape and Area Factors form determines the area of the primary contamination graphically, and not analytically, to this precision. The code recalculates these two values when changes made in the map interface to the direction of groundwater flow and/or the dimensions of the primary contamination. These are shown to a higher precision. The user can input a value for the length of contamination parallel to the aquifer flow.

The entries in the External Radiation Shape and Area Factors form are also initialized by the code. These are updated when changes are made in the Site Layout form or the Map Interface.
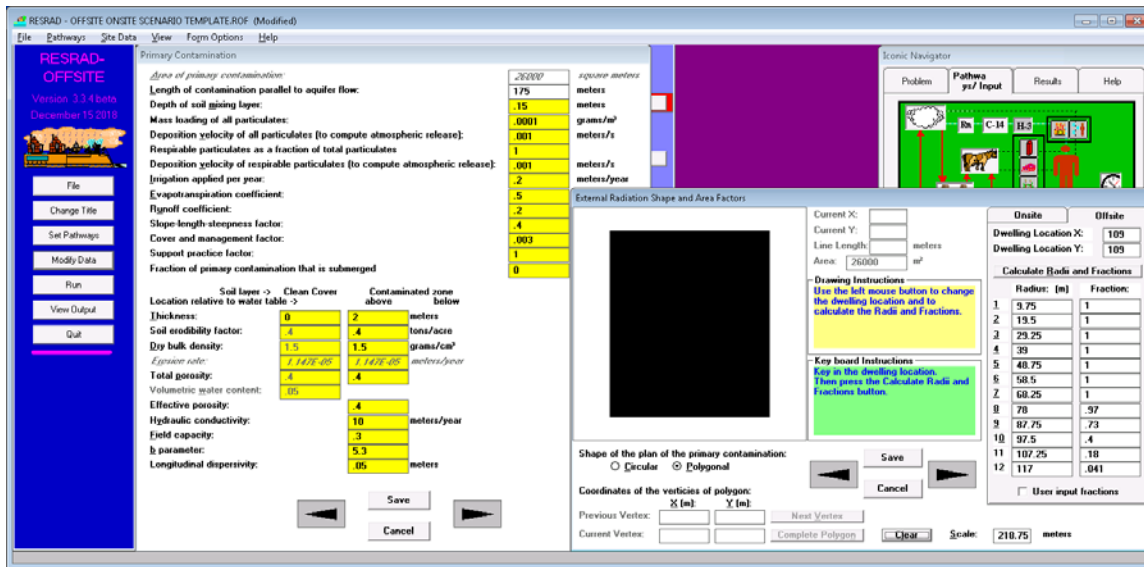
Figure L-4   Primary Contamination Form and the External Radiation Shape and Area Factors Form Initialized by the Onsite Scenario Template

4. The code initializes the overlap between each farmed land and the primary contamination (Figure L-5), assuming that all four farmed lands overlap the primary contamination to the same extent as shown in the initial layouts in Figures L-2 and L-3. If the locations and or the dimensions of the farmed lands or the primary contamination are changed, the code will recalculate the overlaps based on the new dimensions and locations. The user can input values for the fraction of area directly over the primary contamination to override the calculated values.
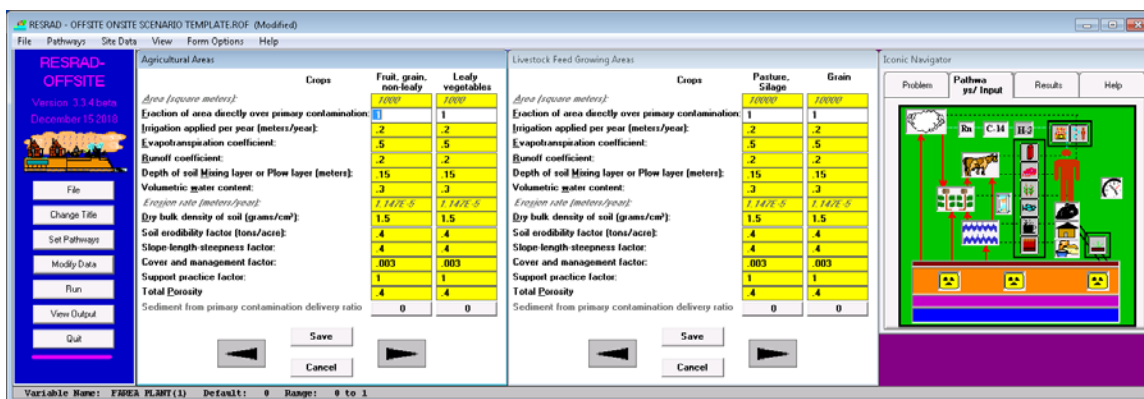
Figure L-5   Physical and Hydrological Properties of Farmed Lands Intialized by the Onsite Scenario Template

The contamination by root uptake from the primary contamination is modeled for the fraction of vegetables and livestock feed grown on the overlapping regions. The contamination by root uptake following accumulation in the soil due to contaminated irrigation and by foliar interception of irrigation water followed by translocation to the edible

L-4

part of the plant are modeled for the vegetables and livestock feed regardless of where it is grown. Because the atmospheric transport is not currently modeled when the agricultural land and primary contamination overlap, contamination by foliar interception of dust followed by translocation is not modeled if the fraction of area directly over the primary contamination is greater than zero.

5. The joint frequencies of wind speed, atmospheric stability, and wind direction are set to give a mean wind speed of 2 m/s (Figure L-6). The mean wind speed will be calculated when site-appropriate data is used. The other inputs in the Atmospheric Transport form are used to model the atmospheric transport to, and the deposition over, the catchment. They will also be used if any of the agricultural lands are entirely outside the primary contamination.
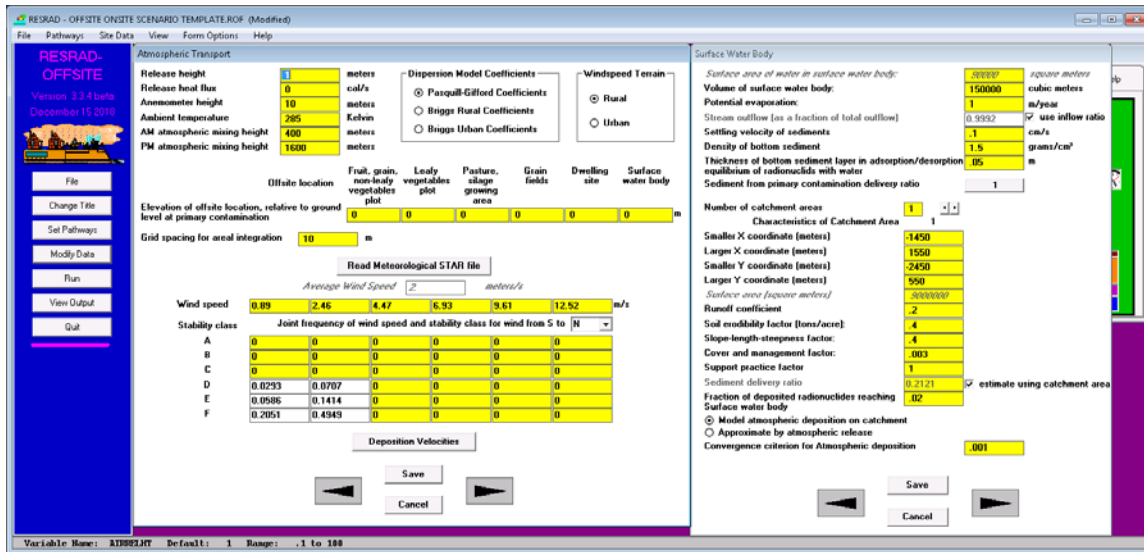
Figure L-6   Atmospheric Transport Form and the Surface Water Body Form Intialized by the Onsite Scenario Template

6. The dispersivities in the saturated zone are initialized based on the average transport distance to the onsite sources of water (Figure L-7). These values are not updated for any changes made in the Site Layout form or the map interface. The user can enter site-appropriate values for these dispersivities.

    The two sources of water, the well and the surface water body, are placed at the down-gradient edge of the primary contamination (Figure L-7). The lateral transport distances to the edges of the surface water body are also initialized. These values are updated based on changes made in the map interface.
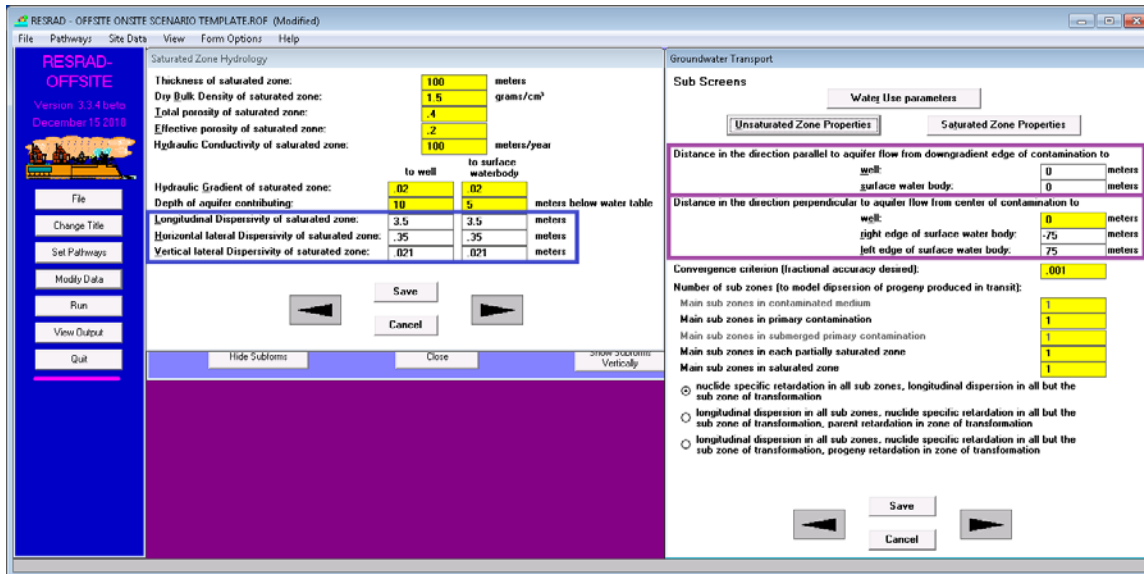
Figure L-7 Saturated Zone Hydrology Form and Groundwater Transport Form Initiallized by the Onsite Scenario Template

7. The occupancies are initialized for onsite exposure (Figure L-8). The outdoor occupancy on the primary contamination could alternatively be distributed between four farmed lands that are situated on the primary contamination. The effects of the choice of how the outdoor occupancy is specified are discussed, among other things, in Section L.2.
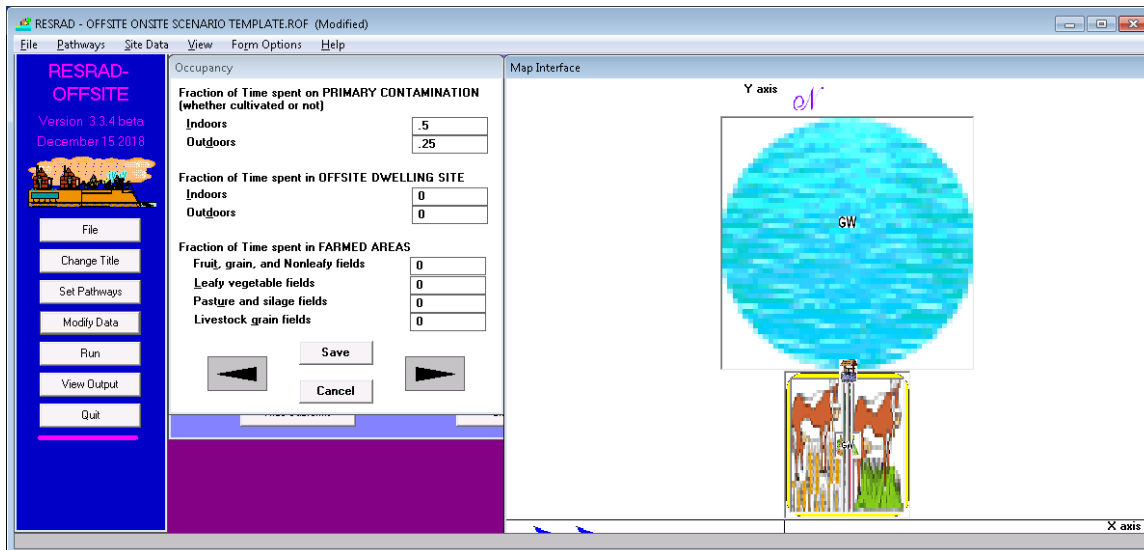
Figure L-8 Occupancy Form Initialized by the Onsite Scenario Template

L.2   Process and Exposure Sub-pathways that Are Modeled when the File Is Created Using the Onsite Scenario Template

1. The **direct exposure from the primary contamination** is computed while indoors and outdoors in the onsite dwelling, outdoors in the farmed lands, and while indoors and outdoors in the offsite dwelling. The receptor is modeled to be at the centers of the dwelling sites or farmed lands for the specified occupancies.

    The onsite scenario template initializes both the onsite and offsite dwellings to the center of the rectangular primary contamination to maximize the computed exposure from direct external radiation. When possible, the four farmed lands are initialized so that their centers have the same coordinate as the center of the primary contamination. The two narrower plots of land where the vegetables are grown are placed close to the center of the primary contamination. The two wider plots of land where the livestock feed is cultivated are placed next to the vegetable plots. This places the centers of the farmed lands as close as possible to the center of the contamination.

2. The **direct exposure from the accumulation in each of the farmlands and in the offsite dwelling site** are computed for the time the receptor occupies that specific farmland, or offsite dwelling site. Accumulation from contaminated irrigation water is modeled for the farmed lands and the offsite dwelling. Accumulation from deposition of particulates transported by air from the primary contamination is modeled if the farmed land or the offsite dwelling site does not overlap the primary contamination. Accumulation on the onsite dwelling site is not modeled.

3a. The exposure from the **inhalation of respirable particulates from the surface layer at the primary contamination** while indoors and outdoors at the onsite dwelling is modeled.

3b. The exposure from the **inhalation of respirable particulates transported from the surface layer at primary contamination** to the offsite dwelling and to the farmed lands by air is modeled, provided that the farmed land or the offsite dwelling does not overlap the primary contamination.

4. The exposure from the **inhalation of respirable particulates re-suspended from accumulation in the offsite dwelling and the farmed lands** is modeled for the occupancy specified for that location. The situations for which accumulation is modeled are described in Item 2 above.

5a. The exposure from the inhalation of short-lived radon progeny from radon released from the primary contamination is modeled while indoors and outdoors at the onsite dwelling.

5b. The exposure from the **inhalation of short-lived progeny of radon released from the primary contamination and transported by air** to the offsite dwelling and the farmed lands by air is modeled, provided that the farmed land or the offsite dwelling does not overlap the primary contamination.

6. The exposure from the inhalation of short-lived progeny of radon release from accumulation of the radon precursors in the offsite dwelling site and the farmed lands is modeled for the occupancy specified for that location. The situations for which accumulation is modeled are described in Item 2 above.

7. The exposure from the inhalation of short-lived progeny of radon released from the water used inside the onsite and offsite dwellings is modeled.

8. The exposure from the **incidental ingestion of soil from the surface layer at the primary contamination** while indoors and outdoors at the onsite dwelling is modeled.

9. The exposure from the **incidental ingestion of soil from the accumulation at the offsite dwelling site** while indoors and outdoors is modeled. The situations for which accumulation is modeled are described in Item 2 above.

10. The exposure from the **incidental ingestion of soil from the accumulation at the agricultural lands** while outdoors is modeled. The situations for which accumulation is modeled are described in Item 2 above.

11. The exposure from the **ingestion of water from a contaminated well or contaminated surface water body** is modeled. The contamination of the well water by radionuclides that were leached by the infiltration through the primary contamination and the contamination of the surface water by radionuclides leached by the infiltration through the primary contamination by radionuclides in the material eroded by runoff from the primary contamination, and by radionuclides in particulates transported by air are modeled.

12. The exposure from the **ingestion of vegetables, meat, milk, and aquatic food** is modeled. The process by which these foods are contaminated are described in the next few items.

13. Contamination of plant food: (a) Root uptake of radionuclide from the primary contamination is modeled for the plants that are grown in part of the farmed land that overlaps the primary contamination. (b) Foliar interception of particulates released from the primary contamination and transported to the farmed land is modeled only if the farm land and the primary contamination overlap. (c) Foliar interception of contaminated irrigation water is modeled regardless of where the plant is grown. (d) Root uptake of radionuclides from the accumulation in the farmed land is modeled. The accumulation in the farmed land is modeled as described in Item 2 above.

14. Contamination of meat and milk: Contamination of meat and milk following ingestion of contaminated water, ingestion of contaminated feed, and ingestion of soil with the animal feed are modeled. The contamination of feed is modeled as described in Item 13 above. The contamination of soil in the farmed land is modeled as described in Item 2 above, with the additional consideration of the concentration in the surface layer of the primary contamination for the part of the farm land that overlaps the primary contamination.

APPENDIX M:
EXAMPLE APPLICATIONS AND BENCHMARKING
WITH DUST-MS OF THE SOURCE TERM MODEL

The source term model in the RESRAD-OFFSITE code Version 4.0 was updated with several new features that allow it to more comprehensively analyze potential releases of radionuclides from the source term to the surrounding environment. This appendix provides eight example applications to demonstrate the use of the new features to evaluate potential human health risks associated with disposal of radioactive wastes. In addition to the example applications, this appendix also documents the comparison of radionuclide release rates predicted by the source term model for each of the eight example applications with the radionuclide release rates predicted by DUST-MS, a computer code with similar functions to the RESRAD-OFFSITE source term model. The added flexibility and more complex source term models in RESRAD-OFFSITE could also be used to derive clean-up levels for complex decommissioning sites including sites with (1) complex source terms, (2) critical receptor groups located offsite, and (3) restricted release sites.

M.1   Features of the RESRAD-OFFSITE Source Term Model

The source term model of RESRAD-OFFSITE tracks the inventory of radionuclides remaining in the original source and provides estimates of radionuclide release rates from the contaminated zone to the surrounding environment as time progresses. The releases of radionuclides from the contaminated zone to the surrounding environment are modeled for the following mechanisms: (1) resuspension, (2) evaporation (for H-3), volatilization (for C-14) or emanation followed by diffusion (for radon), (3) erosion, and (4) leaching. Only radionuclides that are not shielded from interaction with the surrounding environment are susceptible to being released from the contaminated zone and are referred to as "releasable."

Before Version 3.1, the source term considered by RESRAD-OFFSITE is the entity of soil within the volume of the contaminated zone that contains radionuclides distributing homogeneously within its volume. All radionuclides in the soil are considered releasable. In Version 3.1 and the later version, the source term is expanded to include radioactive waste materials that initially could be containerized and/or shielded by engineered barriers and are surrounded by soil in the outside. Under such conditions, the contaminated zone is conceptualized to constitute two domains: the waste domain (including the waste materials and, when applicable, the fill materials within waste containers) and the soil domain (soils that surround the waste materials). Radionuclides initially distribute homogeneously in the waste domain. As long as the containers/barriers remain intact, there is no interaction of the waste materials with the surrounding environment; the fraction of the waste material that is releasable is zero. Over time, some waste containers or engineered barriers would deteriorate or breach, exposing waste materials and radionuclides in the waste materials that are shielded by those containers/barriers to the surrounding environment, rendering them releasable. The cumulative fraction of waste materials becoming releasable would increase with time. The modeling of releases to the surrounding environment via the four mechanisms mentioned above is applied only to the releasable radionuclides in deteriorated/breached containers or engineered barriers.

The updated source term model allows input of up to nine time periods for specifying the change in the cumulative releasable fraction of the source term and provides two options to stipulate the change in releasable fraction between two successive time periods: stepwise at

time vs. linear over time. These input options can be applied to consider the onset of deterioration/breaching in containers or engineered barriers and how the deterioration/breaching of containers progresses over time. For example, when waste materials are contained in multiple containers, the "stepwise at time" option can be applied to consider that containers deteriorate/breach in groups and each group deteriorates/breaches at the same time while the "linear over time" option can be applied to consider containers that deteriorate/breach one by one over time.

While there's no significant change in the modeling of radionuclide releases from the contaminated zone to the surrounding environment via the resuspension, evaporation, volatilization, and emanation followed by diffusion and erosion in the updated source term model, the modeling of radionuclide releases via the leaching mechanism has been improved to be more versatile and comprehensive. The release of radionuclides from the contaminated zone via leaching is modeled as a result of two sequential processes. First, releasable radionuclides transfer to the infiltrating water and are discharged from the initial location in the waste domain (the discharge process). Then radionuclides that are discharged transport from the discharge location to the bottom of the contaminated zone (the transport process). Depending on the mechanism selected for characterizing the discharge of releasable radionuclides in the waste domain after water infiltration, the discharge and transport processes are modeled differently.

The discharge of releasable radionuclides in the waste domain can be characterized as controlled by: (1) first-order dissolution reaction, (2) instantaneous equilibrium desorption, (3) equilibrium solubility, and (4) diffusive transport.

The first option considers the dissolution as a first-order chemical reaction of radionuclides in the waste material with some chemical species in water, and the dissolution rate is linearly proportional to the inventory of releasable radionuclides in the waste materials. The discharge of radionuclides from the initial locations in waste materials is calculated as a function of time with the input first-order rate constant. The second option considers radionuclides, which initially distribute on the surface of the waste materials, that would dissolve in water instantaneously upon contact with water; therefore, the discharge is determined by the amount of radionuclides becoming releasable at any instant. After radionuclides are discharged from their initial locations in the waste material, they would transport with water from the discharge location toward the bottom of the contaminated zone. For transport modeling, the discharge is assumed to distribute evenly along the thickness of the contaminated zone. During the transport process, the discharged radionuclides are considered to redistribute between the surrounding solid materials and water with the redistribution characterized by a sorption-desorption equilibrium constant, Kd. If the waste domain is not conducive, then radionuclides would transport mainly through soils. If the waste domain is conducive, then radionuclides could transport through both soils and materials in the waste domain (including fill materials in containers, if applicable). In the first case, the contaminated zone (i.e., soil) Kd is used to model the transport. In the second case, both the contaminated zone (soil) Kd and the contaminated medium (waste domain) Kd are used to model the transport.

The third option considers that radionuclide concentration in water, no matter if it's in the waste domain or in the soil domain, would not exceed the apportioned limit (calculated by considering the presence of other radioisotopes of the same element) corresponding to the input solubility. As a conservative approach, the radionuclide concentration in leachate (that leaves the contaminated zone) is set to the apportioned limit to calculate a radionuclide discharge rate from the initial locations. The transport that follows the discharge is then considered to go through soils and is modeled with a Kd of 0 g/cm^3 for the radionuclide(s) of concern, so that the loss of

radioactivity due to radiological decay during the transport to the bottom of the contaminated zone is minimized. Under the condition that the solubility is apportioned (almost) entirely to the radionuclide of concern, which has a long radiological half-life, the same radionuclide release rate would persist until the releasable inventory of that radionuclide in the waste domain is depleted.

The last option considers radionuclides in the waste materials would need to diffuse through constrictive channels infiltrated by water in the waste domain to be free for transport. The mathematical equation considering the diffusive transport is solved to obtain the discharge rate of releasable radionuclides, which is then used to model the subsequent transport of radionuclides toward the bottom of the contaminated zone. For this option, the waste domain is not conducive; therefore, discharged radionuclides transport through soils.

Detailed discussions on modeling the discharge and transport processes are provided in Appendix G.

M.2 Site-specific Settings and Disposal Facility Assumed for the Example Applications

For the example applications, different types of radioactive wastes were assumed to be disposed of in a near surface trench that was dug to a depth of 10 m from the ground surface. The trench had a width of 3 m and a length of 40 m. Waste containers were lowered to the trench and were stacked from 5 m to 10 m in depth. Between stacked containers was a layer of backfill soil, which was also used to fill the void space between stacks of containers. After the capacity limit of the trench was reached, the trench was closed and shielded by 5 m of engineered barrier and cover material on the top. See Figure M-1 for a cross-sectional schematic of the waste trench simulated in these benchmarking exercises.
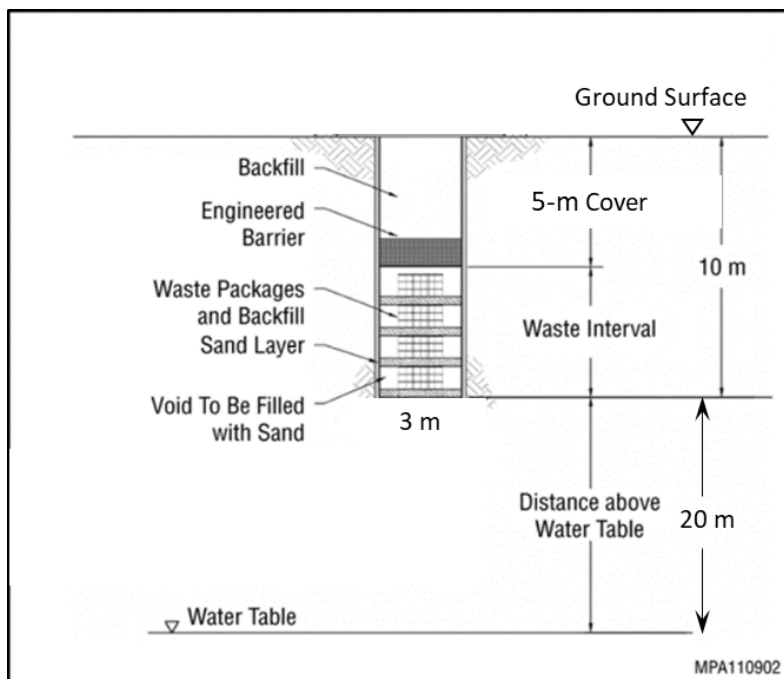
Figure M-1 Cross-sectional Schematic Presentation of the Near Surface Trench Disposal Facility

The disposal facility was assumed to be sited at a location where the annual precipitation rate is 1.2 m, evapotranspiration coefficient is 0.6, and runoff coefficient is 0.22. The groundwater table is 30 m from the ground surface, and the thickness of the groundwater aquifer is 30 m as well. In the RESRAD-OFFSITE analysis, the contaminated zone was placed between 5 and 10 m below the ground surface and assumed an area of 120 m² (3 m × 40 m). The length of the trench parallel to the groundwater flow was 10.95 m. It was assumed that an offsite resident drilled a well at a distance of 300 m from the edge of the disposal facility along the groundwater flow path and the well was the primary source of water. To this offsite resident, the major pathway for potential radiation exposure is through drinking contaminated groundwater, 510 L per year.

Table M-1 lists the site-specific parameters assumed for analyzing the potential groundwater contamination. The soil properties for the unsaturated zone were used for the contaminated zone, except for the thickness, based on the consideration that when the trench was dug, the excavated soil was used as backfill material. The thickness of the contaminated zone was 5 m, with 5 m of cover materials on the top. Input parameters associated with the source term model are discussed in the following sections.

Table M-1 Site-specific Input Parameters Assumed for the Waste Disposal Site

Parameter	Wet Site
Precipitation rate (m/yr)	1.2
Irrigation rate (m/yr)	0
Evapotranspiration coefficient	0.6
Runoff coefficient	0.22
Cover and management factor	0.05
Unsaturated zone characteristics	
Thickness (m)	20
Dry bulk density (g/cm3)	1.62
Soil erodibility factor	0.1
Total porosity	0.4
Effective porosity	0.4
Hydraulic conductivity (m/yr)	30
Soil b parameter	4.1
Longitudinal dispersivity (m)	0
Saturated zone characteristics	
Thickness (m)	30
Dry bulk density (g/cm3)	1.5
Total porosity	0.38
Effective porosity	0.25
Hydraulic conductivity (m/yr)	1200
Hydraulic gradient to well	0.008
Logitudinal dispersivity (m)	30
Horizontal lateral dispersivity	3
Vertical lateral dispersivity	0.3
Distance to well	
In direction parallel to aquifer flow (m)	300
In direction perpendicular to aquifer flow (m)	0

Eight examples were developed to demonstrate the applications of the source term model features to evaluate the potential release of radionuclides to groundwater from the waste disposal facility. Table M-2 summarizes the type of waste material considered, the integrity of the containers/engineered barriers assumed, and the release-controlled mechanism utilized in each example.

Table M-2 Summary of Assumptions and Considerations for the Eight Example Applications

Example No.	Waste Material	Duration of Integrity of Containers and Barriers	Release-Controlled Mechanism
I	Activated metals	500 years	Metal dissolution with a constant rate for 1,000 years
II	Activated metals	1,000 years	Metal dissolution with a constant rate for 10,000 years
III	Activated metals	500 years	Metal dissolution with varied rates for 1,000 years
IV	Transuranic wastes	500 years	Instantaneous equilibrium desorption
V	Grouted transuranic wastes	500 years	Instantaneous equilibrium desorption
VI	Grouted transuranic wastes	500 years	Diffusion
VII	Sealed sources	300 years, 800 years	First-order rate controlled
VIII	Sealed sources	300 years	Solubility controlled

M.3   Example Application I—Disposal of Activated Metals—Delayed Releases for 500 Years

The first example application of the updated source term model considers the disposal of activated metals in the trench described above. Many radionuclides could be found in activated metals, but not every radionuclide has implication in potential groundwater contamination. Those that could contribute to radiation exposure within 10,000 years were selected for analysis, based on previous analysis results for activated metals (ANL 2010). The radionuclides selected include Am-241, C-14, Cs-137, Nb-94, Ni-59, and Tc-99. Table M-3 lists the total inventory and soil Kd values assumed for these radionuclides.

Radionuclides in activated metals embed in the metal structure and cannot be released unless the structure dissolves, which happens when the metals corrode. It was assumed that the activated metals were protected against contact with water for 500 years after the closure of the trench. At 500 years, the integrity of the containers starts to compromise, letting in water from surrounding soils. With water contact, the activated metals would corrode, and the embedded radionuclides would be released. A constant metal corrosion rate of 0.1% per year was assumed for the entire inventory, so it would take 1,000 years for all the metals to corrode and all radionuclides within to be released to the surrounding soils.

Table M-3 Radioactivity Inventory and Kd Values
for Radionuclides in Activated Metals

Radionuclide	Initial conc. based on the entire primary contamination	Total Inventory	Kd (cm3/g)
	pCi/g	Ci	
Am-241	3930	3.82	1000
C-14	290000	281.88	0
Cs-137	561000	545.29	100
Nb-94	42000	40.82	100
Ni-59	7.99E+06	7766.28	50
Np-237	0	0.00	5
Tc-99	86400	83.98	0.1
Th-229	0	0.00	1000
U-233	0	0.00	200

M.3.1 RESRAD-OFFSITE Dose Analysis

Figure M-2 shows the input settings of the source term model to analyze the release of radionuclides from the contaminated zone due to leaching. By choosing the option, "specify initial activity based on mass of entire primary contamination," the input concentration for each radionuclide was determined by dividing the initial inventory by the total mass of materials in the contaminated zone. Take Am-241, for example, the input concentration was calculated as (3.82 Ci × 10^{12} pCi/Ci) / (3 m × 40 m × 5 m × 1,000,000 cm^3/m^3 × 1.62 g/cm^3) = 3,930 pCi/g, where 1.62 g/cm^3 is the bulk density of the entire contaminated zone.

Although "constant dissolution of waste materials" is not an option under release mechanisms, the condition can be established with specific input settings. To result in a constant corrosion rate for the activated metals, the "cumulative fraction of radionuclide-bearing material that is releasable" was set to increase from 0 at 500 years to 1 at 1,500 years linearly, so each year 0.1% of the metals would corrode and become releasable. Then by choosing "equilibrium desorption transfer" as the release mechanism for radionuclides, radionuclides would be released and discharged to the soil domain as soon as the metal structure dissolves, i.e., corrodes. (Note: The Kds of radionuclides for the waste domain cannot be specified, essentially treated as 0s, because the input concentrations are based on the mass of the entire primary contamination.) In this way, the same discharge rate of radionuclides from the waste domain to the soil domain, if decay and ingrowth were neglected, would be observed between 500 and 1,500 years. (Note: In actual modeling, decay and ingrowth were considered, so the discharge rates of radionuclides would change with time.)

Figure M-2 Source Term Model Input Settings for Disposal of Activated Waste

Figure M-3 shows the radiation dose profile calculated by RESRAD-OFFSITE for the drinking water exposure pathway. C-14 and Tc-99 contribute to the first peak, which would occur slightly after 500 years, the time the breaching of containers would begin. The C-14 and Tc-99 released from the waste domain would reach the offsite well location rather quickly, because both have a small Kd value for soil, 0 cm^3/g for C-14 and 0.1 cm^3/g for Tc-99. Cs-137 would not contribute to the radiation exposure, because it would decay away before reaching the offsite well. The dose contribution from Am-241 is small, because its initial activity is much lower than other radionuclides. The dose contribution from Nb-94 is also small, because it has a soil Kd of 100 cm^3/g, which is significantly greater than C-14 and Tc-99. The second peak in the dose profile is contributed by Ni-59, which has a Kd of 50 cm^3/g for soils.

**Figure M-3 Potential Radiation Dose Associated with Disposal of Activated Metals—
Delayed Releases for 500 years**

M.3.2 Comparison with DUST-MS

The DUST-MS code (Sullivan 2006) was developed by Brookhaven National Laboratory and is mostly used for evaluating radionuclide release rates from disposal units buried underground; the release rates can be input to a groundwater transport model for further evaluation of potential groundwater contamination. Unlike RESRAD-OFFSITE, which analytically solves the mathematical equations describing the transport of radionuclides in soils, DUST-MS implements a one-dimensional (1-D) numerical analysis method called finite difference (FD) to solve the same equations. To use the 1-D FD method, users are required to subdivide the contaminated zone with a number of grids (or nodes), which can be associated with release from radioactive waste materials. The distribution of waste materials into grids is determined by the users, with the amount over the grids adding up to the total inventory. The number of grids subdividing the contaminated zone will affect the precision of the calculation results.

To calculate radionuclide release rates from the bottom of the disposal unit, i.e., the bottom of the contaminated zone for RESRAD-OFFSITE, three different grids schemes each with 111, 221, and 451 grids were used to obtain calculation results with DUST-MS. For each grids scheme, the domain of analysis was 105-m long, with the top 5 m in the waste disposal area and the following 100 m simply in the transit area. The addition of the 100-m long transit area was to satisfy the lower boundary condition assumed for the analysis that the radionuclide concentrations at the lower end of the analysis domain were zero at all times. The spacing between grids was narrower within the disposal area than within the transit area. For the three grids schemes, the spacing between grids within the disposal area was 50 cm, 25 cm, and 10 cm, respectively. Each grid within the disposal area was associated with a container containing the same amount of waste material, except for the first one, which was at the upper

end of the analysis domain. There would not be any radionuclides moving across the top of the disposal area.

To model the delayed release of radionuclides, all the containers were assumed to fail at the same time, at 500 years. "Dissolution" was selected as the sole release mechanism for DUST-MS to consider the release due to metal corrosion, with a fractional release rate of 0.001/yr. The fluxes of radionuclides across the bottom of the disposal area were obtained and multiplied by the area of the disposal unit, which is 120 m^2, to get the radionuclide release rates for comparison with those calculated by RESRAD-OFFITE, listed in the file AQFLUXIN.dat that was generated after each RESRAD-OFFSITE run. Figures M-4 to M-12 show the comparisons.

Figure M-4 Comparison of Calculated Am-241 Release Rates Associated with Disposal of Activated Metals—Delayed Releases for 500 Years

Figure M-5 Comparison of Calculated C-14 Release Rates Associated with Disposal of Activated Metals—Delayed Releases for 500 Years

Figure M-6 Comparison of Calculated Cs-137 Release Rates Associated with Disposal of Activated Metals—Delayed Releases for 500 Years

Figure M-7 Comparison of Calculated Nb-94 Release Rates Associated with Disposal of Activated Metals—Delayed Releases for 500 Years
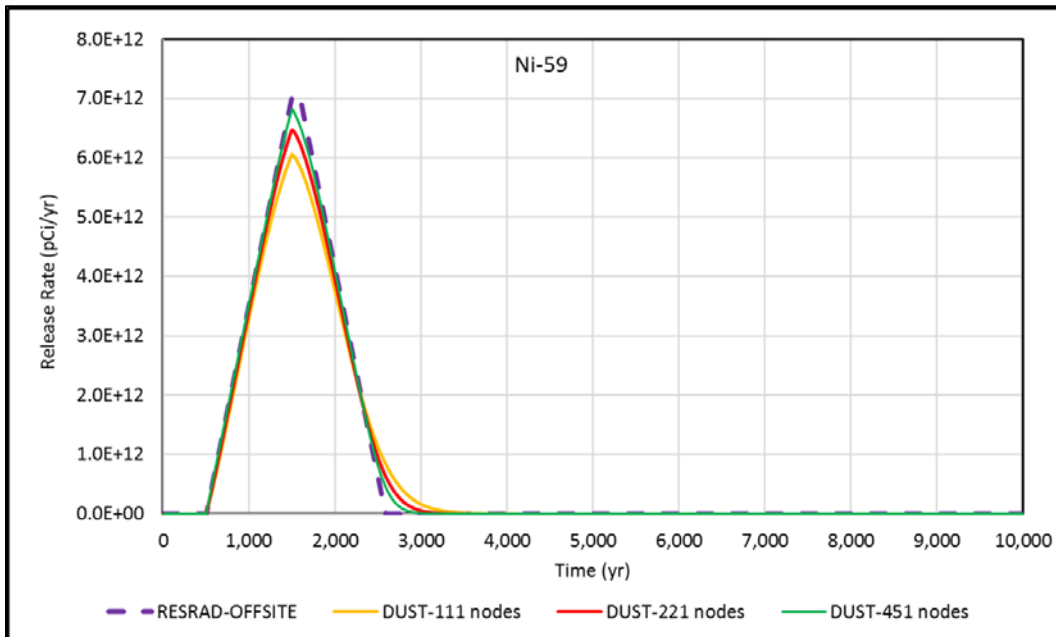
Figure M-8 Comparison of Calculated Ni-59 Release Rates Associated with Disposal of Activated Metals—Delayed Releases for 500 Years
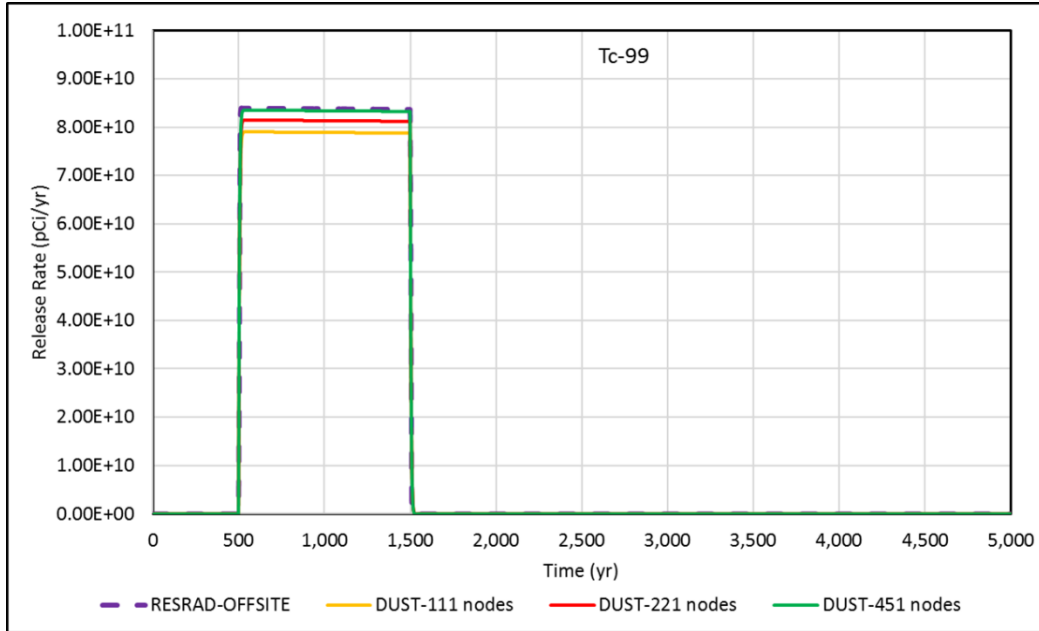
Figure M-9 Comparison of Calculated Tc-99 Release Rates Associated with Disposal of Activated Metals—Delayed Releases for 500 Years
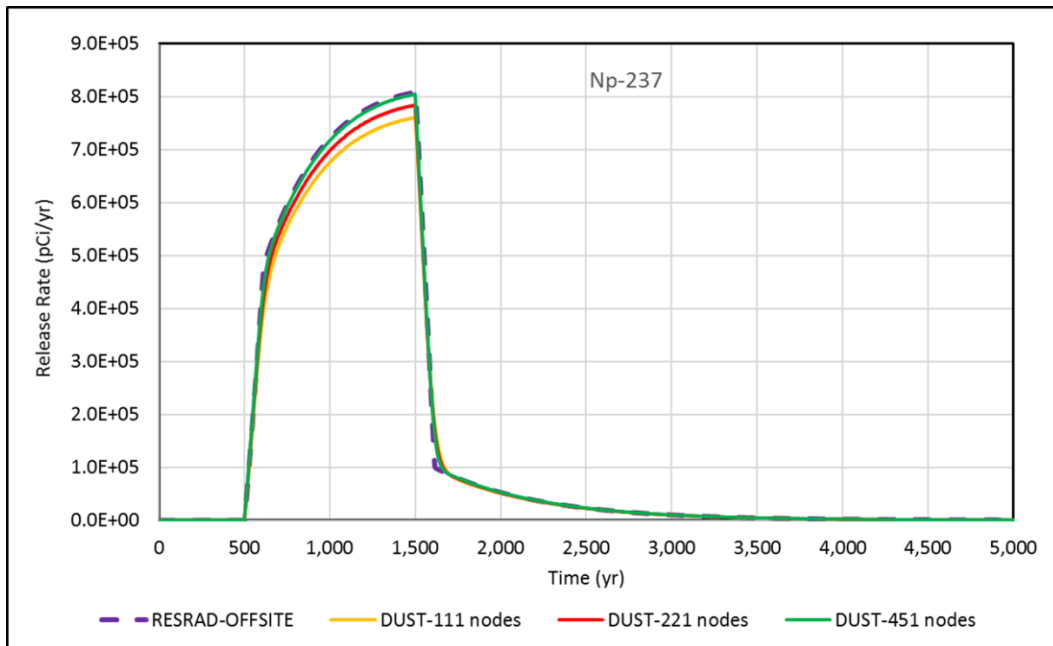
Figure M-10 Comparison of Calculated Np-237 Release Rates Associated with Disposal of Activated Metals—Delayed Releases for 500 Years
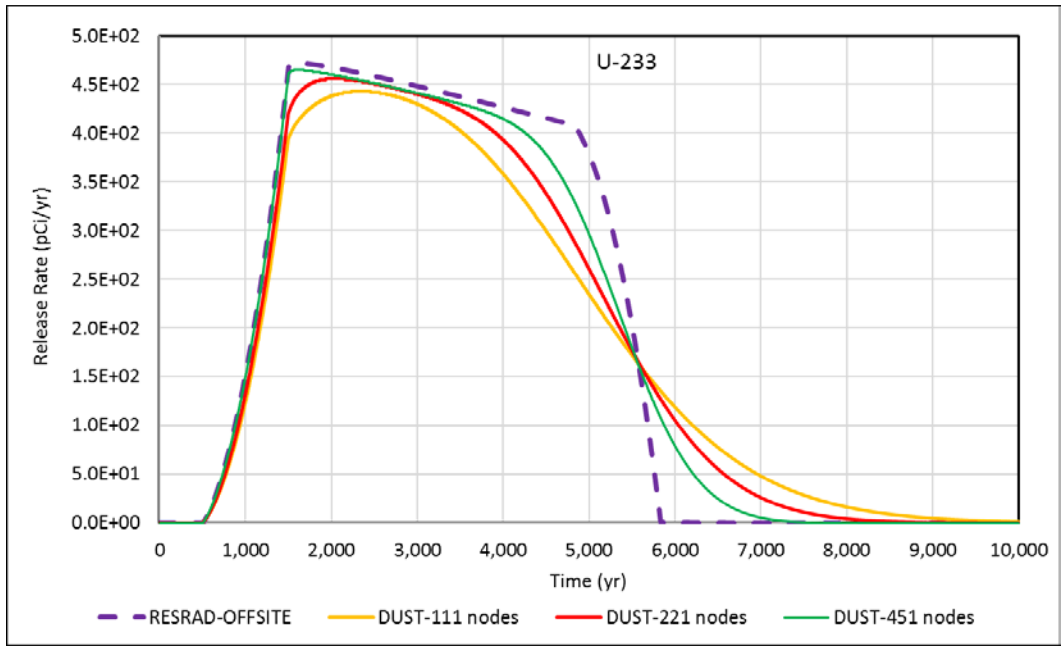
Figure M-11 Comparison of Calculated U-233 Release Rates Associated with Disposal of Activated Metals—Delayed Releases for 500 Years
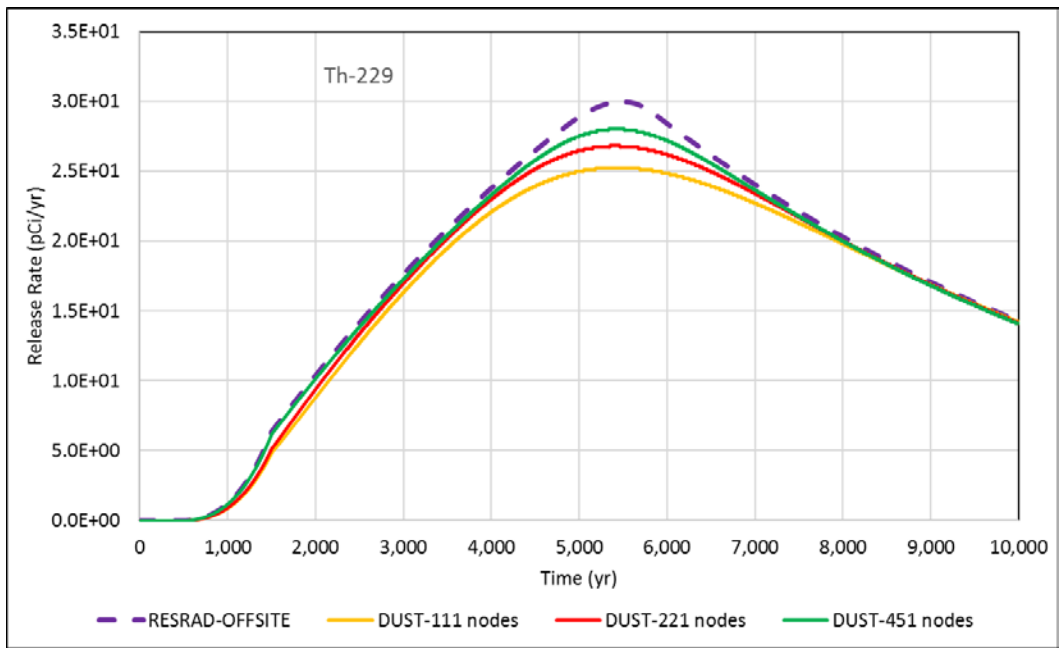
Figure M-12 Comparison of Calculated Th-229 Release Rates Associated with Disposal of Activated Metals—Delayed Releases for 500 Years

In general, the radionuclide release rates calculated by RESRAD-OFFSITE agree well with those calculated by DUST-MS, for both parent and progeny radionuclides. In the analyses, Np-237, U-233, and Th-229 are progenies of Am-241. The release rate profiles shown in the above figures indicate that the results produced by DUST-MS would approach those produced by RESRAD-OFFSITE as the number of grids is increased. Nevertheless, the precision in results gained by increasing the number of grids could be offset by the accumulation of rounding errors, which is commonly seen with numerical analysis methods, and is the explanation that for Cs-137; the results obtained with the 451 grids scheme are not closer to the RESRAD-OFFSITE results than the results obtained with the 221 grids scheme (Figure M-6).

M.4   Example Application II—Disposal of Activated Metals—Delayed Releases for 1,000 Years

The protection provided by the containers/engineered barriers in Example Application I for activated metals was assumed to last longer, 1,000 years, in Example Application II. After water infiltrated the containers, the activated metals were assumed to corrode with a constant rate for 10,000 years, i.e., 0.01% per year.

M.4.1 RESRAD-OFFSITE Dose Analysis

The input settings of the source term model to analyze the release of radionuclides from the contaminated zone due to leaching were essentially the same as shown in Figure M-2, except that the inputs for "time at which release begins or changes (year)" were changed from 500 and 1,500 to 1,000 and 11,000.

Figure M-13 shows the radiation dose profile associated with the drinking water pathway calculated by RESRAD-OFFSITE. Due to the smaller corrosion rate of activated metals (compared with that assumed in Example Application I), the peak dose reduced from 26 mrem/yr (in Example Application I) to 6.3 mrem/yr. The two distinct peaks observed in Figure M-3 are now connected, because the releases of C-14 and Tc-99 would last for 10,000 years.
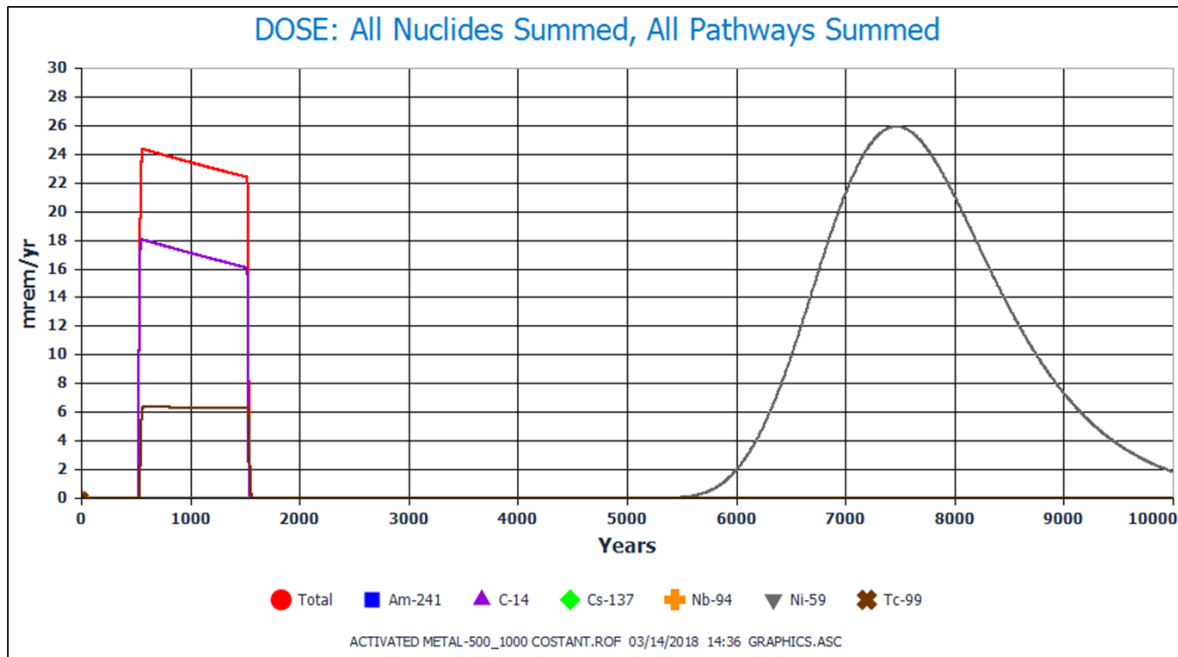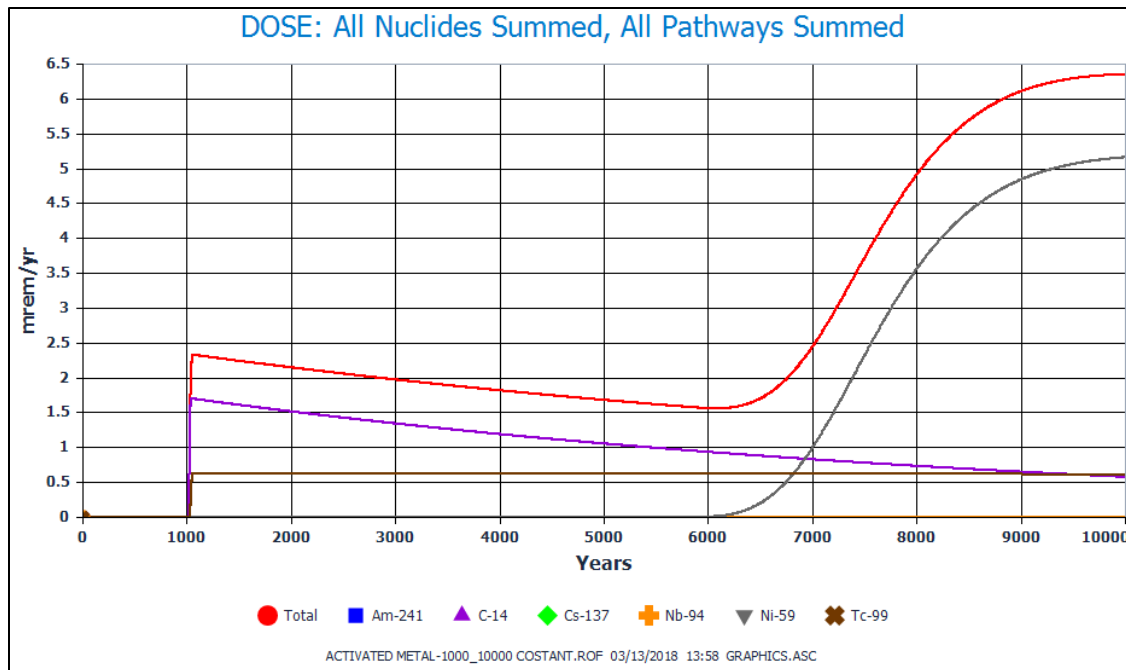
Figure M-13 Potential Radiation Dose Associated with Disposal of Activated Metals—Delayed Releases for 1,000 years

M.4.2 Comparison with DUST-MS

To calculate flux rate of radionuclides from the bottom of the disposal unit with DUST-MS, the 451 grids scheme was used. Each grid in the disposal area (except for the first one) was associated with a waste container. Each container contained the same amount of radioactivity, and all the containers would fail at the same time, at 1000 years. The "dissolution" mechanism was selected as the sole release mechanism with a fractional release rate of 0.0001/yr.

Figures M-14 to M-22 compare the radionuclide release rates calculated by DUST-MS and RESRAD-OFFSITE for each of the radionuclides analyzed. The comparisons show very good agreement between RESRAD-OFFSITE and DUST-MS, for both parent and progeny radionuclides.
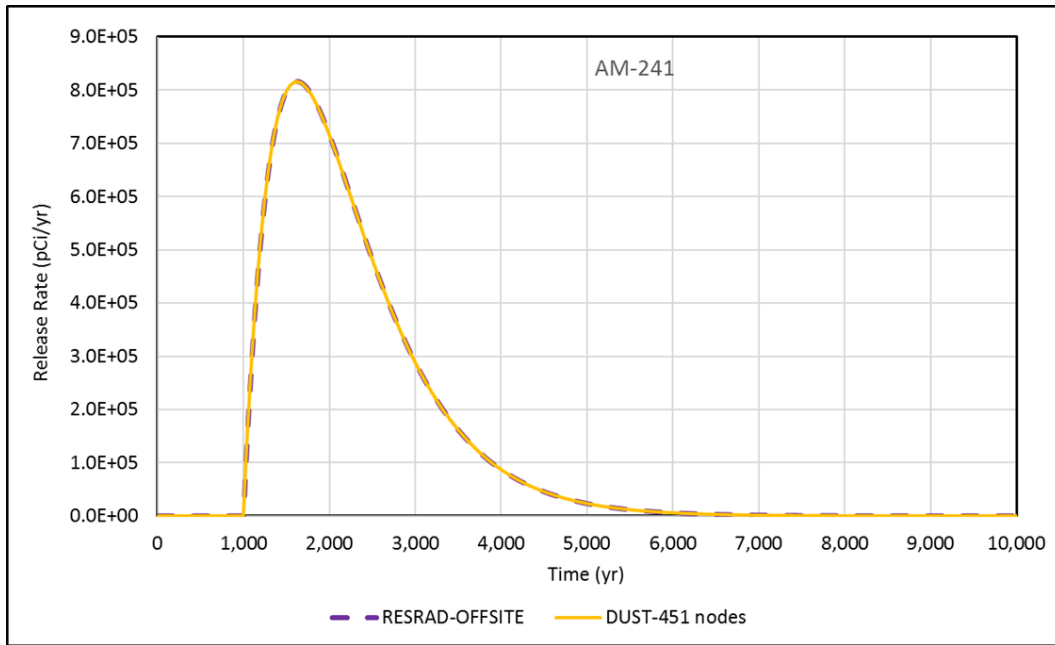
Figure M-14 Comparison of Calculated Am-241 Release Rates Associated with Disposal of Activated Metals—Delayed Releases for 1,000 Years
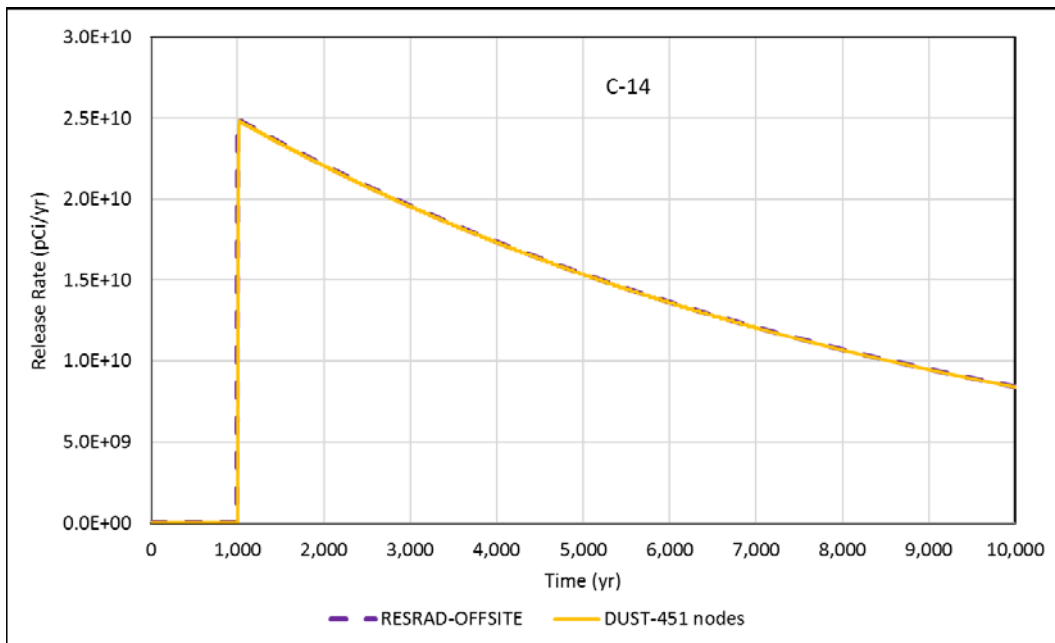
Figure M-15 Comparison of Calculated C-14 Release Rates Associated with Disposal of Activated Metals—Delayed Releases for 1,000 Years
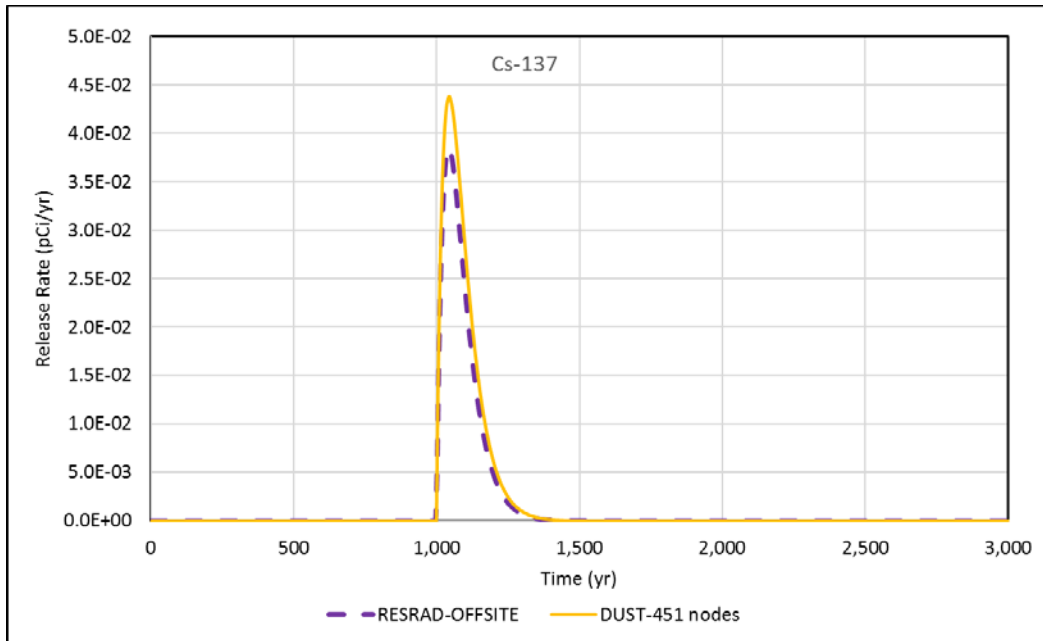
Figure M-16 Comparison of Calculated Cs-137 Release Rates Associated with Disposal of Activated Metals—Delayed Releases for 1,000 Years
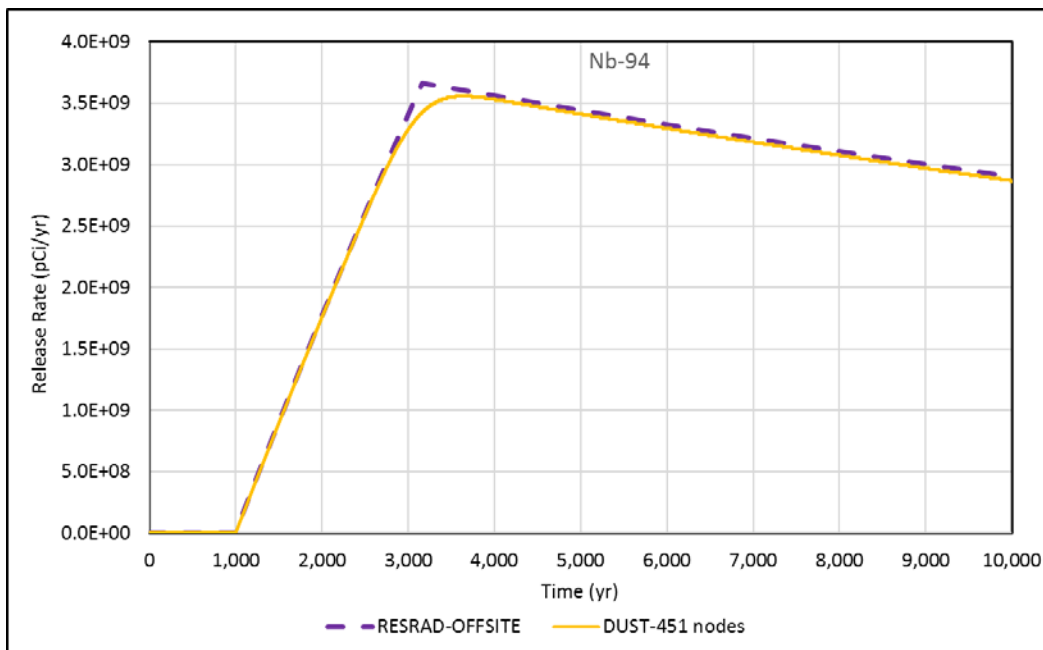
Figure M-17 Comparison of Calculated Nb-94 Release Rates Associated with Disposal of Activated Metals—Delayed Releases for 1,000 Years
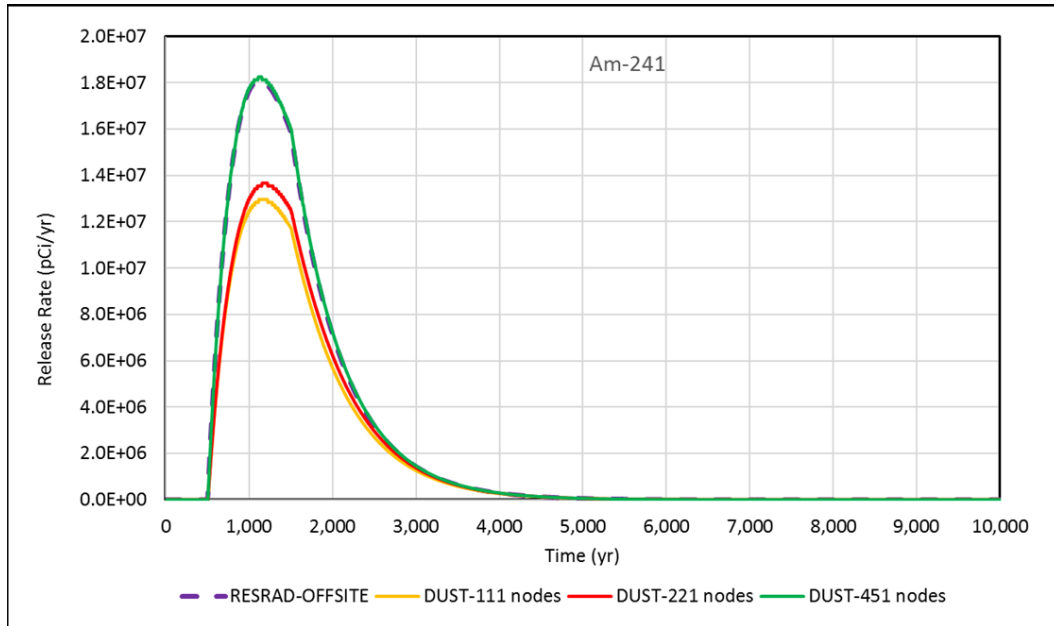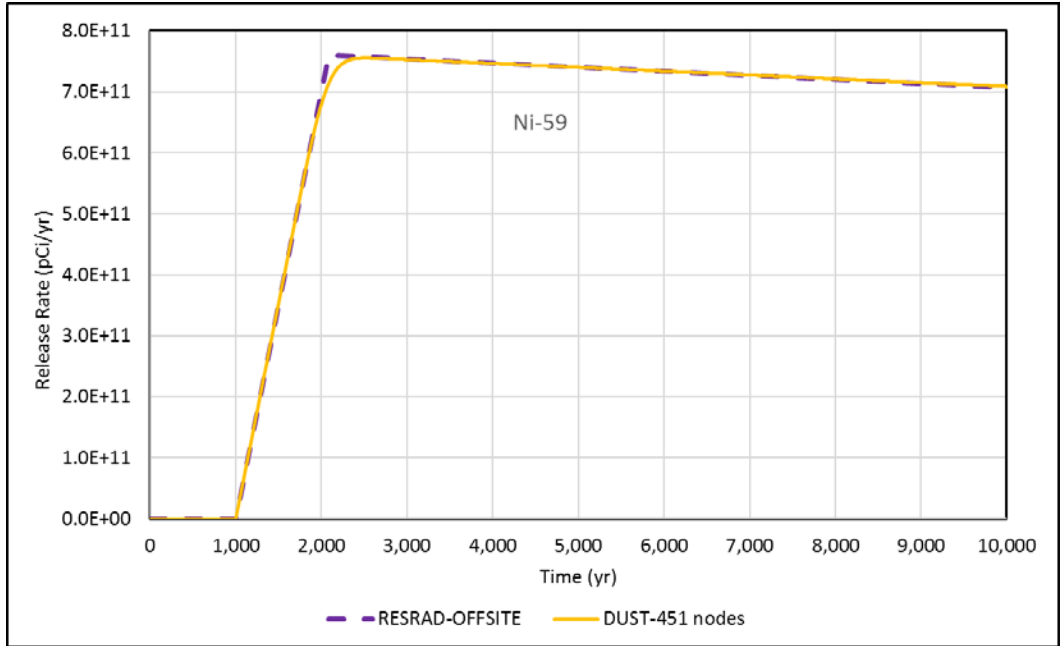
Figure M-18 Comparison of Calculated Ni-59 Release Rates Associated with Disposal of Activated Metals—Delayed Releases for 1,000 Years
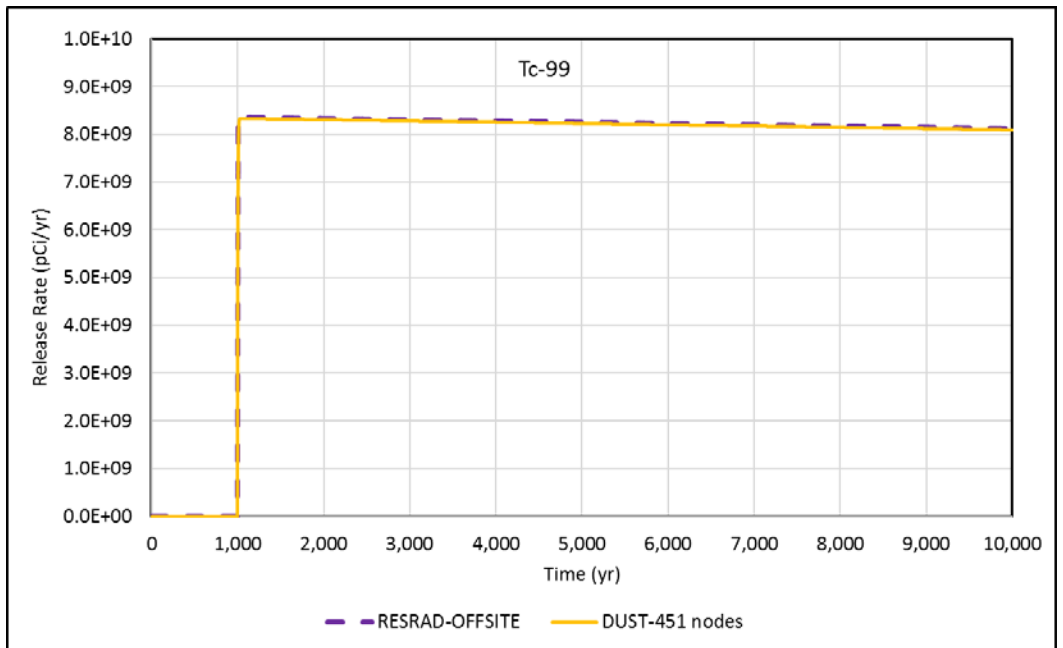
Figure M-19 Comparison of Calculated Tc-99 Release Rates Associated with Disposal of Activated Metals—Delayed Releases for 1,000 Years
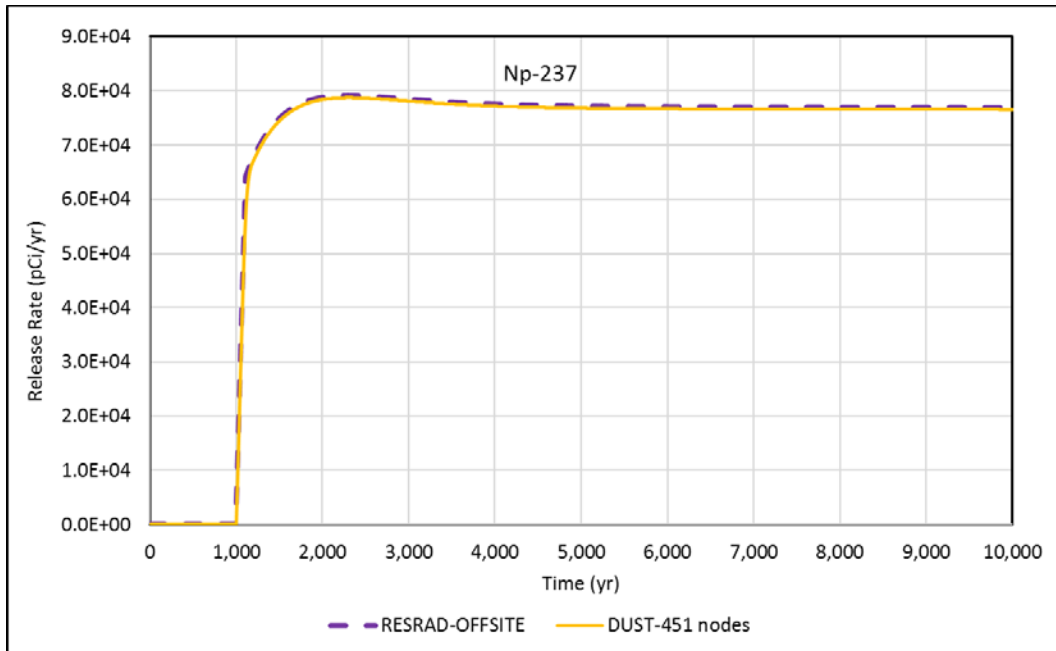
Figure M-20 Comparison of Calculated Np-237 Release Rates Associated with Disposal of Activated Metals—Delayed Releases for 1,000 Years
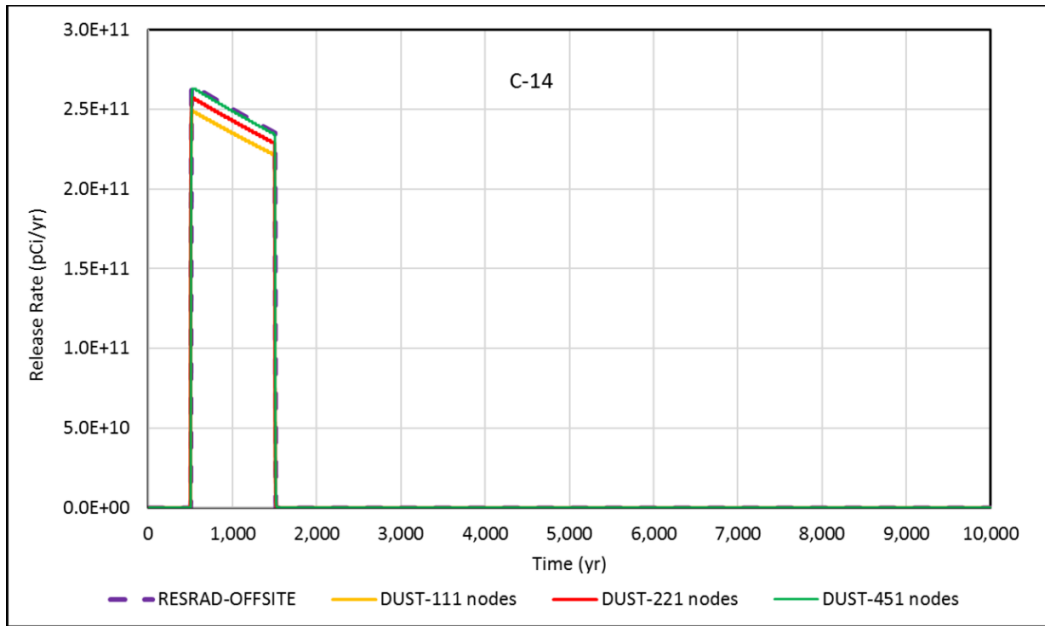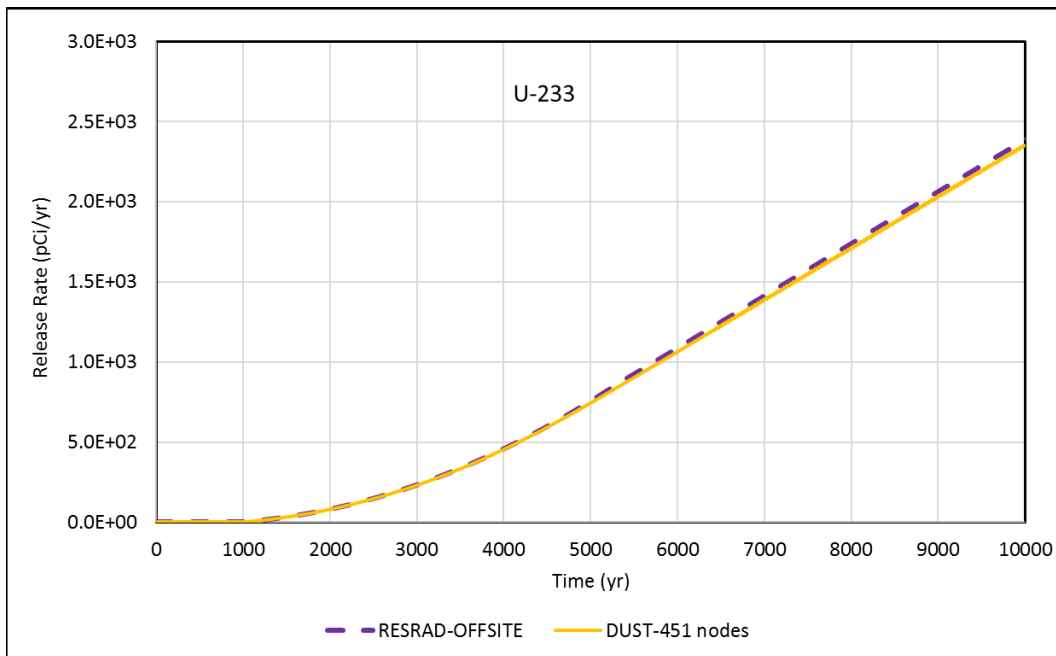

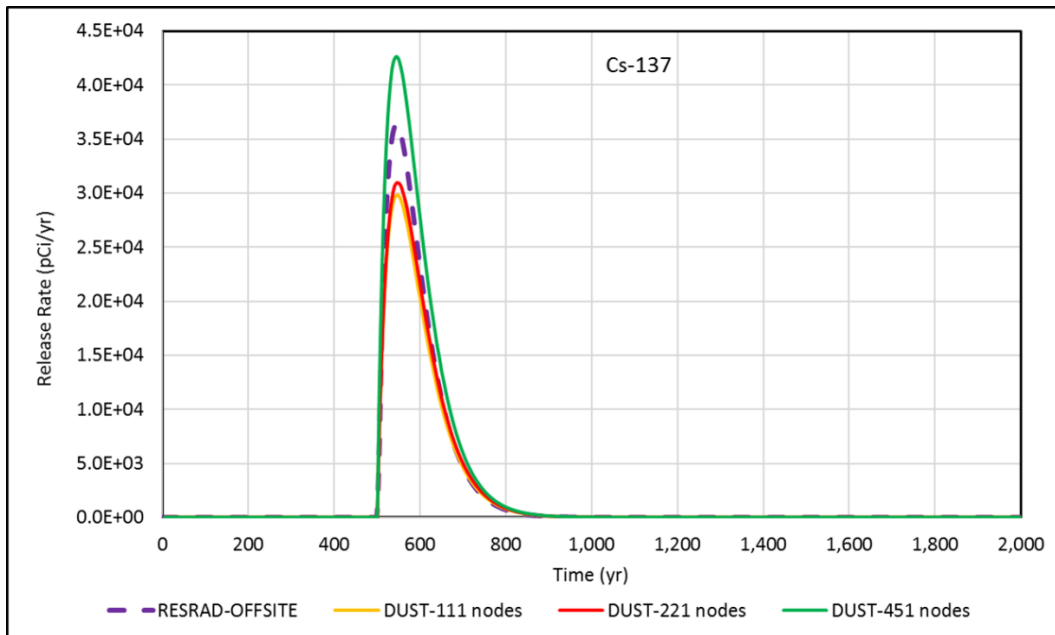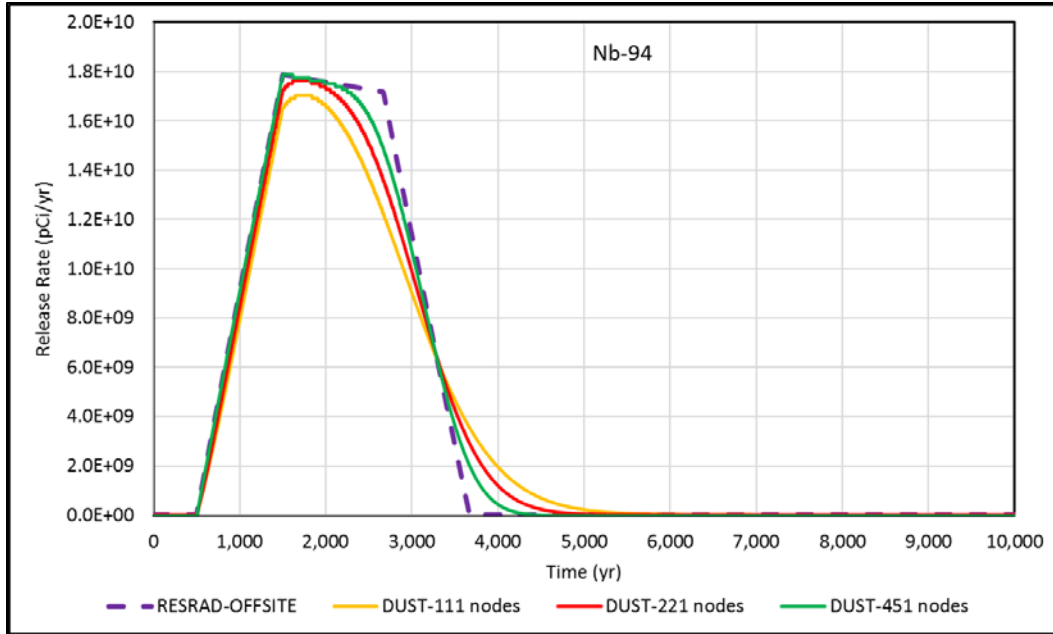**Figure M-21 Comparison of Calculated U-233 Release Rates Associated with Disposal of Activated Metals—Delayed Releases for 1,000 Years**
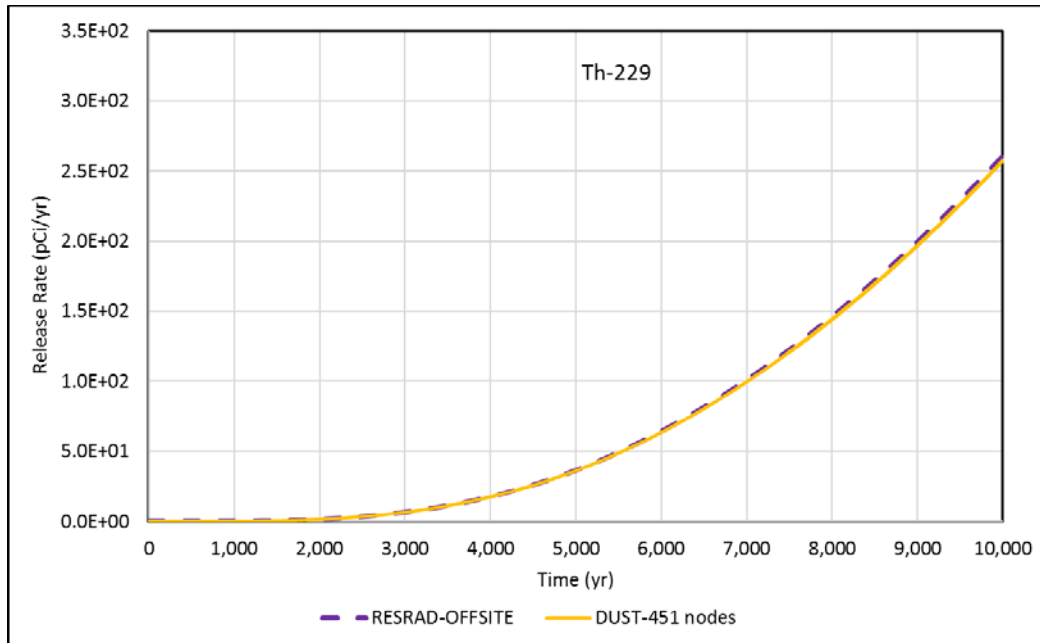
Figure M-22 Comparison of Calculated Th-229 Release Rates Associated with Disposal of Activated Metals—Delayed Releases for 1,000 Years

M.5   Example Application III—Disposal of Activated Metals—Delayed Releases for 500 Years with an Increasing Corrosion Rate

In Example Application III, the activated metals disposed of in the near surface trench as considered in Example Applications I and II were assumed to corrode with an increasing rate over time, after being exposed to water. The corrosion was assumed to begin at 500 years and to complete at 1,500 years.

M.5.1 RESRAD-OFFSITE Dose Analysis

Figure M-23 shows the input settings for the source term model. The corrosion rate of the activated metals was 0.05% per year between 500 and 700 years, 0.075% per year between 700 and 900 years, 0.1% per year between 900 and 1,100 years, 0.125% per year between 1,100 and 1,300 years, and 0.15% per year between 1,300 and 1,500 years.

Figure M-24 shows the radiation dose profile associated with the drinking water pathway calculated by RESRAD-OFFSITE. Due to the step increases in the release rate over a 1,000-year period, the radiation doses contributed by C-14 and Tc-99 would also increase by steps over a 1,000-year period. However, the dose contributed by Ni-59 has the same smooth profile and with about the same peak magnitude as the dose contribution obtained in Example Application I (Figure M-3). The effect of step increases in the release rate from the contaminated zone was diluted by the effects of radiological decay and dispersion during the long transport times in the unsaturated zone and in the groundwater aquifer.

Figure M-23 Source Term Model Input Settings for Disposal of Activated Waste

Figure M-24 Potential Radiation Dose Associated with Disposal of Activated Metals—Delayed Releases for 500 Years with an Increasing Corrosion Rate

M.5.2 Comparison with DUST-MS

To calculate flux rate of radionuclides from the bottom of the disposal unit with DUST-MS, a 481-grid scheme was used. The 5-m thick disposal area was subdivided by 101 grids (with first grid at the upper end of the analysis domain), and the spacing between grids was 5 cm. The other 380 grids spanned the transit area that was added below the disposal area to satisfy the boundary condition that radionuclide concentrations at the lower end of the analysis domain were zero at all times. Same as the analyses for Example Applications I and II, the initial radioactivity inventory was evenly divided, enclosed in waste containers, and associated with the grids (1-100) that spanned the disposal area.

For the same type of radioactive waste material in each waste container, DUST-MS accepts only one fractional release rate to be used with the "dissolution" mechanism over the time frame of analysis—10,000 years in this case. To consider the same amount of activated metal corroding over time as did by RESRAD-OFFSITE, the 100 containers assumed in this analysis were set to fail at five different times in groups (500, 700, 900, 1100, and 1300 years, corresponding to the beginning of each step increase in the corrosion rate). The "fractional release rate" was set to 0.5% per year, so the activated metal contained in each of the 100 containers would corrode completely in 200 years after the container failed. This fractional release rate for each container translated to 0.005% per year for the entire activated metal inventory disposed of in the trench, which was used to determine the number of containers to fail at the five different times. According to the annual corrosion rate on the basis of the entire activated metal inventory as discussed in Section M.5.1, the number of containers to fail at 500, 700, 900, 1100, and 1300 years were determined to be 10, 15, 20, 25, and 30, respectively. The 100 containers were grouped by the determined numbers sequentially in two different ways, first from the top to the bottom, and then from the bottom up. Each group of containers was assigned the corresponding failure time. Using this approach, two different input files were created to obtain radionuclide flux rates and to calculate radionuclide release rates for comparison with those calculated by RESRAD-OFFSITE.

Figures M-25 to M-33 show the comparison of the release rates from DUST-MS and RESRAD-OFFSITE analyses for each of the radionuclides analyzed. In the figures, DUST-MS1 denotes the release rate profile from the DUST-MS analysis that grouped containers from the top to the bottom so that upper container groups would fail earlier than lower container groups. DUST-MS2 denotes the release rate profile from the DUST-MS analysis that grouped containers in the opposite way, so lower container groups would fail earlier than upper container groups. In the figures, the release of radionuclides (from the bottom of the contaminated zone) always starts earlier with DUST-MS2 than with DUST-MS1, as expected. The peak release rate with DUST-MS1 is greater than with DUST-MS2, except for Am-241 and Cs-137, because the arrival time periods at the bottom of the disposal unit for the releases from different container groups have more overlap with DUST-MS1 than with DUST-MS2. In another words, with DUST-M2, the arrival of the releases from different container groups at the bottom of the disposal unit tend to spread out in time. The exceptions observed for Am-241 and Cs-137 were due to their shorter radiological half-life than the transport time needed to reach the bottom of the disposal unit. Therefore, a significant fraction of the released radionuclides would decay away during the transport.
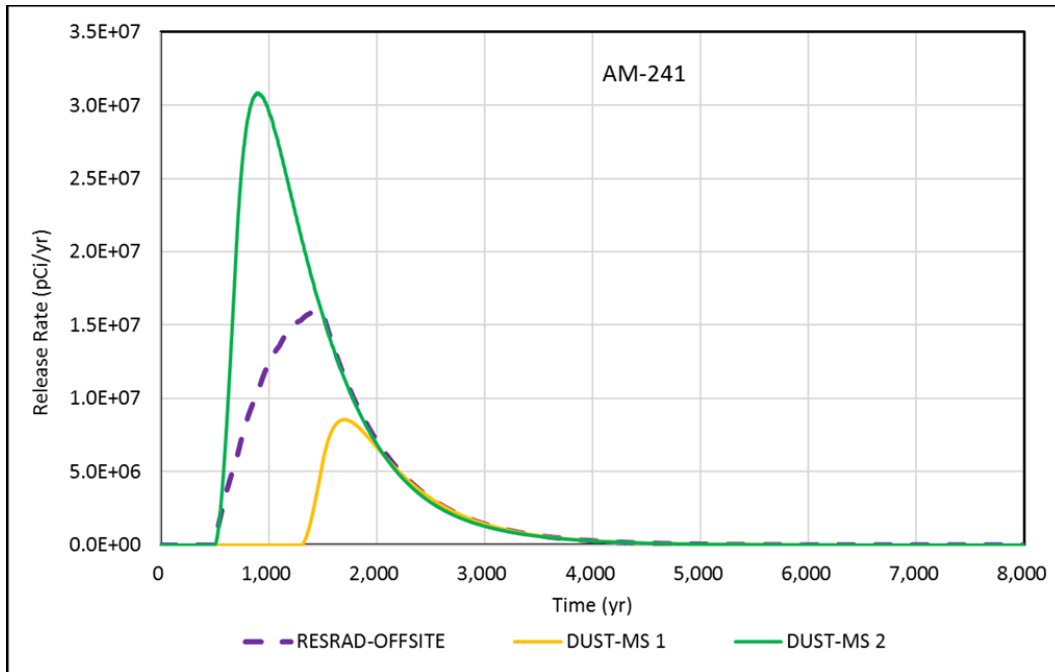
Figure M-25 Comparison of Calculated Am-241 Release Rates Associated with Disposal of Activated Metals—Increasing Corrosion Rate
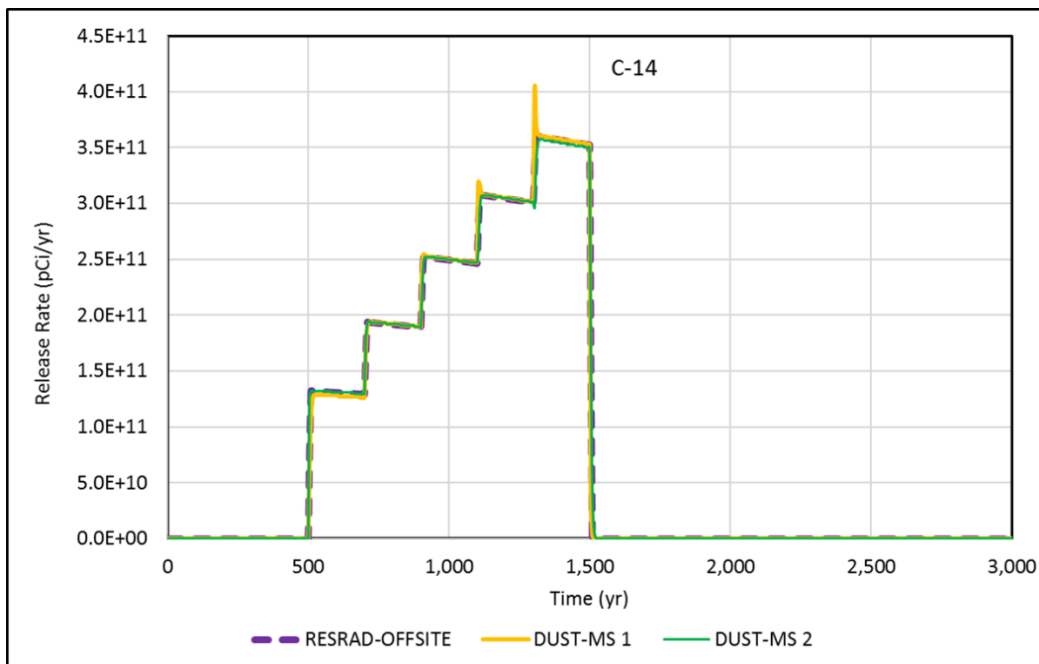
Figure M-26 Comparison of Calculated C-14 Release Rates Associated with Disposal of Activated Metals—Increasing Corrosion Rate
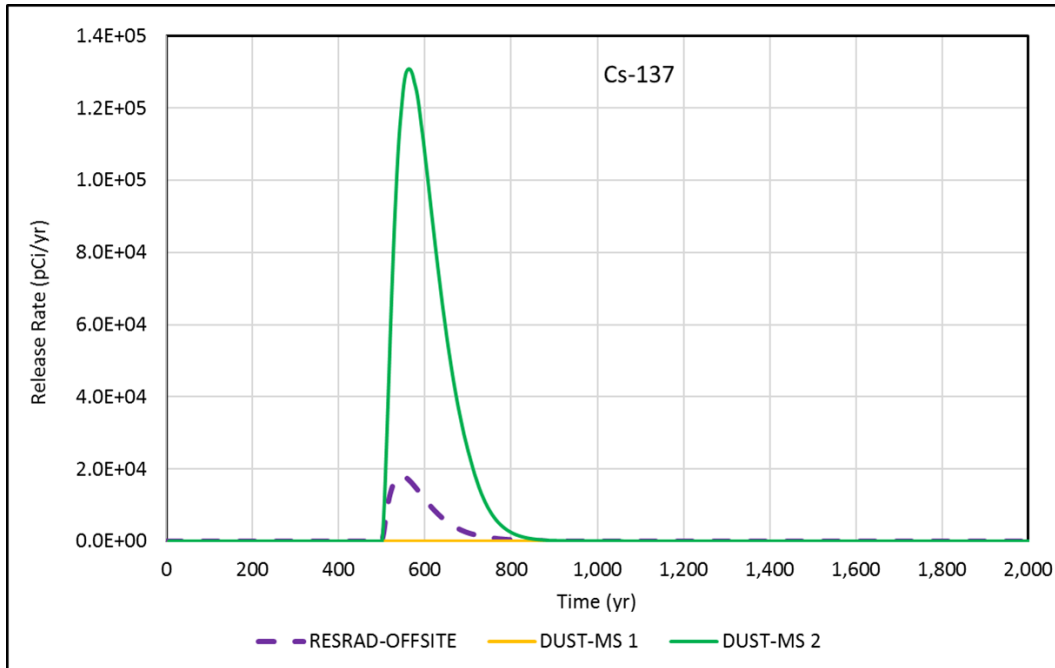
Figure M-27 Comparison of Calculated Cs-137 Release Rates Associated with Disposal of Activated Metals—Increasing Corrosion Rate
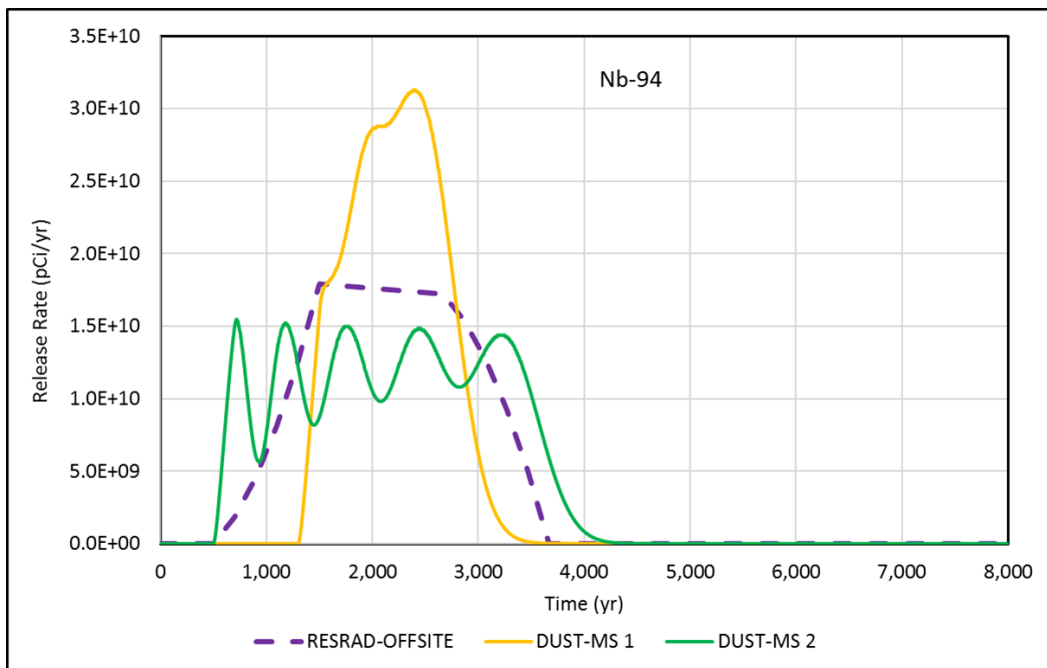
Figure M-28 Comparison of Calculated Nb-94 Release Rates Associated with Disposal of Activated Metals—Increasing Corrosion Rate
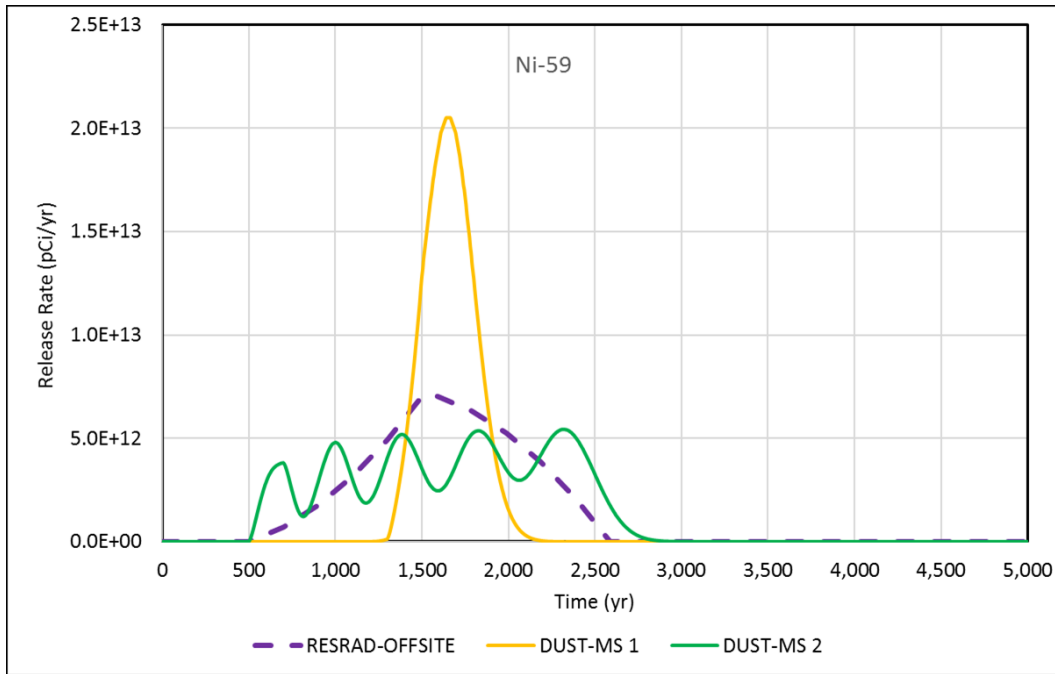
Figure M-29 Comparison of Calculated Ni-59 Release Rates Associated with Disposal of Activated Metals—Increasing Corrosion Rate
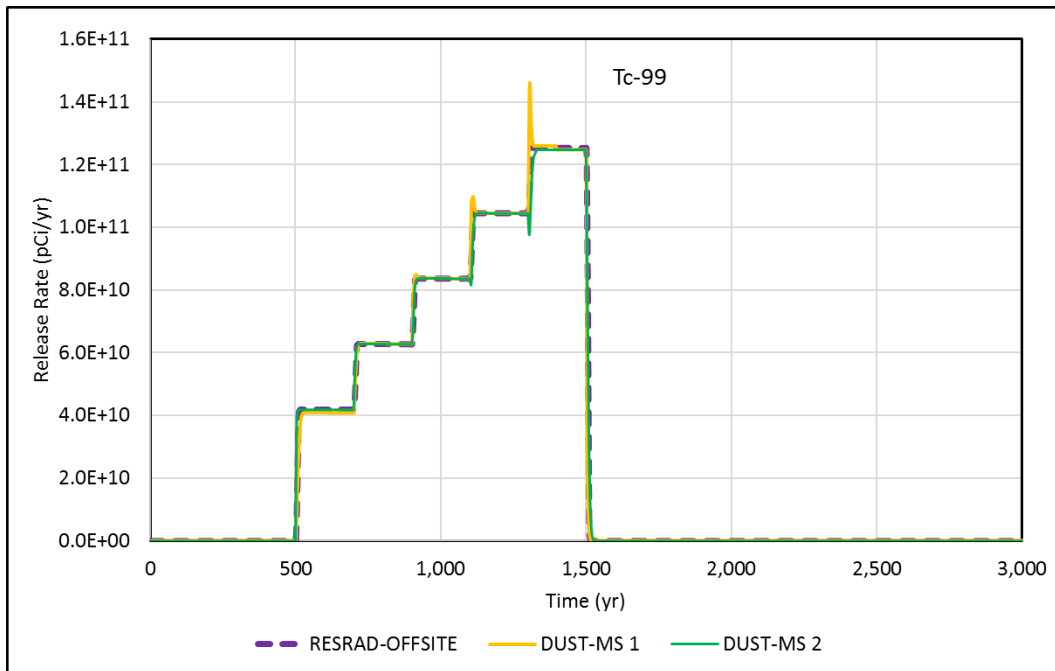
Figure M-30 Comparison of Calculated Tc-99 Release Rates Associated with Disposal of Activated Metals—Increasing Corrosion Rate
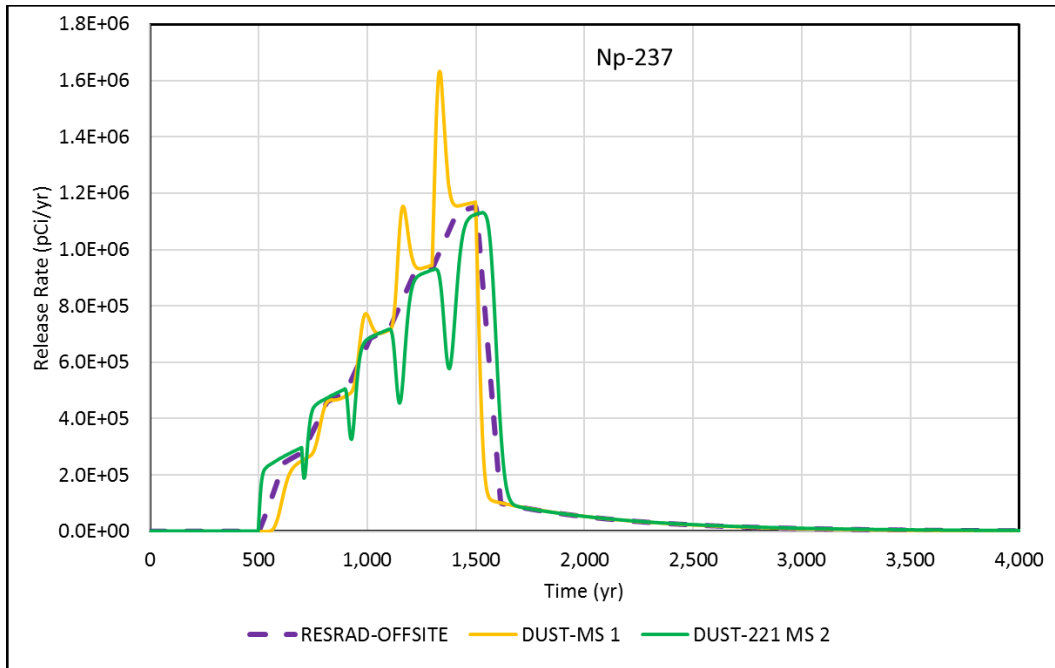
Figure M-31 Comparison of Calculated Np-237 Release Rates Associated with Disposal of Activated Metals—Increasing Corrosion Rate
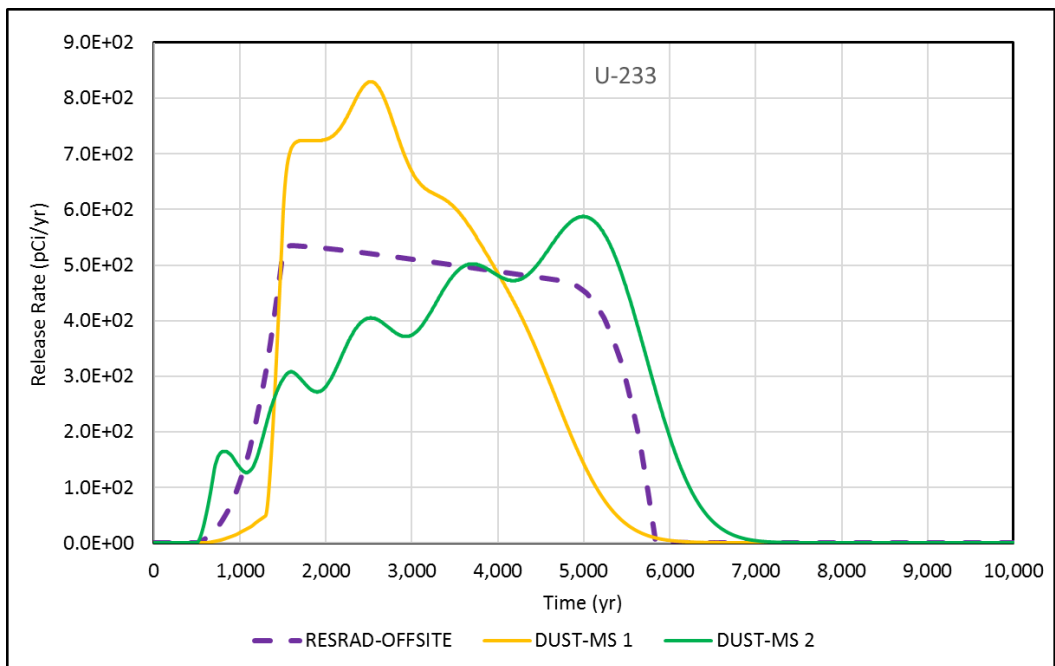
Figure M-32 Comparison of Calculated U-233 Release Rates Associated with Disposal of Activated Metals—Increasing Corrosion Rate
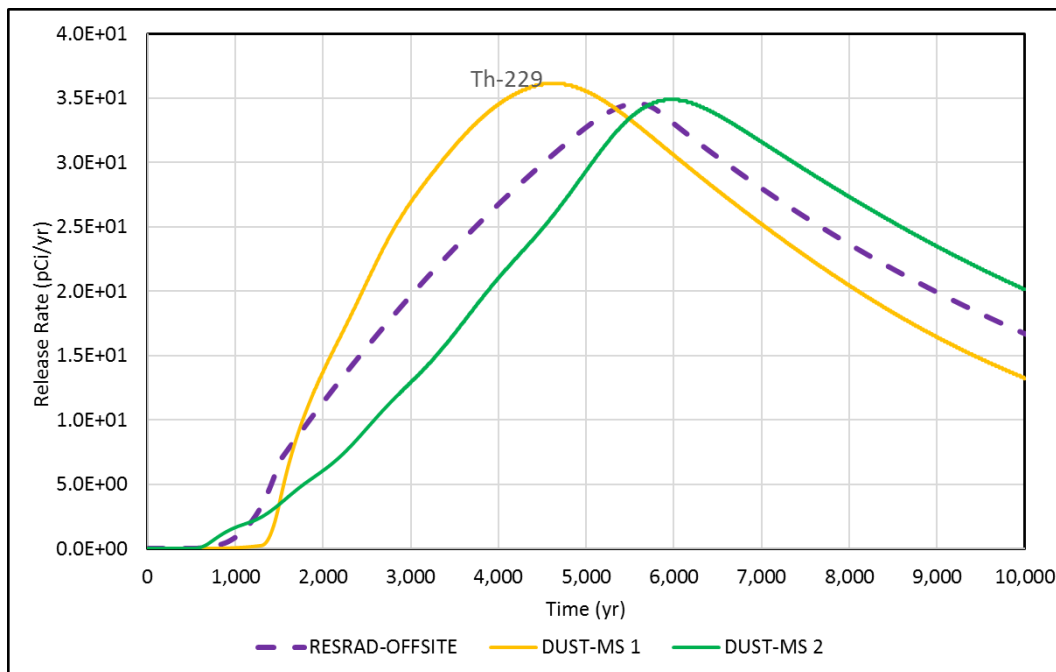
**Figure M-33 Comparison of Calculated Th-229 Release Rates Associated
with Disposal of Activated Metals—Increasing Corrosion Rate**

According to Figures M-25 to M-33, the radionuclide release rates with RESRAD-OFFSITE are between the release rates with DUST-MS1 and DUST-MS2, which conforms to expectation, because RESRAD-OFFSITE assumes the discharge of radionuclides from the waste domain to the soil domain is even along the depth of the contaminated zone.

The discussions above provide the rationale employed to design DUST-MS input files to match the RESRAD-OFFSITE analysis. The rationale can be applied conversely to design RESRAD-OFFSITE input files to analyze realistic waste disposal situations in which multiple containers at different locations within the disposal unit would fail at different times.

M.6   Example Application IV—Disposal of Transuranic (TRU) Wastes

Example Application IV concerns the disposal of TRU wastes, which could be different materials such as clothes, papers, gloves, etc., that contain transuranic radionuclides on their surfaces. Many radionuclides could be present in these waste materials. However, to simplify the analysis, three radionuclides that were found to potentially impact the groundwater in a previous waste disposal performance assessment (ANL 2010) were considered. These three radionuclides were Np-237, Pu-241, and Am-241. They belong to the same decay chain; Pu-241 decays to Am-241, which decays to Np-237; Np-237 then decays to U-233 and Th-229. Table M-4 lists the total inventory, soil Kds, and other properties assumed for these radionuclides.

Table M-4 Radioactivity Inventory and Kd Values for Radionuclides in TRU Wastes

Radionuclide	Initial inventory (Ci)	Initial conc. based on the entire primary contamination (pCi/g)	Initial concentration based on mass of grouted waste (pCi/g)	Kd (cm3/g) for soil	Kd (cm3/g) for cement	Effective diffusion coefficient in cement (cm2/s)	Effective diffusion coefficient in cement (m2/yr)
Np-237	0.75	7.72E+02	2.36E+03	5	300	5.00E-10	1.58E-06
Pu-241	8000	8.23E+06	2.52E+07	270	1000	5.00E-11	1.58E-07
Am-241	2650	2.73E+06	8.33E+06	1000	1000	5.00E-13	1.58E-09
U-233	0	0.00E+00	0.00E+00	200	1000	1.00E-12	3.15E-09
Th-229	0	0.00E+00	0.00E+00	1000	1000	1.00E-12	3.15E-09

The TRU wastes were assumed to be packaged in multiple waste containers and disposed of in the trench. The total volume of the waste containers was assumed to be 120 m³, which was 20% the volume of the disposal cell. The bulk density of the waste materials based on the total volume of the waste containers was assumed to be 1.8 g/cm³. Radionuclides were assumed to loosely attach to the surface of the waste materials and would dissolve in water when they have contact with water, which was assumed to occur 500 years after the waste disposal.

M.6.1 RESRAD-OFFSITE Dose Analysis

Figure M-34 shows the input settings of the source term model to analyze the releases of radionuclides from the contaminated zone due to leaching. Considering the loose attachment between radionuclides and the waste materials, the "equilibrium desorption transfer" was selected as the release mechanism, and the change from 0 to 1 in the "cumulative fraction of radionuclide-bearing material that is releasable" was stepwise at 500 years.

The input concentrations were based on the entire primary contamination, so the value for each radionuclide was calculated by dividing the initial inventory by the total mass of materials in the contaminated zone, i.e., 3 m × 40 m × 5 m × 1,000,000 cm³/m³ × 1.62 g/cm³ = 9.72 × 10⁸ g, where 1.62 g/cm³ is the bulk density of the entire contaminated zone. Because of this selection, the input of Kds for the contaminated medium was not available. Essentially, when radionuclides on the waste materials had contact with water, they would all dissolve in water and be discharged to the surrounding soil domain for subsequent transport to the bottom of the contaminated zone.

Figure M-34 Source Term Model Input Settings for Disposal of TRU Waste

Figure M-35 shows the radiation dose profile associated with the drinking water pathway calculated by RESRAD-OFFSITE. The peak radiation dose associated with Am-241 or Pu-241 was contributed by Np-237, a common progeny that had a much smaller soil Kd of 5 cm³/g compared with the soil Kds of other radionuclides. The narrow peak in the dose profile results from the pulse discharge of all radionuclides from the waste domain to the surrounding soil domain at 500 years.
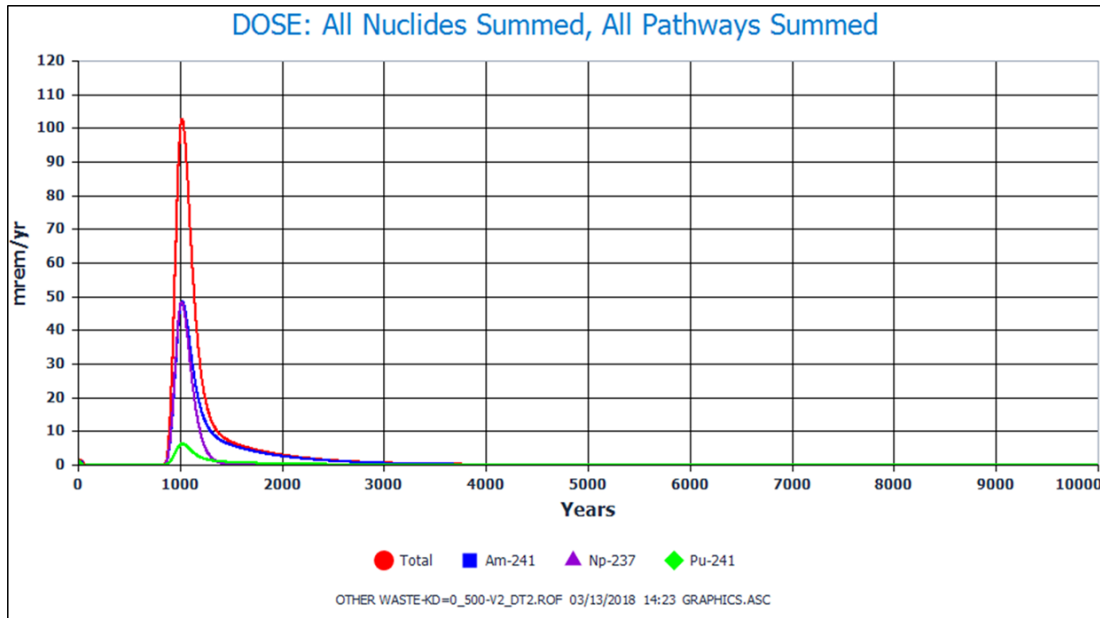
Figure M-35 Potential Radiation Dose Associated with Disposal of TRU Waste—Delayed Releases for 500 Years

M.6.2 Comparison with DUST-MS

Two input files with the 451 and 481 grids schemes as discussed in Section 3.2 and Section 5.2, respectively, were used when running the DUST-MS code to analyze the releases of radionuclides associated with the TRU waste disposal. With the 451 grids scheme, the total inventory of radionuclides was equally distributed to 50 containers associated with the grids that spanned the disposal area. With the 481 grids scheme, the total inventory was equally distributed to 100 containers. Surface rinse was selected to be the release mechanism, and the partitioning coefficient (i.e., Kd in RESRAD-OFFSITE) for the wasteform was set to 0 g/cc.

Figures M-36 to M-40 compare the radionuclide release rates calculated by DUST-MS and RESRAD-OFFSITE for each of the radionuclides analyzed. In general, the DUST-MS results and RESRAD-OFFSITE results are in good agreement. Greater discrepancy is seen with the release profiles of Pu-241, which has a short half-life of 14.4 years, than with the release profiles of Am-241, Np-237, U-233, and Th-229. This might be due to the more significant rounding errors with the Pu-241 results than with the results of the other four radionuclides from DUST-MS.
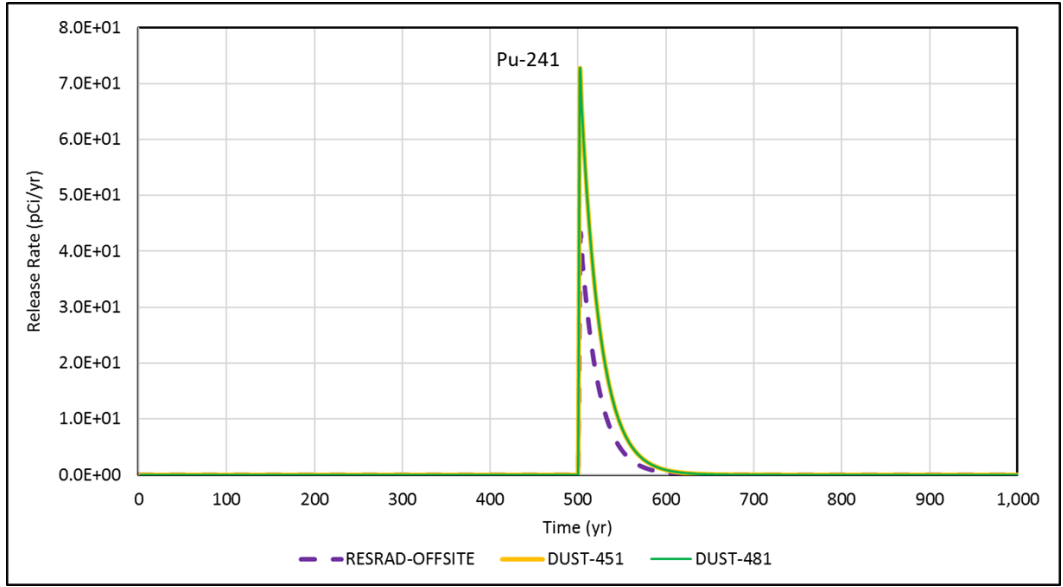
Figure M-36 Comparison of Calculated Pu-241 Release Rates Associated with Disposal of TRU Wastes
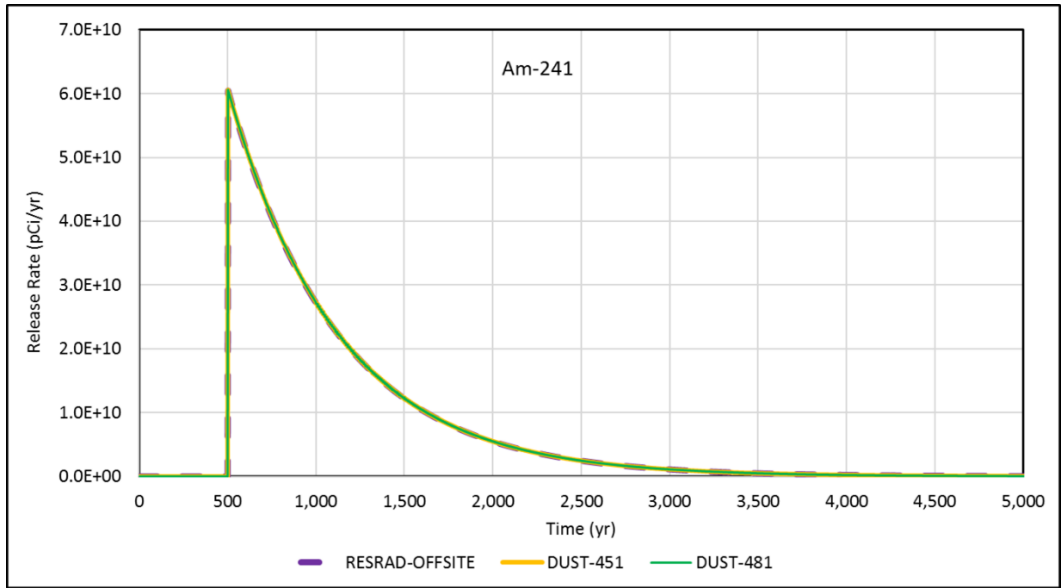
Figure M-37 Comparison of Calculated Am-241 Release Rates Associated with Disposal of TRU Wastes
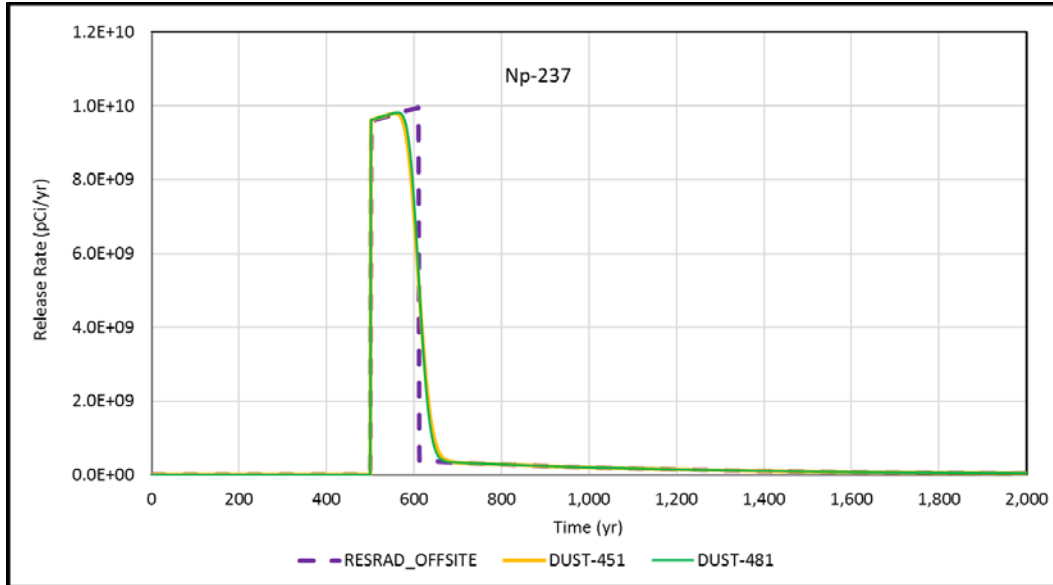
Figure M-38 Comparison of Calculated Np-237 Release Rates Associated with Disposal of TRU Wastes
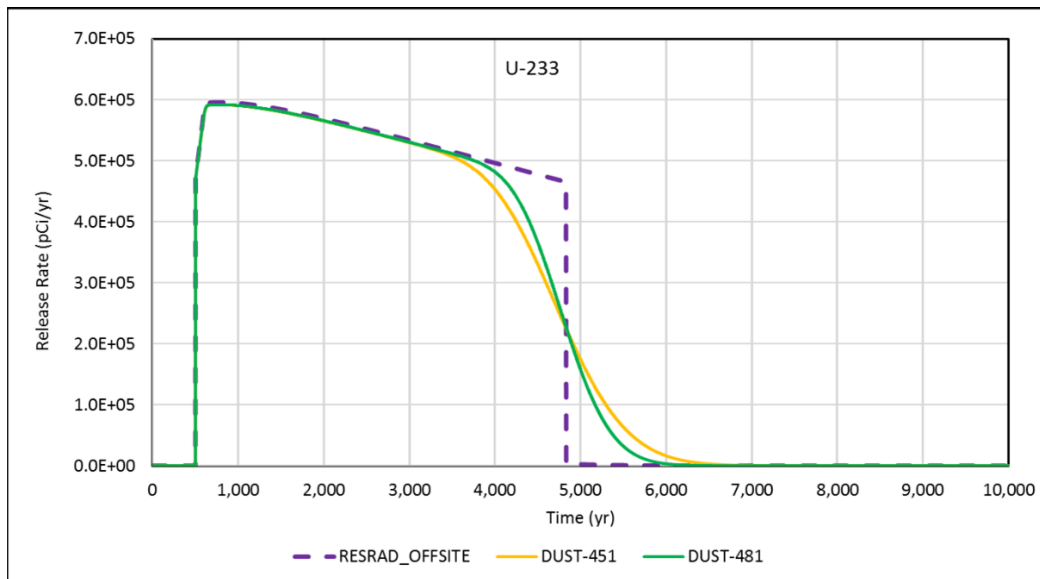
Figure M-39 Comparison of Calculated U-233 Release Rates Associated with Disposal of TRU Wastes
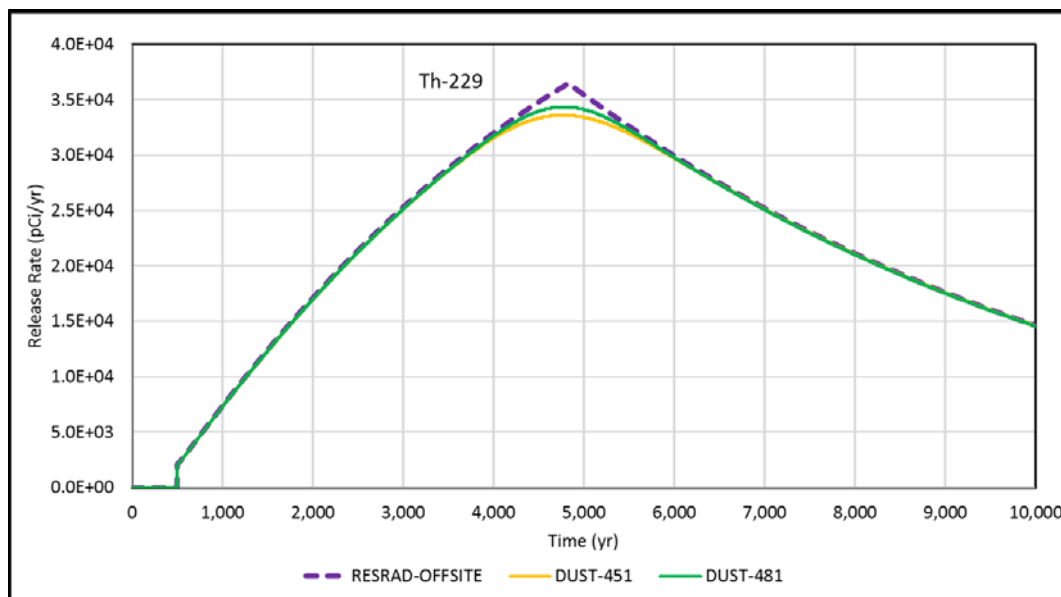
Figure M-40 Comparison of Calculated Th-229 Release Rates Associated with Disposal of TRU Wastes

M.7 Example Application V—Disposal of Grouted TRU Wastes

The TRU wastes concerned in Example Application IV were assumed to be grouted with cement to increase physical stability and reduce potential releases of radionuclides in Example Application V. The radionuclide mix and inventory were the same as listed in Table M-4. The bulk density of the grouted waste was assumed to be 2.65 g/cm³ based on the volume of the waste container. When containers fail (at 500 years), water would enter the containers, move along cracks in the cement matrix, and contact the waste materials. Upon contact with water, radionuclides would detach from the surface of the waste materials and dissolve in water. The dissolved radionuclides, while moving with water toward the bottom of the disposal cell, could adsorb to the cement or soil particles and the distributions of radionuclides among cement, soil particles, and water were assumed to reach equilibrium instantaneously. The soil Kds and cement Kds of radionuclides used for the analysis are listed in Table M-4.

M.7.1 RESRAD-OFFSITE Dose Analysis

In order to consider radionuclides adsorbing to cement in the waste domain, input concentrations were specified based on the mass of the contaminated medium. For example, the initial radioactivity of Np-237 was 0.75 Ci; the input concentration was calculated as 0.75 Ci × 10¹² pCi/Ci / (120 m³ × 10⁶ cm³/m³ × 2.65 g/cm³) = 2,360 pCi/g, where 120 m³ was the total volume of the waste containers and 2.65 g/cm³ was the bulk density of the grouted waste.

"Equilibrium Desorption Transfer" was selected as the release mechanism for radionuclides to consider their loose attachment to the waste materials. The "cumulative fraction of radionuclide-bearing material that is releasable" was increased stepwise to 1 at 500 years when all containers were assumed to fail. The total mass (318,000 kg) and volume (120 m³) were specified for the contaminated medium (i.e., the grouted waste including the waste materials and the cement matrix). (Note: the total mass was used to calculate the input concentrations of

radionuclides.) The bulk density of the contaminated zone was calculated to be 1.826 g/cm^3, based on the mass and volume of the contaminated medium and the mass (777,600 kg) and volume (480 m^3) of the surrounding soil, which was assumed to have a bulk density of 1.62 g/cm^3. Figure M-41 shows the input settings of the source term model.

Figure M-41 Source Term Model Input Settings for Disposal of Grouted TRU Waste

Figure M-42 shows the radiation dose profile associated with the drinking water pathway calculated by RESRAD-OFFSITE. Here the peaks are wider and the total peak dose is lower than those in Figure M-35. These are due to the additional retardation provided by the cement matrix to the movement of radionuclides detaching from the waste materials.
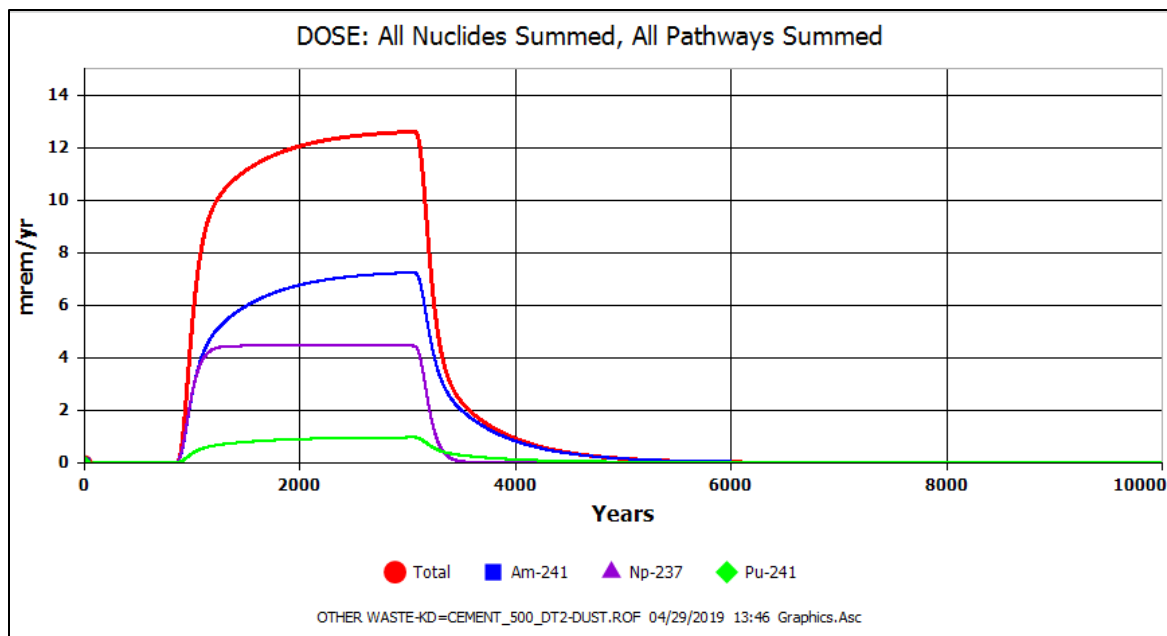
Figure M-42 Potential Radiation Dose Associated with Disposal of Grouted TRU Waste

M.7.2 Comparison with DUST-MS

The 481 grids scheme as discussed in Section 5.2 was used when employing DUST-MS to analyze the releases of radionuclides associated with the disposal of grouted TRU waste. The disposal area (5 m in depth) was subdivided by 101 grids (with the first grid at the top and 101th grid at the bottom) with a 5-cm spacing. The grouted waste was assumed being contained in 40 containers which were associated with 40 of the 101 grids (or nodes). Two different ways were used to assign the associations and create two input files. In the first input file, the containers were associated with grids 4, 6, 9, 11, 14, 16, 19, …, 94, 96, 99, and 101. In the second input file, each container was moved up by one grid, so they were associated with grids 3, 5, 8, 10, 13, 15, 18, …, 93, 95, 98, and 100. As in Example Application IV, surface rinse was selected as the release mechanism, but the partitioning coefficient (i.e., Kd in RESRAD-OFFSITE) for the wasteform was set to the value for cement (see Table M-4) rather than 0. The flux of radionuclides at grid 101 was obtained from the DUST-MS analyses to determine the radionuclide release rates at the bottom of the disposal area.

Specific input values were used in DUST-MS analyses to consider the retardation from soils and cement to the transport of radionuclides in water toward the bottom of the contaminated zone, as considered in the RESRAD-OFFSITE analysis. These specific input values were developed by taking into account the input limitations in DUST-MS, which are detailed as follows. First, DUST-MS accepts the input of bulk density and Kd for "the material" in which radionuclides transport (in this case, the soils surrounding the waste containers), but it accepts only the input of Kd for the wasteform (in this case, the cement grouted waste). In the DUST-MS analyses, the input bulk density of soil was used as the bulk density of the cement-grouted waste. In RESRAD-OFFSITE analysis, soils and the cement-grouted matrix (i.e., the contaminated medium) had different bulk densities. Secondly, DUST-MS accepts the input of facility dimensions, including the area and the spacing between grids (nodes), to determine the

controlled volume associated with each grid, which is the controlled volume of soil. However, there is no provision in DUST-MS to accept the input of wasteform dimensions. In the DUST-MS analyses, the controlled volume with each grid was used as the volume of the wasteform in the associated container. In the RESRAD-OFFSITE code, the total volume (and mass) of the wasteform (i.e., the contaminated medium) was specified, which was different from the total volume of soils in the contaminated zone.

To produce radionuclide release rates for comparison with those calculated by RESRAD-OFFSITE, the total mass of soils and the total mass of wasteform in the disposal area as considered in the DUST-MS analyses had to equal those considered in the RESRAD-OFFSITE analysis. To achieve this objective, the area of the disposal facility was set to 96 m^2, which was 80% the area of the contaminated zone (3 m × 40 m = 120 m^2) used in RESRAD-OFFITE analysis. With this setting, the total volume of soils was 96 m^2 × 5 m = 480 m^3, same as that considered in the RESRAD-OFFSITE analysis (600 m^3 – 120 m^3 = 480 m^3, where 600 m^3 was the volume of the contaminated zone and 120 m^3 was the volume of the contaminated medium.) The bulk density of soil was 1.62 g/cm^3, same as that assumed in RESRAD-OFFSITE analysis. The total mass of the wasteform should equal 318,000 kg (see Figure M-41). Because the bulk density DUST-MS used for the wasteform was also 1.62 g/cm^3, the total volume of wasteform, based on this bulk density, would be 196 m^3. The controlled volume associated with each grid was 96 m^2 × 0.05 m = 4.8 m^3, which was also the volume of the wasteform considered by DUST-MS. To attain the total volume of 196 m^3, the number of containers should be 196 m^3/4.8 m^3 = 40.

Figures M-43 to M-47 compare the radionuclide release rates from the DUST-MS and RESRAD-OFFSITE analyses for each of the radionuclides concerned. In the figures, "DUST-MS 2" denotes the results obtained with the input file that associated the lowest container with grid 101, at which the flux of radionuclides was calculated. "DUST-MS 1" denotes the results obtained with the other input file in which all the containers were moved up by 1 grid so the lowest container was associated with grid 100. In general, radionuclides released from the waste materials would need to travel longer distances to reach the bottom of the disposal area with the container distributions in DUST-MS 1 than in DUST-MS 2. Due to additional radiological decay associated with longer travel time, the radionuclide release rate is expected to be smaller with DUST-MS 1 than with DUST-MS 2, which is observed in Figure M-43 for Pu-241 and Figure M-44 for Am-241. The difference in release rate is not visible in Figures M-45, M-46, and M-47, for Np-237, U-233, and Th-229, respectively, because these three radionuclides have a much longer decay half-life than Pu-241 and Am-241. Different from the DUST-MS analyses, in which the source of radionuclides for transport came from several discrete locations, in RESRAD-OFFSITE analysis, the source of radionuclides, after they detached from the waste materials, was evenly distributed along the depth of the contaminated zone from where they transport to the bottom of the contaminate zone. This fundamental difference caused the discrepancy between the RESRAD-OFFSITE results and DUST-MS results.
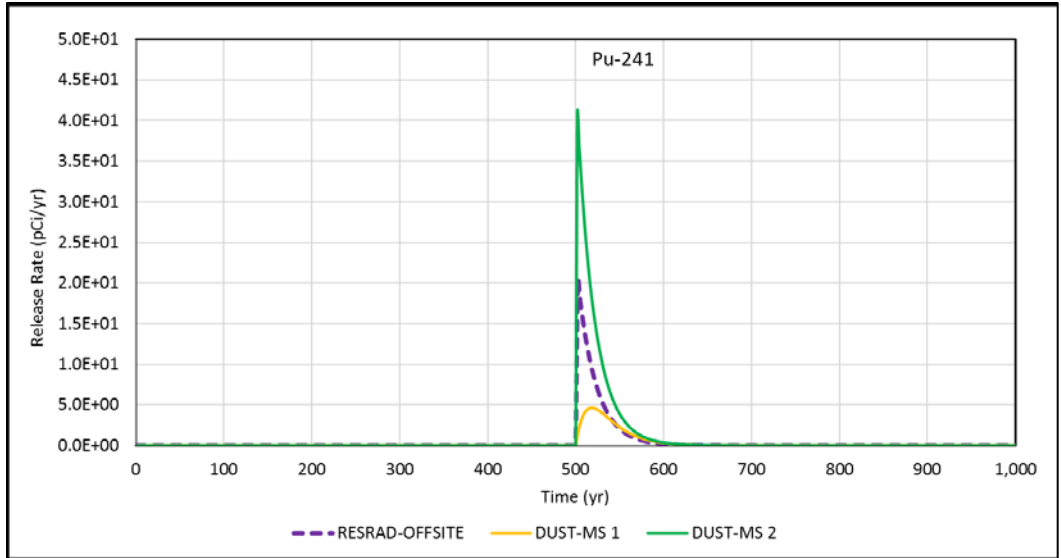
Figure M-43 Comparison of Calculated Pu-241 Release Rates Associated with Disposal of Grouted TRU Wastes
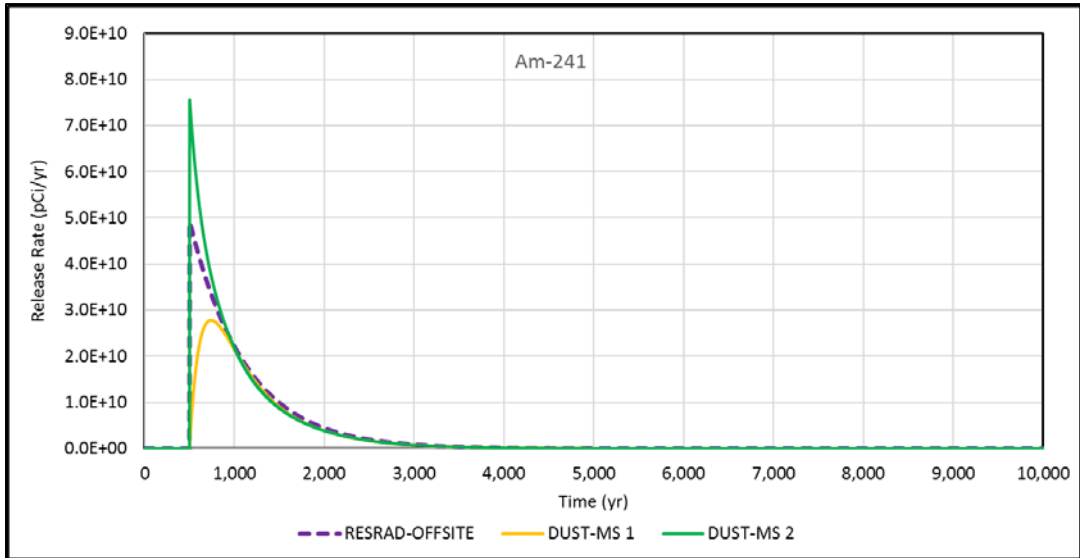
Figure M-44 Comparison of Calculated Am-241 Release Rates Associated with Disposal of Grouted TRU Wastes
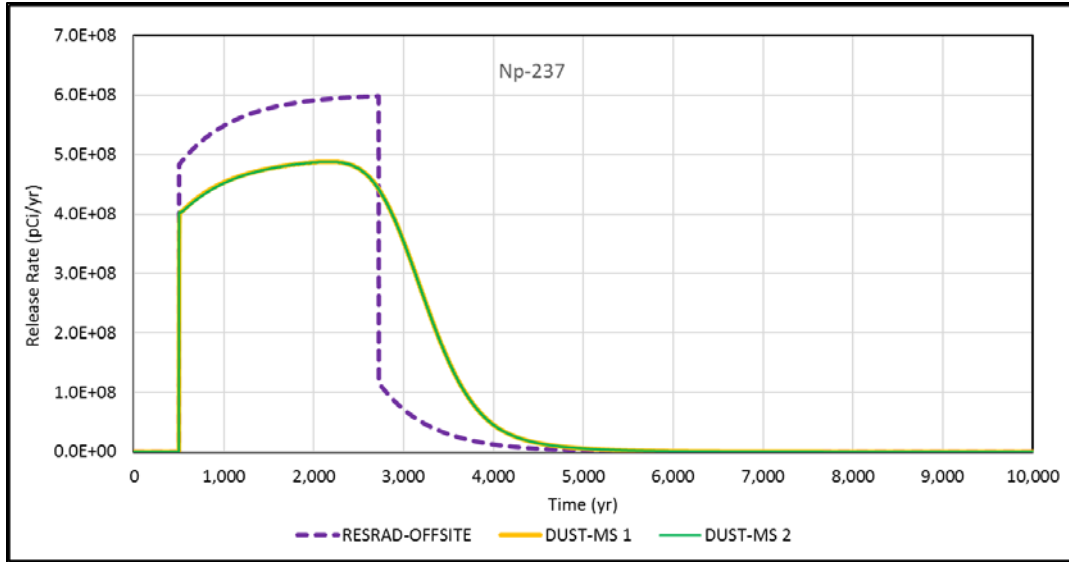
Figure M-45 Comparison of Calculated Np-237 Release Rates Associated with Disposal of Grouted TRU Wastes
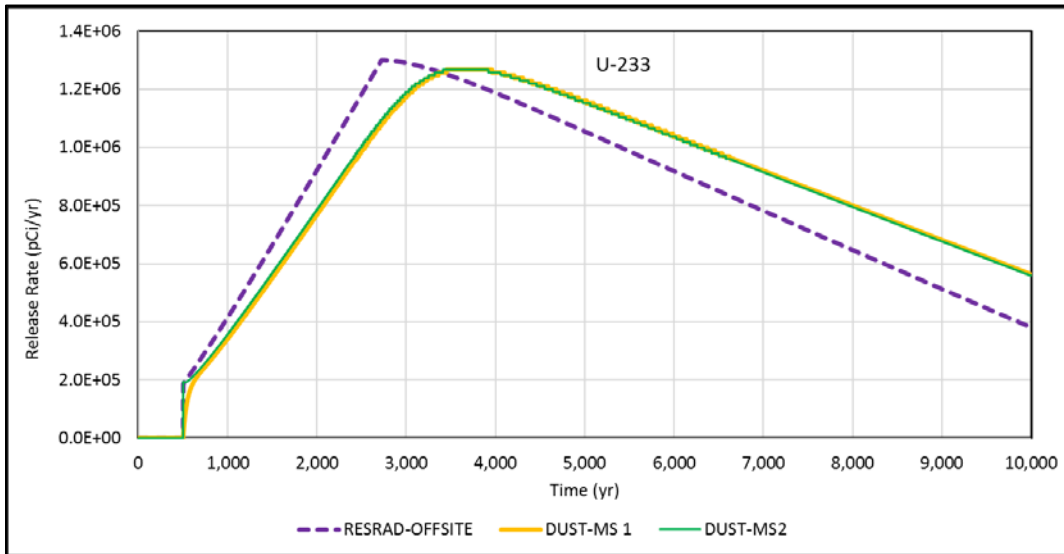
Figure M-46 Comparison of Calculated U-233 Release Rates Associated with Disposal of Grouted TRU Wastes
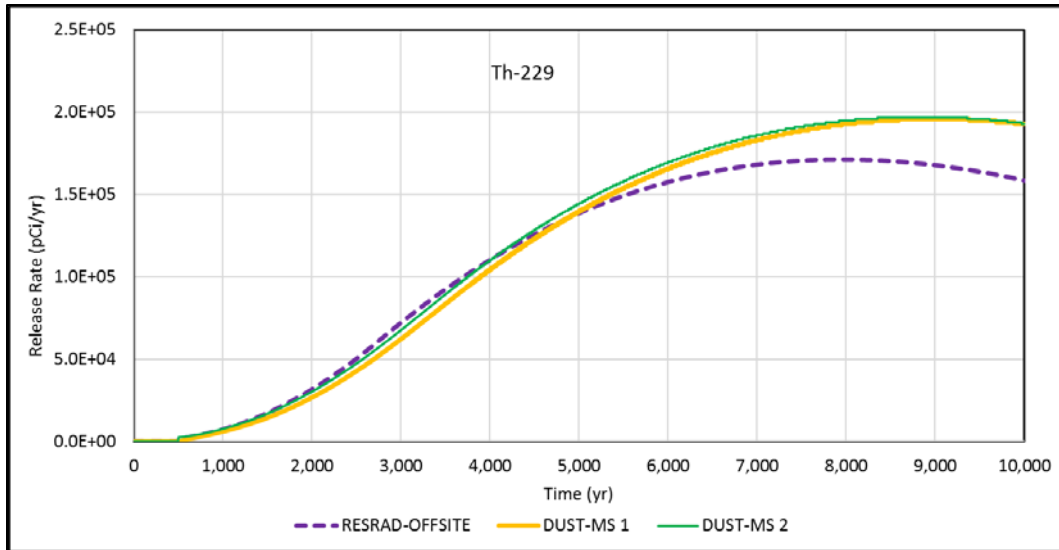
**Figure M-47 Comparison of Calculated Th-229 Release Rates Associated
with Disposal of Grouted TRU Wastes**

M.8 Example Application VI—Disposal of Grouted TRU Wastes—Release through Diffusion

In Example Application VI, the release rates of radionuclides from the grouted TRU wastes considered in Example Application V were assumed to be controlled by diffusive transport. Although cracks would form in the cement matrix as it deteriorates over time, there are intact fragments where only tiny pores or microcracks are present. In the tiny pores or microcracks, the movement of water is restricted, so radionuclides that partition to the pore water upon contact with water would need to diffuse to the larger cracks, then migrate to the surfaces of the cement matrix by advection. Both the diffusive and advective transport could affect the radionuclide release rate from the waste domain to the soil domain. However, in Example Application VI, the diffusive transport is considered to proceed much more slowly than the advective transport; therefore, it determines the release rate of radionuclides to the surrounding soil.

M.8.1 RESRAD-OFFSITE Dose Analysis

Figure M-48 shows the input settings of the source term model. After the "Model diffusive transport out of contaminated medium" option was selected, the initial radionuclide concentrations input to RESRAD-OFFSITE must be specified on the basis of the contaminated medium. The initial concentrations were the same as those used in Example Application V (see Table M-4).

Figure M-48 Source Term Model Input Settings for Disposal of Grouted TRU Waste—Diffusion Controlled Release with 10-cm Fragments

"Equilibrium Desorption Transfer" was the mechanism associated with the "diffusive transport" option. A Kd value for the contaminated medium is required for each radionuclide of concern, which is used to determine the partitioning of radionuclides between the waste materials and the pore water assuming instantaneous equilibrium. A Kd value of 0 cm^3/g was used for all radionuclides of concern so that all the releasable radionuclide inventory would dissolve in pore water when the waste material became releasable. This set up the initial radionuclide concentrations in water for the diffusive transport. The diffusion flux of radionuclides in pore water across each of the surfaces of intact fragments was calculated using the diffusion coefficient in a contaminated medium (i.e., the cement matrix) and the dimensions specified for individual fragments, which were assumed to be 10 cm in all x, y, and z directions in this analysis. Most of the literature data on diffusion coefficients for different radionuclides were obtained by conducting leaching experiments in laboratories, specifically by measuring the

amount of radionuclides released from contaminated materials to the leachate used and then fitting the measurement data to the mathematical formulation for diffusion to obtain an "effective" diffusion coefficient. The effective diffusion coefficient obtained could include the effect of equilibrium desorption or other interaction that occurs simultaneously with diffusion, depending on the mathematical formula selected for data fitting. With this consideration, the Kds for the contaminated medium were set to 0 cm^3/g in this example application.

Figure M-49 shows the radiation dose profile associated with the drinking water pathway calculated by RESRAD-OFFSITE. Comparing with the dose profile in Figure M-42, the peak in Figure M-49 is narrower and the peak dose is greater. This indicates the assumption that diffusive transport controls the release rate of radionuclides from the waste domain may not reflect the actual situation, and further investigation is needed. The dimensions of individual fragments in which diffusion would take place were assumed to be 10 cm in x, y, and z directions, which were much smaller than the dimensions of the waste container. The use of smaller fragments for diffusion was based on the consideration that there would be larger cracks in the cement matrix in which the movement of radionuclides (in water) would not be restricted to diffusion. On the other hand, the effective diffusion coefficients used in this analysis were at the upper end of their range; had smaller values been used, the dose profile would have shown a peak with a longer tail and with a smaller peak value.
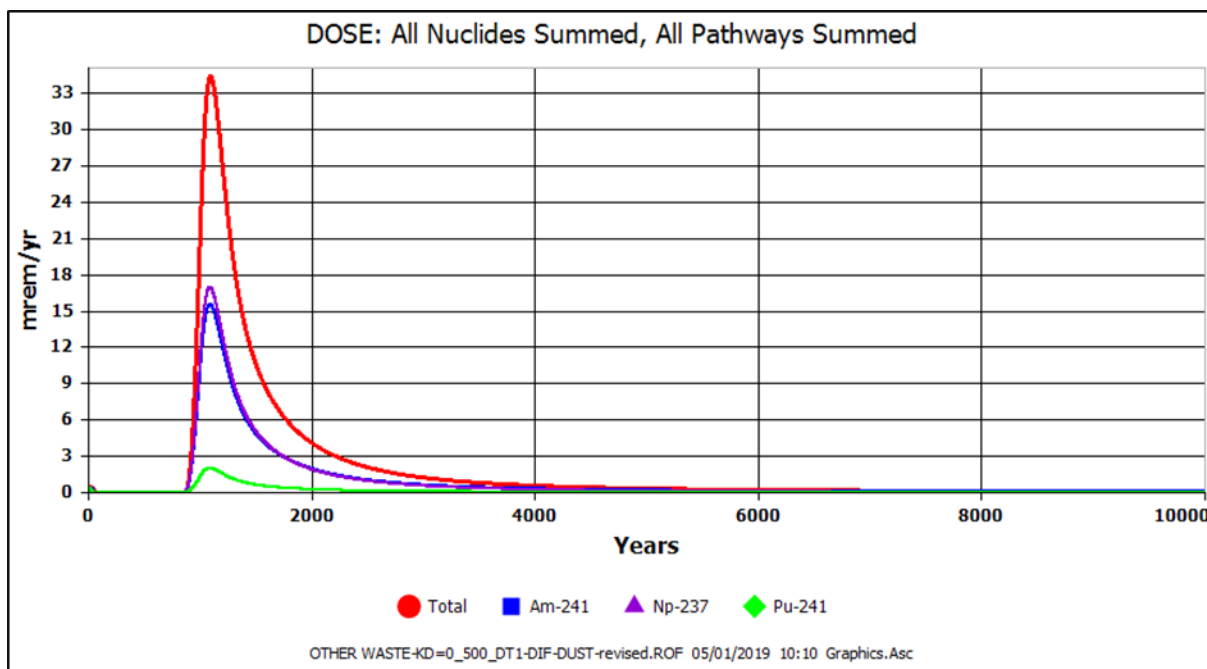
Figure M-49 Potential Radiation Dose Associated with Disposal of TRU Waste—Diffusion Controlled Release with 10-cm Fragments

M.8.2 Comparison with DUST-MS

The 481 grids scheme with 40 waste containers and the lowest container being associated with grid 100 as discussed in Section M.7.2 was used in the DUST-MS analysis for Example Application VI. 100% of the release of radionuclides from the waste form was considered to occur through diffusion. There are two options for modeling diffusive transport; one solves the

governing equation analytically and the other solves the governing equation numerically with the finite difference (FD) method. According to the available guidance document (Sullivan 2006), the analytical option has limitation—it cannot handle the ingrowth of progenies properly, perhaps when the progenies diffuse with a different speed than the parent nuclide. It is not clear how the fluxes of progenies are calculated with the analytical method. Even with the FD method, there are no discussions on how progenies are accounted for in the guidance document (Sullivan, 2006). The boundary condition at the surface of individual fragments for diffusion assumes the radionuclide concentration in pore water would be zero. Two DUST-MS runs were performed; one chose the analytical option and the other chose the numerical option.

The RESRAD-OFFSITE code solves the governing equation for diffusive transport analytically. Unlike the assumption adopted by DUST-MS, RESRAD-OFFSITE considers a zero radionuclide concentration in pore water at an infinite distance from the center of each individual fragment.

Figures M-50 to M-54 compare the release rates of radionuclides from the bottom of the contaminated zone for each of the radionuclides concerned. In the figures, the radionuclide release profile calculated by RESRAD-OFFSITE is denoted as "RESRAD-OFFSITE." "DUST-analytical" and "DUST-FD" denote the results from DUST-MS with the analytical and finite difference options. In general, the DUST-MS results obtained with the FD option agree better with the RESRAD-OFFSITE results than the DUST-MS results obtained with the analytical option. As mentioned previously, the boundary conditions assumed by RESRAD-OFFSITE and DUST-MS for solving the governing equation for diffusive transport are different, which could be the main reason for the discrepancies in their results, although the different ways of handling the ingrowth and transport of progenies could contribute to the discrepancies as well.
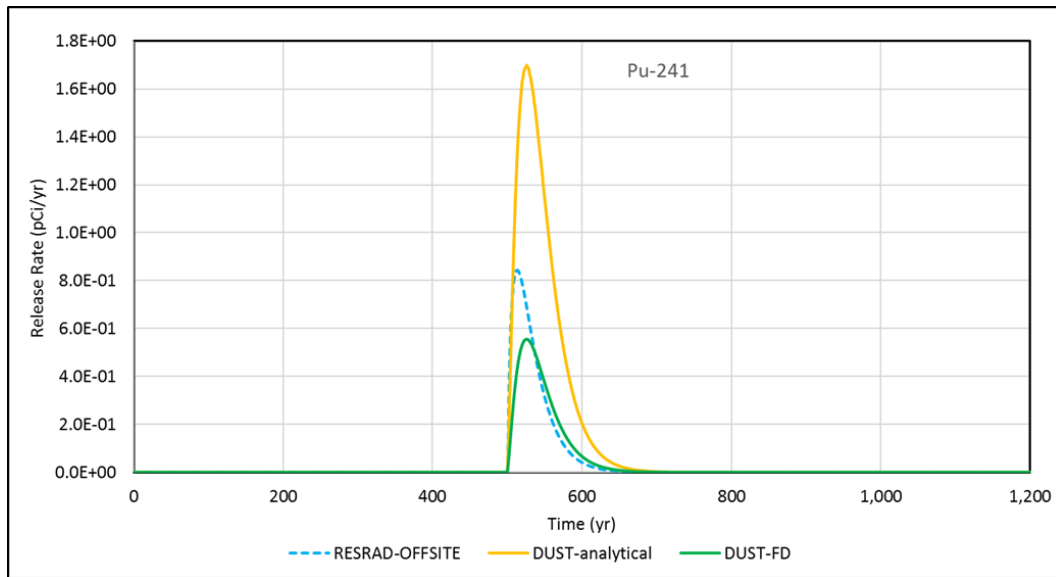
Figure M-50 Comparison of Calculated Pu-241 Release Rates Associated with Disposal of Grouted TRU Wastes—Diffusive Transport within 10-cm Fragments
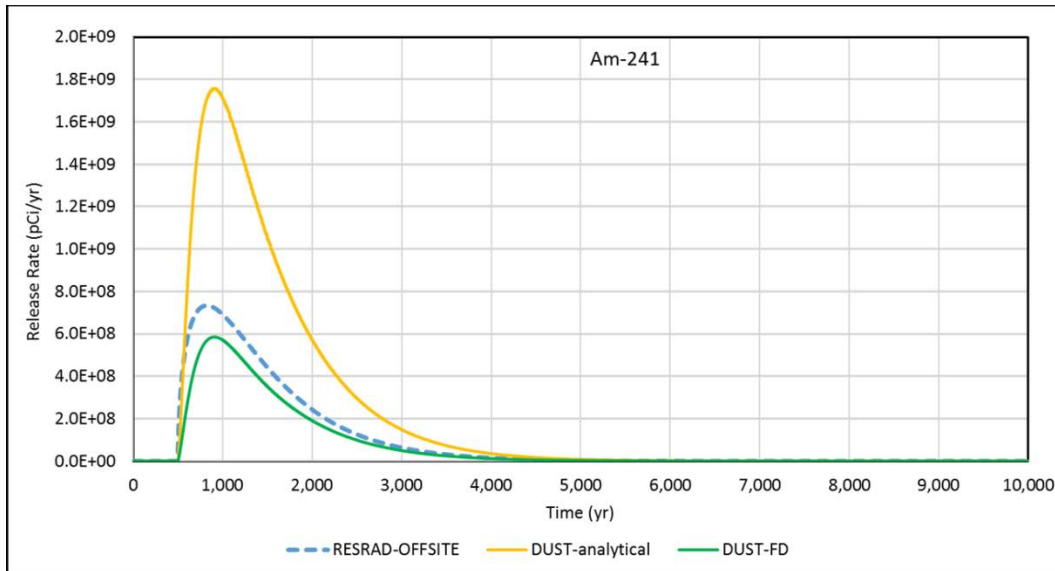
Figure M-51 Comparison of Calculated Am-241 Release Rates Associated with Disposal of Grouted TRU Wastes—Diffusive Transport within 10-cm Fragments
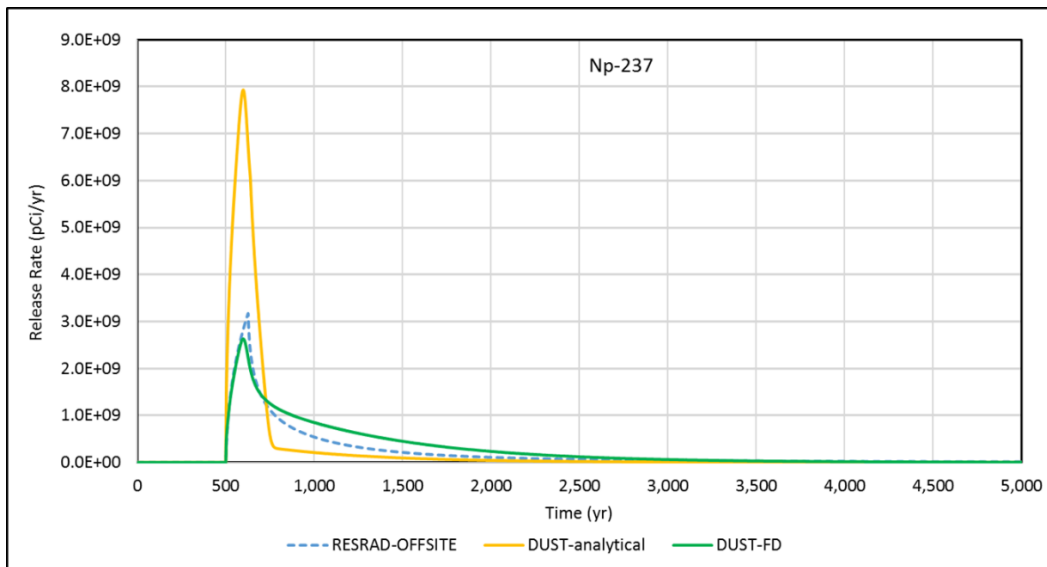
Figure M-52 Comparison of Calculated Np-237 Release Rates Associated with Disposal of Grouted TRU Wastes—Diffusive Transport within 10-cm Fragments
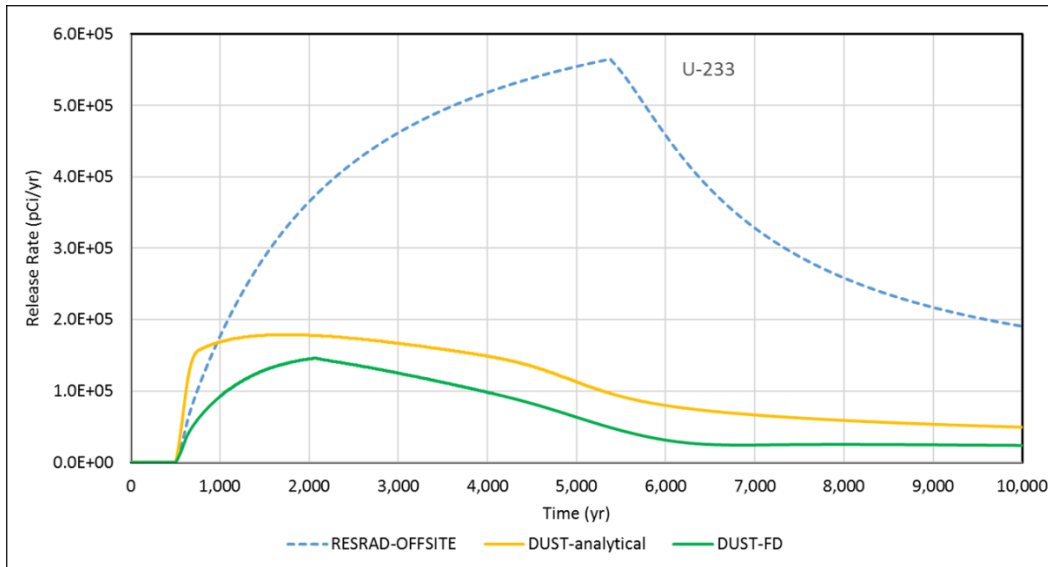
**Figure M-53 Comparison of Calculated U-233 Release Rates Associated
with Disposal of Grouted TRU Wastes—Diffusive Transport
within 10-cm Fragments**
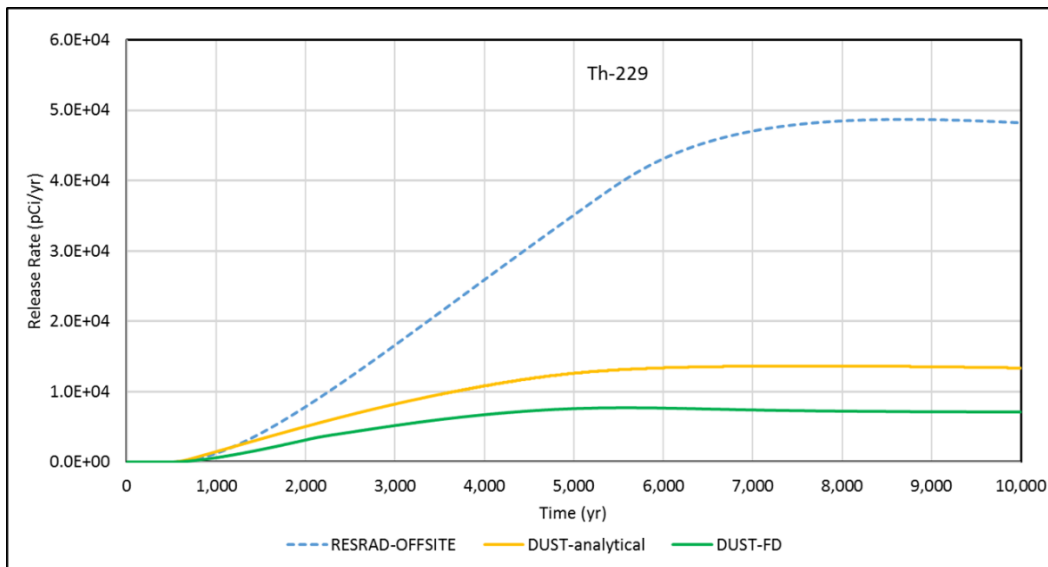
**Figure M-54 Comparison of Calculated Th-229 Release Rates Associated
with Disposal of Grouted TRU Wastes—Diffusive Transport
within 10-cm Fragments**

M.9 Example Application VII – Disposal of Sealed Sources Waste – First-Order Rate-Controlled Release

In Example Application VII, the release rates of radionuclides from sealed sources waste assumed to be disposed of in the near surface trench were analyzed. Table M-5 lists the

radionuclides of concern (Pu-238, Pu-239, and Am-241) that were selected on the basis of potential impact to groundwater, and their initial inventory was assumed in the analysis.

It is assumed that when the waste materials are in contact with water, chemical interaction between species (containing the radionuclide of concern) in the waste materials and in water would occur, causing radionuclides to dissolve into the water. The dissolution rate at any time is linearly proportional to the releasable inventory of radionuclide in the waste materials. Once radionuclides dissolve in water, they would be discharged to the soil domain and transported to the bottom of the contaminated zone. The first-order rate constant for dissolution is usually determined by carrying out leaching experiments and fitting mathematical formulation with the measured radionuclide release rates. The assumed values for this analysis are listed in the last column of Table M-5.

Table M-5 Radioactivity Inventory and Kd Values for Radionuclides in Sealed Sources Waste

Radionuclide	Initial inventory (Ci)	Initial conc. based on the entire primary contamination (pCi/g)	Kd for soil (cm3/g)	1st order leach rate constant (1/yr)
Pu-238	50000	5.14E+07	100	2.08E-03
Pu-239	35000	3.60E+07	100	2.08E-03
Am-241	6250	6.43E+06	100	2.08E-03
Ac-227	0	0.00E+00	100	2.08E-03
Np-237	0	0.00E+00	10	2.05E-02
U isotopes	0	0.00E+00	100	2.08E-03
Th isotopes	0	0.00E+00	250	8.32E-04
Pa-231	0	0.00E+00	35	5.92E-03
Pb-210	0	0.00E+00	100	2.08E-03
Po-210	0	0.00E+00	100	2.08E-03
Ra-226	0	0.00E+00	50	4.15E-03

Am-241 sealed sources and Pu-238 and Pu-239 sealed sources were assumed to be packaged in different waste containers, which, in conjunction with the original package of the sealed sources, provide different levels of protection for the radioactive materials. The release of Am-241 was assumed to begin at 800 years, while the release of Pu-238 and Pu-239 was assumed to begin at 300 years after the waste disposal.

M.9.1 RESRAD-OFFSITE Dose Analysis

Figure M-55 shows the input settings of the source term model. The sealed sources were not considered to be grouted, and the retardation to radionuclide transport toward the bottom of the contaminated zone was primarily caused by adsorption to soil particles; therefore, the input radionuclide concentration was "based on the mass of the entire primary contamination." The release of Am-241 and the release of Pu-238 and Pu-239 were delayed by different numbers of

years, so the specifications for "cumulative fraction of radionuclide bearing material that is releasable" are different for Am-241 and for Pu-238 and Pu-239, as shown in Figure M-55. The linearity of the dissolution rate of radionuclide to the releasable inventory was assumed unchanged with time, so the same first-order rate constant (i.e., the leach rate in the source term model) was specified for both times, 300 years and 800 years.

Figure M-55 Source Term Model Input Settings for Disposal of Sealed Sources Waste—First-Order Rate-Controlled Release

Figure M-56 shows the radiation dose profile associated with the drinking water pathway calculated by RESRAD-OFFSITE. The arrival of radionuclides at the well location would take several thousand years, and the total dose would result primarily from Pu-239. Figure M-57 provides a breakdown of the total dose by the initially existing radionuclides and their decay progenies. The contribution to the total dose attributed to Am-241 was actually from Np-237, its progeny, because Np-237 has a smaller Kd than Am-241, so it would reach the well location earlier than would Am-241; furthermore, due to the shorter decay half-life of Am-241 (432 years), most of its radioactivity would decay away before reaching the well location. The contribution to the total dose attributed to Pu-238 came from U-234, Po-210, Pb-210, and Ra-226, all decay progenies of Pu-238. Their contributions peaked at 10,000 years, with a total slightly greater than 140 mrem/yr. The contribution to the total dose attributed to Pu-239 came from Pu-239 itself, because it has a long decay half-life (24,100 years) so the amount of progenies generated within 10,000 years would be much less than the amount of Pu-239 remaining, which also has a much larger ingestion dose conversion factor than the first decay progeny, U-235.
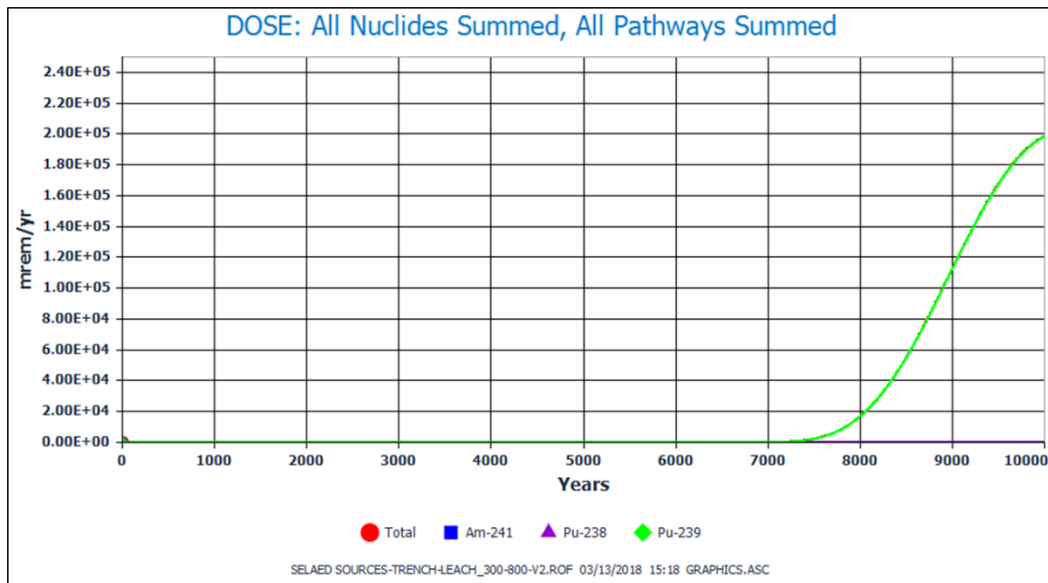
Figure M-56 Potential Radiation Dose Associated with Disposal of Sealed Sources Waste—First-Order Rate-Controlled Release
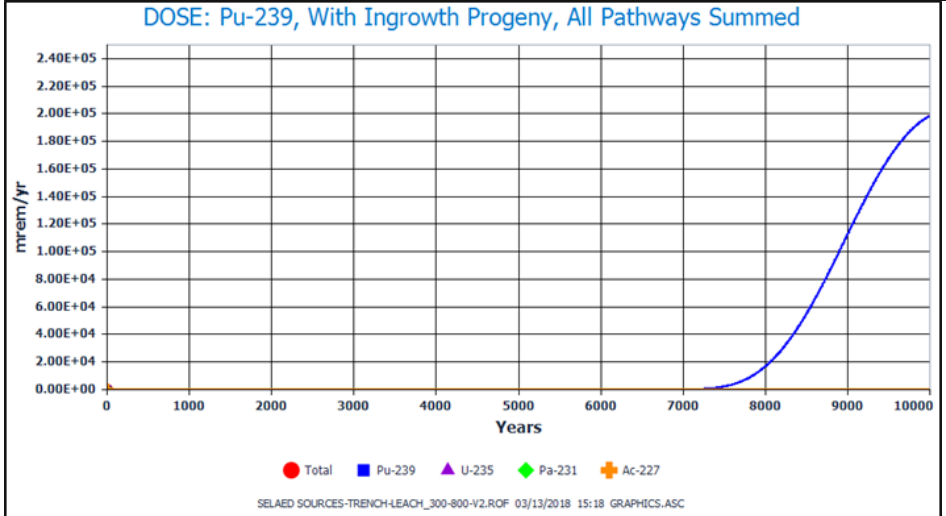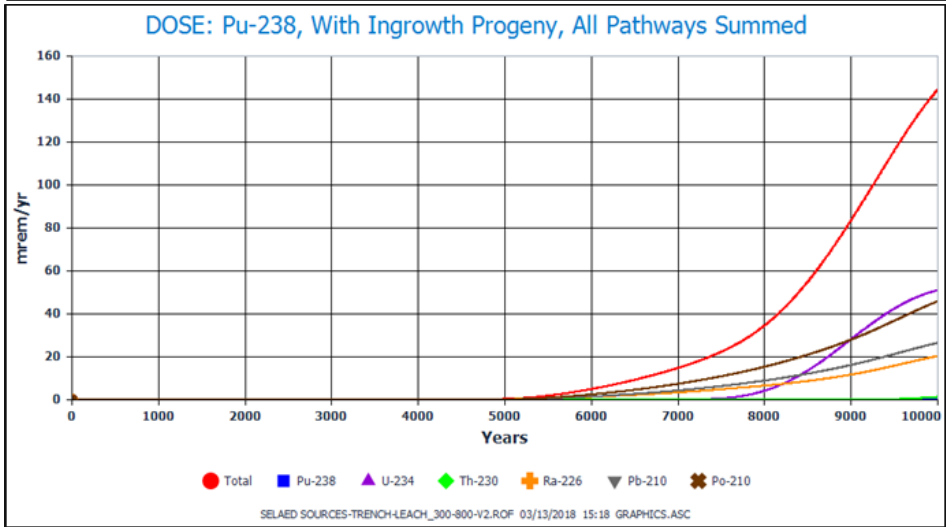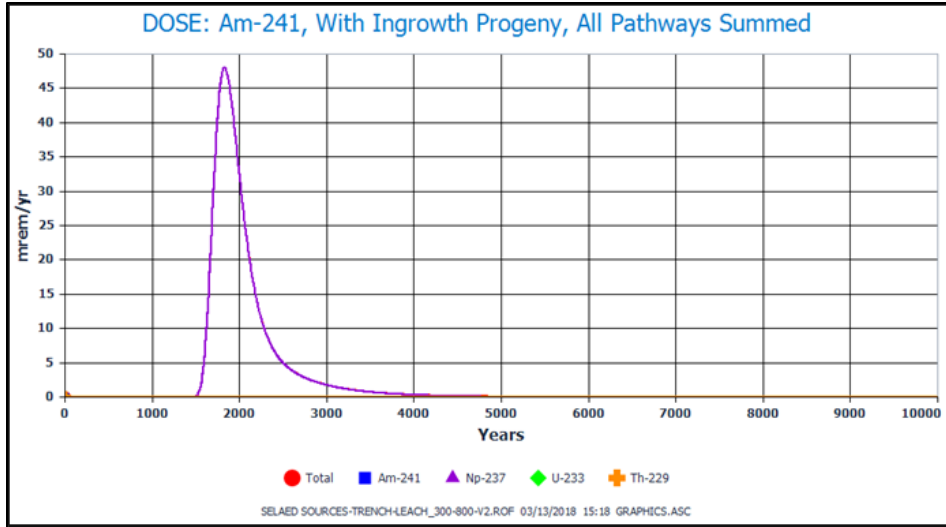
Figure M-57 Breakdown of Total Radiation Dose Associated with Disposal of Sealed Sources Waste—First-Order Rate-Controlled Release

The predicted total dose contribution from Pu-239 was extremely high, peaking at about 200,000 mrem/yr within 10,000 years. Such a high dose contribution would be caused by a high concentration of Pu-239 in the well water, which indicated a high concentration of Pu-239 in the leachate (i.e., soil water) that would leave the contaminated zone. Table M-6 lists the calculated leachate concentrations of each individual radionuclide in each decay chain simulated by the RESRAD-OFFSITE code. They were obtained by dividing the radionuclide release rates from the bottom of the contaminated zone by the water flow rate (i.e., the water infiltration rate times the area of the contaminated zone). As shown by the listed values, the concentrations of Pu-239 would greatly exceed the solubility of Pu, when no limitation to the leachate concentration is imposed during the simulation.

Table M-6 Calculated Concentrations of Individual Radionuclides of Each Decay Chain in Leachate That Would Leave the Contaminated Zone

Concentration of Pu-239 greatly exceeds the solubility limit

Conc. in the water (mole/L) leaving the contaminated zone

time (yr)	Am-241	Np-237	U-233	Th-229	Pu-238	Pu-238	U-234	Th-230	Ra-226	Pb-210	Po-210	Pu-239	U-235	Pa-231	Ac-227
280	0.00E+00	0.00E+00	0.00E+00	0.00E+00	0.00E+00	0.00E+00	0.00E+00	0.00E+00	0.00E+00	0.00E+00	0.00E+00	0.00E+00	0.00E+00	0.00E+00	0.00E+00
285	0.00E+00	0.00E+00	0.00E+00	0.00E+00	0.00E+00	0.00E+00	0.00E+00	0.00E+00	0.00E+00	0.00E+00	0.00E+00	0.00E+00	0.00E+00	0.00E+00	0.00E+00
290	0.00E+00	0.00E+00	0.00E+00	0.00E+00	0.00E+00	0.00E+00	0.00E+00	0.00E+00	0.00E+00	0.00E+00	0.00E+00	0.00E+00	0.00E+00	0.00E+00	0.00E+00
295	0.00E+00	0.00E+00	0.00E+00	0.00E+00	0.00E+00	0.00E+00	0.00E+00	0.00E+00	0.00E+00	0.00E+00	0.00E+00	0.00E+00	0.00E+00	0.00E+00	0.00E+00
300	0.00E+00	0.00E+00	0.00E+00	0.00E+00	1.65E-19	8.95E-11	2.50E-07	2.76E-10	1.73E-15	2.86E-17	1.01E-19	1.85E-07	1.61E-09	1.92E-15	1.44E-19
305	0.00E+00	0.00E+00	0.00E+00	0.00E+00	4.77E-19	2.59E-10	7.24E-07	8.29E-10	5.35E-15	8.67E-17	3.34E-19	5.53E-07	4.88E-09	5.81E-15	4.96E-19
310	0.00E+00	0.00E+00	0.00E+00	0.00E+00	7.62E-19	4.14E-10	1.16E-06	1.38E-09	9.25E-15	1.46E-16	6.12E-19	9.17E-07	8.21E-09	9.75E-15	9.35E-19
315	0.00E+00	0.00E+00	0.00E+00	0.00E+00	1.02E-18	5.55E-10	1.55E-06	1.93E-09	1.34E-14	2.08E-16	9.30E-19	1.28E-06	1.16E-08	1.38E-14	1.45E-18
320	0.00E+00	0.00E+00	0.00E+00	0.00E+00	1.26E-18	6.83E-10	1.91E-06	2.48E-09	1.79E-14	2.71E-16	1.28E-18	1.63E-06	1.51E-08	1.78E-14	2.03E-18
325	0.00E+00	0.00E+00	0.00E+00	0.00E+00	1.47E-18	7.98E-10	2.23E-06	3.02E-09	2.26E-14	3.37E-16	1.67E-18	1.99E-06	1.86E-08	2.20E-14	2.68E-18
330	0.00E+00	0.00E+00	0.00E+00	0.00E+00	1.66E-18	9.03E-10	2.52E-06	3.56E-09	2.76E-14	4.04E-16	2.09E-18	2.33E-06	2.23E-08	2.62E-14	3.37E-18
335	0.00E+00	0.00E+00	0.00E+00	0.00E+00	1.83E-18	9.96E-10	2.78E-06	4.10E-09	3.28E-14	4.73E-16	2.54E-18	2.68E-06	2.59E-08	3.04E-14	4.11E-18
340	0.00E+00	0.00E+00	0.00E+00	0.00E+00	1.99E-18	1.08E-09	3.01E-06	4.64E-09	3.83E-14	5.44E-16	3.01E-18	3.02E-06	2.97E-08	3.48E-14	4.89E-18
345	0.00E+00	0.00E+00	0.00E+00	0.00E+00	2.12E-18	1.15E-09	3.22E-06	5.18E-09	4.41E-14	6.17E-16	3.51E-18	3.36E-06	3.35E-08	3.92E-14	5.71E-18
775	0.00E+00	0.00E+00	0.00E+00	0.00E+00	4.76E-19	2.59E-10	7.22E-07	3.69E-08	1.28E-12	1.76E-14	1.37E-16	2.22E-05	5.00E-07	7.15E-13	1.53E-16
780	0.00E+00	0.00E+00	0.00E+00	0.00E+00	4.61E-19	2.50E-10	6.99E-07	3.72E-08	1.30E-12	1.80E-14	1.40E-16	2.23E-05	5.06E-07	7.26E-13	1.55E-16
785	0.00E+00	0.00E+00	0.00E+00	0.00E+00	4.45E-19	2.42E-10	6.76E-07	3.74E-08	1.32E-12	1.83E-14	1.43E-16	2.25E-05	5.13E-07	7.37E-13	1.58E-16
790	0.00E+00	0.00E+00	0.00E+00	0.00E+00	4.31E-19	2.34E-10	6.53E-07	3.76E-08	1.34E-12	1.86E-14	1.45E-16	2.26E-05	5.19E-07	7.49E-13	1.60E-16
795	0.00E+00	0.00E+00	0.00E+00	0.00E+00	4.16E-19	2.26E-10	6.32E-07	3.78E-08	1.36E-12	1.90E-14	1.48E-16	2.27E-05	5.25E-07	7.61E-13	1.63E-16
800	1.66E-10	4.19E-08	7.01E-14	1.37E-17	4.02E-19	2.19E-10	6.11E-07	3.81E-08	1.38E-12	1.93E-14	1.51E-16	2.28E-05	5.32E-07	7.72E-13	1.66E-16
805	4.92E-10	1.22E-07	2.19E-13	4.20E-17	3.89E-19	2.11E-10	5.90E-07	3.83E-08	1.40E-12	1.97E-14	1.54E-16	2.30E-05	5.38E-07	7.84E-13	1.68E-16
810	8.10E-10	1.94E-07	3.81E-13	7.20E-17	3.76E-19	2.04E-10	5.71E-07	3.85E-08	1.42E-12	2.00E-14	1.57E-16	2.31E-05	5.44E-07	7.96E-13	1.71E-16
815	1.12E-09	2.59E-07	5.53E-13	1.04E-16	3.63E-19	1.98E-10	5.51E-07	3.87E-08	1.45E-12	2.04E-14	1.60E-16	2.32E-05	5.50E-07	8.06E-13	1.74E-16
820	1.42E-09	3.19E-07	7.36E-13	1.37E-16	3.51E-19	1.91E-10	5.33E-07	3.89E-08	1.47E-12	2.07E-14	1.62E-16	2.33E-05	5.57E-07	8.14E-13	1.76E-16

The DUST-MS code does not provide the option of considering releases of radionuclides controlled by first-order dissolution reaction. Therefore, comparison between RESRAD-OFFSITE and DUST-MS results was not attempted.

M.10 Example Application VIII—Disposal of Sealed Sources Waste—Solubility Controlled Release

As discussed in Section M.9.1 concerning the RESRAD-OFFSITE analysis for Example Application VII, the predicted Pu-239 concentration in leachate would greatly exceed its solubility, if its release from the waste domain was controlled by a first-order dissolution reaction with the specified first-order rate constant. Therefore, in Example Application VIII, a different option provided by the updated source term model of RESRAD-OFFSITE, the equilibrium

solubility release, was considered for Pu-238 and Pu-239. The solubility for Pu was assumed to be 1×10^{-10} g atomic weight/L (mole/L), which is about 2.39×10^{-8} g/L.

M.10.1 RESRAD-OFFSITE Dose Analysis

The input settings of the source term model to analyze Example Application VIII are shown in Figure M-58. Because Pu-238 and Pu-239 are isotopes of Pu, the "equilibrium solubility release" option was selected for both radionuclides. For other radionuclides, the release mechanism remained "first-order rate-controlled release."

In the RESRAD-OFFSITE analysis, the (mass) concentration of Pu in the leachate, which was the (mass) concentration of Pu-238 and Pu-239 combined, would be set equal to the solubility until the releasable inventories of Pu-238 and Pu-239 in the waste domain were exhausted. The (mass) concentration ratio of Pu-238 to Pu-239 in the leachate was the same as the (mass) ratio of releasable inventory of Pu-238 to Pu-239 in the waste domain. Because the initial mass inventory of Pu-238 in the waste domain was much smaller than that of Pu-239, in addition, Pu-238 would decay away very quickly (the decay half-life of Pu-238 is 87.7 years), as a result, the mass concentration of Pu-239 in the leachate would be essentially the same as the solubility of Pu, starting at 300 years until the time the releasable Pu-239 is depleted.

Figure M-59 shows the radiation dose profile associated with the drinking water pathway calculated by RESRAD-OFFSITE. The peak total dose at 10,000 years was reduced to 140 mrem/yr (from 200,000 mrem/yr, as seen in Figure M-56) and was mainly attributed to Pu-238. Figure M-60 provides a breakdown of the total dose by the initially existing radionuclides and their decay progenies. The maximum contribution from Pu-239 to the total dose was less than 2 mrem/yr.

Figure M-58 Source Term Model Input Settings for Disposal of Sealed Sources Waste—Solubility Controlled Release for Pu

Figure M-59 Potential Radiation Dose Associated with Disposal of Sealed Sources Waste—Solubility Controlled Release for Pu
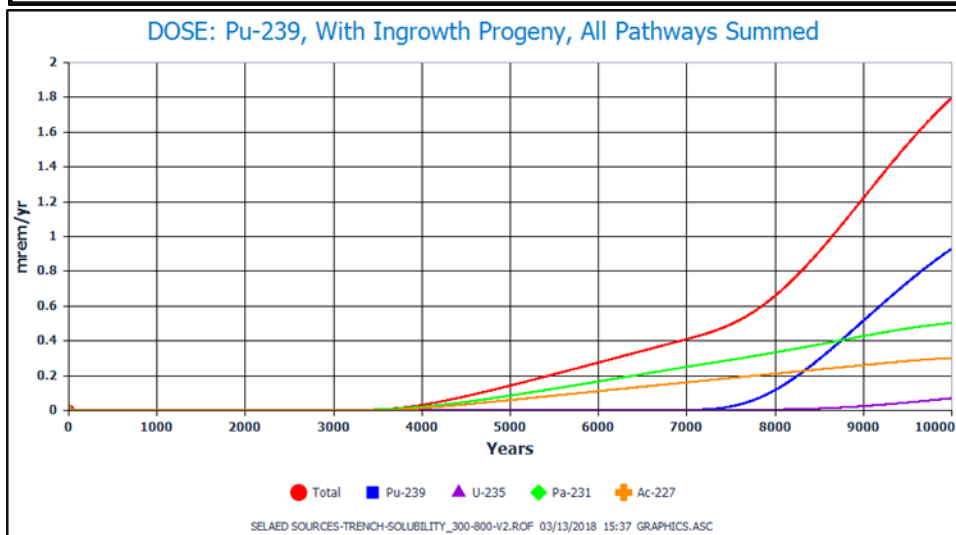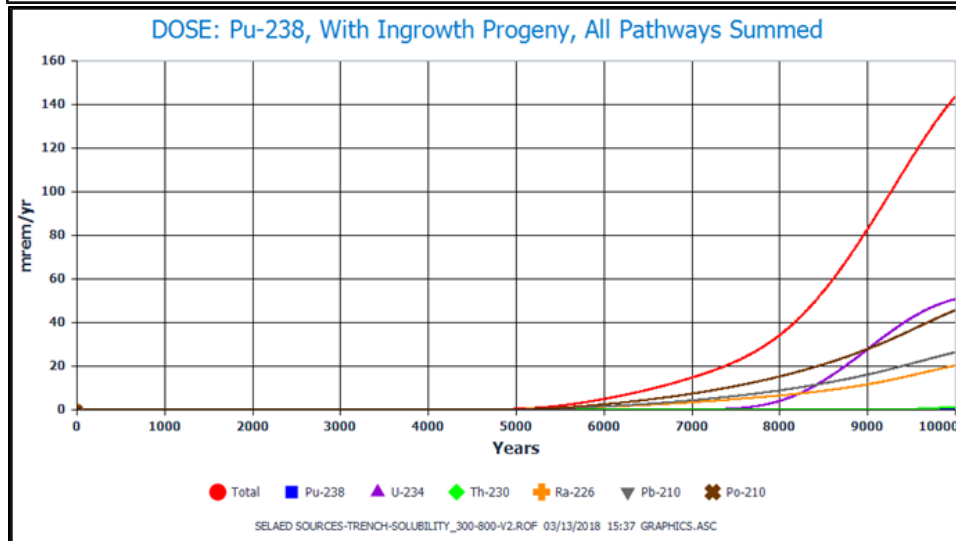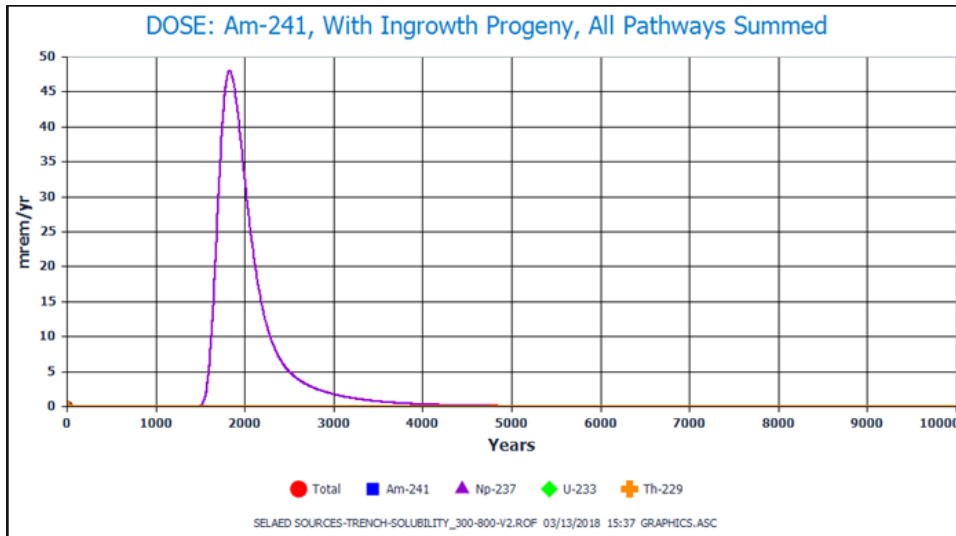
Figure M-60 Breakdown of Total Radiation Dose Associated with Disposal of Sealed Sources Waste—Solubility Controlled Release

M.10.2   Comparison with DUST-MS

In DUST-MS, each individual radionuclide requires an input of solubility to limit its concentration in leachate; the input solubility is used exclusively for the designated radionuclide. In addition to the requirement for solubility, DUST-MS does not have provision for considering a first-order dissolution reaction as the control mechanism for the releases of radionuclides from the waste domain. Therefore, to compare calculated radionuclide release rates from RESRAD-OFFSITE and DUST-MS when solubility is taken into account, the analysis of leaching of Pu-238 and its decay progenies and of Pu-239 and its progenies were conducted separately. In each analysis, a solubility of 1×10^{-10} mole/L was assumed for the parent nuclide (i.e., Pu-238 or Pu-239) and the releases of decay progenies were assumed to be controlled by equilibrium desorption (for RESRAD-OFFSITE) or surface rinse (for DUST-MS). The input Pu-238 and Pu-239 concentrations based on the entire contamination and the Kds of decay progenies for soils as listed in Table M-5 were used in the analyses. The releases of radionuclides from the waste domain were assumed to occur 300 years after the disposal of sealed sources waste.

Figures M-61 to M-66 compare the release rates of Pu-238 and its decay progenies, U-234, Th-230, Ra-226, Pb-210, and Po-210 from the bottom of the contaminated zone. The disagreement in the release rates of Pu-238 is mainly due to the different ways of using the input solubility by DUST-MS and RESRAD-OFFSITE. In DUST-MS, the concentration in leachate is calculated with the soil Kd, which is then set equal to the solubility if the calculated value is greater, while in RESRAD-OFFSITE, the leachate concentration is set to the solubility until the releasable inventory is depleted. The release rate of Pu-238 would affect the inventory of Pu-238 remaining in the waste domain, which then would affect the amount of its decay progenies in the waste domain and subsequently, their release rates at the bottom of the contaminated zone.

Figures M-67 to M-69 compare the release rate of Pu-239 and two of its decay progenies, U-235, and Ac-227. With a leachate concentration equivalent to the solubility, the release of Pu-239 would last for more than 10,000 years; therefore, as shown in Figure M-67, the RESRAD-OFFSITE results and DUST-MS results of Pu-239 release rates agree well with each other, which then result in good agreement in the release rates of U-235 (Figure M-68). In Figure M-69, only the release rate profile generated with the RESRAD-OFFSITE results is displayed; no release rates were calculated for Ac-227 by DUST-MS because Ac-227 is not included in its radionuclide database.
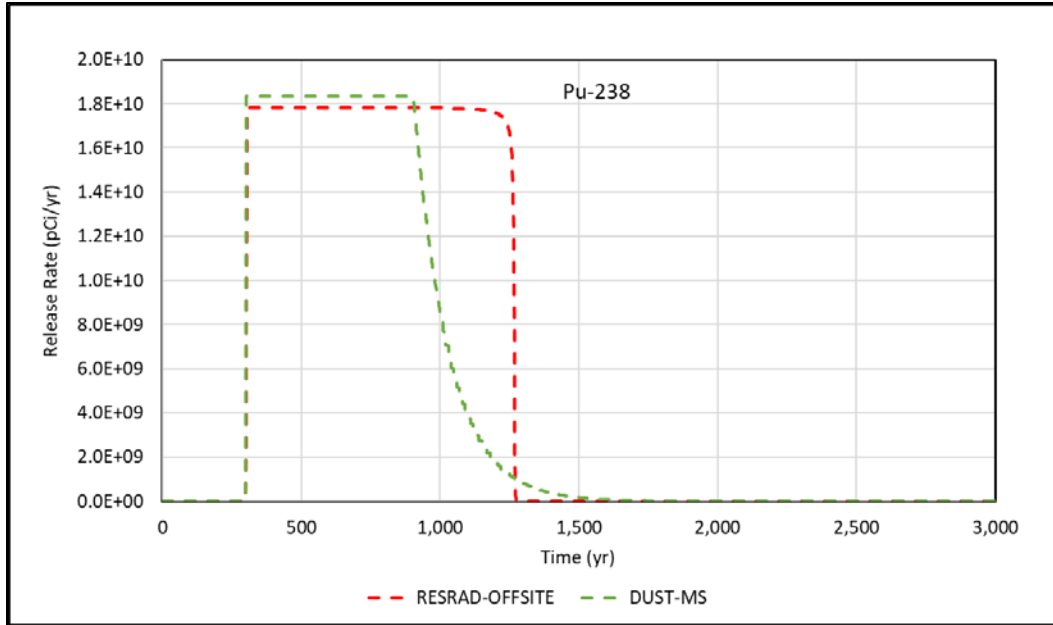
Figure M-61 Comparison of Calculated Pu-238 Release Rates Associated with Disposal of Sealed Sources Wastes—Solubility Input for Pu-238
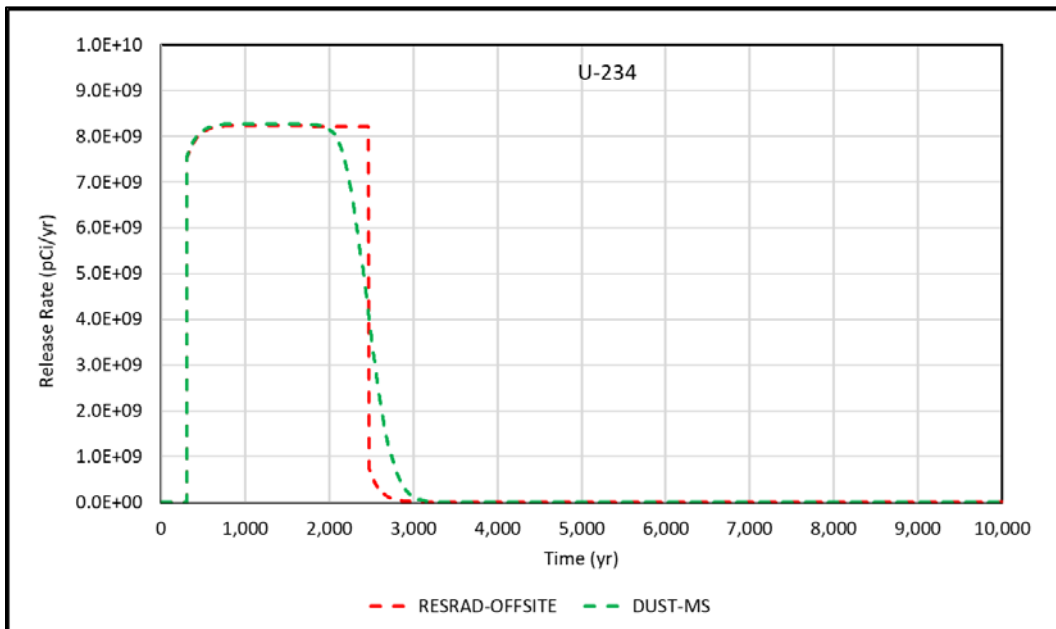
Figure M-62 Comparison of Calculated U-234 Release Rates Associated with Disposal of Sealed Sources Wastes—Solubility Input for Pu-238
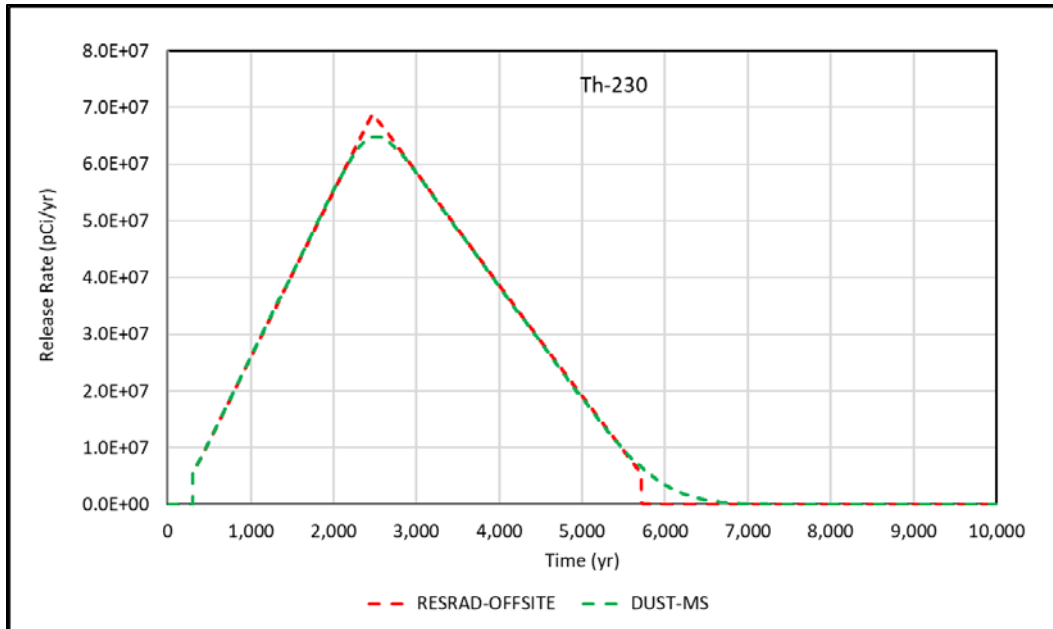
Figure M-63 Comparison of Calculated Th-230 Release Rates Associated with Disposal of Sealed Sources Wastes—Solubility Input for Pu-238
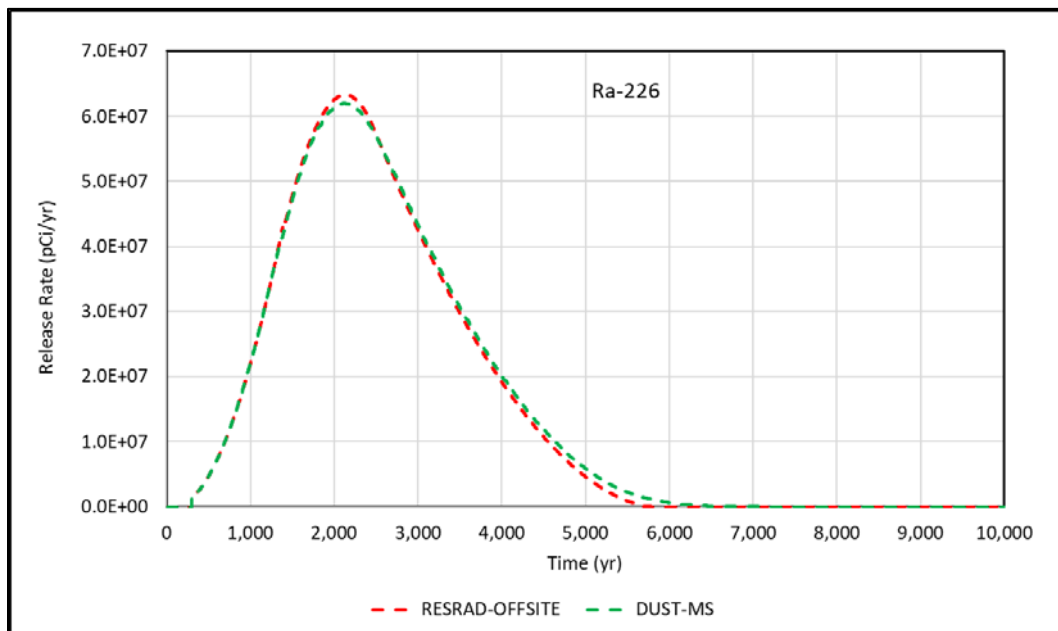
Figure M-64 Comparison of Calculated Ra-226 Release Rates Associated with Disposal of Sealed Sources Wastes—Solubility Input for Pu-238
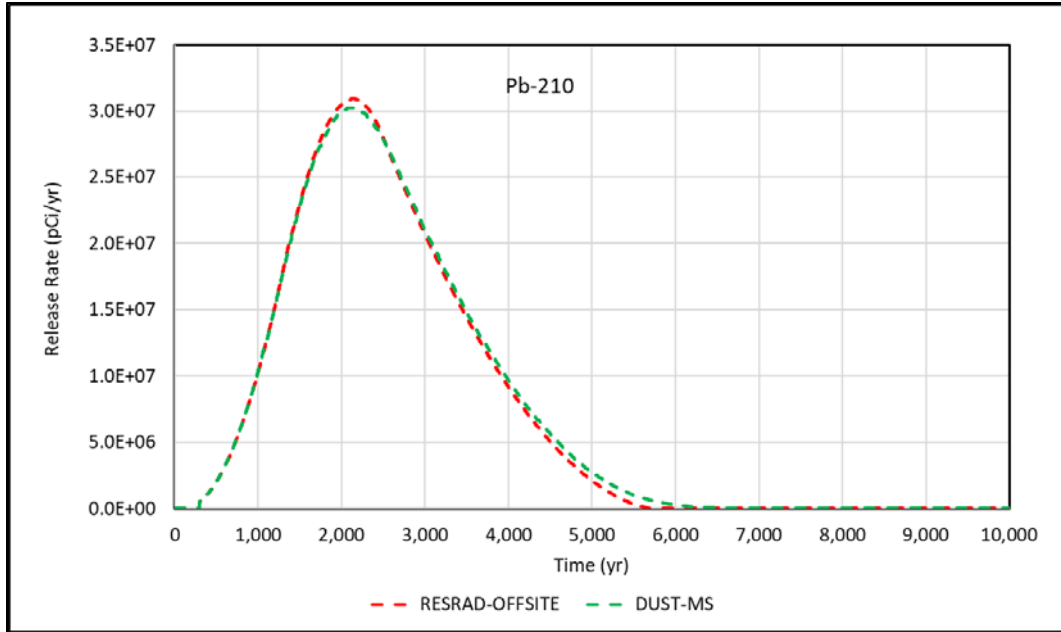
Figure M-65 Comparison of Calculated Pb-210 Release Rates Associated with Disposal of Sealed Sources Wastes—Solubility Input for Pu-238
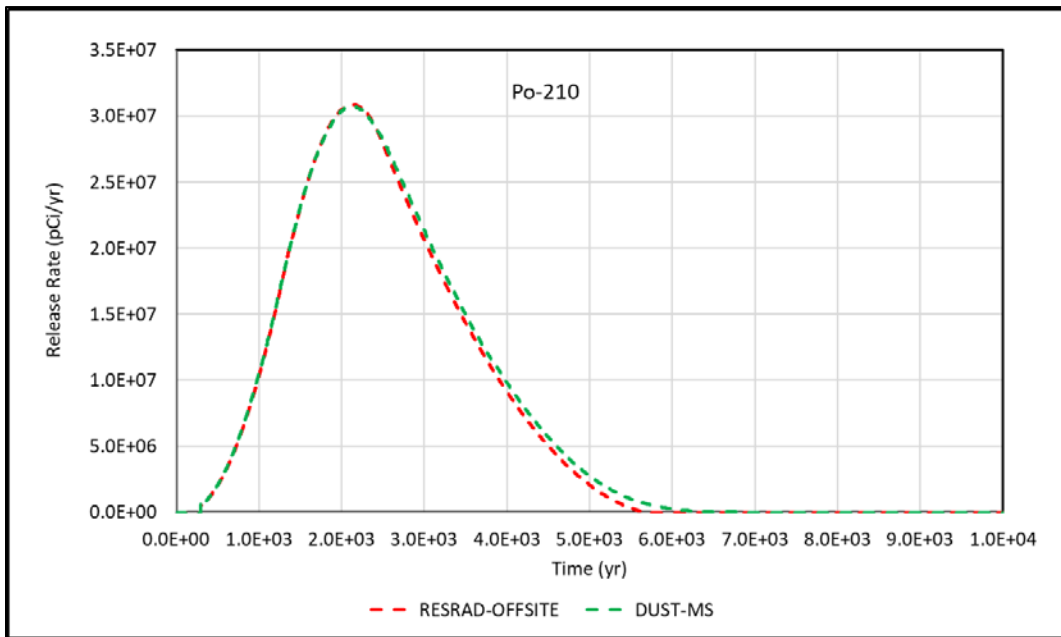
Figure M-66 Comparison of Calculated Po-210 Release Rates Associated with Disposal of Sealed Sources Wastes—Solubility Input for Pu-238
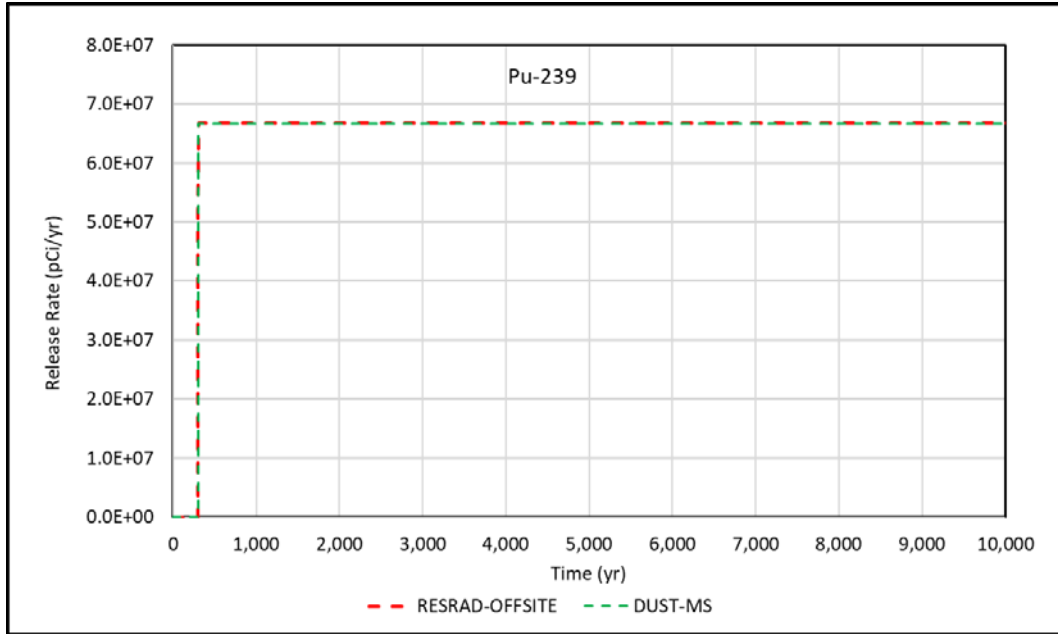
Figure M-67 Comparison of Calculated Pu-239 Release Rates Associated with Disposal of Sealed Sources Wastes—Solubility Input for Pu-239
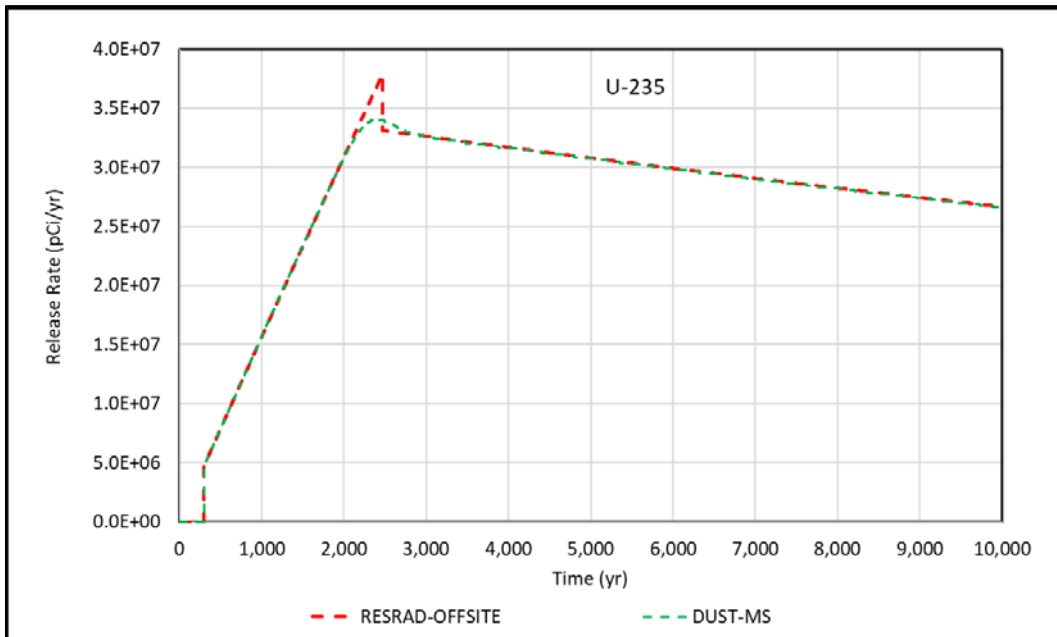
Figure M-68 Comparison of Calculated U-235 Release Rates Associated with Disposal of Sealed Sources Wastes—Solubility Input for Pu-239
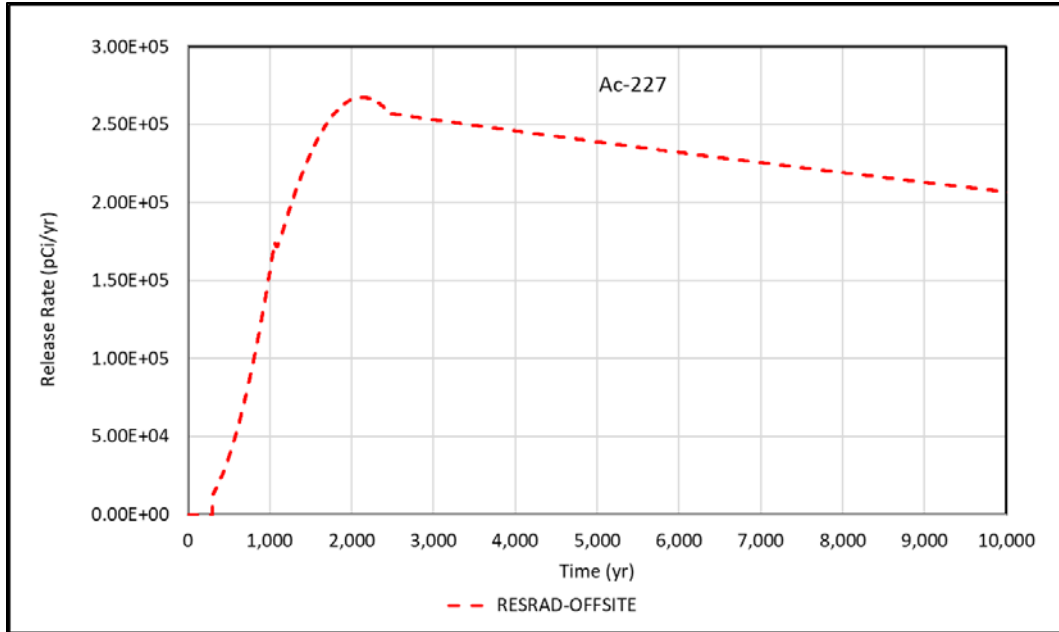
**Figure M-69 Calculated U-235 Release Rates Associated with Disposal of
Sealed Sources Wastes by RESRAD-OFFSITE—Solubility
Input for Pu-239**

M.11 <u>References</u>

Argonne (Argonne National Laboratory), 2010*, Post-closure Performance Analysis of the
Conceptual Disposal Facility Designs at the Sites Considered for the Greater-than-Class C
Environmental Impact Statement*, ANL/EVS/R-10/8, prepared by Environmental Science
Division, Oct.

Sullivan, T.M., 2006, *DUSTMS-D Disposal Unit Source Term‒ Multiple Species-Distributed
Failure Data Input Guide*, BNL-75554-2006, Brookhaven National Laboratory, Upton, N.Y., Jan.

APPENDIX N:
RISK ESTIMATION METHODOLOGY
AND RISK COEFFICIENT LIBRARIES

This appendix describes the risk estimation methodology and risk coefficient (slope factor) libraries in the RESRAD-OFFSITE code. The risk assessment methodology can be employed with different risk coefficient libraries.

N.1   RISK Estimation Methodology

RESRAD-OFFSITE uses the U.S. Environmental Protection Agency (EPA) risk coefficients with the exposure rate (for the external radiation pathways) and the total intake amount (for internal exposure pathways) to estimate the radiation risk. EPA calculates radionuclide risk coefficients using health effects data and dose and risk models from a number of national and international scientific advisory commissions and organizations. The risk coefficients are calculated for each radionuclide individually based on its unique chemical, metabolic, and radioactive properties.

For the purpose of computing the risk coefficients, it is assumed the concentration of the radionuclide in the environmental medium remains constant and all persons in the population are exposed to that environmental medium throughout their lifetimes. The risk coefficients are derived using the age and gender distributions of a hypothetical closed "stationary" population. The population is referred to as "stationary" because the gender-specific birth rates and survival functions are assumed to remain invariant over time. Risk coefficient estimates need the following:

- Age-dependent organ-specific cancer risk models; the age-at-exposure groups considered in the models are 0–9 years, 10–19 years, 20–29 years, 30–39 years, and 40+ years, which is an absolute risk model or a relative risk model for 14 cancer sites;

- Age-specific biokinetic and dosimetric models;

- U.S. decennial life tables and the cancer mortality/morbidity data for the same period; and

- Age- and gender-dependent usage of contaminated media.

For each type of cancer, values for lifetime risk per unit absorbed dose were used to convert the absorbed dose rates into lifetime cancer risk as a function of age. This calculation involves the absorbed dose as a function of age, the time-dependent intake of radionuclides, and the population's survival function. The survival function is the age-dependent probability that a person will die at a particular age. It was assumed that the radiation dose to the population does not significantly alter the survival function.

Age- and gender-specific radiation risk models were taken from the EPA report, *Estimating Radiological Cancer Risks*, which was based on data from Japanese atomic bomb survivors as well as other study groups (EPA 1994). Figure N-1 shows the steps involved in estimating risk coefficients. A total risk coefficient is derived by first adding the risk estimates for the different cancer sites in each gender and then calculating a weighted mean of the coefficients for males and females.
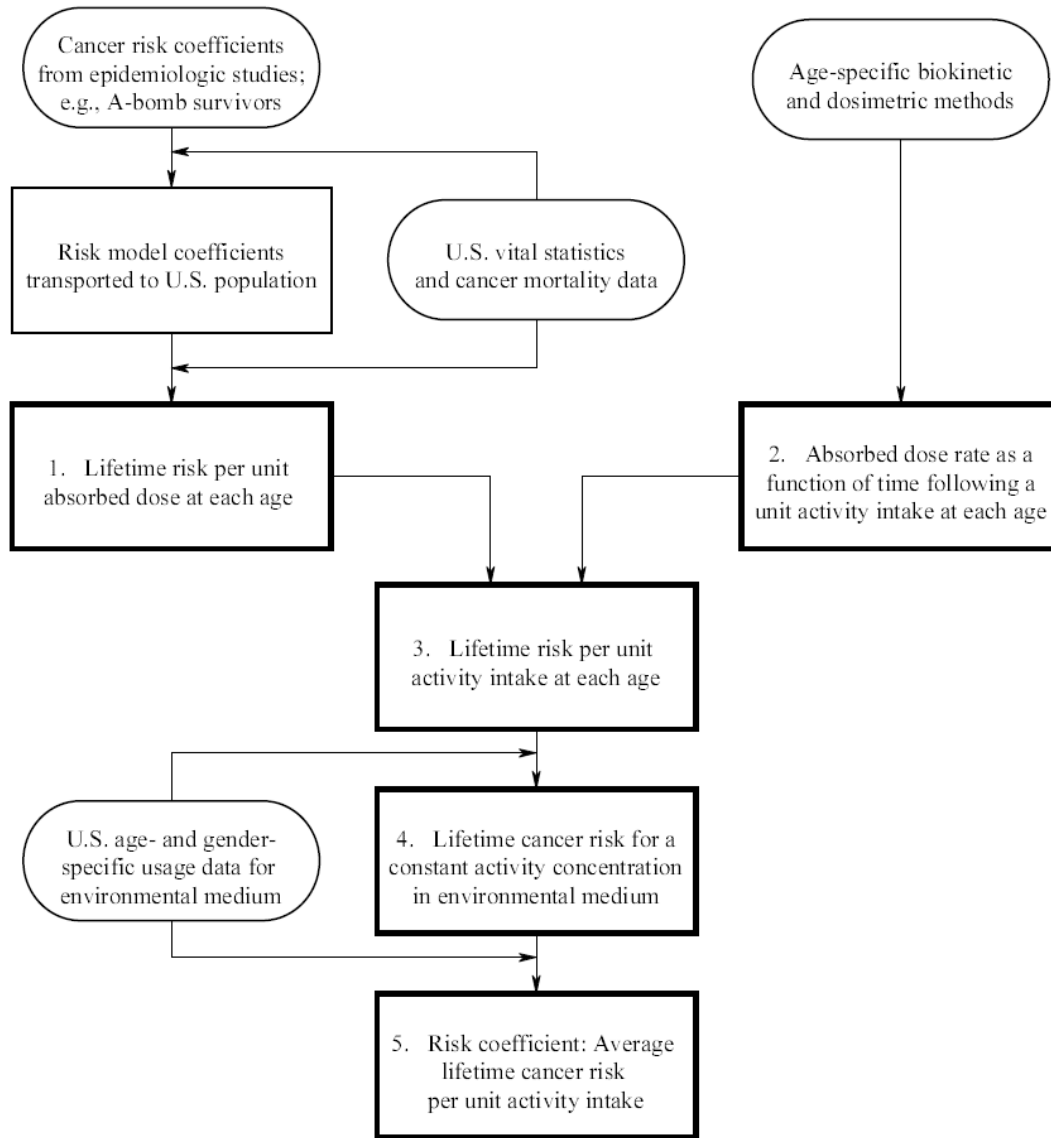
Figure N-1   Steps Involved in Computation of Risk Coefficients

Step 1. Lifetime risk per unit absorbed dose at each age

For each of 14 cancer sites in the body, radiation risk models are used to calculate gender-specific values for the lifetime risk per unit absorbed dose received at each age. The cancer sites considered are esophagus, stomach, colon, liver, lung, bone, skin, breast, ovary, bladder, kidney, thyroid, red marrow (leukemia), and residual (all remaining cancer sites combined). The computation involves an integration over age, beginning at the age at which the dose is received, product of the age-specific risk model coefficient, and the survival function.

Step 2. Absorbed dose rate as a function of time post acute intake at each age

This step involves using the age-specific biokinetic models to calculate time-dependent inventories of Activity in various regions of the body following acute intake of a unit Activity of the radionuclide. For a given radionuclide and intake mode, this calculation is performed for each of six "basic" ages at intake: infancy (100 days); 1, 5, 10, and 15 years; and maturity (usually 20 years, but 25 years in the biokinetic models for some elements).

Age-specific dosimetric models are used to convert the calculated time-dependent regional activities in the body to absorbed dose rates (per unit intake) to radiosensitive tissues as a function of age at intake and time after intake. Absorbed dose rates for intake ages intermediate to the six basic ages at intake are determined by interpolation.

Step 3. Lifetime cancer risk per unit intake at each age

This step involves integration over age of the product of the absorbed dose rate at age *y* for a unit intake at age *yi*, the lifetime risk per unit absorbed dose received at age *y*, and the value of the survival function at age *y* divided by the value at age *yi*. The survival function is used to account for the probability that a person exposed at age *yi* is still alive at age *y* to receive the absorbed dose. It assumes the radiation dose received is low, and it does not change the survival function.

Step 4. Lifetime cancer risk for chronic intake

This step takes into account the variation in environmental media usage with age and gender. For each cancer site and each gender, the lifetime cancer risk for chronic exposure is obtained by integration over age *y* of the product of the lifetime cancer risk per unit intake at age *y* and the expected intake of the environmental medium at age *y*. The expected intake at a given age is the product of the usage rate of the medium and the value of the survival function at that age.

Step 5. Average lifetime cancer risk per unit activity intake

The average lifetime cancer risk is calculated by dividing the calculated lifetime cancer risk for chronic intake calculated in step 4 by the expected lifetime media usage.

The computation of risk coefficients for external exposure involves fewer steps because age-specific organ dose rates due to external exposure are not available.

N.2   Risk Coefficient Libraries

Three sets of risk coefficients obtained from different sources are included in the RESRAD-OFFSITE code. Two sets of risk libraries are based on the ICRP 38 radionuclide transformation database (ICRP 1983), and one set of risk libraries is based on the ICRP 107 radionuclide transformation database (ICRP 2008). Users can also create their own libraries starting with the base libraries available for the ICRP 38 and ICRP 107 transformation databases.

N.2.1   FGR-13 Risk Coefficients

The first set of risk coefficients was obtained primarily from Federal Guidance Report No. 13 (FGR 13) (EPA 1999). FGR 13 includes risk coefficients for latent cancer morbidity (called slope factors) and for cancer mortality from six different modes of exposure. The six modes are inhalation of air, ingestion of food, ingestion of tap water, and external exposure from submersion in air, from a surface source of soil, and from an infinite volume source of soil. Risk coefficients for four of the exposure modes (inhalation, ingestion of food, ingestion of tap water, and external exposure from an infinite source of soil) are used in RESRAD-OFFSITE for risk calculations. Table N-1 lists the default morbidity and mortality risk coefficients used in the code for radionuclides with a 30-day cutoff half-life. Note that FGR 13 provides separate inhalation risk coefficients for particulate aerosols of type F, type M, and type S, which represent fast, medium, and slow absorption to blood, respectively. The inhalation risk coefficients listed in Table N-1 are the most conservative values.

Table N-1 FGR-13 Morbidity and Mortality Risk Coefficients from Different Modes of Exposure

| Radionuclide[a] | External (risk/yr per Bq/g) | | Inhalation (risk/Bq) | | Ingestion | | | | | |
| | | | | | Food (risk/Bq) | | Water (risk/Bq) | | Soil[b] (risk/Bq) | |
	Morbidity	Mortality	Morbidity	Mortality	Morbidity	Mortality	Morbidity	Mortality	Morbidity	Mortality
Ac-227+D	3.97E-05	2.70E-05	5.75E-06	5.45E-06	1.76E-08	1.20E-08	1.31E-08	9.15E-09	1.76E-08	1.20E-08
Ag-105	5.81E-05	3.95E-05	8.54E-11	7.11E-11	6.73E-11	4.03E-11	4.78E-11	2.89E-11	6.73E-11	4.03E-11
Ag-108m+D	1.94E-04	1.32E-04	2.81E-09	2.42E-09	3.03E-10	1.92E-10	2.20E-10	1.42E-10	3.03E-10	1.92E-10
Ag-110m+D	3.51E-04	2.39E-04	1.22E-09	1.03E-09	3.70E-10	2.30E-10	2.67E-10	1.68E-10	3.70E-10	2.30E-10
Al-26	3.59E-04	2.44E-04	7.84E-09	7.03E-09	6.73E-10	3.84E-10	4.68E-10	2.68E-10	6.73E-10	3.84E-10
Am-241	7.46E-07	5.03E-07	1.02E-06	9.03E-07	3.62E-09	2.56E-09	2.81E-09	2.01E-09	3.62E-09	2.56E-09
Am-242m+D	9.69E-07	6.57E-07	9.32E-07	7.29E-07	2.44E-09	1.84E-09	1.96E-09	1.50E-09	2.44E-09	1.84E-09
Am-242m+D1	9.69E-07	6.57E-07	9.32E-07	7.29E-07	2.44E-09	1.84E-09	1.96E-09	1.50E-09	2.44E-09	1.84E-09
Am-242m+D2	7.08E-05	4.79E-05	9.30E-07	7.27E-07	2.58E-09	1.92E-09	2.06E-09	1.55E-09	2.58E-09	1.92E-09
Am-243+D	1.72E-05	1.17E-05	1.00E-06	8.57E-07	3.82E-09	2.65E-09	2.92E-09	2.08E-09	3.82E-09	2.65E-09
As-73	1.56E-07	1.05E-07	1.35E-10	1.23E-10	6.16E-11	3.49E-11	4.22E-11	2.39E-11	6.16E-11	3.49E-11
Au-195	3.73E-06	2.53E-06	1.75E-10	1.58E-10	5.92E-11	3.30E-11	4.05E-11	2.27E-11	5.92E-11	3.30E-11
Ba-133	3.89E-05	2.64E-05	8.78E-10	7.73E-10	2.55E-10	1.73E-10	1.84E-10	1.27E-10	2.55E-10	1.73E-10
Be-10	2.01E-08	1.36E-08	2.54E-09	2.38E-09	2.76E-10	1.56E-10	1.90E-10	1.07E-10	2.76E-10	1.56E-10
Be-7	5.76E-06	3.92E-06	5.76E-12	4.59E-12	3.24E-12	1.91E-12	2.34E-12	1.39E-12	3.24E-12	1.91E-12
Bi-207	1.91E-04	1.30E-04	2.97E-09	2.60E-09	2.20E-10	1.25E-10	1.53E-10	8.76E-11	2.20E-10	1.25E-10
Bi-210m+D	2.75E-05	1.86E-05	7.89E-07	7.51E-07	2.10E-09	1.21E-09	1.49E-09	8.62E-10	2.10E-09	1.21E-09
Bk-247	8.35E-06	5.68E-06	1.29E-06	1.07E-06	4.32E-09	3.22E-09	3.35E-09	2.54E-09	4.32E-09	3.22E-09
Bk-249	7.11E-11	4.70E-11	3.14E-09	2.58E-09	4.24E-11	2.55E-11	3.00E-11	1.82E-11	4.24E-11	2.55E-11
Bk-249+D	2.81E-06	1.92E-06	3.14E-09	2.58E-09	5.11E-11	3.09E-11	3.60E-11	2.19E-11	5.11E-11	3.09E-11
C-14 (particulates)	2.12E-10	1.41E-10	4.57E-10	4.30E-10	5.41E-11	3.68E-11	4.19E-11	2.89E-11	5.41E-11	3.68E-11
C-14 (gas)	0.00E+00	0.00E+00	5.38E-13	3.68E-13	0.00E+00	0.00E+00	0.00E+00	0.00E+00	0.00E+00	0.00E+00
Ca-41	0.00E+00	0.00E+00	1.37E-11	1.27E-11	1.18E-11	1.04E-11	9.54E-12	8.57E-12	1.18E-11	1.04E-11
Ca-45	1.07E-09	7.19E-10	3.46E-10	3.22E-10	9.11E-11	6.27E-11	6.68E-11	4.73E-11	9.11E-11	6.27E-11

Table N-1 FGR-13 Morbidity and Mortality Risk Coefficients from Different Modes of Exposure (Cont.)

Radionuclide[a]	External (risk/yr per Bq/g) Morbidity	External (risk/yr per Bq/g) Mortality	Inhalation (risk/Bq) Morbidity	Inhalation (risk/Bq) Mortality	Ingestion Food (risk/Bq) Morbidity	Ingestion Food (risk/Bq) Mortality	Ingestion Water (risk/Bq) Morbidity	Ingestion Water (risk/Bq) Mortality	Ingestion Soil[b] (risk/Bq) Morbidity	Ingestion Soil[b] (risk/Bq) Mortality
Cd-109	2.36E-07	1.56E-07	5.92E-10	5.43E-10	1.81E-10	1.14E-10	1.35E-10	8.65E-11	1.81E-10	1.14E-10
Cd-113	1.99E-09	1.34E-09	3.03E-09	2.18E-09	7.84E-10	5.49E-10	6.16E-10	4.35E-10	7.84E-10	5.49E-10
Cd-113m	1.20E-08	8.16E-09	3.51E-09	2.51E-09	9.84E-10	6.73E-10	7.76E-10	5.35E-10	9.84E-10	6.73E-10
Cd-115m	3.05E-06	2.09E-06	7.89E-10	6.92E-10	6.65E-10	3.76E-10	4.59E-10	2.62E-10	6.65E-10	3.76E-10
Ce-139	1.23E-05	8.32E-06	1.86E-10	1.67E-10	5.27E-11	2.97E-11	3.65E-11	2.05E-11	5.27E-11	2.97E-11
Ce-141	6.14E-06	4.16E-06	3.65E-10	3.30E-10	1.83E-10	1.02E-10	1.25E-10	6.92E-11	1.83E-10	1.02E-10
Ce-144+D	6.60E-06	4.52E-06	4.87E-09	4.49E-09	1.40E-09	7.76E-10	9.54E-10	5.29E-10	1.40E-09	7.76E-10
Cf-248	1.28E-09	7.54E-10	6.92E-07	6.57E-07	1.68E-09	1.03E-09	1.20E-09	7.46E-10	1.68E-09	1.03E-09
Cf-249	3.70E-05	2.50E-05	1.31E-06	1.08E-06	4.41E-09	3.27E-09	3.43E-09	2.60E-09	4.41E-09	3.27E-09
Cf-250	1.21E-09	7.16E-10	9.95E-07	9.43E-07	3.03E-09	2.15E-09	2.33E-09	1.70E-09	3.03E-09	2.15E-09
Cf-251	1.02E-05	6.92E-06	1.33E-06	1.10E-06	4.59E-09	3.41E-09	3.57E-09	2.67E-09	4.59E-09	3.41E-09
Cf-252	2.34E-09	1.49E-09	7.03E-07	2.12E-06	4.86E-09	1.46E-08	4.86E-09	1.46E-08	4.86E-09	1.46E-08
Cl-36	4.70E-08	3.22E-08	2.73E-09	2.58E-09	1.20E-10	7.92E-11	8.92E-11	5.95E-11	1.20E-10	7.92E-11
Cm-241	5.24E-05	3.57E-05	3.30E-09	3.11E-09	1.90E-10	1.06E-10	1.31E-10	7.32E-11	1.90E-10	1.06E-10
Cm-242	2.09E-09	1.29E-09	5.43E-07	5.16E-07	1.48E-09	8.65E-10	1.04E-09	6.16E-10	1.48E-09	8.65E-10
Cm-243	1.13E-05	7.70E-06	9.92E-07	9.38E-07	3.32E-09	2.30E-09	2.56E-09	1.81E-09	3.32E-09	2.30E-09
Cm-244	1.31E-09	7.76E-10	9.62E-07	9.08E-07	2.92E-09	2.02E-09	2.26E-09	1.59E-09	2.92E-09	2.02E-09
Cm-245	6.43E-06	4.38E-06	1.03E-06	8.81E-07	3.65E-09	2.57E-09	2.81E-09	2.02E-09	3.65E-09	2.57E-09
Cm-246	1.24E-09	7.35E-10	1.02E-06	8.81E-07	3.54E-09	2.51E-09	2.76E-09	1.98E-09	3.54E-09	2.51E-09
Cm-247+D	3.69E-05	2.51E-05	9.43E-07	7.86E-07	3.53E-09	2.45E-09	2.70E-09	1.93E-09	3.53E-09	2.45E-09
Cm-248	9.24E-10	5.49E-10	4.05E-06	2.23E-05	3.51E-08	1.84E-07	3.51E-08	1.84E-07	3.51E-08	1.84E-07
Co-56	4.86E-04	3.32E-04	6.92E-10	5.73E-10	3.86E-10	2.35E-10	2.73E-10	1.67E-10	3.86E-10	2.35E-10
Co-57	9.59E-06	6.54E-06	1.01E-10	8.73E-11	4.03E-11	2.43E-11	2.81E-11	1.70E-11	4.03E-11	2.43E-11
Co-58	1.21E-04	8.27E-05	2.15E-10	1.81E-10	1.13E-10	6.81E-11	7.97E-11	4.84E-11	1.13E-10	6.81E-11
Co-60	3.35E-04	2.28E-04	2.73E-09	2.32E-09	6.03E-10	3.89E-10	4.24E-10	2.76E-10	6.03E-10	3.89E-10
Cs-134	1.92E-04	1.31E-04	1.89E-09	1.66E-09	1.39E-09	9.57E-10	1.14E-09	7.92E-10	1.39E-09	9.57E-10

Table N-1 FGR-13 Morbidity and Mortality Risk Coefficients from Different Modes of Exposure (Cont.)

Radionuclide[a]	External (risk/yr per Bq/g) Morbidity	External Mortality	Inhalation (risk/Bq) Morbidity	Inhalation Mortality	Food (risk/Bq) Morbidity	Food Mortality	Water (risk/Bq) Morbidity	Water Mortality	Soil[b] (risk/Bq) Morbidity	Soil Mortality
Cs-135	6.38E-10	4.27E-10	6.73E-10	6.30E-10	1.59E-10	1.07E-10	1.28E-10	8.73E-11	1.59E-10	1.07E-10
Cs-137+D	6.88E-05	4.68E-05	3.03E-09	2.76E-09	1.01E-09	6.89E-10	8.22E-10	5.65E-10	1.01E-09	6.89E-10
Dy-159	8.62E-07	5.76E-07	4.51E-11	3.95E-11	2.08E-11	1.16E-11	1.43E-11	8.05E-12	2.08E-11	1.16E-11
Es-254+D	1.15E-04	7.77E-05	7.00E-07	6.65E-07	2.13E-09	1.27E-09	1.50E-09	9.09E-10	2.13E-09	1.27E-09
Eu-148	2.66E-04	1.81E-04	3.38E-10	2.51E-10	1.63E-10	9.49E-11	1.16E-10	6.81E-11	1.63E-10	9.49E-11
Eu-149	3.84E-06	2.61E-06	3.43E-11	2.92E-11	2.00E-11	1.12E-11	1.39E-11	7.81E-12	2.00E-11	1.12E-11
Eu-150b	1.75E-04	1.19E-04	7.14E-09	5.57E-09	1.64E-10	9.76E-11	1.17E-10	7.03E-11	1.64E-10	9.76E-11
Eu-152	1.43E-04	9.76E-05	5.14E-09	4.11E-09	2.35E-10	1.35E-10	1.64E-10	9.51E-11	2.35E-10	1.35E-10
Eu-154	1.58E-04	1.07E-04	5.70E-09	4.70E-09	4.03E-10	2.29E-10	2.78E-10	1.59E-10	4.03E-10	2.29E-10
Eu-155	3.35E-06	2.28E-06	5.16E-10	4.68E-10	7.49E-11	4.19E-11	5.14E-11	2.89E-11	7.49E-11	4.19E-11
Fe-55	0.00E+00	0.00E+00	4.00E-11	3.30E-11	3.14E-11	2.39E-11	2.33E-11	1.81E-11	3.14E-11	2.39E-11
Fe-59	1.58E-04	1.07E-04	3.97E-10	3.49E-10	3.00E-10	1.91E-10	2.13E-10	1.36E-10	3.00E-10	1.91E-10
Fe-60+D	5.03E-07	3.41E-07	1.00E-08	7.81E-09	6.46E-09	4.95E-09	4.86E-09	3.76E-09	6.46E-09	4.95E-09
Fe-60+D1	5.03E-07	3.41E-07	1.00E-08	7.81E-09	6.46E-09	4.95E-09	4.86E-09	3.76E-09	6.46E-09	4.95E-09
Fm-257+D	8.31E-06	5.65E-06	1.18E-06	1.12E-06	3.25E-09	1.85E-09	2.25E-09	1.29E-09	3.25E-09	1.85E-09
Fm-257+D1	8.31E-06	5.65E-06	1.18E-06	1.12E-06	3.24E-09	1.85E-09	2.24E-09	1.29E-09	3.24E-09	1.85E-09
Gd-146+D	3.29E-04	2.24E-04	7.89E-10	6.82E-10	3.70E-10	2.10E-10	2.59E-10	1.48E-10	3.70E-10	2.10E-10
Gd-148	0.00E+00	0.00E+00	4.14E-07	3.92E-07	1.49E-09	1.08E-09	1.14E-09	8.54E-10	1.49E-09	1.08E-09
Gd-151	3.24E-06	2.19E-06	9.97E-11	8.89E-11	4.46E-11	2.49E-11	3.08E-11	1.71E-11	4.46E-11	2.49E-11
Gd-152	0.00E+00	0.00E+00	2.46E-07	2.20E-07	1.04E-09	7.65E-10	8.03E-10	6.03E-10	1.04E-09	7.65E-10
Gd-153	4.38E-06	2.95E-06	2.32E-10	2.09E-10	6.00E-11	3.35E-11	4.11E-11	2.31E-11	6.00E-11	3.35E-11
Ge-68+D	1.13E-04	7.68E-05	2.92E-09	2.70E-09	2.78E-10	1.58E-10	1.96E-10	1.12E-10	2.78E-10	1.58E-10
H-3	0.00E+00	0.00E+00	2.30E-11	2.12E-11	3.89E-12	2.66E-12	3.03E-12	2.09E-12	3.89E-12	2.66E-12
Hf-172+D	2.40E-04	1.63E-04	2.44E-09	2.13E-09	4.10E-10	2.34E-10	2.85E-10	1.65E-10	4.10E-10	2.34E-10
Hf-175	3.65E-05	2.50E-05	1.45E-10	1.25E-10	7.65E-11	4.30E-11	5.30E-11	3.00E-11	7.65E-11	4.30E-11
Hf-178m	2.59E-04	1.76E-04	1.00E-08	8.11E-09	5.76E-10	3.49E-10	4.08E-10	2.51E-10	5.76E-10	3.49E-10

Table N-1 FGR-13 Morbidity and Mortality Risk Coefficients from Different Modes of Exposure (Cont.)

| Radionuclide[a] | External (risk/yr per Bq/g) | | Inhalation (risk/Bq) | | Ingestion | | | | | |
| | | | | | Food (risk/Bq) | | Water (risk/Bq) | | Soil[b] (risk/Bq) | |
	Morbidity	Mortality	Morbidity	Mortality	Morbidity	Mortality	Morbidity	Mortality	Morbidity	Mortality
Hf-181	6.05E-05	4.14E-05	5.76E-10	5.19E-10	2.50E-10	1.40E-10	1.72E-10	9.62E-11	2.50E-10	1.40E-10
Hf-182	2.46E-05	1.67E-05	9.22E-09	7.73E-09	1.96E-10	1.34E-10	1.45E-10	1.01E-10	1.96E-10	1.34E-10
Hg-194+D	1.33E-04	9.08E-05	2.06E-09	1.72E-09	2.93E-09	2.02E-09	2.23E-09	1.55E-09	2.93E-09	2.02E-09
Hg-203	2.49E-05	1.69E-05	6.62E-10	5.95E-10	2.06E-10	1.37E-10	1.54E-10	1.03E-10	2.06E-10	1.37E-10
Ho-166m	2.08E-04	1.42E-04	2.06E-08	1.56E-08	3.08E-10	1.84E-10	2.17E-10	1.31E-10	3.08E-10	1.84E-10
I-125	1.96E-07	1.23E-07	7.49E-10	7.76E-10	1.70E-09	1.76E-10	6.86E-10	7.14E-11	1.70E-09	1.76E-10
I-129	1.65E-07	1.05E-07	4.32E-09	5.97E-10	8.70E-09	8.86E-10	4.00E-09	4.08E-10	8.70E-09	8.86E-10
In-114m+D	1.00E-05	6.81E-06	8.84E-10	7.57E-10	9.73E-10	5.54E-10	6.70E-10	3.84E-10	9.73E-10	5.54E-10
In-115	7.30E-09	4.95E-09	1.09E-08	9.84E-09	1.17E-09	9.95E-10	9.14E-10	7.86E-10	1.17E-09	9.95E-10
Ir-192	9.19E-05	6.24E-05	6.51E-10	5.81E-10	2.89E-10	1.62E-10	1.99E-10	1.12E-10	2.89E-10	1.62E-10
Ir-192m	1.46E-05	9.92E-06	2.76E-09	2.49E-09	3.57E-11	2.34E-11	2.65E-11	1.76E-11	3.57E-11	2.34E-11
Ir-194m	2.73E-04	1.86E-04	1.24E-09	1.08E-09	3.41E-10	1.97E-10	2.40E-10	1.39E-10	3.41E-10	1.97E-10
K-40	2.15E-05	1.47E-05	6.00E-09	5.62E-09	9.27E-10	5.89E-10	6.68E-10	4.30E-10	9.27E-10	5.89E-10
La-137	1.82E-07	1.17E-07	3.76E-10	3.11E-10	1.35E-11	7.78E-12	9.41E-12	5.46E-12	1.35E-11	7.78E-12
La-138	1.64E-04	1.12E-04	8.24E-09	6.35E-09	1.34E-10	8.05E-11	9.54E-11	5.81E-11	1.34E-10	8.05E-11
Lu-173	7.89E-06	5.32E-06	2.35E-10	2.09E-10	5.30E-11	2.97E-11	3.65E-11	2.06E-11	5.30E-11	2.97E-11
Lu-174	1.15E-05	7.86E-06	3.84E-10	3.46E-10	5.73E-11	3.22E-11	3.95E-11	2.23E-11	5.73E-11	3.22E-11
Lu-174m	2.67E-06	1.81E-06	4.08E-10	3.73E-10	1.34E-10	7.43E-11	9.14E-11	5.08E-11	1.34E-10	7.43E-11
Lu-176	4.95E-05	3.38E-05	4.73E-09	4.11E-09	3.65E-10	2.06E-10	2.51E-10	1.42E-10	3.65E-10	2.06E-10
Lu-177m+D	9.88E-05	6.75E-05	1.57E-09	1.42E-09	3.97E-10	2.21E-10	2.73E-10	1.53E-10	3.97E-10	2.21E-10
Md-258	3.54E-08	2.32E-08	5.84E-07	5.54E-07	1.69E-09	9.70E-10	1.17E-09	6.76E-10	1.69E-09	9.70E-10
Mn-53	0.00E+00	0.00E+00	2.62E-11	2.43E-11	6.08E-12	3.51E-12	4.22E-12	2.46E-12	6.08E-12	3.51E-12
Mn-54	1.05E-04	7.16E-05	3.27E-10	2.67E-10	8.41E-11	5.30E-11	6.16E-11	3.95E-11	8.41E-11	5.30E-11
Mo-93	5.86E-09	3.38E-09	1.55E-10	1.45E-10	1.13E-10	1.01E-10	9.05E-11	8.22E-11	1.13E-10	1.01E-10
Na-22	2.78E-04	1.90E-04	2.63E-09	2.31E-09	3.41E-10	2.34E-10	2.60E-10	1.80E-10	3.41E-10	2.34E-10
Nb-93m	1.04E-09	5.97E-10	1.53E-10	1.42E-10	3.16E-11	1.77E-11	2.17E-11	1.21E-11	3.16E-11	1.77E-11

Table N-1 FGR-13 Morbidity and Mortality Risk Coefficients from Different Modes of Exposure (Cont.)

Radionuclide[a]	External (risk/yr per Bq/g)		Inhalation (risk/Bq)		Ingestion Food (risk/Bq)		Water (risk/Bq)		Soil[b] (risk/Bq)	
	Morbidity	Mortality	Morbidity	Mortality	Morbidity	Mortality	Morbidity	Mortality	Morbidity	Mortality
Nb-94	1.97E-04	1.34E-04	3.65E-09	3.19E-09	3.00E-10	1.73E-10	2.10E-10	1.22E-10	3.00E-10	1.73E-10
Nb-95	9.54E-05	6.51E-05	1.74E-10	1.50E-10	9.46E-11	5.41E-11	6.62E-11	3.81E-11	9.46E-11	5.41E-11
Ni-59	0.00E+00	0.00E+00	6.51E-11	4.57E-11	1.05E-11	6.27E-12	7.41E-12	4.43E-12	1.05E-11	6.27E-12
Ni-63	0.00E+00	0.00E+00	1.56E-10	1.09E-10	2.57E-11	1.53E-11	1.81E-11	1.08E-11	2.57E-11	1.53E-11
Np-235	5.76E-08	3.84E-08	5.24E-11	4.84E-11	1.37E-11	7.59E-12	9.35E-12	5.19E-12	1.37E-11	7.59E-12
Np-236a	8.78E-06	5.97E-06	6.32E-08	4.62E-08	3.89E-10	2.42E-10	2.84E-10	1.78E-10	3.89E-10	2.42E-10
Np-237+D	2.15E-05	1.46E-05	7.76E-07	7.33E-07	2.46E-09	1.56E-09	1.82E-09	1.18E-09	2.46E-09	1.56E-09
Os-185	8.41E-05	5.70E-05	1.66E-10	1.38E-10	7.30E-11	4.27E-11	5.19E-11	3.05E-11	7.30E-11	4.27E-11
Os-194+D	1.11E-05	7.53E-06	6.98E-09	6.52E-09	9.43E-10	5.28E-10	6.46E-10	3.63E-10	9.43E-10	5.28E-10
Pa-231	3.76E-06	2.55E-06	2.06E-06	1.52E-06	6.11E-09	4.30E-09	4.68E-09	3.30E-09	6.11E-09	4.30E-09
Pb-202+D	4.95E-05	3.38E-05	9.28E-10	8.00E-10	8.46E-10	6.24E-10	6.40E-10	4.78E-10	8.46E-10	6.24E-10
Pb-205	9.46E-11	5.81E-11	6.38E-11	5.97E-11	2.23E-11	1.73E-11	1.71E-11	1.37E-11	2.23E-11	1.73E-11
Pb-210+D	1.13E-07	7.79E-08	4.39E-07	4.17E-07	3.22E-08	2.33E-08	2.41E-08	1.76E-08	3.22E-08	2.33E-08
Pd-107	0.00E+00	0.00E+00	4.57E-11	4.22E-11	9.92E-12	5.49E-12	6.76E-12	3.73E-12	9.92E-12	5.49E-12
Pm-143	3.59E-05	2.44E-05	2.45E-10	1.86E-10	3.35E-11	1.93E-11	2.36E-11	1.37E-11	3.35E-11	1.93E-11
Pm-144	1.86E-04	1.27E-04	1.49E-09	1.13E-09	1.26E-10	7.41E-11	9.03E-11	5.32E-11	1.26E-10	7.41E-11
Pm-145	4.35E-07	2.86E-07	3.46E-10	2.97E-10	2.18E-11	1.24E-11	1.51E-11	8.62E-12	2.18E-11	1.24E-11
Pm-146	8.89E-05	6.05E-05	2.78E-09	2.23E-09	1.62E-10	9.24E-11	1.13E-10	6.49E-11	1.62E-10	9.24E-11
Pm-147	8.68E-10	5.84E-10	4.35E-10	4.05E-10	6.70E-11	3.73E-11	4.57E-11	2.55E-11	6.70E-11	3.73E-11
Pm-148m+D	2.46E-04	1.68E-04	5.86E-10	5.07E-10	3.42E-10	1.93E-10	2.37E-10	1.35E-10	3.42E-10	1.93E-10
Po-210	1.07E-09	7.27E-10	3.92E-07	3.70E-07	6.08E-08	4.43E-08	4.78E-08	3.54E-08	6.08E-08	4.43E-08
Pt-193	7.51E-11	4.57E-11	5.30E-11	4.95E-11	8.35E-12	4.62E-12	5.70E-12	3.16E-12	8.35E-12	4.62E-12
Pu-236	3.22E-09	2.07E-09	8.00E-07	7.57E-07	2.68E-09	1.87E-09	2.02E-09	1.44E-09	2.68E-09	1.87E-09
Pu-237	3.03E-06	2.06E-06	4.03E-11	3.57E-11	2.27E-11	1.27E-11	1.56E-11	8.73E-12	2.27E-11	1.27E-11
Pu-238	1.95E-09	1.22E-09	1.41E-06	1.19E-06	4.57E-09	3.51E-09	3.54E-09	2.76E-09	4.57E-09	3.51E-09
Pu-239	5.41E-09	3.62E-09	1.49E-06	1.26E-06	4.70E-09	3.62E-09	3.65E-09	2.84E-09	4.70E-09	3.62E-09

Table N-1 FGR-13 Morbidity and Mortality Risk Coefficients from Different Modes of Exposure (Cont.)

Radionuclide[a]	External (risk/yr per Bq/g)		Inhalation (risk/Bq)		Ingestion					
					Food (risk/Bq)		Water (risk/Bq)		Soil[b] (risk/Bq)	
	Morbidity	Mortality	Morbidity	Mortality	Morbidity	Mortality	Morbidity	Mortality	Morbidity	Mortality
Pu-240	1.89E-09	1.19E-09	1.50E-06	1.26E-06	4.70E-09	3.62E-09	3.65E-09	2.84E-09	4.70E-09	3.62E-09
Pu-241	1.11E-10	7.54E-11	2.34E-08	1.98E-08	6.16E-11	5.08E-11	4.76E-11	3.95E-11	6.16E-11	5.08E-11
Pu-241+D	1.02E-05	6.92E-06	2.36E-08	2.00E-08	2.55E-10	1.58E-10	1.79E-10	1.12E-10	2.55E-10	1.58E-10
Pu-242	1.69E-09	1.07E-09	1.42E-06	1.19E-06	4.46E-09	3.46E-09	3.46E-09	2.70E-09	4.46E-09	3.46E-09
Pu-244	8.14E-10	4.86E-10	1.35E-06	1.14E-06	4.86E-09	3.62E-09	3.70E-09	2.81E-09	4.86E-09	3.62E-09
Pu-244+D	4.08E-05	2.79E-05	1.35E-06	1.14E-06	5.14E-09	3.78E-09	3.89E-09	2.92E-09	5.14E-09	3.78E-09
Ra-226+D	2.29E-04	1.56E-04	7.64E-07	7.26E-07	1.39E-08	9.58E-09	1.04E-08	7.17E-09	1.39E-08	9.58E-09
Ra-228+D	1.22E-04	8.32E-05	1.18E-06	1.12E-06	3.87E-08	2.73E-08	2.82E-08	2.00E-08	3.87E-08	2.73E-08
Rb-83+D	5.89E-05	4.00E-05	1.48E-10	1.19E-10	2.03E-10	1.39E-10	1.54E-10	1.06E-10	2.03E-10	1.39E-10
Rb-84	1.14E-04	7.76E-05	2.51E-10	2.12E-10	3.16E-10	2.15E-10	2.38E-10	1.64E-10	3.16E-10	2.15E-10
Rb-87	2.46E-09	1.66E-09	1.17E-09	1.09E-09	1.91E-10	1.28E-10	1.41E-10	9.54E-11	1.91E-10	1.28E-10
Re-184	1.06E-04	7.27E-05	2.23E-10	1.94E-10	1.19E-10	7.19E-11	8.54E-11	5.19E-11	1.19E-10	7.19E-11
Re-184m	4.11E-05	2.78E-05	9.49E-10	8.57E-10	1.88E-10	1.12E-10	1.32E-10	7.95E-11	1.88E-10	1.12E-10
Re-186m+D	1.96E-06	1.33E-06	4.61E-09	4.34E-09	5.01E-10	2.92E-10	3.49E-10	2.06E-10	5.01E-10	2.92E-10
Re-187	0.00E+00	0.00E+00	3.19E-12	2.97E-12	6.92E-13	4.03E-13	4.84E-13	2.84E-13	6.92E-13	4.03E-13
Rh-101	2.39E-05	1.62E-05	4.89E-10	4.35E-10	8.14E-11	4.89E-11	5.81E-11	3.51E-11	8.14E-11	4.89E-11
Rh-102	2.63E-04	1.79E-04	1.62E-09	1.34E-09	2.81E-10	1.78E-10	2.08E-10	1.33E-10	2.81E-10	1.78E-10
Rh-102m	5.70E-05	3.89E-05	6.92E-10	6.16E-10	2.36E-10	1.35E-10	1.64E-10	9.43E-11	2.36E-10	1.35E-10
Ru-103+D	5.51E-05	3.76E-05	2.89E-10	2.59E-10	1.50E-10	8.51E-11	1.04E-10	5.91E-11	1.50E-10	8.51E-11
Ru-106+D	2.61E-05	1.78E-05	6.03E-09	5.57E-09	1.65E-09	9.35E-10	1.14E-09	6.46E-10	1.65E-09	9.35E-10
S-35	2.37E-10	1.58E-10	1.77E-10	1.63E-10	1.00E-10	6.73E-11	7.35E-11	5.00E-11	1.00E-10	6.73E-11
Sb-124	2.40E-04	1.64E-04	8.65E-10	7.54E-10	5.00E-10	2.86E-10	3.49E-10	2.00E-10	5.00E-10	2.86E-10
Sb-125	4.89E-05	3.35E-05	1.08E-09	9.73E-10	1.66E-10	1.01E-10	1.18E-10	7.27E-11	1.66E-10	1.01E-10
Sc-46	2.60E-04	1.77E-04	6.68E-10	5.78E-10	2.40E-10	1.36E-10	1.68E-10	9.59E-11	2.40E-10	1.36E-10
Se-75	3.92E-05	2.65E-05	1.35E-10	1.15E-10	2.92E-10	2.04E-10	2.20E-10	1.56E-10	2.92E-10	2.04E-10
Se-79	2.97E-10	1.97E-10	5.38E-10	5.05E-10	2.62E-10	1.82E-10	1.97E-10	1.38E-10	2.62E-10	1.82E-10

Table N-1 FGR-13 Morbidity and Mortality Risk Coefficients from Different Modes of Exposure (Cont.)

| Radionuclide[a] | External (risk/yr per Bq/g) | | Inhalation (risk/Bq) | | Ingestion | | | | | |
| | Morbidity | Mortality | Morbidity | Mortality | Food (risk/Bq) | | Water (risk/Bq) | | Soil[b] (risk/Bq) | |
					Morbidity	Mortality	Morbidity	Mortality	Morbidity	Mortality
Si-32+D	2.55E-07	1.81E-07	8.29E-09	7.82E-09	4.68E-10	3.02E-10	3.35E-10	2.21E-10	4.68E-10	3.02E-10
Sm-145	1.04E-06	6.84E-07	1.61E-10	1.38E-10	4.59E-11	2.57E-11	3.16E-11	1.77E-11	4.59E-11	2.57E-11
Sm-146	0.00E+00	0.00E+00	3.76E-07	3.38E-07	1.42E-09	1.09E-09	1.11E-09	8.70E-10	1.42E-09	1.09E-09
Sm-147	0.00E+00	0.00E+00	3.41E-07	3.05E-07	1.29E-09	9.89E-10	1.01E-09	7.89E-10	1.29E-09	9.89E-10
Sm-151	9.73E-12	5.70E-12	2.48E-10	2.31E-10	2.18E-11	1.23E-11	1.50E-11	8.46E-12	2.18E-11	1.23E-11
Sn-113+D	2.89E-05	1.98E-05	3.93E-10	3.53E-10	1.75E-10	9.77E-11	1.20E-10	6.73E-11	1.75E-10	9.77E-11
Sn-119m	3.24E-08	1.99E-08	3.22E-10	2.97E-10	8.76E-11	4.86E-11	5.97E-11	3.32E-11	8.76E-11	4.86E-11
Sn-121m+D	2.66E-08	1.69E-08	1.19E-09	1.12E-09	1.38E-10	7.75E-11	9.47E-11	5.31E-11	1.38E-10	7.75E-11
Sn-123	1.05E-06	7.16E-07	1.25E-09	1.14E-09	5.54E-10	3.08E-10	3.78E-10	2.10E-10	5.54E-10	3.08E-10
Sn-126+D	2.39E-04	1.63E-04	1.12E-08	1.02E-08	1.06E-09	6.07E-10	7.36E-10	4.23E-10	1.06E-09	6.07E-10
Sr-85	5.95E-05	4.03E-05	8.73E-11	7.16E-11	8.41E-11	5.57E-11	6.11E-11	4.08E-11	8.41E-11	5.57E-11
Sr-89	1.94E-07	1.38E-07	8.16E-10	7.22E-10	4.97E-10	2.97E-10	3.46E-10	2.10E-10	4.97E-10	2.97E-10
Sr-90+D	5.29E-07	3.74E-07	1.17E-08	1.10E-08	2.58E-09	2.02E-09	2.00E-09	1.61E-09	2.58E-09	2.02E-09
Ta-179	9.78E-07	6.59E-07	5.54E-11	4.84E-11	1.35E-11	7.54E-12	9.30E-12	5.22E-12	1.35E-11	7.54E-12
Ta-180	5.49E-05	3.73E-05	1.96E-09	1.76E-09	1.74E-10	9.76E-11	1.20E-10	6.76E-11	1.74E-10	9.76E-11
Ta-182	1.63E-04	1.11E-04	1.01E-09	9.05E-10	3.11E-10	1.75E-10	2.15E-10	1.21E-10	3.11E-10	1.75E-10
Tb-157	4.41E-08	2.95E-08	8.65E-11	7.81E-11	7.30E-12	4.11E-12	5.03E-12	2.84E-12	7.30E-12	4.11E-12
Tb-158	9.65E-05	6.57E-05	4.62E-09	3.76E-09	1.89E-10	1.09E-10	1.32E-10	7.68E-11	1.89E-10	1.09E-10
Tb-160	1.41E-04	9.62E-05	8.11E-10	7.24E-10	3.43E-10	1.91E-10	2.35E-10	1.32E-10	3.43E-10	1.91E-10
Tc-95m+D	8.31E-05	5.67E-05	1.24E-10	1.03E-10	6.87E-11	4.13E-11	4.93E-11	3.01E-11	6.87E-11	4.13E-11
Tc-97	7.95E-09	4.57E-09	1.30E-10	1.22E-10	1.05E-11	6.08E-12	7.30E-12	4.24E-12	1.05E-11	6.08E-12
Tc-97m	2.81E-08	1.83E-08	3.89E-10	3.59E-10	9.30E-11	5.30E-11	6.43E-11	3.68E-11	9.30E-11	5.30E-11
Tc-98	1.74E-04	1.19E-04	3.35E-09	2.97E-09	2.73E-10	1.61E-10	1.92E-10	1.14E-10	2.73E-10	1.61E-10
Tc-99	2.20E-09	1.48E-09	1.03E-09	9.68E-10	1.08E-10	6.16E-11	7.43E-11	4.27E-11	1.08E-10	6.16E-11
Te-121m+D	8.01E-05	5.47E-05	5.92E-10	5.21E-10	2.78E-10	1.85E-10	2.08E-10	1.42E-10	2.78E-10	1.85E-10
Te-123	7.38E-08	4.57E-08	3.22E-10	2.81E-10	1.38E-10	1.18E-10	1.11E-10	9.59E-11	1.38E-10	1.18E-10

Table N-1 FGR-13 Morbidity and Mortality Risk Coefficients from Different Modes of Exposure (Cont.)

Radionuclide[a]	External (risk/yr per Bq/g)		Inhalation (risk/Bq)		Ingestion					
					Food (risk/Bq)		Water (risk/Bq)		Soil[b] (risk/Bq)	
	Morbidity	Mortality	Morbidity	Mortality	Morbidity	Mortality	Morbidity	Mortality	Morbidity	Mortality
Te-123m	1.21E-05	8.24E-06	4.81E-10	4.41E-10	1.53E-10	9.73E-11	1.12E-10	7.27E-11	1.53E-10	9.73E-11
Te-125m	1.88E-07	1.19E-07	3.92E-10	3.62E-10	1.27E-10	7.51E-11	9.00E-11	5.43E-11	1.27E-10	7.51E-11
Te-127m+D	6.28E-07	4.22E-07	9.53E-10	8.73E-10	3.63E-10	2.25E-10	2.59E-10	1.66E-10	3.63E-10	2.25E-10
Te-129m+D	8.03E-06	5.47E-06	8.13E-10	7.18E-10	5.99E-10	3.41E-10	4.17E-10	2.41E-10	5.99E-10	3.41E-10
Th-228+D	2.10E-04	1.43E-04	3.89E-06	3.71E-06	1.14E-08	6.96E-09	8.07E-09	4.98E-09	1.14E-08	6.96E-09
Th-229+D	3.15E-05	2.15E-05	6.21E-06	5.87E-06	1.94E-08	1.28E-08	1.43E-08	9.54E-09	1.94E-08	1.28E-08
Th-230	2.21E-08	1.49E-08	9.19E-07	7.24E-07	3.22E-09	2.16E-09	2.46E-09	1.67E-09	3.22E-09	2.16E-09
Th-232	9.24E-09	6.22E-09	1.17E-06	1.10E-06	3.59E-09	2.45E-09	2.73E-09	1.87E-09	3.59E-09	2.45E-09
Ti-44+D	2.75E-04	1.87E-04	9.23E-09	8.31E-09	1.04E-09	6.14E-10	7.34E-10	4.36E-10	1.04E-09	6.14E-10
Tl-204	7.46E-08	5.08E-08	1.64E-09	1.53E-09	2.23E-10	1.34E-10	1.58E-10	9.57E-11	2.23E-10	1.34E-10
Tm-170	2.73E-07	1.85E-07	9.00E-10	8.22E-10	3.54E-10	1.96E-10	2.41E-10	1.34E-10	3.54E-10	1.96E-10
Tm-171	1.88E-08	1.26E-08	1.18E-10	1.09E-10	2.76E-11	1.54E-11	1.89E-11	1.05E-11	2.76E-11	1.54E-11
U-232	1.62E-08	1.09E-08	2.50E-06	2.37E-06	1.04E-08	7.22E-09	7.89E-09	5.51E-09	1.04E-08	7.22E-09
U-233	2.65E-08	1.80E-08	7.65E-07	7.27E-07	2.62E-09	1.69E-09	1.94E-09	1.26E-09	2.62E-09	1.69E-09
U-234	6.81E-09	4.54E-09	7.51E-07	7.14E-07	2.58E-09	1.66E-09	1.91E-09	1.24E-09	2.58E-09	1.66E-09
U-235+D	1.47E-05	9.99E-06	6.76E-07	6.43E-07	2.64E-09	1.67E-09	1.94E-09	1.24E-09	2.64E-09	1.67E-09
U-236	3.38E-09	2.22E-09	6.97E-07	6.62E-07	2.44E-09	1.57E-09	1.81E-09	1.17E-09	2.44E-09	1.57E-09
U-238	1.35E-09	8.51E-10	6.38E-07	6.08E-07	2.34E-09	1.51E-09	1.73E-09	1.13E-09	2.34E-09	1.51E-09
U-238+D	3.07E-06	2.10E-06	6.39E-07	6.09E-07	3.26E-09	2.02E-09	2.35E-09	1.48E-09	3.26E-09	2.02E-09
V-49	0.00E+00	0.00E+00	7.62E-12	6.78E-12	4.84E-12	2.68E-12	3.30E-12	1.83E-12	4.84E-12	2.68E-12
W-181	1.31E-06	8.84E-07	2.89E-11	2.47E-11	1.54E-11	8.73E-12	1.07E-11	6.08E-12	1.54E-11	8.73E-12
W-185	7.89E-09	5.32E-09	3.68E-10	3.41E-10	1.16E-10	6.43E-11	7.92E-11	4.41E-11	1.16E-10	6.43E-11
W-188+D	6.62E-06	4.51E-06	1.56E-09	1.41E-09	7.45E-10	4.05E-10	5.10E-10	2.78E-10	7.45E-10	4.05E-10
Y-88	3.70E-04	2.51E-04	5.49E-10	4.00E-10	1.58E-10	9.27E-11	1.13E-10	6.68E-11	1.58E-10	9.27E-11
Y-91	6.78E-07	4.68E-07	9.08E-10	8.05E-10	6.35E-10	3.51E-10	4.32E-10	2.39E-10	6.35E-10	3.51E-10
Yb-169	2.09E-05	1.42E-05	2.92E-10	2.61E-10	1.58E-10	8.78E-11	1.08E-10	6.05E-11	1.58E-10	8.78E-11

Table N-1 FGR-13 Morbidity and Mortality Risk Coefficients from Different Modes of Exposure (Cont.)

| Radionuclide[a] | External (risk/yr per Bq/g) | | Ingestion | | | | | | | |
| | | | Inhalation (risk/Bq) | | Food (risk/Bq) | | Water (risk/Bq) | | Soil[b] (risk/Bq) | |
	Morbidity	Mortality	Morbidity	Mortality	Morbidity	Mortality	Morbidity	Mortality	Morbidity	Mortality
Zn-65	7.59E-05	5.16E-05	2.05E-10	1.66E-10	4.16E-10	2.81E-10	3.16E-10	2.16E-10	4.16E-10	2.81E-10
Zr-88	4.46E-05	3.03E-05	3.65E-10	3.03E-10	5.89E-11	3.57E-11	4.27E-11	2.61E-11	5.89E-11	3.57E-11
Zr-93	0.00E+00	0.00E+00	4.11E-10	3.81E-10	3.89E-11	2.84E-11	3.00E-11	2.26E-11	3.89E-11	2.84E-11
Zr-95+D	9.19E-05	6.25E-05	5.71E-10	5.06E-10	1.79E-10	1.02E-10	1.25E-10	7.12E-11	1.79E-10	1.02E-10

a   Radionuclides with a half-life greater than 30 days. If short-lived progeny are involved, the symbol "+D" is added to the radionuclide name, for example, Ac-227+D. To distinguish between different associated radionuclides or terminal radionuclides, a different +D symbol, for example, "+D1," "+D2," is used. See Appendix A for associated progeny and their branching fractions.

b   Food ingestion risk coefficients are also used for soil ingestion risk calculations.

N.2.2 HEAST Risk Coefficients

The second set of risk coefficients in the database was obtained from the EPA's Health Effects Assessment Summary Tables (EPA 1997). Table N-2 lists external, inhalation, and ingestion risk coefficients for total cancer morbidity for 30-day cutoff half-life radionuclides. The ingestion risk coefficients are for food ingestion, water ingestion, and soil ingestion.

Table N-2 HEAST Morbidity Risk Coefficients from Different Modes of Exposure

Radionuclide[a]	External (risk/yr per Bq/g)	Inhalation (risk/Bq)	Ingestion Food (risk/Bq)	Ingestion Water (risk/Bq)	Ingestion Soil (risk/Bq)
Ac-227+D	3.97E-05	5.64E-06	1.76E-08	1.31E-08	3.14E-08
Ag-105	5.81E-05	7.65E-11	6.73E-11	4.78E-11	1.19E-10
Ag-108m+D	1.94E-04	7.22E-10	3.03E-10	2.2E-10	5.19E-10
Ag-110m+D	3.51E-04	7.65E-10	3.7E-10	2.67E-10	6.41E-10
Al-26	3.59E-04	1.87E-09	6.73E-10	4.68E-10	1.27E-09
Am-241	7.46E-07	7.59E-07	3.62E-09	2.81E-09	5.86E-09
Am-242m+D	9.69E-07	4.23E-07	2.44E-09	1.96E-09	3.63E-09
Am-242m+D1	9.69E-07	4.23E-07	2.44E-09	1.96E-09	3.63E-09
Am-242m+D2	7.08E-05	4.22E-07	2.58E-09	2.06E-09	3.9E-09
Am-243+D	1.72E-05	7.3E-07	3.82E-09	2.92E-09	6.26E-09
As-73	1.56E-07	1.05E-10	6.16E-11	4.22E-11	1.19E-10
Au-195	3.73E-06	1.75E-10	5.92E-11	4.05E-11	1.14E-10
Ba-133	3.89E-05	3.14E-10	2.55E-10	1.84E-10	3.76E-10
Be-10	2.01E-08	2.54E-09	2.76E-10	1.9E-10	5.46E-10
Be-7	5.76E-06	5.76E-12	3.24E-12	2.34E-12	5.46E-12
Bi-207	1.91E-04	5.68E-10	2.2E-10	1.53E-10	4.03E-10
Bi-210m+D	2.75E-05	3.16E-07	2.1E-09	1.49E-09	3.92E-09
Bk-247	8.35E-06	8.81E-07	4.32E-09	3.35E-09	6.73E-09
Bk-249	7.11E-11	1.39E-09	4.24E-11	3E-11	7.97E-11
Bk-249+D	2.81E-06	1.39E-09	5.11E-11	3.6E-11	9.62E-11
C-14 particulates	2.12E-10	1.91E-10	5.41E-11	4.19E-11	7.54E-11
C-14 gaseous	0.00E+00	5.38E-13	0.00E+00	0.00E+00	0.00E+00
Ca-41	0.00E+00	5.65E-12	1.18E-11	9.54E-12	1.55E-11
Ca-45	1.07E-09	2.54E-10	9.11E-11	6.68E-11	1.64E-10
Cd-109	2.36E-07	5.92E-10	1.81E-10	1.35E-10	3.08E-10
Cd-113	1.99E-09	3.03E-09	7.84E-10	6.16E-10	1.04E-09
Cd-113m	1.20E-08	3.51E-09	9.84E-10	7.76E-10	1.38E-09
Cd-115m	3.05E-06	7.89E-10	6.65E-10	4.59E-10	1.28E-09
Ce-139	1.23E-05	1.53E-10	5.27E-11	3.65E-11	1E-10
Ce-141	6.14E-06	3.08E-10	1.83E-10	1.25E-10	3.62E-10
Ce-144+D	6.60E-06	2.97E-09	1.4E-09	9.54E-10	2.76E-09
Cf-248	1.28E-09	4.89E-07	1.68E-09	1.2E-09	3.19E-09
Cf-249	3.70E-05	9.19E-07	4.41E-09	3.43E-09	6.86E-09
Cf-250	1.21E-09	7.19E-07	3.03E-09	2.33E-09	5E-09
Cf-251	1.02E-05	9.19E-07	4.59E-09	3.57E-09	7.22E-09

Table N-2 HEAST Morbidity Risk Coefficients from Different Modes of Exposure (Cont.)

Radionuclide[a]	External (risk/yr per Bq/g)	Inhalation (risk/Bq)	Ingestion Food (risk/Bq)	Water (risk/Bq)	Soil (risk/Bq)
Cf-252	2.34E-09	7.03E-07	4.86E-09	4.86E-09	4.86E-09
Cl-36	4.70E-08	6.76E-10	1.2E-10	8.92E-11	2.07E-10
Cm-241	5.24E-05	2.73E-09	1.9E-10	1.31E-10	3.65E-10
Cm-242	2.09E-09	4.08E-07	1.48E-09	1.04E-09	2.84E-09
Cm-243	1.13E-05	7.27E-07	3.32E-09	2.56E-09	5.54E-09
Cm-244	1.31E-09	6.84E-07	2.92E-09	2.26E-09	4.89E-09
Cm-245	6.43E-06	7.49E-07	3.65E-09	2.81E-09	5.89E-09
Cm-246	1.24E-09	7.49E-07	3.54E-09	2.76E-09	5.73E-09
Cm-247+D	3.69E-05	6.76E-07	3.53E-09	2.7E-09	5.74E-09
Cm-248	9.24E-10	4.05E-06	3.51E-08	3.51E-08	3.51E-08
Co-56	4.86E-04	5E-10	3.86E-10	2.73E-10	6.92E-10
Co-57	9.59E-06	5.65E-11	4.03E-11	2.81E-11	7.51E-11
Co-58	1.21E-04	1.62E-10	1.13E-10	7.97E-11	2.01E-10
Co-60	3.35E-04	9.68E-10	6.03E-10	4.24E-10	1.09E-09
Cs-134	1.92E-04	4.46E-10	1.39E-09	1.14E-09	1.57E-09
Cs-135	6.38E-10	5.03E-11	1.59E-10	1.28E-10	1.94E-10
Cs-137+D	6.88E-05	3.22E-10	1.01E-09	8.22E-10	1.17E-09
Dy-159	8.62E-07	3.46E-11	2.08E-11	1.43E-11	3.97E-11
Es-254+D	1.15E-04	0.0000005	2.13E-09	1.5E-09	4.1E-09
Eu-148	2.66E-04	2.68E-10	1.63E-10	1.16E-10	2.81E-10
Eu-149	3.84E-06	2.89E-11	2E-11	1.39E-11	3.78E-11
Eu-150b	1.75E-04	3.03E-09	1.64E-10	1.17E-10	2.92E-10
Eu-152	1.43E-04	2.46E-09	2.35E-10	1.64E-10	4.38E-10
Eu-154	1.58E-04	3.11E-09	4.03E-10	2.78E-10	7.7E-10
Eu-155	3.35E-06	4E-10	7.49E-11	5.14E-11	1.46E-10
Fe-55	0.00E+00	2.16E-11	3.14E-11	2.33E-11	5.65E-11
Fe-59	1.58E-04	3.59E-10	3E-10	2.13E-10	5.59E-10
Fe-60+D	5.03E-07	4.97E-09	6.46E-09	4.86E-09	9.54E-09
Fe-60+D1	5.03E-07	4.97E-09	6.46E-09	4.86E-09	9.54E-09
Fm-257+D	8.31E-06	9.04E-07	3.25E-09	2.25E-09	6.38E-09
Fm-257+D1	8.31E-06	9.04E-07	3.24E-09	2.24E-09	6.37E-09
Gd-146+D	3.29E-04	6.84E-10	3.7E-10	2.59E-10	6.78E-10
Gd-148	0.00E+00	3.41E-07	1.49E-09	1.14E-09	2.45E-09
Gd-151	3.24E-06	7.89E-11	4.46E-11	3.08E-11	8.65E-11
Gd-152	0.00E+00	2.46E-07	1.04E-09	8.03E-10	1.7E-09
Gd-153	4.38E-06	1.77E-10	6E-11	4.11E-11	1.15E-10
Ge-68+D	1.13E-04	1.32E-09	2.78E-10	1.96E-10	5.19E-10
H-3	0.00E+00	5.38E-12	3.89E-12	3.03E-12	5.95E-12
Hf-172+D	2.40E-04	2.03E-09	4.1E-10	2.85E-10	7.68E-10
Hf-175	3.65E-05	1.16E-10	7.65E-11	5.3E-11	1.43E-10
Hf-178m	2.59E-04	1E-08	5.76E-10	4.08E-10	1.05E-09
Hf-181	6.05E-05	4.76E-10	2.5E-10	1.72E-10	4.84E-10
Hf-182	2.46E-05	9.22E-09	1.96E-10	1.45E-10	3.43E-10
Hg-194+D	1.33E-04	1.97E-09	2.93E-09	2.23E-09	4.3E-09

Table N-2 HEAST Morbidity Risk Coefficients from Different Modes of Exposure (Cont.)

Radionuclide[a]	External (risk/yr per Bq/g)	Inhalation (risk/Bq)	Ingestion Food (risk/Bq)	Ingestion Water (risk/Bq)	Ingestion Soil (risk/Bq)
Hg-203	2.49E-05	6.62E-10	2.06E-10	1.54E-10	3.43E-10
Ho-166m	2.08E-04	8.35E-09	3.08E-10	2.17E-10	5.68E-10
I-125	1.96E-07	7.49E-10	1.7E-09	6.86E-10	1.5E-09
I-129	1.65E-07	4.32E-09	8.7E-09	4E-09	7.32E-09
In-114m+D	1.00E-05	8.11E-10	9.73E-10	6.7E-10	1.9E-09
In-115	7.30E-09	1.09E-08	1.17E-09	9.14E-10	1.58E-09
Ir-192	9.19E-05	6.51E-10	2.89E-10	1.99E-10	5.51E-10
Ir-192m	1.46E-05	2.76E-09	3.57E-11	2.65E-11	5.84E-11
Ir-194m	2.73E-04	1.24E-09	3.41E-10	2.4E-10	6.19E-10
K-40	2.15E-05	2.78E-10	9.27E-10	6.68E-10	1.67E-09
La-137	1.82E-07	3.76E-10	1.35E-11	9.41E-12	2.55E-11
La-138	1.64E-04	8.24E-09	1.34E-10	9.54E-11	2.38E-10
Lu-173	7.89E-06	2.35E-10	5.3E-11	3.65E-11	1.01E-10
Lu-174	1.15E-05	3.84E-10	5.73E-11	3.95E-11	1.11E-10
Lu-174m	2.67E-06	4.08E-10	1.34E-10	9.14E-11	2.63E-10
Lu-176	4.95E-05	3.81E-09	3.65E-10	2.51E-10	7.03E-10
Lu-177m+D	9.88E-05	1.57E-09	3.97E-10	2.73E-10	7.61E-10
Md-258	3.54E-08	4.54E-07	1.69E-09	1.17E-09	3.32E-09
Mn-53	0.00E+00	5.86E-12	6.08E-12	4.22E-12	1.18E-11
Mn-54	1.05E-04	1.59E-10	8.41E-11	6.16E-11	1.39E-10
Mo-93	5.86E-09	3.43E-11	1.13E-10	9.05E-11	1.43E-10
Na-22	2.78E-04	1.05E-10	3.41E-10	2.6E-10	5.32E-10
Nb-93m	1.04E-09	5.14E-11	3.16E-11	2.17E-11	6.24E-11
Nb-94	1.97E-04	1.02E-09	3E-10	2.1E-10	5.54E-10
Nb-95	9.54E-05	1.47E-10	9.46E-11	6.62E-11	1.72E-10
Ni-59	0.00E+00	6.51E-11	1.05E-11	7.41E-12	1.98E-11
Ni-63	0.00E+00	1.56E-10	2.57E-11	1.81E-11	4.84E-11
Np-235	5.76E-08	3.11E-11	1.37E-11	9.35E-12	2.7E-11
Np-236a	8.78E-06	2.64E-08	3.89E-10	2.84E-10	6.92E-10
Np-237+D	2.15E-05	4.79E-07	2.46E-09	1.82E-09	4.38E-09
Os-185	8.41E-05	1.66E-10	7.3E-11	5.19E-11	1.29E-10
Os-194+D	1.11E-05	6.98E-09	9.43E-10	6.46E-10	1.85E-09
Pa-231	3.76E-06	1.23E-06	6.11E-09	4.68E-09	1.01E-08
Pb-202+D	4.95E-05	4.03E-10	8.46E-10	6.4E-10	1.1E-09
Pb-205	9.46E-11	1.74E-11	2.23E-11	1.71E-11	3.41E-11
Pb-210+D	1.13E-07	8.34E-08	3.22E-08	2.41E-08	5.04E-08
Pd-107	0.00E+00	4.57E-11	9.92E-12	6.76E-12	1.96E-11
Pm-143	3.59E-05	1.45E-10	3.35E-11	2.36E-11	5.95E-11
Pm-144	1.86E-04	7.46E-10	1.26E-10	9.03E-11	2.19E-10
Pm-145	4.35E-07	1.78E-10	2.18E-11	1.51E-11	4.16E-11
Pm-146	8.89E-05	1.46E-09	1.62E-10	1.13E-10	3.03E-10
Pm-147	8.68E-10	4.35E-10	6.7E-11	4.57E-11	1.32E-10
Pm-148m+D	2.46E-04	5.86E-10	3.42E-10	2.37E-10	6.37E-10
Po-210	1.07E-09	2.92E-07	6.08E-08	1.02E-08	2.15E-08

Table N-2 HEAST Morbidity Risk Coefficients from Different Modes of Exposure (Cont.)

Radionuclide[a]	External (risk/yr per Bq/g)	Inhalation (risk/Bq)	Ingestion Food (risk/Bq)	Water (risk/Bq)	Soil (risk/Bq)
Pt-193	7.51E-11	3E-12	8.35E-12	5.7E-12	1.66E-11
Pu-236	3.22E-09	6.16E-07	2.68E-09	2.02E-09	4.7E-09
Pu-237	3.03E-06	3.43E-11	2.27E-11	1.56E-11	4.38E-11
Pu-238	1.95E-09	9.08E-07	4.57E-09	3.54E-09	7.35E-09
Pu-239	5.41E-09	0.0000009	4.7E-09	3.65E-09	7.46E-09
Pu-240	1.89E-09	0.0000009	4.7E-09	3.65E-09	7.49E-09
Pu-241	1.11E-10	9.03E-09	6.16E-11	4.76E-11	8.89E-11
Pu-241+D	1.02E-05	9.2E-09	2.55E-10	1.79E-10	4.65E-10
Pu-242	1.69E-09	8.46E-07	4.46E-09	3.46E-09	7.11E-09
Pu-244	8.14E-10	7.92E-07	4.86E-09	3.7E-09	7.95E-09
Pu-244+D	4.08E-05	7.92E-07	5.14E-09	3.89E-09	8.49E-09
Ra-226+D	2.29E-04	3.13E-07	1.39E-08	1.04E-08	1.97E-08
Ra-228+D	1.22E-04	1.41E-07	3.87E-08	2.82E-08	6.18E-08
Rb-83+D	5.89E-05	6.27E-11	2.03E-10	1.54E-10	3.19E-10
Rb-84	1.14E-04	9.7E-11	3.16E-10	2.38E-10	5.16E-10
Rb-87	2.46E-09	5.78E-11	1.91E-10	1.41E-10	3.38E-10
Re-184	1.06E-04	1.82E-10	1.19E-10	8.54E-11	2.07E-10
Re-184m	4.11E-05	6.11E-10	1.88E-10	1.32E-10	3.43E-10
Re-186m+D	1.96E-06	1.24E-09	5.01E-10	3.49E-10	9.41E-10
Re-187	0.00E+00	6.78E-13	6.92E-13	4.84E-13	1.3E-12
Rh-101	2.39E-05	4.89E-10	8.14E-11	5.81E-11	1.45E-10
Rh-102	2.63E-04	1.62E-09	2.81E-10	2.08E-10	4.62E-10
Rh-102m	5.70E-05	6.92E-10	2.36E-10	1.64E-10	4.49E-10
Ru-103+D	5.51E-05	2.41E-10	1.5E-10	1.04E-10	2.84E-10
Ru-106+D	2.61E-05	2.76E-09	1.65E-09	1.14E-09	3.22E-09
S-35	2.37E-10	1.36E-10	1E-10	1.39E-11	3.35E-11
Sb-124	2.40E-04	6.57E-10	5E-10	3.49E-10	9.46E-10
Sb-125	4.89E-05	4.49E-10	1.66E-10	1.18E-10	3.03E-10
Sc-46	2.60E-04	6.68E-10	2.4E-10	1.68E-10	4.38E-10
Se-75	3.92E-05	1.02E-10	2.92E-10	2.2E-10	4.51E-10
Se-79	2.97E-10	9E-11	2.62E-10	1.97E-10	4.32E-10
Si-32+D	2.55E-07	8.25E-09	4.68E-10	3.35E-10	8.62E-10
Sm-145	1.04E-06	1.22E-10	4.59E-11	3.16E-11	8.84E-11
Sm-146	0.00E+00	2.13E-07	1.42E-09	1.11E-09	2.26E-09
Sm-147	0.00E+00	1.86E-07	1.29E-09	1.01E-09	2.05E-09
Sm-151	9.73E-12	1.32E-10	2.18E-11	1.5E-11	4.3E-11
Sn-113+D	2.89E-05	2.72E-10	1.75E-10	1.2E-10	3.36E-10
Sn-119m	3.24E-08	2.11E-10	8.76E-11	5.97E-11	1.72E-10
Sn-121m+D	2.66E-08	4.38E-10	1.38E-10	9.47E-11	2.71E-10
Sn-123	1.05E-06	8.19E-10	5.54E-10	3.78E-10	1.09E-09
Sn-126+D	2.39E-04	2.73E-09	1.06E-09	7.36E-10	2.03E-09
Sr-85	5.95E-05	6.92E-11	8.41E-11	6.11E-11	1.36E-10
Sr-89	1.94E-07	6.32E-10	4.97E-10	3.46E-10	9.38E-10
Sr-90+D	5.29E-07	3.06E-09	2.58E-09	2E-09	3.9E-09

Table N-2 HEAST Morbidity Risk Coefficients from Different Modes of Exposure (Cont.)

Radionuclide[a]	External (risk/yr per Bq/g)	Inhalation (risk/Bq)	Ingestion		
			Food (risk/Bq)	Water (risk/Bq)	Soil (risk/Bq)
Ta-179	9.78E-07	5.54E-11	1.35E-11	9.3E-12	2.57E-11
Ta-180	5.49E-05	1.96E-09	1.74E-10	1.2E-10	3.32E-10
Ta-182	1.63E-04	1.01E-09	3.11E-10	2.15E-10	5.92E-10
Tb-157	4.41E-08	3.95E-11	7.3E-12	5.03E-12	1.43E-11
Tb-158	9.65E-05	2.24E-09	1.89E-10	1.32E-10	3.57E-10
Tb-160	1.41E-04	6.62E-10	3.43E-10	2.35E-10	6.54E-10
Tc-95m+D	8.31E-05	9.22E-11	6.87E-11	4.93E-11	1.17E-10
Tc-97	7.95E-09	2.3E-11	1.05E-11	7.3E-12	2E-11
Tc-97m	2.81E-08	3.03E-10	9.3E-11	6.43E-11	1.79E-10
Tc-98	1.74E-04	8.14E-10	2.73E-10	1.92E-10	4.95E-10
Tc-99	2.20E-09	3.81E-10	1.08E-10	7.43E-11	2.07E-10
Te-121m+D	8.01E-05	4.2E-10	2.78E-10	2.08E-10	4.65E-10
Te-123	7.38E-08	3.22E-10	1.38E-10	1.11E-10	1.83E-10
Te-123m	1.21E-05	3.68E-10	1.53E-10	1.12E-10	2.76E-10
Te-125m	1.88E-07	3.16E-10	1.27E-10	9E-11	2.41E-10
Te-127m+D	6.28E-07	7.13E-10	3.63E-10	2.59E-10	6.84E-10
Te-129m+D	8.03E-06	6.75E-10	5.99E-10	4.17E-10	1.16E-09
Th-228+D	2.10E-04	3.86E-06	1.14E-08	8.1E-09	2.19E-08
Th-229+D	3.15E-05	6.07E-06	1.94E-08	1.43E-08	3.48E-08
Th-230	2.21E-08	7.7E-07	3.22E-09	2.46E-09	5.46E-09
Th-232	9.24E-09	1.17E-06	3.59E-09	2.73E-09	6.24E-09
Ti-44+D	2.75E-04	9.23E-09	1.04E-09	7.34E-10	1.93E-09
Tl-204	7.46E-08	6.62E-11	2.23E-10	1.58E-10	4.16E-10
Tm-170	2.73E-07	6.57E-10	3.54E-10	2.41E-10	7E-10
Tm-171	1.88E-08	9E-11	2.76E-11	1.89E-11	5.46E-11
U-232	1.62E-08	5.27E-07	1.04E-08	7.89E-09	1.55E-08
U-233	2.65E-08	3.14E-07	2.62E-09	1.94E-09	4.32E-09
U-234	6.81E-09	3.08E-07	2.58E-09	1.91E-09	4.27E-09
U-235+D	1.47E-05	2.73E-07	2.64E-09	1.94E-09	4.42E-09
U-236	3.38E-09	2.84E-07	2.44E-09	1.81E-09	4.03E-09
U-238	1.35E-09	2.52E-07	2.34E-09	1.73E-09	3.86E-09
U-238+D	3.07E-06	2.53E-07	3.26E-09	2.35E-09	5.68E-09
V-49	0.00E+00	3.97E-12	4.84E-12	3.3E-12	9.54E-12
W-181	1.31E-06	3.65E-12	1.54E-11	1.07E-11	2.89E-11
W-185	7.89E-09	2.53E-11	1.16E-10	7.92E-11	2.26E-10
W-188+D	6.62E-06	1.85E-10	7.45E-10	5.1E-10	1.45E-09
Y-88	3.70E-04	4.59E-10	1.58E-10	1.13E-10	2.68E-10
Y-91	6.78E-07	9.08E-10	6.35E-10	4.32E-10	1.26E-09
Yb-169	2.09E-05	2.92E-10	1.58E-10	1.08E-10	3.03E-10
Zn-65	7.59E-05	1.57E-10	4.16E-10	3.16E-10	6.62E-10
Zr-88	4.46E-05	2.42E-10	5.89E-11	4.27E-11	1.01E-10
Zr-93	0.00E+00	1.97E-10	3.89E-11	3E-11	5.73E-11
Zr-95+D	9.19E-05	4.47E-10	1.79E-10	1.25E-10	3.34E-10

Footnote on next page.

a   Radionuclides with a half-life greater than 30 days. If short-lived progeny are
    involved, the symbol "+D" symbol is added to radionuclide name, for example,
    Ac-227+D. To distinguish between different associated radionuclides or
    terminal radionuclides, a different +D symbol, for example, "+D1," "+D2," is
    used. See Appendix A for associated progeny and their branching fractions.

N.2.3   DCFPAK3.02 Risk Coefficients

DCFPAK3.02 libraries use the ICRP 107 radionuclide transformation database and ICRP 60
dose estimation methodology (see Section A.3). The methodology used for calculating risk
coefficients is the same as used in FGR 13. Table N-3 lists the default morbidity and mortality
risk coefficients for different modes of exposure from DCFPAK 3.02 libraries used in the code
for radionuclides with a 30-day cutoff half-life in risk calculations.

Table N-3 DCFPAK3.02 Morbidity and Mortality Risk Coefficients from Different Modes of Exposure

Radionuclide[a]	External (risk/yr per Bq/g)		Inhalation (risk/Bq)		Ingestion Food (risk/Bq)		Ingestion Water (risk/Bq)		Ingestion Soil (risk/Bq)	
	Morbidity	Mortality	Morbidity	Mortality	Morbidity	Mortality	Morbidity	Mortality	Morbidity	Mortality
Ac-227+D	4.40E-05	3.00E-05	5.76E-06	5.45E-06	1.77E-08	1.2E-08	1.32E-08	9.16E-09	1.77E-08	1.2E-08
Ag-105	5.68E-05	3.85E-05	8.5E-11	7.07E-11	6.65E-11	3.96E-11	4.73E-11	2.85E-11	6.65E-11	3.96E-11
Ag-108m+D	1.94E-04	1.32E-04	2.84E-09	2.44E-09	3.01E-10	1.91E-10	2.19E-10	1.41E-10	3.01E-10	1.91E-10
Ag-110m+D	3.54E-04	2.40E-04	1.23E-09	1.04E-09	3.76E-10	2.33E-10	2.71E-10	1.7E-10	3.76E-10	2.33E-10
Al-26	3.60E-04	2.44E-04	7.85E-09	7.03E-09	6.71E-10	3.83E-10	4.67E-10	2.68E-10	6.71E-10	3.83E-10
Am-241	7.48E-07	5.02E-07	1.02E-06	9.03E-07	3.61E-09	2.55E-09	2.8E-09	2.01E-09	3.61E-09	2.55E-09
Am-242m+D	9.61E-07	6.54E-07	9.28E-07	7.25E-07	2.43E-09	1.84E-09	1.96E-09	1.49E-09	2.43E-09	1.84E-09
Am-242m+D1	9.61E-07	6.54E-07	9.28E-07	7.25E-07	2.43E-09	1.84E-09	1.96E-09	1.49E-09	2.43E-09	1.84E-09
Am-242m+D2	7.51E-05	5.11E-05	9.26E-07	7.23E-07	2.57E-09	1.91E-09	2.05E-09	1.54E-09	2.57E-09	1.91E-09
Am-243+D	1.80E-05	1.22E-05	0.000001	8.58E-07	3.82E-09	2.66E-09	2.94E-09	2.08E-09	3.82E-09	2.66E-09
As-73	1.55E-07	1.04E-07	1.35E-10	1.23E-10	6.18E-11	3.49E-11	4.24E-11	2.4E-11	6.18E-11	3.49E-11
Au-195	3.69E-06	2.50E-06	1.79E-10	1.61E-10	6.11E-11	3.41E-11	4.19E-11	2.34E-11	6.11E-11	3.41E-11
Ba-133	3.88E-05	2.64E-05	8.89E-10	7.83E-10	2.56E-10	1.74E-10	1.86E-10	1.28E-10	2.56E-10	1.74E-10
Be-10	2.03E-08	1.38E-08	2.54E-09	2.38E-09	2.78E-10	1.56E-10	1.9E-10	1.07E-10	2.78E-10	1.56E-10
Be-7	5.81E-06	3.94E-06	5.82E-12	4.64E-12	3.28E-12	1.93E-12	2.36E-12	1.4E-12	3.28E-12	1.93E-12
Bi-207	1.91E-04	1.30E-04	2.97E-09	2.6E-09	2.23E-10	1.27E-10	1.55E-10	8.87E-11	2.23E-10	1.27E-10
Bi-208	3.85E-04	2.63E-04	2.69E-09	2.24E-09	1.46E-10	8.56E-11	1.05E-10	6.17E-11	1.46E-10	8.56E-11
Bi-210m+D	2.79E-05	1.90E-05	7.89E-07	7.5E-07	2.1E-09	1.21E-09	1.5E-09	8.65E-10	2.1E-09	1.21E-09
Bk-247	1.26E-05	8.55E-06	1.3E-06	1.07E-06	4.34E-09	3.23E-09	3.37E-09	2.55E-09	4.34E-09	3.23E-09
Bk-249	1.27E-10	8.49E-11	3.21E-09	2.65E-09	4.22E-11	2.54E-11	2.98E-11	1.82E-11	4.22E-11	2.54E-11
Bk-249+D	2.81E-06	1.91E-06	3.22E-09	2.65E-09	5.09E-11	3.08E-11	3.58E-11	2.19E-11	5.09E-11	3.08E-11
C-14 (particulates)	2.12E-10	1.41E-10	4.58E-10	4.29E-10	5.4E-11	3.68E-11	4.2E-11	2.89E-11	5.4E-11	3.68E-11
C-14 (gaseous)	0.00E+00	0.00E+00	5.39E-13	3.68E-13	0.00E+00	0.00E+00	0.00E+00	0.00E+00	0.00E+00	0.00E+00
Ca-41	0.00E+00	0.00E+00	1.6E-11	1.49E-11	1.38E-11	1.22E-11	1.12E-11	1.01E-11	1.38E-11	1.22E-11
Ca-45	1.07E-09	7.19E-10	3.47E-10	3.22E-10	9.09E-11	6.26E-11	6.67E-11	4.73E-11	9.09E-11	6.26E-11
Cd-109	2.35E-07	1.56E-07	5.92E-10	5.45E-10	1.81E-10	1.14E-10	1.35E-10	8.64E-11	1.81E-10	1.14E-10

Table N-3 DCFPAK3.02 Morbidity and Mortality Risk Coefficients from Different Modes of Exposure (Cont.)

Radionuclide[a]	External (risk/yr per Bq/g)		Inhalation (risk/Bq)		Ingestion					
					Food (risk/Bq)		Water (risk/Bq)		Soil (risk/Bq)	
	Morbidity	Mortality	Morbidity	Mortality	Morbidity	Mortality	Morbidity	Mortality	Morbidity	Mortality
Cd-113	1.95E-09	1.32E-09	3.01E-09	2.16E-09	7.79E-10	5.44E-10	6.13E-10	4.3E-10	7.79E-10	5.44E-10
Cd-113m	1.84E-08	1.25E-08	3.56E-09	2.54E-09	9.92E-10	6.79E-10	7.84E-10	5.41E-10	9.92E-10	6.79E-10
Cd-115m+D	2.16E-05	1.47E-05	7.94E-10	6.97E-10	6.81E-10	3.85E-10	4.71E-10	2.68E-10	6.81E-10	3.85E-10
Cd-115m+D1	4.48E-06	3.06E-06	7.88E-10	6.92E-10	6.63E-10	3.75E-10	4.59E-10	2.61E-10	6.63E-10	3.75E-10
Ce-139	1.22E-05	8.33E-06	1.87E-10	1.68E-10	5.32E-11	2.98E-11	3.67E-11	2.06E-11	5.32E-11	2.98E-11
Ce-141	6.15E-06	4.20E-06	3.66E-10	3.31E-10	1.84E-10	1.02E-10	1.26E-10	6.95E-11	1.84E-10	1.02E-10
Ce-144+D	6.16E-06	4.22E-06	4.87E-09	4.49E-09	1.4E-09	7.76E-10	9.54E-10	5.29E-10	1.4E-09	7.76E-10
Cf-248	4.58E-08	3.11E-08	6.92E-07	6.57E-07	1.69E-09	1.03E-09	1.2E-09	7.48E-10	1.69E-09	1.03E-09
Cf-249	3.60E-05	2.45E-05	1.31E-06	1.08E-06	4.41E-09	3.28E-09	3.43E-09	2.59E-09	4.41E-09	3.28E-09
Cf-250	1.32E-06	9.02E-07	1.01E-06	9.56E-07	3.12E-09	2.22E-09	2.41E-09	1.75E-09	3.12E-09	2.22E-09
Cf-251	9.78E-06	6.63E-06	1.33E-06	1.1E-06	4.56E-09	3.38E-09	3.54E-09	2.66E-09	4.56E-09	3.38E-09
Cf-252	6.15E-05	4.20E-05	1.2E-06	1.14E-06	4.93E-09	3.09E-09	3.6E-09	2.3E-09	4.93E-09	3.09E-09
Cf-254	2.27E-03	1.55E-03	4.12E-06	3.9E-06	8.27E-08	4.69E-08	5.76E-08	3.27E-08	8.27E-08	4.69E-08
Cl-36	4.58E-08	3.13E-08	2.73E-09	2.58E-09	1.2E-10	7.92E-11	8.91E-11	5.93E-11	1.2E-10	7.92E-11
Cm-241	5.24E-05	3.56E-05	3.31E-09	3.12E-09	1.94E-10	1.09E-10	1.34E-10	7.49E-11	1.94E-10	1.09E-10
Cm-242	2.12E-09	1.32E-09	5.42E-07	5.15E-07	1.48E-09	8.65E-10	1.04E-09	6.15E-10	1.48E-09	8.65E-10
Cm-243	1.14E-05	7.73E-06	9.94E-07	9.39E-07	3.34E-09	2.31E-09	2.57E-09	1.81E-09	3.34E-09	2.31E-09
Cm-244	3.79E-09	2.46E-09	9.61E-07	9.09E-07	2.93E-09	2.02E-09	2.26E-09	1.6E-09	2.93E-09	2.02E-09
Cm-245	7.42E-06	5.05E-06	1.03E-06	8.79E-07	3.66E-09	2.58E-09	2.83E-09	2.03E-09	3.66E-09	2.58E-09
Cm-246	4.86E-07	3.31E-07	1.03E-06	8.86E-07	3.59E-09	2.54E-09	2.79E-09	2.01E-09	3.59E-09	2.54E-09
Cm-247+D	3.68E-05	2.51E-05	9.43E-07	7.85E-07	3.51E-09	2.45E-09	2.7E-09	1.92E-09	3.51E-09	2.45E-09
Cm-248	1.77E-04	1.21E-04	3.89E-06	3.04E-06	1.61E-08	1.1E-08	1.23E-08	8.56E-09	1.61E-08	1.1E-08
Cm-250	1.80E-03	1.22E-03	2.67E-05	2.09E-05	1.17E-07	7.94E-08	8.9E-08	6.14E-08	1.17E-07	7.94E-08
Cm-250+D	1.94E-03	1.32E-03	2.67E-05	2.09E-05	1.18E-07	7.98E-08	8.95E-08	6.17E-08	1.18E-07	7.98E-08
Cm-250+D1	1.91E-03	1.30E-03	2.67E-05	2.09E-05	1.17E-07	7.94E-08	8.9E-08	6.14E-08	1.17E-07	7.94E-08
Co-56	4.95E-04	3.38E-04	6.8E-10	5.64E-10	3.85E-10	2.33E-10	2.72E-10	1.66E-10	3.85E-10	2.33E-10
Co-57	9.59E-06	6.53E-06	1.01E-10	8.76E-11	4.03E-11	2.43E-11	2.81E-11	1.7E-11	4.03E-11	2.43E-11

Table N-3 DCFPAK3.02 Morbidity and Mortality Risk Coefficients from Different Modes of Exposure (Cont.)

Radionuclide[a]	External (risk/yr per Bq/g)		Inhalation (risk/Bq)		Ingestion Food (risk/Bq)		Ingestion Water (risk/Bq)		Ingestion Soil (risk/Bq)	
	Morbidity	Mortality	Morbidity	Mortality	Morbidity	Mortality	Morbidity	Mortality	Morbidity	Mortality
Co-58	1.21E-04	8.27E-05	2.14E-10	1.8E-10	1.12E-10	6.81E-11	7.95E-11	4.84E-11	1.12E-10	6.81E-11
Co-60	3.35E-04	2.28E-04	2.72E-09	2.33E-09	6.03E-10	3.88E-10	4.26E-10	2.76E-10	6.03E-10	3.88E-10
Cs-134	1.92E-04	1.31E-04	1.89E-09	1.66E-09	1.4E-09	9.57E-10	1.14E-09	7.91E-10	1.4E-09	9.57E-10
Cs-135	1.58E-09	1.06E-09	9.09E-10	8.53E-10	2.11E-10	1.42E-10	1.7E-10	1.16E-10	2.11E-10	1.42E-10
Cs-137+D	6.85E-05	4.68E-05	3.04E-09	2.78E-09	1.01E-09	6.89E-10	8.24E-10	5.68E-10	1.01E-09	6.89E-10
Dy-154	0.00E+00	0.00E+00	3.53E-07	3.34E-07	1.14E-09	7.66E-10	8.64E-10	5.92E-10	1.14E-09	7.66E-10
Dy-159	8.71E-07	5.81E-07	4.69E-11	4.09E-11	2.14E-11	1.2E-11	1.47E-11	8.26E-12	2.14E-11	1.2E-11
Es-254+D	1.16E-04	7.87E-05	7E-07	6.65E-07	2.14E-09	1.27E-09	1.52E-09	9.14E-10	2.14E-09	1.27E-09
Es-254+D1	2.52E-07	1.70E-07	7E-07	6.65E-07	2.12E-09	1.26E-09	1.5E-09	9.06E-10	2.12E-09	1.26E-09
Es-255+D	9.36E-08	6.38E-08	4.12E-07	3.91E-07	1.12E-09	6.3E-10	7.71E-10	4.34E-10	1.12E-09	6.3E-10
Es-255+D1	7.11E-07	4.82E-07	4.36E-07	4.14E-07	1.72E-09	9.63E-10	1.18E-09	6.62E-10	1.72E-09	9.63E-10
Eu-148	2.73E-04	1.86E-04	3.46E-10	2.56E-10	1.66E-10	9.68E-11	1.19E-10	6.94E-11	1.66E-10	9.68E-11
Eu-149	4.04E-06	2.73E-06	4.67E-11	3.97E-11	3.46E-11	1.93E-11	2.38E-11	1.33E-11	3.46E-11	1.93E-11
Eu-150	1.83E-04	1.24E-04	7.34E-09	5.69E-09	1.52E-10	9.13E-11	1.09E-10	6.61E-11	1.52E-10	9.13E-11
Eu-152	1.46E-04	9.94E-05	5.17E-09	4.12E-09	2.25E-10	1.3E-10	1.58E-10	9.15E-11	2.25E-10	1.3E-10
Eu-154	1.58E-04	1.08E-04	5.57E-09	4.56E-09	3.83E-10	2.18E-10	2.66E-10	1.52E-10	3.83E-10	2.18E-10
Eu-155	3.38E-06	2.30E-06	5.18E-10	4.77E-10	7.64E-11	4.28E-11	5.24E-11	2.94E-11	7.64E-11	4.28E-11
Fe-55	1.29E-14	8.80E-15	4E-11	3.3E-11	3.13E-11	2.39E-11	2.32E-11	1.81E-11	3.13E-11	2.39E-11
Fe-59	1.57E-04	1.07E-04	3.97E-10	3.49E-10	3.01E-10	1.91E-10	2.13E-10	1.36E-10	3.01E-10	1.91E-10
Fe-60+D	4.83E-07	3.28E-07	1.04E-08	8.17E-09	6.74E-09	5.15E-09	5.06E-09	3.92E-09	6.74E-09	5.15E-09
Fe-60+D1	4.83E-07	3.28E-07	1.04E-08	8.17E-09	6.74E-09	5.15E-09	5.06E-09	3.92E-09	6.74E-09	5.15E-09
Fm-257+D	1.33E-05	9.02E-06	7.62E-07	7.24E-07	1.88E-09	1.09E-09	1.31E-09	7.7E-10	1.88E-09	1.09E-09
Fm-257+D1	1.33E-05	9.06E-06	1.19E-06	1.13E-06	3.43E-09	1.96E-09	2.37E-09	1.36E-09	3.43E-09	1.96E-09
Gd-146+D	3.19E-04	2.17E-04	7.63E-10	6.61E-10	3.59E-10	2.03E-10	2.51E-10	1.43E-10	3.59E-10	2.03E-10
Gd-148	0.00E+00	0.00E+00	4.11E-07	3.89E-07	1.47E-09	1.07E-09	1.13E-09	8.44E-10	1.47E-09	1.07E-09
Gd-150	0.00E+00	0.00E+00	3.31E-07	3.13E-07	1.32E-09	9.73E-10	1.02E-09	7.67E-10	1.32E-09	9.73E-10
Gd-151	3.82E-06	2.60E-06	1.18E-10	1.05E-10	5.17E-11	2.88E-11	3.55E-11	1.98E-11	5.17E-11	2.88E-11

Table N-3 DCFPAK3.02 Morbidity and Mortality Risk Coefficients from Different Modes of Exposure (Cont.)

Radionuclide[a]	External (risk/yr per Bq/g)		Inhalation (risk/Bq)		Ingestion					
					Food (risk/Bq)		Water (risk/Bq)		Soil (risk/Bq)	
	Morbidity	Mortality	Morbidity	Mortality	Morbidity	Mortality	Morbidity	Mortality	Morbidity	Mortality
Gd-152	0.00E+00	0.00E+00	2.46E-07	2.2E-07	1.04E-09	7.64E-10	8.02E-10	6.02E-10	1.04E-09	7.64E-10
Gd-153	4.35E-06	2.94E-06	2.32E-10	2.09E-10	6.01E-11	3.36E-11	4.14E-11	2.32E-11	6.01E-11	3.36E-11
Ge-68+D	1.13E-04	7.67E-05	2.8E-09	2.6E-09	2.77E-10	1.58E-10	1.96E-10	1.11E-10	2.77E-10	1.58E-10
H-3	0.00E+00	0.00E+00	2.29E-11	2.11E-11	3.89E-12	2.65E-12	3.03E-12	2.09E-12	3.89E-12	2.65E-12
Hf-172+D	2.48E-04	1.69E-04	2.47E-09	2.16E-09	4.16E-10	2.39E-10	2.91E-10	1.68E-10	4.16E-10	2.39E-10
Hf-174	0.00E+00	0.00E+00	2.73E-07	2.58E-07	2.16E-09	1.51E-09	1.72E-09	1.21E-09	2.16E-09	1.51E-09
Hf-175	3.47E-05	2.36E-05	1.42E-10	1.22E-10	7.49E-11	4.23E-11	5.2E-11	2.95E-11	7.49E-11	4.23E-11
Hf-178m	2.45E-04	1.67E-04	8.76E-09	7.01E-09	4.64E-10	2.82E-10	3.31E-10	2.04E-10	4.64E-10	2.82E-10
Hf-181	5.78E-05	3.94E-05	5.75E-10	5.19E-10	2.52E-10	1.41E-10	1.73E-10	9.67E-11	2.52E-10	1.41E-10
Hf-182	2.46E-05	1.67E-05	8.88E-09	7.4E-09	1.72E-10	1.19E-10	1.28E-10	9.06E-11	1.72E-10	1.19E-10
Hg-194+D	1.29E-04	8.80E-05	2.03E-09	1.68E-09	2.89E-09	2E-09	2.19E-09	1.52E-09	2.89E-09	2E-09
Hg-203	2.49E-05	1.69E-05	6.62E-10	5.95E-10	2.06E-10	1.37E-10	1.54E-10	1.03E-10	2.06E-10	1.37E-10
Ho-163	0.00E+00	0.00E+00	3.23E-11	2.45E-11	7.11E-13	4.1E-13	4.89E-13	2.83E-13	7.11E-13	4.1E-13
Ho-166m	1.93E-04	1.32E-04	2.07E-08	1.57E-08	3.19E-10	1.9E-10	2.24E-10	1.35E-10	3.19E-10	1.9E-10
I-125	1.97E-07	1.23E-07	7.52E-10	7.79E-11	9.34E-10	9.7E-11	6.91E-10	7.19E-11	9.34E-10	9.7E-11
I-129	1.67E-07	1.07E-07	4.42E-09	6.14E-10	5.32E-09	5.43E-10	4.08E-09	4.16E-10	5.32E-09	5.43E-10
In-114m+D	8.57E-06	5.82E-06	1.36E-09	1.21E-09	9.85E-10	5.62E-10	6.78E-10	3.89E-10	9.85E-10	5.62E-10
In-115	7.42E-09	5.02E-09	1.1E-08	9.9E-09	1.17E-09	9.99E-10	9.17E-10	7.91E-10	1.17E-09	9.99E-10
Ir-192	9.15E-05	6.22E-05	6.51E-10	5.8E-10	2.89E-10	1.63E-10	1.99E-10	1.13E-10	2.89E-10	1.63E-10
Ir-192n	3.16E-08	2.15E-08	4.25E-09	3.9E-09	2.06E-10	1.18E-10	1.42E-10	8.18E-11	2.06E-10	1.18E-10
Ir-194m	2.73E-04	1.86E-04	1.18E-09	1.03E-09	3.25E-10	1.89E-10	2.29E-10	1.34E-10	3.25E-10	1.89E-10
K-40	2.16E-05	1.47E-05	6E-09	5.6E-09	9.24E-10	5.88E-10	6.67E-10	4.29E-10	9.24E-10	5.88E-10
La-137	1.86E-07	1.19E-07	3.84E-10	3.17E-10	1.37E-11	7.89E-12	9.52E-12	5.53E-12	1.37E-11	7.89E-12
La-138	1.63E-04	1.11E-04	8.22E-09	6.33E-09	1.34E-10	8.08E-11	9.58E-11	5.83E-11	1.34E-10	8.08E-11
Lu-173	1.21E-05	8.21E-06	3.4E-10	3.02E-10	7.57E-11	4.24E-11	5.22E-11	2.93E-11	7.57E-11	4.24E-11
Lu-174	1.01E-05	6.88E-06	4.06E-10	3.68E-10	6.14E-11	3.44E-11	4.23E-11	2.38E-11	6.14E-11	3.44E-11
Lu-174m	2.48E-06	1.68E-06	4.24E-10	3.87E-10	1.38E-10	7.62E-11	9.39E-11	5.21E-11	1.38E-10	7.62E-11

Table N-3 DCFPAK3.02 Morbidity and Mortality Risk Coefficients from Different Modes of Exposure (Cont.)

Radionuclide[a]	External (risk/yr per Bq/g)		Inhalation (risk/Bq)		Ingestion					
					Food (risk/Bq)		Water (risk/Bq)		Soil (risk/Bq)	
	Morbidity	Mortality	Morbidity	Mortality	Morbidity	Mortality	Morbidity	Mortality	Morbidity	Mortality
Lu-176	4.83E-05	3.28E-05	4.78E-09	4.16E-09	3.7E-10	2.09E-10	2.55E-10	1.45E-10	3.7E-10	2.09E-10
Lu-177m+D	9.88E-05	6.73E-05	1.56E-09	1.41E-09	3.95E-10	2.21E-10	2.72E-10	1.52E-10	3.95E-10	2.21E-10
Mn-53	0.00E+00	0.00E+00	2.6E-11	2.4E-11	6.01E-12	3.48E-12	4.17E-12	2.44E-12	6.01E-12	3.48E-12
Mn-54	1.05E-04	7.16E-05	3.26E-10	2.67E-10	8.39E-11	5.3E-11	6.15E-11	3.94E-11	8.39E-11	5.3E-11
Mo-93	5.74E-09	3.31E-09	1.5E-10	1.41E-10	1.05E-10	9.39E-11	8.44E-11	7.61E-11	1.05E-10	9.39E-11
Na-22	2.79E-04	1.90E-04	2.63E-09	2.31E-09	3.41E-10	2.34E-10	2.6E-10	1.8E-10	3.41E-10	2.34E-10
Nb-91	1.93E-07	1.31E-07	1.35E-10	1.26E-10	1.06E-11	5.93E-12	7.23E-12	4.07E-12	1.06E-11	5.93E-12
Nb-91m	3.28E-06	2.24E-06	3.94E-10	3.64E-10	1.06E-10	5.9E-11	7.26E-11	4.03E-11	1.06E-10	5.9E-11
Nb-92	1.86E-04	1.27E-04	2.01E-09	1.68E-09	1.24E-10	7.49E-11	8.97E-11	5.46E-11	1.24E-10	7.49E-11
Nb-93m	1.03E-09	5.90E-10	1.63E-10	1.51E-10	3.29E-11	1.83E-11	2.25E-11	1.26E-11	3.29E-11	1.83E-11
Nb-94	1.95E-04	1.33E-04	3.62E-09	3.19E-09	3E-10	1.73E-10	2.1E-10	1.22E-10	3E-10	1.73E-10
Nb-95	9.53E-05	6.50E-05	1.73E-10	1.5E-10	9.46E-11	5.42E-11	6.63E-11	3.82E-11	9.46E-11	5.42E-11
Nd-144	0.00E+00	0.00E+00	2.81E-07	2.52E-07	1.06E-09	8.15E-10	8.29E-10	6.5E-10	1.06E-09	8.15E-10
Ni-59	1.83E-09	1.25E-09	6.45E-11	4.52E-11	1.04E-11	6.2E-12	7.34E-12	4.4E-12	1.04E-11	6.2E-12
Ni-63	0.00E+00	0.00E+00	1.59E-10	1.11E-10	2.62E-11	1.55E-11	1.84E-11	1.1E-11	2.62E-11	1.55E-11
Np-235	3.82E-08	2.57E-08	5.53E-11	5.09E-11	1.48E-11	8.18E-12	1.01E-11	5.58E-12	1.48E-11	8.18E-12
Np-235+D	3.82E-08	2.57E-08	5.53E-11	5.09E-11	1.48E-11	8.18E-12	1.01E-11	5.58E-12	1.48E-11	8.18E-12
Np-236	1.05E-05	7.16E-06	9.08E-08	6.61E-08	4.93E-10	3.1E-10	3.6E-10	2.3E-10	4.93E-10	3.1E-10
Np-236+D	1.26E-04	8.61E-05	9.1E-08	6.62E-08	6.29E-10	3.87E-10	4.54E-10	2.83E-10	6.29E-10	3.87E-10
Np-236+D1	1.26E-04	8.61E-05	9.1E-08	6.62E-08	6.29E-10	3.87E-10	4.54E-10	2.83E-10	6.29E-10	3.87E-10
Np-237+D	2.31E-05	1.57E-05	7.75E-07	7.32E-07	2.48E-09	1.57E-09	1.85E-09	1.19E-09	2.48E-09	1.57E-09
Os-185	8.05E-05	5.49E-05	1.6E-10	1.33E-10	7.08E-11	4.13E-11	5.02E-11	2.95E-11	7.08E-11	4.13E-11
Os-186	0.00E+00	0.00E+00	3.24E-07	3.07E-07	2.83E-09	1.92E-09	2.12E-09	1.46E-09	2.83E-09	1.92E-09
Os-194+D	1.12E-05	7.60E-06	7.01E-09	6.54E-09	9.57E-10	5.34E-10	6.55E-10	3.67E-10	9.57E-10	5.34E-10
Pa-231	3.44E-06	2.33E-06	2.06E-06	1.52E-06	6.1E-09	4.29E-09	4.66E-09	3.3E-09	6.1E-09	4.29E-09
Pb-202+D	4.90E-05	3.31E-05	3.77E-09	3.49E-09	1.27E-09	9.31E-10	9.52E-10	7.05E-10	1.27E-09	9.31E-10
Pb-205	8.17E-11	5.02E-11	6.16E-11	5.76E-11	2.17E-11	1.69E-11	1.67E-11	1.33E-11	2.17E-11	1.69E-11

Table N-3 DCFPAK3.02 Morbidity and Mortality Risk Coefficients from Different Modes of Exposure (Cont.)

Radionuclide[a]	External (risk/yr per Bq/g)		Inhalation (risk/Bq)		Ingestion Food (risk/Bq)		Ingestion Water (risk/Bq)		Ingestion Soil (risk/Bq)	
	Morbidity	Mortality	Morbidity	Mortality	Morbidity	Mortality	Morbidity	Mortality	Morbidity	Mortality
Pb-210+D	1.15E-07	7.94E-08	4.41E-07	4.19E-07	3.21E-08	2.33E-08	2.41E-08	1.76E-08	3.21E-08	2.33E-08
Pb-210+D1	4.64E-07	3.22E-07	4.41E-07	4.18E-07	3.21E-08	2.33E-08	2.41E-08	1.76E-08	3.21E-08	2.33E-08
Pd-107	0.00E+00	0.00E+00	4.74E-11	4.39E-11	1.03E-11	5.68E-12	7E-12	3.87E-12	1.03E-11	5.68E-12
Pm-143	3.60E-05	2.44E-05	2.45E-10	1.87E-10	3.35E-11	1.93E-11	2.37E-11	1.37E-11	3.35E-11	1.93E-11
Pm-144	1.86E-04	1.27E-04	1.49E-09	1.13E-09	1.27E-10	7.41E-11	9.04E-11	5.32E-11	1.27E-10	7.41E-11
Pm-145	4.26E-07	2.81E-07	3.36E-10	2.87E-10	2.05E-11	1.17E-11	1.42E-11	8.13E-12	2.05E-11	1.17E-11
Pm-146	8.84E-05	6.03E-05	2.77E-09	2.21E-09	1.59E-10	9.1E-11	1.11E-10	6.38E-11	1.59E-10	9.1E-11
Pm-147	8.71E-10	5.84E-10	4.34E-10	4.05E-10	6.7E-11	3.72E-11	4.57E-11	2.54E-11	6.7E-11	3.72E-11
Pm-148m+D	2.45E-04	1.67E-04	5.8E-10	5.02E-10	3.39E-10	1.91E-10	2.36E-10	1.34E-10	3.39E-10	1.91E-10
Po-208	2.41E-09	1.64E-09	6.1E-07	5.8E-07	7.6E-08	5.55E-08	5.99E-08	4.42E-08	7.6E-08	5.55E-08
Po-209	7.16E-07	4.89E-07	7.62E-07	7.23E-07	7.54E-08	5.51E-08	5.95E-08	4.39E-08	7.54E-08	5.51E-08
Po-210	1.22E-09	8.30E-10	3.92E-07	3.72E-07	6.09E-08	4.45E-08	4.8E-08	3.54E-08	6.09E-08	4.45E-08
Pt-190	0.00E+00	0.00E+00	4.06E-07	3.85E-07	1.14E-09	6.95E-10	8.14E-10	4.99E-10	1.14E-09	6.95E-10
Pt-193	5.18E-11	3.16E-11	5.33E-11	4.95E-11	9.59E-12	5.31E-12	6.54E-12	3.62E-12	9.59E-12	5.31E-12
Pu-236	3.09E-09	1.99E-09	8.01E-07	7.59E-07	2.71E-09	1.9E-09	2.04E-09	1.46E-09	2.71E-09	1.9E-09
Pu-237	3.09E-06	2.10E-06	4.04E-11	3.56E-11	2.53E-11	1.41E-11	1.74E-11	9.7E-12	2.53E-11	1.41E-11
Pu-238	1.87E-09	1.17E-09	1.41E-06	1.19E-06	4.58E-09	3.5E-09	3.55E-09	2.75E-09	4.58E-09	3.5E-09
Pu-239+D	5.65E-09	3.79E-09	1.5E-06	1.26E-06	4.71E-09	3.63E-09	3.65E-09	2.85E-09	4.71E-09	3.63E-09
Pu-240	1.92E-09	1.22E-09	1.5E-06	1.26E-06	4.71E-09	3.63E-09	3.65E-09	2.85E-09	4.71E-09	3.63E-09
Pu-241	1.10E-10	7.45E-11	2.34E-08	1.98E-08	6.17E-11	5.06E-11	4.77E-11	3.94E-11	6.17E-11	5.06E-11
Pu-241+D	1.01E-05	6.85E-06	2.36E-08	2E-08	2.59E-10	1.6E-10	1.83E-10	1.14E-10	2.59E-10	1.6E-10
Pu-242	1.18E-08	7.95E-09	1.42E-06	1.2E-06	4.48E-09	3.45E-09	3.47E-09	2.71E-09	4.48E-09	3.45E-09
Pu-244	2.67E-06	1.82E-06	1.41E-06	1.19E-06	5.08E-09	3.78E-09	3.88E-09	2.93E-09	5.08E-09	3.78E-09
Pu-244+D	4.25E-05	2.90E-05	1.41E-06	1.19E-06	5.35E-09	3.93E-09	4.07E-09	3.03E-09	5.35E-09	3.93E-09
Ra-226+D	2.26E-04	1.54E-04	7.63E-07	7.25E-07	1.39E-08	9.57E-09	1.04E-08	7.18E-09	1.39E-08	9.57E-09
Ra-228+D	1.09E-04	7.45E-05	1.18E-06	1.12E-06	3.86E-08	2.73E-08	2.81E-08	2E-08	3.86E-08	2.73E-08
Rb-83+D	5.74E-05	3.91E-05	1.4E-10	1.12E-10	1.91E-10	1.3E-10	1.45E-10	9.99E-11	1.91E-10	1.3E-10

Table N-3 DCFPAK3.02 Morbidity and Mortality Risk Coefficients from Different Modes of Exposure (Cont.)

Radionuclide[a]	External (risk/yr per Bq/g)		Inhalation (risk/Bq)		Ingestion					
					Food (risk/Bq)		Water (risk/Bq)		Soil (risk/Bq)	
	Morbidity	Mortality	Morbidity	Mortality	Morbidity	Mortality	Morbidity	Mortality	Morbidity	Mortality
Rb-84	1.12E-04	7.64E-05	2.81E-10	2.41E-10	3.21E-10	2.18E-10	2.41E-10	1.66E-10	3.21E-10	2.18E-10
Rb-87	2.74E-09	1.84E-09	1.21E-09	1.13E-09	1.98E-10	1.33E-10	1.45E-10	9.88E-11	1.98E-10	1.33E-10
Re-183	9.59E-06	6.50E-06	3.36E-10	3.05E-10	1.28E-10	7.49E-11	9.01E-11	5.3E-11	1.28E-10	7.49E-11
Re-184	1.06E-04	7.26E-05	2.24E-10	1.95E-10	1.19E-10	7.21E-11	8.57E-11	5.22E-11	1.19E-10	7.21E-11
Re-184m	4.01E-05	2.73E-05	9.62E-10	8.68E-10	1.89E-10	1.12E-10	1.33E-10	7.99E-11	1.89E-10	1.12E-10
Re-186m+D	1.97E-06	1.33E-06	4.54E-09	4.24E-09	4.94E-10	2.88E-10	3.45E-10	2.03E-10	4.94E-10	2.88E-10
Re-186m+D1	1.97E-06	1.33E-06	4.54E-09	4.24E-09	4.94E-10	2.88E-10	3.45E-10	2.03E-10	4.94E-10	2.88E-10
Re-187	0.00E+00	0.00E+00	2.98E-12	2.77E-12	6.47E-13	3.78E-13	4.51E-13	2.66E-13	6.47E-13	3.78E-13
Rh-101	2.57E-05	1.75E-05	4.64E-10	4.08E-10	7.73E-11	4.68E-11	5.54E-11	3.38E-11	7.73E-11	4.68E-11
Rh-102	5.93E-05	4.04E-05	7.02E-10	6.28E-10	2.41E-10	1.38E-10	1.67E-10	9.6E-11	2.41E-10	1.38E-10
Rh-102m	2.64E-04	1.80E-04	1.8E-09	1.49E-09	2.98E-10	1.89E-10	2.2E-10	1.41E-10	2.98E-10	1.89E-10
Ru-103+D	5.81E-05	3.98E-05	2.81E-10	2.5E-10	1.42E-10	8.07E-11	9.87E-11	5.62E-11	1.42E-10	8.07E-11
Ru-106+D	2.63E-05	1.79E-05	6.06E-09	5.59E-09	1.65E-09	9.34E-10	1.14E-09	6.45E-10	1.65E-09	9.34E-10
S-35	2.36E-10	1.57E-10	1.76E-10	1.63E-10	9.99E-11	6.71E-11	7.35E-11	4.98E-11	9.99E-11	6.71E-11
Sb-124	2.45E-04	1.67E-04	8.64E-10	7.53E-10	5E-10	2.86E-10	3.47E-10	1.99E-10	5E-10	2.86E-10
Sb-125	4.95E-05	3.38E-05	1.09E-09	9.84E-10	1.68E-10	1.02E-10	1.2E-10	7.35E-11	1.68E-10	1.02E-10
Sc-46	2.60E-04	1.77E-04	6.67E-10	5.79E-10	2.39E-10	1.36E-10	1.68E-10	9.59E-11	2.39E-10	1.36E-10
Se-75	3.85E-05	2.62E-05	1.33E-10	1.13E-10	2.87E-10	2.01E-10	2.17E-10	1.54E-10	2.87E-10	2.01E-10
Se-79	2.45E-10	1.63E-10	5.03E-10	4.71E-10	2.48E-10	1.72E-10	1.87E-10	1.31E-10	2.48E-10	1.72E-10
Si-32+D	2.55E-07	1.82E-07	8.21E-09	7.76E-09	4.72E-10	3.04E-10	3.38E-10	2.22E-10	4.72E-10	3.04E-10
Sm-145	1.01E-06	6.66E-07	1.57E-10	1.35E-10	4.49E-11	2.51E-11	3.09E-11	1.73E-11	4.49E-11	2.51E-11
Sm-146	0.00E+00	0.00E+00	3.74E-07	3.35E-07	1.41E-09	1.08E-09	1.1E-09	8.64E-10	1.41E-09	1.08E-09
Sm-147	0.00E+00	0.00E+00	3.41E-07	3.06E-07	1.29E-09	9.89E-10	1.01E-09	7.89E-10	1.29E-09	9.89E-10
Sm-148	0.00E+00	0.00E+00	2.93E-07	2.63E-07	1.11E-09	8.5E-10	8.65E-10	6.78E-10	1.11E-09	8.5E-10
Sm-151	1.04E-11	6.12E-12	2.5E-10	2.33E-10	2.2E-11	1.24E-11	1.51E-11	8.54E-12	2.2E-11	1.24E-11
Sn-113+D	2.94E-05	2.00E-05	3.99E-10	3.57E-10	1.78E-10	9.92E-11	1.22E-10	6.83E-11	1.78E-10	9.92E-11
Sn-119m	4.23E-08	2.58E-08	3.31E-10	3.05E-10	8.91E-11	4.97E-11	6.09E-11	3.4E-11	8.91E-11	4.97E-11

Table N-3 DCFPAK3.02 Morbidity and Mortality Risk Coefficients from Different Modes of Exposure (Cont.)

| Radionuclide[a] | External (risk/yr per Bq/g) | | Inhalation (risk/Bq) | | Ingestion | | | | | |
| | Morbidity | Mortality | Morbidity | Mortality | Food (risk/Bq) | | Water (risk/Bq) | | Soil (risk/Bq) | |
					Morbidity	Mortality	Morbidity	Mortality	Morbidity	Mortality
Sn-121m+D	2.69E-08	1.71E-08	1.19E-09	1.12E-09	1.4E-10	7.82E-11	9.55E-11	5.37E-11	1.4E-10	7.82E-11
Sn-123	1.05E-06	7.19E-07	1.26E-09	1.14E-09	5.56E-10	3.09E-10	3.8E-10	2.11E-10	5.56E-10	3.09E-10
Sn-126+D	2.37E-04	1.62E-04	1.15E-08	1.04E-08	1.08E-09	6.14E-10	7.47E-10	4.28E-10	1.08E-09	6.14E-10
Sr-85	5.81E-05	3.94E-05	8.56E-11	7.03E-11	8.24E-11	5.45E-11	6E-11	4.01E-11	8.24E-11	5.45E-11
Sr-89	1.96E-07	1.39E-07	8.18E-10	7.23E-10	4.97E-10	2.98E-10	3.47E-10	2.11E-10	4.97E-10	2.98E-10
Sr-90+D	5.27E-07	3.75E-07	1.17E-08	1.1E-08	2.57E-09	2.01E-09	2E-09	1.61E-09	2.57E-09	2.01E-09
Ta-179	7.57E-07	5.08E-07	4.82E-11	4.23E-11	1.27E-11	7.12E-12	8.77E-12	4.91E-12	1.27E-11	7.12E-12
Ta-182	1.63E-04	1.11E-04	1E-09	8.95E-10	3.05E-10	1.71E-10	2.11E-10	1.19E-10	3.05E-10	1.71E-10
Tb-157	8.11E-08	5.39E-08	1E-10	8.94E-11	8.19E-12	4.62E-12	5.63E-12	3.19E-12	8.19E-12	4.62E-12
Tb-158	9.72E-05	6.63E-05	4.65E-09	3.78E-09	1.86E-10	1.07E-10	1.3E-10	7.53E-11	1.86E-10	1.07E-10
Tb-160	1.42E-04	9.66E-05	8.16E-10	7.27E-10	3.44E-10	1.93E-10	2.37E-10	1.33E-10	3.44E-10	1.93E-10
Tc-95m+D	8.46E-05	5.75E-05	1.25E-10	1.04E-10	6.95E-11	4.19E-11	4.99E-11	3.04E-11	6.95E-11	4.19E-11
Tc-97	7.73E-09	4.45E-09	1.3E-10	1.21E-10	1.06E-11	6.11E-12	7.33E-12	4.26E-12	1.06E-11	6.11E-12
Tc-97m	2.79E-08	1.82E-08	3.92E-10	3.64E-10	9.33E-11	5.31E-11	6.43E-11	3.68E-11	9.33E-11	5.31E-11
Tc-98	1.74E-04	1.19E-04	3.19E-09	2.8E-09	2.54E-10	1.5E-10	1.79E-10	1.07E-10	2.54E-10	1.5E-10
Tc-99	2.24E-09	1.51E-09	1.03E-09	9.67E-10	1.08E-10	6.17E-11	7.44E-11	4.28E-11	1.08E-10	6.17E-11
Te-121m+D	8.02E-05	5.47E-05	6.04E-10	5.3E-10	2.82E-10	1.87E-10	2.11E-10	1.44E-10	2.82E-10	1.87E-10
Te-123	1.27E-10	7.89E-11	8.32E-11	7.63E-11	3.56E-11	3.18E-11	2.93E-11	2.63E-11	3.56E-11	3.18E-11
Te-123m	1.21E-05	8.24E-06	4.79E-10	4.41E-10	1.52E-10	9.68E-11	1.11E-10	7.26E-11	1.52E-10	9.68E-11
Te-125m	1.87E-07	1.19E-07	3.91E-10	3.6E-10	1.27E-10	7.51E-11	9E-11	5.42E-11	1.27E-10	7.51E-11
Te-127m+D	6.27E-07	4.25E-07	9.55E-10	8.76E-10	3.63E-10	2.26E-10	2.61E-10	1.66E-10	3.63E-10	2.26E-10
Te-129m+D	8.13E-06	5.53E-06	8.09E-10	7.12E-10	5.98E-10	3.42E-10	4.17E-10	2.41E-10	5.98E-10	3.42E-10
Th-228+D	1.98E-04	1.35E-04	3.9E-06	3.71E-06	1.14E-08	6.98E-09	8.12E-09	5.01E-09	1.14E-08	6.98E-09
Th-229+D	3.07E-05	2.09E-05	6.2E-06	5.88E-06	1.94E-08	1.28E-08	1.43E-08	9.54E-09	1.94E-08	1.28E-08
Th-230	2.28E-08	1.55E-08	9.21E-07	7.23E-07	3.22E-09	2.17E-09	2.47E-09	1.67E-09	3.22E-09	2.17E-09
Th-232	9.69E-09	6.53E-09	1.17E-06	1.1E-06	3.6E-09	2.45E-09	2.73E-09	1.87E-09	3.6E-09	2.45E-09
Ti-44+D	2.76E-04	1.88E-04	9.32E-09	8.39E-09	1.04E-09	6.13E-10	7.34E-10	4.35E-10	1.04E-09	6.13E-10

Table N-3 DCFPAK3.02 Morbidity and Mortality Risk Coefficients from Different Modes of Exposure (Cont.)

| Radionuclide[a] | External (risk/yr per Bq/g) | | Inhalation (risk/Bq) | | Ingestion | | | | | |
| | | | | | Food (risk/Bq) | | Water (risk/Bq) | | Soil (risk/Bq) | |
	Morbidity	Mortality	Morbidity	Mortality	Morbidity	Mortality	Morbidity	Mortality	Morbidity	Mortality
Tl-204	8.08E-08	5.49E-08	1.63E-09	1.53E-09	2.22E-10	1.34E-10	1.57E-10	9.55E-11	2.22E-10	1.34E-10
Tm-168	1.45E-04	9.85E-05	5E-10	4.36E-10	1.74E-10	9.88E-11	1.21E-10	6.94E-11	1.74E-10	9.88E-11
Tm-170	2.16E-07	1.47E-07	8.85E-10	8.08E-10	3.5E-10	1.94E-10	2.39E-10	1.32E-10	3.5E-10	1.94E-10
Tm-171	1.80E-08	1.21E-08	1.17E-10	1.09E-10	2.76E-11	1.53E-11	1.88E-11	1.05E-11	2.76E-11	1.53E-11
U-232	1.47E-08	9.91E-09	2.5E-06	2.37E-06	1.04E-08	7.19E-09	7.85E-09	5.49E-09	1.04E-08	7.19E-09
U-233	1.92E-08	1.30E-08	7.65E-07	7.27E-07	2.62E-09	1.69E-09	1.94E-09	1.26E-09	2.62E-09	1.69E-09
U-234	6.85E-09	4.58E-09	7.52E-07	7.14E-07	2.58E-09	1.66E-09	1.91E-09	1.24E-09	2.58E-09	1.66E-09
U-235+D	1.56E-05	1.06E-05	6.76E-07	6.42E-07	2.64E-09	1.68E-09	1.94E-09	1.24E-09	2.64E-09	1.68E-09
U-236	3.35E-09	2.20E-09	6.94E-07	6.59E-07	2.43E-09	1.56E-09	1.8E-09	1.17E-09	2.43E-09	1.56E-09
U-238	3.35E-09	2.22E-09	6.39E-07	6.07E-07	2.34E-09	1.51E-09	1.73E-09	1.13E-09	2.34E-09	1.51E-09
U-238+D	3.22E-06	2.20E-06	6.4E-07	6.08E-07	3.26E-09	2.02E-09	2.35E-09	1.47E-09	3.26E-09	2.02E-09
V-49	0.00E+00	0.00E+00	7.58E-12	6.73E-12	4.79E-12	2.66E-12	3.27E-12	1.82E-12	4.79E-12	2.66E-12
V-50	1.95E-04	1.33E-04	2.57E-09	1.93E-09	2.15E-10	1.45E-10	1.6E-10	1.09E-10	2.15E-10	1.45E-10
W-181	1.29E-06	8.71E-07	3.06E-11	2.63E-11	1.76E-11	9.98E-12	1.22E-11	6.93E-12	1.76E-11	9.98E-12
W-185	7.61E-09	5.14E-09	3.69E-10	3.4E-10	1.16E-10	6.44E-11	7.92E-11	4.4E-11	1.16E-10	6.44E-11
W-188+D	7.01E-06	4.80E-06	1.57E-09	1.42E-09	7.43E-10	4.03E-10	5.1E-10	2.78E-10	7.43E-10	4.03E-10
Y-88	3.69E-04	2.51E-04	5.51E-10	4E-10	1.59E-10	9.28E-11	1.14E-10	6.69E-11	1.59E-10	9.28E-11
Y-91	6.15E-07	4.26E-07	9.08E-10	8.06E-10	6.37E-10	3.52E-10	4.34E-10	2.4E-10	6.37E-10	3.52E-10
Yb-169	2.17E-05	1.47E-05	3.36E-10	3E-10	1.84E-10	1.03E-10	1.27E-10	7.06E-11	1.84E-10	1.03E-10
Zn-65	7.57E-05	5.18E-05	2.04E-10	1.65E-10	4.14E-10	2.81E-10	3.14E-10	2.16E-10	4.14E-10	2.81E-10
Zr-88	4.32E-05	2.95E-05	3.63E-10	3.02E-10	5.81E-11	3.51E-11	4.19E-11	2.57E-11	5.81E-11	3.51E-11
Zr-93	0.00E+00	0.00E+00	3.95E-10	3.65E-10	3.8E-11	2.75E-11	2.93E-11	2.19E-11	3.8E-11	2.75E-11
Zr-95+D	9.73E-05	6.62E-05	6.75E-10	5.93E-10	3.36E-10	1.88E-10	2.31E-10	1.31E-10	3.36E-10	1.88E-10
Zr-95+D1	9.09E-05	6.19E-05	5.75E-10	5.11E-10	1.82E-10	1.03E-10	1.26E-10	7.23E-11	1.82E-10	1.03E-10

Footnote on next page.

Table N-3 DCFPAK3.02 Morbidity and Mortality Risk Coefficients from Different Modes of Exposure (Cont.)

a   Radionuclides with a half-life greater than 30 days. If short-lived progeny are involved, the symbol "+D" is added to the radionuclide name, for example, Ac-227+D. To distinguish between different associated radionuclides or terminal radionuclides, a different +D symbol, for example, "+D1," "+D2," is used. See Appendix A for associated progeny and their branching fractions.

N.2.4   User Libraries

Users can also create their own risk coefficient (slope factor) libraries starting with the base libraries available in the DCF Editor. For example, if the inhalation class for a radionuclide is different from the default inhalation class, users can choose inhalation slope factors based on the known inhalation class. Users can create a user library using the DCF Editor. The User's Guide discusses how to create a user library.

N.3   <u>References</u>

EPA (U.S. Environmental Protection Agency), 1994, *Estimating Radiological Cancer Risks*, EPA 402-R-93-076, U.S. Environmental Protection Agency, Washington, D.C., June. Available at: https://www.epa.gov/sites/production/files/2015-05/documents/402-r-93-076.pdf.

EPA, 1997, Health Effects Assessment Summary Tables (HEAST), U.S. Environmental Protection Agency, Washington, D.C. Available at: https://www.epa.gov/sites/production/files/2015-02/documents/heast2_table_4-d2_0401.pdf.

EPA, 1999, *Cancer Risk Coefficients for Environmental Exposure to Radionuclides*, EPA 402-R-99-001, Federal Guidance Report No. 13, prepared for the Office of Radiation and Indoor Air, U.S. Environmental Protection Agency, Washington, D.C., by Oak Ridge National Laboratory, Oak Ridge, Tenn., September. Available at: https://www.epa.gov/sites/production/files/2015-05/documents/402-r-99-001.pdf.

ICRP (International Commission on Radiological Protection), 1983, *Radionuclide Transformations: Energy and Intensity of Emissions*, ICRP Publication 38, Annals of the ICRP, Vol. 11–13, Pergamon Press, New York, N.Y.

ICRP, 2008, *Nuclear Decay Data for Dosimetric Calculations,* ICRP Publication 107, Pergamon Press, New York, N.Y.

APPENDIX O:
AREA FACTORS FOR OFFSITE EXPOSURE SCENARIOS

As shown in Equation (O.1), the area factor computed by RESRAD-OFFSITE is the ratio of the dose from the entire area of primary contamination to the dose from a part of the primary contamination—both doses being computed for the same exposure scenario and using the same initial activity concentrations of the radionuclides. The two situations modeled to obtain a single measure of the area factor are shown in Figure O-1.
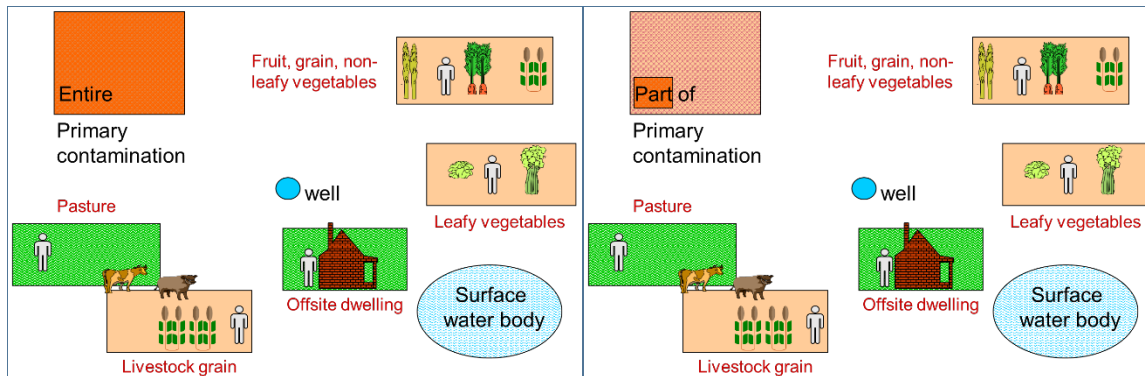
Figure O-1   The Two Scenarios Modeled to Obtain a Measure of the Area Factor

$$Area\ Factor = \frac{Dose\ from\ the\ entire\ area\ of\ the\ primary\ contamination}{Dose\ from\ part\ of\ the\ area\ of\ the\ primary\ contamination} \tag{O.1}$$

In the context of determining the area factor, the entire primary contamination is also referred to as the large area or the wide area. The part of the primary contamination is referred to as a hot spot or a small area of elevated Activity. The latter is referred to as the elevated measurement comparison (EMC) area in the *Multi-Agency Radiation Survey and Site Investigation Manual* (MARSSIM) (2000). The area factor can be used in conjunction with MARSSIM applications to determine the Derived Concentration Guideline Level ($DCGL$) for a small EMC area (i.e., $DCGL_{EMC}$). In MARSSIM terminology, the $DCGL$ for the wide area is called $DCGL_W$.

The dose computed by RESRAD-OFFSITE Version 4 is directly proportional to the Activity concentration in the primary contamination, if the radionuclides follow the equilibrium desorption transfer, the first-order rate-controlled transfer, or the RESRAD-ONSITE exponential release. It will not necessarily be so if any of the radionuclides in the scenario follow the equilibrium solubility transfer. Thus, provided that none of the radionuclides in the scenario follow the equilibrium solubility transfer, the dose in Equation (O.1) can be replaced by the dose per unit Activity.

$$Area\ Factor = \frac{\frac{Dose}{Activity\ concentration}\ from\ the\ entire\ area\ of\ the\ primary\ contamination}{\frac{Dose}{Activity\ concentration}\ from\ part\ of\ the\ area\ of\ the\ primary\ contamination} \tag{O.2}$$

The $DCGL$ is the Activity concentration in the relevant portion of the primary contamination that yields a dose equal to the dose limit; it is inversely proportional to the dose per Activity concentration. Using this inverse relationship gives the desired expression for the area factor.

$$Area\ Factor = \frac{\frac{1}{DCGL_W}}{\frac{1}{DCGL_{EMC}}} = \frac{DCGL_{EMC}}{DCGL_W} \qquad (O.3)$$

The area factors are especially useful in field applications for the quick determination of $DCGL_{EMC}$, which is simply the product of the area factor and the $DCGL_W$. The RESRAD-OFFSITE code provides users with a way to obtain a set of area factors for an offsite receptor scenario, prior to the post-cleanup survey. Because neither the sizes nor the locations of any small areas of elevated measurement are known prior to the final survey, the code uses the probabilistic analysis feature to analyze a number of small areas of elevated measurement, each of a different size and each possibly at a different location within the wide area. The first step is to prepare an input file, just as in the case of a regular RESRAD-OFFSITE run. The layout of the site is specified in the Site Layout form or in the map interface, and site-appropriate values are input for all of the variables in the RESRAD-OFFSITE interface. Then, the "Generate Area Factors" command is chosen in the File menu to display the Area Factors form (Figure O-2). This form is used to specify the parameters related to area factor calculations. The X dimension of the small area of elevated contamination is sampled, as described in Sections O.1, O.3, and O.5. The Y dimension of the small area of elevated contamination can be either sampled or made proportional to the X dimension, as described in Sections O.2, O.3, and O.5. If the Y dimension is to be sampled, the correlation between the samples of the X and Y dimensions must be specified. The location of the small area of elevated contamination can be concentric with the primary contamination or it can be allowed to move within the confines of the original primary contamination, as described in Section O.4.
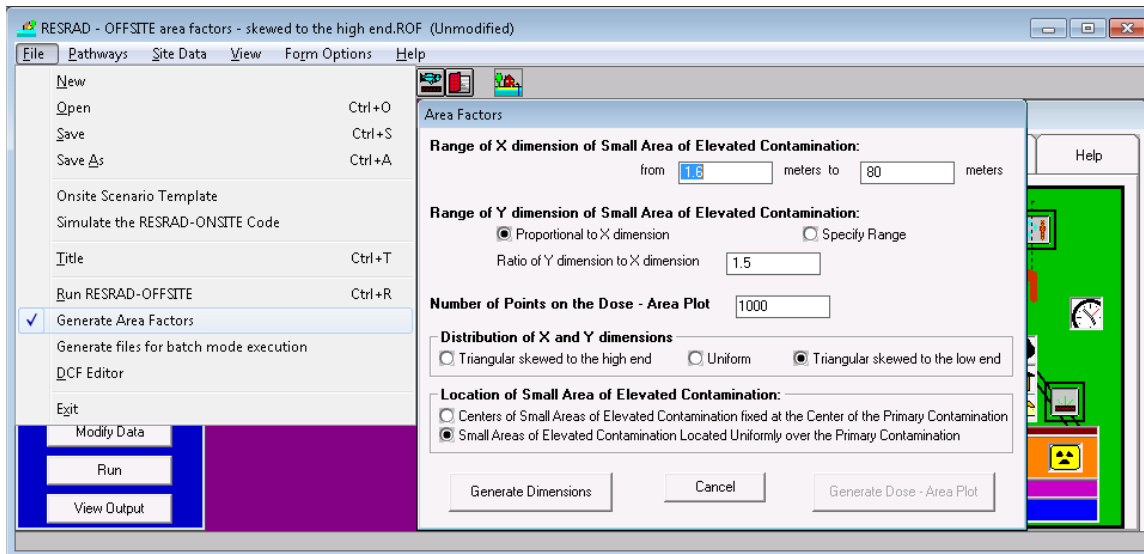
Figure O-2 Displaying the Area Factors Form

O.1   The Range of the X Dimension of the Small Area of Elevated Contamination

By default, the X dimension of the small area of elevated contamination will be obtained by sampling a triangular distribution skewed to the low end ranging from 1/50 to 1 times the X dimension of the primary contamination (Figure O-2). The user can change the lower and upper limits, however, the upper limit may not exceed the X dimension of the primary contamination. That is, the X dimension of the small area of elevated contamination cannot be larger than the X dimension of the primary contamination.

O.2   The Range of the y Dimension of the Small Area of Elevated Contamination

By default, the Y dimension of the small area of elevated contamination is set to be proportional to the X dimension of the small area of elevated contamination. The default proportionality constant is the ratio of the Y dimension of the primary contamination to the X dimension of the primary contamination (Figure O-2). The user may change the proportionality constant; however, the code will not then check to ensure that the resulting Y dimension of the small area of elevated contamination is less than the Y dimension of the primary contamination.

Alternatively, the Y dimension can be sampled in the same manner as the X dimension. If this option is chosen (Figure O-3), by default the Y dimension will be sampled from a uniform distribution ranging from 1/50 to 1 times the Y dimension of the primary contamination. The user can change the lower and upper limits; however, again, the upper limit may not exceed the Y dimension of the primary contamination. In this case, the user must specify the rank correlation coefficient between the X and Y dimensions of the small area of elevated contamination; the default value of 0.99 will produce results that are similar to the default proportionality option. A negative rank correlation coefficient would simulate small areas of elevated contamination that are elongated in either the X or Y directions.

Figure O-3 Option to Specify the Range of the Y Dimension of the Small Area of Elevated Contamination

O.3 Distribution of the X and Y Dimensions of the Small Area of Elevated Contamination

Three options are available for the distribution of the dimensions of the small area of elevated contamination: (1) triangular distribution skewed to the high end, (2) uniform distribution, and (3) triangular distribution skewed to the low end. The distribution of the areas of the small areas of elevated measurement will be uniform when Option 1 (i.e., triangular distribution skewed to the high end) is specified, as is evident from the cumulative distribution function of the areas that were produced under this option (see Figure O-4). Option 2 (i.e., sampling the dimensions uniformly) will result in a distribution of areas that is skewed to the lower end. The distribution of the sampled area will be skewed even more toward the low end if Option 3 (i.e., triangular distribution that is skewed to the low end) is selected. Option 3 would be appropriate if the small areas of elevated contamination are likely to be small in size and, therefore, a user desires to sample a larger number of small areas.
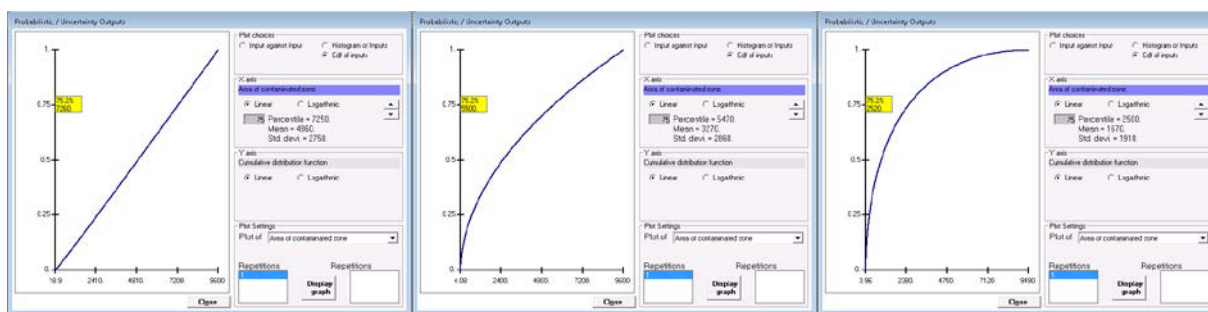
Figure O-4 The Distributions of the Area of the Small Area of Elevated Contamination under the Three Distributions Options for Sampling the Dimensions of the Small Area of Elevated Contamination: *Triangular Skewed to the High End (left), Uniform (center), and Triangular Skewed to the Low End (right)*

O.4 Location of the Small Area of Elevated Contamination

There are two choices for the locations of the small areas of elevated contamination: they can all be concentric with the primary contamination or they can be distributed uniformly over the primary contamination. The small area of elevated contamination is constrained to be within the primary contamination under the distributed option. The code samples two-unit uniform distributions and uses those samples to locate the small area of elevated contamination. A sample value of zero for the X location would place the left edge of the small area of elevated contamination on the left boundary of the primary contamination. A unit value would place the right edge of the small area of elevated contamination on the right boundary of the primary contamination. Likewise, a sample value of zero for the Y location would place the lower edge of the small area of elevated contamination on the lower boundary of the primary contamination. A unit value would place the top edge of the small area of elevated contamination on the upper boundary of the primary contamination. The concentric option will produce a tighter curve between the dose and the small area of elevated contamination. Because the calculated dose will vary with the location of the small area of elevated contamination, the first option (concentric areas) could produce area factors that are higher than reasonable, whereas the second option (distributed areas) will produce conservative area factors.

O.5   Number of Points on the Dose—Area Plot

This specifies the number of times the distribution of the dimensions of the small area of elevated contamination is to be sampled. The default value is 1,000. A smaller value can be used if the dose-area relationship is expected to be in a tight band or a single curve, as would be the case if the Y dimension of the small area of elevated contamination is set to be proportional to the X dimension and the center is fixed. As described in Section O.8, a larger value might be required if the dose-area relationship is expected to be in the shape of a wide band, for example, when both dimensions of the small area of elevated contamination are sampled and/or the location of these small areas of elevated contamination was allowed to vary.

O.6   Generate Dimensions

The Generate Dimensions command button is used to generate the layout—dimensions and location—of each sample of small area of elevated contamination and the offsite transport distances from each sample of small area of elevated contamination to the offsite receptor locations. The Generate Dimension command must be clicked after the user does the following: specifies the limits and type of distribution for the X dimension of the small area of elevated contamination, chooses the method of determining the Y dimension and specifies the values required for that method, selects the desired location option for the small areas of elevated contamination and sets the number of samples. This command button first launches the probabilistic sampling code to sample all the specified distributions. That information is then read by the interface, which uses the sampling results to locate each sample of the small area of elevated contamination and evaluate the relationships for the offsite transport distances for each sample of small area of elevated contamination. Three types of plots of the dimension that were generated can be viewed before proceeding to generate the dose from each small area of elevated contamination—scatter plots, histograms, and cumulative distribution functions. These plots are used to verify that the desired layout and transport distances have been generated. The Generate Dose-Area Plot command button becomes active after the layout and transport distances have been generated (Figure O-5).

Figure O-5   Generate Dose-Area Plot Command Button Enabled in the Area Factors Form

O.7   Generate Dose-Area Plot

This command launches the computational code of RESRAD-OFFSITE to process the inputs for each of the sampled small areas of elevated contamination to generate the dose from each of those small areas of elevated contamination. A scatter plot of dose against the area of elevated contamination and a text report of area factors are displayed for each radionuclide at the end of the run. Four sample plots, obtained by using four options for sizing and locating the small area, for three different radionuclides (i.e., cesium-137 [Cs-137], plutonium-239 [Pu-239], and technetium-99 [Tc-99]) are shown in Figure O-6 through Figure O-8. The four options are case (a) the Y dimensions of the small areas of elevated contamination are proportional to the X dimensions of the small areas of elevated contamination and the small areas of elevated contamination are concentric with the whole contamination; case (b) the Y dimensions of the small areas of elevated contamination are proportional to the X dimensions and the small areas of elevated contamination are located within the whole contamination, but are not constrained to be concentric; case (c) the Y dimensions of the small areas of elevated contamination are sampled and paired with the samples of the X dimension at a specified correlation and the small areas of elevated contamination are concentric with the whole contamination; and case (d) the Y dimensions of the small area of elevated contamination are sampled and paired with the samples of the X dimension at a specified correlation, and the small area of elevated contamination is located within the whole contamination, but is not constrained to be concentric.
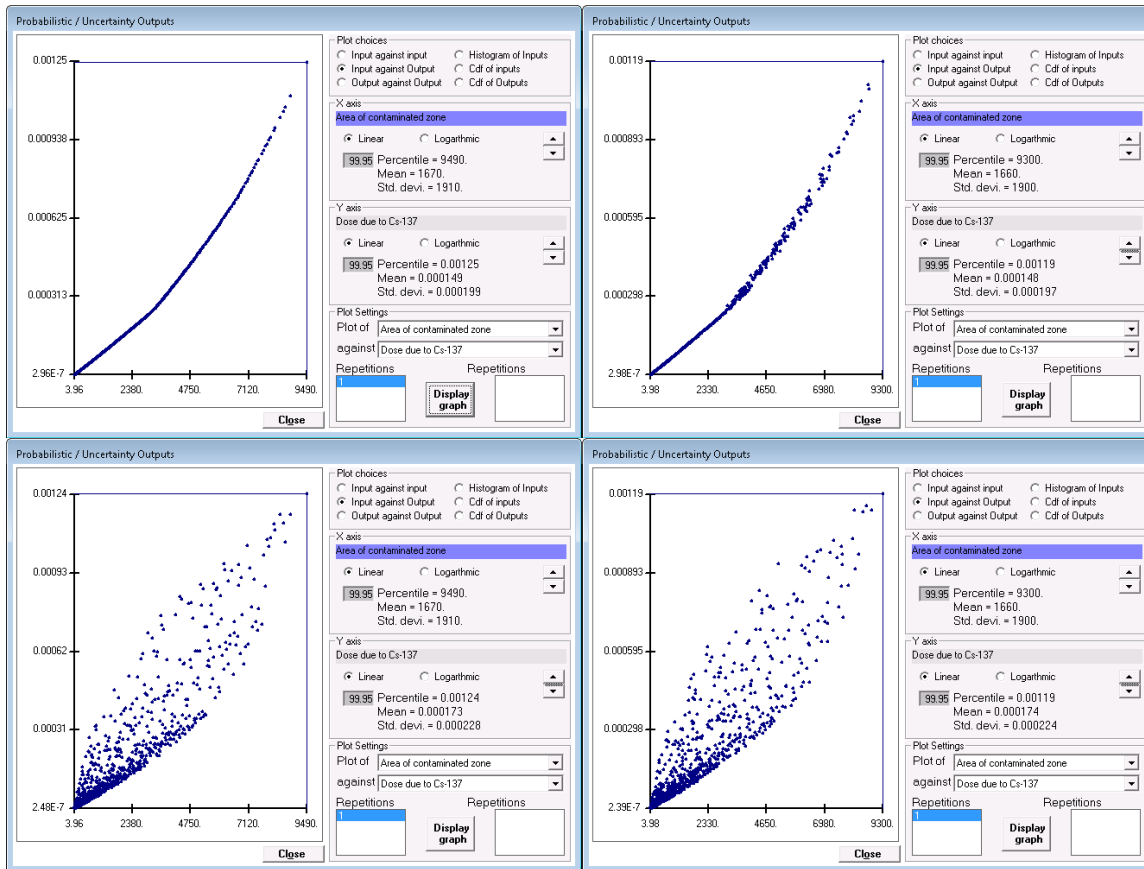
Figure O-6   Scatter Plot of Dose against Area of Contamination for ^{137}Cs where the Direct External Exposure from the Primary Contamination is the Dominant Pathway. *Top left: Case (a): Y dimension is proportional to the X dimension; the small area of elevated contamination is concentric with the primary contamination. Bottom left: Case (b): Y dimension is proportional to the X dimension; the small area of elevated contamination is located anywhere within the primary contamination. Top right: Case (c): X and Y dimensions are highly correlated (rank regression coefficient 0.99); the small area of elevated contamination is concentric with the primary contamination. Bottom right: Case (d): X and Y dimensions are highly correlated (rank regression coefficient 0.99); the small area of elevated contamination is located anywhere within the primary contamination.*

Figure O-7   Scatter Plot of Dose against Area of Contamination for ^{239}Pu for which Atmospheric Transport Is the Dominant Route of Exposure. *Top left: Case (a): Y dimension is proportional to the X dimension; the small area of elevated contamination is concentric with the primary contamination. Bottom left: Case (b): Y dimension is proportional to the X dimension; the small area of elevated contamination is located anywhere within the primary contamination. Top right: Case (c): X and Y dimensions are highly correlated (rank regression coefficient 0.99); the small area of elevated contamination is concentric with the primary contamination. Bottom right: Case (d): X and Y dimensions are highly correlated (rank regression coefficient 0.99); the small area of elevated contamination is located anywhere within the primary contamination.*

Figure O-8   Scatter Plot of Dose against Area of Contamination for ^{99}Tc for which Groundwater Transport Is the Dominant Route of Exposure. *Top left: Case (a): Y dimension is proportional to the X dimension; the small area of elevated contamination is concentric with the primary contamination. Bottom left: Case (b): Y dimension is proportional to the X dimension; the small area of elevated contamination is located anywhere within the primary contamination. Top right: Case (c): X and Y dimensions are highly correlated (rank regression coefficient 0.99); the small area of elevated contamination is concentric with the primary contamination. Bottom right: Case (d): X and Y dimensions are highly correlated (rank regression coefficient 0.99); the small area of elevated contamination is located anywhere within the primary contamination.*

O-9

O.8   Table of Area Factors

The area factor of a nuclide is the ratio of the activity concentration of the nuclide in a small area of elevated contamination located within the primary contamination, $DCGL_{EMC}$, to the activity concentration of the nuclide in the whole primary contamination, $DCGL_W$, both of which result in a peak total dose equal to the basic radiation dose limit to the same offsite receptor. Dose is linearly related to the Activity concentration in the primary contamination under all but the equilibrium solubility transfer model in RESRAD-OFFSITE. Thus, the area factor can be computed by dividing the RESRAD-OFFSITE predicted peak nuclide dose from the entire primary contamination by the RESRAD-OFFSITE predicted peak nuclide dose from a small area of elevated Activity when the same exposure scenario is modeled for both areas at the same Activity concentration, provided the equilibrium solubility transfer option is not specified for any of the radionuclides in the site.

$$Area\ Factor = \frac{DCGL_{EMC}}{DCGL_W}$$

$$= \frac{Dose\ per\ unit\ Activity\ from\ entire\ primary\ contamination}{Dose\ per\ unit\ Activity\ from\ small\ area\ of\ elevated\ Activity} \tag{O.4}$$

The dose versus area plots for case (a) in Figure O-6 through Figure O-8 are all single curves, whereas the plots for cases (b) and (d) are scattered over a wide band. The plots for case (c) are similar to those of case (a), with some scatter that is noticeable at higher doses. In cases (a) and (c), the small area of elevated contamination is constrained to be concentric with the primary contamination. In cases (b) and (d), the small area of elevated contamination is constrained to be within the primary contamination, but it does not have to be concentric with it. The dose from the small area of elevated contamination will be influenced by its location relative to the receptor for almost all exposure pathways. For example, in Figure O-6, where the direct external exposure pathway dominates, a small area of elevated contamination that is located closer to the receptor will subject the receptor to a greater dose than one that is located farther away, all other conditions being equal. Similarly in Figure O-7, where the atmospheric transport is the dominant exposure pathway, a small area of elevated contamination that is located in an unfavorable location with respect to atmospheric stability, wind speed, joint frequency, and distance will subject the receptor to a greater dose than one that is located at a favorable location, all other conditions being equal. Likewise in Figure O-8, where groundwater transport is the dominant exposure pathway, a small area of elevated contamination that has considerable overlap of flow lines with the source of water will subject the receptor to a greater dose than one that has little overlap of flow lines, all other conditions being equal. The transport distance will also influence the dose depending on the relative effects of ingrowth, decay, and dispersion. In cases (a) and (b), the small area of elevated contamination is constrained to be similar in shape to the primary contamination. In cases (c) and (d), the small area of elevated contamination is of a different shape, because its two dimensions are sampled separately and paired according to a user-specified correlation. The small area of elevated contamination will more closely resemble the shape of the primary contamination if the dimensions are directly correlated to a high degree (rank correlation coefficient of almost 1). The dose from the small area of elevated contamination will be influenced by its shape for almost all exposure pathways; the relationship between shape and dose is complex.

Thus, the area factor depends not only on the size of the small area of elevated measurement, but also on its shape and its location within the primary contamination. Because neither the dimensions nor the location of any potential small area of elevated contamination are known prior to the final site survey, the area factor table generated by RESRAD-OFFSITE must be that for the most detrimental location and dimensions. The code will be better able to find the most detrimental location if a sufficiently large number of simulations is performed. The code groups the simulations (the default is 1,000 simulations) into 20 intervals based on the area of the small area of elevated contamination. Then the code determines the simulation within each interval for which the dose/area ratio is the greatest. This method generally allows the code to find the 20 points from the simulations that are closest to the upper boundary of the dose-area curve. The areas and doses of these 20 simulations are used to generate the area factor text report.

The area factors calculated by the RESRAD-OFFSITE code, and the corresponding small areas are output to the file named "AreaFactorText.REP" in the RESRAD-OFFSITE directory. A copy of this file is saved as "inputfilename.AF" to the directory where the input file is saved. This file contains a list of up to 21 pairs of areas and area factors for each radionuclide analyzed—the 20 from the probabilistic run and the one from the whole area deterministic run. The area factors for different radionuclides are listed on separate pages of the text report. Figure O-9 through Figure O-11 show the text reports derived for the information shown in the scatter plots in Figure O-6 through Figure O-8. The user must check the area factor table to see whether the number of simulations was sufficient for the code to determine the upper boundary of the scatter plot. One way to do this is to check whether the area factors are increasing as the area decreases. If they do not, the user could rerun the analysis with a larger number of simulations.

These area factors are for the specific scenario analyzed. They are derived on the basis of pathways selected and parameter values used for that particular scenario. The radionuclide-specific area factor for radionuclide i, $Area\ Factor_i$, can be used with the wide-area radionuclide-specific $DCGL_W^i$ to quickly estimate a conservative value for the small area $DCGL_{EMC}^i$ during the final survey using Equation (O.5).

$$DCGL_{EMC}^i = Area\ Factor_i \times DCGL_W^i \tag{O.5}$$

The location and dimension-specific value of the small-area $DCGL_{EMC}^i$ can be obtained after the final survey by running RESRAD-OFFSITE in the deterministic mode using the information obtained during the final survey. If there are multiple radionuclides in the contaminated area, the sum of fractions rule can be used to determine whether the dose criterion is exceeded.

View - AreaFactorText.REP (top left)

```
RESRAD-OFFSITE Area Factor Report
TITLE : RESRAD-OFFSITE Default Parameters
FILE  : AREA FACTORS Y PROPORTIONAL TO X CENTERED.ROF

Area Factor summary table for Cs-137
Area         Area Factor
3.96         4300.
23.7         717.
67.6         252.
90.1         189.
157.         108.
221.         77.1
422.         40.2
554.         30.5
714.         23.5
905.         18.4
1120.        14.8
1380.        11.9
1690.        9.69
2060.        7.91
2500.        6.47
3020.        5.3
3700.        4.07
4560.        3.03
5850.        2.15
9490.        1.02
9700.        1.0
```

View - AreaFactorText.REP (top right)

```
RESRAD-OFFSITE Area Factor Report
TITLE : RESRAD-OFFSITE Default Parameters
FILE  : AREA FACTORS Y CORRELATED TO X CENTERED.ROF

Area Factor summary table for Cs-137
Area         Area Factor
16.5         1030.
38.8         438.
65.3         260.
103.         164.
207.         82.
234.         72.5
382.         44.1
513.         32.6
668.         25.
811.         20.5
1090.        15.2
1330.        12.3
1530.        10.6
1990.        8.14
2350.        6.8
2870.        5.52
3630.        3.92
4500.        2.98
5710.        2.14
9300.        1.07
9700.        1.0
```

View - AreaFactorText.REP (bottom left)

```
RESRAD-OFFSITE Area Factor Report
TITLE : RESRAD-OFFSITE Default Parameters
FILE  : AREA FACTORS Y PROPORTIONAL TO X DISTRIBUTED.ROF

Area Factor summary table for Cs-137
Area         Area Factor
5.58         250.
39.1         51.2
66.6         42.4
112.         19.1
215.         12.9
310.         7.73
327.         8.75
466.         6.23
600.         4.54
847.         3.93
956.         5.05
1200.        3.53
1640.        2.72
1790.        2.9
2230.        2.44
3020.        1.83
3510.        1.67
4320.        1.52
4650.        1.57
6100.        1.32
9700.        1.0
```

View - AreaFactorText.REP (bottom right)

```
RESRAD-OFFSITE Area Factor Report
TITLE : RESRAD-OFFSITE Default Parameters
FILE  : AREA FACTORS Y CORRELATED TO X DISTRIBUTED.ROF

Area Factor summary table for Cs-137
Area         Area Factor
6.46         251.
35.9         54.4
60.5         31.
124.         23.1
160.         19.3
269.         9.05
348.         7.25
437.         6.22
621.         4.91
727.         5.04
967.         3.88
1210.        4.24
1640.        2.58
1750.        2.51
2290.        2.08
2940.        2.2
3160.        2.03
4040.        1.62
5130.        1.37
6250.        1.34
9700.        1.0
```

Figure O-9   Area Factor Text Report for ^{137}**Cs.** *Top left: Case (a): Y dimension is proportional to the X dimension; the small area of elevated contamination is concentric with the primary contamination. Bottom left: Case (b): Y dimension is proportional to the X dimension; the small area of elevated contamination is located anywhere within the primary contamination. Top right: Case (c): X and Y dimensions are highly correlated (rank regression coefficient 0.99); the small area of elevated contamination is concentric with the primary contamination. Bottom right: Case (d): X and Y dimensions are highly correlated (rank regression coefficient 0.99); the small area of elevated contamination is located anywhere within the primary contamination.*

Top left (Case a):

```
RESRAD-OFFSITE Area Factor Report
TITLE : RESRAD-OFFSITE Default Parameters
FILE  : AREA FACTORS Y PROPORTIONAL TO X CENTERED.ROF

Area Factor summary table for Pu-239
Area        Area Factor
18.6        344.
30.7        209.
88.7        72.2
144.        44.3
150.        42.7
281.        22.9
422.        15.4
546.        11.7
671.        9.41
905.        7.06
1080.       5.93
1160.       5.57
1430.       4.61
1730.       3.84
2070.       3.27
2510.       2.79
3050.       2.37
3700.       2.01
4650.       1.66
5880.       1.4
9700.       1.0
```

Top right (Case c):

```
RESRAD-OFFSITE Area Factor Report
TITLE : RESRAD-OFFSITE Default Parameters
FILE  : AREA FACTORS Y CORRELATED TO X CENTERED.ROF

Area Factor summary table for Pu-239
Area        Area Factor
16.7        385.
28.7        224.
90.1        71.1
148.        43.3
207.        30.3
234.        26.8
317.        20.2
458.        13.7
666.        9.49
904.        7.03
912.        6.99
1130.       5.68
1470.       4.34
1690.       3.89
2350.       2.82
2520.       2.69
3090.       2.27
3750.       1.96
4970.       1.54
5930.       1.36
9700.       1.0
```

Bottom left (Case b):

```
RESRAD-OFFSITE Area Factor Report
TITLE : RESRAD-OFFSITE Default Parameters
FILE  : AREA FACTORS Y PROPORTIONAL TO X DISTRIBUTED.ROF

Area Factor summary table for Pu-239
Area        Area Factor
8.51        354.
20.3        144.
66.6        44.6
112.        26.
187.        17.9
310.        11.2
328.        10.4
466.        6.92
600.        5.36
875.        4.29
1000.       3.98
1200.       3.09
1650.       2.7
1790.       2.51
2230.       2.08
2570.       1.94
3260.       1.63
4320.       1.41
4650.       1.36
5960.       1.26
9700.       1.0
```

Bottom right (Case d):

```
RESRAD-OFFSITE Area Factor Report
TITLE : RESRAD-OFFSITE Default Parameters
FILE  : AREA FACTORS Y CORRELATED TO X DISTRIBUTED.ROF

Area Factor summary table for Pu-239
Area        Area Factor
6.46        424.
21.3        145.
60.5        47.
114.        28.
166.        21.3
234.        13.9
366.        8.76
437.        9.16
621.        5.79
727.        4.74
1120.       3.52
1260.       3.31
1640.       2.53
1800.       2.39
2200.       2.09
2560.       2.06
3010.       1.8
4040.       1.48
4650.       1.38
6190.       1.23
9700.       1.0
```

Figure O-10 Area Factor Text Report for [239]Pu. *Top left: Case (a): Y dimension is proportional to the X dimension; the small area of elevated contamination is concentric with the primary contamination. Bottom left: Case (b): Y dimension is proportional to the X dimension; the small area of elevated contamination is located anywhere within the primary contamination. Top right: Case (c): X and Y dimensions are highly correlated (rank regression coefficient 0.99); the small area of elevated contamination is concentric with the primary contamination. Bottom right: Case (d): X and Y dimensions are highly correlated*
(rank regression coefficient 0.99); the small area of elevated contamination is located anywhere within the primary contamination.

Top left (Case a):

```
RESRAD-OFFSITE Area Factor Report
TITLE : RESRAD-OFFSITE Default Parameters
FILE  : AREA FACTORS Y PROPORTIONAL TO X CENTERED.ROF

Area Factor summary table for Tc-99
Area        Area Factor
3.96        769.
19.4        157.
47.8        64.2
90.1        34.3
147.        21.2
221.        14.3
313.        10.2
424.        7.68
559.        5.95
718.        4.75
906.        3.87
1130.       3.21
1390.       2.7
1700.       2.31
2060.       2.
2500.       1.75
3030.       1.54
3700.       1.37
4580.       1.21
5880.       1.07
9700.       1.0
```

Top right (Case c):

```
RESRAD-OFFSITE Area Factor Report
TITLE : RESRAD-OFFSITE Default Parameters
FILE  : AREA FACTORS Y CORRELATED TO X CENTERED.ROF

Area Factor summary table for Tc-99
Area        Area Factor
4.02        758.
19.4        157.
52.4        58.4
103.        29.8
154.        20.2
234.        13.4
309.        10.3
429.        7.5
580.        5.67
747.        4.48
942.        3.67
1170.       3.04
1440.       2.53
1690.       2.28
2090.       1.92
2520.       1.67
3090.       1.46
3750.       1.32
4650.       1.19
5930.       1.04
9700.       1.0
```

Bottom left (Case b):

```
RESRAD-OFFSITE Area Factor Report
TITLE : RESRAD-OFFSITE Default Parameters
FILE  : AREA FACTORS Y PROPORTIONAL TO X DISTRIBUTED.ROF

Area Factor summary table for Tc-99
Area        Area Factor
8.01        329.
44.2        60.9
62.3        50.2
110.        27.6
164.        16.8
294.        10.9
323.        9.13
497.        6.12
633.        5.18
741.        4.24
1000.       3.31
1320.       2.71
1490.       2.44
1730.       2.27
2310.       1.78
2560.       1.7
3140.       1.49
3750.       1.37
4580.       1.21
5960.       1.06
9700.       1.0
```

Bottom right (Case d):

```
RESRAD-OFFSITE Area Factor Report
TITLE : RESRAD-OFFSITE Default Parameters
FILE  : AREA FACTORS Y CORRELATED TO X DISTRIBUTED.ROF

Area Factor summary table for Tc-99
Area        Area Factor
9.83        297.
33.3        91.3
71.4        39.7
117.        26.1
152.        19.2
244.        12.
315.        9.37
437.        6.65
705.        4.43
729.        4.59
911.        3.67
1290.       2.71
1400.       2.51
1730.       2.2
2350.       1.74
2580.       1.62
3160.       1.41
3680.       1.4
4600.       1.17
5900.       1.06
9700.       1.0
```
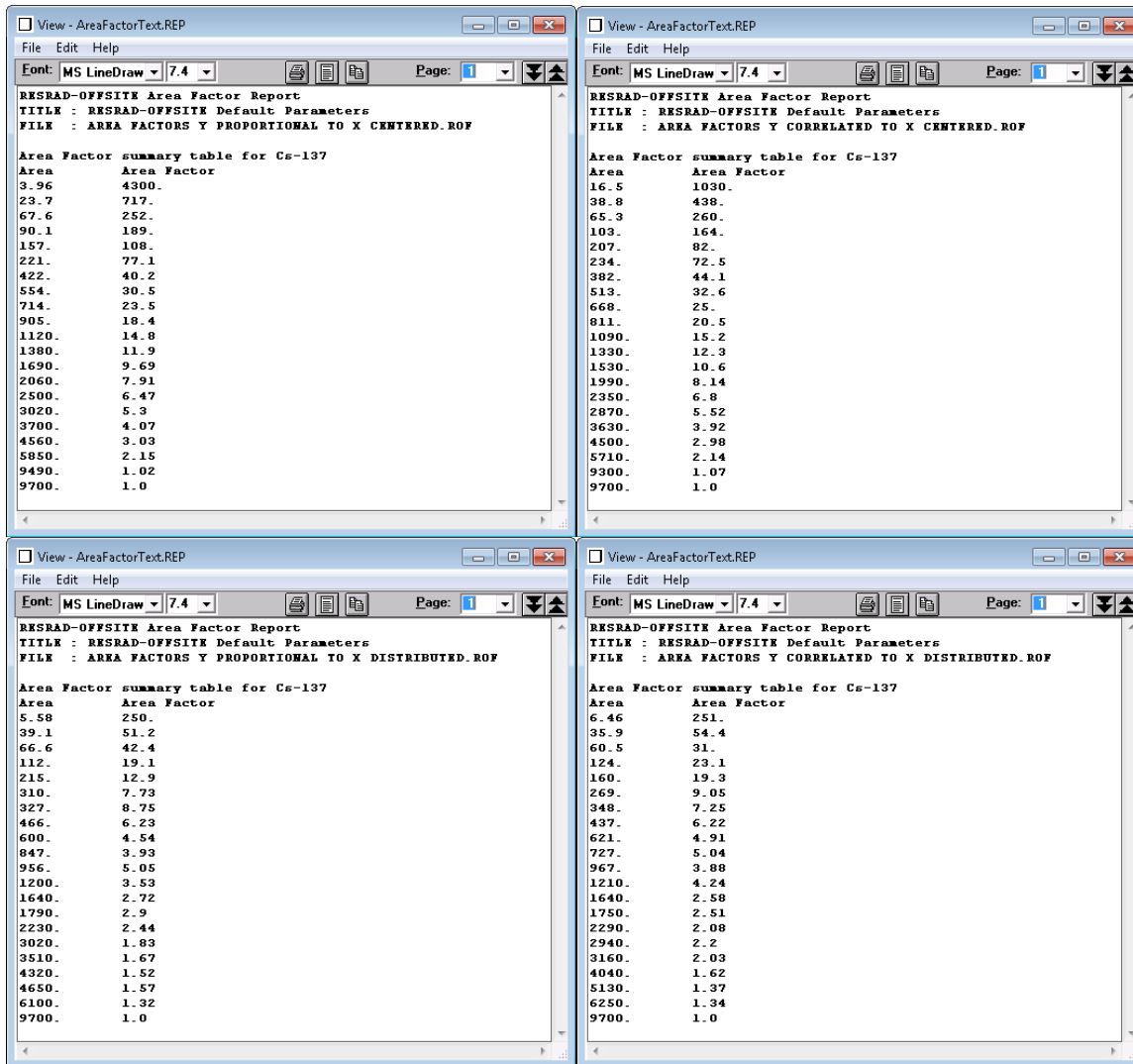
Figure O-11 Area Factor Text Report for ^{99}Tc. *Top left: Case (a): Y dimension is proportional to the X dimension; the small area of elevated contamination is concentric with the primary contamination. Bottom left: Case (b): Y dimension is proportional to the X dimension; the small area of elevated contamination is located anywhere within the primary contamination. Top right: Case (c): X and Y dimensions are highly correlated (rank regression coefficient 0.99); the small area of elevated contamination is concentric with the primary contamination. Bottom right: Case (d): X and Y dimensions are highly correlated (rank regression coefficient 0.99); the small area of elevated contamination is located anywhere within the primary contamination.*
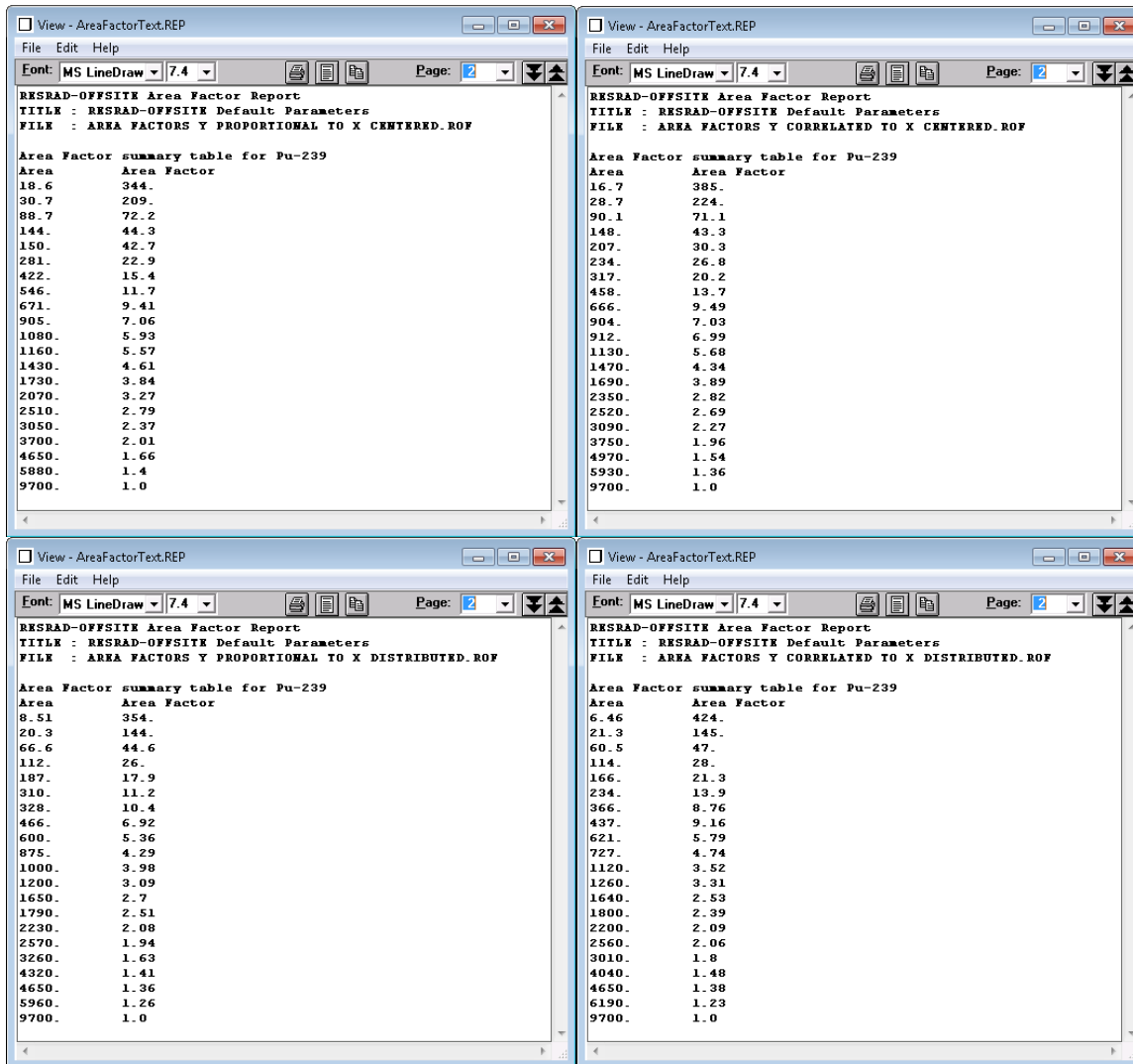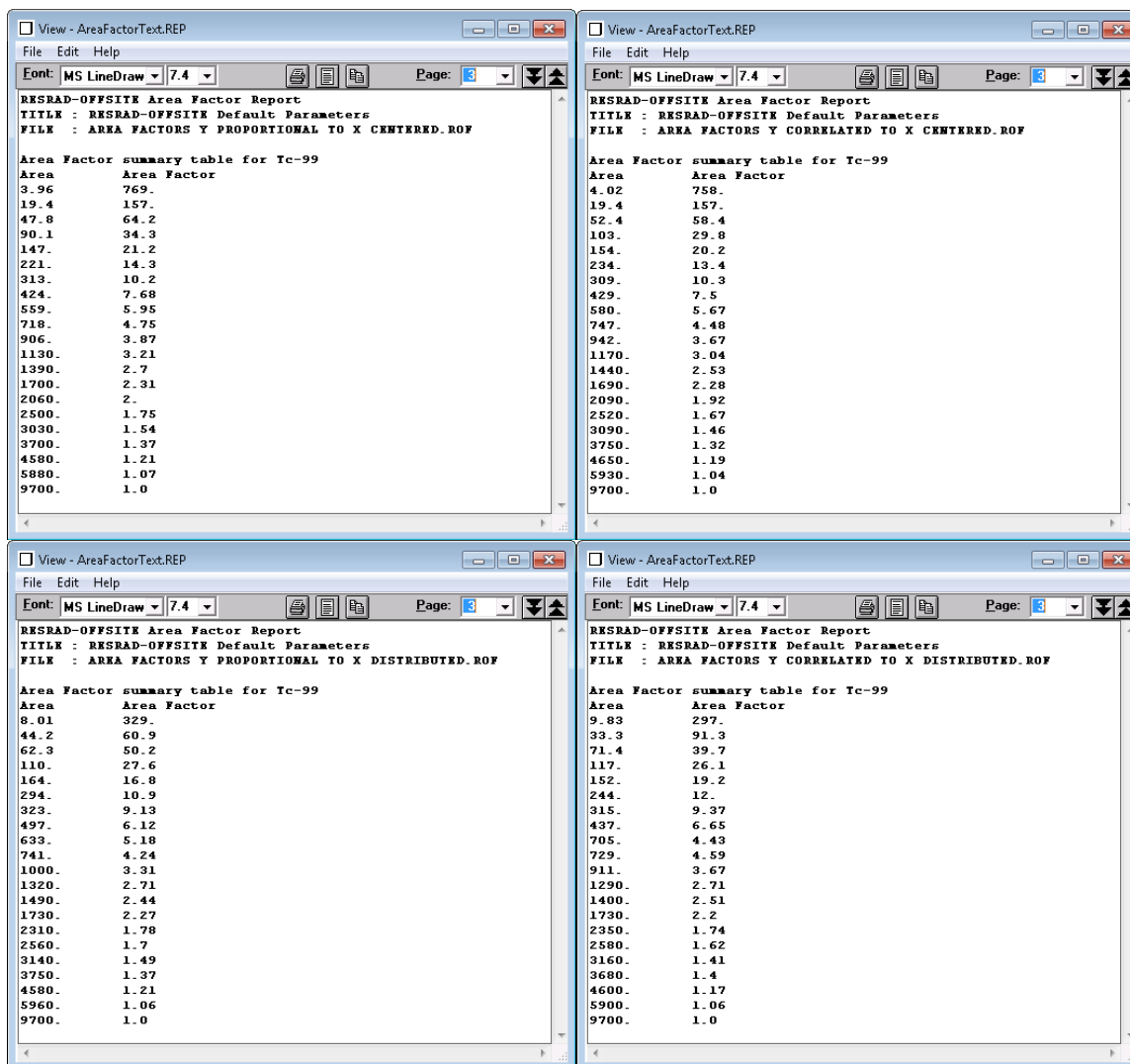
O.9   Reference

MARSSIM, 2000, *Multi-Agency Radiation Survey and Site Investigation Manual (MARSSIM)*, NUREG-1575, Rev. 1, EPA 402-R-97-016, Rev. 1, DOE/EH-0624, Rev. 1, Aug.

NRC FORM 335 (12-2010) NRCMD 3.7	U.S. NUCLEAR REGULATORY COMMISSION **BIBLIOGRAPHIC DATA SHEET** *(See instructions on the reverse)*	1. REPORT NUMBER (Assigned by NRC, Add Vol., Supp., Rev., and Addendum Numbers, if any.) **Volume 1**

2. TITLE AND SUBTITLE	3. DATE REPORT PUBLISHED

	MONTH	YEAR

4. FIN OR GRANT NUMBER

5. AUTHOR(S)	6. TYPE OF REPORT Technical

7. PERIOD COVERED (Inclusive Dates)

8. PERFORMING ORGANIZATION - NAME AND ADDRESS (If NRC, provide Division, Office or Region, U. S. Nuclear Regulatory Commission, and mailing address; if contractor, provide name and mailing address.)

9. SPONSORING ORGANIZATION - NAME AND ADDRESS (If NRC, type "Same as above", if contractor, provide NRC Division, Office or Region, U. S. Nuclear Regulatory Commission, and mailing address.)

10. SUPPLEMENTARY NOTES

11. ABSTRACT (200 words or less)

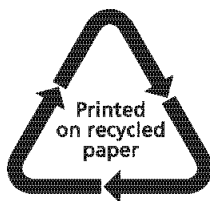| 12. KEY WORDS/DESCRIPTORS (List words or phrases that will assist researchers in locating the report.)	13. AVAILABILITY STATEMENT unlimited
	14. SECURITY CLASSIFICATION
	(This Page) unclassified
	(This Report) unclassified
	15. NUMBER OF PAGES 544
	16. PRICE

UNITED STATES
NUCLEAR REGULATORY COMMISSION
WASHINGTON, DC 20555-0001

OFFICIAL BUSINESS

@NRCgov

NUREG/CR-7269
Volume 1

User's Manual for RESRAD-OFFSITE Code Version 4;
Methodology and Models Used in RESRAD-OFFSITE Code

March 2021